DEVELOPMENT OF NOSCAPINE CONGENER FOR THE MANAGEMENT OF BREAST CANCER

A Thesis Submitted to the Sambalpur University in Partial Fulfilment of the Requirements for the Degree of

DOCTOR OF PHILOSOPHY
IN
BIOTECHNOLOGY

by

PRATYUSH PRAGYANDIPTA

Regd. No. 002/2018/Bio.Tech.

Under the Joint Supervision of

Supervisor: *Dr. Pradeep K. Naik, Professor, Department of Biotechnology & Bioinformatics, Sambalpur University*

Co-supervisor: *Dr. Manu Lopus, Reader, School of Biological Sciences, UM-DAE Center for Excellence in Basic Sciences, Mumbai*

DEPARTMENT OF BIOTECHNOLOGY & BIOINFORMATICS,
SAMBALPUR UNIVERSITY, JYOTIVIHAR, BURLA,
SAMBALPUR- 768019, ODISHA

May, 2022

Dr. Pradeep K. Naik
Professor and Head
Dept. of Biotechnology & Bioinformatics

SAMBALPUR UNIVERSITY
JYOTI VIHAR – 768019
SAMBALPUR, ODISHA
Mob.: +91-9479268802
Fax: (0663) – 2430158
E-mail: *pknaik1973@gmail.com*

CERTIFICATE

*This is to certify that the research work entitled, "**Development of noscapine congener for the management of breast cancer**" submitted by **Pratyush Pragyandipta (Regd No: 002/2018/Bio.Tech.)** at **Sambalpur University, Orissa, India** is a bonafide record of his original work carried out under my supervision. This work has not been submitted partially or wholly to any other University or Institute for any degree or diploma. I recommend this thesis in fulfillment of the award of the degree of **Doctor of Philosophy** in **Biotechnology.***

11/05/2022

Prof. (Dr.) Pradeep Kumar Naik
Dept. of Biotechnology & Bioinformatics,
Sambalpur University, Jyoti Vihar, Burla,
Sambalpur, India.
Date: 11/05/22

Professor and Head
P.G. Dept. of BT & BI
Sambalpur University
Jyoti Vihar-768019,Odisha

UNIVERSITY OF MUMBAI-DEPARTMENT OF ATOMIC ENERGY

CENTRE FOR EXCELLENCE IN BASIC SCIENCES

Nalanda, University of Mumbai, Kalina campus, Mumbai 400098

Phone: 91-22-26532132 Web: www.cbs.ac.in Fax: 91-22-26532134

Nurturing talent...promoting excellence

मौलिक विज्ञान प्रकर्ष केन्द्र

CERTIFICATE

*This is to certify that the research work entitled, "**Development of noscapine congener for the management of breast cancer**" submitted by **Pratyush Pragyandipta (Regd No: 002/2018/Bio.Tech.)** at **Sambalpur University, Orissa, India** is a bonafide record of his original work carried out under my co- supervision. This work has not been submitted partially or wholly to any other University or Institute for any degree or diploma. I recommend this thesis in fulfillment of the award of the degree of **Doctor of Philosophy** in **Biotechnology.***

Dr. Manu Lopus,
School of Biological Sciences,
UM-DAE, Centre for Excellence in Basic Sciences,
Mumbai, India.

Date: 21.3.22

TABLE OF CONTENTS

Chapter 4

In Silico Inspired Design of 1,3-Diynl Congeners of Noscapine as Promising Tubulin-Binding Anticancer Agent: Chemical Synthesis and Cellular Activity with Breast Cancer Cell Lines. **103-144**

Chapter 5

LIST OF FIGURE

LIST OF TABLE

ABSTRACT OF THE DISSERTATION

Drugs that target mitotic spindle, such as taxol, vinca-drugs, and estramustine have been in the clinic for the treatment of different types of breast cancers. However, these drugs are known to cause severe dose-limiting toxicities in patients such as peripheral neuropathy, systemic toxicity, and allergic reactions. More importantly patients are developing resistance against taxol. Thus, wonderful promise of taxol in managing breast cancers justifies further effort to discover novel mitotic inhibitors. Better yet, it would be additionally useful if other novel anti-mitotic agents have less side effects and easily administered. Our initial efforts towards this end have been quite encouraging in that we have rationally designed and chemically synthesized a battery of derivatives of natural lead molecule, Noscapine (opium alkaloid, used as anticough medicine and identified as tubulin binding anticancer agent). Some of these compounds were demonstrated as more potent compared to Noscapine as anticancer agent. In a quest of making novel derivatives of noscapine, the present study focusing on rational design of five new classes of noscapinoids such as (1) 1,3-diynyl-noscapinoids, (2) 9-arylimino noscapinoids, (3) N-arylalkylamino-noscapinoids, (4) N-imidazopyridine-noscapinoids and (5) 9-Urea noscapinoids, followed by chemical synthesis and exhaustive experimental evaluation as potent anticancer agents with little or no toxicity that holds great promise for clinical use.

A novel class of noscapine derivatives known as 9-arylimino noscapinoids was designed by substituting arylimino groups (Schiff bases) at the C-9 position. These molecules were docked with αβ-tubulin complex and a panel of three top-scoring molecules, 9-((E)-((5-bromothiophen-2-yl)methylene)amino)-4-methoxy-6-methyl-5,6,7,8 -tetrahydro-[1,3] dioxolo [4,5-g] isoquinolin-5-yl)-6,7dimethoxyisobenzofuran-1(3H)-one **(4),** 9-((E)-(2,5-difluorobenzylidene)amino)-4-methoxy-6-methyl-5,6,7,8-tetrahydro-[1,3] dioxolo[4,5-g]isoquinolin-5-yl)-6,7-dimethoxyisobenzofuran-1(3H)-one **(5)** and 9-((E)-(4-bromobenzylidene)amino) -4-methoxy-6-methyl-5,6,7,8-tetrahydro-[1,3]dioxolo[4,5-g]iso quinolin-5-yl)-6,7-dimethoxyisobenzofuran-1(3H)-one **(6)** based on docking score were screened out. These molecules bind tubulin with robust predicted binding energy of -37.24 kcal/mol and -45.41 kcal/mol for **4**, -39.73 kcal/mol and -47.74 kcal/mol for **5**, and -43.62 kcal/mol and -49.72 kcal/mol for **6** respectively compared to noscapine (-34.47 kcal/mol and -40.27 kcal/mol) using molecular mechanics/Poisson-Boltzmann surface area (MM/PBSA) and molecular mechanics/generalized Born surface area (MM/GBSA). These three molecules were chemically synthesized and demonstrated experimentally to bind

tubulin with high affinity compared to noscapine. The anti-proliferative activity of **4-6** revealed inhibitory concentration (IC_{50} value) in between 3.6 to 32.6 μM using MCF-7 and MDA-MB-231 human breast cancer cell lines and a group of primary breast tumor cells. All three molecules were shown to inhibit the mitotic progression at the G2/M phase and induce apoptosis to cancer cells at a different level. Thus, we conclude that 9-arylimino noscapinoids **4-6** have tremendous potential as chemotherapeutic agents for the treatment of breast cancer.

In our next attempt, we envisaged developing 9-N-arylmethylamino derivatives of noscapine to enhance the anticancer activity of noscapine. The scaffold structure of noscapine was tailored by inducing a N-aryl methyl pharmacophore at the C-9 position to generate a library of derivatives, followed by a screening of top-ranked three derivatives (S)-3-((R)-9-((Anthracen-9-ylmethyl)amino)-4-methoxy-6-methyl-5,6,7,8-tetrahydro-[1,3] dioxolo[4,5-g]isoquinolin-5-yl)-6,7-dimethoxyisobenzofuran-1(3H)-one **(15)**, (S)-3-((R)-9-(([1,1'-Biphenyl]-4-ylmethyl)amino)-4-methoxy-6-methyl-5,6,7,8-tetrahydro[1,3]dio xolo[4,5-g]isoquinolin-5-yl)-6,7-dimethoxyisobenzofuran-1(3H)-one **(16)** and (S)-3-((R)-9-((2,5-difluorobenzyl)amino)-4-methoxy-6-methyl-5,6,7,8-tetrahydro-[1,3]dioxolo [4,5-g]isoquinolin-5-yl)-6,7-dimethoxyisobenzofuran-1(3H)-one **(17)** using molecular docking. These derivatives were synthesized and analysed for their *in vitro* cytotoxicity against breast cancer cell lines (MCF-7 and MDA-MB-231). Further, inhibition of cell cycle progression and induction of apoptosis to cancer cells was determined using FACS. Antiproliferative activity with the treatment of 15-17 revealed IC_{50} values ranging between 19.4 to 47.3 μM in two human breast cancer cell lines (MCF 7 and MDA-MB-231) without affecting the normal healthy cells (cytotoxicity is < 5% at 100 μM) using human embryonic kidney cell (293T). These derivatives induce apoptosis to cancer cells by arresting the mitotic cell cycle in the G2/M-phase by interfering with microtubules. The 9-(N-arylmethylamino) derivatives of noscapine have a good probability of becoming a novel therapeutic agent for the treatment of breast cancer.

In our further attempt, a panel of 1,3-diynyl-noscapinoids such as (*S*)-3-((*R*)-9-(cyclopropylbuta-1,3-diyn-1-yl)-4-methoxy-6-methyl-5,6,7,8-tetrahydro-[1,3] dioxolo[4,5-*g*]isoquinolin-5-yl)-6,7-dimethoxyisobenzofuran-1(3*H*)-one **(20)**, (*S*)-3-((*R*)-9-((4-fluorophenyl)buta-1,3-diyn-1-yl)-4-methoxy-6-methyl-5,6,7,8-tetrahydro [1,3] dioxolo [4,5-*g*]isoquinolin-5-yl)-6,7-dimethoxyisobenzofuran-1(3*H*)-one **(21)** and (*S*)-6,7-dimethoxy-3-((*R*)-4-methoxy-6-methyl-9-((2-(trifluoromethyl)phenyl)buta-1,3-diyn- 1-yl)-5,6,7,8-tetrahydro-[1,3]dioxolo[4,5-*g*]isoquinolin-5-yl)isobenzofuran-1(3*H*)-one **(22)** were strategically designed to increase the anticancer activity of the lead molecule,

noscapine. Structure-activity analyses revealed strong predicted free energy of binding ($\Delta G_{bind,pred}$) of -6.694, -7.294 and -7.468 kcal/mol, for **20-22** respectively compared to noscapine (experimental free energy of binding ("$\Delta G_{bind,expt}$") is -5.246 kcal/mol). These novel derivatives were demonstrated to bind tubulin by fluorescence quenching assay and Far-UV circular dichroism. Further, they were tested to exhibit potent cytotoxic activity compared to noscapine using two human breast cancer cell lines. The IC_{50} value for noscapine, **20, 21** and **22** has been derived to be 35.2, 27.3, 18.7 and 12.7 µM using MCF7 and 39.6, 31.4, 22.5 and 16.1 µM using MDAMB-231. These derivatives were found to arrest cell cycle in the G2/M-phase followed by apoptosis and appearance of TUNEL-positive cells. Thus, we conclude that 1,3-diynyl derivatives of noscapine have great potential to be a novel therapeutic agent for breast cancers.

In a quest of making a new class of noscapine derivatives, we have developed N-imidazopyridine-noscapinoids (**7-11**) by coupling imidazo[1,2-a]pyridine pharmacophore to the N-atom of the isoquinoline ring based on our *in silico* efforts. These compounds were found to bind with high affinity to tubulin based on molecular docking, MD simulation and MM-PBSA. The predicted $\Delta G_{binding}$ varies from -183.79 to -150.66 KJ/mol for the N-imidazopyridine-noscapinoids which is higher then the lead molecule, noscapine ($\Delta G_{binding}$ is -132.63 KJ/mol) and satisfies all the properties essential for ADME. These novel derivatives were chemically synthesized and validated their anticancer activity based on cellular studies using two human breast cancer cell lines, MCF-7 and MDAMB-231, as well as with a panel of primary breast cancer cells isolated from patients. Interestingly, all these derivatives inhibited cellular proliferation in all cancer cells ranging between 5.3 to 34.0 µM, without affecting the normal healthy cells (IC_{50} value > 1500 µM), indicating that these compounds were not toxic to normal healthy cells. Out of the N-imidazopyridine-noscapinoids **(7-11),** N-5-Bromoimidazopyridine-noscapine **(9)** showed promising antiproliferative activity using both the cell lines (IC_{50} value is 5.3 and 7.8 µM against MCF-7 and MDAMB-231) and was selected for the detailed investigation. Unlike previously reported derivatives of noscapine that arrest cells in the S-phase, this novel derivative effectively inhibit proliferation of cancer cells, perturb cell cycle in the G2/M-phase followed by induction of apoptosis. FACS analysis revealed the percentage of early apoptotic cells to 15% and late apoptotic cells to 35% with treatment of N-5-Bromoimidazopyridine-noscapine **(9)** which were significantly high compared to controlled untreated cells. The induction of apoptosis to MDAMB-231 cells by the treatment of N-5-Bromoimidazopyridine-noscapine at its IC_{50} concentration is revealed from the morphological changes such as membrane blebbing, cellular shrinkage,

chromatin condensation and formation of apoptotic bodies. Moreover, treatment with N-5-Bromoimidazopyridine-noscapine **(9)** significantly elevated the reactive oxygen species and the loss of mitochondrial membrane potential which might have a function in the induction of apoptosis. The compound **9** was also found to significantly regressed the implanted tumour in nude mice as xenografts of MCF-7 cells without any apparent side effects after drug administration. Thus, we conclude that N-imidazopyridine-noscapinoids have great potential to be a novel therapeutic agent for breast cancers.

Additionally, we have present a series of noscapine urea congeners **7a-7h** as potential tubulin binding agents. This series of compounds were designed thorugh in silico combinatorial chemistry by coupling of urea pharmacophore at the C-9 position of the noscapine scaffold. The binding affinity of these urea noscapine congeners **7a-7h** with tubulin was theoretically predicted based on combination of molecular docking, MD simulation and MM-PBSA. Both the docking acore and $\Delta G_{bind,pred}$ reveled strong binding affinity of urea congeners wih tubulin compared to noscapine. The $\Delta G_{bind,pred}$ varies in between – 186.3 to -140.9 KJ/mol, whereas for noscapine it is -132.6 KJ/mol. Further, all these compounds have qualified the ADME and drug like characteristics based on in silico prediction. Inspired by *in silico* predictive activity, we have strategically synthesised these urea noscapine congeners **7a-7h** followed by experimental evaluation using a panel of establiehd breast cancer cell lines (MCF-7 and MDAMB-231, primary breast tumor cells obtained from the patients and normal healthy cell line (293T). Interestingly all these derivatives reduced cellular proliferation in all the cancer cells with a IC_{50} concentration between 4.77 to 48.45 μM, without affecting the normal healthy cells (IC_{50} is > 285.4 μM. In particular, the compound **7g** was found to be most promising among the library based on IC_{50} value (IC_{50} value is 4.77 and 6.56 μM for the MCF-7 and MDAMB-231 cell lines) and was selected for the detailed investigation.The treated breast cancer cell line, MDAMB-231 with IC_{50} value of **7g** underwent several morphological changes such as membrane blebbing, numerous fragmented nuclei, and appearance of apoptotic bodies, indicating induction of apoptosis. It has been further confirmed by flow cytometry analysis which revealed early apoptosis (22%) and late apoptosis (68%) to MDAMB-231 cells. The urea noscapine congener **7g** was also found to arrest cell cycle in the G2/M-phase followed by apoptosis and appearance of TUNEL-positive cells at IC_{50} concentration. Further, treatment with **7g** significantly elevated the reactive oxygen species and the loss of mitochondrial membrane potential which might have a function in the induction of apoptosis. The compound **7g** was also found to significantly regressed the implanted tumour in nude mice as xenografts of MCF-7 cells without any apparent side effects after

drug administration. Although the lead compound, noscapine, is already in clinical trials, urea noscapine congener represents an additional edge over noscapine because of its higher potency, without compromising the nontoxic profile of noscapine.

In conclusion, five different classes of noscapinoids were developed by coupling active pharmacophore such as arylimino groups (Schiff bases), N-aryl methyl, 1,3-diynyl, imidazo[1,2-*a*] pyridine and urea group at the C-9 position with noscapine scaffold based on in silico combinatorial approach. We have primarily focused on these functional groups because they are recognized as key pharmacophores in several anticancer drugs utilized in the clinic. All the noscapinoids developed were found to enhance the anticancer activity to several folds. Thus, these noscapinoids have great potential to be a novel therapeutic agent for breast cancers.

CHAPTER 1

Ph.D. Department of Biotechnology & Bioinformatics
Sambalpur University

Introduction

INTRODUCTION

1.1. Cancer Scenario

Cancer ranks as a primary cause of mortality and a significant impediment to living longer. Different types of cancer are named after the tissues or organs where they develop. According to WHO, cancer is the foremost cause of death globally, with approximately 9.9 million deaths in 2020 and 19.3 million new cases (Figure 1.1). The global cancer burden is expected to be 30.2 million new cases. Cancer death is predicted to be 16.3 million by 2040 due to increasing risk factors associated with modernization and a growing economy (Bray *et al.,* 2018; WHO, Globocan, 2021). According to the latest report released by the National Cancer Institute (NCI), in 2020, an estimated 18,06,590 new cases were reported and the global burden of cancer will be nearly 1.9 million new cases in 2021. As per NCI (National Cancer Institute, 2021), Breast cancer, lung and bronchus cancer, colon and rectum cancer, prostate cancer, bladder cancer, melanoma of the skin, non-Hodgkin lymphoma, endometrial cancer, kidney and pelvis cancer, leukemia, pancreatic cancer, liver and thyroid cancer are the major incidence type of cancer. In males around 26% suffer from prostrate cancer while 12% from lungs and 8% form colorectal cancers. In case of females the most common cancer is breast (30%) followed by lungs (13%) and colorectal (8%). Each year, there are 442.4 new cancer cases for every 100,000 men and women, with men having higher mortality rate (189.5 per 100,000) than females (135.7 per 100,000) (As per cancer incidence cases 2013-17). Cancer mortality was found to be highest in African and American males (239.9 per 100,000) and lowest in Asian/Pacific Islander women when groups were compared based on civilization and gender (83.3 per 100,000) (National cancer institute, 2021).

Cancer mortality tends to be a burden for a country. With a population of 1.3 billion people, India accounts for 7 out of 100 new cancer cases and is likely to rise rapidly with an increase in population, urbanization, and aging (Shin *et al.,* 2012). In India, it is the second deadliest disease responsible for a maximum mortality rate of 0.8 million deaths per year. As per the latest report released by WHO the cancer burden of India is 1.3 million new cases in 2020 (WHO, Globocan, 2021, Figure 1.2). The most common form of cancer among males is mouth, tongue, lungs, prostate, and stomach, constituting about 36% of cancer. While in females, the common form of cancer includes

the breast, ovary, cervix, uteri, corpus and lungs, which constitute about 53% of all cancers (Mathur *et al.*, 2020).

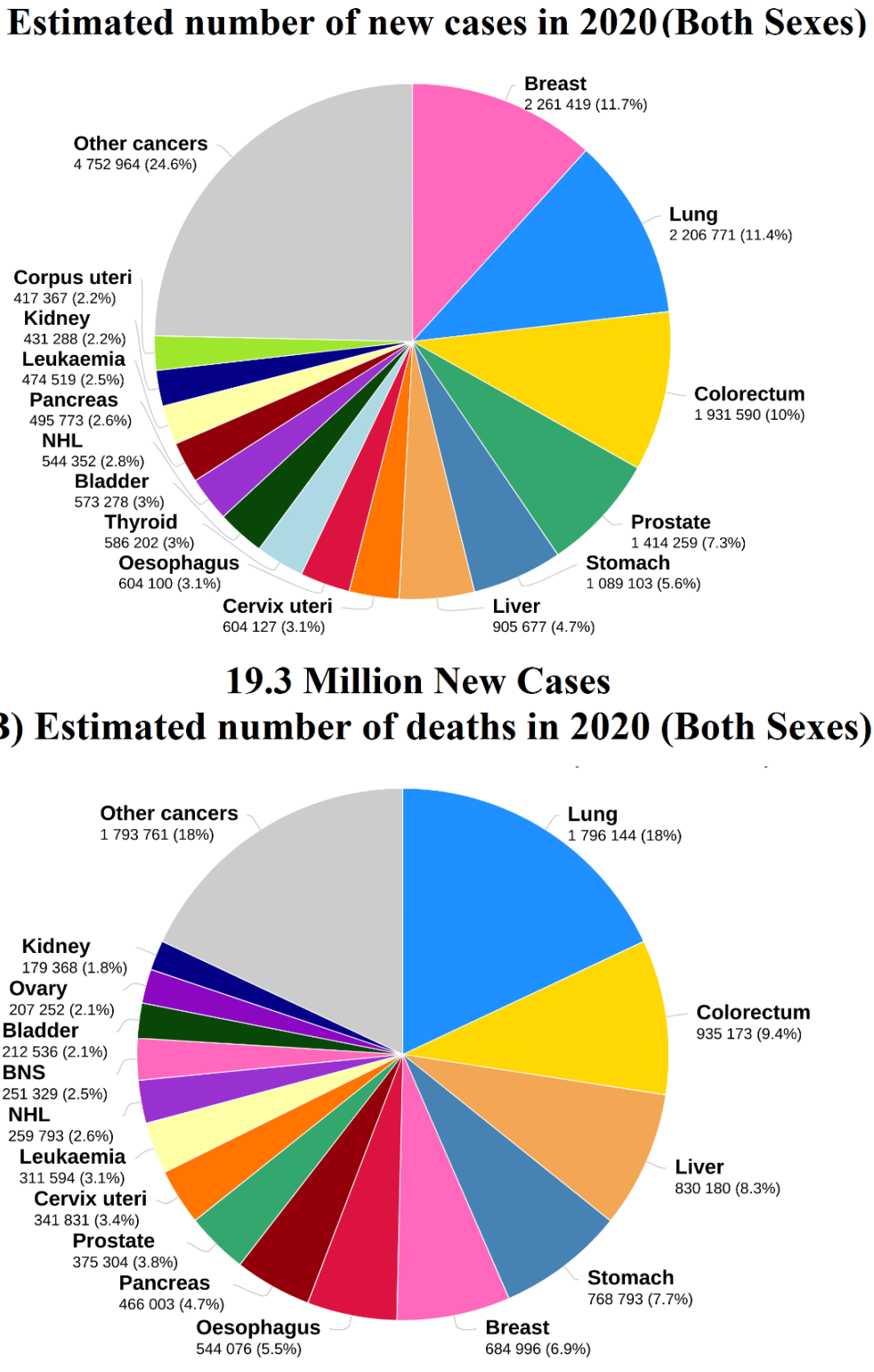

Figure 1.1: *Showing the estimated number of new incidence cases and mortality number, both sexes, all cancer excluding non-melanoma skin cancer, worldwide (Source: WHO, IARC, GLOBOCAN 2020).*

(A) Estimated number of new cases in 2020, India (Both Sexes)

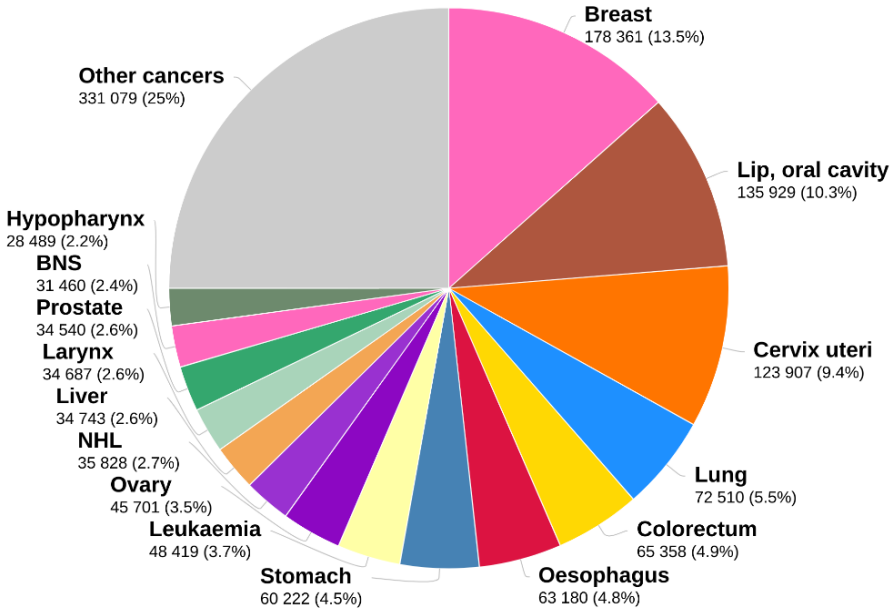

1.3 Million New Cases

(B) Estimated Number of Deaths in 2020, India (Both Sexes)

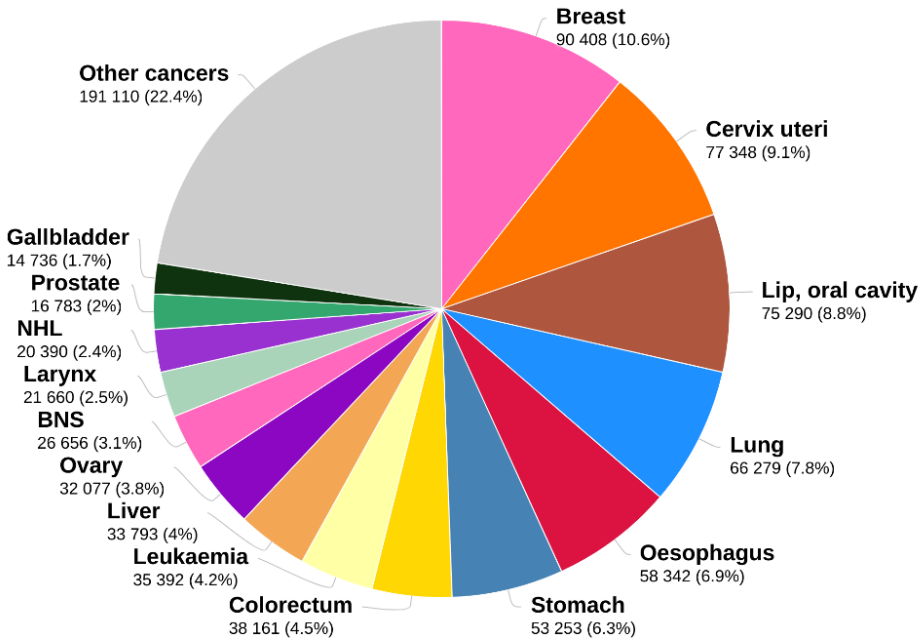

0.8 Million Death

Figure 1.2: *Showing the estimated number of new incidence cases and mortality number, both sexes, all cancer excluding non-melanoma skin cancer, India. (Source: WHO, IARC, GLOBOCAN 2020).*

As per the recent estimation by the Indian Council of Medical Research (ICMR), about 7,84,821 people died of cancer, with incidence cases over 11,57,294 in India (Pilleron *et al.,* 2021). The overall number of new cases is expected to rise from 0.59

million in 2012 to 0.93 million in the case of males, and from 0.60 to 0.94 million in the case of females (Dsouza *et al.*, 2013). As per the ICMR report, the number of incidence cases is likely to increase to 15 lakhs by 2025 and more than 8 lakh deaths with a 12% increase from the current estimated cases. The primary reason behind this increment is increased tobacco consumption (27.1% of the cancer burden is due to tobacco-related cancers). Table 1.1 includes topmost cancer in men and women in India (Saranath and Khanna, 2014).

Table 1.1: The topmost cancer in men and women in India.

Sl.no	Men	Women
01	Lip/Oral Cancer	Breast Cancer
02	Lung Cancer	Cervix Cancer
03	Stomach Cancer	Colorectum Cancer
04	Colorectum Cancer	Ovary Cancer
05	Pharynx Cancer	Lip/Oral Cancer

1.2. Breast Cancer

Breast cancer can be defined as the abnormal growth of the cell lining of breast lobules or ducts characterized by uncontrolled growth leading to the formation of tumours (malignant) in the milk-producing glands or the ducts and having the potential to metastasize. It can either begin in the ducts or the lobules and the growth rate of the tumor is quite slow and by the time lump become too large and can be physically felt or seen it might be developing for a minimum 10 years in the body (Garcia *et al.*, 2007). Generally, all breast cancers are carcinomas in nature. Breast cancer is quite common in females, over 1 million women are being diagnosed and half of them are dying globally, accounting for 25% of all cancer cases and 15% of mortality; and interestingly, it can also affect men, which is quite rare in occurrence (Nounou *et al.*, 2015). Although male and female breast cancer has comparable causes, male breast cancer is caused by hormone-receptor positive cells, which are more susceptible to hormonal treatment, and BRCA2 gene mutations pose a larger risk than BRCA1 gene mutations (Giordano *et al.*, 2002; Gómez-Raposo *et al.*, 2010). The tumour in males expresses the progesterone receptors, estrogen, and is less likely to overexpress HER's-2/neu like women. They are primarily ductal in nature, and 10% are ductal carcinoma *in situ* with a sign of lump or nipple inversion, mostly diagnosed at old age or a later stage (Stage III or IV) than women (Gómez-Raposo *et al.*, 2010).

According to WHO, there are 20 major types and 1 minor subtype of breast cancer. All breast cancers start in the breast and are pretty similar, but they differ in some aspects. On a morphological basis, breast cancers are of two types such as (a) Non-Invasive breast cancer and (b) Invasive breast cancer. When the breast cancer does not spread beyond lobules or ducts from where it originated it is known as Non-Invasive breast cancer. The DCIS or Ductal carcinomas *in situ* and the LCIS or lobular carcinoma *in situ* are the non-invasive breast cancer or *in situ* carcinoma, which could be diagnosed at stage 0 and confined to the ducts (Logan *et al.,* 2015). Invasive breast cancer describes the form of cancer that occurs when abnormal cells break into nearby breast tissue from inside the milk ducts or lobules. In this form of malignancy, the cancer cells have the potential to metastasize i.e., they can spread to different parts of the body via blood circulation or the immune system from breast, which could occur even though the tumor is tiny or large. Invasive or infiltrating lobular carcinoma (ILC) and invasive ductal carcinoma (IDC) are the common forms of invasive breast cancer. Invasive lobular carcinoma is the most frequent histological subtype of invasive breast cancer and accounts for around 5- 15% of all breast cancer incidences. Invasive ductal carcinoma, which is now referred to as 'no special type' (NST), is the most common form of invasive breast cancer accounting for 70-80% of all invasive lesions.

Breast cancer types are generally based on three specific cell surface receptor expression status such as human epidermal growth factor receptor (HER)2/neu receptor, oestrogen receptor (ER), and progesterone receptor (PR). Hormone receptor-positive breast cancer accounting for 75% of all cancer, is the most common form of cancer. Hormones such as progesterone and oestrogen are responsible for the triggering of cancer. HER2- positive breast cancer, caused by overexpression of the protein HER2/neu, accounts for 20% of hormone-receptor-positive breast cancers. HER2-negative tumors do not overexpress HER2/neu. Human epidermal growth factor receptor-2 (HER-2) has a sub-type i.e., triple-negative breast cancer (TNBC), a rarer form of breast cancer that does not overexpress HER-2 and the cells devoid of estrogen and progesterone accounting for 10-20% malignance. This form of malignancy is severe and difficult to treat since it does not succumb to any conventional treatment methods (Harbeck *et al.,* 2019). Some studies also characterize breast cancer as metastatic breast cancer having the potential metastasize and grow uncontrollably, forming new tumours.

1.3. Breast Cancer Scenario

As per WHO, out of the 19.3 million estimated new incidence of cancer in 2020 worldwide, 11.7% are due to breast cancer, making it stand at the first position, followed by lung cancer with a mortality of 6.8 million deaths (Figure 1.3) (WHO, Globocan, 2021). Breast cancer is the most diagnosed cancer among women accounting for 1 in 4 cancer cases. Although breast cancer can occur at any age, it is more common in the case of women aged 40-69, and about 25% are diagnosed at age 70. In the case of men, breast cancer cases are less than 1% (Lukong, 2017). The American Cancer Society estimated about 281,550 and 49,290 new cases of invasive breast cancer and carcinoma in situ (CIS) respectively and the mortality rate is about 43,600 worldwide. In recent years, it has been noted that the incidence rate has increased by 0.5% per year. One remarkable thing to note is that the death rate from breast cancer has dropped to 39% from 1989 to 2015, mainly because of early detection of cancer through screening, increased awareness, and better treatments (American Cancer Society, 2021). Among the top 25 countries with the highest incidence of breast cancer in 2018, Belgium had the highest incidence, followed by Luxembourg and the Netherlands.

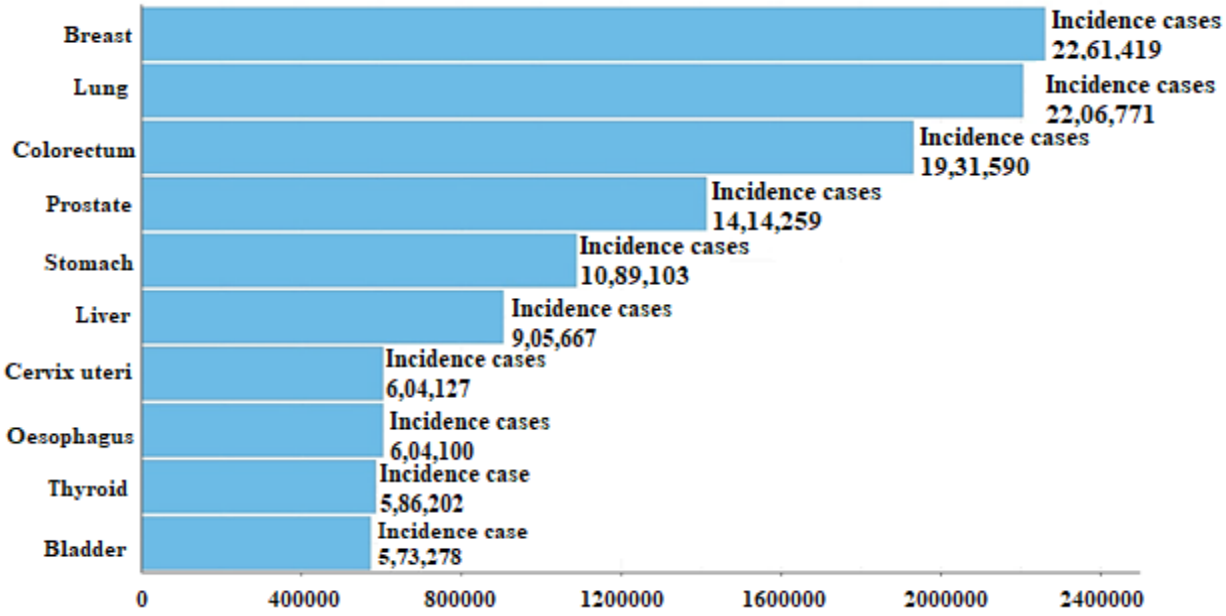

Figure 1.3: *Incidence of different types of cancer. Due to the high incidence rate, breast cancer stands as the deadliest cancer disease worldwide. (Source: WHO, IARC, GLOBOCAN 2020)*

With a population of 1.36 billion, India is a diverse subcontinent regarding ethnicity, culture, economics, religion, and quite variation in the health care system where the benefits of early diagnosis, advanced treatment, and awareness campaigns are

yet to reach everywhere. In India, breast cancer is the most common among females, with a high death rate (Malvia *et al.*, 2017). One woman dies of it among every two women newly diagnosed with breast cancer. In the past few years, there has been a dramatic increase in the incidence of cancer and cancer-related morbidity and death. According to WHO, unlike the developed countries, India is also facing a challenging situation for the increase in incidence (13.54%) and mortality rate (10. 6%) (WHO, Globocan, 2021). The reason behind the highest prevalence could be due to changes in lifestyle, lack of adequate breast cancer screening, detection of cancer at an advanced stage, or absence of adequate medical facilities. The report by ICMR states that breast cancers are estimated to contribute 14.8% of the total cancer burden in India, with a whopping rise of breast cancer incidence in metropolitan cities like Hyderabad, Chennai, Bangalore, Delhi, maybe due to increasing urbanization and adaptation of western styles (ICMR, 2020).

1.4. Breast Cancer Treatments & Sequelae

Treatment for breast cancer is done as soon as possible. Otherwise, the cancer cells keep on growing faster and metastasize to other organs such as lungs, liver, or bones, known as secondary breast cancer or metastatic breast cancer. The treatment for breast cancer aims at removing the cancerous cells. As the biology and behavior of the cancerous cells are quite different certain aspects are taken into consideration before starting the treatment as determining what type of breast cancer one has, its tumor subtype, stages of the tumor, and how fast it tends to grow, the patients' health condition, age, menopausal status (in females), any presence of inherited mutated breast cancer genes like *BRCA1 or BRCA2*. Breast cancer screening is the initial step to finding cancer at an early stage when they are small and have not spread. Early detection of breast cancer is crucial for efficient breast cancer management. The screening may include some of the tests and procedures included as follows**:**

a) **Physical exam and History:** Initially, the body is checked for any general signs of health, such as tumours or anything else abnormal. Extensive health history including prior illnesses and treatments, is also considered.

b) **Clinical Breast Exam (CBE)**: A doctor or other health expert examines the breast and beneath the arms for any lumps or other anomalies.

c) **Mammogram:** An x-ray is used for screening for early detection of breast cancer as it can identify benign or malignant alterations. After compression between two

plates, a small dose of radiation is implied through the breast to get an x-ray showing tumours. Mammograms are used for screening and diagnosis (Bhushan *et al.,* 2021).

d) **Ultrasound examination:** In women with thick breast tissue and suspicious places that are not detectable on mammography, ultrasound can be used to assess some breast abnormalities.

e) **Magnetic Resonance Imaging (MRI):** In order to create a non-invasive, non - ionizing detailed images of the breast, breast MRI uses radiofrequency waves and a magnetic field. This could help determine the size of the tumor (Bhushan *et al.,* 2021).

f) **Dynamic Contrast Enhanced MRI (DCE-MRI):** The DCE-MRI works by analyzing the temporal enhancement pattern of tissue following the intravenous injection of a paramagnetic contrast agent. It is helpful to determine tumor angiogenesis and the likelihood of recurrence and survival. An oestrogen receptor positive (ER+) subtype can be identified by combining DCE-MRI with computer-aided diagnosis technology such as texture analysis (Wang *et al.*, 2020).

g) **Molecular Breast Imaging (MBI):** A molecular-based breast imaging technique that helps detect mammographically occult and sub-centimeter breast cancer with more accuracy and precision than MRI. It is also known as miraluma test, sestamibi test, or breast-specific gamma imaging. This technique mainly depends on Tc-99m sestamibi i.e., approved for breast cancer imaging. This technique is more sensitive than MRI and has a higher specificity for detecting small breast lesions (Wang *et al.,* 2020).

h) **Magnetic Resonance Elastography (MRE):** MRE can be utilized *in vivo* to gather information on tissue mechanical behavior. Breast MRE, a non-invasive, non-ionizing, cross-sectional imaging technique, can quantify the viscoelastic characteristics of breast tissues once external stress is applied. However, due to the increase in the number of cells, collagen and proteoglycans in breast cancer, manual papulation is not possible. Hence, MRE is used due to its high specificity and sensitivity detection capabilities (Wang *et al.,* 2020).

i) **Positron Emission Tomography (PET) Scanning and PET in Conjunction with Computer-aided Tomography (CT) Scanning (PET-CT):** Positron emission tomography (PET) imaging technique is widely used in the field of oncology. As the cancerous cells have higher proliferation and enhanced glucose metabolism, this technique is advantageous for detection. The glucose transporter in cells is the mode

of entry of radiotracers enter cell and are consequently taken up by tumours cells in higher quantities than healthy ones. PET-CT is a combination of PET (Nuclear medicine technique) and CT used to generate highly detailed views of the body (Wang *et al.,* 2020).

j) **Biopsy:** Breast biopsies are the only way to detect breast cancer reliably. It involves the removal of a piece of tissue or cells to analyze under a microscope. Several types of biopsies like bone marrow biopsy, endoscopic biopsy, needle biopsy, skin biopsy are done depending upon the condition and the body area that needs close view.

k) **Receptor Test:** The cancer cells differ in varying numbers and types of receptors. Two types of receptor tests are done as follows:

- **Hormone receptor test:** Estrogen and Progesterone hormone are present in all women but in the case of breast cancer these hormones are attached to the receptors of the cancer cells and cause uncontrolled growth. Immunohistochemistry (IHC) technique is used for the hormone receptor test where it uses antibodies to detect the protein expression. If 1 out of 100 cancer cells stains, positive it is hormone receptor-positive and in the case of a few cells, it is negative (Nounou *et al.,* 2015).
- **HER2 receptor test:** In normal breast cancer cells, HER2 is formed of two copies of the gene. When HER2 lining the cell membrane is activated, it causes uncontrolled growth of the cells and in some cases, more than two copies of genes also make HER2 receptors accounting for rapid uncontrolled growth. IHC is used to determine the amount of HER2 receptors, where a score of 3+ depicts the presence of HER2 receptors. Insitu hybridization (ISU) is also used to count the number of copies of the HER2 gene (Nounou *et al.,* 2015).

After screening types of breast cancer, decisions are taken on the best treatment modality. The current treatment modality starts with surgery, radiotherapy, and systemic therapy that could be used individually or in combination (Nounou *et al.,* 2015).

a) Surgery: Breast cancer surgery is the most common mode of treatment for localized breast cancer. Radiotherapy or chemotherapy can be used consecutively or in conjunction with surgery.

b) Radiation therapy: The main aim is to reduce the chances of cancer recurrence. The cancerous cells are exposed to intense ionizing radiation, causing cellular damage and breaking in the DNA of cancerous cells. These dividing cells fail to repair themselves and undergo apoptosis. If the radiation therapy is given after

surgery it is known as adjuvant treatment and if given in combination with chemotherapy before surgery, it is known as neo-adjuvant therapy. Radiation therapy has high adverse effects on normal, highly dividing cells (Betty Smoot *et al.*, 2009).

c) Systemic Therapy: A mode of treatment where drugs spread throughout the body to kill the cancerous cells. Overall survival for women with breast cancer has increased dramatically because of systemic therapies. However, depending upon the early-stage and locally advanced breast cancer, systemic treatments are of three categories as hormonal therapy, targeted therapy and chemotherapy.

- **Hormonal therapy** is to cease or slow down the growth of hormone-sensitive tumors by limiting the body's ability to generate hormones or interfere with hormones' effects on breast cancer cells. First-line therapy for patients with locally advanced or metastatic breast cancer tested positive for the hormone receptors (ER) is tamoxifen. Fulvestrant, developed by AstraZeneca, was a second-line endocrine therapy approved by FDA in 2002. Aromatase inhibitors class of hormonal therapy limits the supply of estrogen and are more effective than the anti-estrogen tamoxifen in reducing the risk of breast cancer recurrence and spread and are well tolerated. Other drugs like Anastrazole, Aromasin, Raloxifene are also used (Lukong, 2017).

- **Targeted therapy** targets the cancer-specific genes, proteins, or the tissue environment supporting cancer growth and survival. The most common targeted therapy is the drug Herceptin used to treat breast cancer i.e. HER2 positive. Herceptin blocks the power of cancerous cells from growing and dividing while causing less harm to normal cells and is administrated intravenously once a week or every 3 weeks for one year. Targeted therapies also use monoclonal antibodies (Lukong, 2017).

- **Chemotherapy** is a systemic mode of treatment using anticancer drugs aiming to kill the cancerous cells that may have spread outside the breast or armpits. They mainly work by interfering with cell division, primarily aiming at the rapidly dividing cells. Its effectiveness depends upon which stage the cancer is being treated. Chemotherapy is being administrated intravenously (IV), into a muscle (intramuscular) or an injection under the skin (subcutaneous) or a pill or capsule (orally) so that it gets directly into the bloodstream. The regimens are usually divided into cycles that are administered over a set period of time i.e.,

every week or two weeks, or every three or four weeks, depending on the kind of cancer being treated.

Table 1.2.: Drugs being used to treat breast cancer (Betty Smoot *et al.*, 2009; Maughan *et al.*, 2010; NCI, 2021).

Therapy	Drugs Used	Doses Administrated
Chemotherapy	**Anthracyclines**	
	Doxorubicin (Adriamycin)	Intravenously administered every 14 to 21 days for 4-6 cycles. Can be conjugated with paclitaxel, docetaxel or fluorouracil.
	Epirubicin (Ellence)	Intravenously administered every 1 to 8 days for 3-8 cycles. Can be combined with cyclophosphamide.
	Doxorubicin (Doxil)	Intravenously administered on 4th day of each 21-day cycle for eight cycles or until cancer progression.
	Mitoxantrone (Novantrone)	Administrated as a short intravenous infusion every 21days.
	Alkylating Agents	
	Cyclophosphamid (Cytoxan)	Administrated intravenously in divided doses for a period of 2-5 days or orally of 1-5mg per kg per day.
	Thiotepa	Administrated intravenously for 1–4-week interval and given by intravesical mode also.
	Taxanes	
	Docetaxel (Taxotere)	Administrated intravenously for three to four cycles mainly. Could be administrated in conjunction with doxorubicin, epirubicin, cyclophosphamide, and fluorouracil.
	Paclitaxel (Taxol)	Administrated intravenously for every 7 to 21 days for 4 to 12 cycles. Also administrated in combination with doxorubicin and cyclophosphamide.
	Paclitaxel Protein-bound (Abraxane)	Administrated intravenously for every 3 weeks of 30 minutes each or in 1, 8, 15 of each 21- day cycle.
	Platinum Drugs	
	Carboplatin (Paraplatin)	Administrated intravenously on day 1 every 4 weeks for 6 cycles.
	Cisplatin (Platino)	Administrated by slow intravenous infusion for 5 days per cycle.
	Vinca Agents	
	Vinorelbine (Navelbine)	Administrated intravenously over 6-10 minutes once in week. Could be administrated in combination with cisplatin also.
	Oncovin (Vincristine sulfate injection)	Administered by the use of an intact, free-flowing intravenous needle or catheter.
	Vinblastine	Administrated intravenously once in a week.

	Antimetabolites	
	Fluorouracil (5-FU) (Adrucil)	Administrated intravenously once daily for four successive days with maximum up to 12th day.
	Gemcitabine (Gemzar)	Administrated intravenously over 30minutes on days 1 and 8 of 21-day cycle including paclitaxel.
	Methotrexate (Trexall)	Administrated orally for low doses and intramuscularly in 15-30mg daily for 5 days.
	Capecitabine (Xeloda)	Administrated orally twice daily for 2 weeks. In combination with docetaxel can be administrated twice daily for 2 weeks.
	Microtubule Inhibitors	
	Eribulin (Halaven)	Administrated intravenously over 2-5 minutes on days 1 and 8 of 21-day cycle.
	Ixabepilone (Ixempra)	Administrated intravenously over 3 hours every 3 weeks.
Hormonal therapy	**Aromatase inhibitors**	
	Anastrozole (Arimidex)	Administrated orally (tablets) for 5 years. Can be administrated alone or in sequence with in tamoxifen.
	Exemestane (Aromasin)	Administrated orally (tablets) daily for 2 to 5 years after tamoxifen therapy.
	Letrozole (Femara)	Administrated orally (tablets) daily for 2 to 5 years. Should stop administration after tumor relapse.
	Ovarian Suppressors	
	Goserelin (Zoladex)	Administrated subcutaneously every 28 days for 2 years into the anterior abdominal wall under the navel line.
	Busereline (Suprefact)	Administrated subcutaneously in every 8 hours for 7 days.
	Abarelix (Plenaxis)	Administrated intramuscularly to the buttock on day 1, 15, 29 and every 4 weeks thereafter.
	Leuprolide (Lupron)	Administrated intramuscularly for 28 days to 2 years.
	Anti –Estrogen Drugs	
	Tamoxifen (Nolvadex)	Administrated orally in form of tablets daily for 2 to 5 years. Administrated alone or in sequence with in aromatase inhibitor.
	Fulvestrant (Faslodex)	Administrated intramuscularly twice on days 1, 15, 29 and once monthly thereafter. Could be administrated in conjugation with ribociclib, abemaciclib or palbociclib.
	Toremifine (Fareston)	Administrated orally once daily until disease progression is seen.
	Raloxifene (Evista)	Administrated orally one tablet daily up to 5 years.

Targeted Therapy	**Monoclonal antibody**	
	Trastuzumab (Herceptin)	Administrated intravenously with first dose as a chemotherapy regimen for a period of one to three weeks for 1 year.
	Bevacizumab (Avastin)	Administrated intravenously in combination with paclitaxel for up to 6 cycles.
	T-DM1 (Ado-trastuzumab emtansine) (Kadcyla)	Administrated intravenously every 3 weeks of 21 days cycle.
	Pertuzumab (Perjeta)	Administrated intravenously every 3 weeks.
	Kinase Inhibitors	
	Tykerb (Lapatinib)	Administrated orally daily up to 21 days in combination with capecitabine.
	Everolimus (Afinitor)	Administrated orally daily until disease progression or no toxicity.

1.5. Limitations of current anticancer drugs

Chemotherapeutic drugs not only target cancerous cells but also target equally to normal dividing cells, resulting in severe side effects like nausea and vomiting, alopecia, loss of appetite, pulmonary toxicities, sores and ulcers in the mouth and fatigue. Some other major limitations are as follows:

- **Drug Resistance:** A handful of chemotherapeutics are recommended for adjuvant and neoadjuvant therapy of breast cancer subtypes, including TNBCs. Unfortunately, most patients treated with these medications develop resistance, which leads to quicker disease progression and mortality. In addition, drug resistance is a major issue that contributes to the failure of several kinds of chemotherapy (Lukong, 2017).
- **Susceptibility to infections:** Chemotherapeutics target normal cells in addition to cancerous cells, destroying white blood cells that fight infections. Because of a paucity of white blood cells in the body, the immune system is weakened, making the body more susceptible to infections.
- **Myelosuppression:** A decrease in the number of red blood cells, platelets and white blood cells is quite common in chemotherapy, resulting in fatigue or dyspnea or gastrointestinal bleeding (Betty Smoot *et al.,* 2009).
- **Cognitive dysfunction:** Many breast cancer survivors have reported facing impaired concentration and memory during or after chemotherapy. This could be due to the

neurotoxic effects, oxidative stress, reduced oxygenation, anemia, stress or anxiety (Betty Smoot *et al.,* 2009).

- **Cardiac Toxicity:** Certain chemotherapeutics induce severe myocardial damage, resulting in cardiomyopathy.

- **Peripheral Neuropathy:** Chemotherapy-induced peripheral neuropathy (CIPN) is a very common side effect associated with the use of vinca alkaloids, taxanes, and platinum compounds.

1.6. Microtubule and cell cycle progression

The generation of two identical cells from a single cell is the main purpose of cell' cycle. In order to attain this the mother cell must duplicate its chromosomes precisely once more before initiating mitosis. Each daughter cell must have single set of chromosomes at the commencement of mitosis. To do so, the cell must perfectly coordinate a series of complex processes; one must be blocked if the proper completion of a preceding event is interrupted by physical damage or other causes. This is regulated by the cellular surveillance mechanisms called cell cycle check points, proposed first by Mazia (1961) and elucidated by Hartwell and Weinert (1989), and McIntosh (1991). Drugs that block cell cycle progression by activating the checkpoint mechanisms are therefore very useful for chemotherapeutic treatment of various human cancers. Certain drugs that target mitotic spindle's microtubule have shown efficiency in cancer treatment as they can halt cell cycle progression at mitosis and eventually lead to cell death.

1.7. Microtubule Structure and Dynamics

Microtubules are long, hollow cytoskeletal structures with a diameter of 25 nm that play a vital role in numerous cellular functions such as cell shape preservation, intracellular transport of vesicles and organelles, and cilia and flagella beating. Microtubules form a bipolar apparatus termed the mitotic spindle during cell division, which aids in the segregation of chromosomes into two identical daughter cells. (Figure 1.4A).

Microtubules are composed of 13 protofilaments in most cells, and each protofilament is assembled from head-to-tail arrangement of the heterodimer of α- and β-tubulin polypeptides (Amos and Klug, 1974), which are almost 50% similar at the amino acid level (Burns, 1991). The α- and β-tubulin monomer each has a molecular mass of about 50 kDa and each binds a guanosine triphosphate (GTP) molecule

(Weisenberg *et al.,* 1968), nonexchangeable in α-tubulin and exchangeable in β-tubulin (Spiegelman *et al.,* 1977). The head-to-tail association of tubulin dimer gives microtubules an intrinsic polarity in their structure. One end of the microtubule is capped with α-tubulin while the other end is capped with β-tubulin (Song and Mandelkow, 1995; Fan *et al.,*1996a; Mandelkow *et al.,* 1986). The structural polarity of the microtubule influences the dynamic property of its two ends. One end, called the plus end, grows and shortens much faster than the other end, called the minus end (Allen and Borisy, 1974).

Microtubules are intrinsically dynamic polymers (Margolis and Wilson, 1978; Saxton *et al.,* 1984; Mitchison and Kirschner, 1984a, b; Belmont *et al.,* 1990; Schulze and Kirschner, 1986), and switched probabilistically amid growing and shrinking phases. GTP binds to free tubulin in an exchangeable fashion and becomes irreversibly hydrolyzed to guanosine diphosphate (GDP) during the addition of tubulin dimer to the ends of microtubules (David-Pfeuty *et al.,* 1977; MacNeal and Purich, 1978). This gives rise to two unusual dynamic behaviors. Dynamic instability is the sudden and stochastic changes of growth and shortening phase (Mitchison and Kirschner, 1984a, b) while treadmilling depicts the growing of microtubules at one end while shortening at the other ends (Margolis and Wilson, 1978). Several parameters have been used to characterize the dynamics of microtubule assembly (Walker *et al.,* 1988; Jordan and Wilson, 1999). These include the rate of growth, the rate of shortening, the frequency of transitions from growth to shortening (catastrophe frequency), the frequency of transitions from shortening to growth or an attenuated (pause) state (rescue frequency), and the duration of the attenuated state when neither microtubule growth nor shortening can be detected. Microtubule instability is described as the sum of visually detectable tubulin dimer exchange per unit time at the ends of microtubules (Jordan and Wilson, 1999).

The dynamic property is essential for microtubules to accomplish many cellular functions, such as reorienting the microtubule network when cells migrate or encounter morphological changes, and the significant microtubule reorganization at the commencement of mitosis (Joshi, 1998). Mitotic microtubules are 10-100 times more active than interphase microtubules; as in mitosis, they interchange tubulin with the soluble tubulin pool with half-times of 15s, compared to 3 minutes to several hours during interphase (Saxton *et al.,* 1984; Schulze and Kirschner, 1986; Belmont *et al.,* 1990). Rapid microtubule dynamics in mitosis is considered to be crucial for both development and the actions of the mitotic spindle, which leads chromosome

congression to the equatorial plane (also known as the metaphase plate) and their eventual segregation into daughter cells.

Many natural chemical compounds are able to bind to tubulin or microtubules, and they stop cell cycle progression at mitosis by interfering with the mitotic spindle. Several of these compounds, notably paclitaxel, vinblastine, colchicine, and nocodazole, have played important roles in studying basic mechanisms of mitosis. In fact, tubulin was first identified as a high-affinity receptor for colchicine (Borisy and Taylor, 1967a, b; Weisenberg *et al.*, 1968).

Microtubule-interfering agents are classified into two groups. Paclitaxel, for example, promotes microtubule polymerization and bundles the resulting stable microtubules. (Schiff and Horwitz, 1980; Bissery *et al.*, 1991; Jordan and Wilson, 1999). While vinblastine, colchicine, and nocodazole, inhibits microtubule polymerization (Jordan and Wilson, 1999). Although these different microtubule-interfering agents act differently, they all suppress microtubule dynamics, interfere with spindle functions (Figure 1.4B), and arrest cells at mitosis by activating the spindle assembly checkpoint (Rudner and Murray, 1996; Wells, 1996).

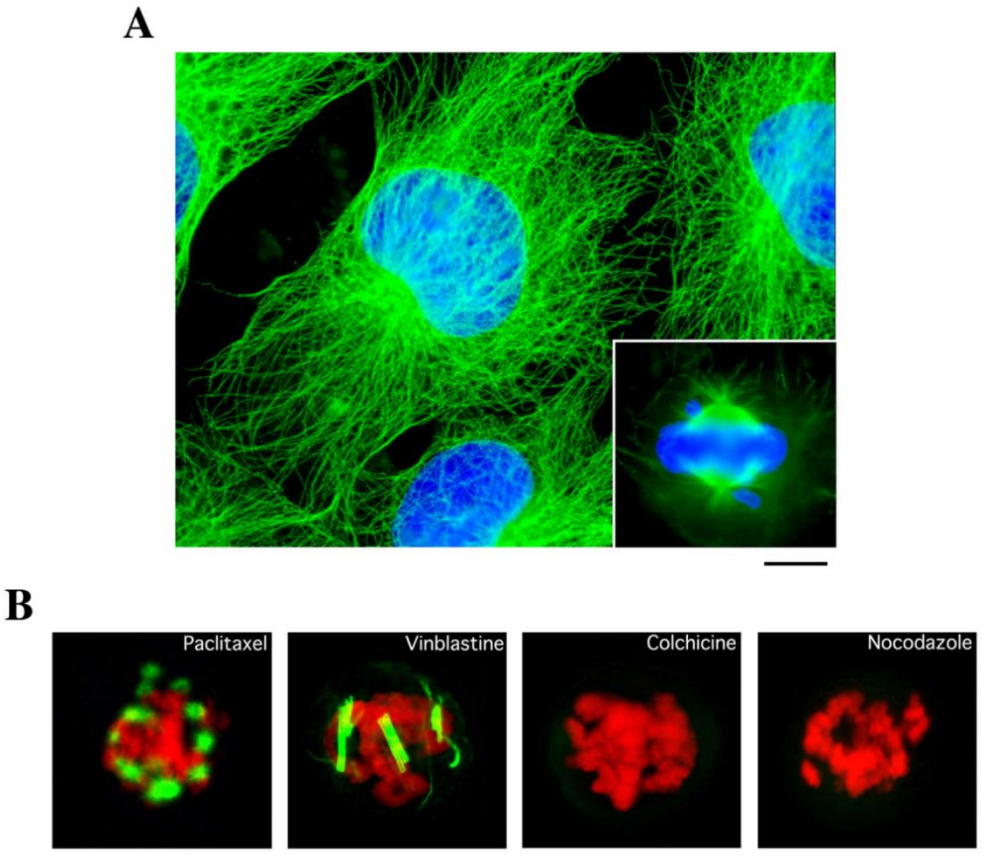

Figure 1.4: *Microtubules (green) are visualized by immunofluorescent staining with a monoclonal antibody against α-tubulin. DNA is visualized by staining with DAPI in A (blue) and propidium iodide in B (red). A, microtubules are precisely organized due to*

their anchorage at the centrosome, the mammalian microtubule-organizing center. Microtubules occur as a radial array in interphase cells. At the onset of mitosis, the radial array of microtubules disappears within minutes and a bipolar array, the mitotic spindle, forms (inset). The mitotic spindle functions in the alignment of chromosomes at the equatorial plane and their final segregation into two daughter cells. Bar, 10 μm. B, microtubule-interfering agents arrest cells at mitosis with distinct spindle defects. In paclitaxel-arrested cells, microtubules form dense asters tethered with chromosomes. In vinblastine-arrested cells, the tubulin subunits resulting from spindle depolymerization form large paracrystalline structures. In cells arrested by colchicine and nocodazole, spindle microtubules are completely depolymerized. Bar, 10 μm.

1.8. Mitotic Arrest and Apoptosis

Typically, cells treated with microtubule-interfering agents arrest at mitosis, resulting from the disruption of spindle functions, and then undergo death (Dustin, 1984). It had therefore been thought that the antitumor activity of microtubule-interfering agents is a consequence of blocking mitotic progression (Milas *et al.,* 1995; Wahl *et al.,* 1996), and the subsequent cell death is a consequence of a catastrophic resolution of the abnormal mitosis, termed mitotic catastrophe (Russel and Nurse, 1986; Russel and Nurse 1987; Heald *et al.,* 1993). Several evidences indicate that microtubule-interfering drugs can elicit morphological and biochemical hallmarks of usual apoptosis, such as chromatin condensation, cell membrane blebbing, and internucleosomal DNA fragmentation (Bhalla *et al.,* 1993; Bonfoco *et al.,* 1995; Woods *et al.,* 1995; Kawamura *et al.,* 1996; Jordan *et al.,* 1996). These results indicated that microtubule-interfering agents and blocking mitosis could induce apoptotic pathways in many types of cells. Now the question was whether the microtubule interfering drugs that caused the mitotic arrest and apoptosis are two distinct events or the result of upsetting the normal physiological balance of microtubule dynamics. Finally, as antimicrotubule drugs cause mitotic arrest, a natural notion that mitotic arrest is the cause of apoptosis has received general acceptance. (King and Cidlowski, 1995).

Nevertheless, recent study indicates that the apoptosis is induced by via signaling pathways by microtubule-interfering agents, independent of mitosis (Long and Fairchild, 1994; Fan *et al.,* 1996b; Lieu *et al.,* 1997; Fan *et al.,* 1998; Miller *et al.,* 1999). For example, in the absence of mitotic block, either a quick exposition to a high concentration of paclitaxel or a lengthy exposition to a low concentration of paclitaxel could cause cells to apoptosis (Long and Fairchild, 1994; Lieu *et al.,* 1997). Furthermore,

baccatin III, the central ring system of the paclitaxel structure, was observed to trigger apoptotic cell death without inducing mitotic arrest; instead, multiple apoptotic events were observed in later phases of the cell cycle (Fan *et al.,* 1998; Miller *et al.,* 1999). Another crucial shred of information confirming the apoptotic pathway independent of mitotic arrest is that glucocorticoids preferentially inhibit paclitaxel-induced apoptosis while not preventing cells from entering mitosis (Fan *et al.,* 1996b). As a result, the particular molecular mechanisms underpinning apoptosis and mitotic arrest caused by microtubule targeting drugs, as well as the link between the two events, still remain unknown.

The potential of microtubule-interfering drugs to trigger apoptosis and pause mitosis provides a mechanistic foundation for their usage in the chemotherapeutic treatment of human cancers. Paclitaxel, docetaxel, and the vinca alkaloids are microtubule agents that are now in clinical use for cancer treatment. Paclitaxel, in particular, has shown to be effective against refractory ovarian cancer, metastatic breast cancer, and non-small-cell lung cancer (Rowinsky, 1997; Crown and O'Leary, 2000), while vinca alkaloids have shown to be effective against cancers such as lymphoma, leukemia, and Kaposi's sarcoma (van Tellingen *et al.,* 1992). Unfortunately, poor water solubility and the toxicity of taxoids and vinca alkaloids have limited their use in anticancer therapy. Furthermore, drug resistance has been impeded by multifactorial factors such as P-glycoprotein overexpression (Gottesman and Pastan, 1993; Bradley and Ling, 1994), changed expression of tubulin isotypes (Burkhart *et al.*, 2001), and the existence of tubulin alterations (Giannakakou *et al.,* 1997). As a result, the development or discovery of microtubule-based molecules is in high demand, particularly for the treatment of human cancers that have become resistant to presently offered drugs.

Noscapine: A new light to the anticancer arsenal

Noscapine (Figure 1.5) is a phthalideiosquinoline alkaloid that occurs in abundance in the opium plant, *Papaver somniferum* L. papaveraceae. It has been used as a cough suppressant in humans and in experimental animals (Chopra *et al.,* 1930; Winter and Flataker, 1954; Empey *et al.,* 1979; Dahlstrom *et al.,* 1982; Karlsson *et al.,* 1990), but the mechanisms for its antitussive action remain largely unknown. A systematic screening based on same structure of known drugs interfering microtubules revealed the opium alkaloid noscapine as a novel microtubule-interfering agent. Noscapine acts mechanistically similar to many other microtubule agents, in that it binds stoichiometrically to the tubulin subunits of microtubules, with one noscapine molecule

per tubulin dimer, and alters the conformation of tubulin upon binding (Ye *et al.,* 1998). In addition, noscapine blocks cell cycle progression at mitosis and causes apoptotic cell death in many cancers cell types (Ye *et al.,* 1998, Ye *et al.,* 2001). It inhibits the progression of murine lymphoma, thymoma, and human breast tumors implanted in nude mice with little or no toxicity to the kidney, heart, liver, bone marrow, spleen, or small intestine and does not inhibit primary humoral immune responses in mice (Ye *et al.,* 1998; Ke *et al.,* 2000). Because noscapine is water-soluble and absorbed after oral administration (Dahlstrom *et al.,* 1982; Haikala *et al.,* 1986; Karlsson *et al.,* 1990), its chemotherapeutic potential in the treatment of human cancers merits thorough evaluation. In both in vivo and in vitro noscapine has shown its efficacy in the treatment of breast cancer. It was found to inhibit the growth of murine and human breast tumours that were implanted in mice by inducing apoptosis (Ye *et al.,* 1998). *In vivo* study of noscapine was found to regress 80% in human breast tumours.

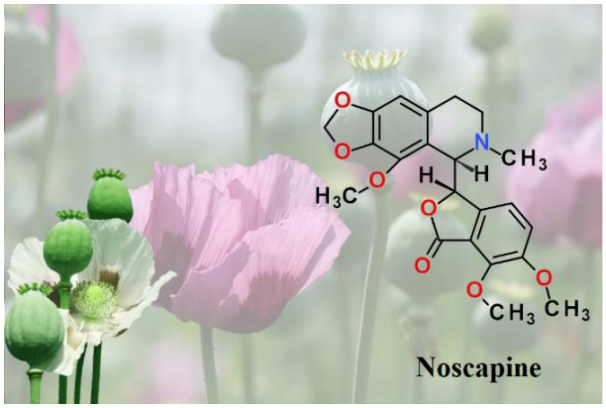

Figure 1.5: *Opium plant and Molecular structure of noscapine. Noscapine structure consists of two ring systems, isoquinoline and isobenzofuranone, linked by a rotatable C–C bond between two chiral centers.*

1.9. Development of Noscapine Analogues

To utilize the complete potential of noscapine and overcome the problem of high micromolar ranges, attempts were made for the development of potent derivatives of noscapine known as noscapinoids. The derivatives synthesized from noscapine have proven to be more potent than that of the parent molecule. These derivatives are categorized into different generations based on sequential synthetic alterations at various places in the scaffold structure of noscapine (Figure 1.6).

1.10. First Generation Noscapinoids:

The first generation of derivatives like halogen derivative (Bromo, Chloro, Fluoro, Iodo) (Aneja *et al.,* 2006a); amino (Naik *et al.,* 2011a), azido (Santoshi *et al.,* 2011) and nitro (Aneja *et al.,* 2006b) were developed by modification at diversity point A (C-9 position) while the reduced oxygen halogenated-noscapine (reduced-

chloronoscapine (Rd-Cl-nos); reduced-iodonoscapine (Rd-I-nos); reduced-fluoronoscapine (Rd-F nos) and reduced-bromonoscapine (Rd-Br-nos) (Aneja *et al.*, 2006c) at diversity point B. These derivatives showed improved anticancer activity compared to noscapine (Aneja *et al.*, 2006a; Naik *et al.*, 2011a; Aneja *et al.*, 2006b; Santoshi *et al.*, 2011; Aneja *et al.*, 2006c) (Figure 1.7 & 1.8).

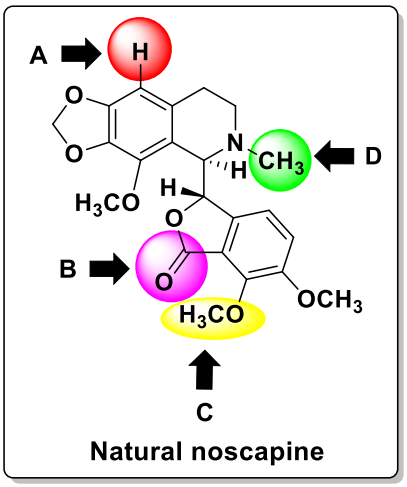

Figure 1.6: *Noscapine showing different diversity points where modifications are done to synthesize potent derivatives.*

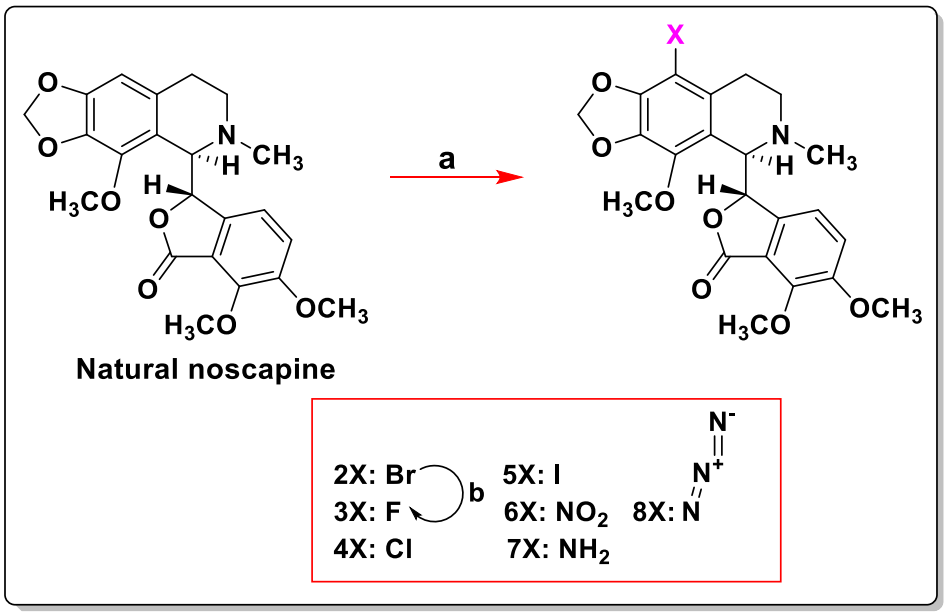

Figure 1.7: *Halogenated derivatives. 'a': Hydrogen bromide & Bromine water for 9-bromo noscapine; Fluorine, Amberlyst & tetrahydrofuran for 9- fluoro noscapine; Chloroform & Sulfuryl chloride for 9- chloro noscapine; Acetonitrile & pyridine-iodine chloride for iodo noscapine; The aromatic nitration of noscapine utilizing silver nitrate in acetonitrile and TFAA at 25°C resulted in nitro noscapine; Noscapine was converted to bromonoscapine followed by synthesis of azido derivative of noscapine in presence of sodium azide and sodium iodide; Amino noscapine was synthesized from azido noscapine (Aneja et al., 2006a; Naik et al., 2011a; Aneja et al., 2006b; Santoshi et al., 2011; Aneja et al., 2006c).*

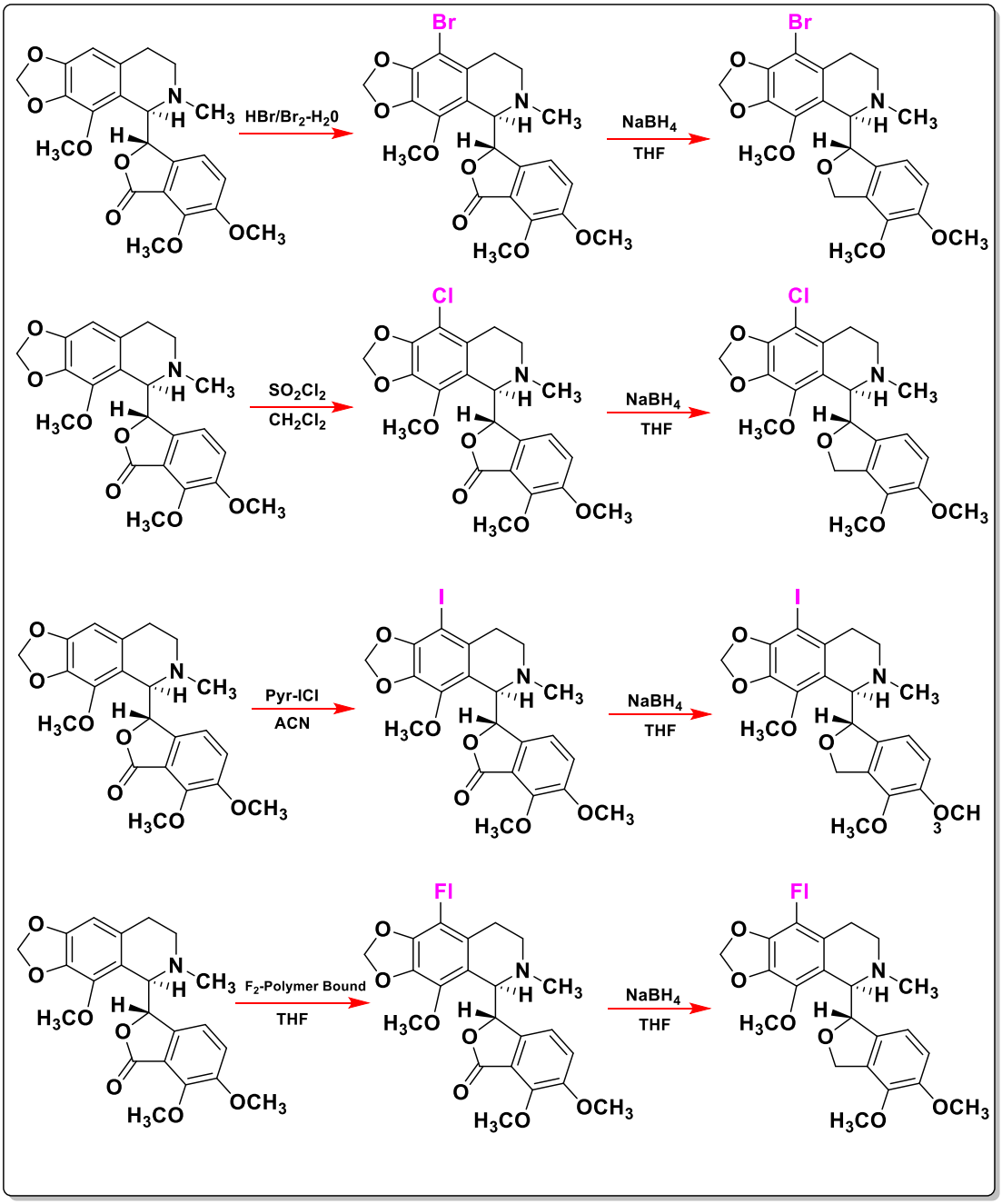

Figure 1.8: *Cyclic ether halogenated derivatives. Rd-9-Br-nos (reduced 9 bromonoscapine); Rd-9-Cl-nos (reduced 9-chloronosapine). Rd-9-I-nos (reduced 9-iodonoscapine); Rd-9-F-nos (reduced 9-fluoronosapine). These were developed from the halogenated derivatives (Aneja et al., 2006c; Lopus and Naik, 2015).*

1.11. Second Generation Noscapinoids

From synthetic perception after the successful development of 1st generation of noscapine, more synthetic analogues were developed from different scaffolds point of noscapine. The benzofuranone ring of noscapine at the diversity point C (7th Position) was modified for the synthesis of more derivatives. Anderson *et al.*, 2005a, b has reported several derivatives by manipulating the benzofuranone ring through regio- and

stereo selective O-demethylation, out of which 3,4,5- trimethoxybenzyl derivative was found to be more potent in arresting the cell cycle at S-Phase. Mishra *et al.*, 2011 synthesized 7-acetyl noscapine and 7-benzoyl noscapine in the first scheme and several carbamate esters in the second scheme, namely 7-ethylcarbamato noscapine, 7-phenyl carbamate noscapine, 7-benzyl carbamate noscapine with 7-hydroxy noscapine as intermediate (Figure 1.9). Peering over to anticancer activity of these compounds, 7-acetyl noscapine was quite effective against most cancer types. Further, Mishra *et al.*, 2019 synthesized a series of novel derivatives known as noscapine glycocojugates at the diversity point C (7th Position). Out of the fourteen derivatives they synthesized, four derivatives, which showed better anticancer activity, are shown (Figure 1.10).

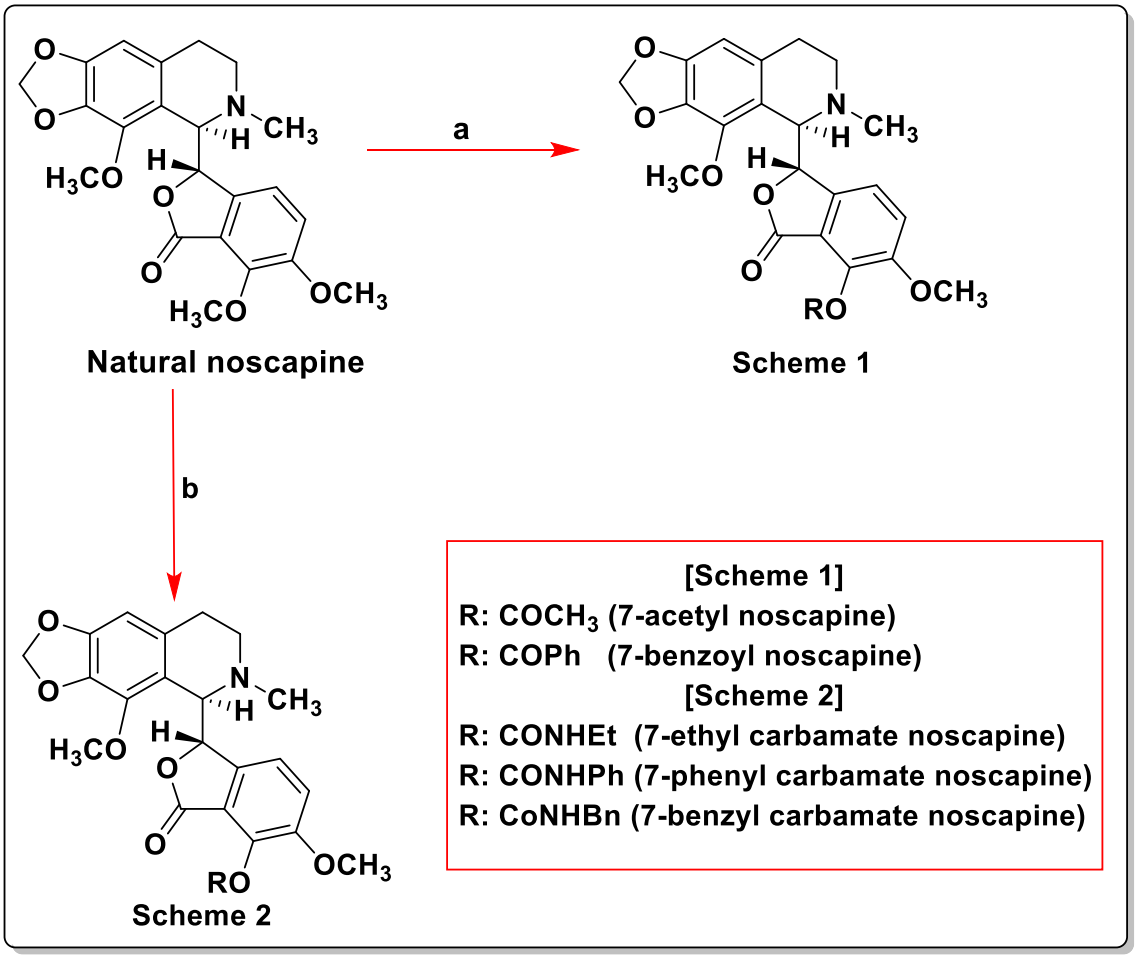

Figure 1.9: *Second generation Noscapinoids synthesized by Mishra et al., 2011* ***(a)****: Dimethylamino pyridine, AC_2O, CH_3CN for 6 h at 50 °C (for 7-acetyl-noscapine); K_2CO_3, benzoyl chloride for 8 h at 80 °C (for 7-benzoyl-noscapine),* ***(b)****: Dimethylamino pyridine, CH_2Cl_2 & isocyanate for 6-8 h at room temeperature (7-ethylcarbamato noscapine, 7-phenyl carbamate noscapine, 7-benzyl carbamate noscapine).*

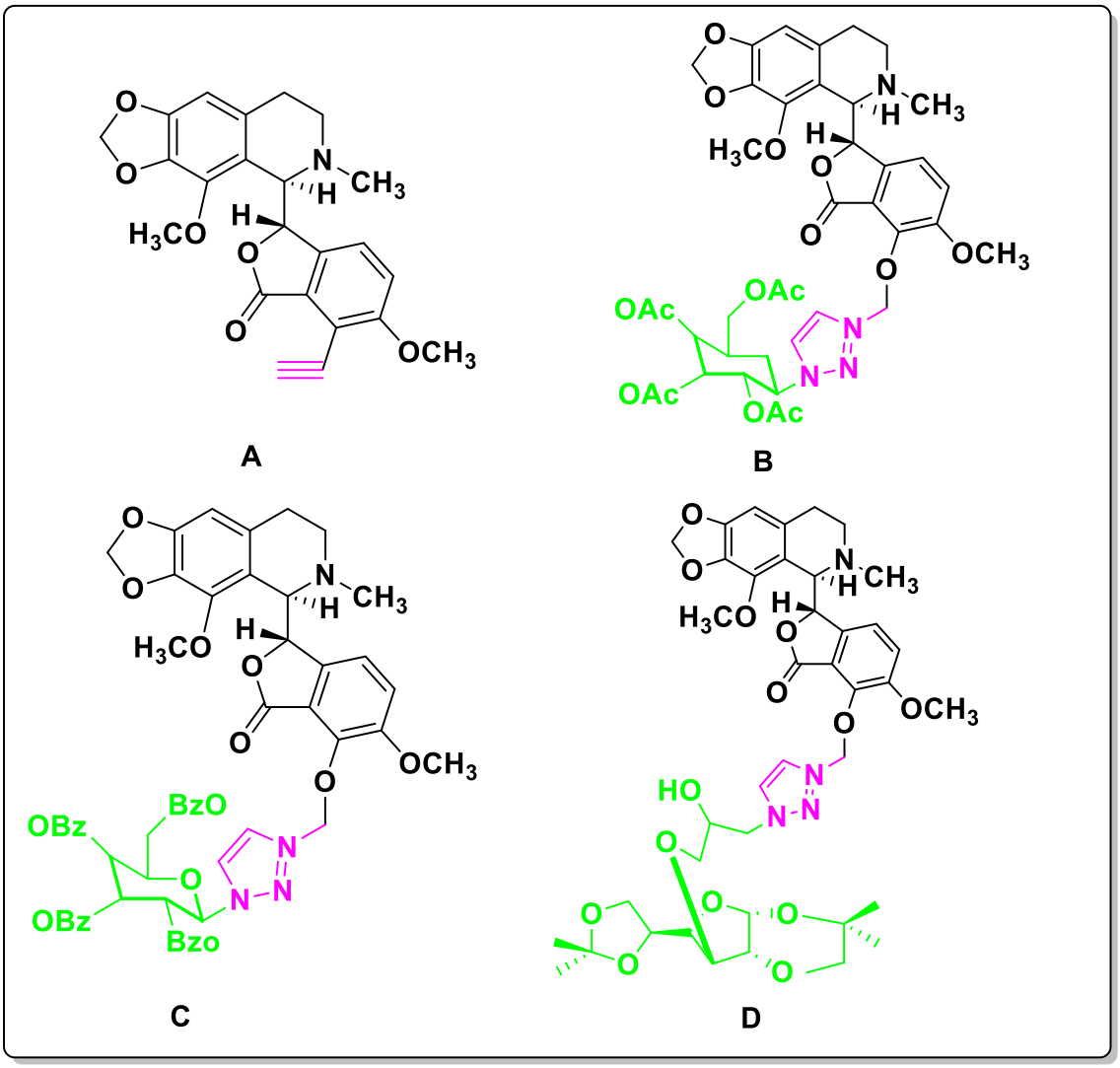

Figure 1.10: *Synthesis of novel derivative of noscapine. (Most prominent one are represented) (Mishra et al., 2019).*

1.12. Third Generation Noscapinoids:

Manchukonda *et al.*, 2013 developed potent aromatic derivatives (third generation of noscapinoids) by bringing changes at the tetrahydroisoquinolone part of noscapine at diversity point D (6th Position) through functionalization of nitrogen (Figure 1.11). All the derivatives showed a better docking score than the parent molecule binding with both α and β-tubulin at a place near the colchicine binding site (*in silico*). The entire derivative showed good potency in inhibiting the proliferation of cancer cells, even better than some of the earlier 1st generation derivatives. They bind with tubulin in a concentration-dependent manner and also delay the cell cycle progression in G2/M phase and triggers apoptosis.

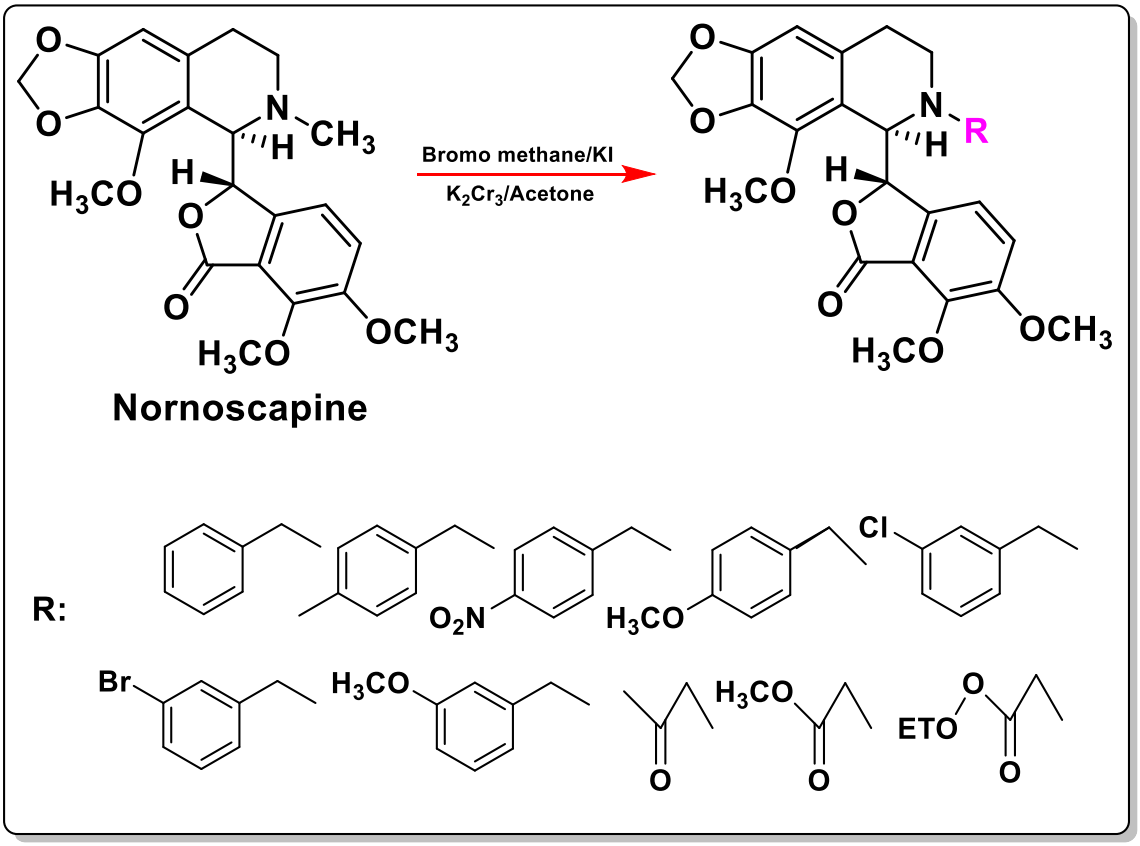

Figure 1.11: *Third generation derivatives. Nornoscapine is the starting material synthesized from noscapine. It is derivatized with benzyl and alky halides in substitution (in presence of base) for development of third generation noscapinoids (Manchukonda et al., 2013).*

1.13. Multi-functionalized Noscapine derivatives:

DeBono *et al.*, 2012; 2014 focused on synthesizing multi-functional derivatives by bringing about modification at the A, B, C & D diversity point (9th, 1st, 7th & 6th position). They synthesized new derivatives (Figure 1.12 & 1.13) by grouping N-ethyl aminocarbonyl with other modifications like nitration and halogenation of noscapine at point A; regioselective *O*- demethylation at C point and reduction of the lactone to the analogous cyclic ether at B point. These newly developed analogues were found to arresting cell cycle at G2/M phase and were quite effective against pancreatic (PANC-1), breast cancer (MCF-7) and prostate cancer (PC3) cell lines in comparison to the parent molecule.

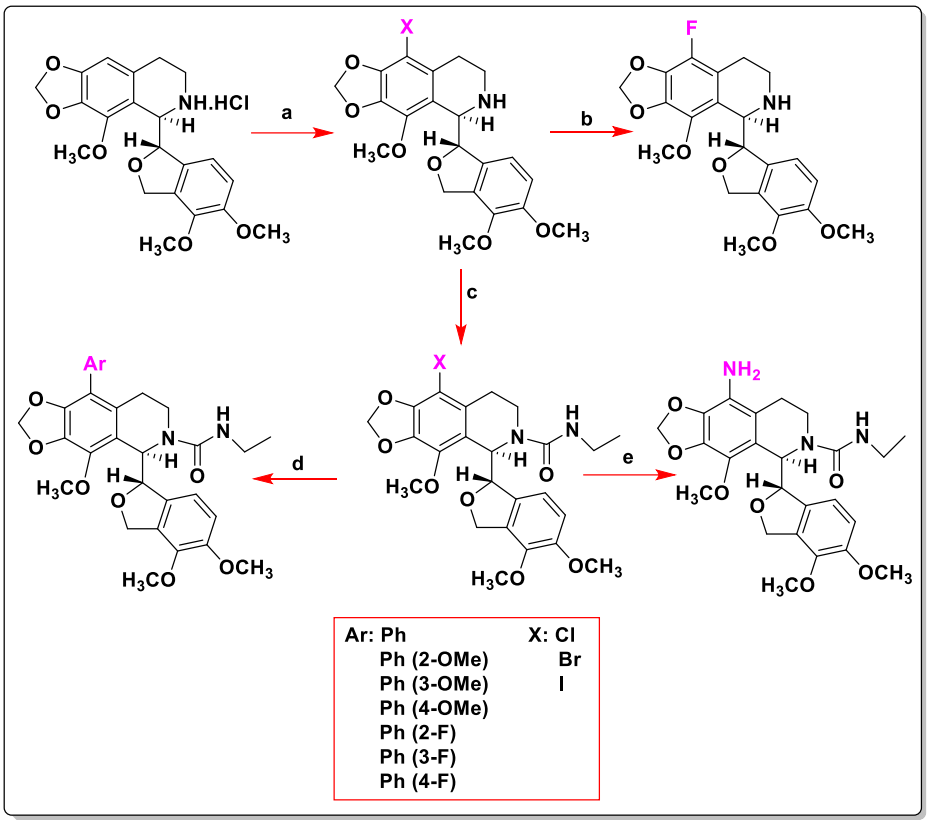

Figure 1.12: *Systematic representations of multi-functional noscapine anlogues. 'a': Cl, $ChCl_3$, SO_2Cl_2 0º (for Cl); Br.NBS, AcOH, room temperature (for Br); I: NIS, TFA, room temperature (for I). 'b': F_2, Amberlyst-A,THF,reflux. 'c': EtNCO, MeCN, room temperature. 'd': $ArB(OH)_2$, $PdCl_2(PPh_3)_2$, THF, 1M Na_2CO_3 at 100ºC. 'e': L-proline, NaN_3, CUI, DMSO, reflux (DeBono et al., 2012; 2014).*

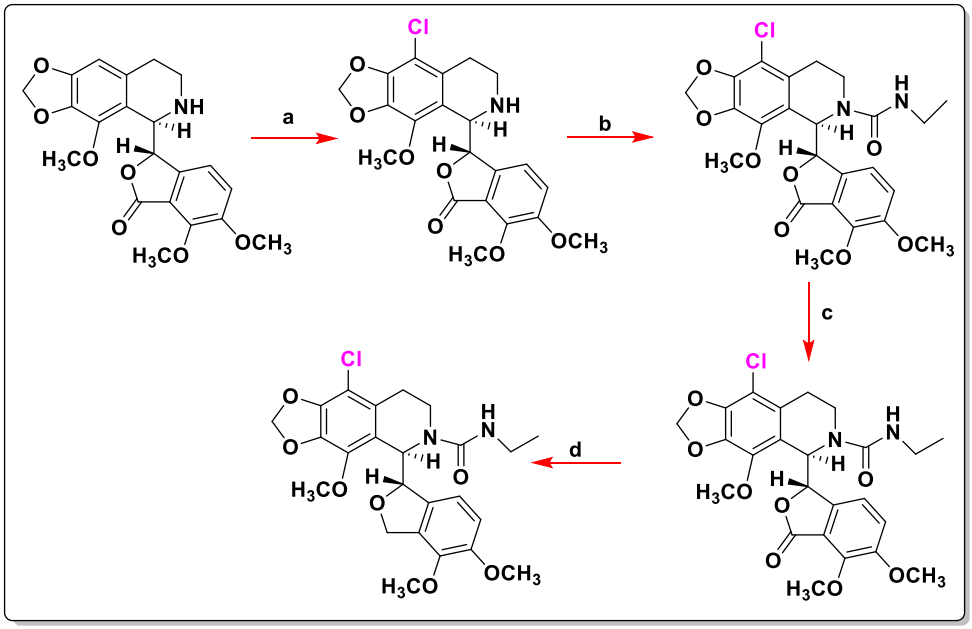

Figure 1.13: *Systematic representations of multi-functional analogues of noscapine. 'a': NCS, TFAA,reflux. 'b': EtNCO, MeCN, -5ºC. 'c': MeMgBr, BnOH, toluene, 120ºC. 'd': $BF_3.Et_2O$, $NaBH_4$ at room temperature (DeBono et al., 2012; 2014).*

1.14. Biaryl Derivatives of Noscapine:

Santoshi *et al.*, 2015 demonstrated the synthesis of six noscapine derivatives (9-arylnoscapines) by implanting the biaryl pharmacophore into the scaffold of noscapine (Figure 1.14). These derivatives were quite efficacious against wide range of cancer cell lines such as MCF-7 (breast cancer), HeLa (cervical cancer), A549 (lung adenocarcinoma), arresting the cell cycle at G2/M phase more efficiently than noscapine.

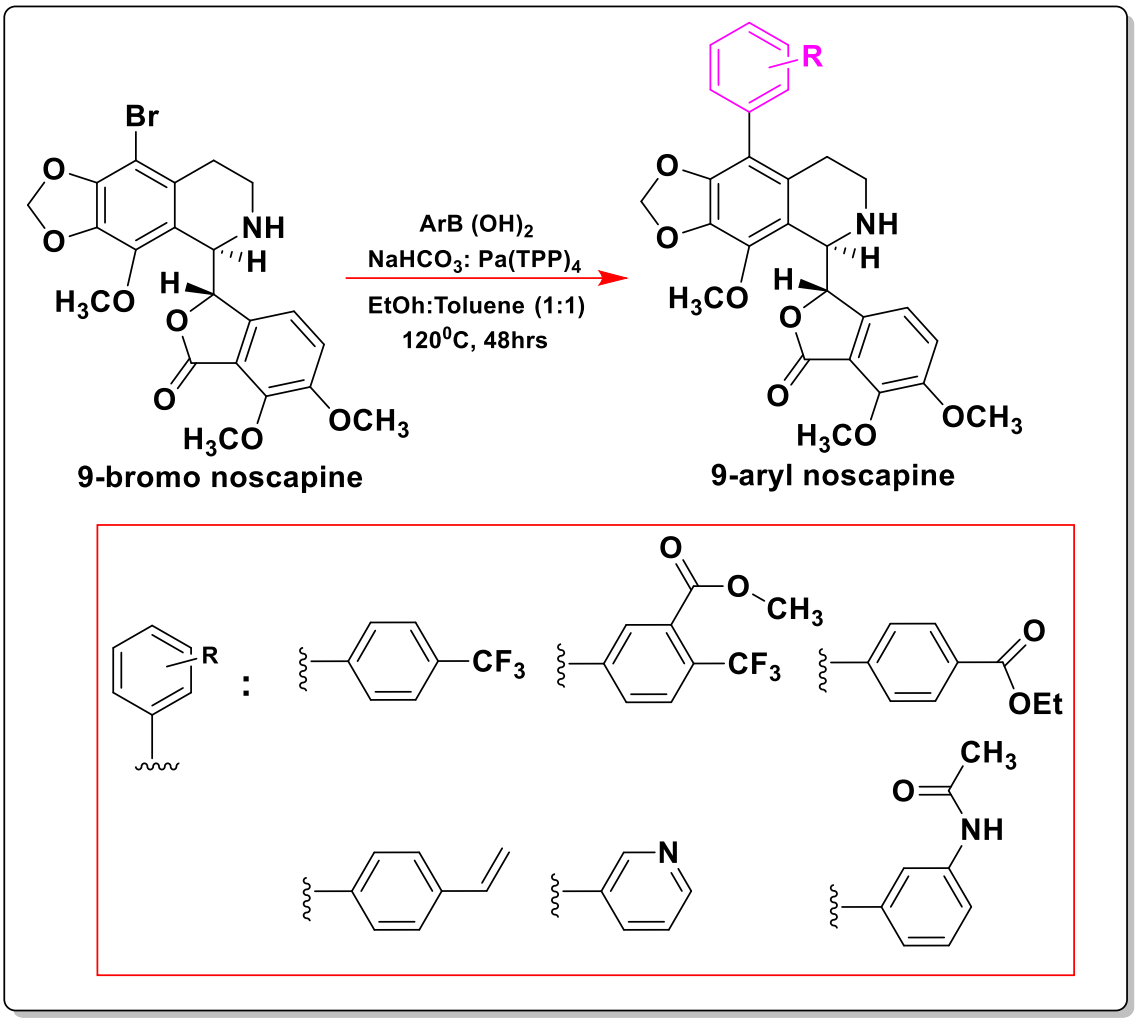

Figure 1.14: *Keeping an eye on computational results this novel biaryl type -noscapine congeners were synthesized from 9-bromo-noscapine utilizing enhanced Suzuki reaction conditions for further experimental assessment (Santoshi et al., 2015).*

1.15. Imidazo [2,1-b] thiazole-Coupled-Noscapine Derivatives:

Nagireddy *et al.*, 2019 described the synthesis of imidazothiazole-coupled noscapine derivatives linked at the 5'-N and 7-O positions (Figure 1.15). The derivatives arrested the cells at G2/M phase, triggered apoptosis by increasing the caspase-3 and PARP levels, and were found effective against prostate cancer cell line with less toxicity.

These derivatives can be further enhanced as a clinical option for treating pancreatic cancer.

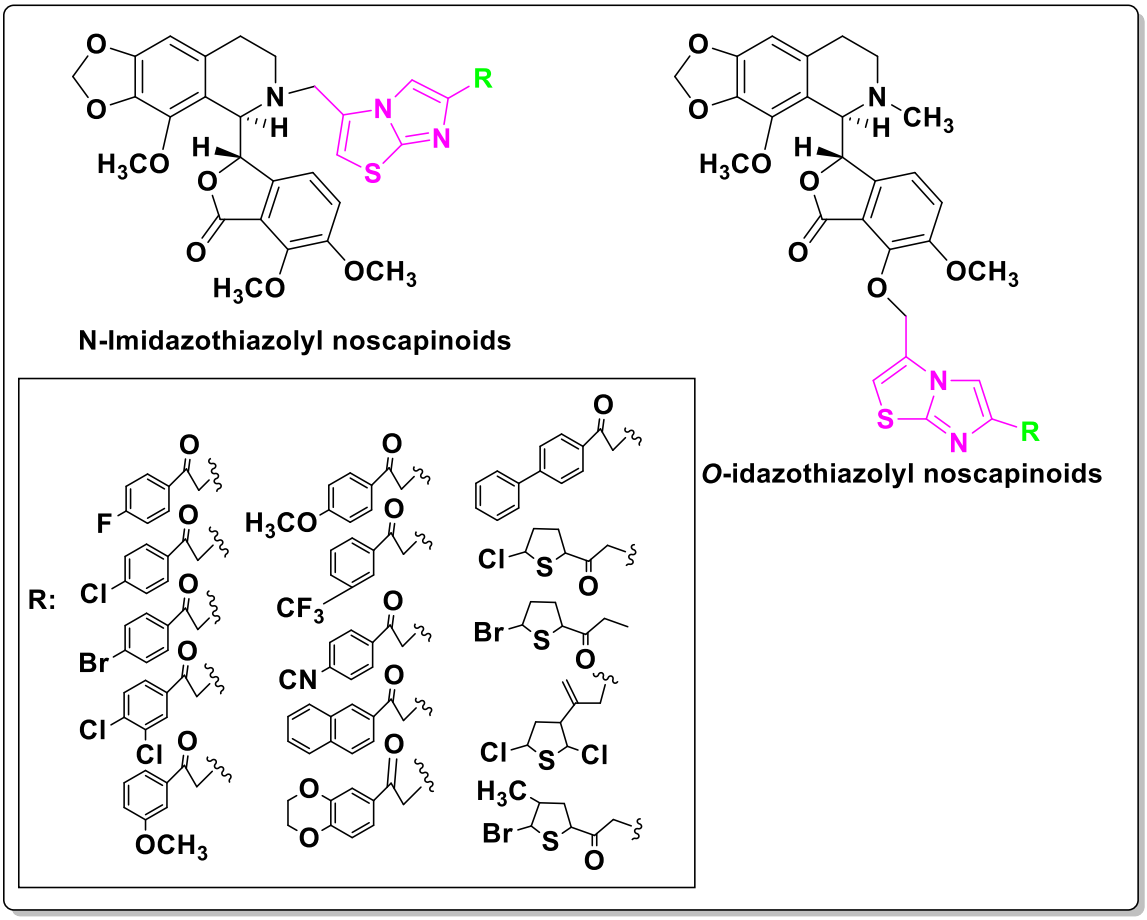

Figure 1.15: *Synthesis of N-Imidazothiazolyl noscapinoids & O-Imidazothiazolyl noscapinoids by bringing changes at the 5'-N and 7-O position (Nagireddy et al., 2019).*

From an ongoing quest to improve our therapeutic arsenal, we have developed a battery of derivatives by modification of its scaffolds and demonstrated to have high tubulin binding and anti-tumor activity compared to noscapine without any debilitating toxicities (Manchukonda *et al.*, 2012; Manchukonda *et al.*, 2013; Manchukonda *et al.*, 2014; Santoshi *et al.*, 2011; Santoshi *et al.*, 2015; Naik *et al.*, 2011a; Naik *et al.*, 2012). While several synthesized derivatives of noscapinoids showed promising *in vitro* activity against a panel of breast tumor cell lines, the antiproliferative activity comes to be in higher concentration (IC_{50} > 20 µM). The status of research in India as well as at international, therefore, reflects that there is an urgent need to take up further optimization of Noscapine towards development of novel and more promising derivatives that should specifically targeted to aggressive carcinomas to obtain the status of an investigational new drug (IND) from the FDA.

1.17. Objectives

- To strategically design congeners of noscapine (we called noscapinoids) through modification of functional groups or appendages attached to its scaffold and screening of promising derivatives by computer aided drug design techniques followed by chemical synthesis, structural characterization and purification.
- To evaluate and establish the *in vitro* anticancer efficacy of novel microtubule-interfering agent using breast cancer cells. Towards this end we will determine the effect of novel noscapine congener to (i) inhibit cellular proliferation, (ii) binding affinity with tubulin, (iii) affect cell cycle kinetics, and (iv) induce apoptosis in breast cancer cells.
- To evaluate the *in vivo* therapeutic efficacy of novel noscapine congener as an anti-tumor agent. We will achieve this by (a) initially implanting solid tumor in mice model followed by administration of drug and by monitoring the decrease in tumor volume; (b) evaluate the toxicity profile by (i) histopathological and (ii) hematological study. By doing so, we aim to assess the clinical potential and potential side effects of the drug molecule.

CHAPTER 2

Structure Based Design of Tubulin Binding 9-Arylimino noscapinoids: Chemical Synthesis and Experimental Validation Against Breast Cancer Cell Lines

2.1. Introduction

Microtubule-interacting drugs, such as taxols and vinca alkaloids, have been used in the clinic to treat various malignancies. However, these drugs are known to cause severe dose-dependent toxicities in patients, such as peripheral neuropathy, systemic toxicity, and allergic reactions (Kavanagh and Kudelka, 1993; Rowinsky and Donehower, 1991). More importantly, patients are developing resistance against taxol. Thus, the wonderful promise of taxol in managing breast cancers justifies further efforts to discover novel mitotic inhibitors. It would be additionally useful if other novel anti-mitotic agents have fewer side effects and are easily administered. In a quest to find such compounds, the natural compounds were screened and Noscapine (an opium alkaloid in the clinic as a safe anti-tussive drug) was discovered (Ye *et al.*, 1998). It was shown to bind tubulin, without interfering with the tubulin organization (monomer/polymer ratio) (Landen *et al.*, 2002). It was found to kill cancer cells of different tissue origins, including those that are resistant to conventional chemotherapeutics. It doesn't show any severe side effects among volunteers (Karlsson *et al.*, 1990). It was found to regress the volume of the implanted tumor to a fair degree in xenograft breast cancer animal models at a high dosage of 600 mg/kg.

From an ongoing quest to improve our therapeutic arsenal, we have developed a battery of derivatives by modification of its scaffolds and demonstrated to have high tubulin binding and anti-tumor activity compared to Noscapine without any debilitating toxicities (Manchukonda *et al.*, 2012; Santoshi *et al.*, 2015; Manchukonda *et al.*, 2013). While several synthesized derivatives of noscapinoids showed promising *in vitro* activity against breast tumor cell lines, the antiproliferative activity comes to be in higher concentration. Therefore, there is an urgent need to take up further optimization of Noscapine towards the development of novel and more promising derivatives.

In this study we appeal to develop 9-arylimino congeners of Noscapine by substituting arylimino groups at the C-9 position of the noscapine scaffold. The promising analogues were then chemically synthesized and their anticancer activity was evaluated using two human breast cancer cell lines (MCF-7 and MDA-MB-231). The 9-arylimino derivatives of Noscapine were found to bind tubulin heterodimer with enhanced binding affinity, efficiently suppress cancer cell growth, and successfully trigger cancer cell apoptosis by the arrest of cancer cells at the G2/M phase.

2.2. Materials and Methods

2.2.1. Refinement of the crystal structure of tubulin

The co-complex structure of tubulin-amino noscapine was downloaded from the PDB data bank (PDB ID: 6Y6D). This structure of tubulin was obtained at a higher resolution of 2.20 Å through X-ray crystallography (Oliva *et al.*, 2020). The structure was visualized using Maestro (Schrodinger software package) and the tubulin heterodimer consisting of α- and β- tubulin was prepared based on the multistep procedure of the protein preparation wizard (Schrodinger software package).

2.2.2. Design of 9-arylimino congeners of Noscapine

Based on *in silico* combinatorial approach 9-arylimino congeners of Noscapine were designed by hybridizing with arylimino groups (Schiff bases) as depicted in Figure 2.1 and a library of 17 compounds was developed (Figure 2.2). It was reported previously that Schiff base analogs have impressive anticancer activity. As an example, Schiff bases from coumarin and pyrazole aldehyde have been tested against cancer cell lines that showed mild anticancer activities (Ali *et al.*, 2013). Furthermore, mono and bis-Schiff bases have been reported efficacious against five cancer cell lines (Sondhi *et al.*, 2012).

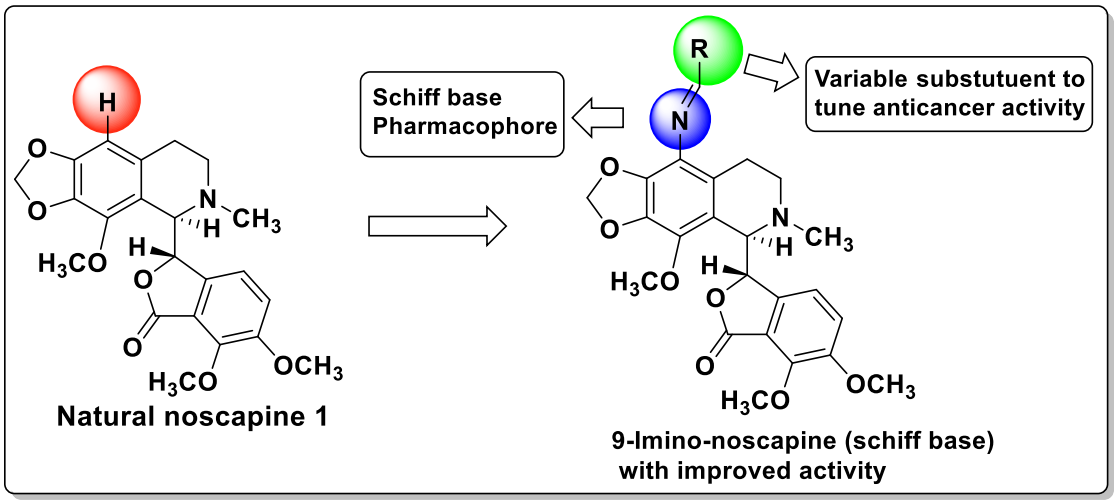

Figure 2.1: *Strategic development of 9-arylimino noscapinoids by hybridizing Schiff base at C-9 position of the isoquinoline ring system of Noscapine.*

2.2.3. Preparation of ligands and optimization

We have built the molecular structures of 9-arylimino derivatives of Noscapine (Figure 2.2) using ISIS draw and converted them into 3D structures using Chemsketch. Macromodel (Schrodinger software package) and OPLS 2005 force field was used for

energy minimization of build structures using PRCG algorithm. A simulation of 1000 steps and an energy gradient of 0.001 were used for energy minimization. The molecules were also geometrically refined using Jaguar (version 17.4, Schrödinger, LLC) with a basis set of 3-21G* (Gordon *et al.,* 1982) using Becke's three-parameter exchange potential and the Lee-Yang-Parr correlation functional (B3LYP) (Beck, 1993). Ligprep (Schrödinger software package) was used to generate ionization states at physiological pH, generation of possible tautomers, and minimization of the ring conformations for each molecule.

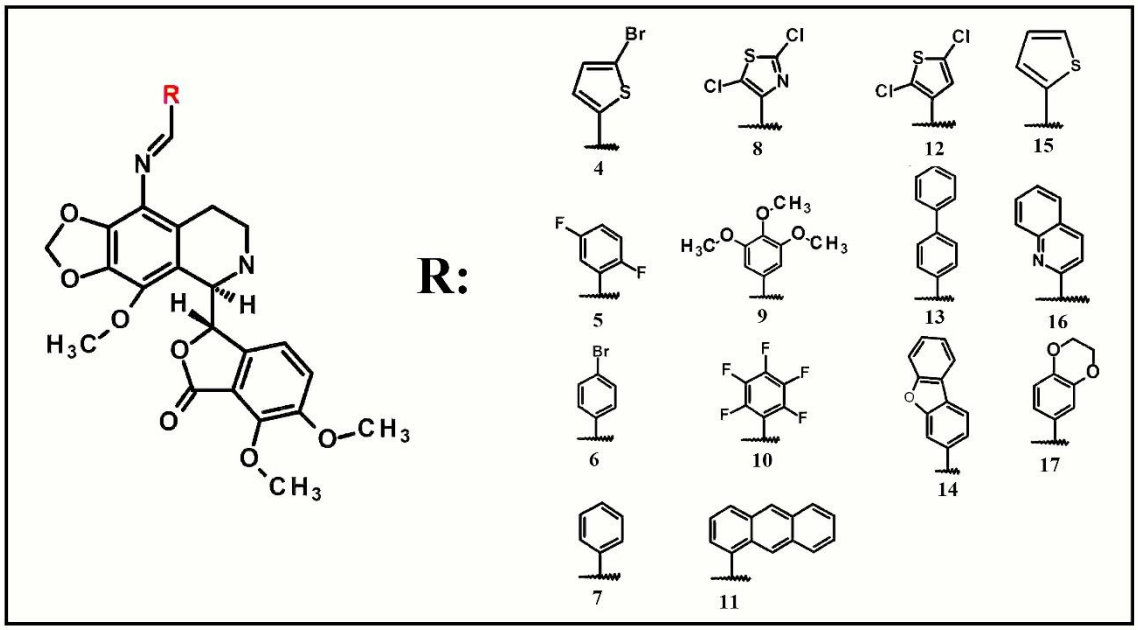

Figure 2.2: *The library of 9-arylimino derivatives of noscapine design based on in silico combinatorial approach to screen out the promising derivatives based on molecular docking for chemical synthesis and experimental evaluation.*

2.2.4. Molecular docking

The docking protocol used was validated by the superimposition of the crystal structure of amino-noscapine with its docked structure and calculating the root mean square deviation (RMSD) between them. The RMSD value of 0.806 between crystal and docked structures validated the docking protocol. After validating the docking protocol the library of 9-arylimino derivatives of noscapine designed above was docked onto the noscapinoids binding site (Oliva *et al.,* 2020) located at α- and β- tubulin interface. The noscapinoids binding site was selected based on the co-crystal structure of tubulin and one of the derivatives of noscapine, amino- noscapine (PDB ID: 6Y6D) (Oliva *et al.,* 2020). Further, the binding site was specified by generating two grid boxes as described earlier (Dash *et al.,* 2021) by selecting the co-crystal ligand, amino-noscapine using the

Glide Grid generation programme. The molecules were docked using Glide-XP algorithm (Halgren *et al.*, 2004) (Schrodinger software package) and evaluated using Glide XP_{Score} function (Halgren *et al.*, 2004) with similar parameters set up as mentioned earlier (Dash *et al.*, 2021). All the molecules in the library were sorted based on their docking score (Table 2.1) and finally, the best three molecules **4-6** (Figure 2.3) based on their docking score were selected for chemical synthesis and experimental evaluation to confirm their anticancer potential.

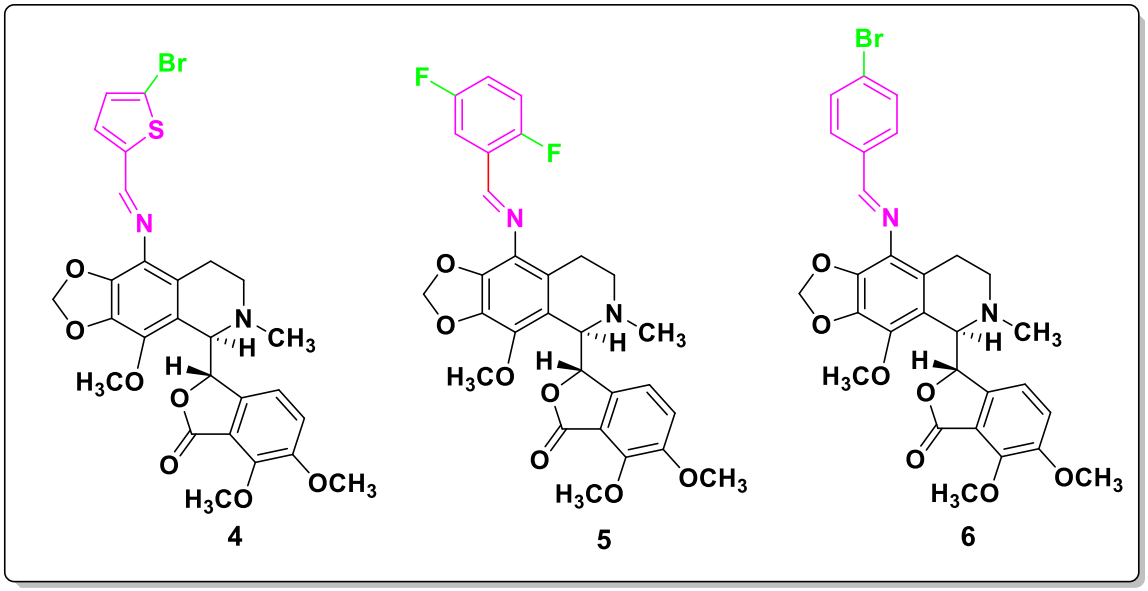

Figure 2.3: *Molecular structure of three top ranked 9-arylimino noscapinoids,* ***4-6*** *screened out from the library based on the docking score.*

Table 2.1: The Glide XP docking score of the 9-arylimino derivatives of noscapine design based on *in silico* combinatorial approach. The three derivatives **4-6** based on better docking score were selected for chemical synthesis and experimental evaluation.

Noscapine and its derivatives	**Docking score (Kcal/Mol)**	**Noscapine and its derivatives**	**Docking score (Kcal/Mol)**
1 (Noscapine)	-3.856	10	-4.137
2	-3.966	11	-3.463
3	-4.002	12	-2.871
4	-4.219	13	-2.918
5	-4.367	14	-3.822
6	-5.135	15	-3.491
7	-2.862	16	-4.031
8	-3.001	17	-4.033
9	-3.948		

2.2.5. Molecular dynamics simulation

The docked complexes of tubulin and 9-arylimino noscapinoids, **4-6** in the presence of GTP, GDP and magnesium were used for molecular dynamics simulation using GROMACS 2019.2 package. The parameter files for tubulin and the ligands were generated as mentioned earlier (Meher *et al.,* 2021). Topologies for ligands were generated using tleap program of Amber18 and ACPYPE software. TIP3P water model with dissolved counter ions were added to neutralize the system. The energy minimization and molecular dynamic simulation of the system for 100 ns with a time step of 2 fs were performed with similar parameters set up as mentioned earlier (Dash *et al.,* 2021). Gromacs tools were used to analyze trajectories for root mean square deviation (RMSD) and root mean square fluctuation (RMSF). All plots were generated using GRACE software.

2.2.6. Prediction of binding free energy using MM-PBSA and MM-GBSA technique

The molecular mechanics Poisson-Boltzmann surface area (MM/PBSA) and molecular mechanics generalized Born surface area (MM/GBSA) methods (Kollman *et al.,* 2000; Massova *et al.,* 2000) were used for predicting the binding free energy ($\Delta G_{bind,pred}$) of 9-arylimino noscapinoids, **4-6** with tubulin using AMBER 16.0. We have used both approaches because many studies have compared the accuracy of MM/PBSA and MM/GBSA, indicating better results for MM/PBSA (Weis *et al.,* 2006; Xu *et al.,* 2013). It was also found that MM/PBSA results are worse (Hou *et al.,* 2011) or equally good (Sun *et al.,* 2014) compared to MM/GBSA, depending on the studied systems. From the last 10 ns of the MD trajectory, 500 snapshots of the structure were collected at an interval of 20 ps to determine $\Delta G_{bind,pred}$ of the molecules.

2.2.7. General procedure for chemical synthesis of 9-arylimino noscapinoids, 4-6

Amino-noscapine **3** was synthesized from the natural α-noscapine as reported earlier (Santoshi *et al.,* 2015). Form the amino-noscapine, the selected 9-arylimino noscapinoids **4-6** were synthesized as per the synthetic scheme (Figure 2.4) as mentioned earlier (Meher *et al.,* 2021). Structural elucidation of intermediates and final products **4-6** were performed using NMR (^{1}H and ^{13}C), IR spectroscopy and mass (HRMS) spectrometry techniques (Appendix A2.1-A2.11). The final products were purified through HPLC using C18 column (acetonitrile: water, 90:10) and were > 96.5% pure.

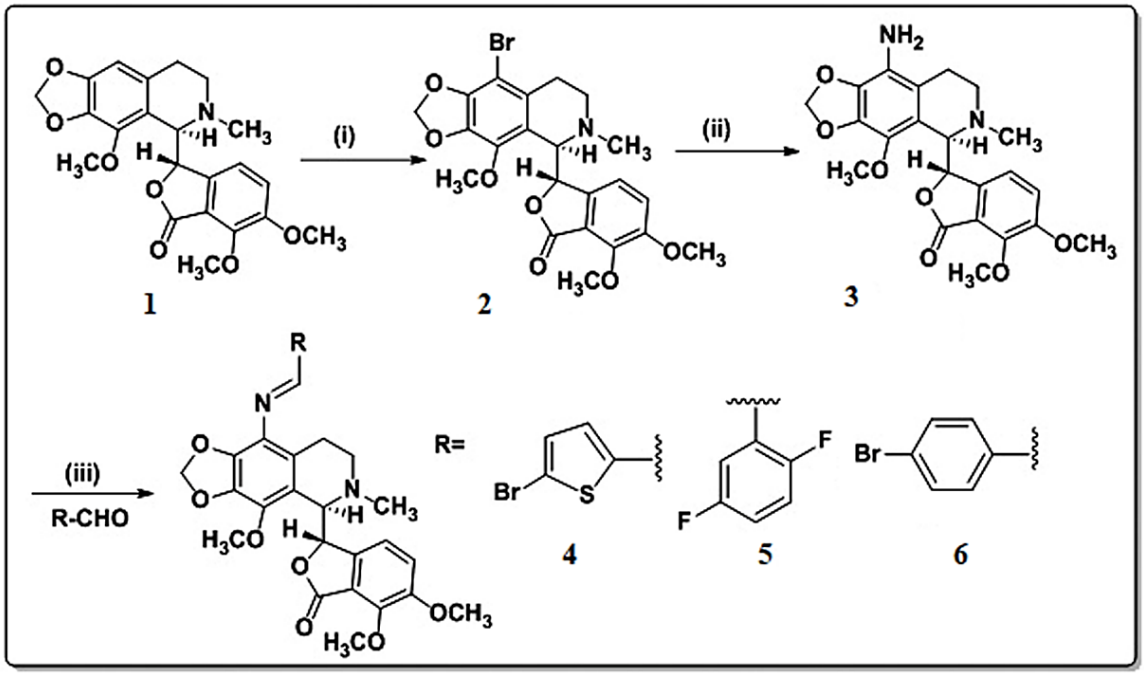

Figure 2.4: *General chemical reaction for chemical synthesis of 9-arylimino noscapinoids 4-6, rationally design in the study. Reaction conditions: (i) 48% HBr, Br2-water, rt, 2h (ii) CuI, NaN3, L-Proline, DMF, 140 °C, 4h, (iii) RCHO, EtOH, Reflux, 24h.*

2.2.8. Structural characterization of 9-arylimino noscapinoids, 4-6

(S)-3-((R)-9-((E)-((5-bromothiophen-2-yl)methylene)amino)-4-methoxy-6-methyl-5,6,7,8-tetrahydro-[1,3]dioxolo[4,5-g]isoquinolin-5-yl)-6,7dimethoxyisobenzofuran-1(3H)-one (4):

Yield: 82%. Nature: White solid. Mp. 94-96 °C. IR (KBr): 3448, 2929, 1758, 1623, 1497, 1424, 1381, 1267, 1209, 1121, 1035, 970, 887, 795, 736, 696, 501 cm^{-1}. ^{1}H NMR (500 MHz, $CDCl_3$) : δ 8.88 (s, 1H, N=CH), 7.14 (d, *J* = 3.8 Hz, 1H, Ar-H), 7.07 (d, *J* = 3.8 Hz, 1H, Ar-H), 7.01 (d, *J* = 8.2 Hz, 1H, Ar-H), 6.36 (d, *J* = 8.2 Hz, 1H, Ar-H), 5.98 (dd, *J* = 1.3, 16.0 Hz, 2H, O-C*H*2-O), 5.55 (d, *J* = 4.5 Hz, 1H, Ar-CH, (C3-phthalide)), 4.36 (d, *J* = 4.5 Hz, 1H, Ar-CH, (C5'-isoquinoline)), 4.10 (s, 3H, -OCH3), 4.02 (s, 3H, -OCH3), 3.86 (s, 3H, -OCH3), 2.98-2.91 (m, 1H, -C*H*H-*N*-CH3 (C7'-isoquinoline)), 2.75-2.69 (m, 1H, -CH*H*-*N*-CH3 (C7'-isoquinoline)), 2.53 (s, 3H, *N*-C*H*3), 2.44-2.38 (m, 1H, Ar-C*H*H (C8'-isoquinoline)), 2.08-2.01 (m, 1H, Ar-CH*H* (C8'- isoquinoline)). ^{13}C NMR (100 MHz, CDCl3) : δ 168.0, 152.0, 147.4, 145.5, 140.7, 137.1, 135.3, 134.8, 129.4, 125.3, 122.9, 120.9, 119.9, 117.9, 117.7, 110.8, 100.6, 81.7, 62.1, 60.7, 59.6, 56.7, 49.1, 45.9, 22.3. MS (ESI-MS) *m/z*: 603 [M+H]+ HRMS (ESI): Calcd for $C_{27}H_{26}BrN_2O_7S$[M+H]+: 603.06116, found: 603.06173.

(S)-3-((R)-9-((E)-(2,5-difluorobenzylidene)amino)-4-methoxy-6-methyl-5,6,7,8tetra hydro-[1,3]dioxolo[4,5-g]isoquinolin-5-yl)-6,7-dimethoxyisobenzofuran-1(3H)-one (5):

Yield: 74%. Nature: White solid. mp: 145-147 °C. IR (KBr): 33571, 2944, 2793, 1762, 1628, 1491, 1428, 1387, 1272, 1142, 1043, 965, 813, 725 cm^{-1}. ^{1}H NMR (400 MHz, $CDCl_3$) : δ 9.13 (d, *J*= 2.4 Hz, 1H, N=CH), 7.87-7.81 (m, 1H, Ar-H), 7.14-7.07 (m, 2H, Ar-H), 7.00 (d, *J* = 8.3 Hz, 1H, Ar-H), 6.33 (d, *J* = 8.3 Hz, 1H, Ar-H), 6.02 (dd, *J* = 1.3, 15.6 Hz, 2H, O-C*H*2-O), 5.57 (d, *J* = 4.4 Hz, 1H, Ar-CH, (C3-phthalide)), 4.39 (d, *J* = 4.4 Hz, 1H, Ar-CH, (C5'-isoquinoline)), 4.10 (s, 3H, -OCH3), 4.04 (s, 3H, -OCH3), 3.86 (s, 3H, -OCH3), 3.05-2.95 (m, 1H, -C*H*H-*N*-CH3 (C7'-isoquinoline)), 2.77-2.69 (m, 1H, -CH*H*-*N*-CH3 (C7'-isoquinoline)), 2.55 (s, 3H, *N*C*H*3), 2.46-2.37 (m, 1H, Ar-C*H*H (C8'-isoquinoline)), 2.11-2.00 (m, 1H, Ar-CH*H* (C8'-isoquinoline)). ^{13}C NMR (125 MHz, $CDCl_3$) : δ 168.0, 159.8 (d, *J*C-F = 31.7 Hz), 157.9(d, *J*C-F= 38.1 Hz), 153.2, 152.1, 147.6, 141.3, 139.47, 139.43, 134.4, 129.8, 126.1 (dd, *J*C-F = 8.1, 11.8 Hz), 124.9, 119.8, 119.1 (dd, *J*C-F = 9.0, 25.4 Hz), 117.8, 117.6, 117.1 (dd, *J*C-F = 8.1, 23.6 Hz), 112.9 (dd, *J*C-F = 2.7, 25.4 Hz), 101.1, 81.7, 62.2, 60.8, 59.5, 56.7, 49.3, 45.8, 22.8. MS (ESI-MS) *m/z*: 553 [M+H]+ HRMS (ESI) : Calcd for $C_{29}H_{27}F_2N_2O_7$ [M+H]+: 553.17808, found: 553.17669.

(S)-3-((R)-9-((E)-(4-bromobenzylidene)amino)-4-methoxy-6-methyl-5,6,7,8-tetrahydro-[1,3]dioxolo[4,5-g]isoquinolin-5-yl)-6,7-dimethoxyisobenzofuran-1(3H)-one (6):

Yield: 76%. Nature: White solid. mp: 93-95 °C. IR (KBr): 3449, 2936, 2795, 1758, 1626, 1494, 1383, 1267, 1124, 1034, 970, 821 cm-1. ^{1}H NMR (500 MHz, $CDCl_3$) : δ 8.84 (s, 1H, N=CH), 7.76 (d, *J* = 8.5 Hz, 2H, Ar-H), 7.58 (d, *J* = 8.5 Hz, 2H, Ar-H), 6.99 (d, *J* = 8.3 Hz, 1H, Ar-H), 6.34 (d, *J* = 8.3 Hz, 1H, Ar-H), 5.99 (dd, *J* = 1.3, 14.9 Hz, 2H, O-C*H*2-O), 5.57 (d, *J* = 4.4 Hz, 1H, Ar-CH, (C3-phthalide)), 4.38 (d, *J* = 4.4 Hz, 1H, Ar-CH, (C5'-isoquinoline)), 4.10 (s, 3H, -OCH3), 4.03 (s, 3H, -OCH3), 3.85 (s, 3H, -OCH3), 3.04-2.93 (m, 1H, -C*H*H-*N*-CH3 (C7'-isoquinoline)), 2.75-2.68 (m, 1H, -CH*H*-*N*-CH3 (C7'-isoquinoline)), 2.54 (s, 3H, *N*C*H*3), 2.46-2.37 (m, 1H, Ar-C*H*H (C8'-isoquinoline)), 2.10-2.00 (m, 1H, Ar-CH*H* (C8'-isoquinoline)). ^{13}C NMR (100 MHz, CDCl3) : δ 168.1, 160.1, 152.1, 147.6, 141.4, 139.2, 139.0, 135.9, 134.5, 131.8, 129.6, 129.3, 125.4, 125.2, 119.8, 118.3, 117.8, 117.6, 100.9, 81.7, 62.2, 60.9, 59.5, 56.7, 49.3, 45.8, 22.7. MS (ESI-MS) *m/z*: 595 [M+H]+ HRMS (ESI) : Calcd for $C_{29}H_{28}BrN_2O_7$ [M+H]+: 595.10744, found: 595.10635.

2.2.9. Cell culture and reagents

The human breast cancer cell lines, MCF-7 and MDA-MB-231 were acquired from the Institute of Life Science, Bhubaneswar, India. The normal human embryonic kidney cell (293T) (passage number 12) was obtained from Dr. S. K. Singh, King George's Medical University, Lucknow, India. Stock solution (100 mM) of 9-arylimino noscapinoids, **4-6** were prepared with 1% dimethyl sulfoxide (DMSO). The cells were grown in a 5% CO_2 and 95% humidity in Dulbecco's modified Eagle medium (DMEM) at a temperature of 37 °C, supplemented with 10 % fetal bovine serum (FBS) and antibiotics. Cells with a 70-80 % confluence were subcultured for bioassays using trypsin-EDTA (0.25 %).

2.2.10. Cellular proliferation assay

The cell proliferation assay was performed using two human breast cancer cell lines MCF-7 and MDA-MB-231 as well as a normal human embryonic kidney cell (293T) as described previously (Meher *et al.*, 2021). Briefly, the cells were seeded at a density of $5x10^3$ cells per well in 96-well plates. The cells were treated with 5 to 100 µM of noscapine and 9-arylimino noscapinoids, **4-6**. After 72h of treatment, the viability of the cell was checked by sulforhodamine B assay. The plate was read at a wavelength of 564 nm using a SPECTRAmax PLUS 384 microplate spectrophotometer. Fifty percent inhibitory concentration (IC_{50}) of molecules was determined using the online tool Quest GraphTM IC_{50} Calculator (AAT Bioquest, Inc., Sunnyvale, CA, USA, https://www.aatbio.com/tools/ic50-calculator).

2.2.11. Cell cycle progression assay

The progression in the mitotic cell cycle with the treatment of 9-arylimino noscapinoids, **4-6** was performed as reported earlier (Patel *et al.*, 2021). Briefly, MDA-MB-231 cells were seeded at a density of $1x10^5$ in a 6-well culture plate overnight and were treated with IC_{50} concentration of noscapine (51.6 µM) and 9-arylimino noscapinoids, **4-6** (32.6, 15.4 and 7.7 µM respectively). After 72 h of treatment, cells were analyzed using flow cytometry (BD FACS Aria-III) to estimate the percentage of cells in the different stages of the cell cycle.

2.2.12. Apoptosis assay

Induction of apoptosis was performed as described earlier (Patel *et al.*, 2021). The breast cancer cells, MDA- MB-231 ($3x10^4$) were seeded on 12 well culture plate and incubated for 24 h with a complete medium. The cells were treated with IC_{50}

concentration of noscapine (51.6 µM) and 9- arylimino noscapinoids, **4-6** (32.6, 15.4 and 7.7 µM respectively) and were harvested at 72 h. The apoptotic cells were detected using an apoptosis detection kit based on the manufacturer's instruction (Sigma–Aldrich, USA) using flow cytometry (BD FACS Aria- III). Viable cells (Annexin V− / PI−), early apoptotic cells (Annexin V+ / PI−), late apoptotic/necrotic cells (Annexin V+ / PI+) and late necrotic cells (Annexin V− / PI+) were identified and determined their percentage.

2.2.13. Extraction and purification of tubulin

Microtubule from the goat brain was isolated by two cycles of temperature and GTP-dependent polymerization and depolymerization (Hamel and Linn, 1981). It was then purified by phosphocellulose chromatography as reported earlier (Panda *et al.*, 2000) and the amount of purified tubulin was estimated using the Bradford method (Bradford, 1976). Aliquots were frozen in liquid nitrogen and preserved at -80 ^{o}C until used.

2.2.14. Tryptophan quenching assay

A fluorescence quenching assay was performed to determine the binding of a chemical onto tubulin (Dash *et al*., 2020). It is because tubulin is autofluorescence in nature due to the presence of several tryptophan amino acids and it was reduced when a molecule binds on it. Tubulin (2 µM) was treated with 9-arylimino noscapinoids **4-6** at a concentration of 25 µM in PEM buffer (50 mM pipes, 3 mM $MgSO_4$, 1 mM EGTA, pH 6.8) in a water bath (35 °C; 45 min). They were then excited at 295 nm and the emission reading at 310–400 nm was obtained. A FlouroMax® 4 spectrofluorometer (Horiba Scientifc, Edison, NJ) supported by FluorEssence 3.5 software was used for the spectrofluorimetric titrations.

2.3. Results and Discussion

Many derivatives of noscapine have been developed to increase its therapeutic outcome (Aneja *et al.,* 2006b; Santoshi *et al.,* 2015; Aneja *et al.,* 2006c; Sondhi *et al.*, 2012; Aneja *et al.*, 2006d; Dash *et al.*, 2020). These derivatives were demonstrated to bind tubulin, perturb cell-cycle progression, inhibit cell proliferation and induce apoptosis in a variety of cancer cells of different tissue origin (Manchukonda *et al.*, 2014). The derivatives generated by modification of the C-9 position on the isoquinoline ring system of noscapine were shown to possess superior activity (Aneja *et al.,* 2006a; Aneja *et al.*, 2006b). Based upon this momentum, we have rationally designed a new

series of derivatives of noscapine by substituting arylimino groups (Schiff bases) at C-9 position to examine their anticancer potential.

2.3.1. Molecular dynamics simulation

The library composed of 9-arylimino derivatives of noscapine was docked onto αβ-tubulin heterodimer and ranked according to docking score. The top ranked three noscapinoids **4-6** (Figure 2.3) having lowest docking scores ranging from -4.219 to -5.135 kcal/mol in comparison to noscapine (-3.586 kcal/mol) (Table 2.1) were selected. The αβ-tubulin heterodimer bound to molecules **4-6** were MD simulated for 100 ns. The system's stability during the period of the simulation was monitored by the root means square deviations (RMSD) of Cα-carbons (Figure 2.5). The deviations in the RMSD plot were very small after equilibration and were found to be stable after 20 ns of simulation. Similarly, the root mean square fluctuations (RMSF) of amino acids in the bound form with ligands and in the free form were not so much different (within the range of 1 to 2.5 Å) indicating that the residues were more rigid (Figure 2.6). The top 5 complex structures of tubulin and 9-arylimino noscapinoids, **4-6** having the lowest total energy from the MD trajectory were used to generate the average structure to elucidate their binding mode. All the three 9- arylimino noscapinoids accommodated well inside the noscapinoids binding pocket (Figure 2.7) between α- and β- tubulin interface. Their interactions with the binding site amino acids are shown in the ligplot (Figure 2.8). The 9-arylimino noscapinoid, **6** binds with 2 hydrogen bonds (represented by a dashed line and the number indicated the bond length) (Figure 2.8c). In contrast, the 9-arylimino noscapinoids, **4** and **5** revealed only 1 hydrogen bond with the binding site residues (Figure 2.8a, b). Besides hydrogen bonding, a good number of hydrophobic interactions were involved in the binding of 9-arylimino noscapinoids **4-6** with binding site residues (Appendix table A2.12-A2.15).

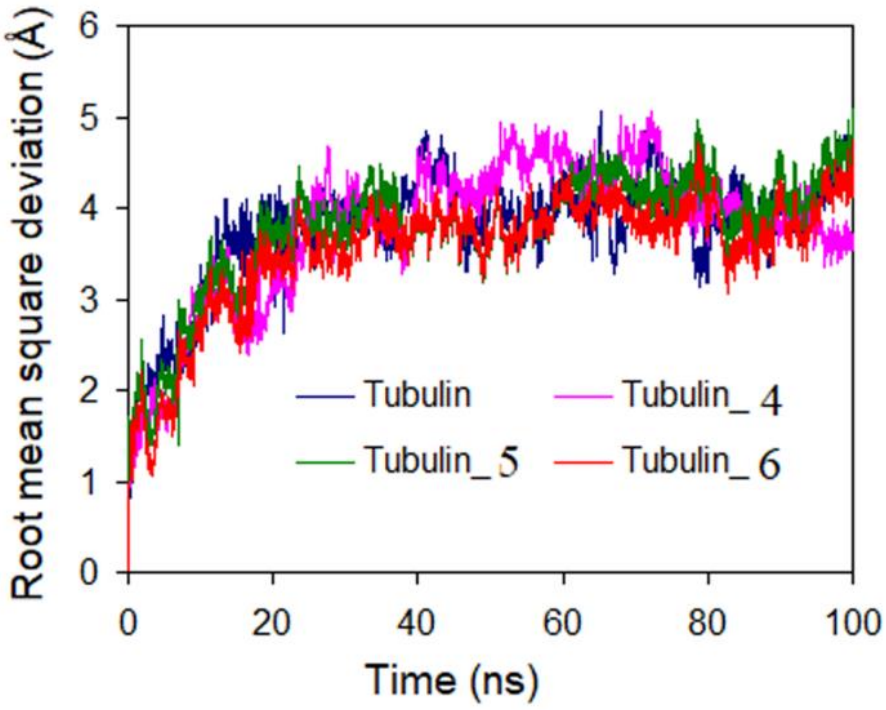

Figure 2.5: *Root mean square deviations (RMSD) of Cα carbon of tubulin in unbound and bound form with 9-arylimino noscapinoids,* ***4-6*** *during 100 ns of MD simulation. The relative fluctuation in the RMSD is very small after ~ 20 ns of the simulation, indicating the systems' stability.*

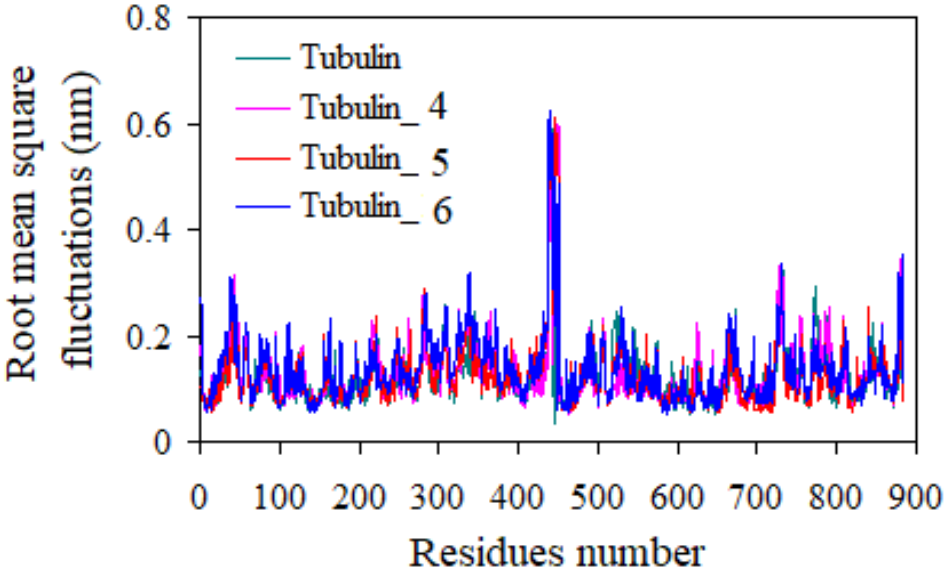

Figure 2.6: *Root mean square fluctuation (RMSF) of the amino acids of tubulin in unbound and bound form with 9-arylimino noscapinoids,* ***4-6*** *during 100 ns of MD simulation. Different levels of flexibility of amino acids were noticed. Most of them showed flexibilities < 3 Å, whereas only few amino acids showed fluctuation >5 Å, indicating that these are more flexible.*

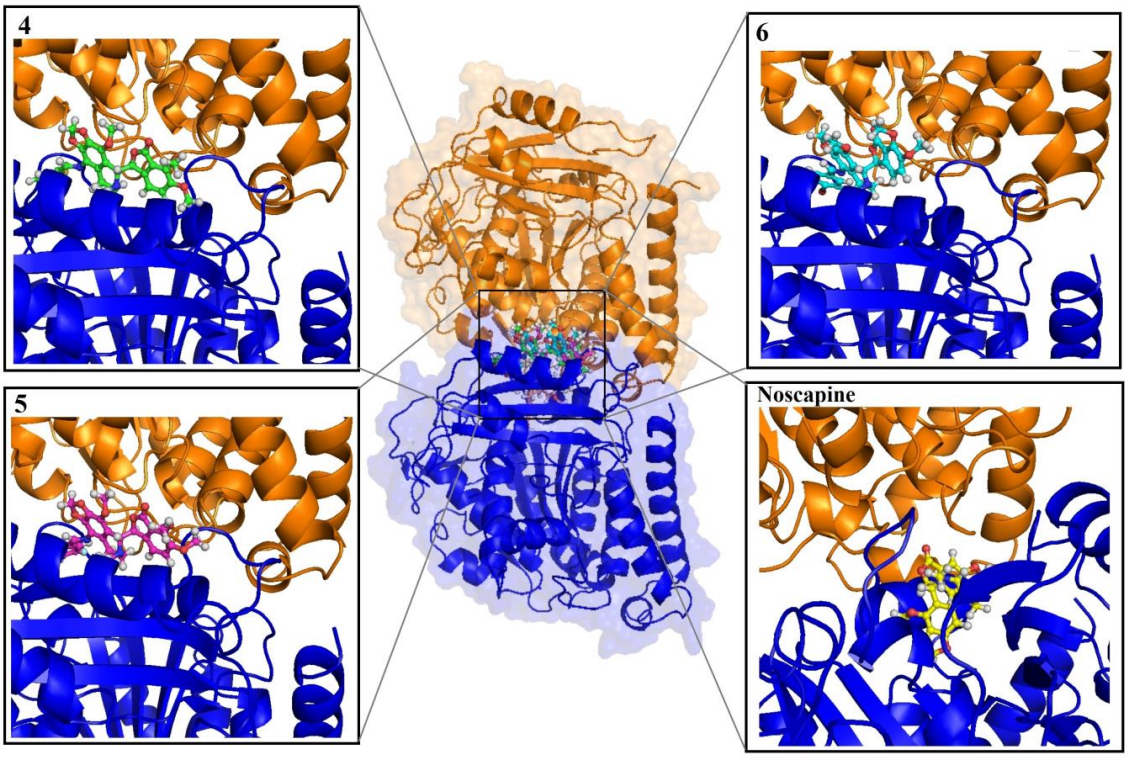

Figure 2.7: *The newly designed 9-arylimino noscapinoids* ***4-6*** *are accomodated well inside the binding site at the interface of α- and β- tubulin. α-tubulin is represented in blue colour and β-tubulin is represented in brown colour.*

2.3.2. Theoretical binding affinity calculation

The binding affinity of all the three 9-arylimino noscapinoids **4-6** was calculated using MM-PBSA and MM-GBSA methods. All three noscapinoids displayed stable interaction throughout the simulation. Among them, the 9-arylimino noscapinoid **6** showed the best binding affinity with the predicted free energy of binding ($\Delta G_{bind,pred}$) of -49.72 kcal/mol followed by **5** with -47.74 kcal/mol and **4** with -45.41 kcal/mol using the MM-PBSA method (Table 2.2a). Using the MM-GBSA method, 9-arylimino noscapinoid **6** showed the highest binding affinity with the value of -43.62 kcal/mol followed by **5** with -39.73 kcal/mol and **4** with -37.24 kcal/mol (Table 2.2b). Overall, all three 9-arylimino noscapinoids **4-6** revealed better binding affinity compared to noscapine (-34.47 and -40.27 kcal/mol), respectively, using both MM-GBSA and MM-PBSA (Table 2.2a & b). This could be attributed to the formation of both hydrogen bonds and hydrophobic interaction of 9-arylimino noscapinoids with surrounding amino acids in the binding pocket. A similar study has been performed earlier for designing novel derivatives of noscapine based on a combination approach of molecular docking and MD simulation. A panel of three different 9-arylimino noscapinoids has been designed *in silico*. These noscapinoids were predicted to have a better binding affinity

with tubulin based on molecular docking and LIE-SGB predicted binding energy (Patel *et al.*, 2021). In contrast, the three new 9-arylimino derivatives of noscapine screened out in this study from the library were predicted to have better binding affinity compared to the previously reported 9-arylimino noscapinoids. A combination of MD simulation and MM-PBSA method has been used earlier to identify potential inhibitors against targeted proteins (Bhardwaj *et al.*, 2020; Bhardwaj and Purohit, 2021).

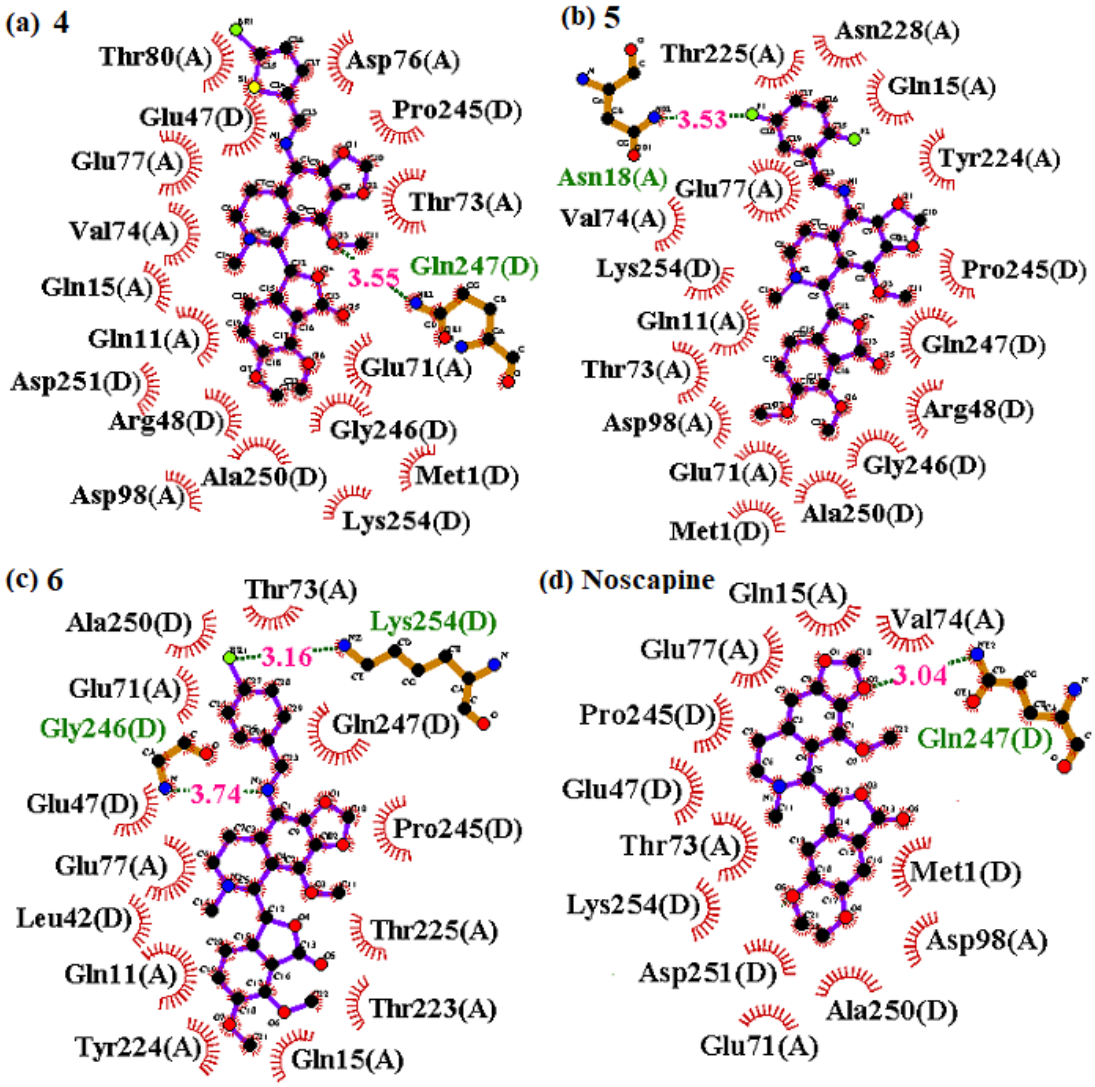

Figure 2.8: *The ligplot analysis showed the interaction of binding site amino acids with the 9-arylimino noscapinoids* ***4-6*** *and noscapine. The binding site residues involved in the interactions are slightly different mainly because of the variation in functional groups. The hydrogen bonds formed (if any) are represented as dotted lines.*

Table 2.2a. Docking score, free energy of binding and its components (kcal/mol) for the 9-arylimino noscapinoids with αβ tubulin dimer using MM-PBSA method.

Energy components (kcal/mol)	Noscapine	4	5	6
Glide XP_{score}	-3.856	-4.219	-4.367	-5.135
ΔE_{ele}	-319.2	-326.5	-338.4	-344.3
ΔE_{vdw}	-65.36	-73.62	-77.27	-79.37
ΔE_{gas}	-383.4	-389.7	-396.2	-409.3
$\Delta G_{sol\text{-}np}$	-7.254	-8.128	-8.927	-9.154
ΔG_{PB}	354.7	359.5	365.2	372.4
$\Delta G_{solv,PB}$	348.3	357.2	362.4	368.2
$\Delta G_{ele,PB}$	33.74	41.43	46.31	48.19
$\Delta G_{bind,PB}$	**-34.47**	**-37.24**	**-39.73**	**-43.62**

Table 2.2b. Free energy of binding and its components (kcal/mol) for the 9-arylimino noscapinoids with αβ tubulin dimer using MM-GBSA method.

Energy components (kcal/mol)	Noscapine	4	5	6
ΔE_{ele}	-319.2	-326.5	-338.4	-344.3
ΔE_{vdw}	-65.36	-73.62	-77.27	-79.37
ΔE_{gas}	-383.4	-389.7	-396.2	-409.3
$\Delta G_{sol\text{-}np}$	-7.254	-8.128	-8.927	-9.154
ΔG_{GB}	349.4	351.3	347.5	364.3
$\Delta G_{solv,GB}$	341.7	344.6	347.4	358.7
$\Delta G_{ele,GB}$	28.95	32.74	34.73	36.44
$\Delta G_{bind,GB}$	**-40.27**	**-45.41**	**-47.74**	**-49.72**

2.3.3 Arylimino noscapinoids, 4-6 inhibits proliferation of MCF-7 and MDA-MB-231

The 9-arylimino noscapinoids, **4-6** inhibited proliferation of MCF-7 and MDA-MB-231 cells in a dose-dependent manner (Figure 2.9). The 9-arylimino derivatives of noscapine, **4-6** revealed promising anti-proliferative activity compared to noscapine. The IC_{50} value was 45.2 µM, 26.8 µM, 11.6 µM and 3.0 µM for noscapine, **4, 5** and **6**, respectively for MCF-7 cells (Table 2.3). In contrast, IC_{50} value of 51.6 µM, 32.6 µM, 15.4 µM and 7.7 µM was measured for noscapine, **4, 5** and **6**, respectively for MDA-MB-231 cells. The differences in IC_{50} values obtained using MCF-7 (a triple positive for receptor proteins) and MDA-MB- 231 (a triple negative for receptor proteins) cell lines revealed that the anti-proliferative activity for these 9-arylimino noscapinoids were cell-type dependent. Further, the toxicity if any to the normal healthy cells with the treatment of noscapine and its 9-arylimino derivatives, **4-6** was determined using normal human

embryonic kidney cells (293T). It was found that noscapine and its 9-arylimino derivatives, **4-6** revealed < 5% cell killing to normal cells even at a high concentration of 100 µM (Figure 2.10), indicating that the molecules are not affecting the normal cells and only selectively inhibiting the proliferation of cancer cells. In contrast, the 9-arylimino derivatives of noscapine, **4-6** at relatively low concentrations (5.0 µM) significantly stimulated proliferation of 293T cells, while at higher concentrations (100 µM) inhibited proliferation of 293T cells (< 5%).

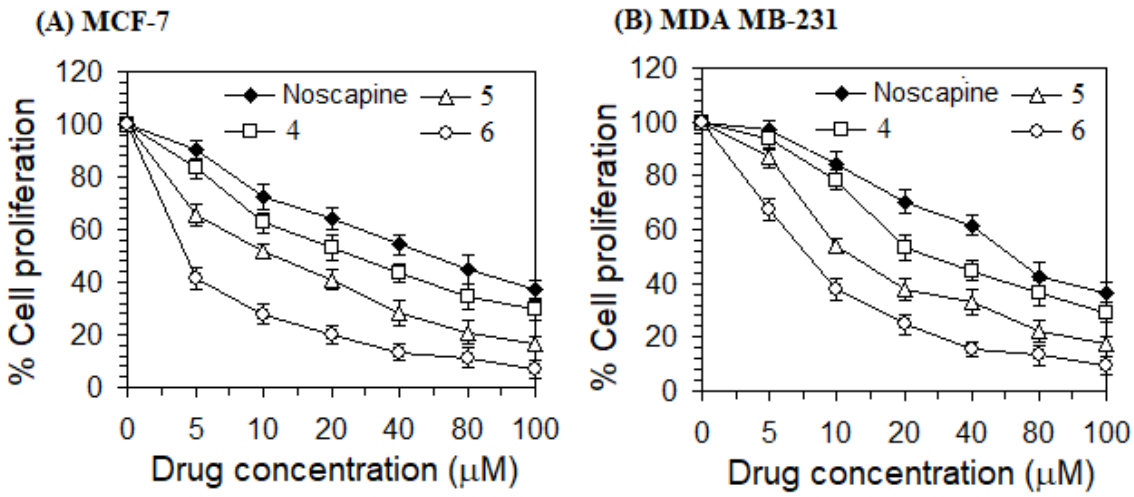

Figure ***2.9:*** *The 9-arylimino noscapinoids* ***4-6*** *have better anti-proliferative activity compared to Noscapine using (a) MCF-7 and (b) MDA-MB-231 human breast cancer cell lines. Both MCF-7 and MDA-MB-231cell lines were treated with Noscapine and its 9-arylimino derivatives* ***4-6*** *at a gradient of concentration ranging from 0 µM to 100 µM for 72h and percentage of cell proliferation was measured using a plate reader. Each value represents the average of 3 independent experiments.*

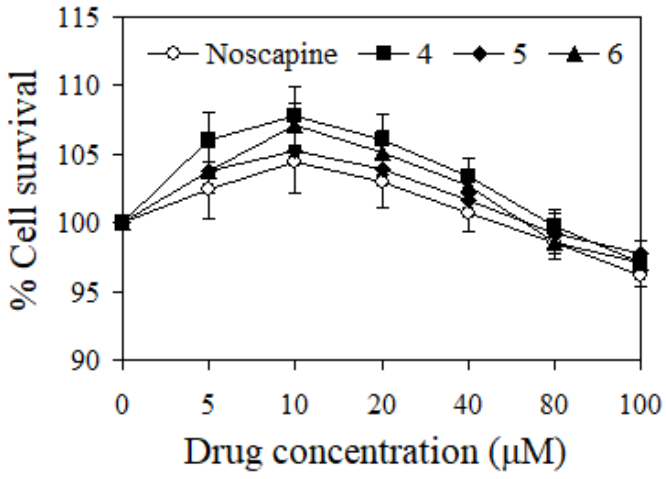

Figure 2.10: *Normal human embryonic kidney cells (293T) revealed < 5% cell death with the treatment of noscapine and 9-arylimino noscapinoids 4-6. The normal cell was*

treated with Noscapine and its 9-arylimino derivatives 4-6 at a gradient of concentration ranging from 0 µM to 100 µM for 72h and percentage of cell proliferation was measured using a plate reader. Each value represents the average of 3 independent experiments.

Table 2.3: IC_{50} values of designed 9-arylimino noscapinoids, **4-6** using two human breast cancer cell lines MCF-7 and MDA-MB-231 and a normal human embryonic kidney cell (293T). The molecules screened out **4-6** have better anti-proliferative activity compared to noscapine without any significant toxicity to normal healthy cells.

	IC_{50} (µM)			
	Noscapine	**4**	**5**	**6**
MCF-7	45.2±4.3	26.8±2.6	11.6±1.6	3.0±0.9
MDA-MB-231	51.6±4.7	32.6±3.2	15.4±1.9	7.7 ±1.3
293T normal cell	212.5±2.7	172.1±4.6	167.4±3.9	152.5±4.8

2.3.4. 9- Arylimino noscapinoids, 4-6 induced apoptosis to cancer cells

The apoptotic cells were easily quantified using FACS analysis using fluorescent dyes, Annexin V and propidium iodide. The percentage of early apoptotic and late apoptotic cells using MDA-MB-231 cell lines for the treatment of noscapine and 9-arylimino noscapinoids, **4-6** with IC_{50} concentration for 72h were collated in Table 2.4. A representative figure of flow cytometry analysis is shown in Figure 2.11. After 72 h, the untreated control cells contained only very few early apoptotic (2.3%) and late apoptotic cells (1.2%), which were considered as the background cell death due to regular trauma during cell culture (Table 2.4). In contrast, the percentage of early apoptotic cells of 14%, 18%, 55%, and 20%; late apoptotic cells of 31%, 40%, 12% and 20% as well as necrotic cells of 1.1%, 2.3%, 3.4% and 20% with treatments of noscapine and its 9-arylimino noscapinoids, **4-6**, respectively were found to be significantly high compared to untreated cells (Table 2.4).

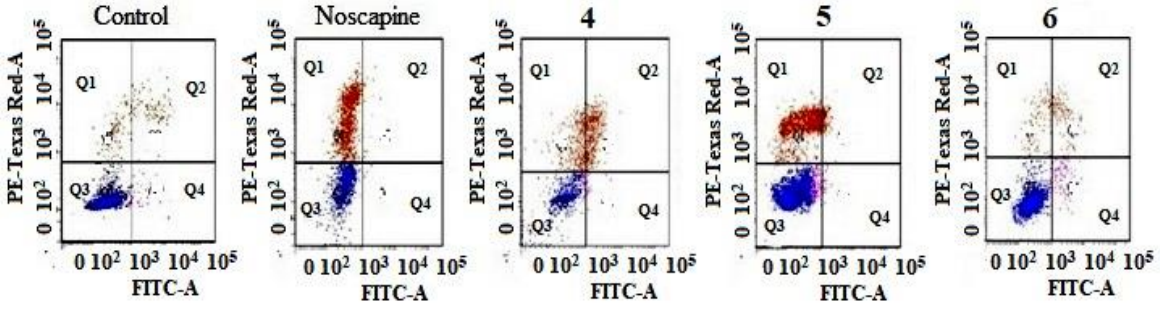

Figure 2.11: *Analysis of apoptosis to MDA-MB-231 cells treated with noscapine and 9-arylimino noscapinoids,* ***4-6*** *based on flow cytometry analysis. The cells were treated with IC_{50} concentration for 72 hours and compared with non-treated control cells.*

Annexin-V in combination with propidium iodide (PI) were used to distinguish among 3 sub-populations of cells: PI- and AnnexinV- cells indicates viable cells (Q3), PI- and Annexin V+ cells indicates early apoptotic cells (Q1), whereas PI+ and Annexin V+ cells indicates late apoptotic cells (Q2).

Table 2.4: Quantification of viable (Q3), early apoptotic (Q1), late apoptotic (Q2) and necrotic (Q4) cells after treatment with noscapine and 9-arylimino noscapinoids, **4-6** by flow cytometry.

Viability/Apoptotic	Untreated	Noscapine	4	5	6
Q1	2.3%	14%	18%	55%	20%
Q2	1.2%	31%	40%	12%	20%
Q3	93%	49%	40%	37%	24%
Q4	0.5%	1.1%	2.3%	3.4%	20%

2.3.5. Inhibition of cell cycle progression

The inhibition in cell cycle progression with the treatment of noscapine and 9-arylimino noscapinoids, **4-6** at IC_{50} concentration using MDA-MB-231 is represented in Figure 2.12. The amount of DNA accumulated in a cell with the treatment of noscapinoids is detected by the fluorescence dye, propidium iodide using flow cytometer. The cells with 2N DNA are in the G1 phase while with 4N DNA are in G2 and M phases. DNA content between 2N and 4N peaks represents that the cells are in the S phase. In contrast, less than 2N DNA indicates the apoptotic cells in which the DNA is degraded to different extents. Treatment of MDA-MB- 231 cells with the 9-arylimino derivatives, **4-6**, inhibited cell cycle progression in the G2/M phase. There was a high accumulation of cells in the G2/M phase compared to untreated cells (Table 2.5). In contrast to the G2/M block, a characteristic hypodiploid DNA content peak (sub-G1) was seen to rise at 72 h of treatment, indicating dying cells.

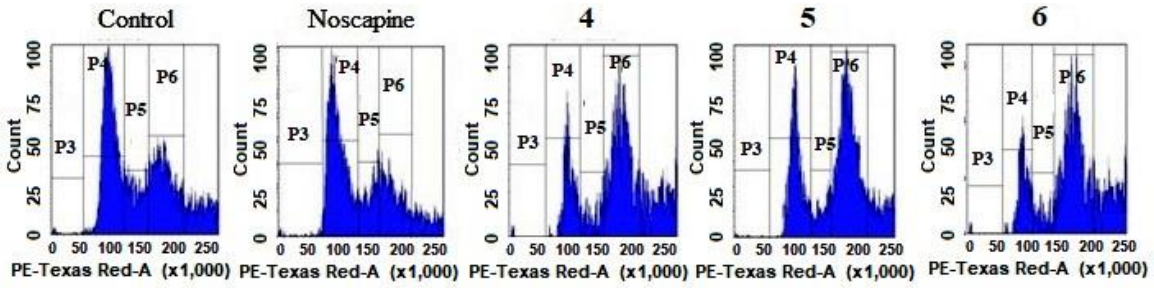

Figure 2.12: *A representative figure of cell cycle distribution as determined by flow cytometry in MDA-MB-231 cells treated with IC_{50} concentration of Noscapine and its 9-arylimino derivatives* ***4-6****. The test compounds inhibit cell cycle progression at mitosis followed by the appearance of a characteristic hypodiploid (sub-G1) DNA peak,*

indicative of apoptosis. P3: sub-G1 phase, P4: G1 phase, P5: S-phase and P6: G2/M phase.

Table 2.5: Effect of Noscapine and its 9-arylimino noscapinoids, **4-6** on cell cycle profile of MDA-MB-231 cells treated with IC_{50} concentration for 72 hour.

	72 hours			
	Sub-G_1	G_0/G_1	S	G_2/M
Control	0.7	20	22.4	7.2
Noscapine	4.9	17.5	15.1	15.5
4	7.5	13.8	10	28.1
5	8.9	14	8.2	34.7
6	10.8	25	10.0	39.7

2.3.6. Tubulin binding assay

Intrinsic fluorescence of tubulin is primarily due to the presence of aromatic amino acid, tryptophan. It is measured by exciting at 295 nm. The decreased fluorescence intensity in the presence of 9-arylimino noscapinoids, **4-6** suggests the binding of these compounds to tubulin. The relative percentage of decrease in fluorescence intensity was 10.92%, 16.42%, 23.28% and 31.64% in presence of 25 µM of noscapine and its 9-arylimino noscapinoids, **4-6** respectively (Fig. 2.13), compared to control. These 9-arylimino noscapinoids revealed increased binding affinity with tubulin compared to noscapine.

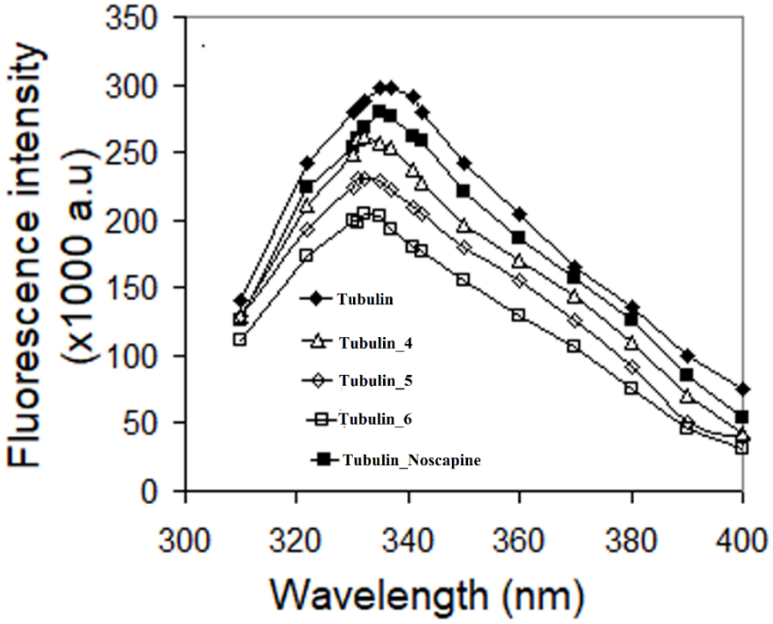

Figure 2.13: *Treatment of Noscapine and its 9-arylimino derivatives,* ***4-6*** *with purified tubulin showed quenching of the intrinsic tubulin fluorescence emission intensity to different extents, indicating binding of these noscapinoids to tubulin.*

2.4. CONCLUSION

In conclusion, a new series of derivatives of noscapine, 9-imine-noscapinoids was developed to accelerate its anticancer activity. This series of noscapine derivatives were developed by substitution of arylimino groups at C-9 position of noscapine scaffold by *in silico* combinatorial approach. Through *in silico* screening, three top ranked molecules were finally screened out for chemical synthesis and experimental evaluation of anticancer activity. These 9-arylimino noscapinoids, **4-6** have shown improved anti-proliferative activity to breast cancer cells compared to noscapine. Therefore, these derivatives may prove efficacious not only in the treatment of breast cancer but also for other types of cancers. Our results compel us to continue to examine the effects of these novel compounds on *in vivo* animal experiments with the final goal of taking it to the human clinical study.

Appendix

A2.1: ^{1}H NMR of 9-arylimino noscapinoid, 4

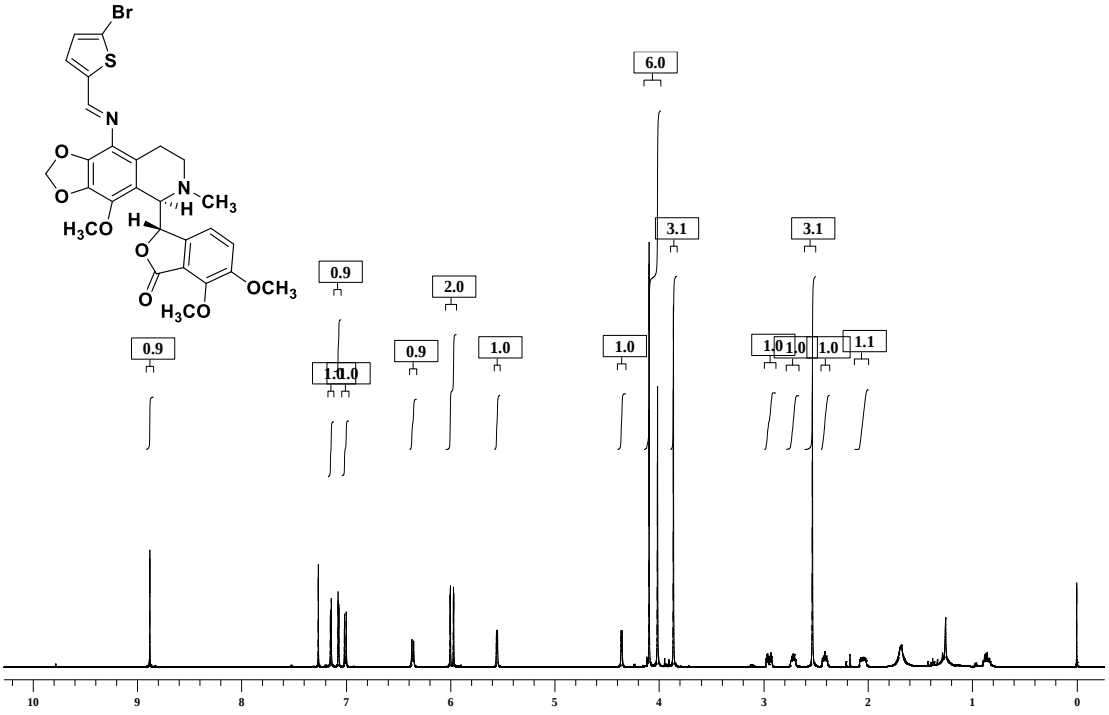

A2.2: ^{13}C NMR of 9-arylimino noscapinoid, 4

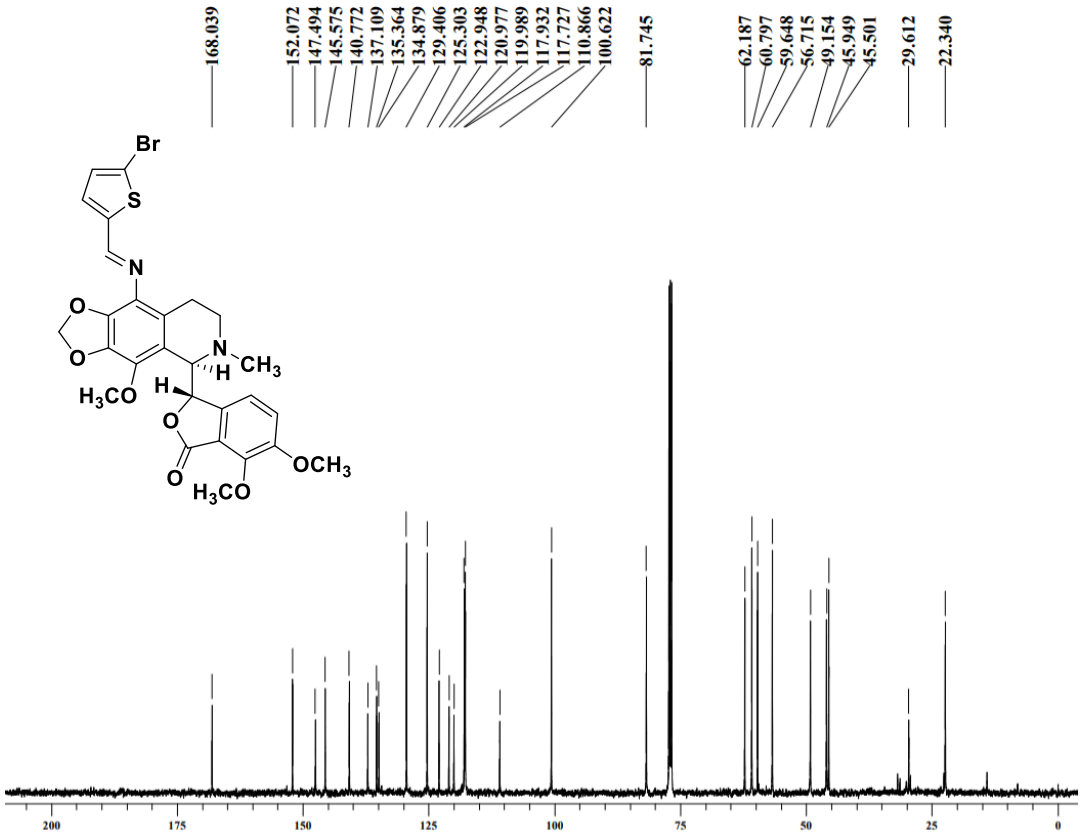

A2.3: ESI-mass spectra of 9-arylimino noscapinoid, 4

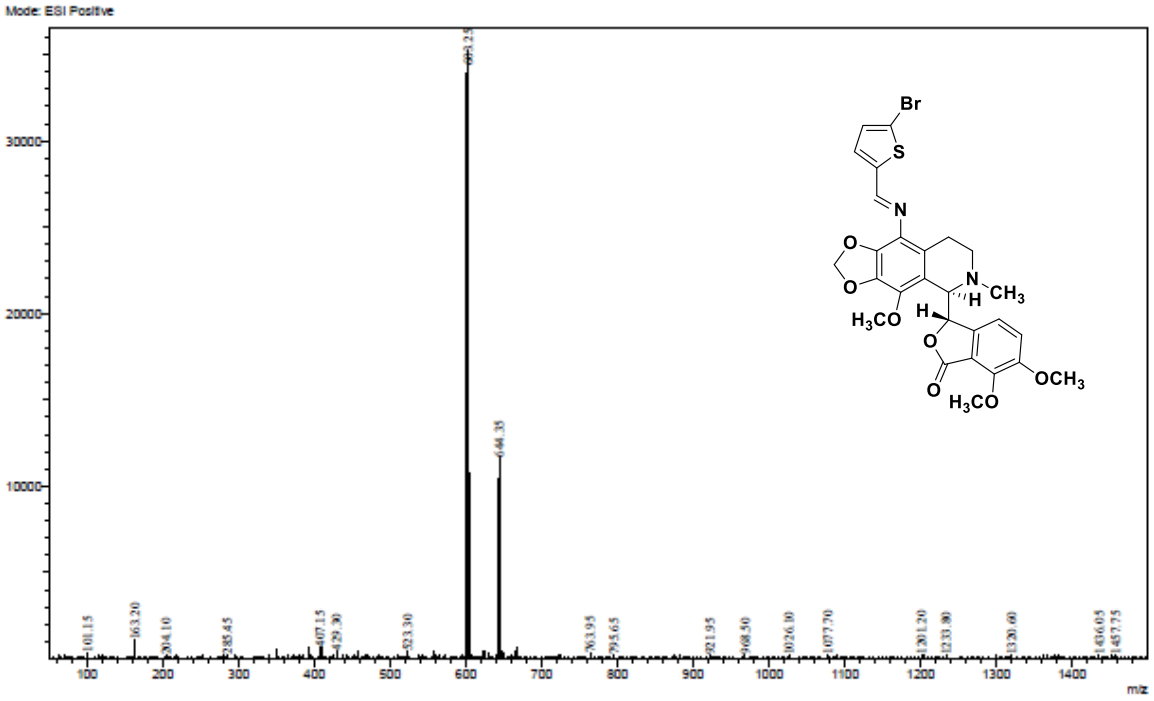

A2.4: ^{1}H NMR of 9-arylimino noscapinoid, 5

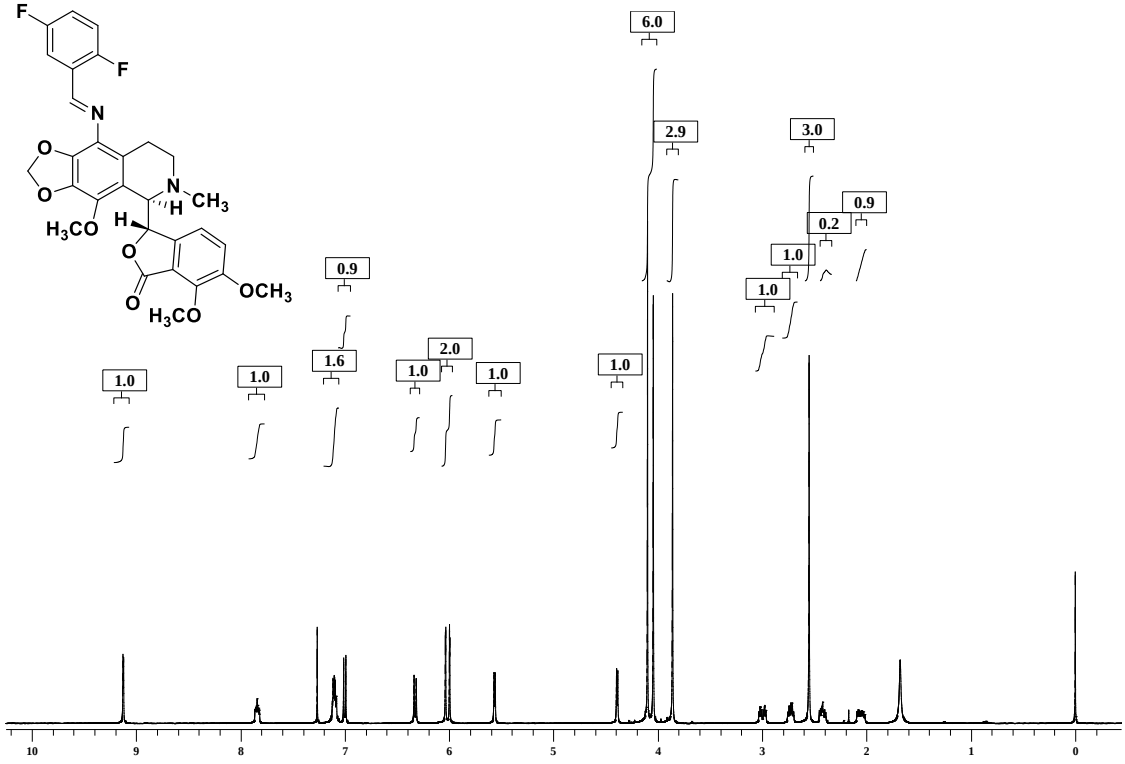

A2.5: ^{13}C NMR of 9-arylimino noscapinoid, 5

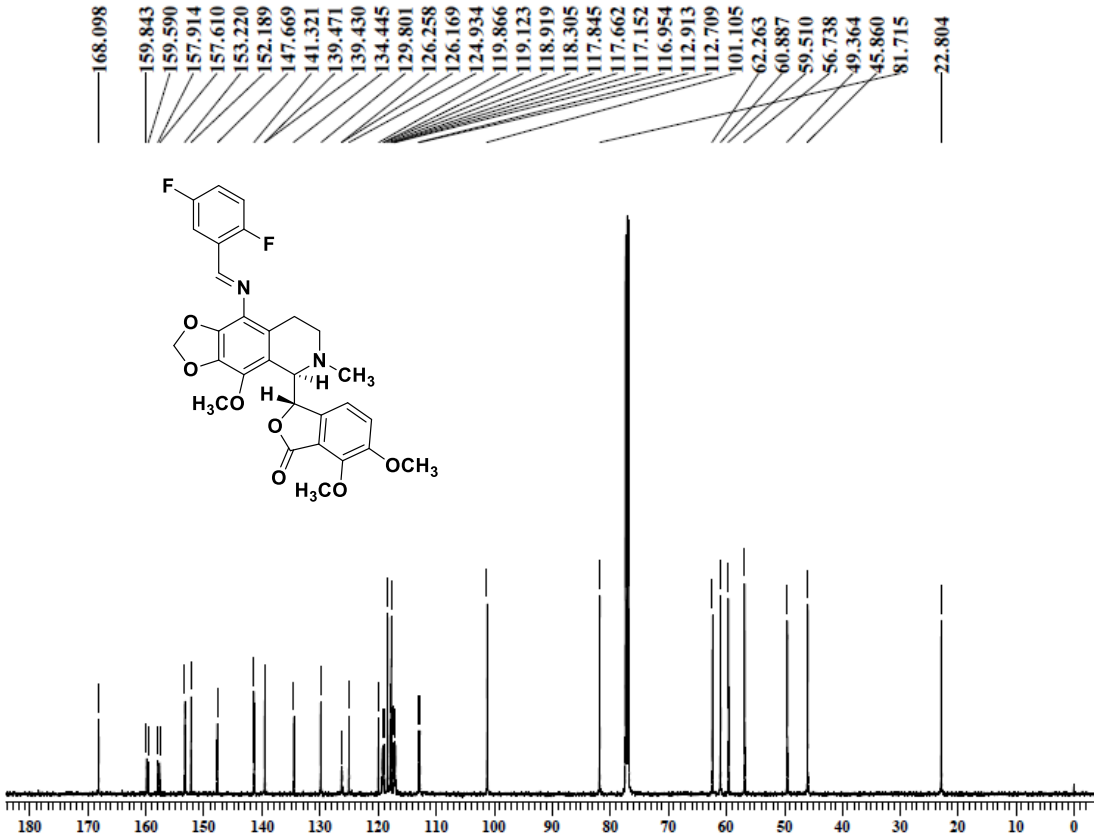

A2.6: ESI- mass spectra of 9-arylimino noscapinoid, 5

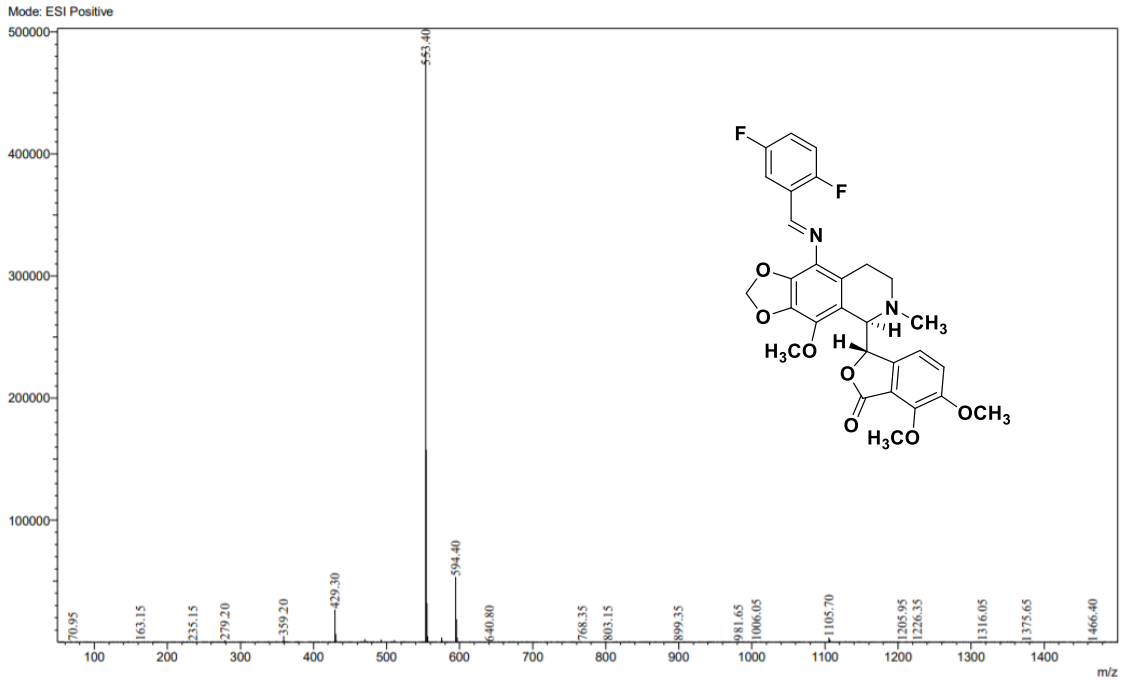

A2.7: HRMS of 9-arylimino noscapinoid, 5

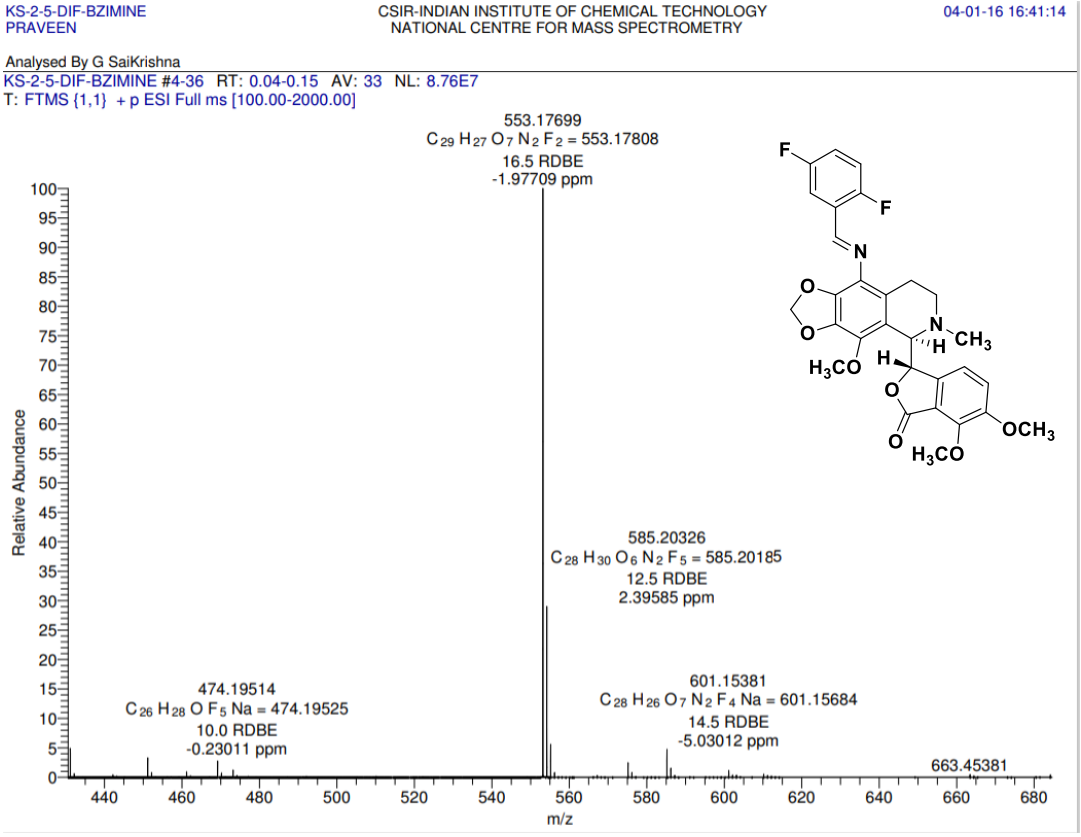

A2.8: ^{1}H NMR of 9-arylimino noscapinoid, 6

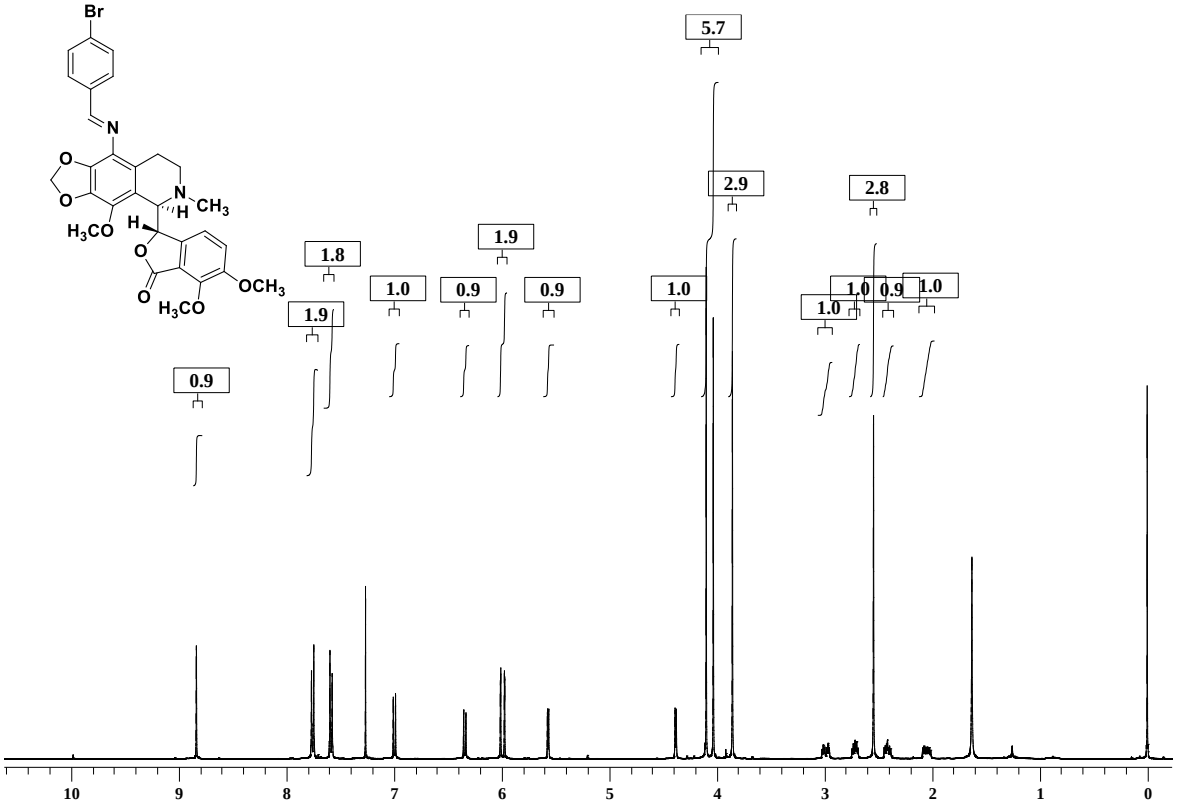

A2.9: ^{13}C NMR of 9-arylimino noscapinoid, 6

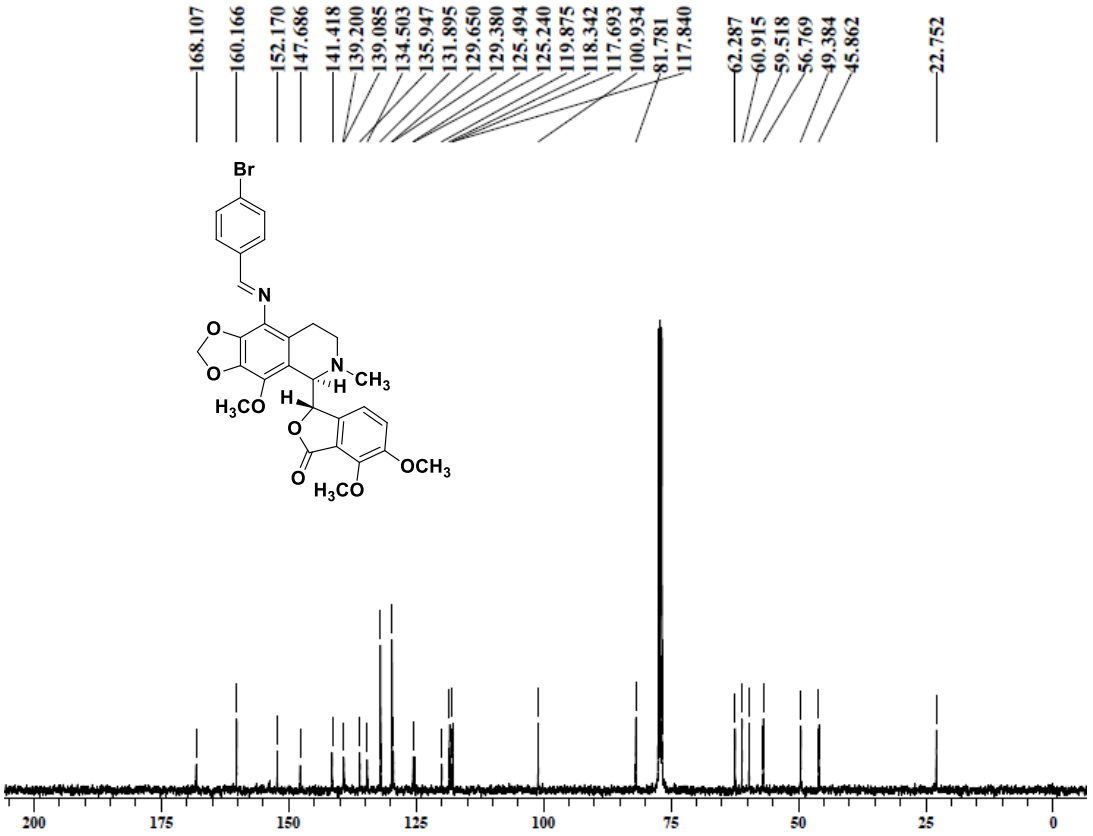

A2.10: HRMS of 9-arylimino noscapinoid, 6

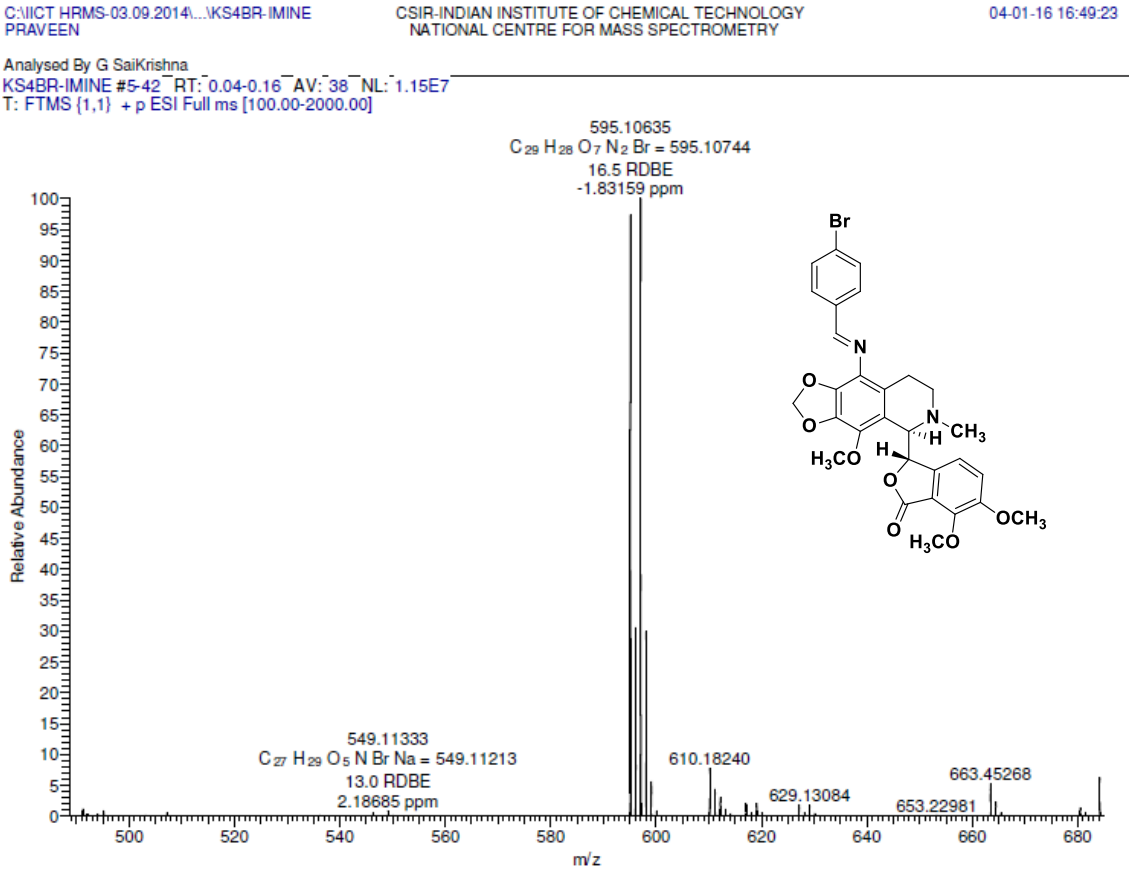

A2.11: ESI- mass spectra of 9-arylimino noscapinoid, 6

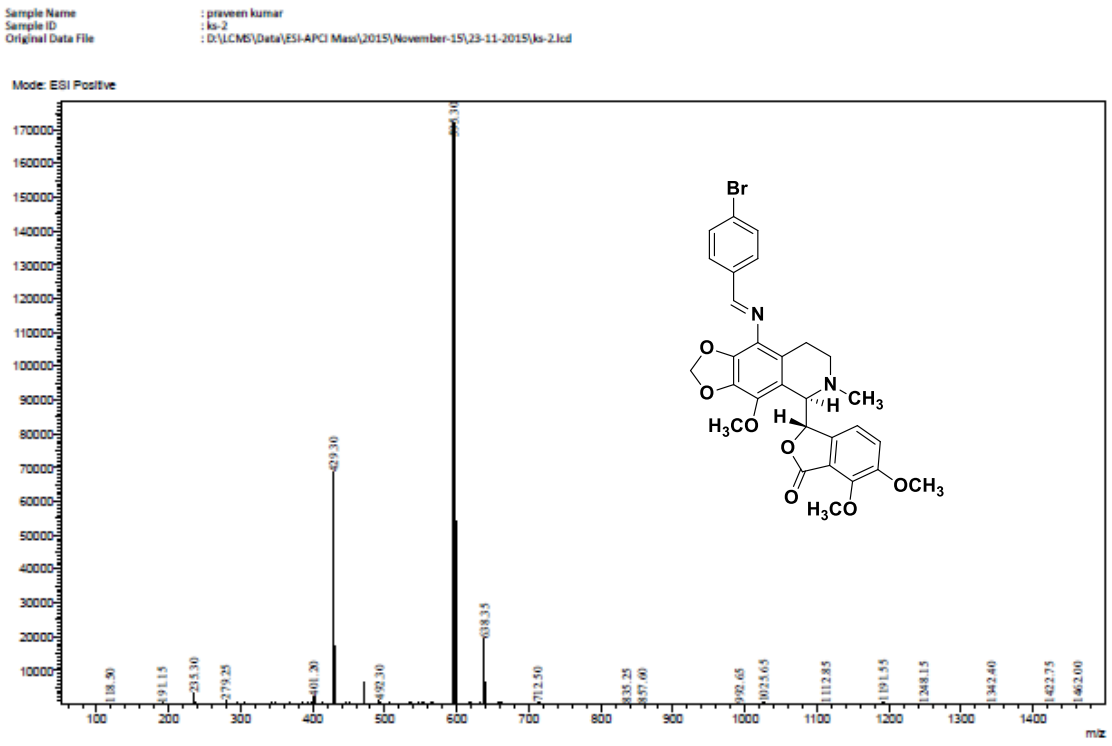

Table A2.12-A2.15: Geometry of hydrogen bonds and hydrophobic interaction of 9-arylimino noscapinoids **4-6** with the binding site residues of tubulin.

Table A2.12			**Table A2.13**		
9-arylimino noscapinoid 4_Tubulin			**9-arylimino noscapinoid 5_Tubulin**		
Hydrogen bonding			**Hydrogen bonding**		
Hydrogen Donor (D)	**Hydrogen Acceptor (A)**	**Distance (D-A) in Å**	**Hydrogen Donor (D)**	**Hydrogen Acceptor (A)**	**Distance (D-A) in Å**
LYS D 254 NZ	4 Br1	3.16	GLN D 247 NE2	5 O3	3.55
GLY D 246 N	4 N1	3.74			
Hydrophobic interaction			**Hydrophobic interaction**		
4	**Tubulin**	**Distance**	**5**	**Tubulin**	**Distance**
C27	LYS D 254 NZ	4.51	C21	GTP A 501 O1G	4.54
C26	LYS D 254 NZ	4.71	C21	LYS D 254 NZ	3.32
C29	ALA D 250 CB	4.65	C19	LYS D 254 NZ	4.23
C28	ALA D 250 CB	4.35	C18	LYS D 254 NZ	4.09
C27	ALA D 250 CB	3.77	C21	LYS D 254 CE	4.19
C26	ALA D 250 CB	3.47	O7	LYS D 254 CE	4
C25	ALA D 250 CB	3.86	C21	LYS D 254 CD	4.58
C24	ALA D 250 CB	4.42	O7	LYS D 254 CD	4.08
C26	ALA D 250 CA	4.97	C21	ASP D 251 OD2	4.41
C26	GLN D 247 OE1	4.92	C22	ALA D 250 CB	4.69
C25	GLN D 247 OE1	4.67	C21	ALA D 250 CB	4.61
C25	GLN D 247 NE2	4.42	O7	ALA D 250 CB	3.54
C23	GLN D 247 NE2	4.85	O6	ALA D 250 CB	3.34
C21	GLN D 247 NE2	4.1	O5	ALA D 250 CB	4.92
C20	GLN D 247 NE2	4.42	C19	ALA D 250 CB	4.48
C19	GLN D 247 NE2	3.65	C18	ALA D 250 CB	3.64
C18	GLN D 247 NE2	3.97	C17	ALA D 250 CB	3.52
C17	GLN D 247 NE2	4.95	C16	ALA D 250 CB	4.29
C10	GLN D 247 NE2	4.82	C13	ALA D 250 CB	4.94
C9	GLN D 247 NE2	4.11	O6	ALA D 250 C	4.81
C8	GLN D 247 NE2	4.95	O7	ALA D 250 CA	4.97
C3	GLN D 247 NE2	4.96	O6	ALA D 250 CA	4.65
C1	GLN D 247 NE2	4.13	C17	ALA D 250 CA	4.99
C25	GLN D 247 CD	4.55	C20	GLN D 247 OE1	3.72
N1	GLN D 247 CD	4.6	C19	GLN D 247 OE1	4.44
C21	GLN D 247 CD	4.88	C15	GLN D 247OE1	4.63
O7	GLN D 247 CD	4.8	C12	GLN D 247 OE1	4.87
C19	GLN D 247 CD	4.93	C20	GLN D 247 NE2	3.76
O1	GLN D 247 CD	4.37	C19	GLN D 247 NE2	5
C9	GLN D 247 CD	4.85	C15	GLN D 247 NE2	4.02
N1	GLN D 247 CG	4.9	C14	GLN D 247 NE2	4.49
C10	GLN D 247 CG	4.28	C12	GLN D 247 NE2	3.54
O1	GLN D 247 CG	3.8	C11	GLN D 247NE2	4.11
C9	GLN D 247 CG	4.64	C5	GLN D 247 NE2	3.54
O1	GLN D 247 CB	4.55	C4	GLN D 247 NE2	4.57
C26	GLN D 247 O	4.53	C2	GLN D 247 NE2	4.52
C25	GLN D 247 O	4.81	C20	GLN D 247 CD	3.91
C26	GLN D 247 C	4.98	C19	GLN D 247 CD	4.89
C25	GLN D 247 C	4.91	C15	GLN D 247 CD	4.47
C26	GLN D 247 CA	4.59	C12	GLN D 247 CD	4.35
C25	GLN D 247 CA	4.15	C11	GLN D 247 CD	5
N1	GLN D 247 CA	4.87	O3	GLN D 247 CD	4.7
O1	GLN D 247 CA	4.4	C5	GLN D 247 CD	4.66
C25	GLN D 247 N	4.39	C20	GLN D 247 CG	5
C10	GLN D 247 N	4.28	C11	GLN D 247 CG	4.94
C9	GLN D 247 N	4.67	C20	GLN D 247 O	4.98
C29	GLY D 246 O	4.66	C19	GLN D 247 O	4.66
C27	GLY D 246 O	4.77	C20	GLN D 247 CA	4.53

C26	GLY D 246 O	3.66	C19	GLN D 247 CA	4.9
C25	GLY D 246 O	2.87	C15	GLN D 247 CA	4.93
C24	GLY D 246 O	3.51	C20	GLY D 246 O	4.3
C23	GLY D 246 O	3.7	C19	GLY D 246 O	4.6
C9	GLY D 246 O	4.71	C18	GLY D 246 O	4.62
C1	GLY D 246 O	4.55	C17	GLY D 246 O	4.28
C26	GLY D 246 C	4.73	C16	GLY D 246 O	3.9
C25	GLY D 246 C	3.87	C15	GLY D 246 O	3.95
C24	GLY D 246 C	4.5	C13	GLY D 246 O	4.08
C23	GLY D 246 C	4.4	C12	GLY D 246 O	4.24
N1	GLY D 246 C	3.82	C16	GLY D 246 C	4.96
C10	GLY D 246 C	4.39	C15	GLY D 246 C	4.81
O1	GLY D 246 C	3.44	O4	GLY D 246 C	4.99
C9	GLY D 246 C	4.39	C12	GLY D 246 C	4.84
C1	GLY D 246 C	4.61	C11	GLY D 246 C	4.99
C23	GLY D 246 CA	4.97	C13	GLY D 246 N	4.88
N1	GLY D 246 CA	4.36	C11	GLY D 246 N	4.49
C10	GLY D 246 CA	4.13	O4	PRO D 245 CB	4.75
O1	GLY D 246 CA	3.47	C11	PRO D 245 CB	3.41
C9	GLY D 246 CA	4.44	O3	PRO D 245 CB	4.56
C1	GLY D 246 CA	4.86	O2	PRO D 245 CB	4.32
C25	GLY D 246 N	4.97	C10	PRO D 245 CB	4.77
C24	GLY D 246 N	4.89	C8	PRO D 245 CB	4.49
C23	GLY D 246 N	4.21	C2	PRO D 245 CB	4.63
C10	GLY D 246 N	4.09	C11	PRO D 245 CG	4.68
C9	GLY D 246 N	3.89	O2	PRO D 245 CG	4.69
C8	GLY D 246 N	4.79	C10	PRO D 245 CG	4.68
C1	GLY D 246 N	4.12	C8	PRO D 245 CG	4.96
N2	PRO D 245 CB	5	C11	PRO D 245 O	4.31
C23	PRO D 245 CB	4.53	C11	PRO D 245 C	4.11
N1	PRO D 245 CB	4.03	O5	PRO D 245 CA	4.82
C11	PRO D 245 CB	3.64	O4	PRO D 245 CA	4.83
O3	PRO D 245 CB	4.1	C11	PRO D 245 CA	4.24
O2	PRO D 245 CB	3.88	C22	ARG D 48 NH2	4.62
C10	PRO D 245 CB	4.19	C13	ARG D 48 NH1	4.92
O1	PRO D 245 CB	3.84	O6	ARG D 48 CZ	4.94
C9	PRO D 245 CB	3.24	O5	ARG D 48 CZ	3.76
C8	PRO D 245 CB	3.28	C13	ARG D 48 CZ	4.86
C7	PRO D 245 CB	4.43	C13	ARG D 48 NE	4.98
C5	PRO D 245 CB	4.72	O5	ARG D 48 CD	4.16
C4	PRO D 245 CB	3.62	C23	GLU D 47 OE2	4.28
C3	PRO D 245 CB	3.52	C10	GLU D 47 OE2	3.31
C2	PRO D 245 CB	3.46	C9	GLU D 47 OE2	3.39
C1	PRO D 245 CB	3.35	C8	GLU D 47 OE2	4.05
C11	PRO D 245 CD	4.87	C3	GLU D 47 OE2	4.93
N2	PRO D 245 CG	4.96	C1	GLU D 47 OE2	3.9
C11	PRO D 245 CG	3.72	C10	GLU D 47 OE1	4.09
O3	PRO D 245 CG	4.58	C10	GLU D 47 CD	4.09
C9	PRO D 245 CG	4.62	O1	GLU D 47 CD	4.01
C8	PRO D 245 CG	4.46	C9	GLU D 47 CD	4.57
C7	PRO D 245 CG	4.94	C22	MET D 1 CE	4.69
C5	PRO D 245 CG	4.94	C21	MET D 1 CE	3.97
C4	PRO D 245 CG	4.25	O7	MET D 1 CE	4.94
C3	PRO D 245 CG	4.36	O6	MET D 1 CE	4.89
C2	PRO D 245 CG	4.25	C21	ASP A 98 OD2	2.86
C1	PRO D 245 CG	4.56	C21	ASP A 98 OD1	4.71
C10	PRO D 245 O	3.17	C21	ASP A 98 CG	4.01
C9	PRO D 245 O	3.77	C21	ASP A 98 CB	4.99
C8	PRO D 245 O	4.02	C25	THR A 80 CG2	4.44
C1	PRO D 245 O	4.57	S1	THR A 80 CG2	4.4

C23	PRO D 245 C	4.67	C23	GLU A 77 OE2	4.57
N1	PRO D 245 C	4.06	C14	GLU A 77 OE2	3.34
O2	PRO D 245 C	4.19	C9	GLU A 77 OE2	3.93
C10	PRO D 245 C	3.66	C8	GLU A 77 OE2	4.34
O1	PRO D 245 C	3.22	C7	GLU A 77 OE2	3.23
C9	PRO D 245 C	3.57	C6	GLU A 77 OE2	4.15
C8	PRO D 245 C	4.13	C5	GLU A 77 OE2	4.38
C3	PRO D 245 C	4.94	C4	GLU A 77 OE2	3.66
C1	PRO D 245 C	4	C3	GLU A 77 OE2	3.15
C23	PRO D 245 CA	4.44	C2	GLU A 77 OE2	4.27
N1	PRO D 245 CA	4.13	C1	GLU A 77 OE2	3.32
O2	PRO D 245 CA	4.7	C14	GLU A 77 OE1	3.72
C10	PRO D 245 CA	4.57	C7	GLU A 77 OE1	4.63
O1	PRO D 245 CA	4.05	N2	GLU A 77 CD	4.61
C9	PRO D 245 CA	3.87	N1	GLU A 77 CD	4.42
C8	PRO D 245 CA	4.29	C14	GLU A 77 CD	3.67
C4	PRO D 245 CA	4.92	C7	GLU A 77 CD	3.76
C3	PRO D 245 CA	4.48	C6	GLU A 77 CD	4.55
C2	PRO D 245 CA	4.79	C4	GLU A 77 CD	4.72
C1	PRO D 245 CA	3.92	C3	GLU A 77 CD	4.1
C14	GLU D 47 OE2	2.9	C1	GLU A 77 CD	4.32
C11	GLU D 47 OE2	4.65	S1	GLU A 77 CG	4.76
C7	GLU D 47 OE2	4.03	C24	GLU A 77 CG	4.74
C6	GLU D 47 OE2	3.64	C23	GLU A 77 CG	4.55
C5	GLU D 47 OE2	3.66	N1	GLU A 77 CG	4.18
C4	GLU D 47 OE2	4.12	C14	GLU A 77 CG	4.76
C3	GLU D 47 OE2	4.41	C7	GLU A 77 CG	3.97
C2	GLU D 47 OE2	4.98	C6	GLU A 77 CG	4.95
C14	GLU D 47 OE1	4.47	C3	GLU A 77 CG	4.55
C11	GLU D 47 OE1	4.43	C1	GLU A 77 CG	4.53
C5	GLU D 47 OE1	4.96	S1	GLU A 77 CA	4.87
N2	GLU D 47 CD	3.94	C25	GLU A 77 N	4.81
C14	GLU D 47 CD	3.91	S1	GLU A 77 N	4.72
C11	GLU D 47 CD	4.93	C27	ASP A 76 OD2	3.98
C6	GLU D 47 CD	4.89	C26	ASP A 76 OD2	3.65
C5	GLU D 47 CD	4.69	C25	ASP A 76 OD2	4.78
C14	GLU D 47 CG	4.98	C26	ASP A 76 OD1	4.88
C11	LEU D 42 CD2	3.52	C27	ASP A 76 CG	4.33
O3	LEU D 42 CD2	4.94	C26	ASP A 76 CG	3.8
C11	LEU D 42 CG	5	C25	ASP A 76 CG	4.63
C22	THR A 225 OG1	2.82	C27	ASP A 76 CB	3.61
C17	THR A 225 OG1	4.99	C26	ASP A 76 CB	3.1
C22	THR A 225 CG2	5	C25	ASP A 76 CB	3.62
C22	THR A 225 CB	3.96	S1	ASP A 76 CB	4.63
C22	THR A 225 CA	4.79	C24	ASP A 76 CB	4.38
C22	THR A 225 N	4.4	C26	ASP A 76 O	4.46
C21	TYR A 224 CE1	4.81	C25	ASP A 76 O	3.86
C21	TYR A 224 CD1	3.73	S1	ASP A 76 O	4.37
O7	TYR A 224 CD1	4.01	C27	ASP A 76 C	4.87
C21	TYR A 224 CG	4.09	C26	ASP A 76 C	4.42
O7	TYR A 224 CG	4.56	C25	ASP A 76 C	4.13
C21	TYR A 224 CB	3.65	S1	ASP A 76 C	4.51
O7	TYR A 224 CB	4.11	C24	ASP A 76 C	4.92
C21	TYR A 224 CA	4.93	C27	ASP A 76 CA	4.85
C22	THR A 223 OG1	4.59	C26	ASP A 76 CA	4.37
C22	THR A 223 CB	4.89	C25	ASP A 76 CA	4.53
C20	GLU A 77 OE2	2.86	N2	VAL A 74 CG2	3.79
C19	GLU A 77 OE2	3.64	C20	VAL A 74 CG2	4.99
C18	GLU A 77 OE2	4.68	C14	VAL A 74 CG2	3.76
C16	GLU A 77 OE2	4.44	C7	VAL A 74 CG2	4.85

C15	GLU A 77 OE2	3.38	C6	VAL A 74 CG2	3.69
C14	GLU A 77 OE2	4.65	N2	VAL A 74 CG1	4.95
C12	GLU A 77 OE2	3.64	C14	VAL A 74 CG1	4.11
C7	GLU A 77 OE2	4.63	N2	VAL A 74 CB	4.62
C6	GLU A 77 OE2	3.74	C14	VAL A 74 CB	4.23
C5	GLU A 77 OE2	4.59	C6	VAL A 74 CB	4.36
C20	GLU A 77 OE1	4.39	N2	VAL A 74 CA	4.54
C19	GLU A 77 OE1	4.53	C14	VAL A 74 CA	4.22
C20	GLU A 77 CD	3.95	C7	VAL A 74 CA	4.28
C19	GLU A 77 CD	4.47	C6	VAL A 74 CA	3.89
C15	GLU A 77 CD	4.55	C14	VAL A 74 N	4.88
C12	GLU A 77 CD	4.83	C7	VAL A 74 N	4.15
C6	GLU A 77 CD	4.78	C6	VAL A 74 N	3.73
C29	THR A 73 OG1	3.32	C22	THR A 73 OG1	3.34
C28	THR A 73 OG1	3.27	C18	THR A 73 OG1	4.93
C27	THR A 73 OG1	4.41	C17	THR A 73 OG1	4.2
C24	THR A 73 OG1	4.48	C16	THR A 73 OG1	4.07
C29	THR A 73 CG2	4.77	C15	THR A 73 OG1	4.62
C28	THR A 73 CG2	4.79	C13	THR A 73 OG1	4.22
C29	THR A 73 CB	4.4	C7	THR A 73 OG1	3.78
C28	THR A 73 CB	4.52	C6	THR A 73 OG1	3.07
C29	GLU A 71 OE2	4.8	C3	THR A 73 OG1	4.96
C28	GLU A 71 OE2	3.83	C27	THR A 73 CG2	4.69
C27	GLU A 71 OE2	4.6	C22	THR A 73 CG2	3.92
C29	GLU A 71 OE1	4.88	C27	THR A 73 CB	4.29
C28	GLU A 71 OE1	3.96	C24	THR A 73 CB	4.9
C27	GLU A 71 OE1	4.49	C23	THR A 73 CB	4.63
C28	GLU A 71 CD	3.99	C22	THR A 73 CB	4.22
C27	GLU A 71 CD	4.51	C7	THR A 73 CB	3.99
C28	GLU A 71 CG	4.98	C6	THR A 73 CB	3.79
C21	GLN A 15 OE1	3.15	C27	THR A 73 O	3.82
C20	GLN A 15 OE1	4.79	C26	THR A 73 O	4.58
C19	GLN A 15 OE1	3.89	S1	THR A 73 O	4.96
C18	GLN A 15 OE1	4.54	C24	THR A 73 O	3.9
C21	GLN A 15 NE2	2.93	C23	THR A 73 O	3.87
C21	GLN A 15 CD	3.31	C7	THR A 73 O	3.13
O7	GLN A 15 CD	4.66	C6	THR A 73 O	3.59
C19	GLN A 15 CD	4.76	C3	THR A 73 O	4.52
C21	GLN A 15 CG	4.62	C1	THR A 73 O	4.97
C27	GLN A 11 OE1	4.65	N2	THR A 73 C	4.88
C26	GLN A 11 OE1	4.26	C27	THR A 73 C	4.54
C25	GLN A 11 OE1	4.8	C24	THR A 73 C	4.86
C21	GLN A 11 NE2	4.83	C23	THR A 73 C	4.77
C28	THR A 73 OG1	3.27	C7	THR A 73 C	3.63
C27	THR A 73 OG1	4.41	C6	THR A 73 C	3.59
C24	THR A 73 OG1	4.48	C27	THR A 73 CA	4.28
C29	THR A 73 CG2	4.77	C24	THR A 73 CA	4.99
C28	THR A 73 CG2	4.79	C7	THR A 73 CA	4.43
C29	THR A 73 CB	4.4	C6	THR A 73 CA	4.33
C28	THR A 73 CB	4.52	C22	GLU A 71 OE2	3.06
C29	GLU A 71 OE2	4.8	C21	GLU A 71 OE2	3.8
C28	GLU A 71 OE2	3.83	C17	GLU A 71 OE2	4.71
C27	GLU A 71 OE2	4.6	C22	GLU A 71 OE1	4.1
C29	GLU A 71 OE1	4.88	C21	GLU A 71 OE1	4
C28	GLU A 71 OE1	3.96	C18	GLU A 71 OE1	4.87
C27	GLU A 71 OE1	4.49	C17	GLU A 71 OE1	4.84
C28	GLU A 71 CD	3.99	C22	GLU A 71 CD	3.75
C27	GLU A 71 CD	4.51	C21	GLU A 71 CD	3.55
C28	GLU A 71 CG	4.98	O7	GLU A 71 CD	4.75
C21	GLN A 15 OE1	3.15	O6	GLU A 71 CD	4.57

C20	GLN A 15 OE1	4.79	C18	GLU A 71 CD	4.9
C19	GLN A 15 OE1	3.89	C17	GLU A 71 CD	4.84
C18	GLN A 15 OE1	4.54	C22	GLU A 71 CG	4.83
C21	GLN A 15 NE2	2.93	C21	GLU A 71 CG	3.52
C21	GLN A 15 CD	3.31	O7	GLU A 71 CG	4.9
O7	GLN A 15 CD	4.66	C21	GLU A 71 CB	4.81
C19	GLN A 15 CD	4.76	C14	GLN A 15 OE1	2.92
C21	GLN A 15 CG	4.62	C14	GLN A 15 NE2	4.98
C27	GLN A 11 OE1	4.65	C14	GLN A 15 CD	4.15
C26	GLN A 11 OE1	4.26	C20	GLN A 11 OE1	3.06
C25	GLN A 11 OE1	4.8	C19	GLN A 11 OE1	3.11
C21	GLN A 11 NE2	4.83	C18	GLN A 11 OE1	4.36
C28	THR A 73 OG1	3.27	C15	GLN A 11 OE1	4.31
C27	THR A 73 OG1	4.41	C14	GLN A 11 OE1	4.7
C24	THR A 73 OG1	4.48	C20	GLN A 11 NE2	4.43
C29	THR A 73 CG2	4.77	C19	GLN A 11 NE2	4.82
C28	THR A 73 CG2	4.79	C20	GLN A 11 CD	4.03
C29	THR A 73 CB	4.4	C19	GLN A 11 CD	4.27
C28	THR A 73 CB	4.52	C14	GLN A 11 CD	4.8
C29	GLU A 71 OE2	4.8	C14	GLN A 11 CG	4.92
C28	GLU A 71 OE2	3.83			
C27	GLU A 71 OE2	4.6			
C29	GLU A 71 OE1	4.88			
C28	GLU A 71 OE1	3.96			
C27	GLU A 71 OE1	4.49			
C28	GLU A 71 CD	3.99			
C27	GLU A 71 CD	4.51			
C28	GLU A 71 CG	4.98			
C21	GLN A 15 OE1	3.15			
C20	GLN A 15 OE1	4.79			
C19	GLN A 15 OE1	3.89			
C18	GLN A 15 OE1	4.54			
C21	GLN A 15 NE2	2.93			
C21	GLN A 15 CD	3.31			
O7	GLN A 15 CD	4.66			
C19	GLN A 15 CD	4.76			
C21	GLN A 15 CG	4.62			
C27	GLN A 11 OE1	4.65			
C26	GLN A 11 OE1	4.26			
C25	GLN A 11 OE1	4.8			
C21	GLN A 11 NE2	4.83			

Table A2.14

9-arylimino noscapinoid 6_Tubulin

Hydrogen bonding		
Hydrogen Donor (D)	**Hydrogen Acceptor (A)**	**Distance (D-A) in Å**
ASN A 18 ND2	6 F1	3.53
Hydrophobic interaction	**Hydrophobic interaction**	
6	**Tubulin**	**Distance**
C21	LYS D 254 NZ	3.6
C19	LYS D 254 NZ	4.6
C18	LYS D 254 NZ	4.58
C21	LYS D 254 CE	4.64
O7	LYS D 254 CE	4.61
O7	LYS D 254 CD	4.63
C22	ALA D 250 CB	4.55
C21	ALA D 250 CB	4.82
O7	ALA D 250 CB	3.45
O6	ALA D 250 CB	3.28

Table A2.15

Noscapine_Tubulin

Hydrogen bonding		
Hydrogen Donor (D)	**Hydrogen Acceptor (A)**	**Distance (D-A) in Å**
GLN D 247 NE2	O2	3.04
Noscapine	**Tubulin**	**Distance**
C20	LYS D 254 NZ	3.42
C16	LYS D 254 NZ	4.9
C20	LYS D 254 CE	3.9
C20	LYS D 254 CD	3.94
C20	LYS D 254 CG	4.95
C20	ASP D 251 OD2	3.2
C17	ASP D 251 OD2	4.65
C20	ASP D 251 CG	4.32
O4	ASP D 251 CG	4.49
C20	ASP D 251 CB	5

O5	ALA D 250 CB	4.85	O4	ASP D 251 CB	4.73
C19	ALA D 250 CB	4.42	C20	ALA D 250 CB	3.93
C18	ALA D 250 CB	3.51	O6	ALA D 250 CB	4.52
C17	ALA D 250 CB	3.35	O5	ALA D 250 CB	4.8
C16	ALA D 250 CB	4.13	O4	ALA D 250 CB	3.77
C15	ALA D 250 CB	4.96	C19	ALA D 250 CB	4.48
C13	ALA D 250 CB	4.82	C18	ALA D 250 CB	4.05
O6	ALA D 250 C	4.67	C17	ALA D 250 CB	3.45
O7	ALA D 250 CA	4.93	C16	ALA D 250 CB	3.26
O6	ALA D 250 CA	4.49	C15	ALA D 250 CB	3.7
C17	ALA D 250 CA	4.76	C14	ALA D 250 CB	4.32
C20	GLN D 247 OE1	3.75	C13	ALA D 250 CB	4.3
C19	GLN D 247 OE1	4.49	C18	ALA D 250 O	4.52
C15	GLN D 247 OE1	4.58	C17	ALA D 250 O	4.73
C12	GLN D 247 OE1	4.81	O4	ALA D 250 C	4.75
C4	GLN D 247 OE1	4.92	C18	ALA D 250 C	4.98
C20	GLN D 247 NE2	3.6	C17	ALA D 250 C	4.83
C19	GLN D 247 NE2	4.86	O4	ALA D 250 CA	4.92
C15	GLN D 247 NE2	3.82	C17	ALA D 250 CA	4.76
C12	GLN D 247 NE2	3.37	C16	ALA D 250 CA	4.76
C11	GLN D 247 NE2	4.84	C13	GLN D 247 OE1	4.68
C10	GLN D 247 NE2	4.59	C13	GLN D 247 NE2	4.22
C9	GLN D 247 NE2	3.43	C10	GLN D 247 NE2	3.63
C8	GLN D 247 NE2	3.14	C9	GLN D 247 NE2	3.91
C7	GLN D 247 NE2	3.95	C8	GLN D 247 NE2	3.42
C6	GLN D 247 NE2	4.74	C4	GLN D 247 NE2	4.81
C5	GLN D 247 NE2	3.51	C2	GLN D 247 NE2	4.78
C4	GLN D 247 NE2	2.79	C1	GLN D 247 NE2	3.94
C3	GLN D 247 NE2	3.14	O7	GLN D 247 CD	4.87
C2	GLN D 247 NE2	2.88	O6	GLN D 247 CD	3.59
C1	GLN D 247 NE2	3.51	C13	GLN D 247 CD	4.49
C20	GLN D 247 CD	3.82	O3	GLN D 247 CD	4.71
C19	GLN D 247 CD	4.84	O2	GLN D 247 CD	4.24
C15	GLN D 247 CD	4.28	C10	GLN D 247 CD	4.85
C12	GLN D 247 CD	4.15	C8	GLN D 247 CD	4.69
O3	GLN D 247 CD	4.42	O6	GLN D 247 CG	4.41
O2	GLN D 247 CD	4.68	O6	GLN D 247 CB	4.52
C9	GLN D 247 CD	4.51	O6	GLN D 247 C	4.48
C8	GLN D 247 CD	4.19	O6	GLN D 247 CA	3.65
C5	GLN D 247 CD	4.64	C13	GLN D 247 CA	4.39
C4	GLN D 247 CD	4.09	O3	GLN D 247 CA	4.82
C3	GLN D 247 CD	4.45	C13	GLN D 247 N	4.6
C2	GLN D 247 CD	4.04	C16	GLY D 246 O	4.45
C1	GLN D 247 CD	4.71	C15	GLY D 246 O	3.74
C20	GLN D 247 CG	4.85	C14	GLY D 246 O	4.16
C12	GLN D 247 CG	4.74	C13	GLY D 246 O	3.15
O3	GLN D 247 CG	4.42	C12	GLY D 246 O	4.08
O2	GLN D 247 CG	4.48	O6	GLY D 246 C	4.06
C8	GLN D 247 CG	4.41	C15	GLY D 246 C	4.88
C4	GLN D 247 CG	4.88	C13	GLY D 246 C	4.09
C2	GLN D 247 CG	4.39	O3	GLY D 246 C	4.03
C19	GLN D 247 O	4.83	C12	GLY D 246 C	4.91
C20	GLN D 247 CA	4.41	O3	GLY D 246 CA	4.87
C19	GLN D 247 CA	4.89	C12	GLY D 246 N	4.63
C15	GLN D 247 CA	4.59	N1	PRO D 245 CB	4.9
C12	GLN D 247 CA	4.86	C12	PRO D 245 CB	4.89
C20	GLN D 247 N	5	C7	PRO D 245 CB	3.79
C15	GLN D 247 N	4.76	C6	PRO D 245 CB	3.58
C12	GLN D 247 N	4.73	C3	PRO D 245 CB	4.63
C20	GLY D 246 O	4.04	C6	PRO D 245 CD	4.92

C19	GLY D 246 O	4.4	C7	PRO D 245 CG	4.07
C18	GLY D 246 O	4.32	C6	PRO D 245 CG	3.73
C17	GLY D 246 O	3.83	C12	PRO D 245 CA	4.74
C16	GLY D 246 O	3.31	C7	PRO D 245 CA	4.82
C15	GLY D 246 O	3.49	C6	PRO D 245 CA	4.2
C13	GLY D 246 O	3.48	C21	ARG D 48 NH2	4.66
C12	GLY D 246 O	3.82	C19	ARG D 48 NH2	3.73
O5	GLY D 246 C	4.82	C18	ARG D 48 NH2	3.75
C20	GLY D 246 C	4.83	C17	ARG D 48 NH2	4.76
C16	GLY D 246 C	4.34	C14	ARG D 48 NH2	4.68
C15	GLY D 246 C	4.29	C19	ARG D 48 NH1	4.4
C13	GLY D 246 C	4.32	C18	ARG D 48 NH1	4.94
O4	GLY D 246 C	4.21	C14	ARG D 48 NH1	4.74
C12	GLY D 246 C	4.29	O5	ARG D 48 CZ	4.23
O3	GLY D 246 C	4.88	C19	ARG D 48 CZ	3.85
O5	GLY D 246 CA	5	C18	ARG D 48 CZ	4.32
C13	GLY D 246 CA	4.79	C14	ARG D 48 CZ	4.56
O4	GLY D 246 CA	4.65	C19	ARG D 48 NE	4.07
C16	GLY D 246 N	4.78	C18	ARG D 48 NE	4.78
C13	GLY D 246 N	3.97	C14	ARG D 48 NE	4.84
C12	GLY D 246 N	4.63	C11	ARG D 48 NE	4.33
C11	GLY D 246 N	4.91	C19	ARG D 48 CD	4.88
O5	PRO D 245 CB	4.52	C11	ARG D 48 CD	4.28
C13	PRO D 245 CB	4.61	C6	ARG D 48 CD	4.62
O4	PRO D 245 CB	3.92	C11	ARG D 48 CG	4.55
C12	PRO D 245 CB	4.98	C11	GLU D 47 OE2	4.56
C11	PRO D 245 CB	3.34	C7	GLU D 47 OE2	3.02
O3	PRO D 245 CB	3.99	C6	GLU D 47 OE2	3.07
O4	PRO D 245 CG	4.99	C3	GLU D 47 OE2	4.47
C11	PRO D 245 CG	4.5	C7	GLU D 47 OE1	4.89
C11	PRO D 245 O	4.23	C6	GLU D 47 OE1	4.95
O5	PRO D 245 C	4.48	C7	GLU D 47 CD	4.17
C13	PRO D 245 C	4.54	C6	GLU D 47 CD	4.05
O4	PRO D 245 C	4.14	C6	GLU D 47 CG	4.57
C11	PRO D 245 C	4.29	C21	MET D 1 CE	3.79
O3	PRO D 245 C	4.46	C20	MET D 1 CE	3.31
O5	PRO D 245 CA	3.93	O5	MET D 1 CE	4.27
C13	PRO D 245 CA	4.25	O4	MET D 1 CE	3.06
O4	PRO D 245 CA	3.94	C18	MET D 1 CE	4.78
C11	PRO D 245 CA	4.39	C17	MET D 1 CE	4.32
O3	PRO D 245 CA	4.72	C20	MET D 1 SD	4.82
C22	ARG D 48 NH2	4.4	O4	MET D 1 SD	4.79
C13	ARG D 48 NH1	4.36	C21	MET D 1 O	3.36
C22	ARG D 48 CZ	4.88	C18	MET D 1 O	4.95
O6	ARG D 48 CZ	4.27	C21	MET D 1 C	4.4
O5	ARG D 48 CZ	3.36	O5	MET D 1 C	4.85
C13	ARG D 48 CZ	4.51	C21	MET D 1 N	4.37
C13	ARG D 48 NE	4.68	C20	ASP A 98 OD2	2.95
O5	ARG D 48 CD	3.64	C20	ASP A 98 OD1	4.3
C13	ARG D 48 CD	4.79	C20	ASP A 98 CG	3.93
O5	ARG D 48 CG	4.84	O4	ASP A 98 CG	4.94
C22	MET D 1 CE	4.91	C10	GLU A 77 OE2	3.79
C21	MET D 1 CE	4.5	C9	GLU A 77 OE2	3.33
O7	MET D 1 CE	4.86	C8	GLU A 77 OE2	3.55
C27	ASN A 228 ND2	3.94	C4	GLU A 77 OE2	4.39
C26	ASN A 228 ND2	3.23	C3	GLU A 77 OE2	4.19
C25	ASN A 228 ND2	4.09	C2	GLU A 77 OE2	3.67
C26	ASN A 228 CG	4.36	C1	GLU A 77 OE2	4.1
C26	ASN A 228 CB	4.68	C10	GLU A 77 OE1	4.34
C27	THR A 225 OG1	4.66	C9	GLU A 77 OE1	4.89

C26	THR A 225 OG1	3.87	C8	GLU A 77 OE1	4.73
C25	THR A 225 OG1	3.69	O2	GLU A 77 CD	4.63
C24	THR A 225 OG1	4.35	C10	GLU A 77 CD	4.46
C23	THR A 225OG1	4.93	O1	GLU A 77 CD	4.65
C26	THR A 225 CB	4.58	C9	GLU A 77 CD	4.42
C25	THR A 225 CB	4.7	C8	GLU A 77 CD	4.4
C26	THR A 225 CA	4.12	C2	GLU A 77 CD	4.89
C25	THR A 225 CA	4.47	C1	GLU A 77 CD	4.88
C26	THR A 225 N	4.28	C22	VAL A 74 CG2	3.12
C25	THR A 225 N	4.3	O7	VAL A 74 CG2	3.85
O1	TYR A 224 CD1	4.84	C1	VAL A 74 CG2	4.88
C26	TYR A 224 CB	4.96	C22	VAL A 74 CB	4.27
C25	TYR A 224 CB	4.46	O7	VAL A 74 CB	4.93
N1	TYR A 224 CB	4.99	C22	VAL A 74 CA	4.29
C26	TYR A 224 O	4.45	C22	VAL A 74 N	4.03
C25	TYR A 224 O	4.85	C22	THR A 73 OG1	2.91
C26	TYR A 224 C	4.44	C21	THR A 73 OG1	4.34
C25	TYR A 224 C	4.51	C19	THR A 73 OG1	3.93
C21	ASP A 98 OD2	3.33	C18	THR A 73 OG1	4.17
C21	ASP A 98 CG	4.51	C17	THR A 73 OG1	4.42
C29	GLU A 77 OE2	4.49	C16	THR A 73 OG1	4.5
C24	GLU A 77 OE2	4.61	C15	THR A 73 OG1	4.32
C23	GLU A 77 OE2	3.66	C14	THR A 73 OG1	3.99
C14	GLU A 77 OE2	4.61	C12	THR A 73 OG1	4.52
C7	GLU A 77 OE2	3.2	C11	THR A 73 OG1	4.25
C6	GLU A 77 OE2	2.86	C5	THR A 73 OG1	3.84
C5	GLU A 77 OE2	4.66	C4	THR A 73 OG1	4.68
C4	GLU A 77 OE2	4.46	C1	THR A 73 OG1	4.76
C3	GLU A 77 OE2	3.74	C21	THR A 73 CG2	3.71
C1	GLU A 77 OE2	4.3	O5	THR A 73 CG2	4.51
C29	GLU A 77 OE1	3.15	C19	THR A 73 CG2	4.47
C28	GLU A 77 OE1	4.2	C18	THR A 73 CG2	4.59
C24	GLU A 77 OE1	3.69	C11	THR A 73 CG2	4.2
C23	GLU A 77 OE1	3.41	N1	THR A 73 CB	4.51
C7	GLU A 77 OE1	3.77	C22	THR A 73 CB	4.08
C6	GLU A 77 OE1	3.91	C21	THR A 73 CB	4.68
C3	GLU A 77 OE1	4.74	C19	THR A 73 CB	4.66
N2	GLU A 77 CD	4.87	C18	THR A 73 CB	4.98
C29	GLU A 77 CD	4.09	C14	THR A 73 CB	4.94
C24	GLU A 77 CD	4.52	C11	THR A 73 CB	4.15
C23	GLU A 77 CD	3.92	C5	THR A 73 CB	4.42
N1	GLU A 77 CD	4.9	C22	THR A 73 O	4.61
C7	GLU A 77 CD	3.74	C22	THR A 73 C	4.22
C6	GLU A 77 CD	3.47	C22	THR A 73 CA	4.74
C3	GLU A 77 CD	4.6	C21	GLU A 71 OE2	2.71
C6	GLU A 77 CG	4.4	C20	GLU A 71 OE2	4.28
N2	VAL A 74 CG2	4.6	C19	GLU A 71 OE2	4.72
C14	VAL A 74 CG2	4.7	C18	GLU A 71 OE2	3.86
C7	VAL A 74 CG2	4.72	C17	GLU A 71 OE2	3.76
C6	VAL A 74 CG2	4.34	C16	GLU A 71 OE2	4.61
C7	VAL A 74 CG1	4.85	C22	GLU A 71 OE1	4.22
C6	VAL A 74 CG1	4.92	C21	GLU A 71 OE1	4.66
C6	VAL A 74 CB	4.79	C20	GLU A 71 OE1	4.98
C14	VAL A 74 CA	4.98	C17	GLU A 71 OE1	4.61
C6	VAL A 74 CA	4.45	C16	GLU A 71 OE1	4.82
C14	VAL A 74 N	4.64	C21	GLU A 71 CD	3.88
C6	VAL A 74 N	4.86	C20	GLU A 71 CD	4.32
C22	THR A 73 OG1	3.44	O5	GLU A 71 CD	4.82
C21	THR A 73 OG1	4.69	O4	GLU A 71 CD	4
C18	THR A 73 OG1	4.71	C18	GLU A 71 CD	4.6

C17	THR A 73 OG1	4.41	C17	GLU A 71 CD	4.19
C16	THR A 73 OG1	4.64	C16	GLU A 71 CD	4.72
C14	THR A 73 OG1	3.15	C21	GLU A 71 CG	4.81
C6	THR A 73 OG1	4.94	C20	GLU A 71 CG	4.22
C22	THR A 73 CG2	4.02	O4	GLU A 71 CG	4.31
C14	THR A 73 CG2	4.97	C17	GLU A 71 CG	4.9
C22	THR A 73 CB	4.3	C10	GLN A 15 OE1	3.24
C14	THR A 73 CB	3.84	C9	GLN A 15 OE1	4.95
C14	THR A 73 O	4.23	C8	GLN A 15 OE1	4.15
C6	THR A 73 O	4.55	C1	GLN A 15 OE1	4.93
C14	THR A 73 C	4.29	C10	GLN A 15 NE2	4.39
C6	THR A 73 C	4.88	O2	GLN A 15 CD	4.11
C14	THR A 73 CA	4.72	C10	GLN A 15 CD	4.08
C22	GLU A 71 OE2	3.37	C22	GLN A 11 OE1	4.29
C21	GLU A 71 OE2	3.68	C13	GLN A 11 OE1	4.75
C22	GLU A 71 OE1	4.36	O7	GLN A 11 CD	4.64
C21	GLU A 71 OE1	3.58	O6	GLN A 11 CD	4.79
C18	GLU A 71 OE1	4.94	O2	GLN A 11 CD	4.7
C22	GLU A 71 CD	4.05			
C21	GLU A 71 CD	3.32			
O7	GLU A 71 CD	4.46			
C18	GLU A 71 CD	4.98			
C21	GLU A 71 CG	3.48			
O7	GLU A 71 CG	4.79			
C21	GLU A 71 CB	4.89			
C28	ASN A 18 ND2	4.84			
C29	GLN A 15 OE1	4.3			
C25	GLN A 15 OE1	4.08			
C24	GLN A 15 OE1	3.65			
C23	GLN A 15 OE1	3.3			
C7	GLN A 15 OE1	2.88			
C6	GLN A 15 OE1	4.02			
C3	GLN A 15 OE1	3.86			
C1	GLN A 15 OE1	4			
C29	GLN A 15 NE2	4.92			
C26	GLN A 15 NE2	4.27			
C25	GLN A 15 NE2	3.62			
C24	GLN A 15 NE2	4.01			
C23	GLN A 15 NE2	4.17			
C7	GLN A 15 NE2	4.71			
C1	GLN A 15 NE2	4.84			
C29	GLN A 15 CD	4.23			
C28	GLN A 15 CD	4.8			
C27	GLN A 15 CD	4.83			
C26	GLN A 15 CD	4.32			
C25	GLN A 15 CD	3.64			
C24	GLN A 15 CD	3.59			
C23	GLN A 15 CD	3.71			
N1	GLN A 15 CD	3.96			
C7	GLN A 15 CD	4.04			
C3	GLN A 15 CD	4.86			
C1	GLN A 15 CD	4.72			
C29	GLN A 15 CG	4			
C28	GLN A 15 CG	4.19			
C27	GLN A 15 CG	4.26			
C26	GLN A 15 CG	4.15			
C25	GLN A 15 CG	3.93			
C24	GLN A 15 CG	3.85			
C23	GLN A 15 CG	4.4			
C29	GLN A 15 CB	4.55			

C28	GLN A 15 CB	4.3			
C27	GLN A 15 CB	3.91			
C26	GLN A 15 CB	3.79			
C25	GLN A 15 CB	4.04			
C24	GLN A 15 CB	4.42			
C28	GLN A 15 O	4.35			
C27	GLN A 15 O	3.5			
C26	GLN A 15 O	4.01			
C28	GLN A 15 C	4.9			
C27	GLN A 15 C	4.21			
C26	GLN A 15 C	4.55			
C28	GLN A 15 CA	4.44			
C27	GLN A 15 CA	4.12			
C26	GLN A 15 CA	4.47			
C21	GLN A 11 OE1	4.98			
C20	GLN A 11 OE1	3.41			
C19	GLN A 11 OE1	3.31			
C18	GLN A 11 OE1	4.6			
C15	GLN A 11 OE1	4.75			
C20	GLN A 11 NE2	4.67			
C19	GLN A 11 NE2	5			
C20	GLN A 11 CD	4.32			
C19	GLN A 11 CD	4.45			
C25	GLN A 15 NE2	3.62			
C24	GLN A 15 NE2	4.01			
C23	GLN A 15 NE2	4.17			
C7	GLN A 15 NE2	4.71			
C1	GLN A 15 NE2	4.84			
C29	GLN A 15 CD	4.23			
C28	GLN A 15 CD	4.8			
C27	GLN A 15 CD	4.83			
C26	GLN A 15 CB	3.79			
C25	GLN A 15 CB	4.04			
C24	GLN A 15 CB	4.42			
C28	GLN A 15 O	4.35			
C27	GLN A 15 O	3.5			
C26	GLN A 15 O	4.01			
C28	GLN A 15 C	4.9			
C27	GLN A 15 C	4.21			
C26	GLN A 15 C	4.55			
C28	GLN A 15 CA	4.44			
C27	GLN A 15 CA	4.12			
C26	GLN A 15 CA	4.47			
C21	GLN A 11 OE1	4.98			
C20	GLN A 11 OE1	3.41			
C19	GLN A 11 OE1	3.31			
C18	GLN A 11 OE1	4.6			
C15	GLN A 11 OE1	4.75			
C20	GLN A 11 NE2	4.67			
C19	GLN A 11 NE2	5			
C20	GLN A 11 CD	4.32			
C19	GLN A 11 CD	4.45			

CHAPTER 3

Development of 9-(N-Arylmethylamino) derivatives of noscapine: The Tubulin Binding Anticancer Agent for the Treatment of Breast Cancer

3.1. Introduction:

The plant alkaloid, noscapine has been administered orally as a safe antitussive drug for over 40 years. It is non-sedative, non-narcotic and lacks respiratory-depressant properties without causing any exhilaration or dependency (Dahlström *et al.,* 1982; Karlsson *et al.,* 1990). It was found that noscapine binds to tubulin and subdues its dynamic instability, leading to inhibition of cell cycle progression at the mitotic phase of both dividing cancer cells and normal cells (Ye *et al.,* 1998; Landen *et al.,* 2002). Cancer cells, perhaps due to their mutations lead to compromised cell cycle checkpoints and fail to arrest mitosis for a long duration and undergo apoptosis. In contrast, the arrested normal cells resume mitosis after drug removal (Zhou *et al.,* 2002a; Aneja *et al.,* 2007a). In comparison to the other microtubule binding drugs like taxanes and vinca alkaloids, noscapine has numerous advantages as an anticancer agent: (a) it arrests a variety of cancer cells including drug resistant variants in mitosis and targets them for apoptosis (Ke *et al.,* 2000; Zhou *et al.,* 2002a; Aneja *et al.,* 2007a; Zhou *et al.,* 2006), (b) it is a poor substrate for drug pumps (poly glycoproteins and MDR-related proteins) which constitute a major cause of drug resistance (Zhou *et al.,* 2006), (c) it inhibits progression of murine melanoma, lymphoma, glioblastoma and human breast tumors implanted in nude mice without detectable toxicity to the rapidly dividing cells and post mitotic cells such as neurons (Ke *et al.,* 2000; Zhou *et al.,* 2002a; Aneja *et al.,* 2007a; Zhou *et al.,* 2006), (d) it does not hinder primary humoral and cellular responses in mice (Ye *et al.,* 1998; Ke *et al.,* 2000; Krishna *et al.,* 2000), (e) it does not cause measurable immunological and neurological toxicity in mice (Aneja *et al.,* 2007a; Landen *et al.,* 2004; Aneja *et al.,* 2010a), (f) it is orally administered as opposed to other anti-MT drugs that require peritoneal injections or intravenous infusions with a risk of anaphylactic reactions (Aneja *et al.,* 2007a), (g) it has a mean bioavailability of ~30-32 percent over a dose range of 10 mg/kg to 300 mg/kg in mice (Jensen *et al.,* 1992; Aneja *et al.,* 2007b). To further improve its efficacy, efforts were based on rational drug design and synthesis of new generations of noscapine derivatives for better therapeutic outcomes. Several derivatives of noscapine were synthesized and evaluated for their antiproliferative activity, ability to suppress tumor size in xenograft animal models and side effects (Zhou *et al.,* 2003; Aneja et al 2006a; Naik *et al.,* 2011a; Santoshi *et al.,* 2011; Mishra *et al.,* 2011; Aneja *et al.,* 2006b; Manchukonda *et al.,* 2013; Santoshi *et al.,* 2015).

In this study, we envisage to develop 9-N-arylmethylamino derivatives of noscapine by substituting alkyl or arylalkyl groups at the C-9 position of the noscapine scaffold. The potential compounds were subsequently synthesized and their anticancer activity was assessed using two human breast cancer cell lines (MCF-7 and MDA-MB-231). The 9-(N-arylmethylamino) derivatives of noscapine were found to bind tubulin heterodimer with

improved binding affinity, significantly decrease cancer cell growth, and successfully induce cancer cell apoptosis by the arrest of cancer cells at G2/M phase.

3.2. Materials and Methods

3.2.1. Preparation of crystal structure of tubulin

The co-complex structure of tubulin-amino noscapine was downloaded from PDB data bank (PDB ID: 6Y6D). X-ray crystallography was used to get this structure of tubulin at a resolution of 2.20 Å (Oliva *et al.,* 2020). The tubulin αβ-heterodimer was obtained after visualizing the structure in Maestro (Schrodinger software package). The missing side-chain atoms of the amino acids were identified using Prime side-chain prediction tool and repaired using Prime (Schrödinger, Inc., NY). Further, the protein preparation wizard (Schrodinger software package) was used to prepare the tubulin structure by adding hydrogen atoms and refining hydrogen-bonding networks.

3.2.2. Preparation of chemical structure of noscapinoids

Chemical structures of the noscapinoids (Figure 3.1) that had been reported earlier (Aneja *et al*., 2006a; Naik *et al*., 2011a; Santoshi and Naik, 2014; Manchukonda *et al*., 2013) and the newly designed 9-(N-arylalkylamino) derivatives of noscapine (Figure 3.2) were built using ISIS draw and transformed into the 3D structure using Chemsketch. Energy minimization of these structures was done using Macromodel (Schrodinger software package) and OPLS 2005 force field. A PRCG algorithm with 1000 steps and an energy gradient of 0.001 was used for energy minimization. Further geometric optimization was done by Jaguar (version 17.4, Schrödinger, LLC) with a basic set of 3-21G* (Binkley *et al.,* 1980; Gordon *et al.,* 1982), using Becke's three-parameter exchange potential and the Lee-Yang-Parr correlation functional (B3LYP) (Lee *et al.,* 1988; Beck, 1993). In order to generate ionization states at physiological pH, possible tautomer's and minimize ring conformation for each molecule Ligprep (Schrödinger software package) was employed.

3.2.3. Molecular docking

The 9-(N-arylalkylamino) derivatives of noscapine were docked onto the noscapinoids binding site (Oliva *et al.,* 2020), at the interface of α- and β- tubulin. The binding site was specified by selecting the ligand, amino noscapine, and creating two grid boxes. An inner grid box of size 12 Å x 12 Å x 12 Å was made using the Glide grid-receptor generating algorithm at the centroid of the binding site indicating that each docked ligand's diameter midpoint must be present in the search space. Along with this box an outer grid box was also formed with a size of ≤ 24 Å of the co-complexed amino noscapine specifying the volume in which the ligand's must restrain. The Glide XP method (Schrodinger software package) was used to

dock the molecules, and their binding poses were evaluated using the GlideXPScore function (Friesner *et al.*, 2004; Halgren *et al.*, 2004). Protein atoms with precise partial charges less than or equal to 0.25 was used as a scaling factor and 0.4 for van der Waals radii. Out of the 10,000 poses evaluated, 1000 were choosen using energy minimization (conjugate gradients), and the 30 structures with the lowest energy conformation were used to determine Glide docking score. For future investigations, the single optimal conformation for each molecule was chosen. The single best conformation for each molecule was chosen. Finally, we filtered out the top three 9-(N-arylmethylamino) derivatives of noscapine, **15-17** (Figure 3.3) from the library for chemical synthesis and experimental evaluation to validate their anticancer potential.

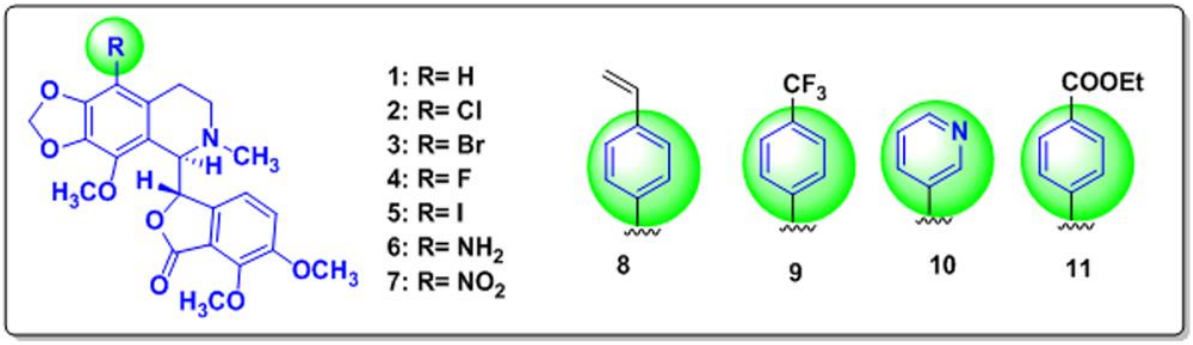

Figure 3.1: *Molecular structures of noscapine derivatives that have already been experimentally proved to bind tubulin with known binding free energy and are taken as a training set for establishing the prediction model.*

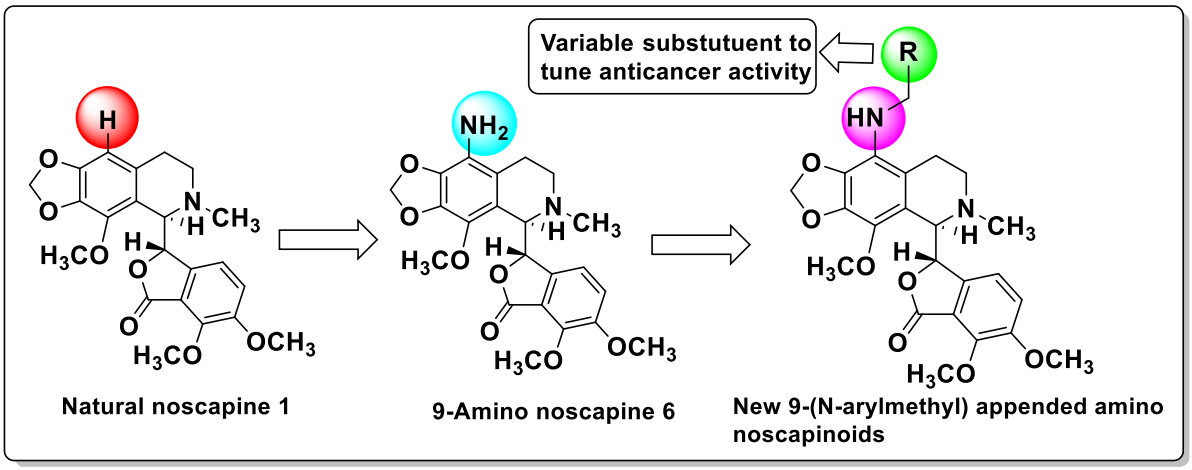

Figure 3.2: *In silico combinatorial derivatization of the scaffold structure of noscapine with alkyl or arylalkyl units to develop a library of 9-(N-arylalkylamino) derivatives of noscapine.*

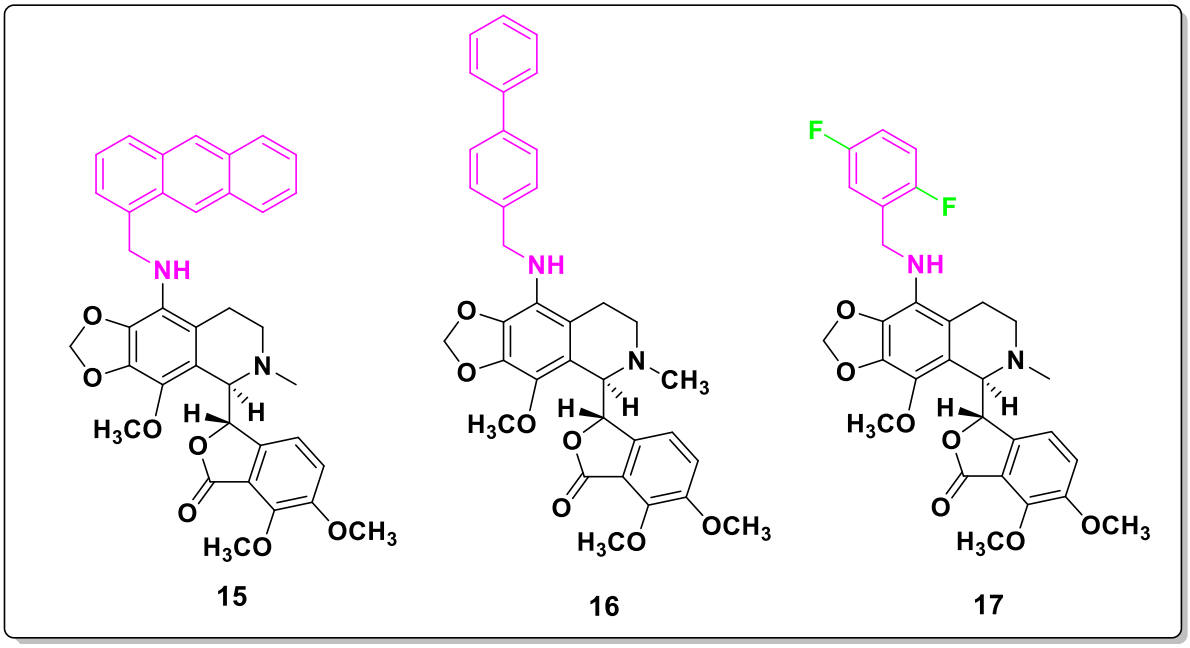

Figure 3.3: *Molecular structure of three top-ranked 9-(N-arylmethylamino) noscapinoids,* ***15-17****, screened out from the library with better tubulin binding affinity.*

3.2.4. LIE-SGB model building

To anticipate the free energy of binding (*ΔGbind,pred*) of 9-(N-arylalkylamino) noscapinoids with tubulin, a linear interaction energy (LIE) with a surface generalised Born (SGB) continuum solvation model (Zhou *et al*., 2001) was developed as reported already (Santoshi *et al*., 2015). The experimental binding free energy (*ΔGbind,expt*) of 9-(N-arylalkylamino) noscapiniods with tubulin (Figure 3.1) and other predicted energy paramters like Coulumbic (U_{coul}), cavity energy (U_{cav}), van der Waals (U_{vdw}) and reaction field (U_{rxn}) was used to develop a multiple linear regression model without intercept for the prediction of binding free energy. Hybrid Monte Carlo simulation approach with comparable settings set up as mentioned before was utilised to estimate the above energy parameters from docked complexes of the noscapinoids using Liaison (Schrödinger package).

$$\Delta G_{bind,pred} = \alpha\left(\langle U^b_{vdw}\rangle - \langle U^f_{vdw}\rangle\right) + \beta\left(\langle U^b_{coul}\rangle - \langle U^f_{coul}\rangle\right) + \gamma\left(\langle U^b_{rxn}\rangle - \langle U^f_{rxn}\rangle\right) + \delta\left(\langle U^b_{cav}\rangle - \langle U^f_{cav}\rangle\right)$$

Here $\langle\ \rangle$ is the ensemble average, b represents the ligand's bound form, f represents the ligand's free form, and α, β, γ and δ are the energy parameter values.

3.2.5. General procedure for chemical synthesis of 15-17

Noscapine was used as a starting material for the synthesis of 9-amino-noscapine through 2 reaction phases such as (a) bromination of noscapine with aqueous HBr/Br_2-H_2O and (b) amination of noscapine with CuI, NaN_3, and L-Proline in DMSO (Naik *et al.*, 2011a). The solution of 9-amino-noscapine **6** (1.0 mmol) was refluxed in ethanol (15 mL) with various substituted aromatic aldehydes (1.0mmol) for 24 hr. The solvent was evaporated under vacuum until the reaction consumed all of the starting material (as suggested by TLC). The crude residue was extracted using dichloromethane (2 x 15 mL) and by washing in a brine solution. After being collected and passed through Na_2SO_4 bed the organic layer was removed at a lower pressure. The crude residue was chromatographed across a triethylamine silica bed using petroleum ether/ethyl acetate (7:3) as eluents to form 9-(arylimino) derivatives of noscapine **12-14** as solid compounds in high yields. The intermediate products **12-14** (1.0 mmol) were reduced to their respective 9-(N-arylmethylamino) derivatives, **15-17**, by treating them with sodium cyanoborohydride (1.2 mmol) in methanol (10 mL) for 4 hours at room temperature (Figure 3.4). NMR (^1H and ^{13}C), IR spectroscopy, and mass (HRMS) spectrometry were used to characterize all intermediates and end products. The spectroscopy data of all the intermediates and final products are included in the Appendix 3.1 to 3.19.

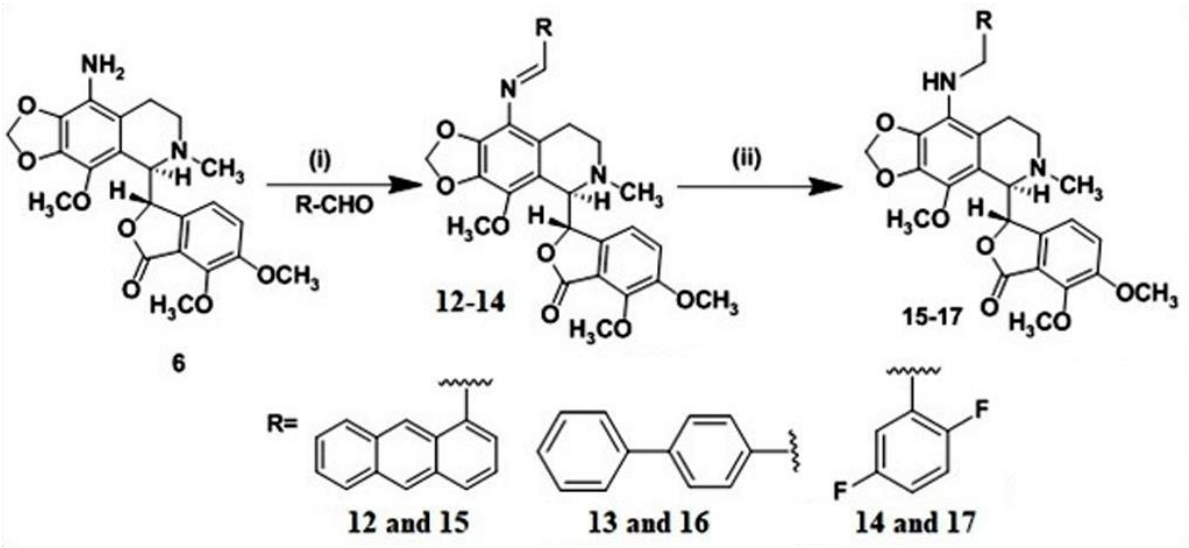

Figure 3.4: *Chemical synthesis of screened out 9-(N-arylmethylamino) derivatives of noscapine* ***15-17****. Reaction Conditions: i) RCHO, EtOH, Reflux, 24 hr; (ii) NaCNBH3, Methanol, RT, 4 h. 9-amino-noscapine was transformed to 9-(arylimino) derivatives of noscapine* ***12-14****, which were subsequently reduced to 9-(N-arylmethylamino) derivatives of noscapine* ***15-17****.*

(S)-3-((R)-9-((E)-(Anthracen-9-ylmethylene)amino)-4-methoxy-6-methyl-5,6,7,8-tetra hydro[1,3]dioxolo[4,5-g]isoquinolin-5-yl)-6,7-dimethoxyisobenzofuran-1(3H)-one(12):

Yield: 72%, mp: 200-202 °C, IR (KBr): 3423, 2935, 1764, 1625, 1495, 1388, 1250, 1135, 1032, 1032, 889, 737, 668 cm-1. 1H NMR (500 MHz, CDCl3) : δ 10.06 (s, 1H, N=CH), 8.82 (d, J = 8.8 Hz, 2H, Ar-H), 8.55 (s, 1H, Ar-H), 8.05 (d, J = 8.2 Hz, 2H, Ar-H), 7.60-7.56 (m, 2H, Ar-H), 7.54-7.50 (m, 2H, Ar-H), 7.01 (d, J = 8.2 Hz, 1H, Ar-H), 6.41 (d, J = 8.2 Hz, 1H, Ar-H), 6.13 (dd, J = 1.3, 19.6 Hz, 2H, OCH2-O), 5.63(d, J = 4.5 Hz, 1H, Ar-CH, (C3-phthalide)), 4.46 (d, J = 4.5 Hz, 1H, Ar-CH, (C5'-isoquinoline)), 4.11 (s, 3H, -OCH3), 4.08 (s, 3H, -OCH3), 3.82 (s, 3H, -OCH3), 3.10-3.03 (m, 1H, -CHH-N-CH3 (C7'-isoquinoline)), 2.80-2.73 (m, 1H, -CHH-N-CH3 (C7'-isoquinoline)), 2.59 (s, 3H, NCH3), 2.53-2.47 (m, 1H, Ar-CHH (C8'-isoquinoline)), 2.24-2.16 (m, 1H, Ar-CHH (C8'-isoquinoline)). 13C NMR (125 MHz, CDCl3): δ 168.0, 152.0, 147.5, 140.9, 137.8, 135.6, 134.9, 131.5, 130.6, 130.2, 129.1, 127.7, 126.4, 125.1(X2), 123.9, 120.9, 119.9, 117.9, 117.7, 100.8, 81.8, 80.8, 62.2, 60.9, 59.7, 56.6, 49.0, 45.7, 22.1. MS (ESI-MS) m/z: 617 [M+H]+ HRMS (ESI): Calcd for C37H33N2O7 [M+H]+: 617.22823, found: 617.22769.

(S)-3-((R)-9-((E)-([1,1'-biphenyl]-4-ylmethylene)amino)-4-methoxy-6-methyl-5,6,7,8 tetrahydro-[1,3]dioxolo[4,5-g]isoquinolin-5-yl)-6,7-dimethoxyisobenzofuran-1(3H)-one(13):

Yield: 76%. mp: 95-97°C. IR (KBr): 3447, 2933, 1759, 1626, 1491, 1436, 1384, 1122, 1033, 969, 840, 763, 695 cm-1. 1H NMR (400 MHz, CDCl3) : δ 8.90 (s, 1H, N=CH), 7.96 (d, J = 8.3 Hz, 2H, Ar-H), 7.69 (d, J = 8.3 Hz, 2H, Ar-H), 7.65 (d, J = 7.2 Hz, 2H, Ar-H), 7.50-7.44 (m, 2H, Ar-H), 7.39 (t, J = 7.3 Hz, 1H, Ar-H), 7.00 (d, J = 8.3 Hz, 1H, Ar-H), 6.32 (d, J = 8.3 Hz, 1H, Ar-H), 6.00 (dd, J = 1.3, 16.2 Hz, 2H, O-CH2-O), 5.59 (d, J = 4.2 Hz, 1H, Ar-CH, (C3-phthalide)), 4.40 (d, J = 4.2 Hz, 1H, Ar-CH, (C5'-isoquinoline)), 4.10 (s, 3H, -OCH3), 4.05 (s, 3H, -OCH3), 3.86 (s, 3H, -OCH3), 3.05-2.97 (m, 1H, -CHH-N-CH3 (C7'-isoquinoline)), 2.74-2.66 (m, 1H, -CHH-N-CH3 (C7'-isoquinoline)), 2.56 (s, 3H, N-CH3), 2.45-2.38 (m, 1H, Ar-CHH (C8'-isoquinoline)), 2.09-2.00 (m, 1H, Ar-CHH (C8'-isoquinoline)). 13C NMR (100MHz, CDCl3): δ 168.1, 161.2, 152.1, 147.6, 143.7, 141.3, 140.2, 139.1, 138.7, 135.8, 134.5, 130.1, 129.1, 128.8, 128.7, 127.7, 127.2, 125.8, 119.8, 118.3, 117.7, 100.8, 81.8, 62.2, 59.4, 56.7, 49.4, 45.9, 22.8. MS (ESI-MS) m/z: 593 [M+H]+ HRMS (ESI): Calcd for C35H33N2O7 [M+H]+: 593.22823, found: 593.22731.

(S)-3-((R)-9-((E)-(2,5-Difluorobenzylidene)amino)-4-methoxy-6-methyl-5,6,7,8 tetrahydro-[1,3]dioxolo[4,5-g]isoquinolin-5-yl)-6,7-dimethoxyisobenzofuran-1(3H)-one (14):

Yield: 74%. mp: 145-147°C. IR (KBr): 33571, 2944, 2793, 1762, 1628, 1491, 1428, 1387, 1272, 1142, 1043, 965, 813, 725 cm-1. 1H NMR (400 MHz, CDCl3): δ 9.13 (d, J= 2.4 Hz, 1H, N=CH), 7.87-7.81 (m, 1H, Ar-H), 7.14-7.07 (m, 2H, Ar-H), 7.00 (d, J = 8.3 Hz, 1H, Ar-H), 6.33 (d, J = 8.3 Hz, 1H, Ar-H), 6.02 (dd, J = 1.3, 15.6 Hz, 2H, O-CH2-O), 5.57 (d, J = 4.4 Hz, 1H, Ar-CH, (C3-phthalide)), 4.39 (d, J = 4.4 Hz, 1H, Ar-CH, (C5'-isoquinoline)), 4.10 (s, 3H, -OCH3), 4.04 (s, 3H, -OCH3), 3.86 (s, 3H, -OCH3), 3.05-2.95 (m, 1H, -CHH-N-CH3 (C7'-isoquinoline)), 2.77-2.69 (m, 1H, -CHH-N-CH3 (C7'-isoquinoline)), 2.55 (s, 3H, NCH3), 2.46-2.37 (m, 1H, Ar-CHH (C8'-isoquinoline)), 2.11-2.00 (m, 1H, Ar-CHH (C8'-isoquinoline)). 13C NMR (125 MHz, CDCl3) : δ 168.0, 159.8 (d, JC-F = 31.7 Hz), 157.9(d, JC-F= 38.1 Hz), 153.2, 152.1, 147.6, 141.3, 139.47, 139.43, 134.4, 129.8, 126.1 (dd, JC-F = 8.1, 11.8 Hz), 124.9, 119.8, 119.1 (dd, JC-F = 9.0, 25.4 Hz), 117.8, 117.6, 117.1 (dd, JC-F = 8.1, 23.6 Hz), 112.9 (dd, JC-F = 2.7, 25.4 Hz), 101.1, 81.7, 62.2, 60.8, 59.5, 56.7, 49.3, 45.8, 22.8. MS (ESI-MS) m/z: 553 [M+H]+ HRMS (ESI): Calcd for C29H27F2N2O7 [M+H]+: 553.17808, found: 553.17669.

(S)-3-((R)-9-((Anthracen-9-ylmethyl)amino)-4-methoxy-6-methyl-5,6,7,8-tetrahydro-[1,3]dio xolo[4,5-g]isoquinolin-5-yl)-6,7-dimethoxyisobenzofuran-1(3H)-one (15):

Yield: 62%. mp. 172-174°C. IR (KBr): 3399, 2927, 2851, 1756, 1616, 1490, 1448, 1326, 1269, 1069, 1032, 967, 738, 663 cm-1. 1H NMR (500 MHz, CDCl3): δ 8.46 (s, 1H, Ar-H), 8.38 (d, J = 8.8 Hz, 2H, Ar-H), 8.04 (d, J = 8.2 Hz, 1H, Ar-H), 7.55 (t, J = 7.1 Hz, 2H, Ar-H), 7.49 (t, J = 7.7 Hz, 2H, Ar-H), 6.81 (d, J = 8.2 Hz, 1H, Ar-H), 6.15-6.05 (m, 3H, Ar-H, OCH2-O), 5.58 (d, J = 3.9 Hz, 1H, Ar-CH, (C3-phthalide)), 5.41 (d, J = 12.3 Hz, 1H, N-CH2H), 5.19 (d, J = 12.3 Hz, 1H, N-CH2H), 4.42 (d, J = 3.9 Hz, 1H, Ar-CH, (C5'-isoquinoline)), 4.06 (s, 3H, -OCH3), 4.00 (s, 3H, -OCH3), 3.76 (s, 3H, -OCH3), 2.53-2.46 (m, 4H, -CHH-N-CH3 (C7'-isoquinoline), N-CH3), 2.29-2.16 (m, 2H, CHH-N-CH3 (C7'-isoquinoline), Ar-CHH (C8'-isoquinoline)), 1.55-1.45 (m, 1H, Ar-CHH (C8'-isoquinoline)) 13C NMR (100 MHz, CDCl3): δ 168.0, 152.0, 147.5, 140.9, 137.8, 135.6, 134.9, 131.5, 130.6, 129.1, 127.7, 126.3, 125.1, 125.0, 123.8, 120.9, 119.9, 117.9, 117.6, 100.8, 81.8, 62.2, 60.8, 59.7, 56.6, 49.0, 45.8, 43.8, 22.2. MS (ESI-MS) m/z: 619 [M+H]+ HRMS (ESI): Calcd for C37H34N2O8 [M+H]+: 619.24388, found: 619.24477.

(S)-3-((R)-9-(([1,1'-Biphenyl]-4-ylmethyl)amino)-4-methoxy-6-methyl-5,6,7,8tetra hydro[1,3]dioxolo[4,5-g]isoquinolin-5-yl)-6,7-dimethoxyisobenzofuran-1(3H)-one (16):

Yield: 65%. mp: 70-72°C. IR (KBr): 3389, 2932, 1756, 1620, 1496, 1441, 1384, 1267, 1119, 1036, 1010, 970, 761, 698 cm-1. 1H NMR (400 MHz, CDCl3) : δ 7.61-7.55 (m, 4H, Ar-H), 7.46-7.33 (m, 5H, Ar-H), 6.76 (d, J= 8.3 Hz, 1H, Ar-H), 6.00-5.93 (m, 3H, Ar-H), 5.57 (d, J = 4.0 Hz, 1H, Ar-CH, (C3-phthalide)), 4.48 (d, J = 14.0 Hz, 1H, N-CHH), 4.41 (d, J = 4.0 Hz,

1H, Ar-CH, (C5'-isoquinoline)), 4.34 (d, J = 14.0 Hz, 1H, N-CHH) 4.06 (s, 3H, -OCH3), 3.95 (s, 3H, -OCH3), 3.70 (s, 3H, -OCH3), 2.60-2.48 (m, 4H, CHHN-CH3 (C7'-isoquinoline), N-CH3), 2.39-2.27 (m, 2H, CHH-N-CH3 (C7'-isoquinoline), Ar-CHH (C8'-isoquinoline)), 1.69-1.57 (m, 1H, Ar-CHH (C8'-isoquinoline)). 13C NMR (100MHz, CDCl3) : δ 168.0, 152.0, 147.5, 140.8, 140.5, 140.0, 139.4, 137.3, 135.4, 134.6, 128.7, 128.1, 127.3, 127.1, 126.8, 124.1, 120.8, 119.9, 117.9, 117.6, 100.6, 81.8, 62.1, 60.8, 59.6, 56.5, 50.6, 49.2, 45.9, 22.4. MS (ESI-MS) m/z: 595 [M+H]+ HRMS (ESI): Calcd for C35H35N2O7 [M+H]+: 595.24388, found:595.24458.

(S)-3-((R)-9-((2,5-difluorobenzyl)amino)-4-methoxy-6-methyl-5,6,7,8-tetrahydro-[1,3]dioxolo [4,5-g]isoquinolin-5-yl)-6,7-dimethoxyisobenzofuran-1(3H)-one (17):

Yield: 82%. mp: 148-150°C. IR (KBr): 3408, 2948, 2897, 2848, 1760, 1620, 1495, 1452, 1383, 1266, 1226, 1039, 876, 821, 752, 643 cm-1. 1H NMR (400 MHz, CDCl3): δ 7.11-6.85 (m, 4H, Ar-H), 5.99-5.89 (m, 3H, Ar-H, O-CH2-O), 5.56 (d, J = 4.1 Hz, 1H, Ar-CH, (C3-phthalide)), 4.47-4.33 (m, 3H, Ar-CH, (C5'-isoquinoline), N-CH2), 4.08 (s, 3H, -OCH3), 3.95 (s, 3H, -OCH3), 3.85 (s, 3H, -OCH3), 2.59-2.49 (m, 4H, CHH-N-CH3 (C7'-isoquinoline), N-CH3), 2.37-2.24 (m, 2H, CHH-N-CH3 (C7'-isoquinoline), Ar-CHH (C8'-isoquinoline)), 1.66-1.55 (m, 1H, Ar-CHH (C8'-isoquinoline)). 13C NMR (100 MHz, CDCl3) : δ 168.0, 159.7 (d, JC-F = 242.0 Hz), 157.8 (d, JC-F = 242.0 Hz), 152.0, 147.5, 140.8, 137.2, 135.2, 134.8, 129.3 (dd, JC-F = 7.3, 17.6 Hz), 123.3, 121.1, 120.0, 117.8, 117.5, 116.2 (d, JC-F = 8.8 Hz), 116.0 (d, JC-F = 8.8 Hz), 115.7(d, JC-F = 5.1 Hz), 115.0(dd, JC-F = 8.8, 24.2 Hz), 100.6, 81.7, 62.1, 60.8, 59.6, 56.6, 49.3, 46.0, 44.3, 22.4. MS (ESI-MS) m/z: 555 [M+H]+ HRMS (ESI) : Calcd for C29H29F2N2O7 [M+H]+: 555.19133, found: 555.19285.

3.2.6. Cancer cell lines and reagents

MCF-7 and MDA-MB-231 (Human Breast cancer cell line) were obtained from the National Center for Cell Science in Pune, Maharashtra, India. The stock solutions (100 mM) of **15-17** were prepared with DMSO (Dimethyl sulfoxide) and kept at 4 ^{o}C until used. The cells were cultured in DMEM (Dulbecco's modified Eagle medium) accompanied with 10% FBS (fetal bovine serum) and antibiotics at 37 °C in a 5% CO_2 and 95% humidity environment. The cells were passage using trypsin-EDTA (0.25%) and used for cellular study after cells showed 70-80% confluency.

3.2.7. Proliferation assay using breast cancer cells

MCF-7 and MDA-MB-231 human breast cancer cell lines as well as a normal human embryonic kidney cell (293T) were used for the cell proliferation experiment. Cells were seeded at a density of 5 x 10^3 per well in a 96 well plate. The cells were treated with escalating

dosages of noscapine and its derivatives **15-17** from 5 to 100 µM. After 72 h of treatment the cell viability was determined using Sulforhodamine B assay. The plate's reading was taken in a microplate spectrophotometer (SPECTRAmax PLUS 384) at 564 nm wavelength. The online tool Quest GraphTM IC_{50} Calculator (AAT Bioquest, Inc., Sunnyvale, CA, USA, https://www.aatbio.com/tools/IC50-calculator) was used to determine the fifty percent inhibitory concentration (IC_{50}) of the molecules.

3.2.8. Cell cycle progression assay

The progression of the mitotic cell cycle with the administration of 9-(N-arylmethylamino) derivatives of noscapine, **15-17**, was analyzed as previously described (Patel *et al.*, 2021). The MDA-MB-231 breast cancer cells were plated in a 6 well culture plate overnight at a density of $1x10^5$ and treated with fifty percent inhibitory concentration (IC_{50}) of noscapine and its derivatives **15-17**. The proportion of cells in each stage of the cell cycle was assessed using flow cytometry (BD FACS Aria-III) after 72 h of treatment. The experiment was done in triplicates.

3.2.9. Apoptosis assay

The induction of apoptosis was carried out as previously reported (Patel *et al.*, 2021). In general, MDA-MB-231 breast cancer cells (3×10^4) were plated on a 12 well culture plate and incubated for 24h in a complete medium. The cells were treated with IC_{50} concentrations of noscapine and its derivatives **15-17** and after 72 h they were analysed using a flow cytometer. The apoptosis detection kit (consisting of FITC-conjugated streptavidin, biotin-conjugated Annexin V and propidium iodide (PI) (Sigma- Aldrich, USA) was used to detect the apoptotic cells. Percentage of viable cells (Annexin V−/PI−), early apoptotic cells (Annexin V+/PI−), late apoptotic/necrotic cells (Annexin V+ / PI+) and late necrotic cells (Annexin V−/PI+) were determined.

3.2.10. Tubulin purification

Microtubules were separated and purified from the goat brain using GTP-dependent polymerization and depolymerization alternative cycles in PEM buffer (50 mM pipes, 3 mM $MgSO_4$, 1 mM EGTA, pH 6.8) (Panda et al., 2000; Hamel and Linn, 1981). The purified microtubules were stored at -86°C until use. The purified tubulin was quantified using the Bradford method (Bradford, 1976) and SDS PAGE.

3.2.11. Tubulin binding assay

Tubulin (2 µM) was incubated for 45 min at 35 °C in a water bath with 9-(N-arylmethylamino) derivatives of noscapine, **15-17** at a concentration of 25 µM in PEM buffer

(50 mM pipes, 3 mM $MgSO_4$, 1 mM EGTA, pH 6.8). The samples were excited at 295 nm, and the emission range was 310-400 nm. A FlouroMax® 4 spectrofluorometer (Horiba Scientific, Edison, NJ) with Fluor Essence 3.5 software was used for the spectrofluorometric titrations. The experiments were carried out twice.

3.3. RESULTS AND DISCUSSION

3.3.1. Development of combinatorial library and screening of promising 9-(N-arylmethylamino) derivatives of noscapine

In the past few decades, a series of noscapine derivatives belonging to various categories (collectively known as noscapinoids) have been developed and chemically synthesized. Some of these derivatives appear to more potent than the parent molecule (Zhou *et al.,* 2003; Aneja et al 2006a; Aneja *et al.,* 2006b; Naik *et al.,* 2011a; Santoshi *et al.,* 2011; Mishra *et al.,* 2011; Manchukonda *et al.,* 2013; Santosi *et al.,* 2015). The availability of structure-activity data for reported noscapine derivatives (Figure 3.1) assists in the development of a good prediction model for anticipating the binding free energy of newly synthesized 9-(N-arylalkylamino) noscapine derivatives with tubulin. In this study, we envisaged to generate a library of 9-(N-arylalkylamino) derivatives of noscapine by functionalizing the 9-amino group of noscapine with alkyl or arylalkyl units, as illustrated in Figure 3.2. The library was docked onto the noscapinoid binding site (Oliva *et al.,* 2020), and evaluated using a Glide XP_{score} function (Friesner *et al.,* 2004; Halgren *et al.,* 2004). The optimum binding poses of the ligand inside the binding pocket of a protein were determined via molecular docking. In comparison to noscapine with a docking score -1.975 kcal/mol, all 9-(N-arylalkylamino) derivatives of noscapine docked well inside the binding pocket with an enhanced docking score (ranging from –2.364 to -5.695 kcal/mol). Finally, three top-ranked derivatives **15-17** (Figure 3.3) based on the docking score (-4.586, -5.003 and -5.695 kcal/mol) (Table 3.1) were selected for chemical synthesis. All three derivatives fit well inside the binding pocket (Figure 3.5).

Table 3.1. Glide XP_{score} as well as various energy parameters such as van der Waals energy (U_{vdw}), Columbic energy (U_{coul}), reaction energy (U_{rxn}) and cavity energy (U_{cav}), calculated using Liasion programme (Schrodinger package) of noscapine and its derivatives. The predicted binding free energy ($\Delta G_{bind,pred}$) was calculated based on LIE-SGB prediction model. In comparison to parent molecule noscapine, the newly synthesized 9-(N-arylmethylamino) noscapinoids **15-17** showed better $\Delta G_{bind,pred.}$

Ligand	Glide XP_{score} (kcal/mol)	$<U_{vdw}>$ (kcal/mol)	$<U_{coul}>$ (kcal/mol)	$<U_{rxn}>$ (kcal/mol)	$<U_{cav}>$ (kcal/mol)	$\Delta G_{bind,expt}$ (kcal/mol)	$\Delta G_{bind,pred}$ (kcal/mol)
1	-1.975	-45.43	-331.08	135.31	2.171	-5.246	-5.016
2	-2.086	-49.29	-210.48	115.81	3.357	-6.006	-6.122
3	-2.814	-42.79	-362.38	155.71	4.282	-5.827	-5.973
4	-2.988	-48.35	-356.08	168.51	2.622	-5.587	-5.707
5	-3.311	-47.98	-285.98	135.31	3.177	-6.360	-5.873
6	-4.539	-47.73	-177.58	118.01	4.028	-6.628	-6.458
7	-2.653	-33.68	-332.18	176.51	4.539	-5.551	-5.644
8	-2.335	-45.86	-278.18	112.11	3.359	-5.665	-5.609
9	-2.398	-33.76	-324.78	152.31	3.841	-5.783	-5.097
10	-3.727	-45.72	-471.48	152.61	3.743	-5.673	-5.579
11	-4.435	-42.98	-267.88	129.71	3.539	-5.518	-5.657
15	-4.586	-52.63	-280.98	145.41	3.027	Nd	-6.279
16	-5.003	-50.01	-305.38	149.51	4.891	Nd	-6.984
17	-5.695	-56.2	-274.78	140.61	4.622	Nd	-7.360

$<U_{vdw}>$, $<U_{coul}>$, $<U_{rxn}>$ and $<U_{cav}>$ energy terms represents the ensemble average energy calculated as the difference between bound and free state of the ligands and its environment. Experimental ΔG_{bind} was calculated from the dissociation constant (K_d value) using the relationship: $\Delta G_{bind} = RT\ln K_d$ where T = 298 K and R = 0.00199 (kcal/mol.K). Nd: not determined.

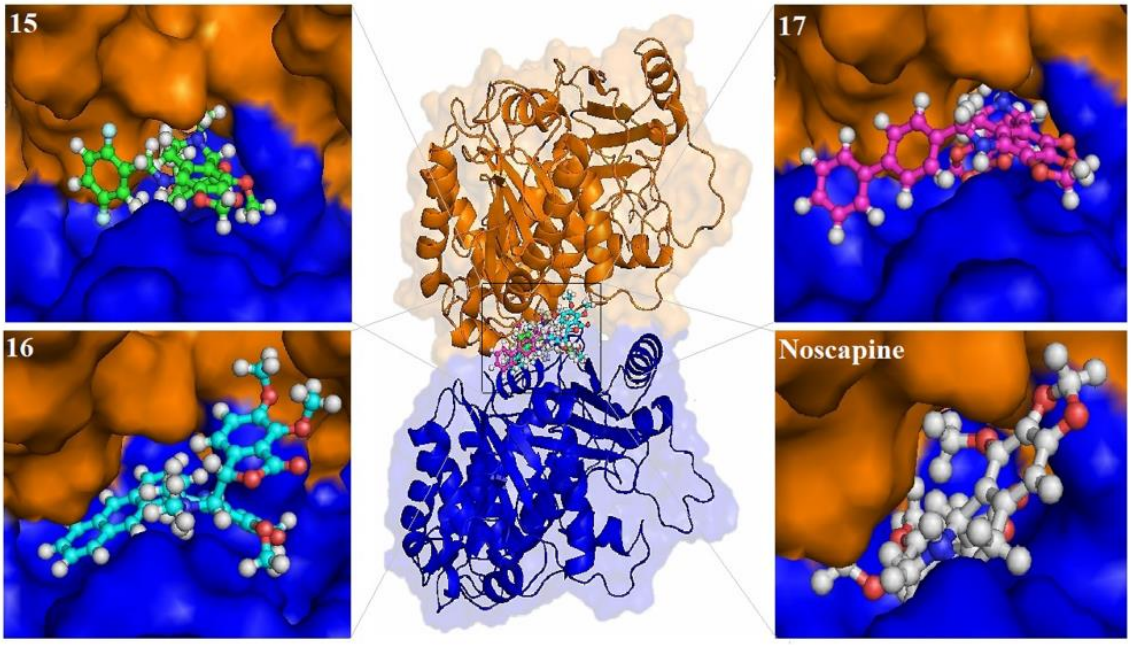

Figure 3.5: *Noscapine and its three derivatives* ***15–17*** *were found to be accommodated well inside the binding pocket at the interface of α-and β-tubulin. α-tubulin is labeled in blue color and β-tubulin is labeled in brown color. The binding domain is represented as a macromodel surface.*

3.3.2. Predicted free energy of binding for 9-(N-arylmethylamino) noscapinoids with tubulin

An empirical linear interaction energy (LIE) with a surface generalised Born (SGB) continuum solvation model (Kollman *et al.,* 2000) (equation 1) was developed to determine the predicted free energy of binding ($\Delta G_{bind,pred}$) of 9-(N-arylmethylamino) noscapinoids with tubulin and included in Table 3.1. The $\Delta G_{bind,pred}$ was found to be remarkably close to $\Delta G_{bind,expt}$ (root mean square error was 0.334 kcal/mol). The values of the coefficients α, β, γ and δ for nonbonding interactions terms van der Waals (U_{vdw}), Coulumbic (U_{coul}), reaction field (U_{rxn}) and cavity energy (U_{cav}) are 0.081, -0.003, -0.009, and -0.512, respectively.

$$\Delta G_{bind,pred} = 0.081\langle U_{vdw}\rangle - 0.003\langle U_{coul}\rangle - 0.009\langle U_{rxn}\rangle - 0.512\langle U_{cav}\rangle \qquad (1)$$

$$(n = 11, R^2 = 0.998, s = 0.334, F = 830.6, P \leq 0.001)$$

In respect to noscapine (-5.016 kcal/mol), the 9-(N-arylmethylamino) noscapinoids exhibited improved $\Delta G_{bind,pred}$ of -6.279 kcal/mol for **15**, -6.984 kcal/mol for **16** and -7.360 kcal/mol for **17.**

3.3.3. Ligplot analysis revealed the binding modes of the ligands

The binding modes of noscapine and its derivatives **15-17**, with the binding site amino acids were shown in the ligplot (Figure 3.6a-d). The binding site amino acids form four hydrogen bonds (dashed line) with the most promising derivative (**17**). The oxygen atoms O3, O4, O5, and O7 of **17** hydrogen-bonded with the side-chain nitrogen atoms of Gln D247 (bond length 2.93 Å), Gln A11 (bond length 4.71 Å), Lys D254 (bond length 4.08 Å), and Arg D48 (bond length 3.74 Å), respectively (Figure 3.6d). In contrast, the derivative **16** forms 3 hydrogen bonds with the binding site amino acids. The oxygen atoms O3 and O4 of **16** hydrogen-bonded with the side-chain nitrogen atom (NE2) of Gln D247 (bond length 2.97 Å) and the main chain nitrogen atom (N) of Gly D246 (bond length 4.87 Å), respectively; whereas the nitrogen atom (N1) of **16** hydrogen-bonded with a side-chain oxygen atom (OE2) of Glu D47 (bond length 2.84 Å) (Figure 3.6c). The derivative **15** forms only 2 hydrogen bonds with the binding site amino acids. Both the nitrogen atoms N1 and N2 of **15** hydrogen-bonded with the side-chain nitrogen atom (NE2) of Gln D247 (bond length 3.34 Å) and a side-chain oxygen atom (OE2) of Glu A77, respectively (Figure 3.6b). Only three hydrogen bonds were generated by the lead molecule, noscapine, with the binding site amino acids Gln D247, Glu D47, and Arg D47 (Figure 3.6a). The binding of noscapine and its derivatives **15-17** to the binding site amino acids was also aided by a series of hydrophobic interactions (Appendix table A3.20 – A3.23).

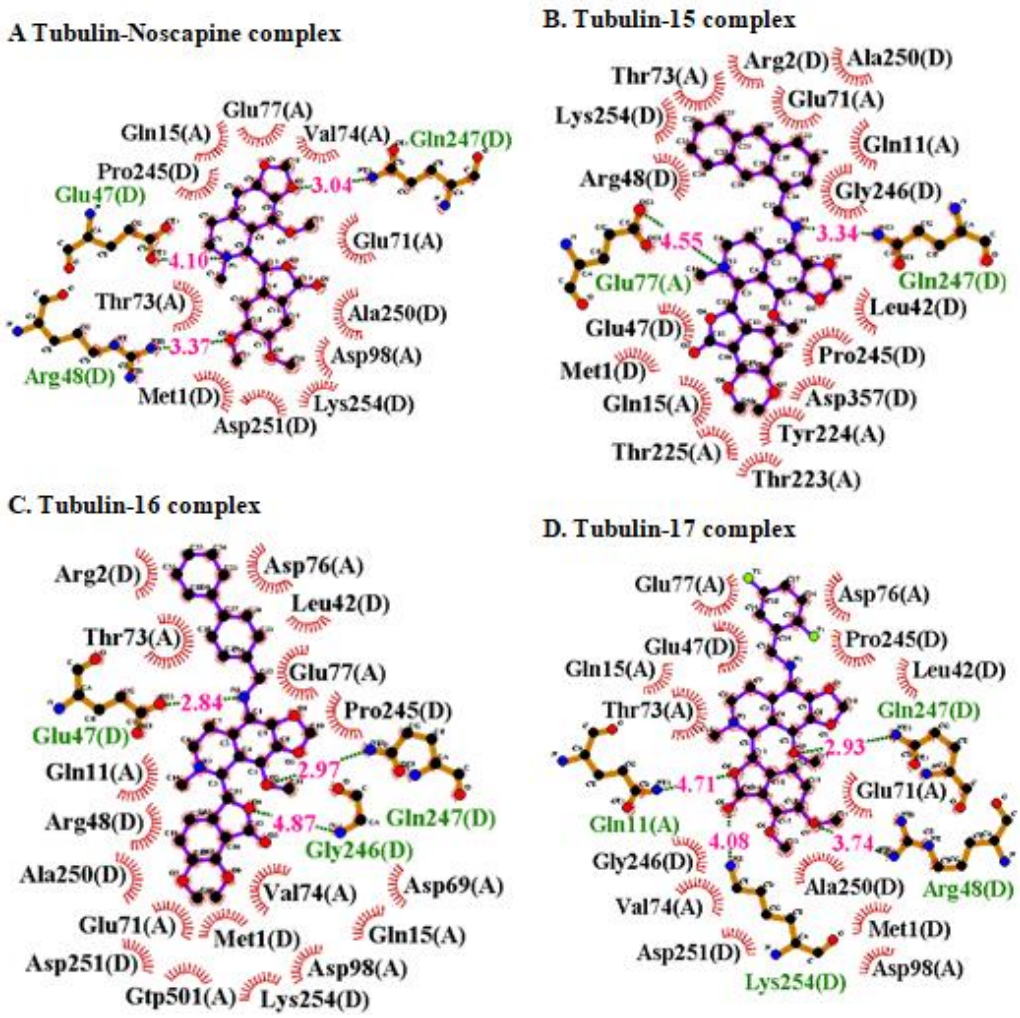

Figure 3.6: *Ligplot analysis demonstrating the interaction between the binding site amino acids of tubulin with (a) Noscapine, (b)* ***15****, (c)* ***16*** *and (d)* ***17****. Hydrogen bonds are represented by dashed lines and numbers represent hydrogen bond lengths in Å. Interactions among hydrophobic molecules are shown as arcs with radial spokes. LIGPLOT was used to develop the graphic. Only the residues within 5 Å of the docked ligands were shown in the images.*

3.3.4. 9-(N-arylmethylamino) derivatives 15-17 inhibits proliferation of cancer cells

The anti-proliferative effect of noscapine and its derivatives **15-17** was investigated using two human breast cancer cells, MCF-7 (estrogen- and progesterone-receptor positive) and MDA-MB-231 (estrogen- and progesterone- receptor negative). All the three noscapinoids **15-17** hindered cancer cell proliferation at a lower dosage than the noscapine (Figure 3.7). In MCF-7 cell line the IC_{50} value was 45.3 µM, 37.2 µM, 30.9 µM and 19.4 µM for noscapine, **15, 16** and **17**, respectively whereas the IC_{50} value for noscapine, **15, 16**, and **17** in MDA-MB-231 cells was measured to be 59.3 µM, 47.3 µM, 33.7 µM, and 24.1 µM, respectively (Table 3.2). Both the MCF-7 and MDA-MB-231 cell lines had different IC_{50} values indicating that the sensitivity of cancer cells to these compounds is cell type-dependent. Furthermore, the toxicity of noscapine and its 9-(N-arylmethylamino) derivatives to normal

healthy cells if any, was assessed using normal human embryonic kidney cells (293T). The anti-proliferative activity was found to be < 5% with the treatment of these compounds at a high concentration of 100 µM (Figure 3.8), indicating very negligible or no toxicity to healthy normal cells.

Table 3.2: IC_{50} values of 9-(N-arylmethylamino) derivatives of noscapine **15-17** in MCF-7 and MDA-MB-231 human breast cancer cell lines. When compared to noscapine, these analogues showed enhanced anti-proliferative efficacy.

Breast cancer cell lines	IC_{50} (µM)			
	Noscapine	**15**	**16**	**17**
MCF-7	45.3 ± 4.2	37.2 ± 3.2	30.9 ± 2.5	19.4 ± 1.9
MDAMB-231	59.3 ± 4.6	47.3 ± 3.5	33.7 ± 2.5	24.1 ± 2.4

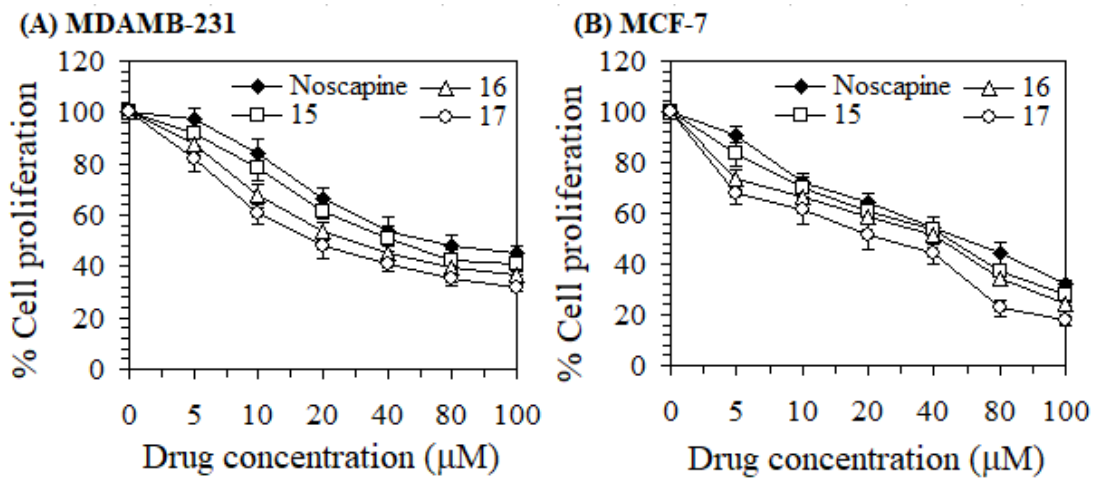

Figure 3.7: *Inhibiting the proliferation of (A) MDA-MB-231 and (B) MCF-7 cancer cells with the treatment of increasing concentration of noscapine and its 9-(N-arylmethylamino) derivatives* ***15-17*** *for 72 h. Each value is the average of three independent trials.*

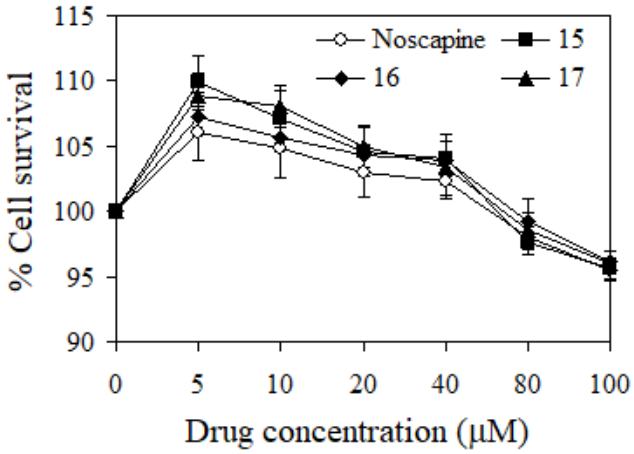

Figure 3.8: *Normal human embryonic kidney cells (293T) revealed < 5% cell death with the treatment of noscapine and 9-(N-arylmethylamino) derivatives* ***15-17*** *for 72 h. Each value represents the average of 3 independent trials.*

3.3.5. 9-(N-arylmethylamino) derivatives 15-17 induced apoptosis to cancer cells

The induction of apoptosis in breast cancer cells after treatment with 9-(N-arylmethylamino) derivatives **15-17** was done by FACS using annexin V and propidium iodide (PI). Annexin V is used to identify the phosphatidylserine that is translocated to the cell membrane's outer leaflet during apoptosis and the propidium iodide to DNA. Table 3.3 shows the proportion of early and late apoptotic cells after treatment with IC_{50} concentrations of noscapine and its derivatives **15-17** for 72 h using the MDA-MB-231 breast cancer cell line. Figure 3.9 illustrates a representative flow cytometry study. After 72 h of culture, the untreated control cell had only a small percentage of early (3.5%) and late (2.0%) apoptotic cells, which were deemed background cell death due to normal necrosis of cells (Table 3.3). In contrast, with treatments of noscapine and its derivatives **15-17**, the percentages of early apoptotic cells of 20%, 40%, 35%, and 30%, as well as late apoptotic cells of 28%, 36%, 43%, and 50% were found to be significantly higher than control untreated cells. (Table 3.3).

Table 3.3: Flow cytometry was used to determine the percentage of cells that were early apoptotic (Q1), late apoptotic (Q2), viable (Q3), and necrotic (Q4).

Viability/Apoptotic	Control	Noscapine	15	16	17
Viable Cell	94%	40%	10%	15%	10%
Early Apoptotic	2%	20%	40%	35%	30%
Late Apoptotic	4%	28%	36%	43%	50%
Necrotic	0%	0%	10%	10%	10%

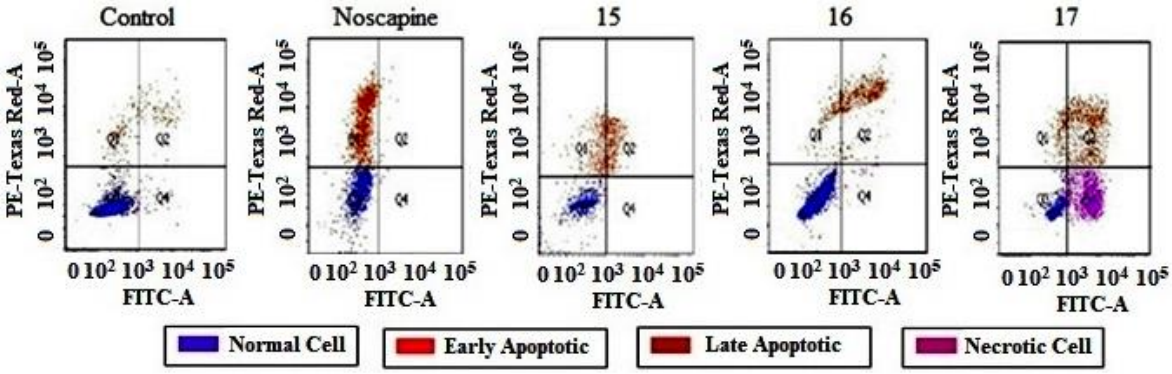

Figure 3.9: *Flow cytometry investigation of MDA-MB-231 cells treated with noscapine and its derivatives* ***15-17*** *and compared to non-treated cells. The fluorescent dye, propidium iodide (PI) was used in combination with the Alexa Fluor 488 conjugate of Annexin-V to discern between three sub-populations: PI-positive and Alexa Fluor 488-positive, indicating late apoptotic cells (PI+, Alexa Fluor 488+), PI-negative and Alexa Fluor 488-negative, indicating viable cells (PI-, Alexa Fluor 488-), PI-negative and Alexa Fluor 488-positive, indicating early apoptotic cells (PI-, Alexa Fluor 488+).*

3.3.6. Inhibition of cell cycle progression by noscapine and its derivatives, 15-17

The impact of noscapine and its derivatives **15-17** (with the treatment of IC_{50} concentration) in cell cycle progression of MDA-MB-231 cells is illustrated in Figure 3.10. The deposition of fluorescently tagged DNA in the presence of **15-17** reveals that cell cycle progression has been disrupted. The presence of 2N DNA suggests that the cells are in the G1 phase, whereas the aggregation of duplicated 4N DNA indicates that they are in the G2 and M phases, respectively. The cells in the S phase (in which DNA is being synthesized) are evidenced by DNA accumulation between the 2N and 4N peaks. On the other hand, less than 2N DNA suggests apoptotic cells in which DNA is degraded to varying extents. The cell cycle profile of MDA-MB-231 cells was significantly inhibited after 72 h of treatment with IC_{50} concentrations of noscapine and its derivatives **15-17** (Table 3.4). A significant amount of cells were accumulated in the G2/M phase. A hypodiploid DNA content peak (sub-G1) was found to rise in the G2/M phase, indicating dead cells.

Table 3.4: The effects of noscapine and its derivatives **15-17** on cell cycle progression in MDA-MB-231 cells treated with IC_{50} concentration for 72 h.

	72 hours			
	Sub-G_1	G_0/G_1	S	G_2/M
Control	0.7	20	22.4	11.2
Noscapine	4.9	17.5	15.1	17.5
15	7.5	13.8	10	19.1
16	8.9	14	8.2	35.7
17	10.8	25	10.0	43.2

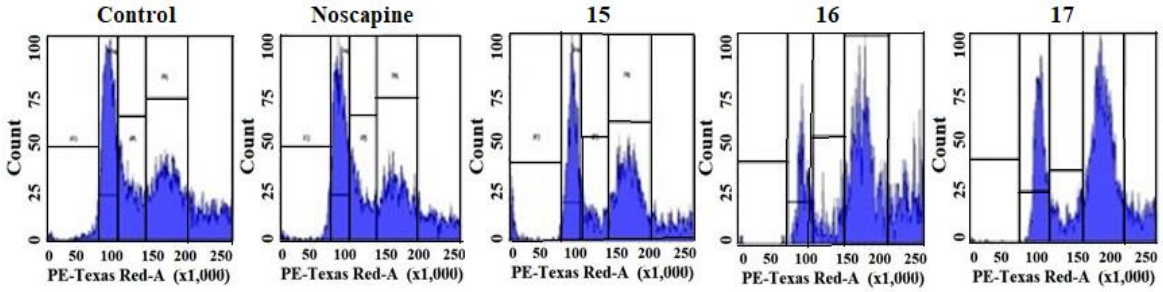

Figure 3.10: *Noscapine and its derivatives* ***15-17*** *disrupt cell cycle progression during the G2/M phase, followed by the emergence of a hypodiploid (sub-G1) DNA peak, suggesting apoptotic cells.*

3.3.7. 9-(N-arylmethylamino) derivatives of noscapine 15-17 were found to bind tubulin

Due to the inclusion of numerous tryptophan amino acids, tubulin is autofluorescent in nature, hence a drop in emission fluorescence associated with ligand binding owing to conformational changes might be beneficial in monitoring ligand binding. In the presence of 25 µM concentration of 9-(N-arylmethylamino) derivatives of noscapine **15-17**, the

fluorescence intensity was reduced by 38%, 17.39%, and 25.47%, respectively, indicating these compounds bind to tubulin and altered its conformation (Figure 3.11).

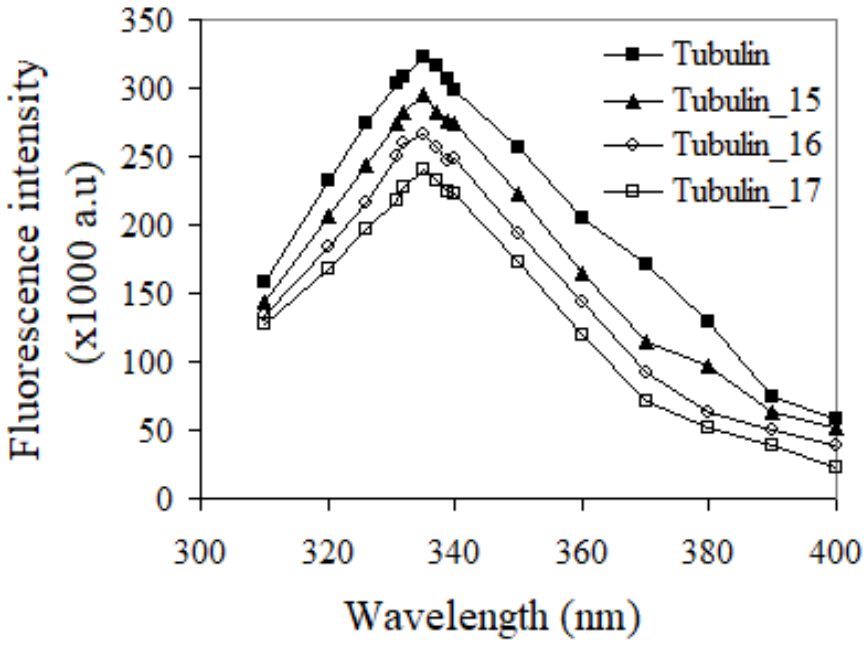

Figure 3.11: *Decrease of fluorescence intensity of tubulin by 9-(N-arylmethylamino) noscapinoids, 15-17. Tubulin (2.0 μM) was incubated with compounds* ***15-17*** *(25 μM) and the emission spectra were collected (310 nm – 400 nm). All the three compounds showed a quenching of the intrinsic tubulin fluorescence emission intensity, indicating their binding to tubulin. The graph is a representative of three independent experiments.*

3.4. Conclusion

A series of 9-(N-arylmethylamino) derivatives of noscapine were designed in order to enhance the activity of noscapine. For the synthesis of the selected molecules from the library the N-aryl methyl pharmacophore was substituted at the C-9 position of the isoquinoline ring of noscapine. When tested against the two human breast cancer cell lines MCF-7 and MDA-MB-231, the three screened derivatives showed a significant increase in the antiproliferative activity to cancerous cells without causing any harm to the normal cells. As a result, this class of compounds may be quite beneficial in the treatment of breast cancer along with other cancer types also. Our findings encourage us to keep looking into the impacts of these new compounds in vivo animal research, with the ultimate goal of moving on to a human clinical trial.

Appendix

A3.1: ^{1}H NMR of 9-arylimino noscapinoid, 12

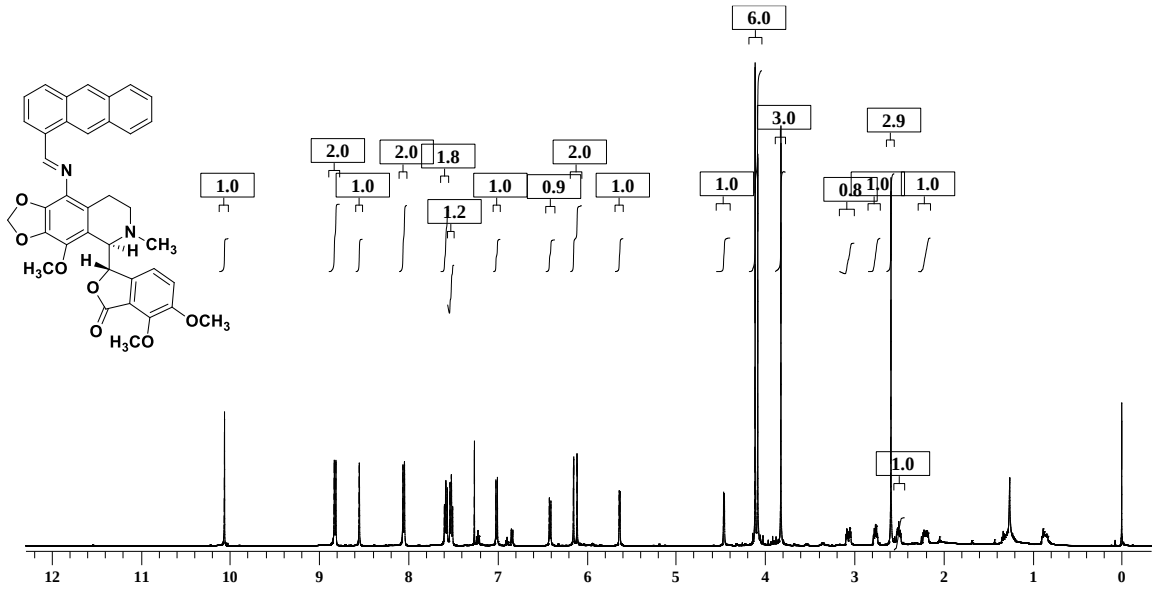

A3.2: ^{13}C NMR of 9-arylimino noscapinoid, 12

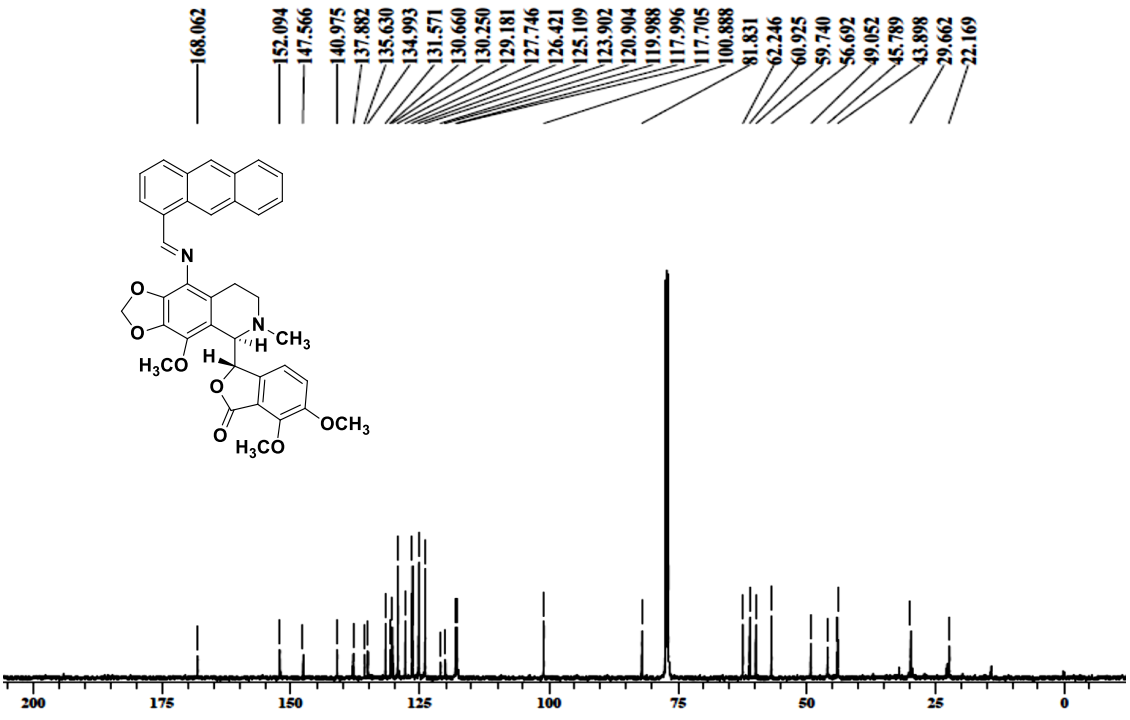

.

A3.3: HRMS of 9-arylimino noscapinoid, 12

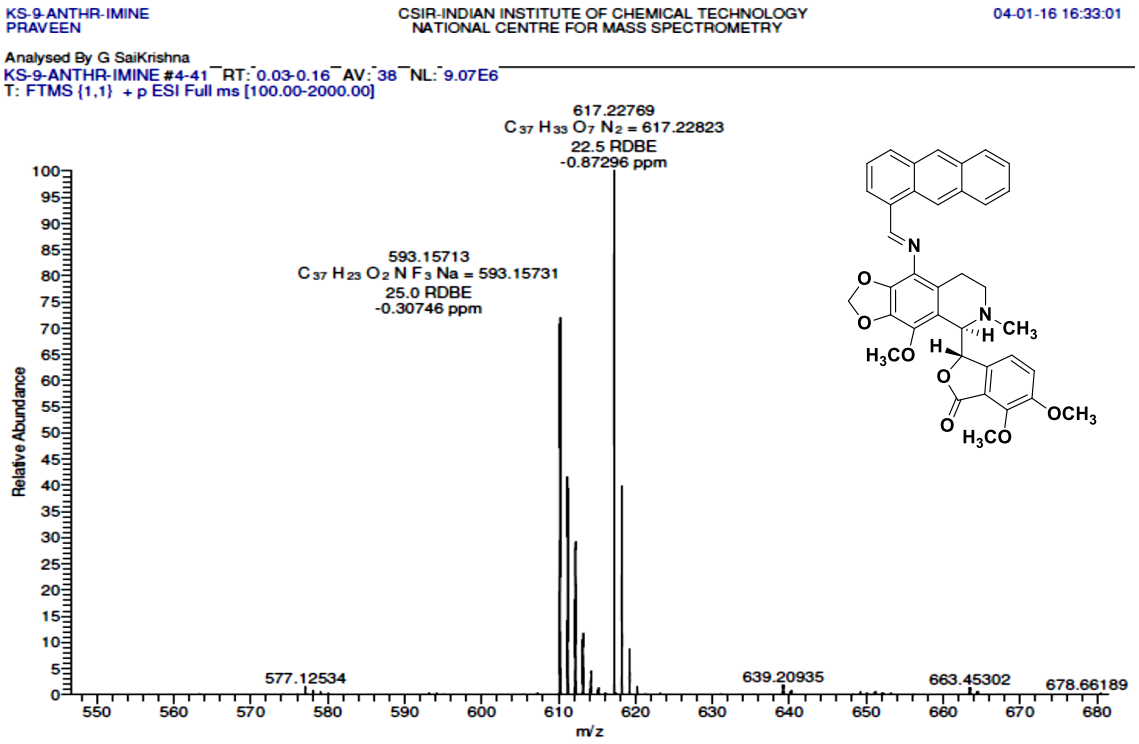

A3.4: ^{1}H NMR of 9-(N-Arylmethylamino), 15

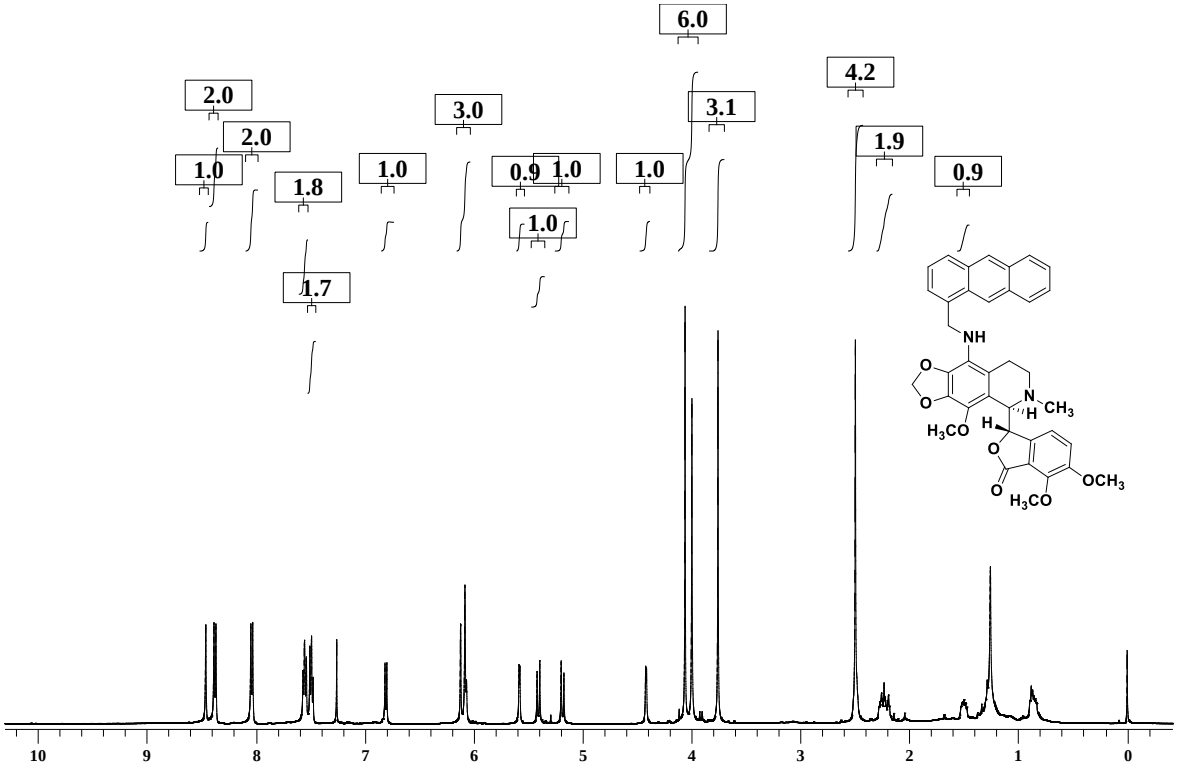

A3.5: ^{13}C NMR of 9-(N-Arylmethylamino), 15

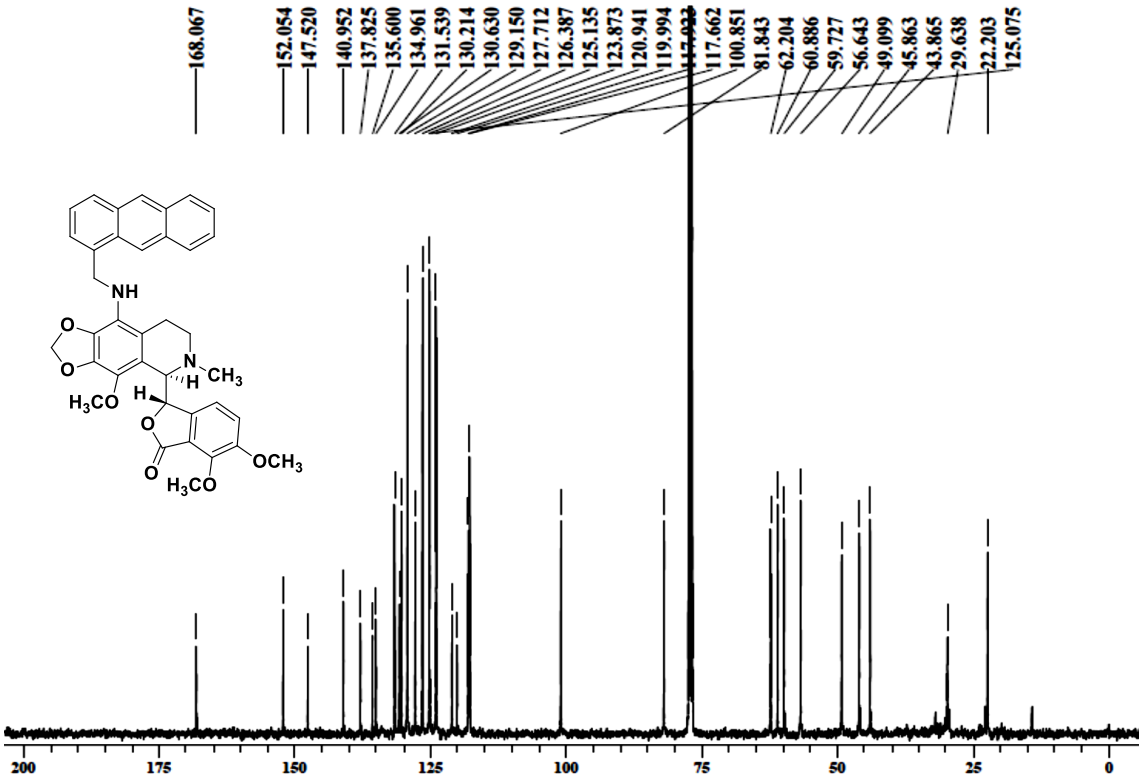

A3.6: HRMS of 9-(N-Arylmethylamino), 15

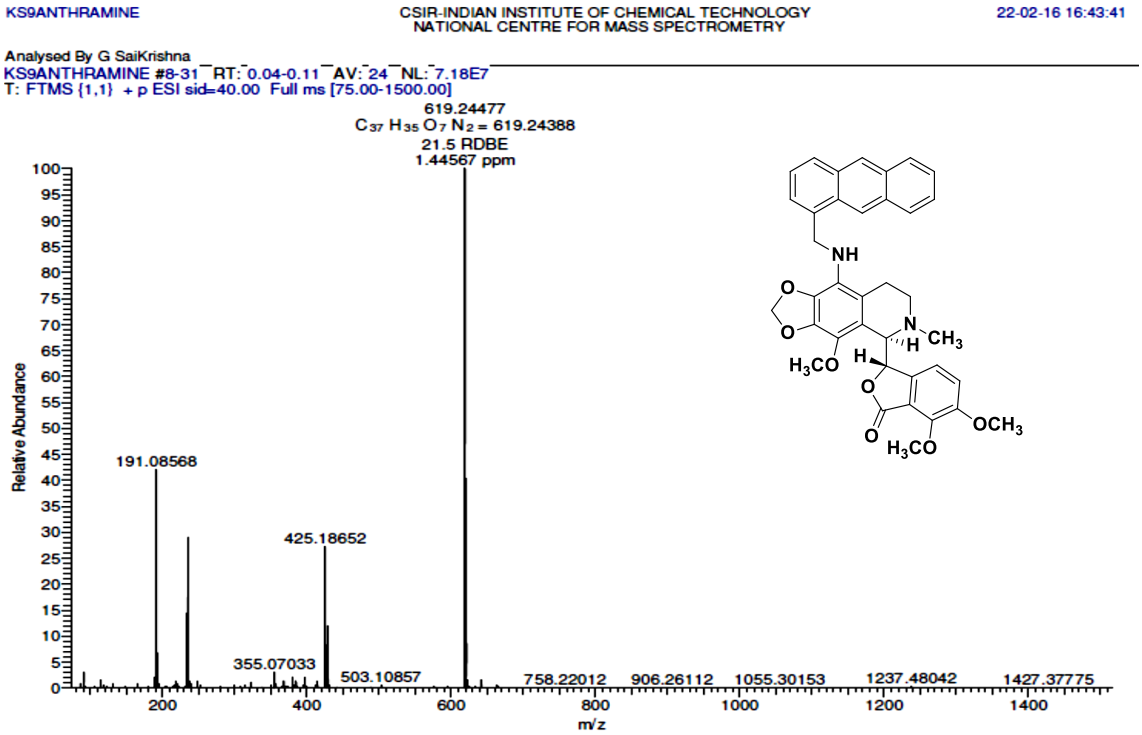

A3.7: ^{1}H NMR of 9-arylimino noscapinoid, 13

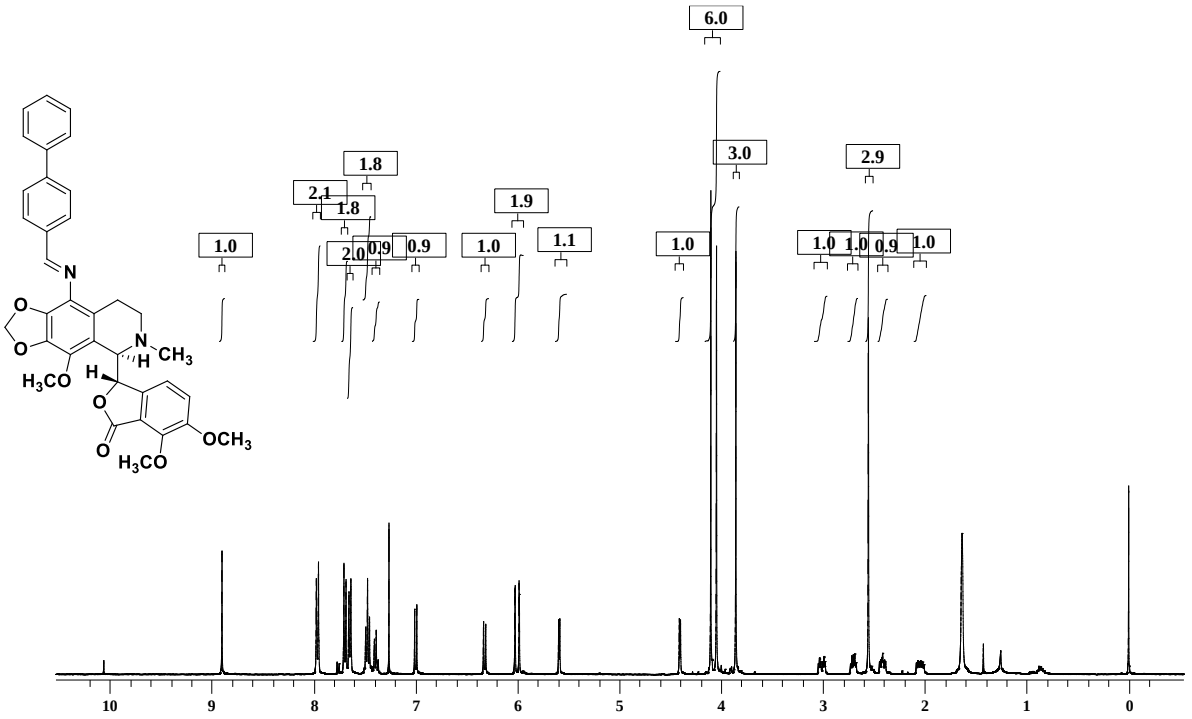

A3.8: : ^{13}C NMR of 9-arylimino noscapinoid, 13

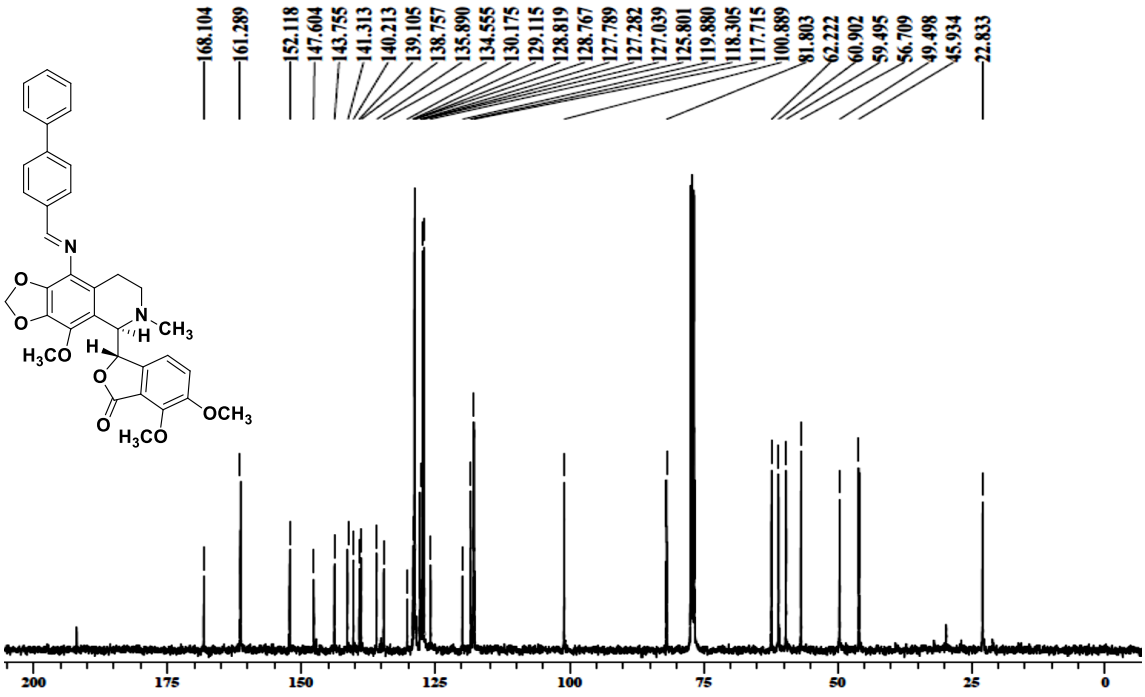

A3.9: HRMS of of 9-arylimino noscapinoid, 13

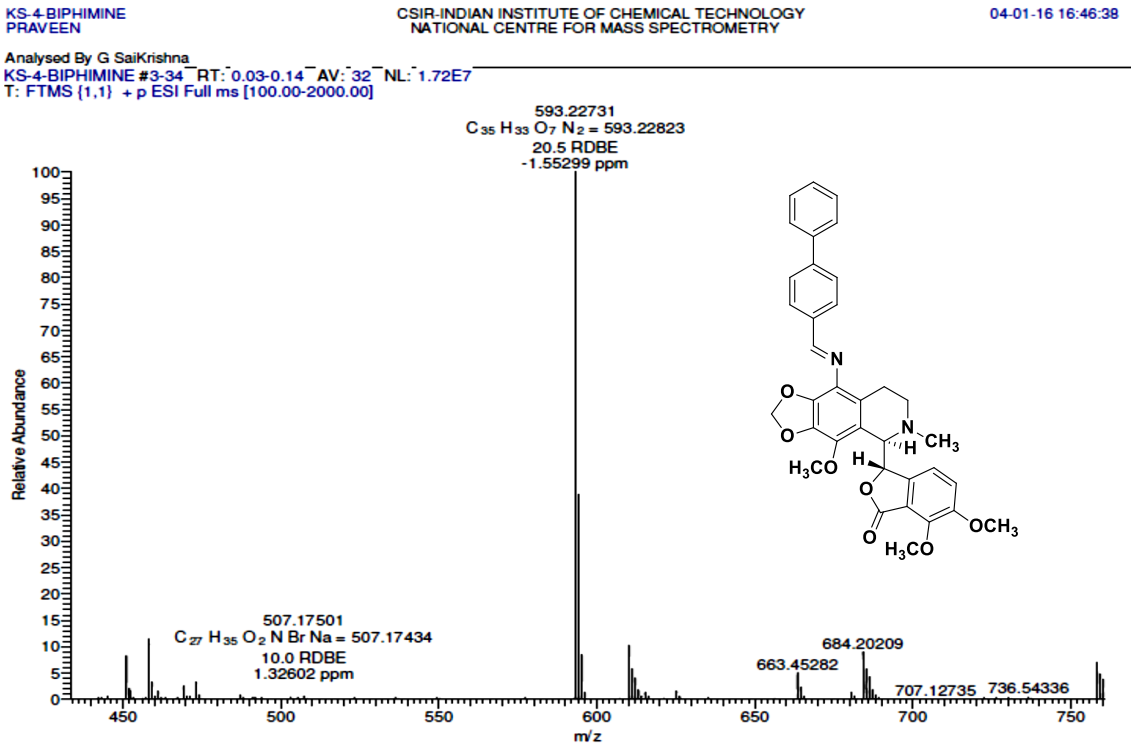

A3.10: ^{1}H NMR of 9-N-Arylmethylamino, 16

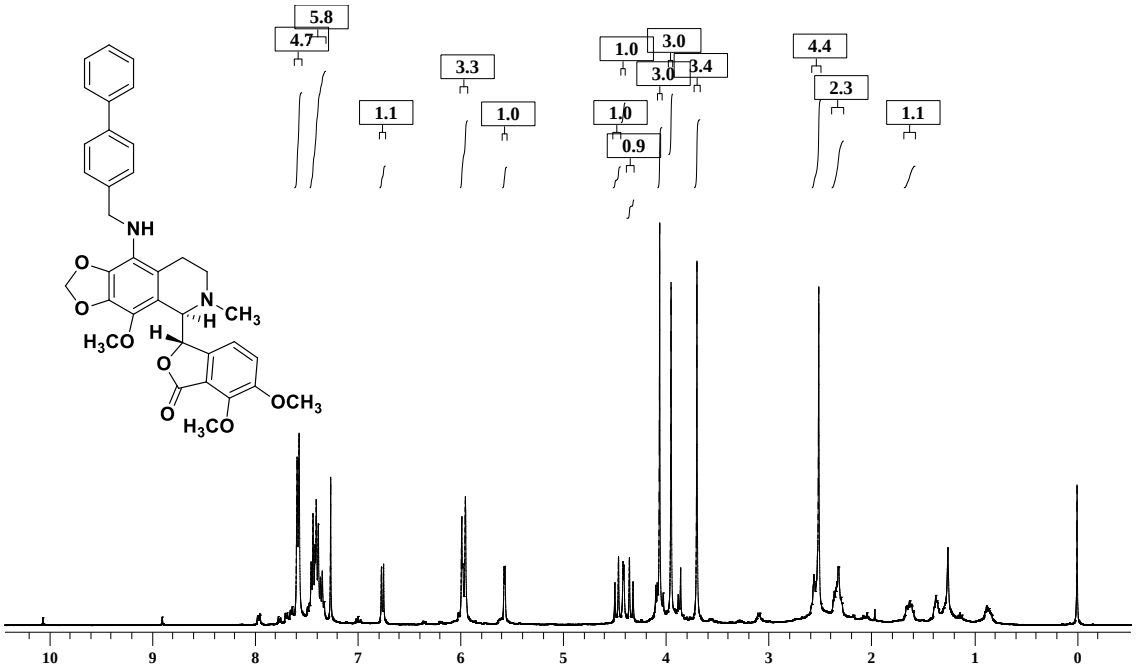

A3.11: ^{13}C NMR of 9-N-Arylmethylamino, 16

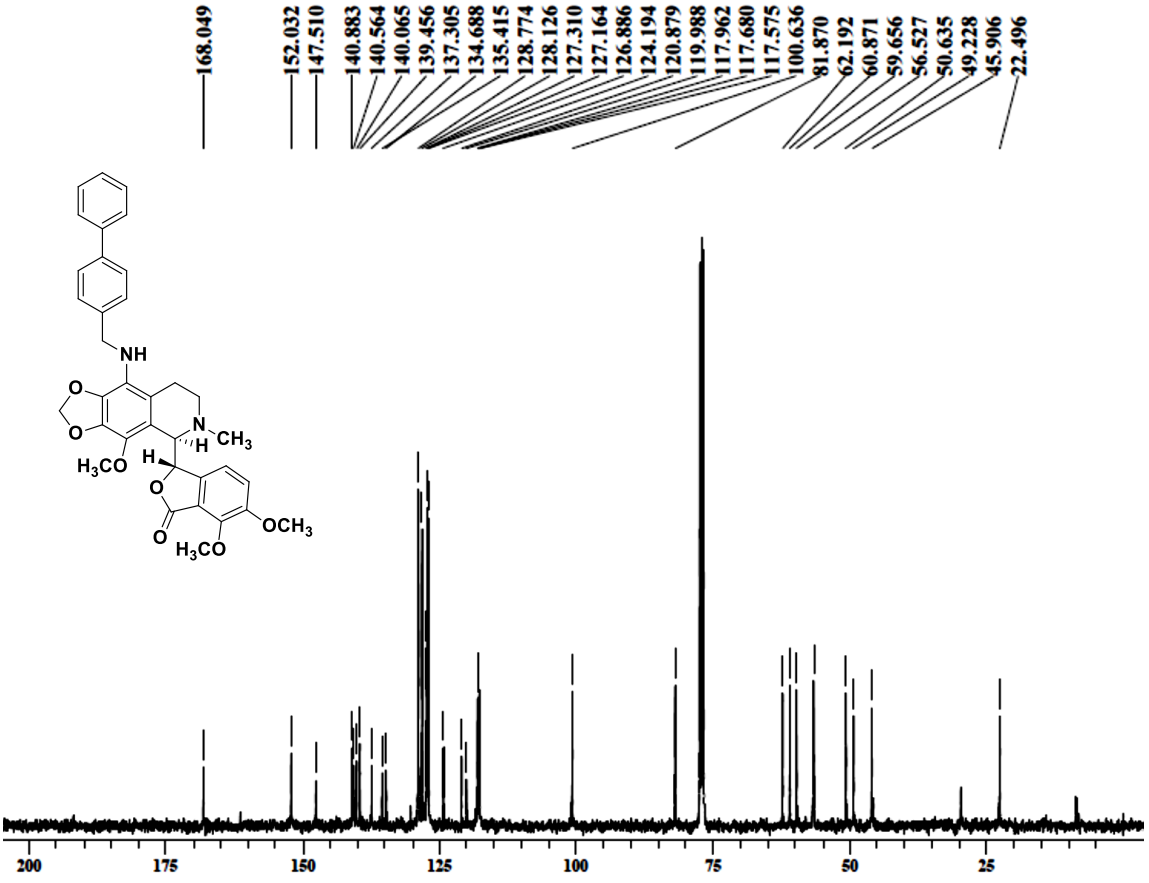

A3.12: HRMS of 9-N-Arylmethylamino, 16

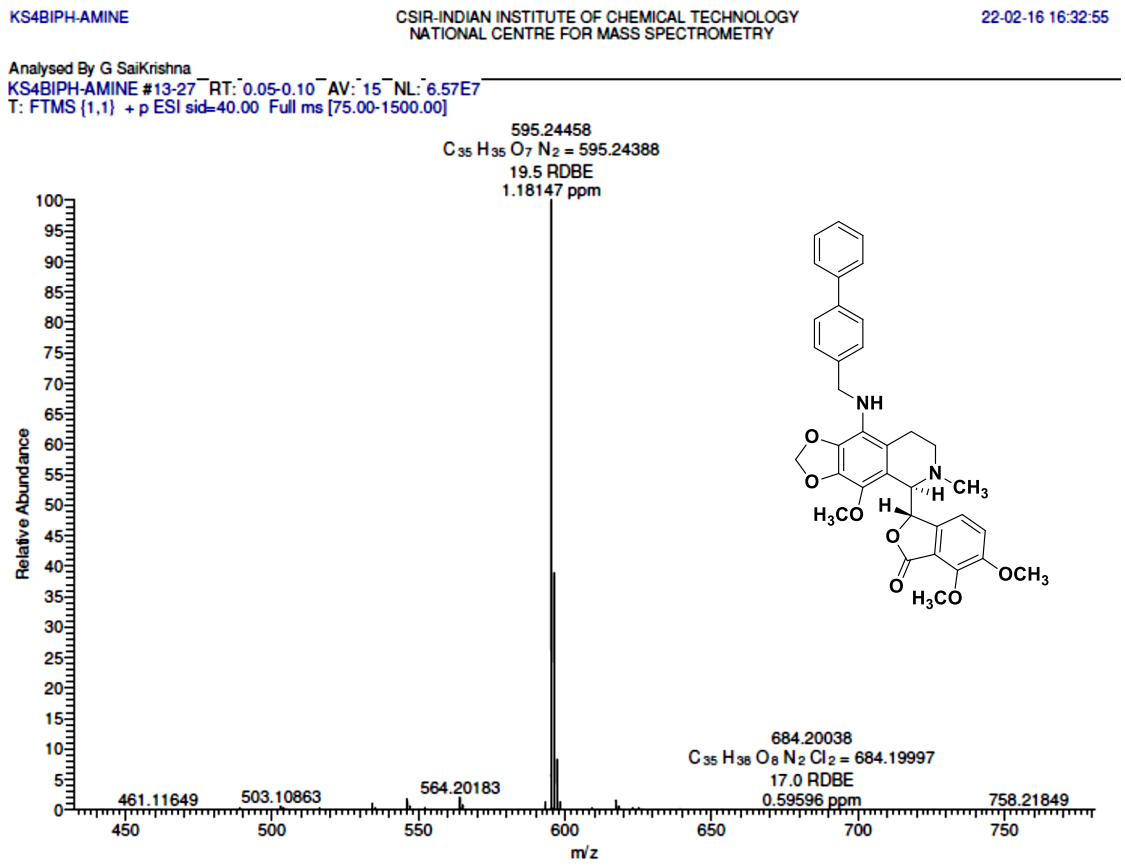

A3.13: ^{1}H NMR of 9-arylimino noscapinoid, 14

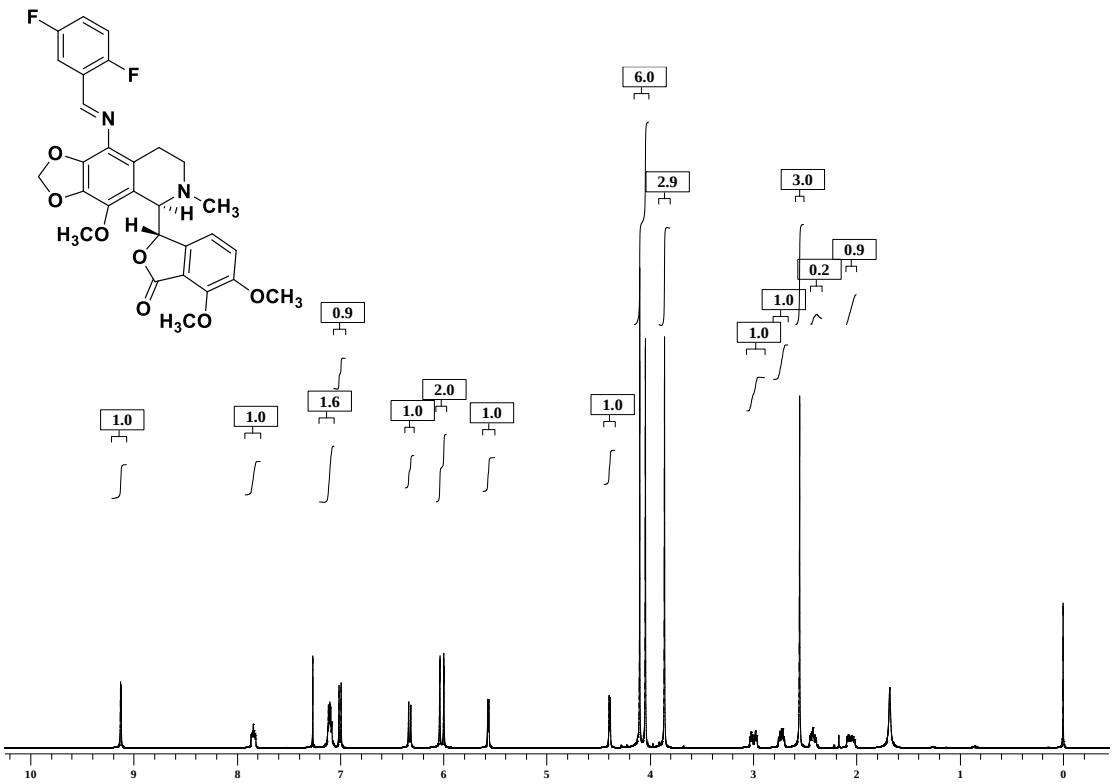

A3.14: ^{13}C NMR of 9-arylimino noscapinoid, 14

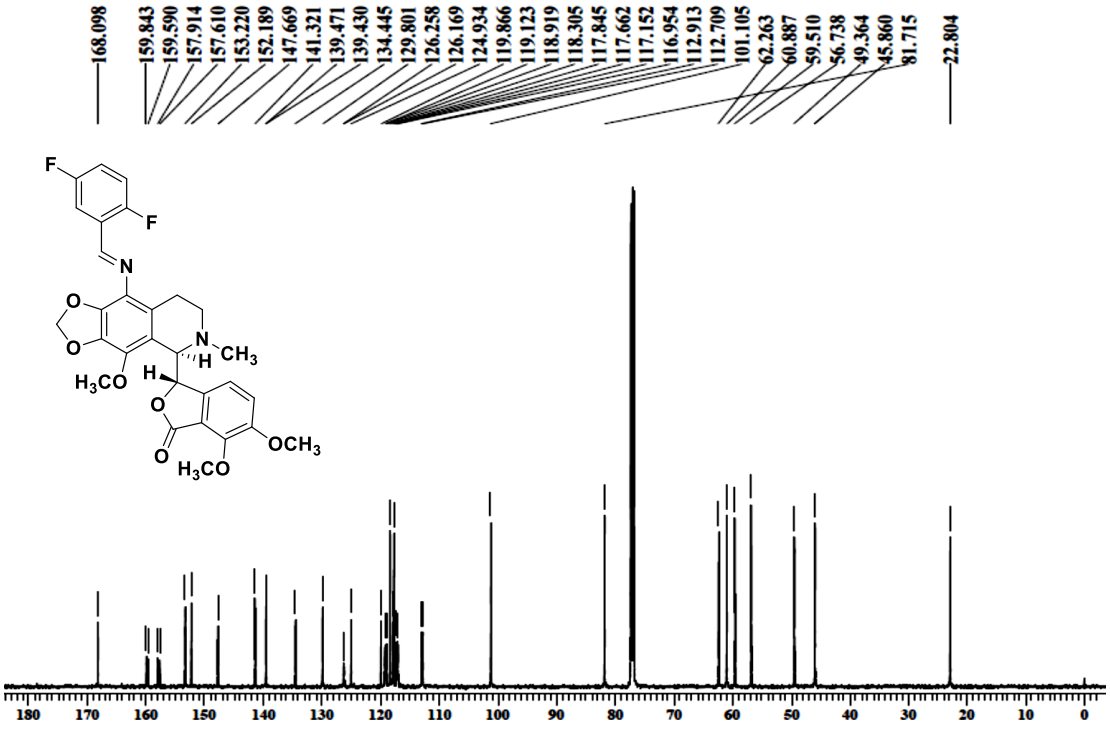

A3.15: ESI- mass spectra of 9-arylimino noscapinoid,14

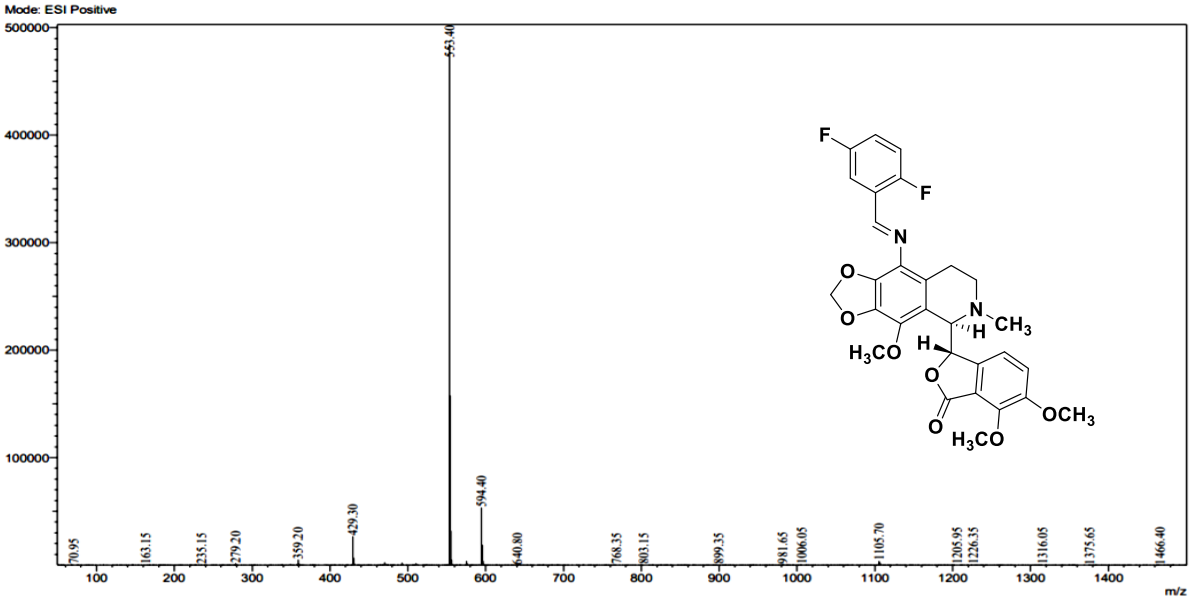

A3.16: HRMS of 9-arylimino noscapinoid, 14

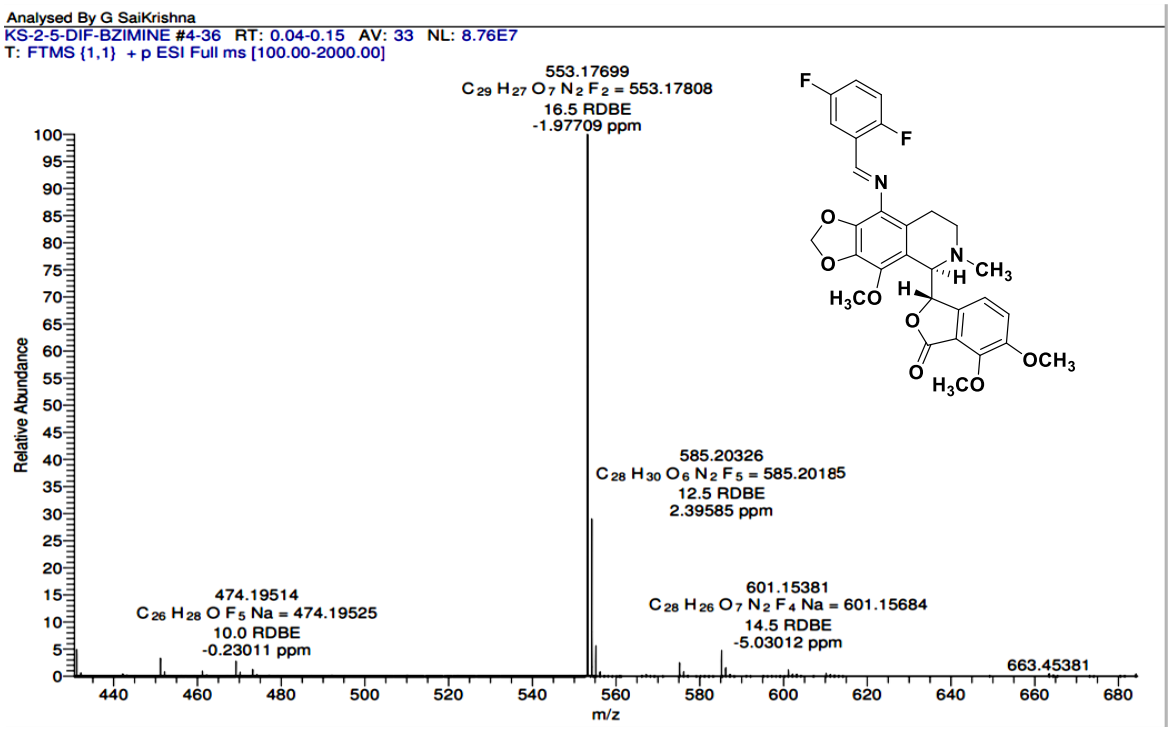

A3.17: ^{1}H NMR of 9-N-Arylmethylamino, 17

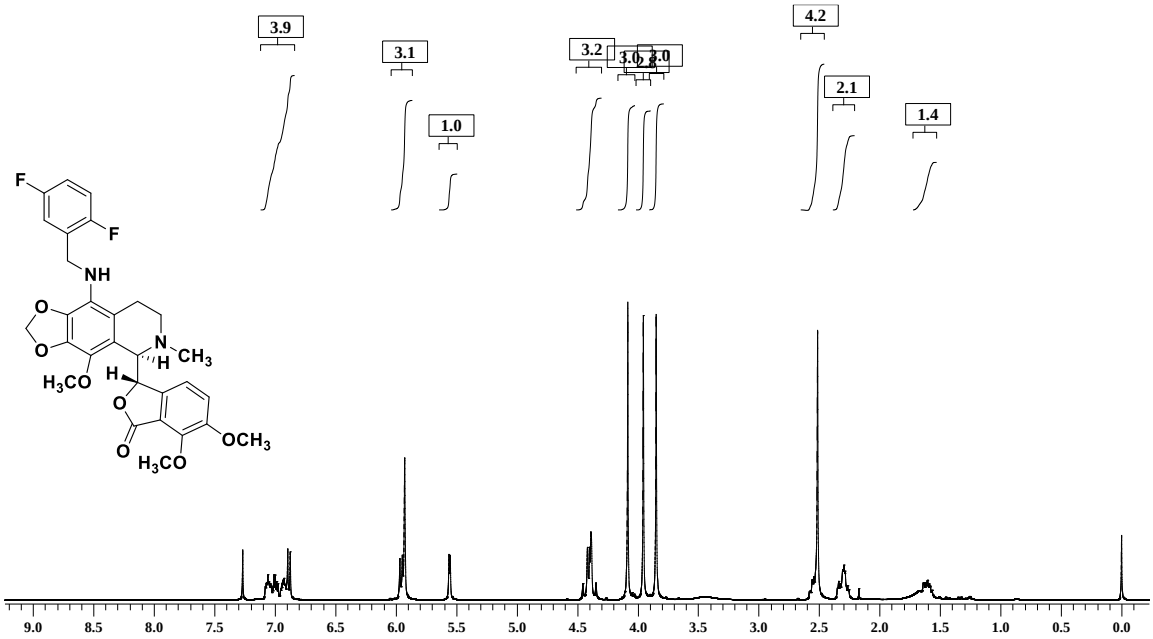

A3.18: ^{13}C NMR of 9-N-Arylmethylamino, 17

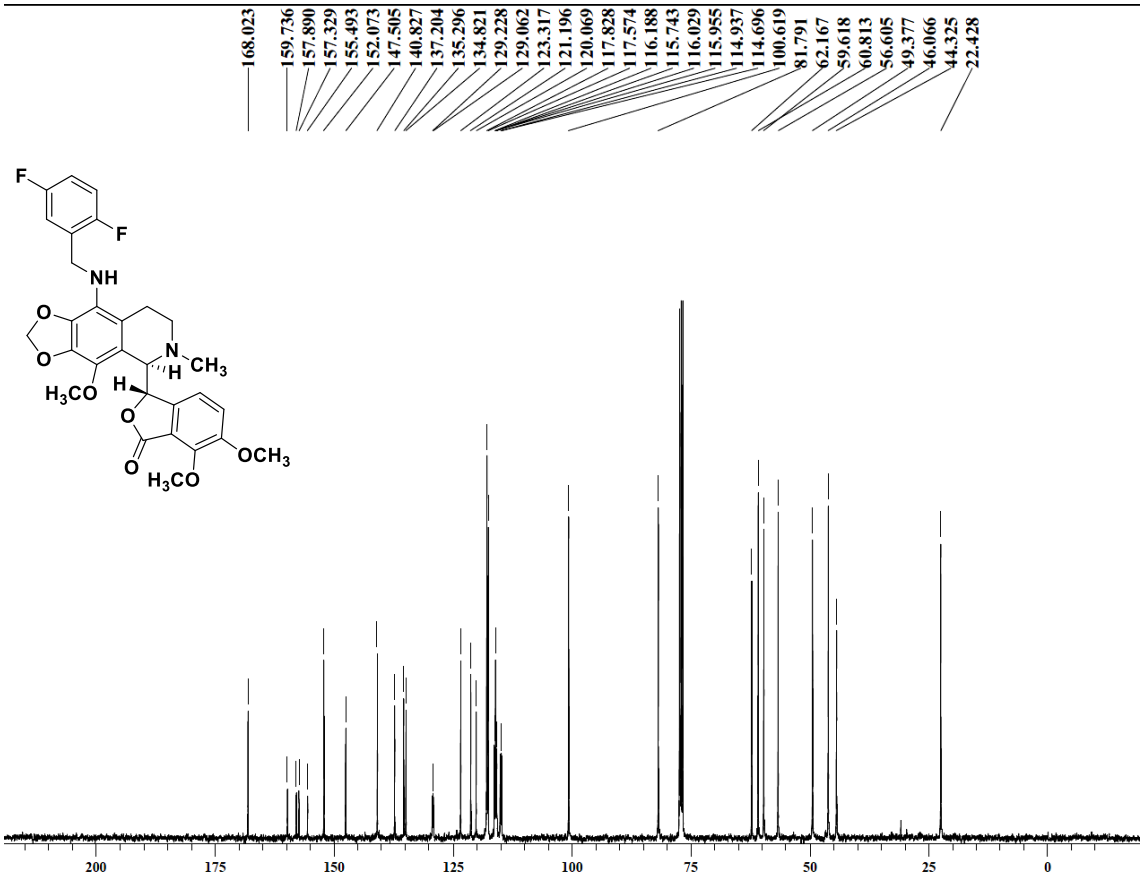

A3.19: ESI- mass spectra of 9-N-Arylmethylamino, 17

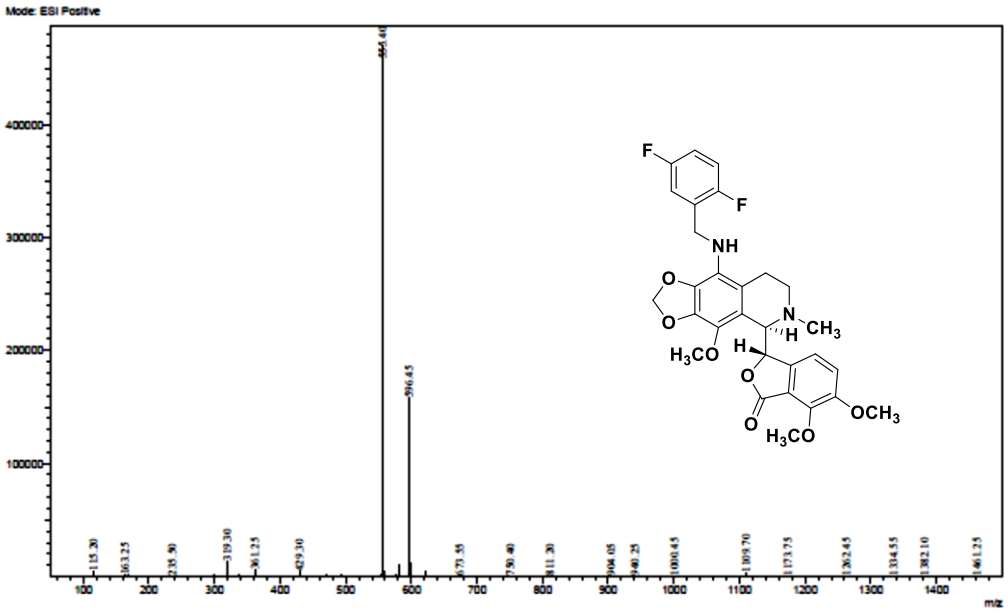

Table A3.20-A3.23: Geometry of hydrogen bonds and hydrophobic interaction of 9-(N-Arylmethylamino) noscapinoids, **15-17** and the lead molecule, noscapine with the binding site residues of tubulin.

Table A3.20			**Table A3.21**		
(a) Noscapine_Tubulin			**(b) 15_Tubulin**		
Hydrogen bonding			**Hydrogen bonding**		
Hydrogen Donor (D)	**Hydrogen Acceptor (A)**	**Distance (D-A) in Å**	**Hydrogen Donor (D)**	**Hydrogen Acceptor (A)**	**Distance (D-A) in Å**
GLN D 247 NE2	Noscapine O2	3.04	GLN D 247 NE2	15 N1	3.34
GLU D 47 OE2	Noscapine N1	4.10	15 N2	GLU A 77 OE2	4.55
ARG D 48 NH2	Noscapine O5	3.37			
Hydrophobic interaction			**Hydrophobic interaction**		
Noscapine	**Tubulin**	**Distance**	**15**	**Tubulin**	**Distance**
C20	LYS D 254 NZ	3.42	C11	ASP D 357 OD1	4.8
C16	LYS D 254 NZ	4.9	C26	LYS D 254 NZ	4.69
C20	LYS D 254 CE	3.9	C25	LYS D 254 NZ	4.45
C20	LYS D 254 CD	3.94	C32	ALA D 250 CB	4.78
C20	LYS D 254 CG	4.95	C31	ALA D 250 CB	4
C20	ASP D 251 OD2	3.2	C30	ALA D 250 CB	4.83
C17	ASP D 251 OD2	4.65	C29	ALA D 250 CB	4.06
C20	ASP D 251 CG	4.32	C28	ALA D 250 CB	3.6
O4	ASP D 251 CG	4.49	C27	ALA D 250 CB	4.28
C20	ASP D 251 CB	5	C26	ALA D 250 CB	3.87
O4	ASP D 251 CB	4.73	C25	ALA D 250 CB	3.5
C20	ALA D 250 CB	3.93	C24	ALA D 250 CB	4.37
O6	ALA D 250 CB	4.52	C32	ALA D 250 O	4.89
O5	ALA D 250 CB	4.8	C31	ALA D 250 O	4.9
O4	ALA D 250 CB	3.77	C27	GLN D 247 OE1	4.35
C19	ALA D 250 CB	4.48	C26	GLN D 247 OE1	4.69
C18	ALA D 250 CB	4.05	C27	GLN D 247 NE2	4.09
C17	ALA D 250 CB	3.45	C26	GLN D 247 NE2	5
C16	ALA D 250 CB	3.26	C24	GLN D 247 NE2	4.85
C15	ALA D 250 CB	3.7	C23	GLN D 247 NE2	4.61
C14	ALA D 250 CB	4.32	C20	GLN D 247 NE2	4.44
C13	ALA D 250 CB	4.3	C19	GLN D 247 NE2	3.75
C18	ALA D 250 O	4.52	C18	GLN D 247 NE2	3.95
C17	ALA D 250 O	4.73	C17	GLN D 247 NE2	4.78
O4	ALA D 250 C	4.75	C10	GLN D 247 NE2	4.71
C18	ALA D 250 C	4.98	C9	GLN D 247 NE2	3.86
C17	ALA D 250 C	4.83	C8	GLN D 247 NE2	4.77
O4	ALA D 250 CA	4.92	C3	GLN D 247 NE2	4.7
C17	ALA D 250 CA	4.76	C1	GLN D 247 NE2	3.74
C16	ALA D 250 CA	4.76	C27	GLN D 247 CD	4.26
C13	GLN D 247 OE1	4.68	C26	GLN D 247 CD	4.95
C13	GLN D 247 NE2	4.22	N1	GLN D 247 CD	4.11
C10	GLN D 247 NE2	3.63	O7	GLN D 247 CD	4.92
C9	GLN D 247 NE2	3.91	C10	GLN D 247 CD	4.9
C8	GLN D 247 NE2	3.42	O1	GLN D 247 CD	4.15
C4	GLN D 247 NE2	4.81	C9	GLN D 247 CD	4.55
C2	GLN D 247 NE2	4.78	C1	GLN D 247 CD	4.66
C1	GLN D 247 NE2	3.94	N1	GLN D 247 CG	4.53
O7	GLN D 247 CD	4.87	C10	GLN D 247 CG	3.97
O6	GLN D 247 CD	3.59	O1	GLN D 247 CG	3.54
C13	GLN D 247 CD	4.49	C9	GLN D 247 CG	4.32
O3	GLN D 247 CD	4.71	C1	GLN D 247 CG	4.88
O2	GLN D 247 CD	4.24	C10	GLN D 247 CB	4.67
C10	GLN D 247 CD	4.85	O1	GLN D 247 CB	4.24
C8	GLN D 247 CD	4.69	C27	GLN D 247 O	4.88
O6	GLN D 247 CG	4.41	C26	GLN D 247 O	4.63
O6	GLN D 247 CB	4.52	C27	GLN D 247 CA	4.19

O6	GLN D 247 C	4.48	C26	GLN D 247 CA	4.66
O6	GLN D 247 CA	3.65	N1	GLN D 247 CA	4.75
C13	GLN D 247 CA	4.39	C10	GLN D 247 CA	4.8
O3	GLN D 247 CA	4.82	O1	GLN D 247 CA	4.07
C13	GLN D 247 N	4.6	C27	GLN D 247 N	4.54
C16	GLY D 246 O	4.45	C23	GLN D 247 N	4.93
C15	GLY D 246 O	3.74	C10	GLN D 247 N	3.84
C14	GLY D 246 O	4.16	C9	GLN D 247 N	4.44
C13	GLY D 246 O	3.15	C30	GLY D 246 O	4.85
C12	GLY D 246 O	4.08	C29	GLY D 246 O	4.07
O6	GLY D 246 C	4.06	C28	GLY D 246 O	4.64
C15	GLY D 246 C	4.88	C27	GLY D 246 O	3.21
C13	GLY D 246 C	4.09	C26	GLY D 246 O	3.92
O3	GLY D 246 C	4.03	C25	GLY D 246 O	4.57
C12	GLY D 246 C	4.91	C24	GLY D 246 O	3.3
O3	GLY D 246 CA	4.87	C23	GLY D 246 O	3.5
C12	GLY D 246 N	4.63	C10	GLY D 246 O	4.89
N1	PRO D 245 CB	4.9	C9	GLY D 246 O	4.59
C12	PRO D 245 CB	4.89	C1	GLY D 246 O	4.62
C7	PRO D 245 CB	3.79	C27	GLY D 246 C	4.14
C6	PRO D 245 CB	3.58	C26	GLY D 246 C	4.94
C3	PRO D 245 CB	4.63	C24	GLY D 246 C	4.27
C6	PRO D 245 CD	4.92	C23	GLY D 246 C	4.14
C7	PRO D 245 CG	4.07	N1	GLY D 246 C	4.03
C6	PRO D 245 CG	3.73	C10	GLY D 246 C	4.01
C12	PRO D 245 CA	4.74	O1	GLY D 246 C	3.17
C7	PRO D 245 CA	4.82	C9	GLY D 246 C	4.23
C6	PRO D 245 CA	4.2	C1	GLY D 246 C	4.65
C21	ARG D 48 NH2	4.66	C23	GLY D 246 CA	4.72
C19	ARG D 48 NH2	3.73	N1	GLY D 246 CA	4.71
C18	ARG D 48 NH2	3.75	O2	GLY D 246 CA	4.89
C17	ARG D 48 NH2	4.76	C10	GLY D 246 CA	3.79
C14	ARG D 48 NH2	4.68	O1	GLY D 246 CA	3.3
C19	ARG D 48 NH1	4.4	C9	GLY D 246 CA	4.35
C18	ARG D 48 NH1	4.94	C1	GLY D 246 CA	4.98
C14	ARG D 48 NH1	4.74	C24	GLY D 246 N	4.73
O5	ARG D 48 CZ	4.23	C23	GLY D 246 N	4.01
C19	ARG D 48 CZ	3.85	C10	GLY D 246 N	3.9
C18	ARG D 48 CZ	4.32	C9	GLY D 246 N	3.91
C14	ARG D 48 CZ	4.56	C8	GLY D 246 N	4.66
C19	ARG D 48 NE	4.07	C1	GLY D 246 N	4.35
C18	ARG D 48 NE	4.78	N2	PRO D 245 CB	4.86
C14	ARG D 48 NE	4.84	C23	PRO D 245 CB	4.41
C11	ARG D 48 NE	4.33	N1	PRO D 245 CB	4.48
C19	ARG D 48 CD	4.88	C11	PRO D 245 CB	3.89
C11	ARG D 48 CD	4.28	O3	PRO D 245 CB	4.3
C6	ARG D 48 CD	4.62	O2	PRO D 245 CB	4.02
C11	ARG D 48 CG	4.55	C10	PRO D 245 CB	4.41
C11	GLU D 47 OE2	4.56	O1	PRO D 245 CB	4.07
C7	GLU D 47 OE2	3.02	C9	PRO D 245 CB	3.51
C6	GLU D 47 OE2	3.07	C8	PRO D 245 CB	3.46
C3	GLU D 47 OE2	4.47	C7	PRO D 245 CB	4.43
C7	GLU D 47 OE1	4.89	C5	PRO D 245 CB	4.7
C6	GLU D 47 OE1	4.95	C4	PRO D 245 CB	3.72
C7	GLU D 47 CD	4.17	C3	PRO D 245 CB	3.7
C6	GLU D 47 CD	4.05	C2	PRO D 245 CB	3.61
C6	GLU D 47 CG	4.57	C1	PRO D 245 CB	3.7
C21	MET D 1 CE	3.79	N2	PRO D 245 CG	4.88
C20	MET D 1 CE	3.31	C11	PRO D 245 CG	4.27
O5	MET D 1 CE	4.27	O3	PRO D 245 CG	4.92
O4	MET D 1 CE	3.06	C9	PRO D 245 CG	4.92
C18	MET D 1 CE	4.78	C8	PRO D 245 CG	4.71

C17	MET D 1 CE	4.32	C7	PRO D 245 CG	4.99
C20	MET D 1 SD	4.82	C4	PRO D 245 CG	4.44
O4	MET D 1 SD	4.79	C3	PRO D 245 CG	4.59
C21	MET D 1 O	3.36	C2	PRO D 245 CG	4.5
C18	MET D 1 O	4.95	C1	PRO D 245 CG	4.93
C21	MET D 1 C	4.4	C11	PRO D 245 O	4.97
O5	MET D 1 C	4.85	C10	PRO D 245 O	3.13
C21	MET D 1 N	4.37	C9	PRO D 245 O	3.83
C20	ASP A 98 OD2	2.95	C8	PRO D 245 O	3.87
C20	ASP A 98 OD1	4.3	C2	PRO D 245 O	4.85
C20	ASP A 98 CG	3.93	C1	PRO D 245 O	4.76
O4	ASP A 98 CG	4.94	C23	PRO D 245 C	4.46
C10	GLU A 77 OE2	3.79	N1	PRO D 245 C	4.54
C9	GLU A 77 OE2	3.33	O2	PRO D 245 C	4
C8	GLU A 77 OE2	3.55	C10	PRO D 245 C	3.6
C4	GLU A 77 OE2	4.39	O1	PRO D 245 C	3.29
C3	GLU A 77 OE2	4.19	C9	PRO D 245 C	3.66
C2	GLU A 77 OE2	3.67	C8	PRO D 245 C	4.04
C1	GLU A 77 OE2	4.1	C2	PRO D 245 C	4.95
C10	GLU A 77 OE1	4.34	C1	PRO D 245 C	4.26
C9	GLU A 77 OE1	4.89	C23	PRO D 245 CA	4.33
C8	GLU A 77 OE1	4.73	N1	PRO D 245 CA	4.68
O2	GLU A 77 CD	4.63	O2	PRO D 245 CA	4.68
C10	GLU A 77 CD	4.46	C10	PRO D 245 CA	4.63
O1	GLU A 77 CD	4.65	O1	PRO D 245 CA	4.19
C9	GLU A 77 CD	4.42	C9	PRO D 245 CA	4.07
C8	GLU A 77 CD	4.4	C8	PRO D 245 CA	4.36
C2	GLU A 77 CD	4.89	C3	PRO D 245 CA	4.68
C1	GLU A 77 CD	4.88	C2	PRO D 245 CA	4.87
C22	VAL A 74 CG2	3.12	C1	PRO D 245 CA	4.29
O7	VAL A 74 CG2	3.85	C37	ARG D 48 NH2	3.94
C1	VAL A 74 CG2	4.88	C36	ARG D 48 NH2	3.9
C22	VAL A 74 CB	4.27	C35	ARG D 48 NH2	3.69
O7	VAL A 74 CB	4.93	C34	ARG D 48 NH2	3.5
C22	VAL A 74 CA	4.29	C33	ARG D 48 NH2	3.51
C22	VAL A 74 N	4.03	C32	ARG D 48 NH2	3.76
C22	THR A 73 OG1	2.91	C31	ARG D 48 NH2	4.54
C21	THR A 73 OG1	4.34	C30	ARG D 48 NH2	4.07
C19	THR A 73 OG1	3.93	C29	ARG D 48 NH2	4.8
C18	THR A 73 OG1	4.17	C34	ARG D 48 NH1	4.61
C17	THR A 73 OG1	4.42	C33	ARG D 48 NH1	4.5
C16	THR A 73 OG1	4.5	C30	ARG D 48 NH1	4.34
C15	THR A 73 OG1	4.32	C29	ARG D 48 NH1	4.92
C14	THR A 73 OG1	3.99	C37	ARG D 48 CZ	4.81
C12	THR A 73 OG1	4.52	C36	ARG D 48 CZ	4.68
C11	THR A 73 OG1	4.25	C35	ARG D 48 CZ	4.08
C5	THR A 73 OG1	3.84	C34	ARG D 48 CZ	3.56
C4	THR A 73 OG1	4.68	C33	ARG D 48 CZ	3.7
C1	THR A 73 OG1	4.76	C32	ARG D 48 CZ	4.38
C21	THR A 73 CG2	3.71	C30	ARG D 48 CZ	3.91
O5	THR A 73 CG2	4.51	C29	ARG D 48 CZ	4.77
C19	THR A 73 CG2	4.47	C36	ARG D 48 NE	4.58
C18	THR A 73 CG2	4.59	C35	ARG D 48 NE	3.63
C11	THR A 73 CG2	4.2	C34	ARG D 48 NE	3.11
N1	THR A 73 CB	4.51	C33	ARG D 48 NE	3.71
C22	THR A 73 CB	4.08	C32	ARG D 48 NE	4.67
C21	THR A 73 CB	4.68	C30	ARG D 48 NE	3.99
C19	THR A 73 CB	4.66	C35	ARG D 48 CD	4.66
C18	THR A 73 CB	4.98	C34	ARG D 48 CD	3.95
C14	THR A 73 CB	4.94	C33	ARG D 48 CD	4.61
C11	THR A 73 CB	4.15	C30	ARG D 48 CD	4.55
C5	THR A 73 CB	4.42	C35	ARG D 48 CG	4.85

C22	THR A 73 O	4.61	C34	ARG D 48 CG	4.41
C22	THR A 73 C	4.22	C14	GLU D 47 OE2	3.06
C22	THR A 73 CA	4.74	C7	GLU D 47 OE2	4.13
C21	GLU A 71 OE2	2.71	C6	GLU D 47 OE2	3.68
C20	GLU A 71 OE2	4.28	C5	GLU D 47 OE2	4.08
C19	GLU A 71 OE2	4.72	C4	GLU D 47 OE2	4.56
C18	GLU A 71 OE2	3.86	C3	GLU D 47 OE2	4.7
C17	GLU A 71 OE2	3.76	C14	GLU D 47 OE1	4.34
C16	GLU A 71 OE2	4.61	N2	GLU D 47 CD	4.1
C22	GLU A 71 OE1	4.22	C14	GLU D 47 CD	3.99
C21	GLU A 71 OE1	4.66	C6	GLU D 47 CD	4.92
C20	GLU A 71 OE1	4.98	C11	LEU D 42 CD2	4.01
C17	GLU A 71 OE1	4.61	C36	ARG D 2 NE	4.69
C16	GLU A 71 OE1	4.82	C35	ARG D 2 NE	4.57
C21	GLU A 71 CD	3.88	C35	ARG D 2 CD	4.85
C20	GLU A 71 CD	4.32	C36	ARG D 2 CG	4.34
O5	GLU A 71 CD	4.82	C35	ARG D 2 CG	4.34
O4	GLU A 71 CD	4	C36	ARG D 2 CB	4.17
C18	GLU A 71 CD	4.6	C35	ARG D 2 CB	4.66
C17	GLU A 71 CD	4.19	C36	ARG D 2 CA	4.33
C16	GLU A 71 CD	4.72	C36	ARG D 2 N	4.64
C21	GLU A 71 CG	4.81	C37	MET D 1 CE	4.13
C20	GLU A 71 CG	4.22	C32	MET D 1 CE	4.73
O4	GLU A 71 CG	4.31	C31	MET D 1 CE	4.32
C17	GLU A 71 CG	4.9	C37	MET D 1 O	3.21
C10	GLN A 15 OE1	3.24	C36	MET D 1 O	3.17
C9	GLN A 15 OE1	4.95	C35	MET D 1 O	4.44
C8	GLN A 15 OE1	4.15	C32	MET D 1 O	4.49
C1	GLN A 15 OE1	4.93	C37	MET D 1 C	4.33
C10	GLN A 15 NE2	4.39	C36	MET D 1 C	4.12
O2	GLN A 15 CD	4.11	C37	MET D 1 N	4.7
C10	GLN A 15 CD	4.08	C36	MET D 1 N	4.9
C22	GLN A 11 OE1	4.29	C22	THR A 225 OG1	2.82
C13	GLN A 11 OE1	4.75	C21	THR A 225 OG1	4.24
O7	GLN A 11 CD	4.64	C17	THR A 225 OG1	4.8
O6	GLN A 11 CD	4.79	C22	THR A 225 CG2	4.99
O2	GLN A 11 CD	4.7	C22	THR A 225 CB	3.82
			C22	THR A 225 CA	4.54
			C22	THR A 225 N	4.01
			C21	THR A 225 N	4.54
			O7	TYR A 224 CE1	4.98
			C21	TYR A 224 CD1	4.49
			O7	TYR A 224 CD1	3.85
			C18	TYR A 224 CD1	4.99
			C21	TYR A 224 CG	4.54
			O7	TYR A 224 CG	4.31
			C22	TYR A 224 CB	4.88
			C21	TYR A 224 CB	3.69
			O7	TYR A 224 CB	3.8
			C22	TYR A 224 C	4.91
			C21	TYR A 224 C	4.67
			C21	TYR A 224 CA	4.71
			O7	TYR A 224 CA	4.87
			C22	TYR A 224 N	4.65
			C22	THR A 223 OG1	4.09
			C22	THR A 223 CB	4.32
			O6	THR A 223 CB	4.8
			C20	GLU A 77 OE2	3
			C19	GLU A 77 OE2	3.72
			C18	GLU A 77 OE2	4.91
			C16	GLU A 77 OE2	4.9
			C15	GLU A 77 OE2	3.77

			C14	GLU A 77 OE2	4.81
			C12	GLU A 77 OE2	4.1
			C7	GLU A 77 OE2	4.41
			C6	GLU A 77 OE2	3.61
			C5	GLU A 77 OE2	4.85
			C20	GLU A 77 OE1	4.46
			C19	GLU A 77 OE1	4.52
			C20	GLU A 77 CD	4.08
			C19	GLU A 77 CD	4.52
			C15	GLU A 77 CD	4.89
			C6	GLU A 77 CD	4.73
			C37	THR A 73 OG1	4.69
			C34	THR A 73 OG1	4.59
			C33	THR A 73 OG1	3.96
			C32	THR A 73 OG1	3.99
			C31	THR A 73 OG1	3.98
			C30	THR A 73 OG1	3.98
			C29	THR A 73 OG1	4
			C28	THR A 73 OG1	3.97
			C25	THR A 73 OG1	4.64
			C24	THR A 73 OG1	4.72
			C37	THR A 73 CG2	4.04
			C36	THR A 73 CG2	3.99
			C35	THR A 73 CG2	3.92
			C34	THR A 73 CG2	3.89
			C33	THR A 73 CG2	3.96
			C32	THR A 73 CG2	4.01
			C31	THR A 73 CG2	4.69
			C30	THR A 73 CG2	4.65
			C34	THR A 73 CB	4.62
			C33	THR A 73 CB	4.42
			C32	THR A 73 CB	4.6
			C31	THR A 73 CB	4.95
			C30	THR A 73 CB	4.66
			C37	GLU A 71 OE2	3.42
			C36	GLU A 71 OE2	4.35
			C33	GLU A 71 OE2	4.58
			C32	GLU A 71 OE2	3.56
			C31	GLU A 71 OE2	3.36
			C28	GLU A 71 OE2	4.28
			C25	GLU A 71 OE2	4.77
			C32	GLU A 71 OE1	4.93
			C31	GLU A 71 OE1	4.39
			C28	GLU A 71 OE1	4.66
			C25	GLU A 71 OE1	4.74
			C37	GLU A 71 CD	4.56
			C32	GLU A 71 CD	4.46
			C31	GLU A 71 CD	3.95
			C28	GLU A 71 CD	4.56
			C25	GLU A 71 CD	4.72
			C31	GLU A 71 CG	4.82
			C21	GLN A 15 OE1	3.53
			C20	GLN A 15 OE1	4.81
			C19	GLN A 15 OE1	3.83
			C18	GLN A 15 OE1	4.46
			C21	GLN A 15 NE2	3.22
			C19	GLN A 15 NE2	4.93
			C18	GLN A 15 NE2	4.94
			C21	GLN A 15 CD	3.48
			O7	GLN A 15 CD	4.31
			C19	GLN A 15 CD	4.65
			C18	GLN A 15 CD	4.99

			C21	GLN A 15 CG	4.47
			C21	GLN A 15 CB	4.96
			C27	GLN A 11 OE1	4.38
			C26	GLN A 11 OE1	3.87
			C25	GLN A 11 OE1	4.76
			C26	GLN A 11 CD	5
Table A3.22			**Table A3.23**		
c) 16-Tubulin			**(d) 17_Tubulin**		
Hydrogen bonding			**Hydrogen bonding**		
Hydrogen Donor (D)	**Hydrogen Acceptor (A)**	**Distance (D-A) in Å**	**Hydrogen Donor (D)**	**Hydrogen Acceptor (A)**	**Distance (D-A) in Å**
GLN D 247 NE2	16 O3	2.97	LYS D 254 NZ	17 O5	4.08
GLY D 246 N	16 O4	4.87	GLN D 247 NE2	17 O3	2.93
16 N1	GLU D 47 OE2	2.84	ARG D 48 NH2	17 O7	3.74
			GLN A 11 NE2	17 O4	4.71
Hydrophobic interaction			**Hydrophobic interaction**		
16	**Tubulin**	**Distance**	**Noscapine**	**Tubulin**	**Distance**
C21	LYS D 254 NZ	3.18	C22	LYS D 254 NZ	4.11
C19	LYS D 254 NZ	4.15	C21	ASP D 251 OD2	4.48
C18	LYS D 254 NZ	4.06	C21	ASP D 251 CB	4.81
C21	LYS D 254 CE	4.44	C22	ALA D 250 CB	4.94
O7	LYS D 254 CE	4.25	C21	ALA D 250 CB	4.41
O7	LYS D 254 CD	4.71	O7	ALA D 250 CB	4.62
C22	ASP D 251 OD2	4.21	O6	ALA D 250 CB	3.67
C22	ALA D 250 CB	3.78	O5	ALA D 250 CB	3.93
O7	ALA D 250 CB	4.69	C19	ALA D 250 CB	4.95
O6	ALA D 250 CB	4.51	C18	ALA D 250 CB	4.16
C19	ALA D 250 CB	4.75	C17	ALA D 250 CB	3.63
C18	ALA D 250 CB	4.36	C16	ALA D 250 CB	3.96
C17	ALA D 250 CB	4.25	C15	ALA D 250 CB	4.78
C16	ALA D 250 CB	4.58	C13	ALA D 250 CB	4.18
C15	ALA D 250 CB	5	C21	ALA D 250 O	4.48
C22	ALA D 250 O	4.77	C21	ALA D 250 C	4.87
C22	ALA D 250 C	4.87	C13	GLN D 247 OE1	4.24
C22	ALA D 250 CA	4.98	C12	GLN D 247 OE1	4.43
C20	GLN D 247 OE1	3.79	C5	GLN D 247 OE1	4.76
C19	GLN D 247 OE1	4.59	C15	GLN D 247 NE2	4.85
C15	GLN D 247 OE1	4.7	C14	GLN D 247 NE2	4.25
C12	GLN D 247 OE1	4.91	C13	GLN D 247 NE2	4.39
C20	GLN D 247 NE2	3.91	C12	GLN D 247 NE2	3.35
C15	GLN D 247 NE2	4.17	C11	GLN D 247 NE2	3.74
C14	GLN D 247 NE2	4.77	C5	GLN D 247 NE2	3.18
C12	GLN D 247 NE2	3.67	C4	GLN D 247 NE2	3.99
C11	GLN D 247 NE2	3.54	C2	GLN D 247 NE2	3.86
C5	GLN D 247 NE2	3.48	O5	GLN D 247 CD	4.69
C4	GLN D 247 NE2	4.27	C13	GLN D 247 CD	4.4
C2	GLN D 247 NE2	4.04	O4	GLN D 247 CD	3.35
C20	GLN D 247 CD	4.02	C12	GLN D 247 CD	3.99
C15	GLN D 247 CD	4.59	C11	GLN D 247 CD	4.35
C12	GLN D 247 CD	4.42	O3	GLN D 247 CD	3.91
C11	GLN D 247 CD	4.27	C5	GLN D 247 CD	4.23
O3	GLN D 247 CD	4.05	C2	GLN D 247 CD	4.99
C5	GLN D 247 CD	4.57	O4	GLN D 247 CG	4.32
C11	GLN D 247 CG	4.07	C12	GLN D 247 CG	4.77
O3	GLN D 247 CG	4.33	C11	GLN D 247 CG	4.04
C20	GLN D 247 O	4.93	O3	GLN D 247 CG	4.08
C19	GLN D 247 O	4.96	O4	GLN D 247 CB	4.68
C20	GLN D 247 CA	4.56	C11	GLN D 247 CB	4.98
C11	GLN D 247 N	4.44	C13	GLN D 247 O	4.57
C20	GLY D 246 O	4.31	O5	GLN D 247 C	4.47
C19	GLY D 246 O	4.96	C13	GLN D 247 C	4.92
C16	GLY D 246 O	4.41	O4	GLN D 247 C	4.99

C15	GLY D 246 O	4.04	O5	GLN D 247 CA	4.23
C13	GLY D 246 O	4.57	C13	GLN D 247 CA	4.31
C12	GLY D 246 O	4.1	O4	GLN D 247 CA	4.01
C11	GLY D 246 O	4.7	C12	GLN D 247 CA	4.67
C15	GLY D 246 C	4.93	C11	GLN D 247 CA	4.87
C12	GLY D 246 C	4.74	C13	GLN D 247 N	4.9
C11	GLY D 246 C	4.34	C12	GLN D 247 N	4.78
C11	GLY D 246 CA	4.54	C11	GLN D 247 N	4.16
C11	GLY D 246 N	4.2	C20	GLY D 246 O	4.43
O4	PRO D 245 CB	4.93	C17	GLY D 246 O	4.61
C11	PRO D 245 CB	3.88	C16	GLY D 246 O	3.85
O3	PRO D 245 CB	4.68	C15	GLY D 246 O	3.76
O2	PRO D 245 CB	3.68	C13	GLY D 246 O	3.68
C10	PRO D 245 CB	3.78	C12	GLY D 246 O	3.75
O1	PRO D 245 CB	4.1	C11	GLY D 246 O	4.45
C9	PRO D 245 CB	4.14	O5	GLY D 246 C	4.96
C8	PRO D 245 CB	3.82	C16	GLY D 246 C	4.95
C2	PRO D 245 CB	4.35	C15	GLY D 246 C	4.7
C1	PRO D 245 CB	4.9	C13	GLY D 246 C	4.63
O2	PRO D 245 CG	4.45	O4	GLY D 246 C	4.42
C10	PRO D 245 CG	4.09	C12	GLY D 246 C	4.39
O1	PRO D 245 CG	4.08	C11	GLY D 246 C	4.02
C9	PRO D 245 CG	4.42	O3	GLY D 246 C	4.92
C8	PRO D 245 CG	4.55	C11	GLY D 246 CA	4.16
C11	PRO D 245 O	4.13	C11	GLY D 246 N	3.83
C11	PRO D 245 C	4	C11	PRO D 245 CB	3.71
O4	PRO D 245 CA	4.95	O3	PRO D 245 CB	4.55
C11	PRO D 245 CA	4.45	O2	PRO D 245 CB	3.65
C22	ARG D 48 NH2	4.92	C10	PRO D 245 CB	3.8
O5	ARG D 48 CZ	4.31	O1	PRO D 245 CB	4.02
O5	ARG D 48 CD	4.68	C9	PRO D 245 CB	3.95
C29	GLU D 47 OE2	3.4	C8	PRO D 245 CB	3.73
C28	GLU D 47 OE2	4.36	C4	PRO D 245 CB	4.97
C24	GLU D 47 OE2	4.16	C2	PRO D 245 CB	4.22
C23	GLU D 47 OE2	3.98	C1	PRO D 245 CB	4.71
C10	GLU D 47 OE2	4.33	O2	PRO D 245 CG	4.38
C9	GLU D 47 OE2	3.31	C10	PRO D 245 CG	4.03
C8	GLU D 47 OE2	4.47	O1	PRO D 245 CG	4.03
C3	GLU D 47 OE2	4.53	C9	PRO D 245 CG	4.31
C1	GLU D 47 OE2	3.36	C8	PRO D 245 CG	4.52
C10	GLU D 47 OE1	4.75	C1	PRO D 245 CG	4.99
C9	GLU D 47 OE1	4.82	C11	PRO D 245 O	3.76
C29	GLU D 47 CD	4.12	C11	PRO D 245 C	3.64
C28	GLU D 47 CD	4.82	O3	PRO D 245 C	4.91
N1	GLU D 47 CD	4.06	C11	PRO D 245 CA	4.18
C10	GLU D 47 CD	4.95	C8	PRO D 245 CA	4.94
O1	GLU D 47 CD	3.94	C21	ARG D 48 NH2	4.17
C9	GLU D 47 CD	4.4	C19	ARG D 48 NH2	4.25
C1	GLU D 47 CD	4.59	C18	ARG D 48 NH2	4.2
C29	GLU D 47 CG	4	C19	ARG D 48 NH1	4.61
C28	GLU D 47 CG	4.24	C18	ARG D 48 NH1	4.98
N1	GLU D 47 CG	4.88	O7	ARG D 48 CZ	4.38
C32	GLU D 47 O	4.87	C20	ARG D 48 CZ	4.87
C31	GLU D 47 O	4.27	C19	ARG D 48 CZ	4.15
C28	GLU D 47 O	4.47	C18	ARG D 48 CZ	4.5
C10	LEU D 42 CD2	4.75	C20	ARG D 48 NE	4.89
C35	ARG D 2 NH2	4.86	C19	ARG D 48 NE	4.2
C34	ARG D 2 NH2	3.88	C18	ARG D 48 NE	4.86
C33	ARG D 2 NH2	3.45	C19	ARG D 48 CD	4.78
C32	ARG D 2 NH2	4.17	C29	GLU D 47 OE2	3.62
C33	ARG D 2 NH1	4.92	C28	GLU D 47 OE2	4.73
C34	ARG D 2 CZ	4.67	C24	GLU D 47 OE2	4.01

C33	ARG D 2 CZ	3.87	C23	GLU D 47 OE2	3.64
C32	ARG D 2 CZ	4.25	C10	GLU D 47 OE2	4.08
C34	ARG D 2 NE	4.73	C9	GLU D 47 OE2	3.43
C33	ARG D 2 NE	3.79	C8	GLU D 47 OE2	4.6
C32	ARG D 2 NE	3.69	C3	GLU D 47 OE2	4.7
C31	ARG D 2 NE	4.57	C1	GLU D 47 OE2	3.45
C33	ARG D 2 CD	4.86	C10	GLU D 47 OE1	4.54
C32	ARG D 2 CD	4.46	C9	GLU D 47 OE1	4.92
C22	MET D 1 CE	3.55	C29	GLU D 47 CD	4.47
O7	MET D 1 CE	4.91	C24	GLU D 47 CD	5
O6	MET D 1 CE	4.61	C23	GLU D 47 CD	4.77
C22	MET D 1 O	5	N1	GLU D 47 CD	3.92
C22	ASP A 98 OD2	4.67	C10	GLU D 47 CD	4.71
C21	ASP A 98 OD2	3.12	O1	GLU D 47 CD	3.84
C18	ASP A 98 OD2	4.72	C9	GLU D 47 CD	4.5
C21	ASP A 98 CG	4.31	C1	GLU D 47 CD	4.67
O7	ASP A 98 CG	4.58	C29	GLU D 47 CG	4.37
C21	ASP A 98 CB	4.84	C28	GLU D 47 CG	4.9
C23	GLU A 77 OE2	3.87	N1	GLU D 47 CG	4.78
C14	GLU A 77 OE2	3.22	C28	GLU D 47 O	4.9
C9	GLU A 77 OE2	4.77	C10	LEU D 42 CD2	4.73
C7	GLU A 77 OE2	3.62	C22	MET D 1 CE	4.98
C6	GLU A 77 OE2	4.34	C21	MET D 1 CE	3.29
C5	GLU A 77 OE2	4.6	O7	MET D 1 CE	4.66
C4	GLU A 77 OE2	4.14	O6	MET D 1 CE	4.59
C3	GLU A 77 OE2	3.7	C21	MET D 1 SD	4.98
C2	GLU A 77 OE2	4.85	C21	MET D 1 O	3.75
C1	GLU A 77 OE2	4.06	C21	MET D 1 C	4.93
C14	GLU A 77 OE1	3.81	C22	ASP A 98 OD2	3.99
N2	GLU A 77 CD	4.77	C23	GLU A 77 OE2	4.02
C23	GLU A 77 CD	4.54	C14	GLU A 77 OE2	3.38
C14	GLU A 77 CD	3.59	C9	GLU A 77 OE2	4.87
C7	GLU A 77 CD	4.35	C7	GLU A 77 OE2	3.67
C6	GLU A 77 CD	4.87	C6	GLU A 77 OE2	4.31
C3	GLU A 77 CD	4.75	C5	GLU A 77 OE2	4.92
C25	GLU A 77 CG	4.75	C4	GLU A 77 OE2	4.44
C23	GLU A 77 CG	4.2	C3	GLU A 77 OE2	3.85
C14	GLU A 77 CG	4.53	C1	GLU A 77 OE2	4.16
C7	GLU A 77 CG	4.56	C14	GLU A 77 OE1	3.97
C35	ASP A 76 OD2	3.34	N2	GLU A 77 CD	4.9
C34	ASP A 76 OD2	3.98	C23	GLU A 77 CD	4.77
C30	ASP A 76 OD2	4.39	C14	GLU A 77 CD	3.83
C27	ASP A 76 OD2	4.57	C7	GLU A 77 CD	4.41
C26	ASP A 76 OD2	3.74	C6	GLU A 77 CD	4.82
C25	ASP A 76 OD2	4.64	C3	GLU A 77 CD	4.9
C35	ASP A 76 CG	4.29	C25	GLU A 77 CG	4.62
C34	ASP A 76 CG	4.97	C23	GLU A 77 CG	4.49
C26	ASP A 76 CG	4.29	C14	GLU A 77 CG	4.91
C25	ASP A 76 CG	4.93	C7	GLU A 77 CG	4.71
C35	ASP A 76 CB	4.71	C25	GLU A 77 N	4.92
C27	ASP A 76 CB	4.98	C27	ASP A 76 OD2	4.19
C26	ASP A 76 CB	3.8	C26	ASP A 76 OD2	3.83
C25	ASP A 76 CB	4.06	C25	ASP A 76 OD2	4.98
C25	ASP A 76 C	4.94	C27	ASP A 76 CG	4.94
N2	VAL A 74 CG2	3.96	C26	ASP A 76 CG	4.25
C21	VAL A 74 CG2	4.72	C27	ASP A 76 CB	4.66
C20	VAL A 74 CG2	4.99	C26	ASP A 76 CB	3.61
C19	VAL A 74 CG2	4.88	C25	ASP A 76 CB	4.2
C18	VAL A 74 CG2	4.99	C26	ASP A 76 C	4.97
C14	VAL A 74 CG2	3.67	C25	ASP A 76 C	4.85
C6	VAL A 74 CG2	4.35	C26	ASP A 76 CA	4.88
C14	VAL A 74 CG1	4.24	N2	VAL A 74 CG2	4

N2	VAL A 74 CB	4.81	C22	VAL A 74 CG2	4.85
C14	VAL A 74 CB	4.15	C14	VAL A 74 CG2	3.95
N2	VAL A 74 CA	4.64	C6	VAL A 74 CG2	4.07
C14	VAL A 74 CA	3.99	C14	VAL A 74 CG1	4.45
C6	VAL A 74 CA	4.49	N2	VAL A 74 CB	4.9
C14	VAL A 74 N	4.5	C14	VAL A 74 CB	4.5
C7	VAL A 74 N	4.91	C6	VAL A 74 CB	4.81
C6	VAL A 74 N	4.19	N2	VAL A 74 CA	4.84
C25	THR A 73 OG1	4.9	C14	VAL A 74 CA	4.47
C22	THR A 73 OG1	4.65	C6	VAL A 74 CA	4.37
C18	THR A 73 OG1	4.49	C7	VAL A 74 N	4.89
C17	THR A 73 OG1	3.55	C6	VAL A 74 N	4.15
C16	THR A 73 OG1	3.59	C28	THR A 73 OG1	4.97
C15	THR A 73 OG1	4.5	C27	THR A 73 OG1	4.96
C14	THR A 73 OG1	4.87	C22	THR A 73 OG1	4.11
C13	THR A 73 OG1	3.62	C21	THR A 73 OG1	4.88
C12	THR A 73 OG1	4.98	C20	THR A 73 OG1	4.03
C7	THR A 73 OG1	4	C19	THR A 73 OG1	3.69
C6	THR A 73 OG1	3	C18	THR A 73 OG1	3.68
C35	THR A 73 CG2	4.56	C17	THR A 73 OG1	3.97
C30	THR A 73 CG2	4.54	C16	THR A 73 OG1	4.31
C27	THR A 73 CG2	4.41	C15	THR A 73 OG1	4.33
C26	THR A 73 CG2	4.03	C7	THR A 73 OG1	3.92
C25	THR A 73 CG2	4.62	C6	THR A 73 OG1	3.13
O6	THR A 73 CG2	4.4	C29	THR A 73 CG2	4.85
O5	THR A 73 CG2	4.3	C28	THR A 73 CG2	3.99
C13	THR A 73 CG2	4.95	C27	THR A 73 CG2	3.7
C6	THR A 73 CG2	4.89	C26	THR A 73 CG2	4.39
N2	THR A 73 CB	4.92	C21	THR A 73 CG2	4.96
C27	THR A 73 CB	4.55	O7	THR A 73 CG2	4.14
C26	THR A 73 CB	3.78	C19	THR A 73 CG2	4.4
C25	THR A 73 CB	3.93	C18	THR A 73 CG2	4.48
C24	THR A 73 CB	4.79	C29	THR A 73 CB	4.53
O6	THR A 73 CB	4.43	C28	THR A 73 CB	4.06
O5	THR A 73 CB	4.22	C27	THR A 73 CB	3.76
C17	THR A 73 CB	4.86	C26	THR A 73 CB	4.01
C16	THR A 73 CB	4.82	C25	THR A 73 CB	4.48
C13	THR A 73 CB	4.52	C24	THR A 73 CB	4.72
C7	THR A 73 CB	4.16	O7	THR A 73 CB	4.71
C6	THR A 73 CB	3.65	C20	THR A 73 CB	4.83
C26	THR A 73 O	3.82	C19	THR A 73 CB	4.39
C25	THR A 73 O	3.19	C18	THR A 73 CB	4.6
C24	THR A 73 O	4.22	C7	THR A 73 CB	4.21
C23	THR A 73 O	4.41	C6	THR A 73 CB	3.88
C14	THR A 73 O	4.53	C29	THR A 73 O	4.99
C7	THR A 73 O	3.76	C27	THR A 73 O	4.53
C6	THR A 73 O	3.78	C26	THR A 73 O	3.7
N2	THR A 73 C	4.76	C25	THR A 73 O	3.51
C26	THR A 73 C	4.37	C24	THR A 73 O	4.24
C25	THR A 73 C	4.03	C23	THR A 73 O	4.73
C14	THR A 73 C	4.72	C7	THR A 73 O	3.9
C7	THR A 73 C	4.27	C6	THR A 73 O	3.93
C6	THR A 73 C	3.85	C27	THR A 73 C	4.91
C27	THR A 73 CA	4.99	C26	THR A 73 C	4.36
C26	THR A 73 CA	3.91	C25	THR A 73 C	4.44
C25	THR A 73 CA	4.05	C7	THR A 73 C	4.33
C7	THR A 73 CA	4.84	C6	THR A 73 C	3.95
C6	THR A 73 CA	4.4	C28	THR A 73 CA	4.92
C22	GLU A 71 OE2	3.38	C27	THR A 73 CA	4.22
C21	GLU A 71 OE2	4.51	C26	THR A 73 CA	4.04
C18	GLU A 71 OE2	4.59	C25	THR A 73 CA	4.57
C17	GLU A 71 OE2	4.05	C7	THR A 73 CA	4.91

C22	GLU A 71 OE1	4.5	C6	THR A 73 CA	4.57
C21	GLU A 71 OE1	3.7	C22	GLU A 71 OE2	3.6
C18	GLU A 71 OE1	4.19	C21	GLU A 71 OE2	3.33
C17	GLU A 71 OE1	4	C18	GLU A 71 OE2	4.13
C16	GLU A 71 OE1	4.85	C17	GLU A 71 OE2	4.33
C22	GLU A 71 CD	3.88	C22	GLU A 71 OE1	3.27
C21	GLU A 71 CD	3.72	C21	GLU A 71 OE1	4.97
O7	GLU A 71 CD	3.87	C18	GLU A 71 OE1	4.87
O6	GLU A 71 CD	3.32	C17	GLU A 71 OE1	4.62
C18	GLU A 71 CD	4.29	C22	GLU A 71 CD	3.22
C17	GLU A 71 CD	4.07	C21	GLU A 71 CD	4.2
C22	GLU A 71 CG	4.46	O7	GLU A 71 CD	4.46
C21	GLU A 71 CG	3.49	O6	GLU A 71 CD	3.95
O7	GLU A 71 CG	3.94	C18	GLU A 71 CD	4.7
O6	GLU A 71 CG	4.29	C17	GLU A 71 CD	4.55
C18	GLU A 71 CG	4.79	C22	GLU A 71 CG	3.65
C17	GLU A 71 CG	4.95	C21	GLU A 71 CG	4.88
C21	GLU A 71 CB	4.96	O6	GLU A 71 CG	4.5
C21	ASP A 69 OD2	4.9	C14	GLN A 15 OE1	3.2
C14	GLN A 15 OE1	3.48	C14	GLN A 15 CD	4.43
C14	GLN A 15 CD	4.7	C22	GLN A 11 OE1	4.65
C21	GLN A 11 OE1	4.15	C16	GLN A 11 OE1	4.87
C20	GLN A 11 OE1	3.04	C14	GLN A 11 OE1	4.73
C19	GLN A 11 OE1	2.91	C13	GLN A 11 OE1	3.77
C18	GLN A 11 OE1	4.05	C12	GLN A 11 OE1	4.89
C15	GLN A 11 OE1	4.23	O5	GLN A 11 CD	4.66
C14	GLN A 11 OE1	4.94	C14	GLN A 11 CD	4.88
C20	GLN A 11 NE2	4.46	C13	GLN A 11 CD	4.81
C19	GLN A 11 NE2	4.75	O4	GLN A 11 CD	4.52
C20	GLN A 11 CD	4.04			

CHAPTER 4

In Silico Inspired Design of 1,3-Diynyl Congeners of Noscapine as Promising Tubulin-Binding Anticancer Agent: Chemical Synthesis and Cellular Activity with Breast Cancer Cell Lines

4.1. Introduction

Microtubules (MTs) play a significant role in many of the cellular functions including cell division. Therefore, it has been used as a suitable drug target to develop chemotherapeutic drugs against rapidly dividing cancer cells. The effectiveness of MT targeting drugs has been confirmed by the clinical use of vinca alkaloids and taxanes for the treatment of a wide variety of human cancers. However, these anti-MT agents are known to induce undesired, dose-limiting toxicities in patients (Kavanagh and Kudelka, 1993; Rowinsky and Donehower, 1991). The clinical success of taxanes has impelled worldwide to search for natural compounds targeted to MT but with improved characteristics. In quest for finding such a compound without having any side effects, noscapine (an opium alkaloid) was discovered that binds tubulin dimer with a 1:1 stoichiometry, arrests a variety of mammalian cells in mitosis and causes apoptosis (Ye *et al*., 1998). It has been used as a cough suppressant since the mid 1950s and illustrating a good safety profile. It is also found to be well-tolerated in humans without having any severe toxicity (Dahlström *et al*., 1982; Karlsson *et al*., 1990; Jensen *et al*., 1992). Furthermore, it inhibits the proliferation of cancer cells of different tissue origin and regresses effectively the implanted tumor in animal models without any side effects (Ye *et al*., 1998; Landen *et al*., 2002; Zhou *et al*., 2002b; Zhou *et al.*, 2003; Landen *et al.*, 2004). The minimal side effect of noscapine is due to its selectivity in killing the cancer cells without hampering the normal healthy cells. It was revealed that normal healthy cells respond to noscapine (or its tested derivatives) treatment by arresting mitosis for a long period of time, at least 12 to 24 hours. However, if noscapine exposure is removed prior to this time period by replenishing with a fresh drug-free culture medium, the arrested cells resume the progression of the normal mitosis producing viable daughter cells (Landen *et al*., 2002). This innovative research has prodded an enormous enthusiasm for the scientific world to use noscapine and its synthetic analogues for the therapy of malignancy.

In order to enhance the anti-proliferative activity of noscapine we have tried to develop a new series of its derivatives (called diyne derivatives) by strategically modifying its scaffold structure and supported by our in silico efforts. These derivatives were then chemically synthesized and validated their anti-proliferative activity to cancer cells using two human carcinoma cell lines, MCF-7 and MDA-MB-231. The novel derivatives were found to bind tubulin heterodimer with increased binding affinity,

inhibit proliferation of neoplastic cell and causes selective G2/M arrest in cancer cells. The mitotic catastrophe in cancer cells is then followed by induction of apoptosis.

4.2. Materials and Methods

4.2.1. Protein preparation

The crystal structure of amino noscapine-tubulin complex (PDB ID: 6Y6D, resolution 2.20 Å, (Olive *et al*., 2020), was downloaded from the PDB databank and used for in silico study. The structure was prepared using protein preparation wizard workflow (Schrödinger). Further, it was refined by performing an all atom molecular dynamics (MD) simulation of 100 ns in explicit water using GROMACS 4.5.4 software (Berendsen *et al*., 1995), and the GROMOS96 force field as reported earlier (Santoshi and Naik, 2014). The last 2000 frames from the MD trajectory were used for the generation of an average structure of the tubulin.

4.2.2. Preparation of molecular structure of noscapinoids

A library of molecular structures of C-9 substituted noscapine derivatives (Figure 4.1) that were previously reported (Aneja et al., 2006b; Naik et al., 2011a; Santoshi and Naik, 2014; Manchukonda et al., 2013) and the newly planned derivatives (Figure 4.2) were built using ChemDraw. These structures were imported to Maestro (Schrödinger software package) and were energy minimized using Macromodel (Schrödinger software package). The force field, OPLS 2005 and PRCG algorithm (energy gradient of 0.001) was used for the energy minimization. Each of these structures were refined further by geometric optimization using hybrid density functional theory with Becke's three-parameter exchange potential and the Lee-Yang-Parr correlation functional (B3LYP) with basis set 3-21G* using Jaguar (Schrödinger, software package). The various conformations of molecular structures were generated using Ligprep (Schrödinger software package).

4.2.3. Molecular docking of noscapinoids

Molecular docking of noscapinoids with the refined structure of αβ-tubulin heterodimer was performed using Glide (Schrödinger software package) as reported previously (Naik *et al*., 2011a). A grid box with a dimension of 12Å x 12Å x 12Å was generated by selecting the ligand, amino noscapine in the co-crystal structure of tubulin (PDB ID: 6Y6D) and defined at the centroid of the binding site (Oliva *et al*., 2020; Naik *et al*., 2011b), using Glide grid-receptor generation program. Also, an outer grid box was defined to accommodate all the atoms of noscapinoids with size ≤ 24 Å of the bound

amino noscapine. This grid box size includes all the binding site residues within 6 Å distance of the bound amino-noscapine at the interface of both α- and β- tubulin. The ranges of binding site residues from the α-tubulin include Gly 10-Ala 19, Asp 69-Gly 81, Thr 94-Asn 101, Arg 105, Ile 110, Thr 145, Gly146, Ala 174-Thr 179, Asn 206, Tyr 210, Cys 213, Arg 214, Ile 219-Arg 229; whereas from the β-tubulin are Met 1-Ile 4, His28, Asp 41- Glu 55, Tyr 61, Arg 64, Cys 129-Phe 135, Arg 164, Ile 165, Thr 240-Asn 258, Ala 316-Asp 329, Lys 352-Ile 358. The noscapinoids were docked using Glide XP (extra precision) algorithm and evaluated their binding mode using a Glide XPscore function. One best conformation for every ligand was considered for further analysis.

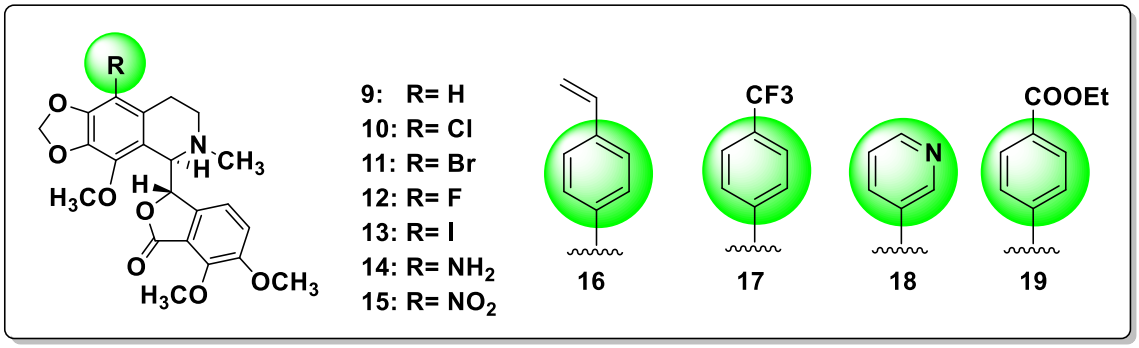

Figure 4.1: *Molecular structures of previously reported noscapine derivatives that have experimentally proven to bind tubulin with known free energy of binding (Table 4.1) and used as training set molecules for LIE-SGB model building.*

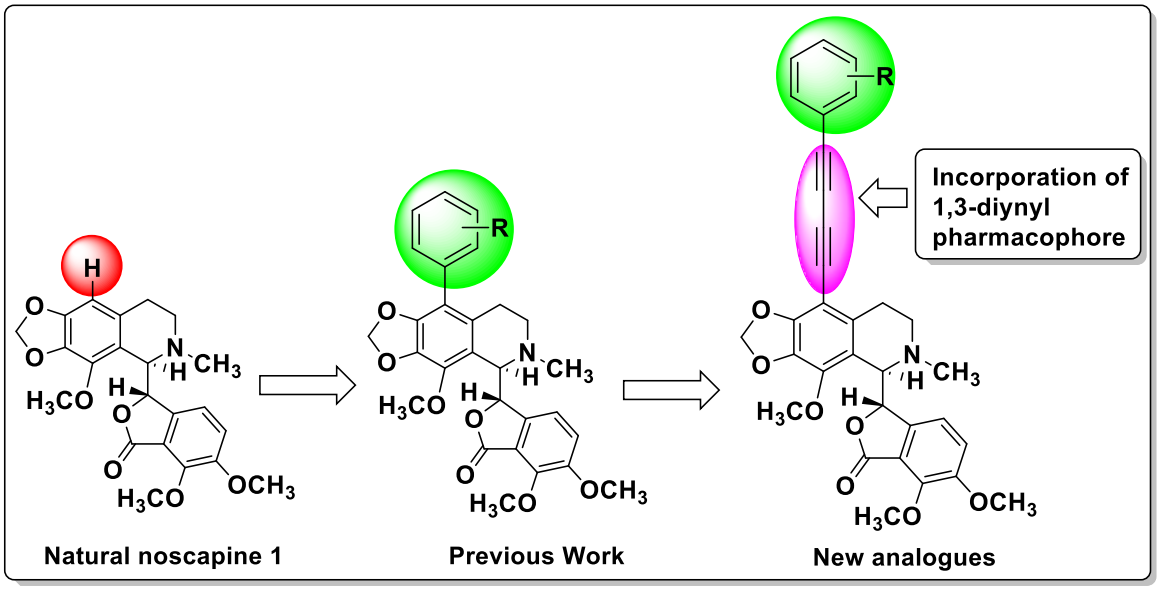

Figure 4.2: *General scheme for strategic development of new noscapine congeners by substitution of various functional groups using in silico combinatorial chemistry.*

4.2.4. LIE-SGB model building

The training data set of previously reported noscapinoids with known experimental binding affinity ($\Delta G_{bind,expt}$) with tubulin (Table 4.1) was used to build a reasonable predictive model for predicting the binding affinity ($\Delta G_{bind,pred}$) of newly designed noscapinoids. A linear interaction energy model (LIE) with a surface generalized Born (SGB) continuum solvation model, proposed by Jorgensen (Zhou *et al*., 2001) was used for building the model. The model used various energy parameters such as van der Waals (U_{vdw}), Columbic (U_{coul}), reaction (U_{rxn}) and cavity energy (U_{cav}) that are calculated from the docked complexes of the noscapinoids using Liaison package (version 5.6, Schrödinger, LLC). Hybrid Monte Carlo simulation technique with similar parameters as reported previously (Santoshi *et al*., 2015) was used.

$$\Delta G_{bind,pred} = \alpha\left(\langle U^{b}_{vdw}\rangle - \langle U^{f}_{vdw}\rangle\right) + \beta\left(\langle U^{b}_{coul}\rangle - \langle U^{f}_{coul}\rangle\right) + \gamma\left(\langle U^{b}_{rxn}\rangle - \langle U^{f}_{rxn}\rangle\right) + \delta\left(\langle U^{b}_{cav}\rangle - \langle U^{f}_{cav}\rangle\right)$$

Here $\langle\ \rangle$ represents the ensemble average, *b* represents the bound form of the ligand, *f* represents the free form of the ligand. The parameters α, β, γ and δ are the coefficients of different energy terms that are determined using Minitab statistical package (Minitab Inc.) by fitting with the experimental binding affinities of training set molecules. Based on the docking score and predictive binding affinity we have finally screened out a panel of 1,3-diynyl derivatives **20-22** (Figure 4.3) for chemical synthesis and experimental evaluation.

4.2.5. Predicted ADME properties

The QikProp program (Schrodinger software package) was used to predict the ADME properties of noscapine and its 1,3-diynyl derivatives **20-22.** All the compounds were imported into the project table, and 44 ADME properties were predicted. Some properties having zero values were manually deleted. The program also evaluates the acceptability of the compounds based on the Lipinski's rule of 5 (number of violations of Lipinski's rule of five) which is essential for rational drug design. Poor absorption or permeation is more likely when a ligand molecule violates Lipinski's rule of five i.e., has more than 5 hydrogen bond donors, the molecular weight is over 500, the log P is over 5 and the sum of N's O's is over 10.

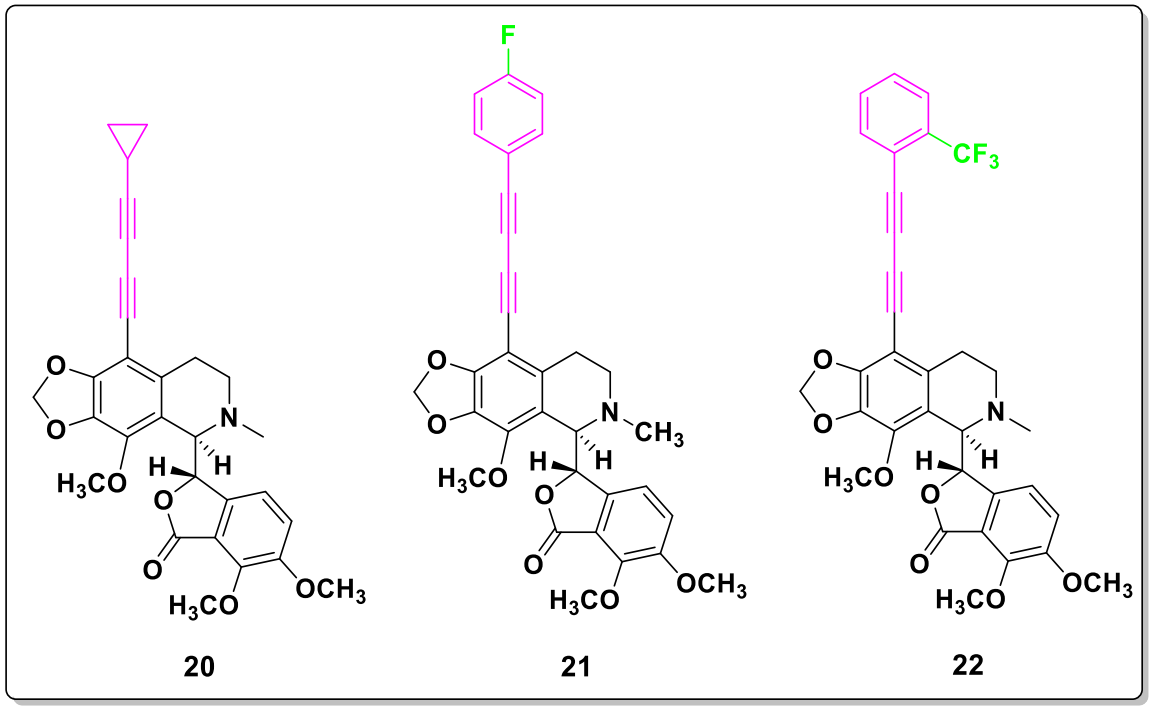

Figure 4.3: *A panel of 1,3-diynyl-noscapinoids developed in the study: 9-cycloro-diyne-noscapine* ***(20),*** *9,4F-ph-diyne-noscapine* ***(21)*** *and 9,2-CF_3-ph-diyne-noscapine* ***(22)***.

4.2.6. Chemical synthesis of 1,3-diynyl-noscapinoids

4.2.6.1. General Method

All the solvents and reagents used are analytically pure. All the reactions were performed in oven-dried flasks with magnetic stirring. Progress of reactions were monitored by thin layer chromatography (TLC) performed on Merck 60 F-254 silica gel pre-coated plates. The TLC plates after elution were visualized illuminating at 254 nm for UV active materials. PMA staining and charring on a hot plate achieved further visualization. Column chromatography was performed using columns packed with slurry of silica gel (200 mesh) in hexane and equilibrated with the appropriate solvent mixture. Compounds were loaded as a concentrated solution or neat and eluted with appropriate solvent system applying pressure with an air pump. Yields refer to chromatographically and spectroscopically pure homogeneous materials unless otherwise stated. Appropriate names for all the new compounds were given with the help of Chem Draw professional 2018. Melting points were determined by CINTEX programmable melting point apparatus and are uncorrected. IR was recorded on Thermo Nicolet nexus-670 spectrometer with reference to KBr. ^{1}H and ^{13}C NMR spectra of samples were recorded on AVANCE- 300 MHz, 400 MHz and 500 MHz spectrometers in $CDCl_3$. Chemical shifts (δ) are described are relative to TMS (δ = 0.0) as the internal standard. Spin multiplicities are described as s (singlet), brs (broad singlet), d (doublet), t (triplet), q

(quartet), or m (multiplet) and coupling constants are reported in hertz (Hz). Mass spectra were recorded in ESI spectrometers. All high-resolution mass spectra were recorded on QSTAR XL hybrid ms/ms system (Applied Bio systems/MDS sciex, foster city, USA), equipped with an ESI source (IICT, Hyderabad). Natural α-noscapine was purchased from Sigma-Aldrich and is used as such.

4.2.6.2. Synthesis protocol of 1,3-diynyl-noscapinoids

Enlivened by our in silico estimations, we next chemically synthesized a panel of novel 9-(1,3-diynyl) noscapinoids through substitution of 1,3-diynyl functional group at the C-9 position of the natural α-noscapine (Figure 4.4). As the starting point, Br-noscapine was synthesized from the noscapine in excellent yield (92%) using bromine water (48% aq. HBr) by modifying the reaction conditions reported earlier (Manchukonda *et al*., 2012). To a solution of 9-bromonoscapine **(9)** (4.0 g, 8.2 mmol) in degassed DMF:Et_3N (1:1 v/v, 10 mL), was added ethyl acrylate, $Pd(OAc)_2$ (1.6 mmol), and Tri(o-tolyl)phosphine (3.2 mmol) under Argon. The contents were stirred at 130 °C for 24 h. Post completion, the reaction was brought to room temperature and DMF was removed under vacuum. Water (20 mL) was added and extracted with dichloromethane (3 x 20 mL), and the combined organic portions were washed with ice cold water, dried over anhydrous Na_2SO_4, and concentrated to give the crude residue which was chromatographed over a triethylamine treated silica gel bed, using 40 % ethyl acetate in *n*-hexanes as eluent, to give pure compound **23** in 75% yield. Compound **23** (2.0 g, 4.6 mmol) in THF:H_2O (9:1, V/V, 10 mL) was reacted with NMO (1.0 g, 9.2 mmol), and OsO_4 (0.4 mmol) at 25 °C for 4 h. After completion of the reaction (judged by TLC), $NaIO_4$ (1.4 g, 7.0 mmol) was added and stirred for another 1 h. To the reaction mixture, water (10 mL) was added, extracted with ethyl acetate (3 x 15 mL) and the combined organic portions were washed with brine, dried over anhydrous Na_2SO_4. The solvent was removed in vacuum to give the crude product, which was chromatographed over a triethylamine treated silica gel bed, using 40% ethyl acetate in *n*-hexanes as eluent, to give pure compound **24** in 78% yield. The obtained compound **24** (1.0 g, 2.2 mmol) was dissolved in anhydrous methanol (10 mL) and to it was added dimethyl(1-diazo-2-oxopropyl) phosphonate (0.6 g, 3.3 mmol) and K_2CO_3 (0.9 g, 6.6 mmol). The reaction mixture was stirred at 25 °C for 4 h; after completion of the reaction (judged by TLC), the reaction mixture was filtered through celite pad and methanol was removed under vacuum. The residue was diluted with water (20 mL), extracted with ethyl acetate (3 x 20 mL), and the combined organic portions were washed with brine, dried over anhydrous

Na_2SO_4. The crude product obtained after solvent evaporation was chromatographed over a triethylamine treated silica gel bed, using 40% ethyl acetate in *n*-hexanes as eluent, to give pure compound **25.** To the solution of 9-ethynylnoscapine **25** (1.0 mmol) in dichloromethane (5 mL), CuI, L-proline, pyrrolidine, and substituted phenyl acetylenes (**26a-c**) (1.2 mmol) were added and stirred at RT for 12 h. The solvent was removed under vacuum. The contents were partitioned between aqueous and dichloromethane (2 x 10 mL); the dichloromethane layer was collected and dried over anhydrous Na_2SO_4 and evaporated on rotary evaporator. The crude residue thus obtained was chromatographed over a triethylamine treated silica gel bed, using 30% EtOAc in *n*-hexane as eluent, to give pure compounds **20-22** as solid products in very good yields (Figure 4.4**)**. All the intermediates and final products **20-22** obtained were structurally characterized by IR, ^{1}H & ^{13}C NMR spectroscopy and mass spectrometry techniques (Appendix A4.1-4.9).

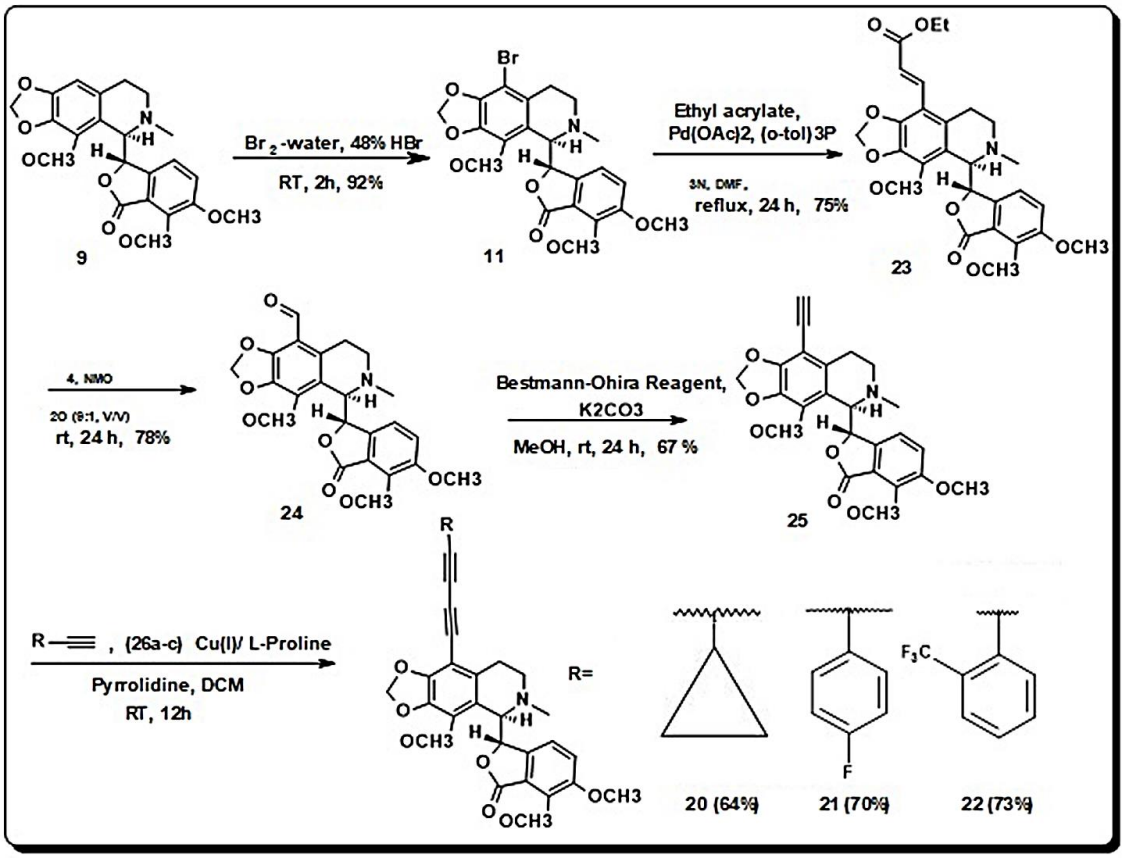

Figure 4.4: *Synthesis of 9-(1, 3-diynyl) noscapinoids* ***20, 21 and 22****.*

4.2.7. Structural characterization of the intermediates and final products:

(E)-ethyl-3-((R)-5-((S)-4,5-dimethoxy-3-oxo-1,3-dihydroisobenzofuran-1-yl)-4-methoxy-6-methyl-5,6,7,8-tetrahydro-[1,3]dioxolo[4,5-g]isoquinolin-9-yl)acrylate (23):

Nature: Yellow solid. M.P : 90-92 °C. IR (KBr) : 2939, 2800, 1761, 1707, 1616, 1498, 1437, 1311, 1270, 1178, 1140, 1034, 980, 887, 732, 664 cm^{-1}. ^{1}H NMR (500 MHz, $CDCl_3$) : δ 7.71 (d, *J* = 15.8 Hz, 1H, Ar-H), 6.99 (d, *J* = 8.1 Hz, 1H, Ar-H), 6.69 (d, *J* = 15.8 Hz, 1H, Ar-H), 6.25 (d, *J* = 8.1 Hz, 1H, Ar-H), 6.05 (s, 2H, O-CH2-O), 5.43 (d, *J* = 4.4 Hz, 1H, Ar-CH, (C3-phthalide)), 4.38 (d, *J* = 4.4 Hz, 1H, Ar-CH, (C5'-isoquinoline)), 4.26 (q, *J* = 7.0 Hz, 2H, -OC*H*$_2$-CH_3), 4.10 (s, 3H, -OCH_3), 4.05 (s, 3H, -OCH_3), 3.88 (s, 3H, -OCH3), 2.79-2.68 (m, 2H, -C*H*$_2$-*N*-CH_3 (C7'-isoquinoline)), 2.53 (s, 3H, -*N*-C*H*$_3$), 2.46-2.38 (m, 1H, Ar-C*H*H (C8'-isoquinoline)), 2.10-2.00 (m, 1H, Ar-CH*H* (C8'-isoquinoline)), 1.33 (t, *J* = 7.0 Hz, 3H, -OCH2-C*H*3). ^{13}C NMR (75 MHz, $CDCl_3$) : δ 167.9, 167.7, 152.1, 148.2, 147.6, 141.6, 141.1, 135.6, 133.6, 131.4, 120.5, 119.6, 118.1, 117.7, 117.3, 109.5, 101.1, 81.4, 62.1, 60.8, 60.3, 59.3, 56.6, 48.8, 45.5, 23.9, 14.2. MS (ESI) *m/z* : 512 [M+H]+ HRMS (ESI) : Calcd for $C_{27}H_{30}NO_9$ [M+H]+: 512.19151, found: 512.19203.

(R)-5-((S)-4,5-dimethoxy-3-oxo-1,3-dihydroisobenzofuran-1-yl)-4-methoxy-6-methyl-5,6,7,8-tetrahydro-[1,3]dioxolo[4,5-g]isoquinoline-9-carbaldehyde (24):

Nature : Off-white solid. M.P : 122 -124 °C. IR (KBr) : 2949, 2842, 2739, 1751, 1677, 1615, 496, 1447, 1270, 1127, 1048, 999, 885, 750, 509 cm^{-1}. ^{1}H NMR (500 MHz, $CDCl_3$) : δ 10.25 (s, 1H, Ar-CH=O), 7.26 (d, *J* = 8.3 Hz, 1H, Ar-H), 6.51 (d, *J* = 8.2 Hz, 1H, Ar-H), 6.08 (s, 2H, O-CH_2-O), 5.44 (d, *J* = 4.8 Hz, 1H, Ar-CH (C3-phthalide)), 4.30 (d, *J* = 4.8 Hz, 1H, Ar-CH (C5'-isoquinoline)), 4.09 (s, 3H, -OCH_3), 4.08 (s, 3H, -OCH_3), 3.89 (s, 3H, -OCH_3), 3.20-3.12 (m, 1H, -C*H*H-*N*-CH_3 ($C_{7'}$-isoquinoline)), 2.87-2.79 (m, 1H, -CH*H*-*N*-CH_3 ($C_{7'}$- isoquinoline), 2.54-2.46 (m, 4H, Ar-C*H*H ($C_{8'}$-isoquinoline), *N*-CH_3), 2.46-2.38 (m, 1H, Ar-CH*H* ($C_{8'}$-isoquinoline)). ^{13}C NMR (125 MHz, $CDCl_3$) : δ 185.9, 166.8, 152.4, 151.3, 146.4, 143.8, 140.3, 132.2, 118.3, 117.7, 116.7, 110.2, 101.2, 80.0, 61.0, 59.8, 58.5, 55.7, 46.8, 44.1, 22.4. MS (ESI) *m/z* : 442 $[M+H]^+$ HRMS (ESI) : Calcd for $C_{23}H_{24}O_8N$ $[M+H]^+$: 442.14964, found:442.15203.

(S)-3-((R)-9-ethynyl-4-methoxy-6-methyl-5,6,7,8-tetrahydro-[1,3]dioxolo[4,5-g]isoquinolin-5-yl)-6,7-dimethoxyisobenzofuran-1(3H)-one (25):

Nature : Off-white solid. M.P. : 98-100 °C. IR (KBr) : 3297, 2948, 2796, 2102, 1757, 1626, 1501, 1463, 1440, 1277, 1119, 1033, 1003, 931, 878, 653, 606 cm^{-1}. ^{1}H NMR (500 MHz, $CDCl_3$): δ 7.02 (d, *J* = 8.1 Hz, 1H, Ar-H), 6.28 (d, *J* = 8.1 Hz, 1H, Ar-H), 6.02 (s, 2H, -OCH2-O), 5.52 (d, *J* = 4.1 Hz, 1H, Ar-CH (C3-phthalide)), 4.33 (d, *J* = 4.1 Hz, 1H, Ar-CH (C5'-isoquinoline)), 4.09 (s, 3H, -OCH3), 4.03 (s, 3H, -OCH3), 3.88 (s, 3H, -OCH3), 3.42 (s, 1H, -C ≡ CH), 2.80-2.65 (m, 2H, -C*H*2-*N*-CH3 (C7'-isoquinoline)), 2.52

(s, 3H, *N*-C*H*3), 2.46-2.38 (m, 1H, Ar-C*H*H (C8'-isoquinoline)), 2.10-1.99 (m, 1H, Ar-CH*H* (C8'-isoquinoline)). ^{13}C NMR (75 MHz, $CDCl_3$): δ 167.9, 152.1, 150.5, 147.6, 141.2, 133.8, 133.1, 119.6, 118.2, 117.4, 101.3, 96.6, 84.3, 81.2, 75.9, 62.1, 60.6, 59.3, 56.7, 48.5, 45.4, 24.7. MS (ESI) *m/z* : 438 [M+H]+HRMS (ESI) : Calcd for $C_{24}H_{24}O_7N$ [M+H]+: 438.15473, found: 438.15521.

(S)-3-((R)-9-(cyclopropylbuta-1,3-diyn-1-yl)-4-methoxy-6-methyl-5,6,7,8-tetrahydro-[1,3] dioxolo[4,5-g]isoquinolin-5-yl)-6,7-dimethoxyisobenzofuran-1(3H)-one (20):

Nature : White solid. M.P. : 134-136 ^{o}C. IR (KBr) : 3418, 2926, 2227, 2145, 1759, 1603, 1497, 1434, 1263, 1118, 1033, 933, 885, 809, 727 cm^{-1}. ^{1}H NMR (300 MHz, $CDCl_3$) : δ 7.01 (d, *J* = 8.2 Hz, 1H, Ar-H), 6.23 (d, *J* = 8.2 Hz, 2H, Ar-H), 6.03 (s, 2H, O-CH2-O), 5.50 (d, *J* = 4.4 Hz, 1H, Ar-CH (C3-phthalide)), 4.31 (d, *J* = 4.4 Hz, 1H, Ar-CH (C5'-isoquinoline)), 4.09 (s, 3H, -OCH3), 4.04 (s, 3H, -OCH3), 3.88 (s, 3H, -OCH3), 2.77-2.60 (m, 2H, -C*H*2-*N*-CH3 (C7'-isoquinoline)), 2.51 (s, 3H, *N*-C*H*3), 2.45-2.33 (m, 1H, Ar-C*H*H (C8'-isoquinoline)), 2.07-1.92 (m, 1H, Ar-CH*H* (C8'-isoquinoline)), 1.46-1.35 (m, 1H, -CH2-C*H*-CH2), 0.91-0.78 (m, 4H, -CH(C*H*2)2). ^{13}C NMR (100 MHz, $CDCl_3$) : δ 167.9, 152.1, 151.3, 147.6, 141.1, 141.0, 134.6, 133.1, 119.6, 118.2, 117.4, 101.3, 96.8, 89.2, 81.3, 81.2, 66.3, 62.1, 60.6, 60.1, 59.3, 56.6, 48.5, 45.4, 24.9, 8.9, 0.3. MS (ESI-MS) *m/z*: 502 [M+H]+HRMS (ESI) : Calcd for $C_{29}H_{29}NO_7$ [M+H]+: 502.18603, found:502.18745.

(S)-3-((R)-9-((4-fluorophenyl)buta-1,3-diyn-1-yl)-4-methoxy-6-methyl-5,6,7,8-tetrahydro [1,3] dioxolo [4,5-g]isoquinolin-5-yl)-6,7-dimethoxyisobenzofuran-1(3H)-one (21):

Nature : White solid. M.P : 118-120 ^{o}C. IR (KBr) : 3418, 2933, 2211, 1758, 1599, 1500, 1434, 1263, 1034, 937, 836, 663, 529, 436 cm^{-1}. ^{1}H NMR (400 MHz, $CDCl_3$) : δ 7.52-7.47 (m, 2H, Ar-H), 7.06-7.01 (m, 3H, Ar-H), 6.31 (dd, *J* = 0.6, 8.1 Hz, 1H, Ar-H), 6.03 (s, 2H, OCH2-O), 5.50 (dd, *J* = 0.6, 4.5 Hz, 1H, Ar-CH (C3-phthalide)), 4.32 (d, *J* = 4.5 Hz, 1H, Ar-CH (C5'-isoquinoline)), 4.10 (s, 3H, -OCH3), 4.05 (s, 3H, -OCH3), 3.89 (s, 3H, -OCH3), 2.81-2.67 (m, 2H, -C*H*2-*N*CH3 (C7'-isoquinoline)), 2.52 (s, 3H, *N*-C*H*3), 2.48-2.40 (m, 1H, Ar-C*H*H (C8'-isoquinoline)), 2.14-2.04 (m, 1H, Ar-CH*H* (C8'-isoquinoline)). ^{13}C NMR (75 MHz, $CDCl_3$) : δ 167.9, 164.1 (d, *J*C-F = 251.6 Hz), 152.2, 151.4, 147.6, 141.6, 141.1, 134.5, 134.3 (d, *J*C-F = 8.8 Hz), 133.5 (d, *J*C-F = 8.0 Hz), 133.2, 119.6, 118.3, 117.7 (d, *J*C-F = 2.9 Hz), 117.6, 117.4, 115.9 (d, *J*C-F = 22.7 Hz), 115.5 (d, *J*CF = 22.0 Hz), 101.4, 96.4, 81.7, 81.1, 80.4, 74.0, 73.5, 62.2, 60.7, 59.4, 56.7,

48.3, 45.3, 24.8. MS (ESI-MS) *m/z* : 556 [M+H]+, HRMS (ESI) : Calcd for $C_{32}H_{27}FNO_7$ [M+H]+: 556.17661, found: 556.17862.

(S)-6,7-dimethoxy-3-((R)-4-methoxy-6-methyl-9-((2-(trifluoromethyl)phenyl)buta-1,3-diyn- 1-yl)-5,6,7,8-tetrahydro-[1,3]dioxolo[4,5-g]isoquinolin-5-yl)isobenzofuran-1(3H)-one (22):

Nature : White solid. M.P: 180-182 °C. IR (KBr) : 3423, 2948, 2793, 1756, 1625, 1497, 1436, 1316, 1265, 1168, 1128, 1078, 1035, 1008, 936, 767 cm^{-1}. ^1H NMR (400 MHz, $CDCl_3$) : δ 7.61 (d, *J* = 7.4 Hz, 2H, Ar-H), 7.55-7.43 (m, 2H, Ar-H), 7.05 (d, *J* = 8.2 Hz, 1H, Ar-H), 6.29 (d, *J* = 8.2 Hz, 1H, Ar-H), 6.04 (s, 2H, O-CH2-O), 5.51 (d, *J* = 4.2 Hz, 1H, Ar-CH (C3-phthalide)), 4.32 (d, *J* = 4.2 Hz, 1H, Ar-CH (C5'-isoquinoline)), 4.10 (s, 3H, -OCH3), 4.06 (s, 3H, -OCH3), 3.89 (s, 3H, -OCH3), 2.82-2.66 (m, 2H, -C*H*2-*N*-CH3 (C7'-isoquinoline)), 2.52 (s, 3H, *N*-C*H*3), 2.48-2.40 (m, 1H, Ar-C*H*H (C8'-isoquinoline)), 2.14-2.05 (m, 1H, Ar-CH*H* (C8'-isoquinoline)). ^{13}C NMR (100 MHz, $CDCl_3$) : δ 168.0, 152.2, 151.5, 147.7, 141.8, 141.1, 134.9, 134.7, 133.2, 132.3 (d, *J*C-F = 30.07 Hz), 131.4, 128.7, 125.9, 125.9, 120.0, 119.6, 118.3, 117.6, 117.4, 101.5, 96.2, 81.1, 80.2, 78.9, 78.2, 76.0, 62.2, 60.7, 59.4, 56.7, 48.4, 45.4, 24.8. MS (ESI-MS) *m/z* : 606 [M+H] HRMS (ESI) : Calcd for $C_{33}H_{27}F_3NO_7$ [M+H]+: 606.17341, found: 606.17380.

4.2.8. Cell culture and reagents

Noscapine, the chemical reagents and media were obtained from Sigma. Human breast cancer cell line, MCF-7 and MDAMB 231 were obtained from the cell repository of the National Center for Cell Science Pune, Maharashtra, India. Stock solution (100 mM) of the newly synthesized 1,3-diynyl derivatives of noscapine, **20-22** was prepared with dimethyl sulfoxide (DMSO) and stored at 4 ˚C until use. The cells were allowed to grow at a temperature of 37 °C in a 5% CO_2 and 95% humidity in Dulbecco's modified Eagle medium (DMEM, Sigma), supplemented with 10% fetal bovine serum (FBS) and antibiotics. Cells with a 70-80% confluence were sub-cultured for bioassays using trypsin-EDTA (0.25 %).

4.2.9. Cellular proliferation assay

Antiproliferation activity of noscapine and its 1,3-diynyl derivatives **20-22** was performed in 96-well plates as described previously (Naik *et al*., 2011b), using two human breast cancer cell lines, MCF-7 and MDA-MB-231. In brief, cells were grown in DMEM culture medium supplemented with 10% FBS, 1% penicillin/streptomycin and 2

mM l-glutamine at 37 °C in a humidified atmosphere with 5% CO_2. Cells were plated at a density of $5x10^3$ cells per well and were treated with gradient concentrations (5 to 100 µM) of noscapine and its 1,3-diynyl derivatives **20-22** for 72h. The cells were then fixed with 50% trichloroacetic acid and stained with 0.4% sulforhodamine B. The unbound dye was removed by washing. The protein bound dye was then extracted with 10 mM Tris base and measured the optical density at 564 nm using a SPECTRAmax PLUS 384 microplate spectrophotometer. The percentage of cell survival as a function of drug concentration was plotted and the IC_{50} values that stand for the drug concentration required to achieve a cell kill of 50% was determined using the online tool Quest GraphTM IC_{50} Calculator (AAT Bioquest, Inc., Sunnyvale, CA, USA, https://www.aatbio.com/tools/ic50-calculator).

4.2.10. Colony formation assay

Colony formation assay was conducted with a triple negative breast cancer cell line, MDA-MB-231. Briefly, 800 cells were seeded in a 6-well culture plate and incubated for 24 hours. The culture plate containing cells were treated with one of the 1,3-diynyl derivatives of noscapine **22** at three different concentrations such as 1µM, 10 µM and 20 µM. The treated cells were kept for 10 days with similar culture conditions as mentioned above in a CO_2 incubator to allow colony formation. The number of colonies under each treated condition was enumerated using image-J software (National Institute of Health, Bethesda, MD, USA).

4.2.11. DAPI staining

Apoptotic cancer cells were visualized by fluorescence microscopy following DAPI staining. Briefly, MDAMB-231 cells were grown on poly-L-lysine coated cover slips in 6-well plates and were treated with IC_{50} concentration (39.6, 31.4, 22.5 and 16.1 µM**)** of noscapine and its 1,3-diynyl derivatives **20-22** for 72h. After incubation, cover slips were fixed in cold methanol, washed with PBS, stained with DAPI, and mounted on slides. Images were captured using a fluorescent microscope (Nikon Eclipse Ts2R-FL). Apoptotic cells were identified by alterations of morphological features (e.g. nuclear condensation, formation of membrane blebs and apoptotic bodies).

4.2.12. Flow cytometric analysis of cell cycle progression

Inhibition of cell cycle progression with the treatment of noscapine and its 1,3-diynyl derivatives **20-22** was investigated using MCF-7 cells. The cells were maintained in DMEM with 4.5 g/L glucose and L-glutamine supplemented with 10% FBS and 1% penicillin/streptomycin, at 37 ^{0}C in a 5% CO_2 atmosphere. After reaching the 80-90% confluence, cells were treated with noscapine and its 1,3-diynyl derivatives **20-22** dissolved in 1% phosphate buffer saline (PBS). After 72h of treatment, cells were harvested and analysed using flow cytometry. Briefly, 2 x 10^6 cells were centrifuged, washed twice with ice-cold PBS and fixed in 70% ethanol at -20 ^{o}C for 24 h. The cells were centrifuged at 1000 x g for 10 min and the supernatant was discarded. The pellet was resuspended in 30 µl of phosphate/citrate buffer (0.2 M Na_2HPO_4/0.1 M citric acid, pH 7.5) at room temperature for 30 min. The cells were washed with 5 ml of PBS, incubated with 0.5 ml of propidium iodide (20 µg/ml in 0.6% Triton-X in PBS) and 0.5 ml of RNase A (20 µg/ml in PBS) for 45 min. in dark. Samples were analysed on a flow cytometer (BD FACS Aria-III) and the progress in the cell cycle was determined.

4.2.13. Quantitation of apoptosis by flow cytometry

MCF-7 cells were plated at a density of 3x10^4 cells per well on 12 well culture plate and incubated for 24 h with a complete medium. The cells were then treated with 25 µM concentration of noscapine and its 1,3-diynyl derivatives, **20-22** for 72 h. Adherent cells were harvested by mild trypsinization, stained with surface marker antibodies (biotin-conjugated Annexin V, FITC-conjugated streptavidin) and propidium iodide (PI). Cells were allowed to suspend in 1X binding buffer and incubated with Annexin V FITC conjugate for 20 min in dark conditions at room temperature. Flow cytometer data with 488 nm excitation for PI and emission at 530 nm were collected. Viable cells (Annexin V^-/PI^-), early apoptotic cells (Annexin V^+/PI^-), late apoptotic/necrotic cells (Annexin V^+/PI^+) and late necrotic cells (Annexin V^-/PI^+) were identified and determined their percentage.

4.2.14. Terminal deoxynucleotideyltransferase-mediated dUPT nick-end labeling (TUNEL) assay for apoptosis

For the TUNEL assay, 2x10^6 MCF-7 cells in 10 mL of medium were treated with 2 µL of 25 µM noscapine and its 1,3-diynyl derivatives **20-22** for 24 h. Cells were centrifuged, washed with ice cold PBS twice and were fixed in 4% paraformaldehyde in PBS and air-dried. Cells were then fixed in 1% paraformaldehyde and apoptosis was

detected by the TUNEL method using the APO-BrdU TUNEL Assay Kit according to the manufacturer's instructions. The percentage of apoptotic cells was calculated out of the total cells evaluated (>200 cells/sample).

4.2.15. Tubulin purification

Tubulin was purified from the goat brain via temperature cycles and GTP-dependent polymerization and depolymerization (Hamel and Linn, 1981; Panda *et al.*, 2000) using PEM buffer (50 mM pipes, 3 mM $MgSO_4$, and 1 mM EGTA, pH 6.8). The amount of tubulin in the extract was estimated by Bradford method using BSA as the standard (Bradford, 1976). The purified tubulin was quickly frozen and stored at -80 °C for further use.

4.2.16. Tubulin binding assay

Tubulin is auto fluorescence in nature due to presence of several tryptophan amino acids. Therefore, to examine the tubulin binding of chemical compounds, a fluorescence titration was used to analyse the quenching of intrinsic fluorescence of tubulin (Dash *et al.,* 2020). The purified tubulin (2 µM) was treated with 1,3-diynyl derivatives of noscapine **20-22** at a concentration of 25 µM in PEM buffer (50 mM pipes, 3 mM $MgSO_4$, 1 mM EGTA, pH 6.8) for 45 min at 35 ˚C. The samples were excited at 295 nm and emission spectrum was measured at 310-400 nm. For the spectrofluorometric titrations a FlouroMax ® 4 spectrofluorometer (Horiba Scientifc, Edison, NJ) assisted by Fluor Essence 3.5 software was used. The experiments were repeated twice.

4.2.17. Far-UV circular dichroism spectra

Far-UV circular dichroism spectra were used to evident the binding of chemical compounds to protein and their impact on the overall secondary structure conformational changes of the protein. The purified tubulin (5 µM) was incubated with 1,3-diynyl derivatives of noscapine **20-22** at a concentration of 25 µM in 25 mM pipes buffer, pH 7.4 for 45 min at 35 ˚C. Far-UV CD spectra (200–260 nm) were taken using a 0.1 cm path length, quartz cuvette after baseline correction (scan rate, 100 nm/min), using a JASCO CD Polarimeter J-810 (Jasco, Tokyo, Japan).

4.3. Results and Discussion

The anti-proliferative activity and tubulin binding affinity of the lead compound, noscapine, were improved manyfold by orchestrating numerous intense potent derivatives (Naik *et al*., 2012; Aneja *et al*., 2006a; Santoshi *et al*., 2015; Jain *et al*., 2011;

Aneja *et al.,* 2006b). Availability of structure-activity information of these derivatives of noscapine inspired us to build up a sensible predictive model for predicting the binding affinity of newly planned derivatives and screening of potent derivatives. We are reporting in this study a panel of 1,3-diynyl derivatives of noscapine as potent tubulin binding anticancer agents.

4.3.1. Rational design of 1,3-diynyl derivatives of noscapine

In pursuance of our endeavors to create novel Noscapine derivatives with improved binding affinity with tubulin, we have designed a new series of derivatives by coupling ethyne and 1,3-diyne functionality with the α-noscapine scaffold (Figure 4.2) based on in silico combinatorial approach. We have primarily focused on these two functional groups because both of them are recognized as a key pharmacophore in several anticancer drugs utilized in clinics such as erlotinib and icotinib (consists of ethyne group) as well as natural products such as panaxytriol, falcarinol, diplyne, 2-deoxydiplyne D sulfate, etc. (consists of 1,3-diynes group) with anticancer activity (Figure 4.5) (Liang *et al*., 2016; Lee *et al*., 2016).

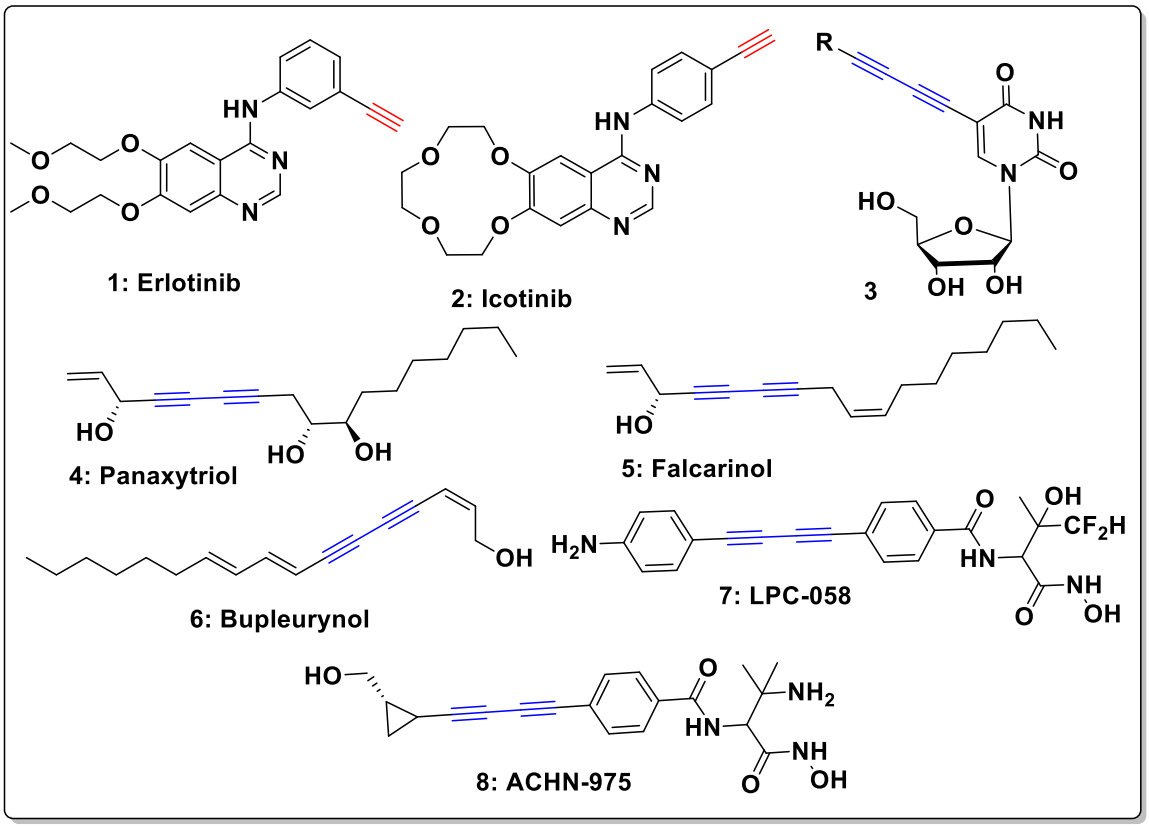

Figure 4.5: *Structures of anticancer drugs* ***1 and 2*** *containing ethyne group and 1,3-diyne containing bioactive natural and synthetic products* ***3-8****.*

4.3.2. Molecular docking and predictive binding affinity of 1,3-diynyl-noscapinoids with tubulin

The noscapinoids, reported earlier (Figure 4.1) and the library of 1,3-diynyl-noscapinoids (Figure 4.2) were docked onto the binding site of tubulin, at the interface between α- and β-tubulin using Glide XP. The predictive free energy of binding *(*$\Delta G_{bind,pred}$) of 1,3-diynyl derivatives of noscapine with tubulin was also calculated based on LIE-SGB predictive model. The reasonably well predictive model was developed by mapping the various energy parameters with the experimental binding affinity of training set molecules. The diverse energy terms used in the predictive model were included in Table 4.1. The values obtained for the coefficients *α, β, γ*, and *δ* are 0.08446, -0.00223, -0.000872 and -0.45601, respectively. The $\Delta G_{bind,pred}$ of the training set molecules were found to be very close to the experimental free energy of binding ($\Delta G_{bind,expt}$) as the mean difference between both the parameters is very small (s = 0.243 kcal/mol). The quality of the fit can also be judged through the value of the squared correlation coefficient (R^2) and analysis of variance (F-value).

$$\Delta G_{bind,pred} = 0.08446\langle U_{vdw}\rangle - 0.00223\langle U_{coul}\rangle - 0.00872\langle U_{rxn}\rangle - 0.45601\langle U_{cav}\rangle$$

$$(n = 11,\ R^2 = 0.998,\ s = 0.243,\ F = 3742.6,\ P \leq 0.001)$$

Because of the robust prediction of free energy of binding, the developed LIE-SGB model was used to determine the $\Delta G_{bind,pred}$ of the newly designed noscapinoids and virtual screening of a panel of highly potent derivatives. Based on the improved $\Delta G_{bind,pred}$ compared to noscapine ($\Delta G_{bind,expt}$ -5.246 kcal/mol), we have selected a panel of three 1,3-diynyl-noscapinoids **20**-**22** (Figure 4.3) having $\Delta G_{bind,pred,}$ value -6.694, -7.294 and -7.468 kcal/mol, respectively. All the three 1,3-diynyl noscapinoids **20**-**22** were accommodated very well inside the binding cavity (Figure 4.6). However, their molecular interactions with the binding site amino acids (within 5 Å) are albeit different as shown in the ligplot (Figure 4.7a-c). This might be due to the different functional groups present among themselves. As shown in the figure, the most potent 1,3-diynyl noscapinoid 22 in terms of docking score interacts more intensely with the residues of tubulin than the other two derivatives. Its binding involved 6 hydrogen bonds (dashed lines): the functional group CF_3 form 3 hydrogen bonds with the amine nitrogen (NE_3) of Glu B247 (bond length 3.34 Å), amine nitrogen (N) of Thr A225 (bond length 4.65 Å) and amine nitrogen (N) of Tyr A224 (bond length 3.04 Å); the nitrogen atom of isoquinoline ring of **22** hydrogen bond with side chain group (OG1) of Thr A73 (bond length 3.59 Å); both the oxygen of isobenzofuranone ring of **22** hydrogen bonds with the side chain group (NH_2) of Arg B2 (bond length 4.43 Å) and side chain group (NE) of

Arg B2 (bond length 2.92 Å) (Figure 4.7a). In contrast the 1,3-diynyl noscapinoids **20** and **21** revealed only 3 hydrogen bonds with the binding site residues (Figure 4.7a,b). Besides hydrogen bonding, a good number of hydrophobic interactions were involved in binding of 1,3-diynyl noscapinoids **20-22** with binding site residues (Appendix Table A4.10-A4.13). Most of the binding site residues are found common in the binding of noscapine and its 1,3-diynyl noscapinoids **20-22** such as Gln B247, Glu A77, Glu B47, Arg B48, Pro B245, Ala B250, Gly B246, Glu A71, Thr A73 and Met B1 (Figure 4.7). The binding site amino acids that are uniquely involved in the binding of 1,3-diynyl noscapinoids **20-22** compared to noscapine are Val B355, Pro A72, Arg B2, Lys A96, Arg A221, Met B325, Thr A223, Tyr A224 and Thr A225 (Figure 4.7). Inspired by our computational findings, we have chemically synthesized the newly designed 1,3-diynyl noscapinoids **20-22** to further evaluate their anticancer potential.

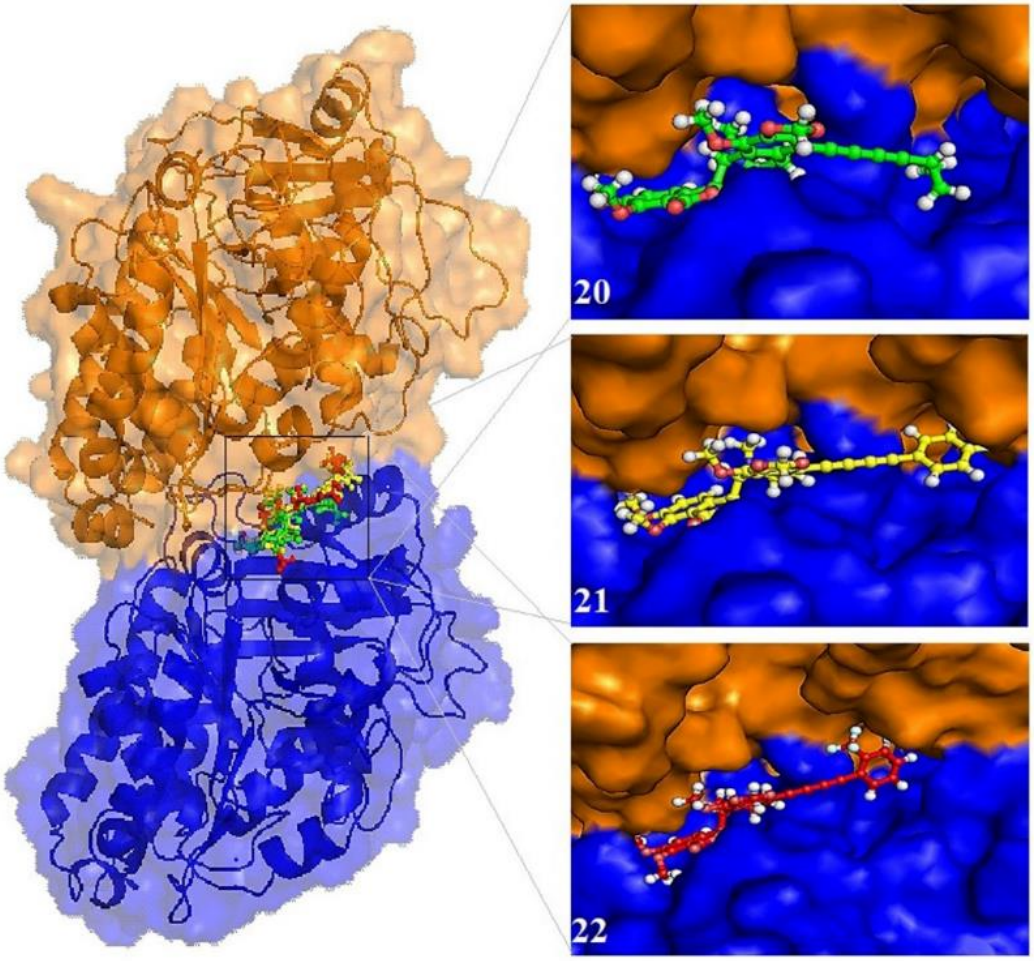

Figure 4.6: *The newly designed 1,3-diynyl noscapinoids **20-22** are well accommodated inside the binding pocket at the interface between α- and β-tubulin. The binding of these noscapinoids are biased more towards β-tubulin.*

Table 4.1: Molecular docking results (Glide XP) as well as calculated energies using Liasion programme (Schrodinger package) of noscapine and its 1,3-diynyl derivatives: van der Waals energy (U_{vdw}), Columbic energy (U_{coul}), reaction energy (U_{rxn}) and cavity energy (U_{cav}) as well as predicted free energy of binding ($\Delta G_{bind,pred}$) based on LIE-SGB prediction model and experimental free energy of binding ($\Delta G_{bind,expt}$). The newly designed 1,3-diynyl noscapinoids, **20-22** revealed improved $\Delta G_{bind,pred}$ compared to the lead molecule, noscapine as well as its previously reported derivatives.

Ligand	Glide XP_{score} (kcal/mol)	$<U_{vdw}>$ (kcal/mol)	$<U_{coul}>$ (kcal/mol)	$<U_{rxn}>$ (kcal/mol)	$<U_{cav}>$ (kcal/mol)	$\Delta G_{bind,\ expt}$ (kcal/mol)	$\Delta G_{bind,pred}$ (kcal/mol)
9	-1.927	-45.14	-330.8	135.5	2.097	-5.246	-5.212
10	-2.038	-49.00	-210.2	116.0	3.283	-6.006	-6.178
11	-2.766	-42.50	-362.1	155.9	4.208	-5.827	-6.060
12	-2.940	-48.06	-355.8	168.7	2.548	-5.587	-5.899
13	-3.263	-47.69	-285.7	135.5	3.103	-6.360	-5.987
14	-4.492	-47.44	-77.3	118.2	3.954	-6.628	-6.668
15	-2.605	-33.39	-331.9	176.7	4.465	-5.551	-5.657
16	-2.287	-45.57	-277.9	112.3	3.285	-5.665	-5.706
17	-2.350	-33.47	-324.5	152.5	3.766	-5.783	-5.151
18	-3.679	-45.41	-471.2	152.8	3.669	-5.673	-5.790
19	-4.687	-42.69	-267.6	129.9	3.465	-5.518	-5.722
20	-3.981	-54.80	-329.0	177.4	2.747	Nd	-6.694
21	-4.770	-53.80	-302.5	123.6	5.147	Nd	-7.294
22	-3.968	-49.87	-301.6	133.9	6.053	Nd	-7.468

$<U_{vdw}>$, $<U_{coul}>$, $<U_{rxn}>$ and $<U_{cav}>$ energy terms represents the ensemble average energy terms calculated as the difference between bound and free state of the ligands and its environment. $\Delta G_{bind,expt}$ was calculated from the dissociation constant (K_d *value*) using the relationship: $\Delta G_{bind,expt}$ = RT ln K_d where T = 298 K and R = 0.00199 (kcal/mol.K). Nd: not determined.

4.3.3. Predicted ADME properties of noscapine and its 1,3-diynyl derivatives 20-22

In order to validate the lead optimization, we have predicted the absorption, distribution, metabolism, and excretion (ADME) properties of noscapine and its 1,3-diynyl derivatives **20-22** using QikProp (Schrodinger software package). A number of ADME properties were predicted viz. molecular weight (*MW*), total solvent accessible surface area (*SASA*), octanol/water partition coefficient (*QPlogPo/w*), octanol/gas partition coefficient (*QPlogPoct*), water/gas partition coefficient (*QPlogPw*), polarizability in cubic angstroms (*QPpolrz*), % human oral absorption in intestine (*QP%*), brain/blood partition coefficient (*QPlogBB*), IC_{50} value for blockage of HERG K+ channel (*QPlogHERG*), skin permeability (*QPlogKp*), prediction of binding to human serum albumin (*QPlogKhsa*), apparent Caco-2 cell permeability in nm/sec

(*QPPCaco*) and apparent MDCK cell permeability in nm/sec (*QPPMDCK*). Caco-2 cells are a model for the gut-blood barrier whereas MDCK cells are considered to be a good mimic for the blood-brain barrier. Also we evaluated the acceptability of noscapine and its 1,3-diynyl derivatives **20-22** based on the Lipinski's rule of 5 (number of violations of Lipinski's rule of five) which is essential for rational drug design. It was interesting to found that noscapine and its 1,3-diynyl derivatives **20-22** revealed significant values for the properties analysed and qualified all the drug like characteristic based on Lipinski's rule of 5 (Table 4.2).

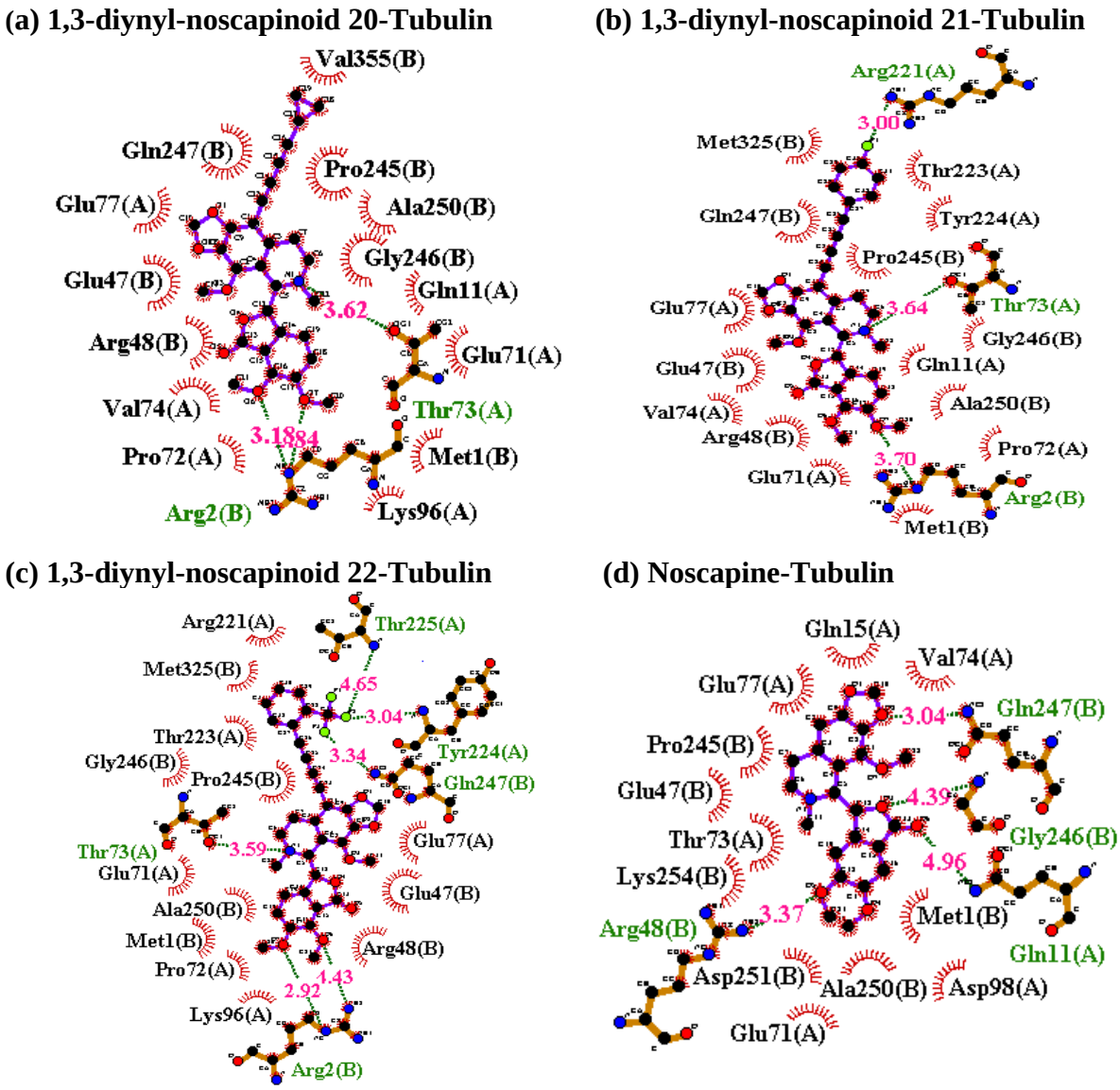

Figure 4.7: *Two dimensional representation of interaction observed between the binding site residues of tubulin with 1,3-diynyl noscapinoids* ***(a) 20, (b) 21, (c) 22*** *and* ***(d) Noscapine****. Dashed lines denote hydrogen bonds and numbers indicate hydrogen bond lengths in Å. Hydrophobic interactions are shown as arcs with radial spokes. The figure was made using LIGPLOT (Wallace et al., 1995). The residues within 5 Å distance from the docked ligands were only shown in the figures.*

Table 4.2: ADME screening of noscapine and its 1, 3-diynyl derivatives **20-22**.

Sl No.	ADME Screening	Noscapine	**20**	**21**	**22**	Recommended values
1	*MW*	413.4	501.5	555.5	605.6	130-725
2	*SASA*	582.6	815.0	860.0	903.8	300-1000
3	*Accpt HB*	8.75	8.75	8.75	8.75	2.0-20.0
4	*QPpolrz*	37.97	51.90	57.65	60.14	13.0-70.0
5	*QPlogPoct*	17.44	21.18	23.72	24.55	8.0-35
6	*QPlogPw*	10.03	10.49	11.85	11.63	4.0-45.0
7	*QPlogPo/w*	1.61	4.13	5.18	5.87	-2.0-6.5
8	*QPlogHERG*	-4.28	-6.58	-7.58	-7.61	Below -5.0
9	*QPPCaco*	770.5	948.4	967.1	1125.8	< 25 poor > 500 great
10	*QPlogBB*	0.34	0.17	0.29	0.49	-3.0-1.2
11	*QPPMDCK*	412.9	516.8	954.7	2304.7	< 25 poor >500 great
12	*QPlogKp*	-3.96	-3.39	-2.73	-2.76	-8.0- -1.0
13	*QPlogKhsa*	-0.57	0.40	0.69	0.91	-1.5-1.5
14	*QP%*	88.05	91.47	84.83	90.04	> 80% high < 25% poor
15	*Rule of Five (No. of violations)*	0	1	2	2	Maximum is 4

4.3.4. 1,3-diynyl noscapinoids inhibits proliferation of cancer cells

Based on our in silico results, we want to determine the anti-proliferative activity of the noscapine and its 1,3-diynyl derivatives **20-22** using two human breast adenocarcinoma cells, MCF-7 (estrogen- and progesterone- receptor positive) and MDAMB-231 (estrogen- and progesterone- receptor negative). The compounds were dissolved in DMSO to make a concentration ranging from 5 μM to 100 μM. Sulforhodamine B (SRB) *in vitro* proliferation assay was used to determine the IC_{50} values (the drug concentration required to achieve a cell kill of 50%). The IC_{50} values for noscapine and its 1,3-diynyl derivatives **20-22** for both the cell lines are assembled in Table 4.3. The rationally designed 1,3-diynyl noscapinoids **20-22** exhibited improved cytotoxic activity compared to noscapine using both the cell lines (Figure 4.8). The IC_{50} value amounted to 35.2, 27.3, 18.7 and 12.7 μM with noscapine, **20, 21** and **22**, respectively, for MCF-7 cells. Parenthetically, a comparable modest IC_{50} value of 39.6, 31.4, 22.5 and 16.1 μM was measured for noscapine, **20, 21** and **22**, respectively for MDAMB-231 cells. The anti-proliferative activity of the newly designed derivatives was improved many fold compared to noscapine using both the cell lines. The close IC_{50} values obtained using MCF-7 and MDAMB-231 suggests that these test compounds inhibit cellular proliferation of cancer cells impartial of hormone receptor status. Despite the fact that a significant correlation on the sensitivity of cancer cells to these

noscapinoids cannot yet be established at this stage, though it is evident that tubulin represents a potential target for these compounds.

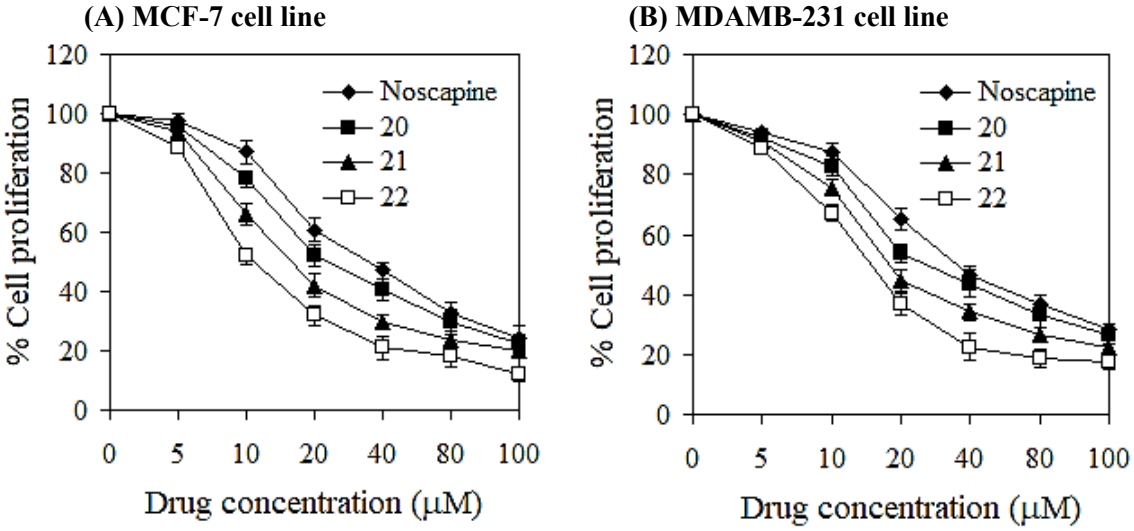

Figure 4.8: *The 1,3-diynyl noscapinoids* ***20-22*** *are more active compared to noscapine in inhibiting the proliferation of human breast cancer cells. Both (A) MCF-7 and (B) MDAMB-231cells were treated with noscapine and its 1,3-diynyl derivatives,* ***20-22*** *for 72 h and* IC_{50} *values were then measured. Each value represents the average of 3 independent experiments.*

Table 4.3: IC_{50} values of 1,3-diynyl noscapinoids **20-22**. All the rationally designed noscapinoids were found to have improved anti-proliferative activity compared to the lead molecule, noscapine.

	IC_{50} (μM)			
	Noscapine	**20**	**21**	**22**
MCF-7	35.2±2.7	27.3±2.4	18.7±1.9	12.7±1.4
MDA-MB-231	39.6±3.5	31.4±2.8	22.5±2.2	16.1±1.8

To further support the anticancer efficacy of the 1,3-diynyl noscapinoids **20-22** we have performed colony formation assay using a triple negative breast cancer cell line MDAMB-231. The cancer cells were treated with increasing concentration of one of the 1,3-diynyl derivatives of noscapine, **22** and incubated the cells at culture conditions for 10 days for colony formation. The number of colonies formed was determined using image-J software. The inhibition in colony formation was found to be concentration dependent (Figure 4.9). The number of colonies formation was significantly inhibited by the treated compound compared to untreated cells. The IC_{50} value was found to be 4.0 μM using colonogenic assay.

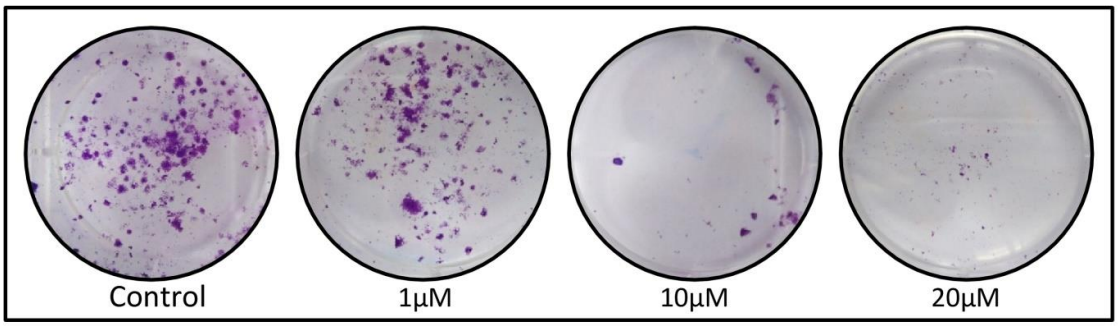

Figure 4.9: *Inhibition in colony formation with the treatment of 1,3-diynyl derivative of noscapine,* ***22****. The triple negative cancer cell line MDAMB-231 was treated with increasing concentration (1 μM, 10 μM and 20 μM) of the compound. The number of colony formation was significantly inhibited by the compound compared to untreated cells.*

Besides, the anti-proliferative activity, morphological examination using DAPI staining under the fluorescence microscope revealed apoptotic cell death to MDAMB-231 cancer cells. Alteration in morphological features such as chromatin condensation, plasma membrane blebbing, and appearance of apoptotic bodies with the treatment of 1,3-diynyl noscapinoids **20-22** indicated apoptotic cells (Figure 4.10).

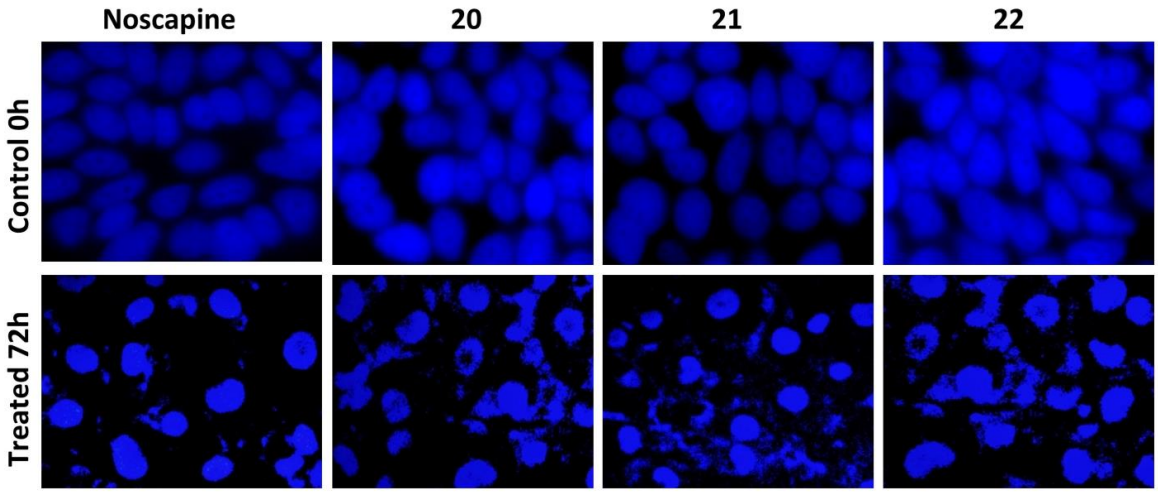

Figure 4.10: *Morphological characterization of MDAMB-231 cancer cells with DAPI staining. Panels show morphological evaluation of nuclei stained with DAPI from control cells (upper panels) and cells treated with* IC_{50} *concentration (39.6, 31.4, 22.5 and 16.1 μM****)*** *of noscapine and its 1,3-diynyl derivatives* ***20-22*** *(lower panels) for 72 hours using fluorescence microscopy.*

4.3.5. 1,3-Diynyl derivatives of noscapine alter the cell cycle progression and cause mitotic arrest

In order to determine the mechanism of cellular apoptosis, we examined the effect of noscapine and its 1,3-diynyl derivatives **20-22** (25 µM concentration) on the mitotic and apoptotic indices as a function of time in MCF-7 cells, using fluorescence activated cell sorting (FACS). The results are collated in Figure 4.11. It is revealed that more number of G2/M cells were accumulated at 24 h of treatment with the test compounds and then a decline upto 72 h. In consistent with this, the apoptotic cells also increased in number during this time period (Figure 4.11). Microtubule-interfering agents, including noscapine (Ye *et al*., 1998; Zhou *et al*., 2002b), are well known to arrest cell cycle progression at the G2/M phase in mammalian cells (Jordan *et al*., 1998). The cell cycle profile of MCF-7 with treatments of noscapine and its 1,3-diynyl derivatives based on FACS analysis is covered in Figure 4.12 (panels A-E). It has been seen that accumulation of fluorescently labeled DNA is a good indicator to observe the cell cycle progression and cell death (Ye *et al*., 1998; Zhou *et al*., 2002b; Aneja *et al*., 2006b). Cells with 2N DNA represent the G1 phase, while cells with duplicated 4N DNA represent G2 and M phases. Cells in the process of DNA replication have peaks between 2N and 4N, which represent S phase. Cells with less than 2N DNA represent dying cells that degrade their DNA to different extents. MCF-7 cells treated with 25 µM of the test compounds for 72 h led to significant perturbations of the cell cycle profile. FACS analysis revealed high accumulation of cells in the G2/M phase at 72 h of treatment of noscapine and its 1,3-diynyl derivatives compared to untreated cells. In contrast to G2/M block, a characteristic peak with hypodiploid DNA content (sub-G1) was seen to appear at 72 hours of treatment.

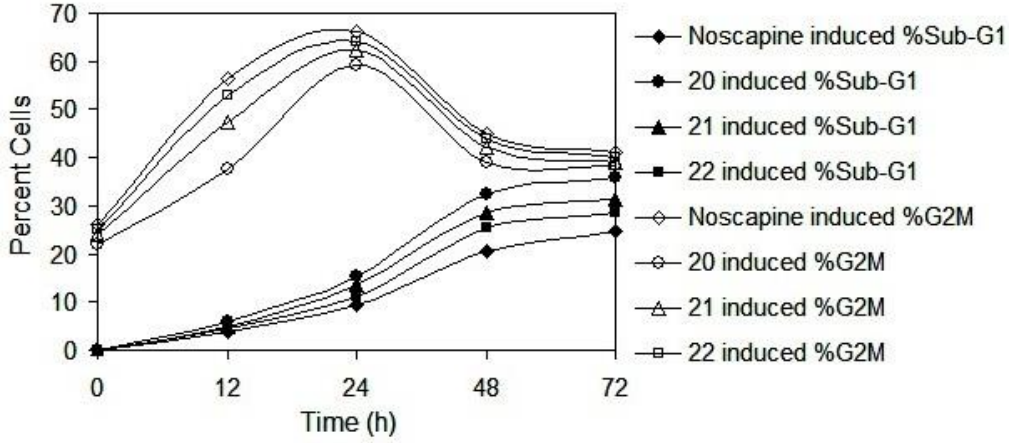

Figure 4.11: *Apoptotic and mitotic index as a function of time of treatment with 25 µM concentrations of noscapine and its 1,3-diynyl derivatives in human breast carcinoma cells (MCF-7). At 24 h, the percentage of G2M (mitotic cells) cells were 66.2%, 59.3%,*

*62.4% and 64.2% respectively for noscapine, **20, 21** and **22**. The increase activity of 1,3-diynyl derivatives compared to noscapine in induction of apoptosis was also evident by the higher percentage of cells with degraded DNA, in that, 24.9%, 35.8%, 31.2% and 28.4% of cells with < 2N DNA (sub-G1) content were seen on treatment of noscapine, **20, 21** and **22**, respectively.*

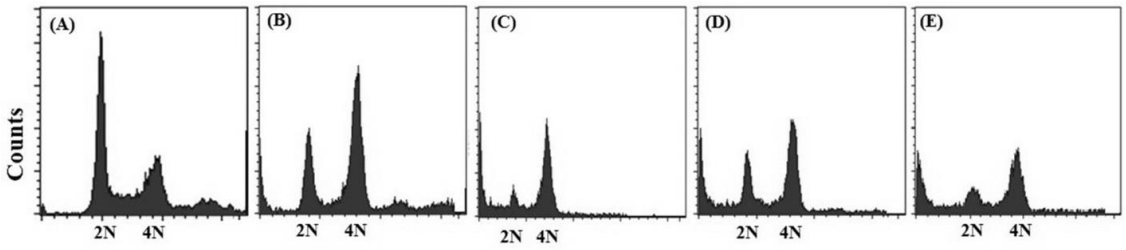

***Figure 4.12:** Noscapine and its 1,3-diynyl derivatives, **20-22** alter the cell cycle profile, followed by the appearance of a characteristic peak of hypodiploid (sub-G1) DNA content, which indicate induction of apoptosis. Panels A-E depicted analyses of cell cycle progression as determined by FACS in MCF-7 cells treated with 25 µM of noscapine and its derivatives **20-22** at 72 hours.*

4.3.6. Induction of apoptosis

We next approached to work out whether or not interference with the cell cycle progression by noscapine and its 1,3-diynyl derivatives led to apoptosis cell death. Biochemically the apoptotic cell death is characterized by alterations of lipid composition of cell membrane, in which the phosphatidylserine (PS), normally located on the inner leaflet of the cell membrane, translocates to the outer leaflet, which can be measured by annexin V binding. Further, a cell-impermeant DNA-binding fluorescent dye, propodium iodide can only enter the cells when it is at the stage of late apoptosis when membrane permeability is compromised. The apoptotic cells can be quantified in large extent by FACS analysis. The percentage of early apoptotic and late apoptotic MCF-7 cells for the treatment of noscapine and its 1,3-diynyl derivatives **20-22** with a concentration of 25 µM for 72 h is collated in Figure 4.13 (panels B-E). After 72 h of culture, the control untreated cell culture contained only very few early apoptotic (2.2%) and late apoptotic cells (4.8%), which were considered as the background cell death due to regular trauma during cell culture (Figure 4.13A). In contrast, the percentage of early apoptotic cells to 5.4%, 13.8%, 16.6% and 24.9% as well as late apoptotic cells to 18.5%, 37.4%, 41.5% and 46.8% with noscapine, **20, 21** and **22**, respectively was found to be significantly high compared to controlled untreated cells (Figure 4.13).

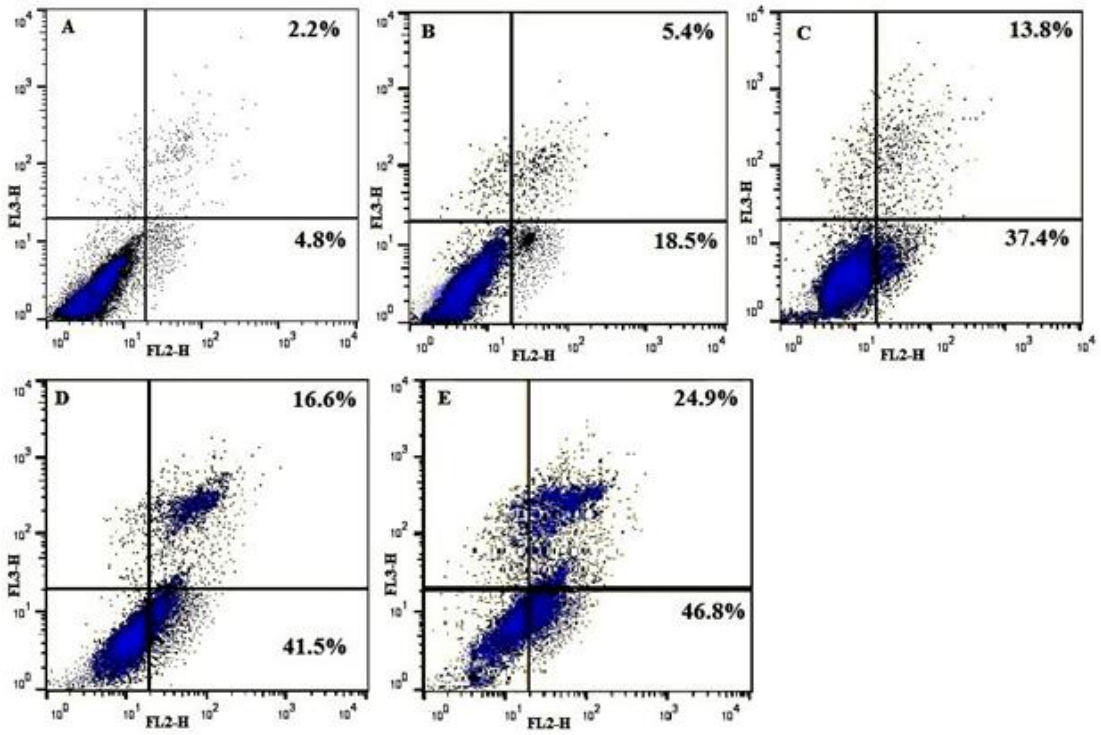

Figure 4.13: *Flow cytometry analysis of phosphatidylserine (PS) exposure in MCF-7 cells treated with noscapine (B) and its derivatives,* ***20*** *(C),* ***21*** *(D) and* ***22*** *(E) with 25 µM for 72 hours and compared with non treated control cells (A). Annexin-V and propidium iodide (PI) were used to distinguish among three sub-populations of cells: PI- and AnnexinV- cells represent viable cells with intact membrane and preserved amino-phospholipid asymmetry, PI- and Annexin V+ cells represent early apoptotic cells with intact cellular membrane exposing phosphatidylserine, whereas PI+ and Annexin V+ cells represent late apoptotic cells with compromised asymmetry and membrane permeability. Representative results of three independent experiments.*

In an effort to characterize induced necrobiosis by noscapine and its 1,3-diynyl derivatives **20-22**, we performed the TUNEL assay on formalin-fixed MCF-7 cells. The terminal stage of apoptosis display cleaved 3' ends of DNA which is visualized by specific labeling by TUNEL assay. The quantitative FACS analysis revealed 57.%, 59.2%, 62.5% and 68.4% TUNEL-positive cells on treatment with 25 µM noscapine, **20, 21** and **22**, respectively (Figure 4.14B-E). In contrast, control untreated cells showed only 3.7% TUNEL-positive cells (Figure 4.14A).

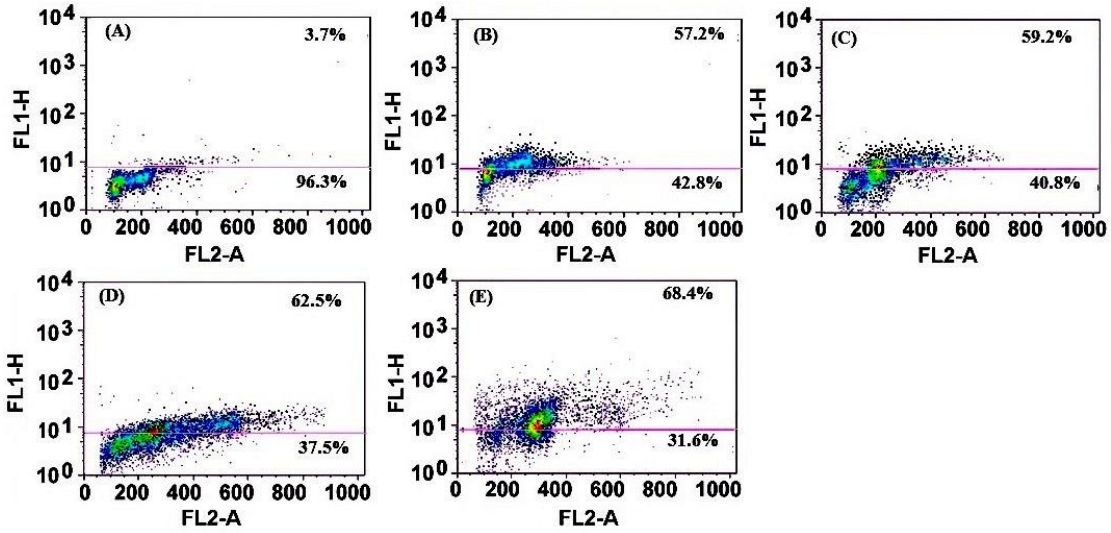

Figure 4.14: *TUNEL analysis reveals induction of apoptosis by (A) untreated cells, (B) noscapine treated cells and its 1,3-diynyl derivatives treated cells: (C)* ***20,*** *(D)* ***21*** *and (E)* ***22****, as evidenced by DNA fragmentation in MCF-7 cells. Number of apoptotic cells is indicated by the number of Alexa Fluor 488 positive cells of the total gated cells. The values presented on cytogram is the percentage of apoptotic cells (top) and normal cells (bottom).*

4.3.7. 1,3- diynyl derivatives of noscapine quenched the intrinsic fluorescence of tubulin

Microtubules are auto fluorescent by nature due to presence of aromatic amino acids, tryptophan which can be selectively measured by exciting at 295 nm. Any chemical compounds that bind with tubulin and alter its conformation lead to decrease in its intrinsic fluorescence (Ye *et al.,* 1998). This is a standard assay to test whether a chemical compound binds to tubulin or not (Zhou *et al.,* 2002b). We have used similar assay to test whether the 1,3-diynyl derivatives of noscapine also bind to tubulin or not. It was revealed that intrinsic fluorescence of tubulin, decreased in presence of 1,3-diynyl derivatives of noscapine **20**–**22**, suggests the binding capability of these compounds to tubulin. The relative percentage of decrease in fluorescence intensity was 12.91 %, 18.87 % and 27.15 % respectively in presence of 25 μM concentration of **20**–**22** (Figure 4.15), compared to control.

4.3.8. 1,3-diynyl derivatives of noscapine alter the secondary structure of tubulin

Circular dichroism is an insightful method of elucidating changes in the secondary structure of the proteins. This can also be used to study the interaction of ligands with protein. The interaction with ligands can influence by various intermolecular as well as

intramolecular forces, affecting the protein 's secondary and tertiary structure (Kelly *et al.,* 2020). The elliptical shifts with the treatment of 1,3-diynyl derivatives of noscapine **20–22** at a 25 µM concentration revealed a marked disturbance in the structure of the alpha helix (Figure 4.16), indicating that these molecules interact with the secondary structure of the tubulin.

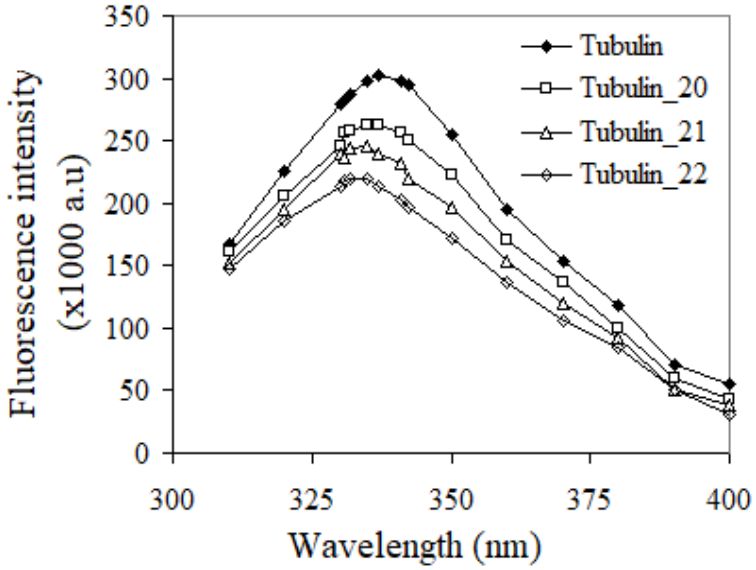

Figure 4.15: *Treatment of purified tubulin with 1,3-diynyl derivatives of noscapine* ***20–22*** *at a concentration of 25 µM quenched the intrinsic fluorescence of tubulin significantly compared to untreated tubulin. The relative percentage of decreased in fluorescence intensity was 12.91 %, 18.87 % and 27.15 % respectively in presence of 25 µM concentration of* ***20–22*** *compared to control.*

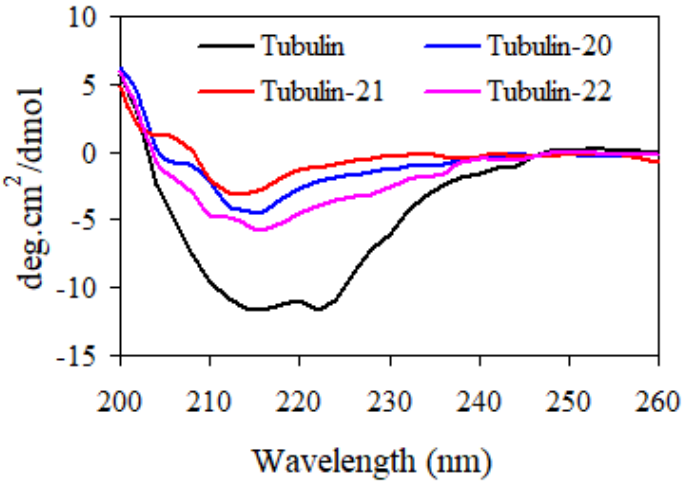

Figure 4.16: *Far-UV circular dichroism spectra indicating disruption of tubulin secondary structure with the treatment of 25 µM concentration of 1,3-diynyl derivatives of noscapine 20–22. The graph represents one of the three independent experiments.*

4.4. Conclusion

In conclusion, we have strategically designed a panel of 1,3-diynyl derivatives of natural lead molecule, noscapine, in a quest to accelerate its anticancer activity. We have also provided the simplest methods for the direct and regioselective modification of noscapine scaffold to produce the 1,3-diynyl derivatives in high yields. All the 1,3-diynyl derivatives developed have showed increase anti-proliferative activity to cancer cells based on our extensive molecular modeling and cellular study using two human breast cancer cell lines, MCF-7 and MDA-MB-231. Therefore, these novel compounds may prove efficacious not only in the treatment of breast carcinoma, but also for other type of cancers. Our results compel us to continue to examine the effects of these novel compounds on *in vivo* animal experiment with the final goal of taking it to the human clinical study.

Appendix

A4.1: ^{1}H NMR of 1,3-diynyl derivatives, 20:

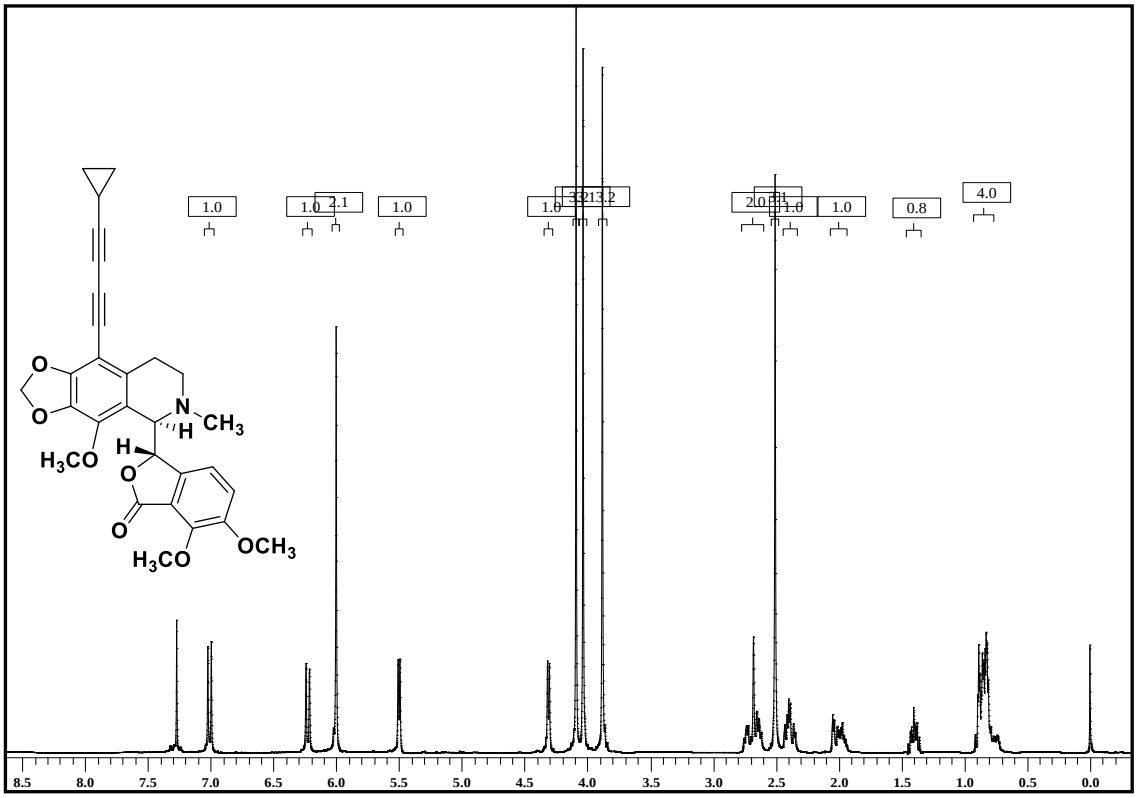

A4.2: ^{13}C NMR of 1,3-diynyl derivatives, 20:

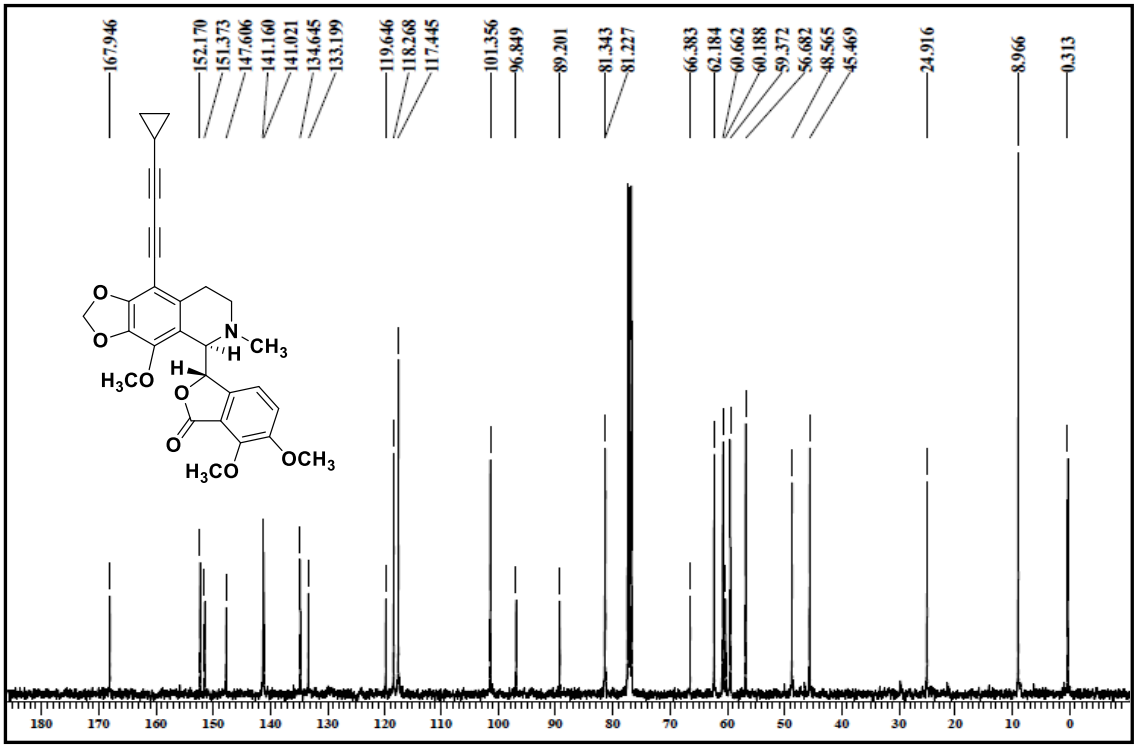

A4.3: HRMS of 1,3-diynyl derivatives, 20:

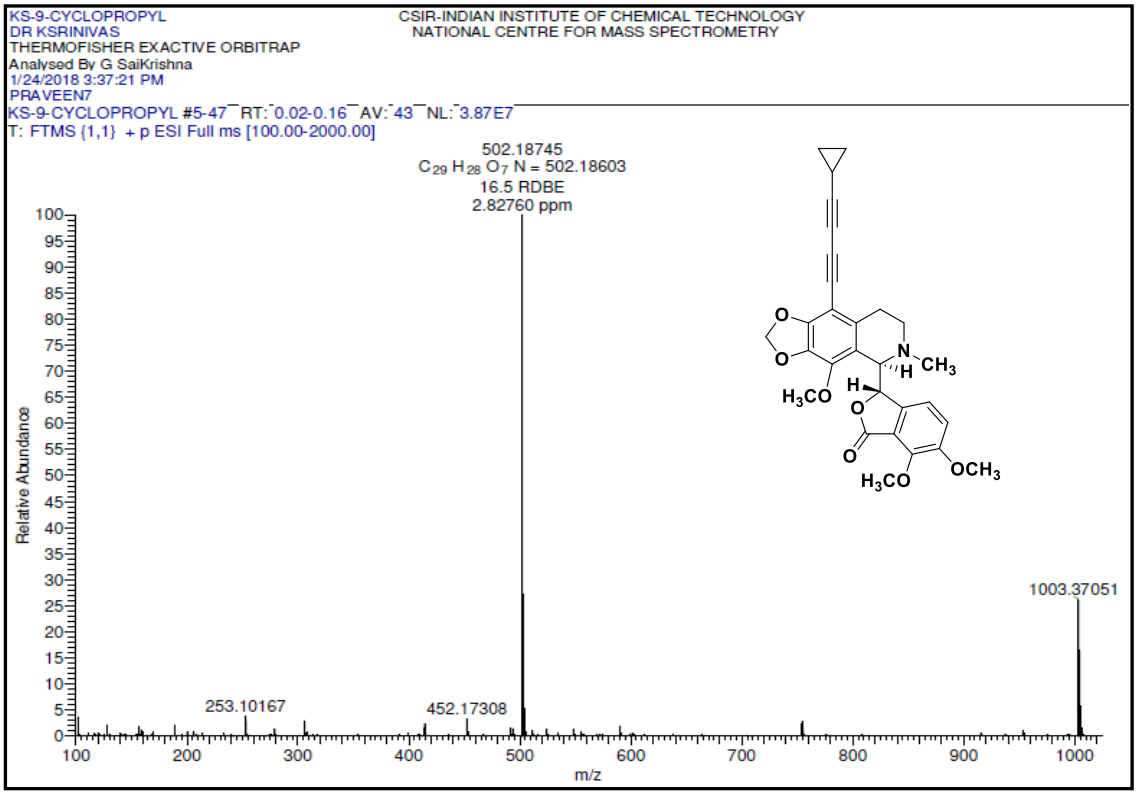

A4.4: ^{1}H NMR of 1,3-diynyl derivatives, 21

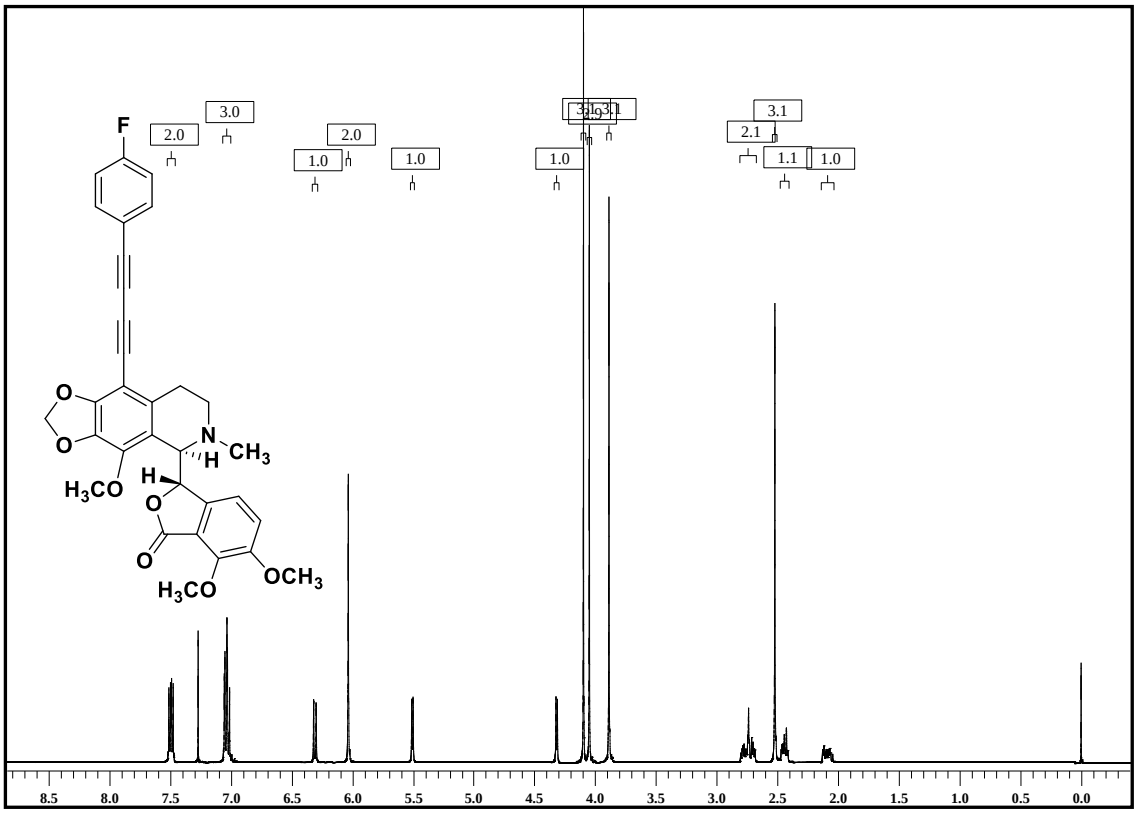

A4.5: ^{13}C NMR of 1,3-diynyl derivatives, 21

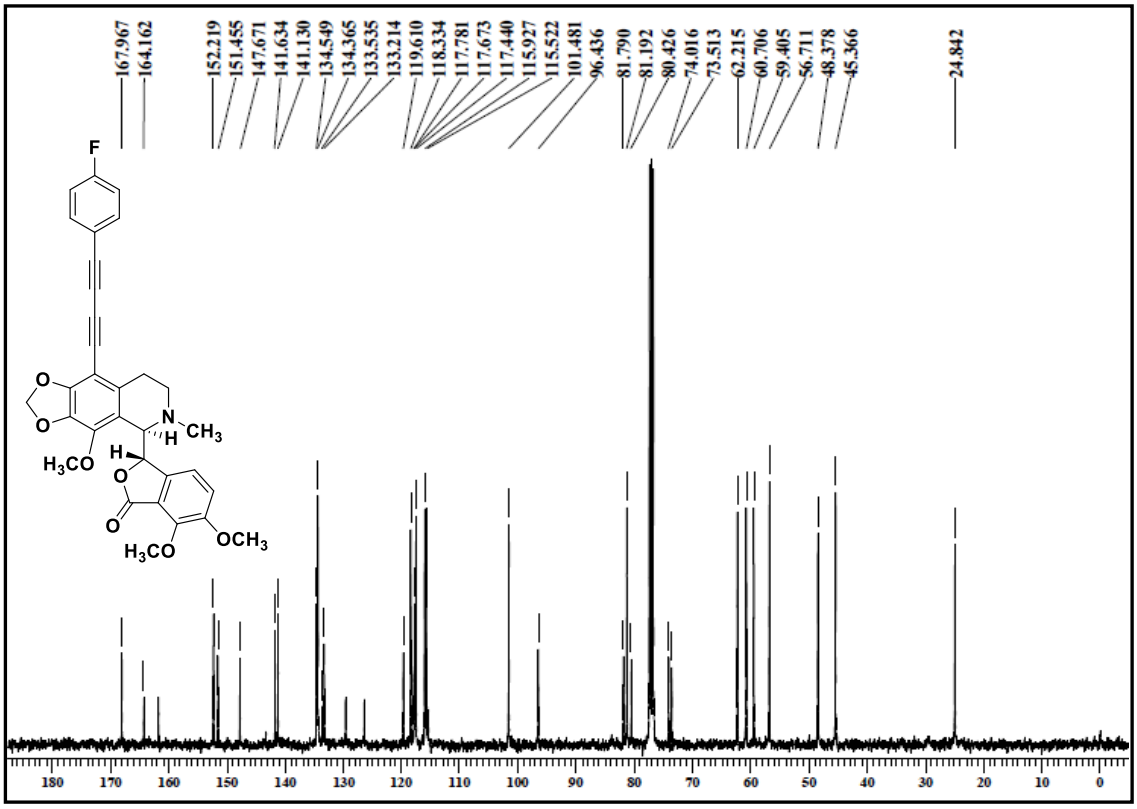

A4.6: HRMS of 1,3-diynyl derivatives, 21

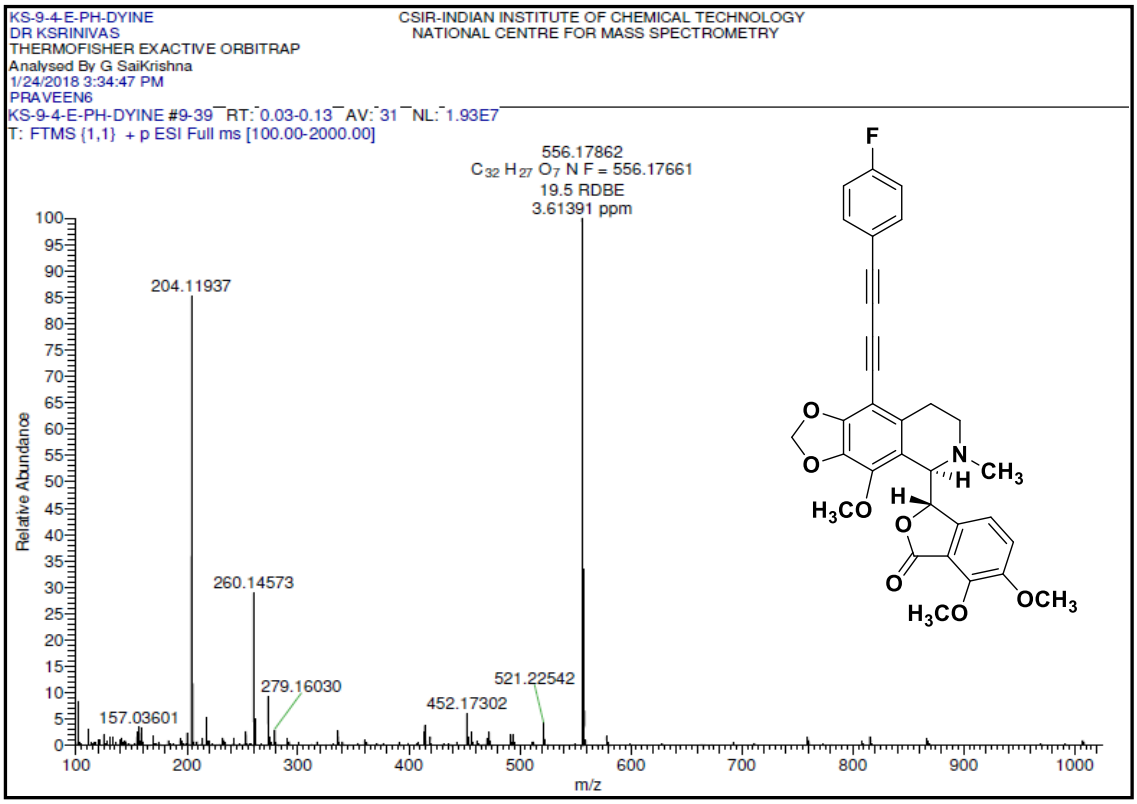

A4.7: ^{1}H NMR of 1,3-diynyl derivatives, 22

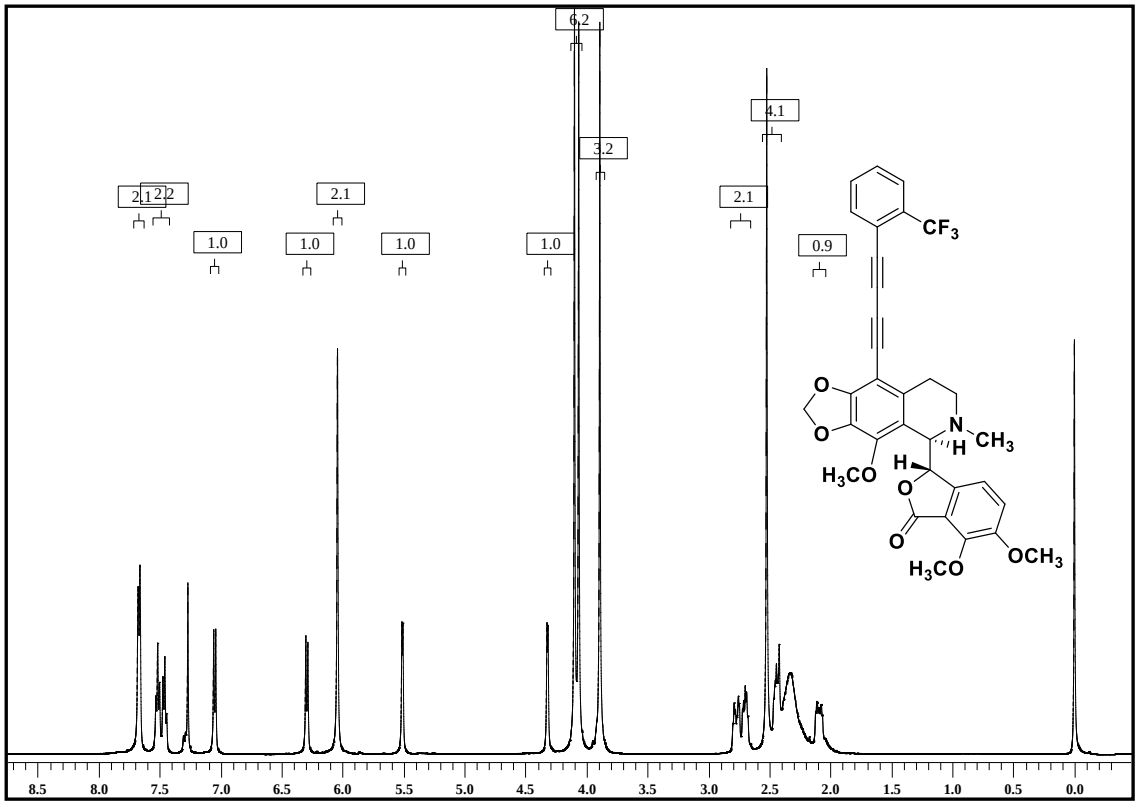

A4.8: ^{13}C NMR of 1,3-diynyl derivatives, 22

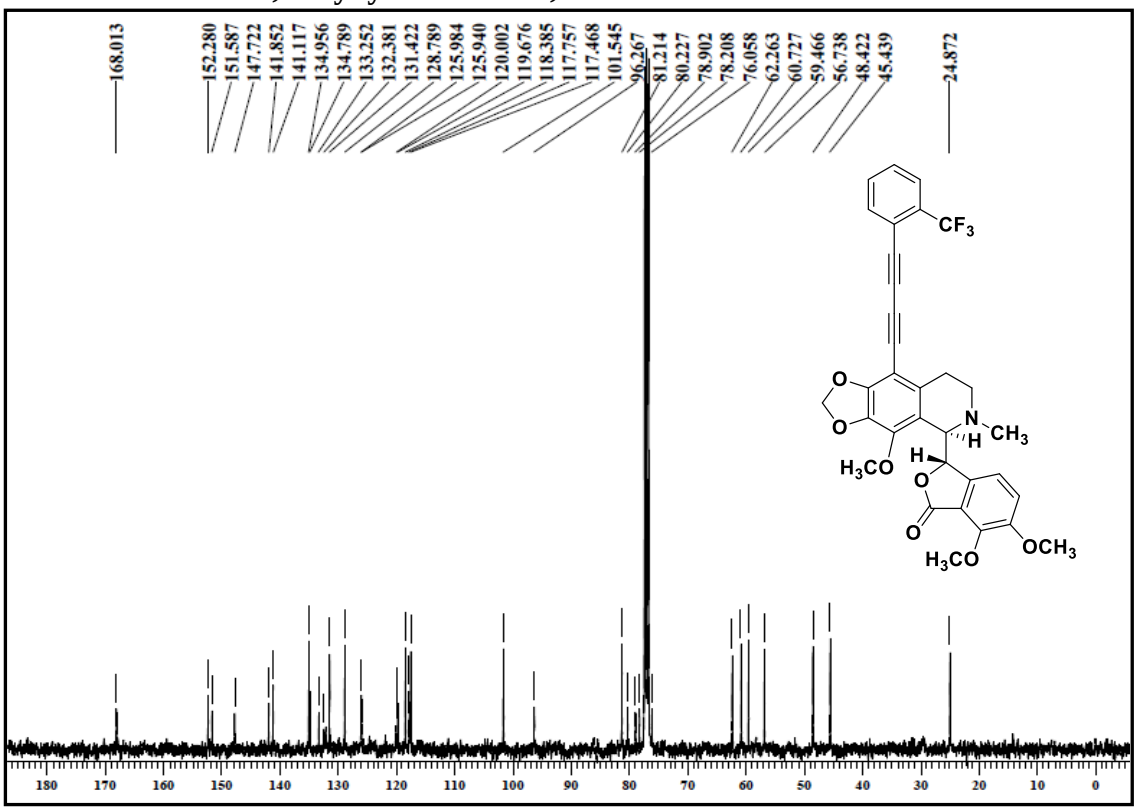

A4.9: HRMS of 1,3-diynyl derivatives, 22

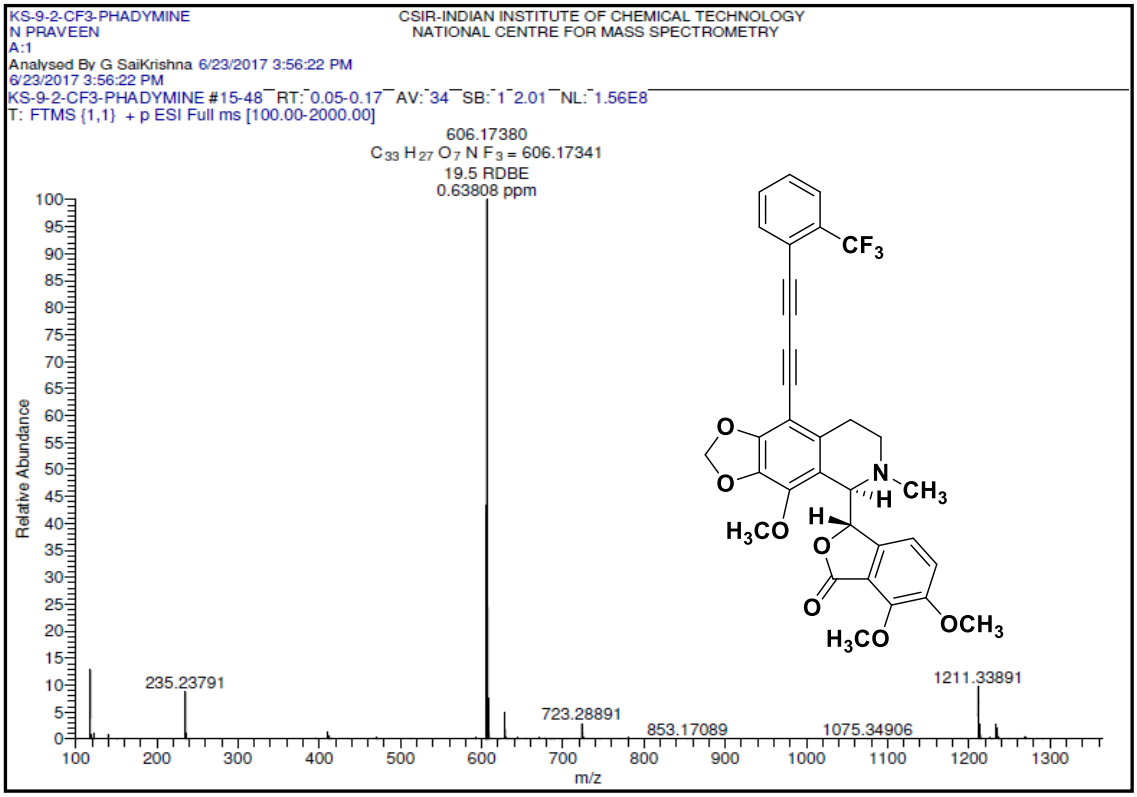

Table A4.10-A4.13: Geometry of hydrogen bonds and hydrophobic interaction of 1,3-diynyl-noscapinoids, **20-22** and the lead molecule, noscapine with the binding site residues of tubulin.

Table A4.10			**Table A4.11**		
(a) 1,3-diynyl noscapinoid 20_Tubulin			**(b) 1,3-diynyl noscapinoid 21_Tubulin**		
Hydrogen bonding			**Hydrogen bonding**		
Hydrogen Donor (D)	**Hydrogen Acceptor (A)**	**Distance (D-A) in Å**	**Hydrogen Donor (D)**	**Hydrogen Acceptor (A)**	**Distance (D-A) in Å**
ARG D 2 NE	20 O7	3.7	ARG D 2 NE	21 O7	2.84
ARG A 221 NH1	20 F1	3	ARG D 2 NE	21 O6	3.18
20 N1	THR A 73 OG1	3.64	21 N1	THR A 73 OG1	3.62
Hydrophobic interaction			**Hydrophobic interaction**		
20	**Tubulin**	**Distance**	**21**	**Tubulin**	**Distance**
C30	MET D 325 CE	4.65	C29	VAL D 355 O	3.13
C29	MET D 325 CE	3.93	C28	VAL D 355 O	4.35
C28	MET D 325 CE	4.79	C27	VAL D 355 O	4.58
C30	MET D 325 SD	4.96	C29	VAL D 355 C	4.21
C29	MET D 325 SD	4.71	C29	VAL D 355 CA	4.82
C30	MET D 325 CG	4.94	C29	VAL D 355 N	4.4
C29	MET D 325 CG	4.99	C28	VAL D 355 N	4.78
N1	ALA D 250 CB	5	N1	ALA D 250 CB	4.6
C19	ALA D 250 CB	4.8	C22	ALA D 250 CB	4.99
C6	ALA D 250 CB	4.44	C7	ALA D 250 CB	4.91
C19	ALA D 250 O	4.97	C6	ALA D 250 CB	3.81
C25	GLN D 247 OE1	4.95	C6	ALA D 250 CA	4.93
C24	GLN D 247 OE1	5	C26	GLN D 247 NE2	4.48
C7	GLN D 247 OE1	4.59	C25	GLN D 247 NE2	3.84
C32	GLN D 247 NE2	4.86	C24	GLN D 247 NE2	3.5
C27	GLN D 247 NE2	4.81	C23	GLN D 247 NE2	3.58
C26	GLN D 247 NE2	3.76	C9	GLN D 247 NE2	4.99
C25	GLN D 247 NE2	3.13	C7	GLN D 247 NE2	4.48
C24	GLN D 247 NE2	2.89	C3	GLN D 247 NE2	4.67
C23	GLN D 247 NE2	3.13	C1	GLN D 247 NE2	4.19
C7	GLN D 247 NE2	3.27	C26	GLN D 247 CD	4.55
C6	GLN D 247 NE2	4.39	C25	GLN D 247 CD	4.18

C3	GLN D 247 NE2	4	C24	GLN D 247 CD	4.13
C1	GLN D 247 NE2	3.92	C23	GLN D 247 CD	4.43
C32	GLN D 247 CD	4.66	C7	GLN D 247 CD	4.96
C27	GLN D 247 CD	4.84	C28	GLN D 247 CG	4.01
C26	GLN D 247 CD	4.08	C27	GLN D 247 CG	4.08
C25	GLN D 247 CD	3.76	C26	GLN D 247 CG	3.5
C24	GLN D 247 CD	3.82	C25	GLN D 247 CG	3.46
C23	GLN D 247 CD	4.23	C24	GLN D 247 CG	3.81
C7	GLN D 247 CD	3.94	C23	GLN D 247 CG	4.49
C6	GLN D 247 CD	4.77	C28	GLN D 247 CB	4.07
C3	GLN D 247 CD	4.99	C27	GLN D 247 CB	4.66
C32	GLN D 247 CG	4	C26	GLN D 247 CB	4.33
C27	GLN D 247 CG	4.08	C25	GLN D 247 CB	4.43
C26	GLN D 247 CG	3.51	C24	GLN D 247 CB	4.82
C25	GLN D 247 CG	3.47	C28	GLN D 247 CA	4.8
C24	GLN D 247 CG	3.84	C26	GLN D 247 CA	4.83
C23	GLN D 247 CG	4.51	C25	GLN D 247 CA	4.67
C7	GLN D 247 CG	4.51	C24	GLN D 247 CA	4.81
C26	GLN D 247 CB	4.87	C7	GLN D 247 CA	4.71
C25	GLN D 247 CB	4.89	C29	GLN D 247 N	4.97
C7	GLN D 247 CA	4.52	C28	GLN D 247 N	4.15
C6	GLN D 247 CA	4.61	C27	GLN D 247 N	4.73
C7	GLN D 247 N	4.41	C26	GLN D 247 N	4.11
C6	GLN D 247 N	4.58	C25	GLN D 247 N	3.96
C7	GLY D 246 O	3.5	C24	GLN D 247 N	4.17
C6	GLY D 246 O	3.01	C23	GLN D 247 N	4.71
C3	GLY D 246 O	4.78	C7	GLN D 247 N	4.35
C7	GLY D 246 C	3.98	C25	GLY D 246 O	4.93
C6	GLY D 246 C	3.92	C24	GLY D 246 O	4.58
C7	GLY D 246 CA	4.85	C23	GLY D 246 O	4.55
C6	GLY D 246 CA	4.89	C22	GLY D 246 O	4.92
C7	GLY D 246 N	4.47	C7	GLY D 246 O	2.86
C6	GLY D 246 N	4.53	C6	GLY D 246 O	3
C23	PRO D 245 CB	4.69	C3	GLY D 246 O	4.31
O4	PRO D 245 CB	4.63	C1	GLY D 246 O	4.95
C9	PRO D 245 CB	4.65	C26	GLY D 246 C	4.6
C4	PRO D 245 CB	4.94	C25	GLY D 246 C	4.21
C3	PRO D 245 CB	4.55	C24	GLY D 246 C	4.13
C1	PRO D 245 CB	4.38	C23	GLY D 246 C	4.42
O4	PRO D 245 CG	4.74	C7	GLY D 246 C	3.55
C7	PRO D 245 C	4.97	C6	GLY D 246 C	4.05
O4	PRO D 245 CA	4.62	C3	GLY D 246 C	4.82
C12	PRO D 245 CA	4.92	C28	GLY D 246 CA	4.97
C3	PRO D 245 CA	4.99	C26	GLY D 246 CA	4.59
C19	ARG D 48 NH2	3.57	C25	GLY D 246 CA	4.3
C18	ARG D 48 NH2	3.57	C24	GLY D 246 CA	4.34
C17	ARG D 48 NH2	3.86	C23	GLY D 246 CA	4.72
C16	ARG D 48 NH2	4.08	C7	GLY D 246 CA	4.24
C15	ARG D 48 NH2	4.06	C6	GLY D 246 CA	4.75
C14	ARG D 48 NH2	3.83	C26	GLY D 246 N	4.91
C13	ARG D 48 NH2	4.93	C25	GLY D 246 N	4.36
C12	ARG D 48 NH2	4.59	C24	GLY D 246 N	4.09
C19	ARG D 48 NH1	4.73	C23	GLY D 246 N	4.19
C15	ARG D 48 NH1	4.87	C7	GLY D 246 N	3.66
C14	ARG D 48 NH1	4.51	C6	GLY D 246 N	4.19
C12	ARG D 48 NH1	4.5	C3	GLY D 246 N	4.46
O6	ARG D 48 CZ	4.93	C1	GLY D 246 N	4.72
C19	ARG D 48 CZ	3.96	C25	PRO D 245 CB	4.65
C18	ARG D 48 CZ	4.29	C24	PRO D 245 CB	4.02
C17	ARG D 48 CZ	4.44	C23	PRO D 245 CB	3.7
C16	ARG D 48 CZ	4.23	O1	PRO D 245 CB	4.54
C15	ARG D 48 CZ	3.9	C9	PRO D 245 CB	4.14
C14	ARG D 48 CZ	3.76	C8	PRO D 245 CB	4.76
C13	ARG D 48 CZ	4.38	C7	PRO D 245 CB	4.61
O4	ARG D 48 CZ	4.4	C4	PRO D 245 CB	4.79
C12	ARG D 48 CZ	4.14	C3	PRO D 245 CB	4.14

C19	ARG D 48 NE	4.16	C1	PRO D 245 CB	3.78
C18	ARG D 48 NE	4.42	C9	PRO D 245 CG	4.86
C17	ARG D 48 NE	4.19	C1	PRO D 245 CG	4.83
C16	ARG D 48 NE	3.59	C29	PRO D 245 O	4.53
C15	ARG D 48 NE	3.27	C27	PRO D 245 O	4.93
C14	ARG D 48 NE	3.57	C26	PRO D 245 O	4.18
C13	ARG D 48 NE	3.48	C25	PRO D 245 O	3.91
C12	ARG D 48 NE	3.94	C24	PRO D 245 O	4
O6	ARG D 48 CD	4.63	C23	PRO D 245 O	4.44
O5	ARG D 48 CD	3.66	C26	PRO D 245 C	4.71
C16	ARG D 48 CD	4.42	C25	PRO D 245 C	4.17
C15	ARG D 48 CD	3.83	C24	PRO D 245 C	3.93
C14	ARG D 48 CD	4.25	C23	PRO D 245 C	4.07
C13	ARG D 48 CD	3.44	C7	PRO D 245 C	4.29
O4	ARG D 48 CD	3.57	C3	PRO D 245 C	4.68
C12	ARG D 48 CD	4.16	C1	PRO D 245 C	4.64
O6	ARG D 48 CG	4.25	C24	PRO D 245 CA	4.51
O5	ARG D 48 CG	3.27	C23	PRO D 245 CA	4.28
C16	ARG D 48 CG	4.49	C7	PRO D 245 CA	4.35
C15	ARG D 48 CG	4.17	C6	PRO D 245 CA	4.96
C14	ARG D 48 CG	4.99	C3	PRO D 245 CA	4.36
C13	ARG D 48 CG	3.57	C1	PRO D 245 CA	4.41
O4	ARG D 48 CG	4.11	C19	ARG D 48 NH2	3.24
O5	ARG D 48 CB	4.67	C18	ARG D 48 NH2	3.9
C13	GLU D 47 OE2	4.67	C17	ARG D 48 NH2	4.79
C10	GLU D 47 OE2	3.98	C15	ARG D 48 NH2	4.52
C9	GLU D 47 OE2	4.57	C14	ARG D 48 NH2	3.7
C8	GLU D 47 OE2	3.89	C12	ARG D 48 NH2	4.19
C2	GLU D 47 OE2	4.25	C6	ARG D 48 NH2	4.77
O5	GLU D 47 CD	4.51	C19	ARG D 48 NH1	4.73
O2	GLU D 47 CD	4.78	C14	ARG D 48 NH1	4.64
O5	GLU D 47 CG	3.83	C12	ARG D 48 NH1	4.34
C13	GLU D 47 CG	4.8	C6	ARG D 48 NH1	4.31
C21	GLU D 47 O	4.6	N1	ARG D 48 CZ	4.91
C13	GLU D 47 O	4.61	C19	ARG D 48 CZ	3.72
O5	GLU D 47 C	4.36	C18	ARG D 48 CZ	4.61
C21	ARG D 2 NH2	4.41	C15	ARG D 48 CZ	4.4
C20	ARG D 2 NH2	4.24	C14	ARG D 48 CZ	3.67
C21	ARG D 2 CZ	4.44	C13	ARG D 48 CZ	4.86
C20	ARG D 2 CZ	4.37	O4	ARG D 48 CZ	4.47
O7	ARG D 2 CZ	4.36	C12	ARG D 48 CZ	3.75
O6	ARG D 2 CZ	4.89	C6	ARG D 48 CZ	4.48
C21	ARG D 2 NE	3.5	C5	ARG D 48 CZ	4.96
C20	ARG D 2 NE	4.14	C19	ARG D 48 NE	3.71
C17	ARG D 2 NE	4.69	C18	ARG D 48 NE	4.51
C16	ARG D 2 NE	4.69	C17	ARG D 48 NE	4.87
C21	ARG D 2 CD	4.19	C16	ARG D 48 NE	4.43
C20	ARG D 2 CD	4.89	C15	ARG D 48 NE	3.6
O7	ARG D 2 CD	4.15	C14	ARG D 48 NE	3.24
O6	ARG D 2 CD	4.03	C13	ARG D 48 NE	3.85
C21	ARG D 2 CG	4.63	C12	ARG D 48 NE	3.32
C20	ARG D 2 CG	4.39	C6	ARG D 48 NE	4.92
O7	ARG D 2 CG	3.53	C5	ARG D 48 NE	4.77
O6	ARG D 2 CG	4.03	O5	ARG D 48 CD	4.4
C17	ARG D 2 CG	4.49	C19	ARG D 48 CD	4.8
C16	ARG D 2 CG	4.71	C15	ARG D 48 CD	4.13
C20	ARG D 2 CB	3.74	C14	ARG D 48 CD	3.98
O7	ARG D 2 CB	3.32	C13	ARG D 48 CD	3.82
O6	ARG D 2 CB	4.81	O4	ARG D 48 CD	3.47
C17	ARG D 2 CB	4.54	C12	ARG D 48 CD	3.61
C20	ARG D 2 CA	4.17	O5	ARG D 48 CG	3.77
O7	ARG D 2 CA	3.76	C16	ARG D 48 CG	4.92
C17	ARG D 2 CA	4.83	C15	ARG D 48 CG	4.13
C20	ARG D 2 N	4.06	C14	ARG D 48 CG	4.49
C20	MET D 1 CE	4.92	C13	ARG D 48 CG	3.62
C18	MET D 1 CE	4.81	O4	ARG D 48 CG	3.73

C20	MET D 1 O	2.96	C12	ARG D 48 CG	4.33
C18	MET D 1 O	3.8	C13	GLU D 47 OE2	4.78
C17	MET D 1 O	3.86	C10	GLU D 47 OE2	3.85
C20	MET D 1 C	3.48	C9	GLU D 47 OE2	4.45
O7	MET D 1 C	3.83	C8	GLU D 47 OE2	3.85
C18	MET D 1 C	4.93	C2	GLU D 47 OE2	4.21
C17	MET D 1 C	4.81	O5	GLU D 47 CD	4.7
C20	MET D 1 CA	4.16	O4	GLU D 47 CD	4.98
O7	MET D 1 CA	4.91	O2	GLU D 47 CD	4.78
C20	MET D 1 N	3.59	C10	GLU D 47 CD	4.96
C32	TYR A 224 CE1	4.12	O5	GLU D 47 CG	3.86
C31	TYR A 224 CE1	4.53	C13	GLU D 47 CG	4.61
C32	TYR A 224 CD1	3.94	O4	GLU D 47 CG	4.72
C31	TYR A 224 CD1	4.43	O5	GLU D 47 CB	4.99
C32	TYR A 224 CG	4.96	C15	GLU D 47 O	4.88
C32	TYR A 224 N	4.83	C13	GLU D 47 O	4.07
C31	TYR A 224 N	4.58	O5	GLU D 47 C	4.22
C32	THR A 223 CG2	4.85	C13	GLU D 47 C	4.99
C31	THR A 223 CG2	4.19	C21	ARG D 2 NH2	4.09
C30	THR A 223 CG2	3.65	C20	ARG D 2 NH2	3.48
C29	THR A 223 CG2	3.89	C17	ARG D 2 NH2	4.53
C28	THR A 223 CG2	4.6	C16	ARG D 2 NH2	4.9
C32	THR A 223 CB	4.65	C20	ARG D 2 NH1	4.69
C31	THR A 223 CB	4.13	C21	ARG D 2 CZ	4.4
C30	THR A 223 CB	4.11	C20	ARG D 2 CZ	3.79
C29	THR A 223 CB	4.62	O7	ARG D 2 CZ	3.31
C31	THR A 223 C	4.87	O6	ARG D 2 CZ	4.19
C32	THR A 223 CA	4.87	C17	ARG D 2 CZ	4.49
C31	THR A 223 CA	4.07	C16	ARG D 2 CZ	4.85
C30	THR A 223 CA	4.25	C21	ARG D 2 NE	3.74
C31	ARG A 221 NH1	3.92	C20	ARG D 2 NE	3.78
C30	ARG A 221 NH1	3.88	C18	ARG D 2 NE	4.99
C31	ARG A 221 CZ	4.79	C17	ARG D 2 NE	3.73
C30	ARG A 221 CZ	4.52	C16	ARG D 2 NE	3.88
C11	GLU A 77 OE2	4.14	C21	ARG D 2 CD	4.69
C10	GLU A 77 OE2	3.78	C20	ARG D 2 CD	4.75
C9	GLU A 77 OE2	4.05	O7	ARG D 2 CD	3.73
C8	GLU A 77 OE2	3.81	O6	ARG D 2 CD	3.81
C2	GLU A 77 OE2	4.44	C17	ARG D 2 CD	4.33
C1	GLU A 77 OE2	4.88	C16	ARG D 2 CD	4.41
C11	GLU A 77 CD	4.62	C20	ARG D 2 CG	4.5
O2	GLU A 77 CD	4.61	O7	ARG D 2 CG	3.59
C10	GLU A 77 CD	4.96	O6	ARG D 2 CG	4.26
C8	GLU A 77 CD	4.92	C18	ARG D 2 CG	4.74
C11	GLU A 77 CG	4.31	C17	ARG D 2 CG	4
O2	GLU A 77 CG	4.89	C16	ARG D 2 CG	4.39
C22	VAL A 74 CG2	4.03	C20	ARG D 2 CB	3.82
C11	VAL A 74 N	4.64	O7	ARG D 2 CB	3.39
C22	THR A 73 OG1	3.27	O6	ARG D 2 CB	4.99
C19	THR A 73 OG1	3.9	C18	ARG D 2 CB	4.62
C18	THR A 73 OG1	4.45	C17	ARG D 2 CB	4.09
C17	THR A 73 OG1	4.94	C16	ARG D 2 CB	4.91
C16	THR A 73 OG1	4.99	C20	ARG D 2 CA	4.49
C15	THR A 73 OG1	4.46	O7	ARG D 2 CA	4.28
C14	THR A 73 OG1	3.9	C18	ARG D 2 CA	4.79
C12	THR A 73 OG1	4.22	C17	ARG D 2 CA	4.71
C11	THR A 73 OG1	3.88	C20	ARG D 2 N	4.34
C5	THR A 73 OG1	3.42	C20	MET D 1 O	3.6
C4	THR A 73 OG1	4.42	C19	MET D 1 O	4.5
C2	THR A 73 OG1	4.67	C18	MET D 1 O	3.5
C21	THR A 73 CG2	3.82	C17	MET D 1 O	4.15
C20	THR A 73 CG2	3.93	C20	MET D 1 C	3.88
O7	THR A 73 CG2	4.19	O7	MET D 1 C	4.42
O6	THR A 73 CG2	4.32	C18	MET D 1 C	4.5
C19	THR A 73 CG2	4.02	C17	MET D 1 C	4.87
C18	THR A 73 CG2	3.86	C20	MET D 1 CA	4.38

C17	THR A 73 CG2	3.67	C20	MET D 1 N	3.72
C16	THR A 73 CG2	3.69	C20	LYS A 96 O	4.8
C15	THR A 73 CG2	3.8	C11	GLU A 77 OE2	4.28
C14	THR A 73 CG2	3.96	C10	GLU A 77 OE2	4
C13	THR A 73 CG2	4.56	C9	GLU A 77 OE2	4.6
C12	THR A 73 CG2	4.85	C8	GLU A 77 OE2	4.16
C11	THR A 73 CG2	4.6	C2	GLU A 77 OE2	4.84
O3	THR A 73 CG2	4.76	C11	GLU A 77 CD	4.76
C5	THR A 73 CG2	4.77	O2	GLU A 77 CD	4.73
N1	THR A 73 CB	4.76	C11	GLU A 77 CG	4.44
C22	THR A 73 CB	4.57	C22	VAL A 74 CG2	4.86
C21	THR A 73 CB	4.96	C11	VAL A 74 N	4.7
C19	THR A 73 CB	4.49	C22	THR A 73 OG1	3.14
C18	THR A 73 CB	4.77	C19	THR A 73 OG1	4.41
C17	THR A 73 CB	4.86	C18	THR A 73 OG1	4.83
C16	THR A 73 CB	4.72	C15	THR A 73 OG1	4.8
C15	THR A 73 CB	4.39	C14	THR A 73 OG1	4.32
C14	THR A 73 CB	4.28	C12	THR A 73 OG1	4.43
C13	THR A 73 CB	4.83	C11	THR A 73 OG1	3.86
C12	THR A 73 CB	4.73	C5	THR A 73 OG1	3.43
C11	THR A 73 CB	3.52	C4	THR A 73 OG1	4.28
O3	THR A 73 CB	3.97	C2	THR A 73 OG1	4.5
C5	THR A 73 CB	4.17	N1	THR A 73 CG2	4.92
C2	THR A 73 CB	4.88	C21	THR A 73 CG2	3.69
C11	THR A 73 O	2.96	C20	THR A 73 CG2	3.92
C11	THR A 73 C	3.65	O7	THR A 73 CG2	3.86
O3	THR A 73 C	4.77	O6	THR A 73 CG2	4.12
C11	THR A 73 CA	4.03	O5	THR A 73 CG2	4.94
O3	THR A 73 CA	4.9	C19	THR A 73 CG2	3.89
C20	PRO A 72 CD	4.98	C18	THR A 73 CG2	3.68
C20	GLU A 71 OE2	3.95	C17	THR A 73 CG2	3.43
C19	GLU A 71 OE2	4.11	C16	THR A 73 CG2	3.48
C18	GLU A 71 OE2	3.78	C15	THR A 73 CG2	3.66
C17	GLU A 71 OE2	4.52	C14	THR A 73 CG2	3.8
C22	GLU A 71 OE1	4.45	C13	THR A 73 CG2	4.37
C19	GLU A 71 CD	4.94	O4	THR A 73 CG2	4.8
C18	GLU A 71 CD	4.86	C12	THR A 73 CG2	4.56
C22	GLN A 11 OE1	4.18	C11	THR A 73 CG2	4.51
			O3	THR A 73 CG2	4.6
			C5	THR A 73 CG2	4.36
			N1	THR A 73 CB	4.61
			C22	THR A 73 CB	4.41
			C21	THR A 73 CB	4.76
			C19	THR A 73 CB	4.69
			C18	THR A 73 CB	4.85
			C17	THR A 73 CB	4.81
			C16	THR A 73 CB	4.67
			C15	THR A 73 CB	4.46
			C14	THR A 73 CB	4.41
			C13	THR A 73 CB	4.81
			O4	THR A 73 CB	4.91
			C12	THR A 73 CB	4.69
			C11	THR A 73 CB	3.46
			O3	THR A 73 CB	3.87
			C5	THR A 73 CB	4.02
			C4	THR A 73 CB	4.81
			C2	THR A 73 CB	4.7
			C11	THR A 73 O	3.02
			C11	THR A 73 C	3.68
			O3	THR A 73 C	4.79
			C11	THR A 73 CA	4.01
			O3	THR A 73 CA	4.85
			C20	PRO A 72 CD	4.52
			C20	PRO A 72 CG	4.45
			C22	GLU A 71 OE2	4.76
			C20	GLU A 71 OE2	4.22

			C19	GLU A 71 OE2	4.39
			C18	GLU A 71 OE2	4.09
			C17	GLU A 71 OE2	4.78
			C22	GLU A 71 OE1	4.39
			C22	GLU A 71 CD	4.77
			C22	GLN A 11 OE1	4.96
Table A4.12			**Table A4.13**		
(c) 1,3-diynyl noscapinoid 22_Tubulin			**(d) Noscapine_Tubulin**		
Hydrogen bonding			**Hydrogen bonding**		
Hydrogen Donor (D)	**Hydrogen Acceptor (A)**	**Distance (D-A) in Å**	**Hydrogen Donor (D)**	**Hydrogen Acceptor (A)**	**Distance (D-A) in Å**
GLN D 247 NE2	F3	3.34	GLN D 247 NE2	O2	3.04
ARG D 2 NH2	O6	4.43	GLY D 246 N	O3	4.39
ARG D 2 NE	O7	2.92	ARG D 48 NH2	O5	3.37
THR A 225 N	F2	4.65	GLN A 11 NE2	O6	4.96
TYR A 224 N	F2	3.04			
20 N1	THR A 73 OG1	3.59			
Hydrophobic interaction			**Hydrophobic interaction**		
22	**Tubulin**	**Distance**	**Noscapine**	**Tubulin**	**Distance**
C31	MET D 325 CE	4.24	C20	LYS D 254 NZ	3.42
C30	MET D 325 CE	4.56	C16	LYS D 254 NZ	4.9
C31	MET D 325 SD	4.6	C20	LYS D 254 CE	3.9
C30	MET D 325 SD	4.8	C20	LYS D 254 CD	3.94
N1	ALA D 250 CB	4.75	C20	LYS D 254 CG	4.95
C22	ALA D 250 CB	4.18	C20	ASP D 251 OD2	3.2
C6	ALA D 250 CB	4.13	C17	ASP D 251 OD2	4.65
C19	ALA D 250 O	4.94	C20	ASP D 251 CG	4.32
C33	GLN D 247 NE2	4.56	O4	ASP D 251 CG	4.49
C28	GLN D 247 NE2	4.88	C20	ASP D 251 CB	5
C27	GLN D 247 NE2	4.56	O4	ASP D 251 CB	4.73
C26	GLN D 247 NE2	3.67	C20	ALA D 250 CB	3.93
C25	GLN D 247 NE2	3.22	O6	ALA D 250 CB	4.52
C24	GLN D 247 NE2	3.13	O5	ALA D 250 CB	4.8
C23	GLN D 247 NE2	3.47	O4	ALA D 250 CB	3.77
C7	GLN D 247 NE2	3.83	C19	ALA D 250 CB	4.48
C6	GLN D 247 NE2	4.94	C18	ALA D 250 CB	4.05
C3	GLN D 247 NE2	4.5	C17	ALA D 250 CB	3.45
C1	GLN D 247 NE2	4.31	C16	ALA D 250 CB	3.26
C33	GLN D 247 CD	4.88	C15	ALA D 250 CB	3.7
C28	GLN D 247 CD	4.9	C14	ALA D 250 CB	4.32
C27	GLN D 247 CD	4.59	C13	ALA D 250 CB	4.3
C26	GLN D 247 CD	4.02	C18	ALA D 250 O	4.52
C25	GLN D 247 CD	3.87	C17	ALA D 250 O	4.73
C24	GLN D 247 CD	4.03	O4	ALA D 250 C	4.75
C23	GLN D 247 CD	4.5	C18	ALA D 250 C	4.98
C7	GLN D 247 CD	4.43	C17	ALA D 250 C	4.83
C33	GLN D 247 CG	4.73	O4	ALA D 250 CA	4.92
C32	GLN D 247 CG	4.03	C17	ALA D 250 CA	4.76
C31	GLN D 247 CG	4.86	C16	ALA D 250 CA	4.76
C28	GLN D 247 CG	4.27	C13	GLN D 247 OE1	4.68
C27	GLN D 247 CG	3.7	C13	GLN D 247 E2	4.22
C26	GLN D 247 CG	3.37	C10	GLN D 247 E2	3.63
C25	GLN D 247 CG	3.52	C9	GLN D 247 NE2	3.91
C24	GLN D 247 CG	3.99	C8	GLN D 247 NE2	3.42
C23	GLN D 247 CG	4.72	C4	GLN D 247 NE2	4.81
C7	GLN D 247 CG	4.93	C2	GLN D 247 NE2	4.78
C32	GLN D 247 CB	4.77	C1	GLN D 247 NE2	3.94
C27	GLN D 247 CB	4.83	O7	GLN D 247 CD	4.87
C26	GLN D 247 CB	4.67	O6	GLN D 247 CD	3.59
C25	GLN D 247 CB	4.84	C13	GLN D 247 CD	4.49
C7	GLN D 247 CA	4.68	O3	GLN D 247 CD	4.71
C6	GLN D 247 CA	4.87	O2	GLN D 247 CD	4.24
C25	GLN D 247 N	4.94	C10	GLN D 247 CD	4.85
C24	GLN D 247 N	5	C8	GLN D 247 CD	4.69
C7	GLN D 247 N	4.48	O6	GLN D 247 CG	4.41
C6	GLN D 247 N	4.74	O6	GLN D 247 CB	4.52

C22	GLY D 246 O	4.88	O6	GLN D 247 C	4.48
C7	GLY D 246 O	3.3	O6	GLN D 247 CA	3.65
C6	GLY D 246 O	2.94	C13	GLN D 247 CA	4.39
C3	GLY D 246 O	4.62	O3	GLN D 247 CA	4.82
C7	GLY D 246 C	3.88	C13	GLN D 247 N	4.6
C6	GLY D 246 C	3.93	C16	GLY D 246 O	4.45
C7	GLY D 246 CA	4.67	C15	GLY D 246 O	3.74
C6	GLY D 246 CA	4.79	C14	GLY D 246 O	4.16
C23	GLY D 246 N	4.96	C13	GLY D 246 O	3.15
C7	GLY D 246 N	4.19	C12	GLY D 246 O	4.08
C6	GLY D 246 N	4.35	O6	GLY D 246 C	4.06
C3	GLY D 246 N	4.81	C15	GLY D 246 C	4.88
C24	PRO D 245 CB	4.61	C13	GLY D 246 C	4.09
C23	PRO D 245 CB	4.12	O3	GLY D 246 C	4.03
O4	PRO D 245 CB	4.95	C12	GLY D 246 C	4.91
O1	PRO D 245 CB	4.72	O3	GLY D 246 CA	4.87
C9	PRO D 245 CB	4.29	C12	GLY D 246 N	4.63
C8	PRO D 245 CB	4.92	N1	PRO D 245 CB	4.9
C7	PRO D 245 CB	4.86	C12	PRO D 245 CB	4.89
C4	PRO D 245 CB	4.91	C7	PRO D 245 CB	3.79
C3	PRO D 245 CB	4.32	C6	PRO D 245 CB	3.58
C1	PRO D 245 CB	3.97	C3	PRO D 245 CB	4.63
O4	PRO D 245 CG	4.93	C6	PRO D 245 CD	4.92
C9	PRO D 245 CG	4.88	C7	PRO D 245 CG	4.07
C1	PRO D 245 CG	4.93	C6	PRO D 245 CG	3.73
C24	PRO D 245 O	5	C12	PRO D 245 CA	4.74
C24	PRO D 245 C	4.93	C7	PRO D 245 CA	4.82
C23	PRO D 245 C	4.79	C6	PRO D 245 CA	4.2
C7	PRO D 245 C	4.72	C21	ARG D 48 NH2	4.66
C3	PRO D 245 C	4.97	C19	ARG D 48 NH2	3.73
C23	PRO D 245 CA	4.88	C18	ARG D 48 NH2	3.75
O4	PRO D 245 CA	4.89	C17	ARG D 48 NH2	4.76
C7	PRO D 245 CA	4.82	C14	ARG D 48 NH2	4.68
C3	PRO D 245 CA	4.65	C19	ARG D 48 NH1	4.4
C1	PRO D 245 CA	4.72	C18	ARG D 48 NH1	4.94
C19	ARG D 48 NH2	3.18	C14	ARG D 48 NH1	4.74
C18	ARG D 48 NH2	3.7	O5	ARG D 48 CZ	4.23
C17	ARG D 48 NH2	4.5	C19	ARG D 48 CZ	3.85
C16	ARG D 48 NH2	4.76	C18	ARG D 48 CZ	4.32
C15	ARG D 48 NH2	4.34	C14	ARG D 48 CZ	4.56
C14	ARG D 48 NH2	3.64	C19	ARG D 48 NE	4.07
C12	ARG D 48 NH2	4.16	C18	ARG D 48 NE	4.78
C19	ARG D 48 NH1	4.66	C14	ARG D 48 NE	4.84
C14	ARG D 48 NH1	4.56	C11	ARG D 48 NE	4.33
C12	ARG D 48 NH1	4.28	C19	ARG D 48 CD	4.88
C19	ARG D 48 CZ	3.69	C11	ARG D 48 CD	4.28
C18	ARG D 48 CZ	4.44	C6	ARG D 48 CD	4.62
C16	ARG D 48 CZ	4.92	C11	ARG D 48 CG	4.55
C15	ARG D 48 CZ	4.23	C11	GLU D 47 OE2	4.56
C14	ARG D 48 CZ	3.64	C7	GLU D 47 OE2	3.02
C13	ARG D 48 CZ	4.67	C6	GLU D 47 OE2	3.07
O4	ARG D 48 CZ	4.26	C3	GLU D 47 OE2	4.47
C12	ARG D 48 CZ	3.75	C7	GLU D 47 OE1	4.89
C21	ARG D 48 NE	4.78	C6	GLU D 47 OE1	4.95
C19	ARG D 48 NE	3.76	C7	GLU D 47 CD	4.17
C18	ARG D 48 NE	4.4	C6	GLU D 47 CD	4.05
C17	ARG D 48 NE	4.63	C6	GLU D 47 CG	4.57
C16	ARG D 48 NE	4.18	C21	MET D 1 CE	3.79
C15	ARG D 48 NE	3.48	C20	MET D 1 CE	3.31
C14	ARG D 48 NE	3.31	O5	MET D 1 CE	4.27
C13	ARG D 48 NE	3.7	O4	MET D 1 CE	3.06
C12	ARG D 48 NE	3.46	C18	MET D 1 CE	4.78
C5	ARG D 48 NE	5	C17	MET D 1 CE	4.32
O5	ARG D 48 CD	4.21	C20	MET D 1 SD	4.82
C19	ARG D 48 CD	4.87	O4	MET D 1 SD	4.79
C16	ARG D 48 CD	4.9	C21	MET D 1 O	3.36

C15	ARG D 48 CD	4.04	C18	MET D 1 O	4.95
C14	ARG D 48 CD	4.08	C21	MET D 1 C	4.4
C13	ARG D 48 CD	3.69	O5	MET D 1 C	4.85
O4	ARG D 48 CD	3.38	C21	MET D 1 N	4.37
C12	ARG D 48 CD	3.79	C20	ASP A 98 OD2	2.95
C21	ARG D 48 CG	4.24	C20	ASP A 98 OD1	4.3
O5	ARG D 48 CG	3.71	C20	ASP A 98 CG	3.93
C16	ARG D 48 CG	4.75	O4	ASP A 98 CG	4.94
C15	ARG D 48 CG	4.15	C10	GLU A 77 OE2	3.79
C14	ARG D 48 CG	4.67	C9	GLU A 77 OE2	3.33
C13	ARG D 48 CG	3.63	C8	GLU A 77 OE2	3.55
O4	ARG D 48 CG	3.79	C4	GLU A 77 OE2	4.39
C12	ARG D 48 CG	4.6	C3	GLU A 77 OE2	4.19
C21	ARG D 48 CB	4.83	C2	GLU A 77 OE2	3.67
C21	ARG D 48 CA	4.54	C1	GLU A 77 OE2	4.1
C21	ARG D 48 N	5	C10	GLU A 77 OE1	4.34
C13	GLU D 47 OE2	4.76	C9	GLU A 77 OE1	4.89
C11	GLU D 47 OE2	4.78	C8	GLU A 77 OE1	4.73
C10	GLU D 47 OE2	3.54	O2	GLU A 77 CD	4.63
C9	GLU D 47 OE2	4.15	C10	GLU A 77 CD	4.46
C8	GLU D 47 OE2	3.63	O1	GLU A 77 CD	4.65
C2	GLU D 47 OE2	4.2	C9	GLU A 77 CD	4.42
O5	GLU D 47 CD	4.59	C8	GLU A 77 CD	4.4
O2	GLU D 47 CD	4.54	C2	GLU A 77 CD	4.89
C10	GLU D 47 CD	4.66	C1	GLU A 77 CD	4.88
C8	GLU D 47 CD	4.86	C22	VAL A 74 CG2	3.12
O5	GLU D 47 CG	3.86	O7	VAL A 74 CG2	3.85
C13	GLU D 47 CG	4.72	C1	VAL A 74 CG2	4.88
O4	GLU D 47 CG	4.95	C22	VAL A 74 CB	4.27
C21	GLU D 47 O	3.42	O7	VAL A 74 CB	4.93
C13	GLU D 47 O	4.33	C22	VAL A 74 CA	4.29
C21	GLU D 47 C	4.54	C22	VAL A 74 N	4.03
O5	GLU D 47 C	4.41	C22	THR A 73 OG1	2.91
C20	ARG D 2 NH2	3.55	C21	THR A 73 OG1	4.34
C17	ARG D 2 NH2	4.78	C19	THR A 73 OG1	3.93
C20	ARG D 2 NH1	4.74	C18	THR A 73 OG1	4.17
C21	ARG D 2 CZ	4.6	C17	THR A 73 OG1	4.42
C20	ARG D 2 CZ	3.83	C16	THR A 73 OG1	4.5
O7	ARG D 2 CZ	3.47	C15	THR A 73 OG1	4.32
O6	ARG D 2 CZ	4.32	C14	THR A 73 OG1	3.99
C17	ARG D 2 CZ	4.69	C12	THR A 73 OG1	4.52
C21	ARG D 2 NE	3.36	C11	THR A 73 OG1	4.25
C20	ARG D 2 NE	3.77	C5	THR A 73 OG1	3.84
C17	ARG D 2 NE	3.9	C4	THR A 73 OG1	4.68
C16	ARG D 2 NE	4.05	C1	THR A 73 OG1	4.76
C21	ARG D 2 CD	3.42	C21	THR A 73 CG2	3.71
C20	ARG D 2 CD	4.71	O5	THR A 73 CG2	4.51
O7	ARG D 2 CD	3.7	C19	THR A 73 CG2	4.47
O6	ARG D 2 CD	3.86	C18	THR A 73 CG2	4.59
C17	ARG D 2 CD	4.41	C11	THR A 73 CG2	4.2
C16	ARG D 2 CD	4.51	N1	THR A 73 CB	4.51
C21	ARG D 2 CG	3.89	C22	THR A 73 CB	4.08
C20	ARG D 2 CG	4.43	C21	THR A 73 CB	4.68
O7	ARG D 2 CG	3.45	C19	THR A 73 CB	4.66
O6	ARG D 2 CG	4.22	C18	THR A 73 CB	4.98
C18	ARG D 2 CG	4.82	C14	THR A 73 CB	4.94
C17	ARG D 2 CG	3.99	C11	THR A 73 CB	4.15
C16	ARG D 2 CG	4.4	C5	THR A 73 CB	4.42
C20	ARG D 2 CB	3.77	C22	THR A 73 O	4.61
O7	ARG D 2 CB	3.27	C22	THR A 73 C	4.22
O6	ARG D 2 CB	4.96	C22	THR A 73 CA	4.74
C18	ARG D 2 CB	4.69	C21	GLU A 71 OE2	2.71
C17	ARG D 2 CB	4.09	C20	GLU A 71 OE2	4.28
C16	ARG D 2 CB	4.92	C19	GLU A 71 OE2	4.72
C20	ARG D 2 CA	4.43	C18	GLU A 71 OE2	3.86
O7	ARG D 2 CA	4.1	C17	GLU A 71 OE2	3.76

C18	ARG D 2 CA	4.79	C16	GLU A 71 OE2	4.61
C17	ARG D 2 CA	4.63	C22	GLU A 71 OE1	4.22
C20	ARG D 2 N	4.31	C21	GLU A 71 OE1	4.66
C20	MET D 1 O	3.53	C20	GLU A 71 OE1	4.98
C19	MET D 1 O	4.49	C17	GLU A 71 OE1	4.61
C18	MET D 1 O	3.43	C16	GLU A 71 OE1	4.82
C17	MET D 1 O	4.03	C21	GLU A 71 CD	3.88
C20	MET D 1 C	3.85	C20	GLU A 71 CD	4.32
O7	MET D 1 C	4.28	O5	GLU A 71 CD	4.82
C18	MET D 1 C	4.47	O4	GLU A 71 CD	4
C17	MET D 1 C	4.8	C18	GLU A 71 CD	4.6
C20	MET D 1 CA	4.39	C17	GLU A 71 CD	4.19
C20	MET D 1 N	3.75	C16	GLU A 71 CD	4.72
C33	TYR A 224 CE1	4.65	C21	GLU A 71 CG	4.81
C29	TYR A 224 CE1	4.99	C20	GLU A 71 CG	4.22
C28	TYR A 224 CE1	4.87	O4	GLU A 71 CG	4.31
C33	TYR A 224 CD1	3.91	C17	GLU A 71 CG	4.9
C29	TYR A 224 CD1	4.78	C10	GLN A 15 OE1	3.24
C28	TYR A 224 CD1	4.53	C9	GLN A 15 OE1	4.95
C33	TYR A 224 CG	4.73	C8	GLN A 15 OE1	4.15
C33	TYR A 224 CB	4.71	C1	GLN A 15 OE1	4.93
C33	TYR A 224 N	4.33	C10	GLN A 15 NE2	4.39
C29	TYR A 224 N	4.86	O2	GLN A 15 CD	4.11
C33	THR A 223 OG1	4.96	C10	GLN A 15 CD	4.08
C33	THR A 223 CG2	4.63	C22	GLN A 11 OE1	4.29
C30	THR A 223 CG2	4.66	C13	GLN A 11 OE1	4.75
C29	THR A 223 CG2	3.97	O7	GLN A 11 CD	4.64
C28	THR A 223 CG2	4.63	O6	GLN A 11 CD	4.79
C33	THR A 223 CB	4.15	O2	GLN A 11 CD	4.7
C29	THR A 223 CB	4.05			
C28	THR A 223 CB	4.56			
C33	THR A 223 CA	4.79			
C29	THR A 223 CA	4.29			
C30	ARG A 221 NH1	4.22			
C29	ARG A 221 NH1	4.58			
C30	ARG A 221 CZ	4.7			
C20	LYS A 96 O	4.9			
C11	GLU A 77 OE2	4.54			
C10	GLU A 77 OE2	3.97			
C9	GLU A 77 OE2	4.38			
C8	GLU A 77 OE2	4.14			
C2	GLU A 77 OE2	4.8			
O2	GLU A 77 CD	4.82			
C11	GLU A 77 CG	4.58			
O2	GLU A 77 CG	5			
C22	THR A 73 OG1	3.41			
C19	THR A 73 OG1	4.4			
C18	THR A 73 OG1	4.89			
C15	THR A 73 OG1	4.67			
C14	THR A 73 OG1	4.19			
C12	THR A 73 OG1	4.32			
C11	THR A 73 OG1	4.27			
C5	THR A 73 OG1	3.37			
C4	THR A 73 OG1	4.21			
C2	THR A 73 OG1	4.41			
C22	THR A 73 CG2	4.83			
C20	THR A 73 CG2	3.88			
O7	THR A 73 CG2	3.95			
O6	THR A 73 CG2	4.08			
O5	THR A 73 CG2	4.87			
C19	THR A 73 CG2	4			
C18	THR A 73 CG2	3.85			
C17	THR A 73 CG2	3.57			
C16	THR A 73 CG2	3.57			
C15	THR A 73 CG2	3.66			
C14	THR A 73 CG2	3.82			

C13	THR A 73 CG2	4.37			
O4	THR A 73 CG2	4.91			
C12	THR A 73 CG2	4.63			
C11	THR A 73 CG2	4.63			
O3	THR A 73 CG2	4.28			
C5	THR A 73 CG2	4.46			
N1	THR A 73 CB	4.66			
C22	THR A 73 CB	4.6			
C19	THR A 73 CB	4.75			
C18	THR A 73 CB	4.98			
C17	THR A 73 CB	4.91			
C16	THR A 73 CB	4.72			
C15	THR A 73 CB	4.41			
C14	THR A 73 CB	4.37			
C13	THR A 73 CB	4.74			
O4	THR A 73 CB	4.98			
C12	THR A 73 CB	4.7			
C11	THR A 73 CB	3.72			
O3	THR A 73 CB	3.55			
C5	THR A 73 CB	4.04			
C4	THR A 73 CB	4.75			
C2	THR A 73 CB	4.56			
C11	THR A 73 O	3.28			
C2	THR A 73 O	4.93			
C11	THR A 73 C	4.02			
O3	THR A 73 C	4.54			
C11	THR A 73 CA	4.24			
O3	THR A 73 CA	4.54			
C20	PRO A 72 CD	4.61			
C20	PRO A 72 CG	4.56			
C22	GLU A 71 OE2	4.15			
C20	GLU A 71 OE2	4.2			
C19	GLU A 71 OE2	4.33			
C18	GLU A 71 OE2	4.13			
C17	GLU A 71 OE2	4.8			
C22	GLU A 71 OE1	4.36			
C22	GLU A 71 CD	4.39			

CHAPTER 5

Rational design of N-imidazopyridine derivatives of noscapine as promising tubulin binding anticancer agents: chemical synthesis and cellular evaluation

5.1. Introduction

Noscapine, an opium alkaloid, was discovered as a small-molecule tubulin-binding agent that arrests cancer cells in mitosis and induces apoptosis (Ye *et al.,* 1998). However, noscapine neither overpolymerize tubulin (unlike taxanes) nor deploymerize tubulin (vincas). In contrast, it delicately attenuate microtubule dynamics and activates the mitotic checkpoints to bring the cell cycle to a halt, allowing other processes reliant upon less dynamic microtubules, such as axonal transport (Ye *et al.,* 1998; Ke *et al.,* 2000; Ye *et al.,* 2001). Because of this unique action, it is devoid of any severe toxicity. In contrast, due to the extreme effect on the microtubule, both taxanes and vincas cause severe toxicities such as leukocytopenia, diarrhea, alopecia and peripheral neuropathies (Rowinsky, 1997; Zhou and Giannakakou, 2005; Theiss and Meller, 2000; Topp *et al.,* 2000). Towards a clinical perspective, the noscapine and its derivatives have been shown to inhibit the proliferation of cancer cells of different tissue origin and regress implanted tumors in animal models with no apparent side effects (Ye *et al.,* 1998; Landen *et al.,* 2002; Zhou *et al.,* 2003). Moreover, it retains activity against cancer cell lines resistant to paclitaxel (1A9/PTX10, 1A9/PTX22) and epothilone (1A9/A8) (Zhou *et al.,* 2002b). Further, it possesses favorable pharmacokinetics (clearance in 6-10 hours, Dahlstrom *et al.,* 1982). All these worthy features of noscapine over the currently used chemotherapeutics, raised a tremendous hope of its potential use as a therapeutic compound and its further development on improving the potency. In quest of increasing its anticancer potential, we approach on rational drug design and chemical synthesis that led to an array of noscapinoids (Manchukonda *et al.,* 2012; Manchukonda *et al.,*2013; Santoshi *et al.,* 2011; Santoshi *et al.,* 2015; Naik *et al.,* 2012), which are at different stages of chemical and biological characterization.

In this study we have focused on developing new derivatives of noscapine by strategically modifying its scaffold by coupling imidazopyridine pharmacophore (called N-imidazopyridine-noscapinoids). These derivatives were then chemically synthesized and validated their anticancer activity based on a cellular study using two human breast cancer cell lines, MCF-7 and MDAMB-231, as well as a panel of primary breast cancer cells obtained from patients. The novel derivatives were found to bind tubulin heterodimer with increased binding affinity, effectively inhibit cancer cell proliferation, cause selective G2/M arrest and induced apoptosis effectively in cancer cells.

5.2. Materials and Methods:

5.2.1. Protein preparation

The PDB (protein data bank) structure of tubulin (PDB ID: 6Y6D, resolution 2.20 Å) (Oliva *et al.*, 2020) was downloaded and used for the molecular modelling study. Although tubulin's crystal structure is generated at high resolution (2.20 Å), it has specific errors like missing hydrogen atoms, and missing side-chain atoms of some amino acids. The multistep procedure of protein preparation wizard (Schrödinger, Inc., NY) was used to add the missing hydrogen atoms. The missing side chain atoms of the amino acids were identified using Prime side chain prediction tool and repaired using Prime (Schrödinger, Inc., NY). Furthermore, the structure was refined by energy minimization using Macromodel (Schrodinger) and OPLS 2005 force field. Polak-Ribiere Conjugate Gradient (PRCG) algorithm with an energy gradient of 0.01 kcal/mol was used for the energy minimization.

5.2.2. Rational design of novel imidazopyridine-noscapinoids

Imidazopyridine (the imidazole moiety fused with the pyridine ring) is a biologically active nitrogen containing heterocycle (Couty *et al.*, 2008; Liu and Chen 2010; Zhou *et al.*, 2009). It displays a wide range of pharmacological activities such as antiprotozoal, antiviral, antifungal, antitumor, antibacterial, anti-inflammatory, antipyretic, antiapoptotic, analgesic, hypnoselective, and anxioselective (Rival *et al.*, 1992; Fisher and Lusi, 1972; Rival *et al.*, 1991; Hamdouchi *et al.*, 1999; Kaminsky and Doweyko, 1999). Several drugs which are in the clinics such as zolpidem (**1),** used in the treatment of insomnia), alpidem (**2),** used as an anxiolytic agent), zolimidine (**3),** used for the treatment of peptic ulcer), necopidem and saripidem (**4)** and (**5)**, used as anxiolytic agents) and GSK812397 (**6)**, used for the treatment of HIV infection) consists of imidazo [1,2-*a*] pyridine (Figure. 5.1) as a pharmacophore (Langer *et al.*, 1990; Almirante *et al.*, 1965; Boerner and Moller, 1997; Gudmundsson and Boggs, 2006).

5.2.3 Preparation of molecular structure of noscapinoids

The newly designed N-imidazopyridine-noscapinoids (Figure 5.3) were built using ChemDraw and imported into Maestro (Schrödinger package). These molecular structures were energy minimized using Macromodel (Schrödinger package) and OPLS 2005 force field with PRCG algorithm (energy gradient of 0.001). The ligand structures were further refined by geometric optimization using hybrid density functional theory with Becke's three-parameter exchange potential and the Lee-Yang-Parr correlation

functional (B3LYP) with basis set 3-21G* using Jaguar (Schrödinger, package). The various conformations of the ligands were generated using Ligprep (Schrödinger package).

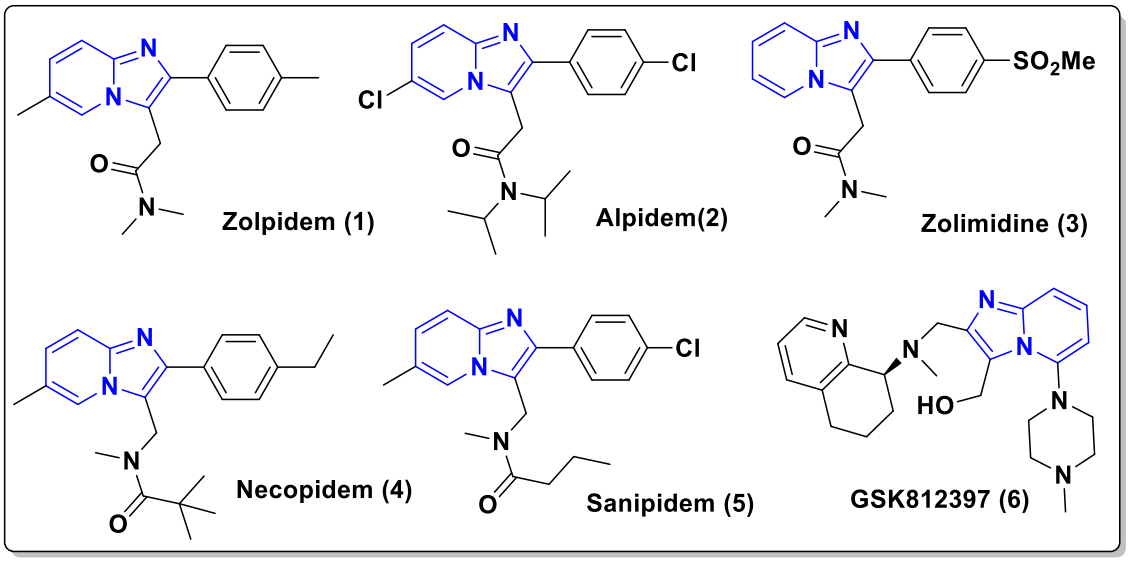

Figure 5.1. *Drugs in the clinics with imidazopyridine pharmacophore.*

In a quest of developing new series of noscapine congeners, we have coupled the imidazo [1,2-*a*] pyridine pharmacophore with noscapine scaffold (Figure 5.2) to design a panel of N-imidazopyridine-noscapinoids by *in silico* as depicted in Figure 5.3.

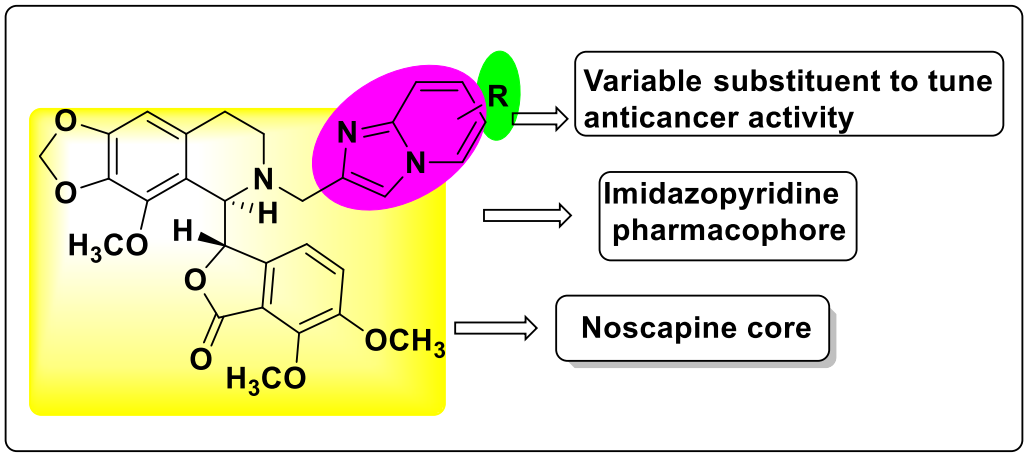

Figure 5.2. *General scheme for strategic development of a panel of N-imidazopyridine-noscapinoids by substitution of various functional groups at 'R'.*

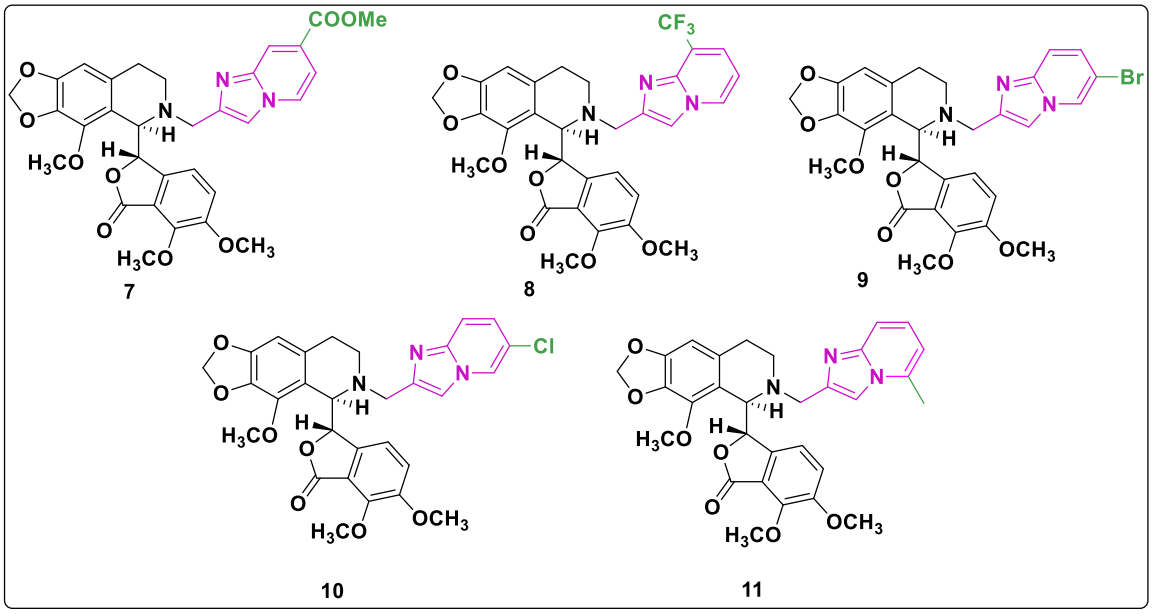

Figure 5.3. *The molecular structure of five N-imidazopyridine-noscapinoids design by substitution of different functional group in the imidazo[1,2-a]pyridine pharmacophore to tune anticancer activity.*

5.2.4. Molecular docking of noscapinoids

The prepared structures of N-imidazopyridine-noscapinoids were docked with αβ-tubulin heterodimer using Glide (Schrödinger package) as reported previously (Naik *et al*, 2011a). Glide grid-receptor generation program was used to create a grid box of size 12Å x 12Å x 12Å at the centroid of the co-crystal ligand, amino-noscapine. Noscapinoids were docked into the binding site using Glide XP (extra precision) and their binding poses were evaluated using a Glide XP_{Score} function (Friesner *et al.*, 2004; Halgren *et al.*, 2004). The single best conformation for each ligand was considered for further analysis.

5.2.5. Molecular dynamics simulation of docked complexes

Molecular dynamics (MD) simulation of the complexes of Tubulin and N-imidazopyridine-noscapinoids in the presence of GTP, GDP and magnesium were carried out using GROMACS 2019.2 package (Abraham *et al.*, 2015). The docked conformation of the complex with the lowest minimum docking score was taken as the initial conformation for MD simulation. The protein was processed by Gromacs with AMBER 999SB force field (Hornak *et al.*, 2006) to generate coordinates and topology files. Parameters for all the 3 ligands (GTP, GDP and **7**) were estimated using a general amber force field (GAFF) (Wang *et al.*, 2004) implemented in antechamber program of Amber 18. All atomic point charges were calculated using AM1-BCC charge model (Jakalian *et al.*, 2002). Topologies and internal coordinates for all ligands were generated

using tleap program of Amber 18 and ACPYPE software (Sousa da Silva and Vranken, 2012). The complex was solvated with TIP3P water model in a truncated octahedron box with the distance of 12 Å between the atoms of protein and the wall of the box. Counter ions at physiological ionic strength (0.15 M) neutralized the system. Energy minimization was performed using the Steepest descent method of 10000 steps to release conflicting contacts. After applying position restraints of 10 kcal/Å^2 on protein and ligands, NVT equilibration of 500 ps run was done at 300 K, followed by NPT equilibration of 500 ps with Parrinello-Rahman barostat at reference pressure of 1 bar. After equilibration, production MD run was performed for 100 ns with a time step of 2 fs. Particle-mesh Ewald algorithm (PME) was used for long-range electrostatic interactions. Short-range electrostatics and van der Waals cut offs were set at 10 Å. The bonds were constrained using a shake algorithm (Ryckaert *et al.,* 1977) and a modified Berendsen thermostat was used to regulate the temperature of the system. The atomic coordinates were recorded every 20 ps during the MD simulation. Gromacs tools were used to analyze trajectories for Root Mean Square Deviation (RMSD), Radius of gyration (Rg) and Root Mean Square Fluctuation (RMSF). All plots were generated using GRACE software. The complex with the lowest minimum total energy from the MD trajectory was used to elucidate the binding mode of the ligand.

5.2.6. Prediction of binding free energy using MM-PBSA technique

Predicted binding free energy of N-imidazopyridine-noscapinoids **7-11** with tubulin was calculated based on Molecular Mechanics Poisson-Boltzmann Surface Area (MM-PBSA) (Kollman *et al.,* 2000). From the last 10 ns of MD trajectory, 500 snapshots were extracted with a time step of 20 ps and the ensemble average of the $\Delta G_{bind,pred}$ was determined using g_mmpbsa tool (Kumari *et al.,* 2014) as follows.

$$\Delta G_{bind,pred} = \Delta G_{complex} - [\Delta G_{Rec} + \Delta G_{lig}]$$

$$G = E_{gas} + G_{sol} - TS.$$

$$E_{gas} = E_{int} + E_{ele} + E_{vdw}$$

$$G_{sol} = G_{PB(GB)} + G_{sol\text{-}np}$$

$$G_{sol\text{-}np} = \gamma SAS$$

Where, G is Gibbs free energy, E_{gas} is the gas phase energy calculated as the sum of internal energy (E_{int}), energy generated as a result of the electrostatic interaction (E_{ele}) and the van der Waals interaction (E_{vdw}). G_{sol} is the solvation free energy calculated as

the sum of polar (G_{PB}) and nonpolar contributions ($G_{sol\text{-}np}$). Polar interaction contribution (G_{PB}) was calculated as the summation of electrostatic contribution (E_{ele}) and polar solvation contribution (G_{PB}). The nonpolar solvation contribution ($G_{sol\text{-}np}$) is approximated as linearly dependent on the solvent accessible surface area (SAS) and γ is the surface tension constant that was set to 0.0072 kcal mol^{-1} $Å^{-2}$. Inspired by the high predicted binding affinity with tubulin compared to noscapine based on the docking score and the predictive free energy of binding using MM-PBSA, we have chemically synthesised all the five N-imidazopyridine-noscapinoids for their experimental validation.

5.2.7. Predicted ADME properties

A set of 44 ADME (absorption, distribution, metabolism, and excretion) properties for N-imidazopyridine-noscapinoids were predicted using the QikProp tool (Schrodinger package). The properties having zero values were manually deleted. The acceptability of the compounds was analysed using Lipinski's rule of 5 (number of violations of Lipinski's rule of five) which is vital for rational drug design. When a ligand molecule violates Lipinski's rule of five, i.e., it contains more than 5 hydrogen bond donors, the molecular weight is over 500, the log P is over 5, and the total of N's and O's is over 10, poor absorption or penetration is more likely.

5.2.8. Chemical synthesis of N-imidazopyridine-noscapinoids

We have attempted to synthesize the designed N-imidazopyridine-noscapinoids chemically, **7-11** by strategically coupling various substituted 2-(chloromethyl) imidazo [1,2-*a*] pyridines with nor-noscapine as depicted in the synthetic scheme (Figure 5.4). Natural noscapine was treated with m-CPBA to give noscapine-N-oxide, then treated with 2N HCl to give noscapine-N-oxide.HCl salt. It is further reacted with $FeSO_4.7H_2O$ to afford nor-noscapine. To a solution of nor-noscapine (1.0 mmol) in acetone (10 mL), K_2CO_3 (2.0 mmol), KI (2.0 mmol) and various substituted 2-(chloromethyl)imidazo [1,2-*a*] pyridine **7-11** (1.1 mmol) were added sequentially, and the contents were stirred for 6h at room temperature. After completion of the reaction, the contents were washed with brine solution. The organic layer was collected and passed through a Na_2SO_4 bed and later removed under reduced pressure. The crude residue was chromatographed over a triethylamine silica bed, using pet.ether/ethyl acetate (3:1) as eluents, to give pure compounds **7-11** as white solid products in 55-72% yields. Structural characterizations of all the intermediates and final products were done using NMR (^1H and ^{13}C), IR

spectroscopy and mass (HRMS) spectrometry techniques. The NMR (^{1}H and ^{13}C) and HRMS spectra are collated in the Appendix material (A5.1-A5.15).

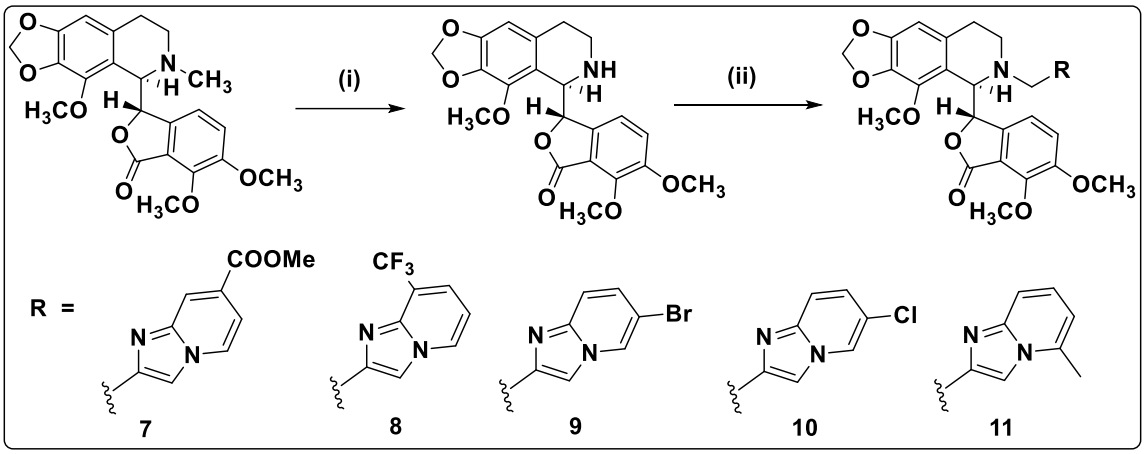

Figure 5.4. *Synthetic scheme 1: General chemical reaction for chemical synthesis of imidazopyridine-noscapinoids (7-11) design in the study. Reaction conditions: (i) a: m-CPBA, DCM; b: 2N HCl; c: $FeSO_4.7H_2O$; (ii) 7-11, K_2CO_3, KI, acetone, rt, 4h, 60%.*

Methyl-2-(((R)-5-((S)-4,5-dimethoxy-3-oxo-1,3-dihydroisobenzofuran-1-yl)-4-methoxy-7,8-di hydro-[1,3]dioxolo[4,5-g]isoquinolin-6(5H)-yl)methyl)imidazo[1,2-a]pyridine-7-carboxylate (7):

Nature: White solid. mp: 95-97 °C. IR (KBr): 3781, 3418, 2930, 1757, 1717, 1620, 1496, 1270, 1036, 932, 815, 763, 435 cm^{-1}. ^{1}H NMR (400 MHz, CDCl3) : δ 8.25-8.22 (m, 1H, Ar-H), 8.16 (dd, *J* = 0.8, 7.0 Hz, 1H, Ar-H), 7.81 (s, 1H, Ar-H), 7.35 (dd, *J* = 1.7, 7.0 Hz, 1H, Ar-H), 6.96 (d, *J* = 8.3 Hz, 1H, Ar-H), 6.33 (s, 1H, Ar-H), 6.07 (dd, *J* = 0.4, 8.3 Hz, 1H, Ar-H), 5.95 (dd, *J* = 1.3, 6.2 Hz, 2H, O-CH2-O), 5.74 (dd, *J* = 0.4, 4.1 Hz, 1H, Ar-CH (C3-pthalide)), 4.69 (d, *J* = 4.1 Hz, 1H, Ar-CH (C5'-isoquinoline)), 4.24 (d, *J* = 14.3 Hz, 1H, -C*H*H*N*-CH2), 4.10 (s, 3H, -OCH3), 4.05 (s, 3H, -OCH3), 3.97-3.92 (m, 4H, -CH*H*-*N*-CH2, -OC*H*3), 3.86 (s, 3H, -OCH3), 2.54-2.39 (m, 3H, -C*H*2-*N*-CH2 (C7'-isoquinoline), Ar-C*H*H (C8'-isoquinoline)), 1.95-1.86 (m, 1H, Ar-CH*H* (C8'-isoquinoline)). ^{13}C NMR (100 MHz, CDCl3): δ 168.0, 165.8, 152.2, 148.4, 148.1, 147.6, 143.3, 140.8, 140.4, 133.9, 131.8, 125.2, 125.1, 120.0, 119.6, 118.1, 117.9, 116.4, 113.1, 111.2, 102.6, 100.7, 81.2, 62.2, 59.4, 59.2, 56.6, 56.0, 52.3, 46.3, 26.4. MS (ESI-MS) *m/z:* 588 $[M+H]^+$ HRMS (ESI) : Calcd for C31H30N3O9 $[M+H]^+$: 588.19766, found: 588.19994.

(S)-6,7-dimethoxy-3-((R)-4-methoxy-6-((8-(trifluoromethyl)imidazo[1,2-a]pyridin-2-yl) methyl)-5,6,7,8-tetrahydro-[1,3]dioxolo[4,5-g]isoquinolin-5-yl)isobenzofuran-1(3H)-one (8):

Nature: White solid.mp: 102-104 ^{o}C. IR (KBr): 3421, 2927, 1759, 1496, 1268, 1214, 1036, 890, 802, 716 cm^{-1}. ^{1}H NMR (400 MHz, CDCl3) : δ 8.29 (s, 1H, Ar-H), 7.65 (s, 1H, Ar-H), 7.40(d, *J* = 9.5 Hz, 1H, Ar-H), 7.16 (d, *J* = 9.5 Hz, 1H, Ar-H), 6.96 (d, *J* = 8.3 Hz, 1H, Ar-H), 6.32 (s, 1H, Ar-H), 6.09 (d, *J* =8.3 Hz, 1H, Ar-H), 5.94 (d, *J* = 5.2 Hz, 2H, O-CH2-O), 5.72 (d, *J* = 4.1 Hz, 1H, Ar-CH (C3-pthalide)), 4.67 (d, *J*= 4.1 Hz, 1H, Ar-CH (C5'-isoquinoline)), 4.19 (d, *J* = 14.4 Hz, 1H, -C*H*H-N-CH2), 4.10 (s, 3H, -OCH3), 4.04 (s, 3H, -OCH3), 3.89-3.84 (m, 4H, -OCH3, -CH*H*-*N*-CH2), 2.54-2.34 (m, 3H, -C*H*2-*N*-CH2 (C7'-isoquinoline), Ar-C*H*H (C8'-isoquinoline)), 1.99-1.83 (m, 1H, Ar-CH*H* (C8'-isoquinoline)). ^{13}C NMR (100 MHz, CDCl3): δ 168.4, 152.1, 148.4, 147.6, 146.0, 142.8, 140.8, 140.4, 133.9, 131.7, 127.3, 125.8, 119.9, 118.1, 117.9, 117.5, 116.5, 111.7, 106.5, 102.4, 100.7, 81.2, 62.2, 59.3, 59.1, 56.6, 55.7, 46.2, 26.3. MS (ESI-MS) *m/z:* 598[M+H]$^{+}$ HRMS (ESI): Calcd for Calcd for $C_{30}H_{27}N_3O_7F_3$[M+H]$^{+}$: 598.1818, found: 598.1795.

(S)-3-((R)-6-((6-bromoimidazo[1,2-a]pyridin-2-yl)methyl)-4-methoxy-5,6,7,8-tetrahydro- [1,3]dioxolo[4,5-g]isoquinolin-5-yl)-6,7-dimethoxyisobenzofuran-1(3H)-one (9):

Nature: White solid. mp: 102-104 ^{o}C. IR (KBr): 3417, 2925, 2850, 1757, 1620, 1489, 1268, 1037, 935, 890, 778, 735cm^{-1}. ^{1}H NMR (500 MHz, $CDCl_3$) : δ 7.88 (s, 1H, Ar-H), 7.51 (d, *J* = 8.3 Hz, 1H, Ar-H), 7.07-6.94 (m, 3H, Ar-H), 6.33 (s, 1H, Ar-H), 6.18 (d, *J* = 8.3 Hz, 1H, Ar-H), 5.94 (dd, *J* = 1.4, 4.8 Hz, 2H, OCH2-O), 5.71 (d, *J* = 4.1 Hz, 1H, Ar-CH (C3-phthalide)), 4.73 (d, *J* = 4.1 Hz, 1H, Ar-CH (C5'-isoquinoline)), 4.22 (d, *J*= 14.3 Hz, 1H, -C*H*H-*N*-CH2), 4.13 (s, 3H, -OCH3), 4.02 (s, 3H, -OCH3), 3.98 (d, *J* = 14.3 Hz, 1H, -CH*H*-*N*CH2), 3.86 (s, 3H, -OCH3), 2.65-2.46 (m, 3H, -C*H*2-*N*CH2 (C7'-isoquinoline), Ar-C*H*H (C8'-isoquinoline)), 2.03-1.92 (m, 1H, Ar-CH*H* (C8'-isoquinoline)). ^{13}C NMR (100 MHz, CDCl3): δ 168.2, 152.1, 148.4, 147.8, 145.1, 144.9, 141.0, 140.5, 133.9, 131.8, 124.1, 119.8, 118.1, 117.8, 116.7, 115.7, 115.6, 114.1, 112.5, 102.4, 100.7, 81.4, 62.5, 59.3, 59.1, 56.7, 55.5, 46.3, 26.6. MS (ESI-MS) *m/z:* 608 [M+H]$^{+}$ HRMS (ESI): Calcd for C29H27BrN3O7 [M+H]+: 608.10269, found: 608.10552.

(S)-3-((R)-6-((6-chloroimidazo[1,2-a]pyridin-2-yl)methyl)-4-methoxy-5,6,7,8-tetrahydro- [1,3]dioxolo[4,5-g]isoquinolin-5-yl)-6,7-dimethoxyisobenzofuran-1(3H)-one (10):

Nature: White solid. mp: 96-98 ºC. IR (KBr): 3390, 2938, 1755, 1621, 1493, 1268, 1214, 1039, 934, 761, 663, 429 cm-1. ^{1}H NMR (400 MHz, $CDCl_3$): δ 8.18 (dd, *J* = 0.8, 2.0 Hz, 1H, Ar-H), 7.66 (s, 1H, Ar- H), 7.43 (dt, *J* = 0.8, 9.5 Hz, 1H, Ar-H), 7.06 (dd, *J* = 2.0, 9.5 Hz, 1H, Ar-H), 6.95 (d, *J* = 8.3 Hz, 1H, Ar-H), 6.32 (s, 1H, Ar-H), 6.08 (dd, *J* = 0.4, 8.3 Hz, 1H, Ar-H), 5.94 (dd, *J* = 1.4, 5.9 Hz, 2H, O-CH2-O), 5.72 (dd, *J* = 0.4, 4.1 Hz, 1H, Ar-CH (C3-pthalide)), 4.67 (d, *J* = 4.1 Hz, 1H, Ar-CH (C5'-isoquinoline)), 4.19 (d, *J* = 14.3 Hz, 1H, -C*H*H N-CH2), 4.10 (s, 3H, -OCH3), 4.04 (s, 3H, -OCH3), 3.90 (d, *J*= 14.30 Hz, 1H, -CH*H*-*N*-CH2), 3.86 (s, 3H, -OCH3), 2.53-2.42 (m, 3H, -C*H*2-*N*-CH2 (C7' isoquinoline), Ar-C*H*H (C8'-isoquinoline)), 1.96-1.86 (m, 1H, Ar-CH*H* (C8'-isoquinoline)).. ^{13}C NMR (100 MHz, $CDCl_3$): δ 168.1, 152.2, 148.4, 147.6, 142.8, 140.8, 140.4, 133.9, 131.8, 125.1, 123.6, 119.9, 119.9, 118.0, 117.9, 117.1, 116.4, 111.8, 102.4, 100.7, 81.2, 62.2,59.3, 59.1, 56.6, 55.7, 46.3, 26.4. MS. (ESI-MS) *m/z*: 564 $[M+H]^+$: HRMS (ESI): Calcd for C29H27ClN3O7 $[M+H]^+$: 564.15320, found:564.15508.

(S)-6,7-dimethoxy-3-((R)-4-methoxy-6-((5-methylimidazo[1,2-a]pyridin-2-yl)methyl)- 5,6,7,8-tetrahydro-[1,3]dioxolo[4,5-g]isoquinolin-5-yl)isobenzofuran-1(3H)-one (11):

Nature : White solid. mp: 100-102 ºC. IR (KBr): 3760, 3447, 2933, 1757, 1652, 1491, 1387, 1269, 1214,1037, 933, 782, 745 cm-1. ^{1}H NMR (400 MHz, $CDCl_3$): δ 7.67 (s, 1H, Ar-CH), 7.45 (d, *J* = 9.0 Hz, 1H, Ar-CH),7.10 (dd, *J* = 6.8, 9.0 Hz, 1H, Ar-CH), 6.96 (d, *J* = 8.3 Hz, 1H, Ar-CH), 6.59 (dt, *J* = 1.1, 6.8 Hz, 1H, Ar-CH), 6.33 (s, 1H, Ar-CH), 6.14 (dd, *J* = 0.4, 8.3 Hz, 1H, Ar-CH), 5.94 (dd, J = 1.4, 5.7 Hz, 2H, O-CH_2-O), 5.74 (dd, *J* = 0.4, 4.1 Hz, 1H, Ar-CH (C_3-phthalide)), 4.67 (d, *J* =4.1 Hz, 1H, Ar-CH (C_5'-isoquinoline)), 4.19 (d, *J* = 14.3 Hz, 1H, -CHH-N-CH_2), 4.10 (s, 3H, -OCH_3), 4.03 (s, 3H, -OCH_3), 3.94 (d, *J*= 14.3 Hz, 1H, -CHH-N-CH_2), 3.86 (s, 3H, -OCH_3), 2.65 (s, 3H, Ar-CH_3), 2.59-2.37 (m, 3H, -CH_2-N-CH_2 (C7'-isoquinoline), Ar-CHH (C8'-isoquinoline)), 1.99-1.90 (m, 1H, Ar-CHH (C8' isoquinoline)). ^{13}C NMR (100 MHz, $CDCl_3$): δ 168.4, 152.1, 148.3, 147.6, 144.8, 144.7, 141.0, 140.4, 134.7, 133.9, 131.6, 124.1, 119.9, 118.0, 117.9, 116.5, 114.0, 111.0, 108.8, 102.5, 100.6, 81.1, 62.2, 59.3, 59.0, 56.6, 55.6, 46.1, 26.0, 18.6. MS. (ESI-MS) *m/z*: 544 $[M+H]^+$: HRMS (ESI): Calcd for $C_{30}H_{30}N_3O_7$ $[M+H]^+$: 544.20783, found:544.20944.

5.2.9. Cell culture and reagents

All the chemical reagents and culture media were obtained from Sigma. Human breast cancer cell lines, MCF-7 and MDA-MB-231 were obtained from the cell repository of the National Center for Cell Science Pune, Maharashtra, India. The selected N-imidazopyridine-noscapinoids were chemically synthesized. Stock solution (100 mM) of the test compounds, **7-11** was prepared with dimethyl sulfoxide (DMSO) and stored at 4˚C until use. The cells were allowed to grow in Dulbecco's modified Eagle medium (DMEM), supplemented with 10% fetal bovine serum (FBS) and antibiotics at a temperature of 37 °C under 5% CO_2 and 95% humidity. Cells with a 70-80% confluence were sub cultured for bioassays using trypsin-EDTA (0.25 %).

5.2.10. In vitro cell proliferation assay using MCF-7 and MDA-MB-231 cell lines

Inhibition of cellular proliferation by the synthesized N-imidazopyridine-noscapinoids **7-11** was carried out using two human breast cancer cell lines, MCF-7 and MDA-MB-231. Cancer cells were grown in DMEM culture medium supplemented with 10% FBS, 1% penicillin/streptomycin and 2 mM l-glutamine at 37 °C with 5% CO_2. Suspension cells were plated into 96-well plates at a density of 5 x 10^3 cells per well and were treated with gradient concentrations (5 to 100 µM) of noscapine and its derivatives **7-11** for 72h. The harvested cells were fixed with 50% trichloroacetic acid, stained with 0.4% sulforhodamine B (dissolved in 1% acetic acid) and then washed with 1% acetic acid to remove unbound dye. The protein bound dye was extracted with 10 mM Tris base and absorbance was measured at 564 nm using a microplate spectrophotometer. The IC_{50} values that stand for the drug concentration required to achieve a cell kill of 50% was determined using the online tool Quest GraphTM IC_{50} Calculator (AAT Bioquest, Inc., Sunnyvale, CA, USA, https://www.aatbio.com/tools/ic50-calculator).

5.2.11. Primary breast cancer cells (PBCs) culture and in vitro cell proliferation assay

Primary breast cancer cells were isolated from the surgically removed breast tumor tissue from the patients (4 nos.) of different stages of cancer. The tumour tissues were treated with 0.25% trypsin and filtered with 70 micron filter followed by centrifugation at 2000 rpm for 3 minutes with serum-free medium. The filtered cells were collected and plated in T25 flask and incubated with a complete DMEM medium, supplemented with 10% FBS and 1% pentrip (mixture of penicillin and streptomycin) at 37 °C under 5% CO_2. Fresh media was replaced every 3-4 days, and subsequent passages were performed under the same conditions as mentioned above. The cultured were

maintained for homogeneous cell type at sub-confluence between 3-8 passages. Cells were allowed to reach 80-90% confluence prior to experimental treatments. After the confluence reached, the primary cells were plated at 2000 cells/well in 96 wells plate with DMEM (low glucose) growth media. The cells were maintained at 37 °C with 5% CO_2 and were treated with gradient concentrations (5 to 100 µM) of noscapine and N-imidazopyridine-noscapinoids, **7-11** for 72 h. Measurement of cell proliferation was performed with a plate reader by sulforhodamine B (SRB) assay, using the CellTiter96 AQueous One Solution Reagent (Sigma). The optical density was measured using a microplate spectrophotometer at a wavelength of 564 nm. The percentage of cell survival as a function of drug concentration was plotted and the IC_{50} value was determined using the online tool, AAT Bioquest.

5.2.12. Flow cytometry analysis of cell cycle progression

MDA-MB-231 cells were grown in DMEM culture media with 4.5 g/L glucose and L-glutamine, supplemented with 10% FBS and 1% penicillin/streptomycin, at 37 ^oC in a 5% CO_2 atmosphere. Cells were treated with noscapine and the most promising N-imidazopyridine-noscapinoid **9** dissolved in 1% phosphate buffer saline (PBS). Cells were sampled after 72 h of treatment, followed by flow cytometry analysis. Briefly, 2 x 10^6 cells were centrifuged, washed twice with ice-cold PBS and fixed in 70% ethanol. The cell pellets in the tubes were stored at -20 ^oC for 24 h. The cell pellets were centrifuged at 1000 x g for 10 min and the supernatant was discarded. The pellet was resuspended in 30 µl of phosphate/citrate buffer (0.2 M Na_2HPO_4/0.1 M citric acid, pH 7.5) at room temperature for 30 min. Cells were then washed with 5 ml of PBS and incubated with 0.5 ml of propidium iodide (20 µg/ml in 0.6% Triton-X in PBS) and 0.5 ml of RNase A (20 µg/ml in PBS) for 45 min. in dark. Samples were analysed on a flow cytometer (BD FACS Aria-III) and the progress in the cell cycle was determined.

5.2.13. Flow cytometry analysis for apoptosis assay

Apoptosis in cancer cells was detected by Annexin-V-FITC apoptosis detection kit (Sigma –Aldrich) based on the manufacturer's instruction. In brief, $3x10^4$ cells per well were seeded on 12 well culture plate and incubated for 24 h with complete medium. The cells were treated with IC_{50} concentration of noscapine and N-imidazopyridine-noscapinoid **9** and were harvested after 48 h. Cells were trypsinized and stained with biotin-conjugated Annexin V FITC-conjugate and propidium iodide (PI). Flow cytometer data with 488 nm excitation for PI and emission at 530 nm were collected. Viable cells (Annexin V^- / PI^-), early apoptotic cells (Annexin V^+ / PI^-), late

apoptotic/necrotic cells (Annexin V^+ / PI^+) and late necrotic cells (Annexin V^- / PI^+) were identified and determined their percentage.

5.2.14. Cellular observation by staining with fluorescent dyes

MDA-MB-231 cancer cells were cultivated in 6-well plates on poly-L-lysine-coated coverslips and treated with the IC_{50} concentration of **9** for 72 hours. After incubation, coverslips were removed, fixed in cold methanol and washed with PBS. It was then stained with 10 µM concentration of DAPI, Hoechst 33342, acridine orange and ethidium bromide dye separately for 15 minutes at room temperature. The stained cells were washed twice in PBS and viewed using a Nikon Eclipse Ts2R-FL inverted fluorescent microscope with standard excitation filters. The excitation and emission wavelengths were 346 nm and 460 nm, respectively. Apoptotic cells in the presence of test compounds were identified by changes in morphological features (e.g. nuclear condensation, formation of membrane blebs and apoptotic bodies) compared to untreated cells.

5.2.15. Measurement of mitochondrial membrane potential (ΔΨm)

The effect of **9** on mitochondrial membrane potential was measured by using three different dyes such as rhodamine-123 (Sigma-Aldrich Co.; Ex/Em = 485 nm/535 nm), JC-1 (Invitrogen Co.; Ex/Em = 515 nm/529 nm) and DAPI (Sigma-Aldrich Co.; Ex/Em = 358 nm/461 nm). Briefly, cells were seeded in 12 well plates followed by treatment with **9** for 48 hours. Cells were washed with PBS and stained with rhodamine-123 (15µg/ml), JC-1 (10 µg/ml) and DAPI (10 µg/ml) for 10 minutes at room temperature. After staining, cells were washed twice with PBS and images were captured using an inverted fluorescence microscope (Nikon Eclipse Ts2R-FL) at 400x magnification. The untreated cells stained with rhodamine-123 appeared light green fluorescence (lower ΔΨm) whereas the treated cells appeared bright green fluorescence (higher ΔΨm). In the case of JC-1 stain, light red fluorescence (lower ΔΨm) was detected in untreated cells, whereas bright red fluorescence (higher ΔΨm) was observed in treated cells. Similarly in DAPI stain relatively light blue with no morphological changes was observed in untreated cells, whereas bright blue with changes in morphological features was observed in treated cells. The intensity was measured using image J software.

5.2.16. Intracellular reactive oxygen species (ROS) detection

An increase in intracellular ROS induces apoptosis in cancer cells. The intracellular ROS concentration was analysed through the oxidative conversion of the sensitive fluorescent probe 2',7'-dichlorofluorescence-diacetate (DCFH-DA) to fluorescent 2',7'-dichlorofluorescein (DCF). Briefly, MDA-MB-231 cells were seeded in 6 well plates containing cover glass and treated with **9** for 48 hours. The treated cells were harvested, washed twice with PBS, resuspended in 500 µL of 10 µM DCFH-DA (purchased from Molecular Probes Inc., Invitrogen) and incubated at room temperature for 30 minutes in the dark. The stained cells were observed under a fluorescent microscope (Nikon Eclipse Ts2R-FL) with standard excitation filters (Nikon). The untreated control cells were observed with low green fluorescence, whereas the treated cells were observed with bright green fluorescence. The results displayed a significant rise in intracellular ROS by **9.**

5.2.17. In vivo antitumor effect against MCF-7 breast tumors

The Institutional Animal Ethics Committee approved the study of National Institute of Pharmaceutical Education and Research (NIPER), Hyderabad (1548/PO/Re/2011/CPCSEA). BALB/c athymic nude female mice of 8 to 10 weeks were housed in the Animal Care Facility. The mice were implanted with $1x10^6$ human epithelial breast adenocarcinoma MCF-7 cells in 0.2 ml of PBS, subcutaneously into the anterior flank. When the implanted tumour was palpable (7-10 days), treatment of the test compound (**9**) was administered by oral gavage. The mice were randomly divided into 2 groups. Group-1 (control) consisted of 5 animals that received daily gavage of vehicle solution (acidified water, pH 4.0) only; group-2 consisted of 5 animals were treated with **9** (50 µM/day). Tumor volumes were estimated on alternate days by measuring tumours in three transverse direction diameters with vernier callipers and calculating their volume as Π/6 (length x width x height) (Tomayko and Reynolds, 1989). The control group of mice was euthanized on day 30 owing to their large tumour volumes and served as the endpoint for control animals. Accordingly, this endpoint was used to evaluate tumour size in untreated mice with those administered with **9**.

5.2.18. Histopathological and hematological analyses

On day 30, both the treated and untreated mice received an overdose (0.2 ml) of 3.5 percent chloral hydrate, blood was drawn from the heart, and CBC analysis was conducted using a CBC analyzer (CDC Technologies, Oxford CT). The animals were

perfused with a 3% paraformaldehyde and 2% glutaraldehyde combination in PBS (pH 7.4). The vital organs like liver, kidney, lung and heart, and tumour were extracted and analyzed for histological investigation. Tissues were mounted in paraffin, sectioned, and stained with hematoxylin and eosin. The tissues were observed under the microscope for toxicity evaluation.

5.3. Results and Discussion

The cell-killing potential of the natural lead molecule, noscapine was improved to many folds by synthesizing several promising derivatives. Many of these derivatives were demonstrated to have increased free energy of binding with tubulin as evident by lowering their dissociation constants (K_d) significantly from 152 μM for noscapine. For example, the halogen derivatives have K_d value in the range of 80 to 22 μM, nitro noscapine has 86 μM and amino noscapine has 14 μM (Aneja *et al.*, 2006a; Naik *et al.*, 2012; Aneja *et al.*, 2006b). Furthermore, we have developed a battery of derivatives by functionalization of 'N' in the isoquinoline unit of natural α-noscapine (Jain *et al.*, 2011) and coupling biaryl pharmacophore (Santoshi *et al.*, 2015). All these derivatives have also shown a lower K_d value compared to noscapine. We are reporting in this study a panel of N-imidazopyridine-noscapinoids, **7-11** as promising tubulin binding anticancer agents.

5.3.1. N-imidazopyridine-noscapinoids docked well inside the binding cavity using molecular docking and MD simulation

The five N-imidazopyridine-noscapinoids, **7-11,** and the lead molecule, noscapine, were docked using Glide XP onto the noscapinoid binding site (Oliva *et al*, 2020) at the interface between α- and β- tubulin. All these molecules were found to fit well inside the binding site. Their binding affinity with tubulin is also evaluated using Glide XP_{score} function (Friesner *et al.*, 2004; Halgren *et al.*, 2004). The N-imidazopyridine-noscapinoids, **7-11** revealed improved docking scores ranging from -8.557 to -8.082 kcal/mol compared to noscapine (docking score is -5.304 kcal/mol) (Table 5.1). The docked complexes of these ligands with tubulin were considered for MD simulation of 100 ns to observe the stability of the complex. The convergence of the MD trajectories was monitored by plotting the root mean square deviation (RMSD) and radius of gyration (Rg) of the backbone C_α atoms with respect to time. The relative fluctuation of the RMSD (0.21 to 0.24 Å) and Rg (0.966 to 0.972 nm) was minimal, suggesting the system's stability (Figure 5.5 and 5.6). Furthermore, the root mean square fluctuations (RMSF) of the residues of tubulin in the bound form with ligands and in the

free form were calculated to reveal the flexibility of these residues (Figure 5.7a&b). It was observed that the RMSF values of the residues in the bound and free form were minimum (0.02 to 0.04 nm) for both α- and β- tubulin, indicating that the residues were more rigid. Overall, the N-imidazopyridine-noscapinoids **7-11** were well accommodated inside the binding site, at the interface between α- and β- tubulin (Figure 5.8). However, their binding modes inside the binding cavity are distinct as shown in the ligplot (Figure 5.9a-d). The differences in binding modes of these noscapinoids are due to various substitutions of functional groups in the scaffold structure and because of differential contribution in binding free energy of amino acids involved in the interactions. As showed in the figure the most potent N-5-Bromoimidazopyridine-noscapine **(9)** in terms of docking score interacts more intensely with the residues of tubulin compared to other derivatives. Its binding involved one hydrogen bond with Lys 352 (bond length 2.9 Å) (Figure 5.9c). Besides, hydrogen bonding, good number of hydrophobic interactions were involved in the binding of N-imidazopyridine-noscapinoids (**7-11**) with binding site residues (Appendix Table A5.16-A5.19).

Table 5.1. Results of molecular docking of N-imidazopyridine-noscapinoids (**7-11**) with tubulin. All the 5 molecules were found to docked well within the binding site with high binding affinity compared to the lead molecule, noscapine.

Ligands ID	Glide XP_{score} (Kcal/mol)	Glide lipo (Kcal/mol)	Glide evdw (Kcal/mol)	Glide ecoul (Kcal/mol)	Glide emodel (Kcal/mol)	Glide energy (Kcal/mol)
7	-8.334	-8.697	-66.458	-7.171	-90.593	-73.630
8	-8.336	-8.869	-64.909	-6.476	-97.341	-71.386
9	-8.557	-8.583	-66.913	-7.819	-102.727	-74.733
10	-8.121	-8.578	-65.140	-5.215	-90.667	-70.355
11	-8.082	-8.393	-64.242	-6.615	-68.275	-70.858
Noscapine	-5.304	-0.589	-35.174	-7.858	-20.456	-43.032

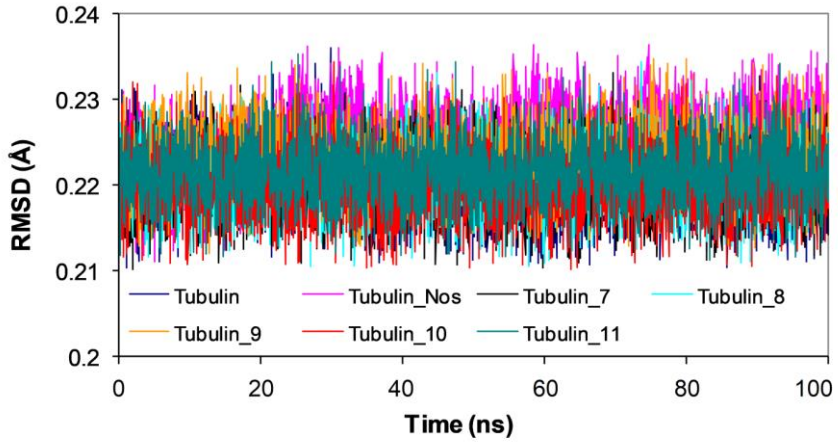

Figure 5.5. *Root mean square deviations (RMSD) of Cα carbon atoms of tubulin only and in complex with N-imidazopyridine-noscapinoids* ***(7-11)*** *during 100 ns of MD simulation. The relative fluctuation in the RMSD of the Cα atoms is very small (0.21 to 0.24 Å) for the entire duration of the simulation.*

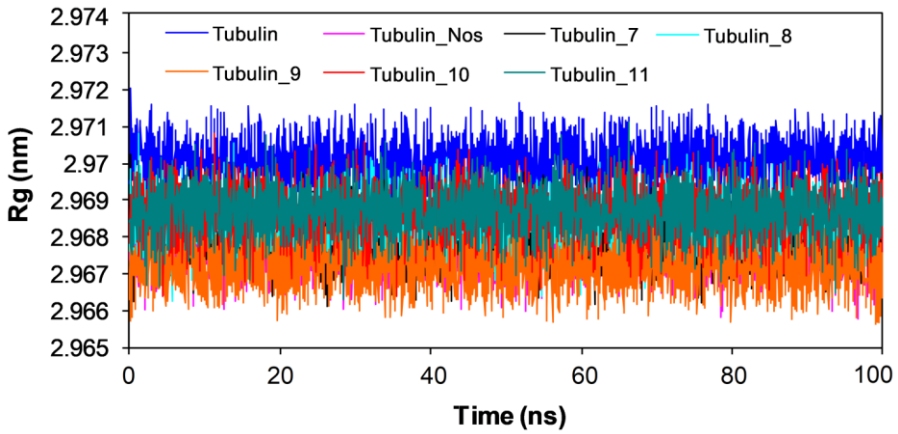

Figure 5.6. *Time evolution of radius of gyration of the tubulin and in complex with N-imidazopyridine-noscapinoids* ***(7-11)*** *over a period of 100 ns of MD simulation. All the molecular systems were found to be stable for the entire duration of the simulation.*

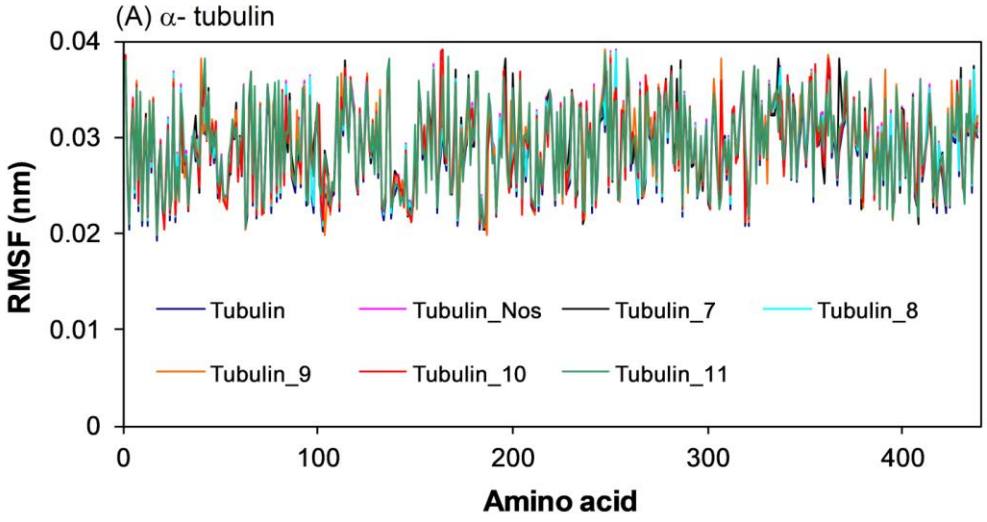

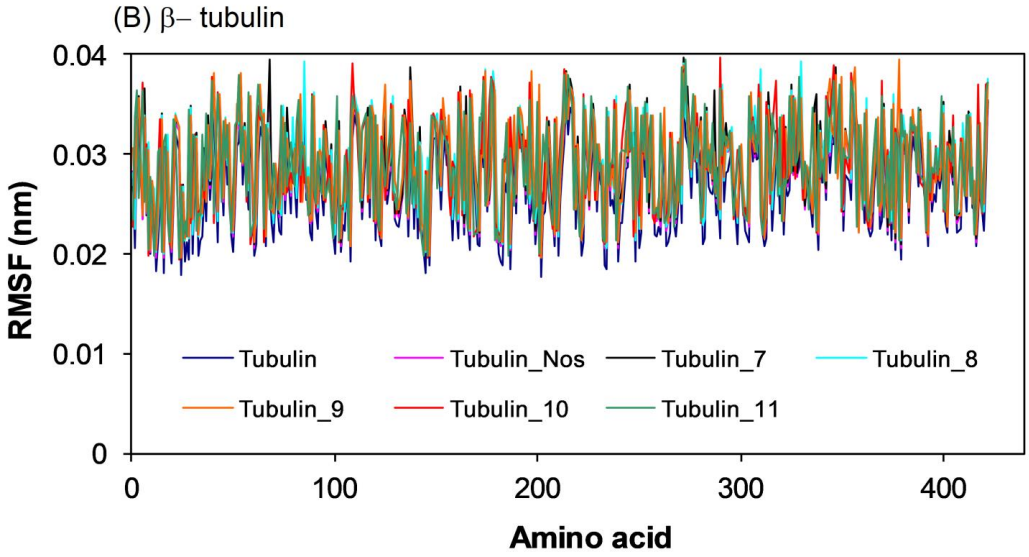

Figure 5.7a&b. *Root mean square fluctuation (RMSF) of the residues of tubulin of the docked ligands in the bound form and in the unbound form of tubulin heterodimer. Different levels of flexibility of these residues were noticed in the free and bound form of tubulin with ligands. All the amino acids showed very low fluctuation (0.02 to 0.04 nm) indicating that most of the residues were rigid both in free and bound form of tubulin.*

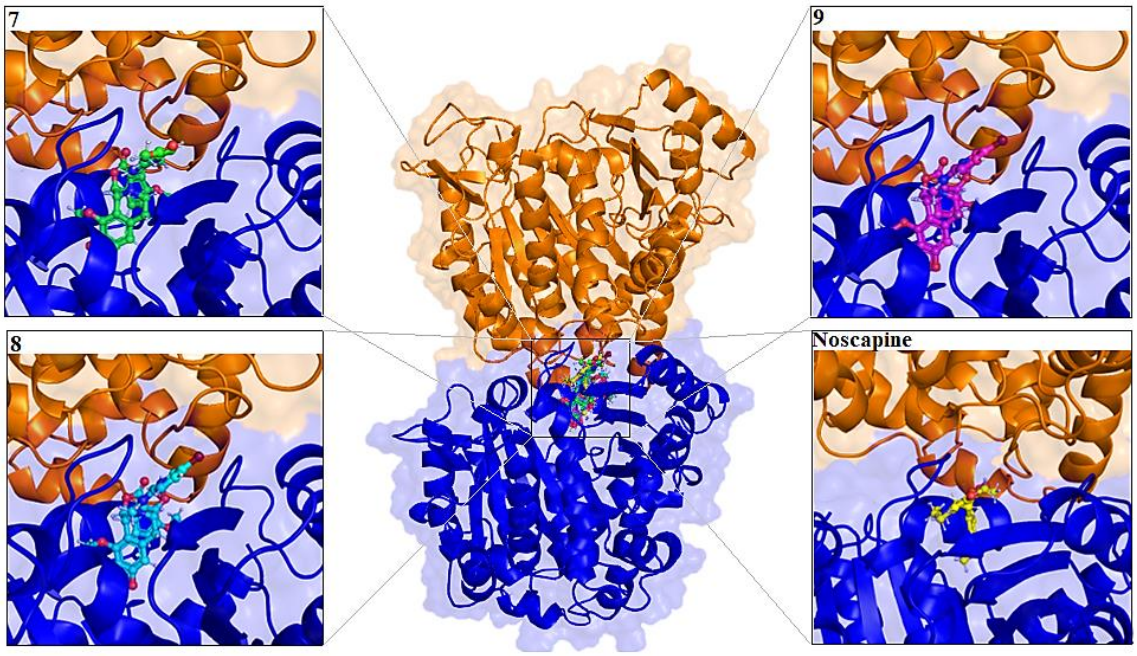

Figure 5.8. *The newly designed N-imidazopyridine-noscapinoids,* ***7-9 & noscapine*** *are well accommodated inside the noscapine binding site at the interface of α- and β-tubulin. The binding site is represented as macromodel surface according to α- and β-tubulin (α-tubulin is represented in brown colour and β-tubulin is represented in blue colour).*

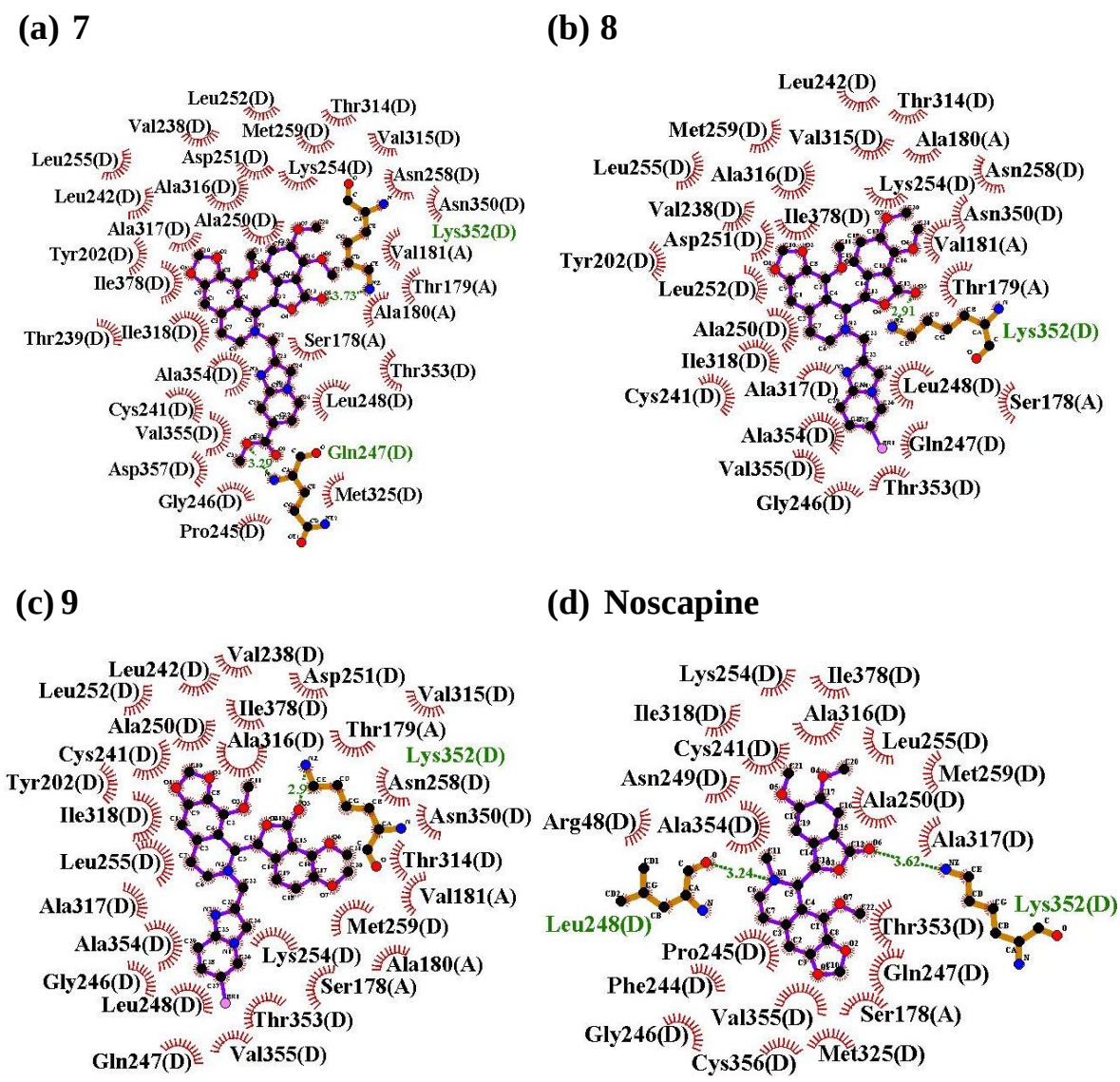

Figure 5.9. *Two dimensional representation of interaction observed between the binding site residues of tubulin with N-imidazopyridine-noscapinoids,* ***(a) 7, (b) 8, (c) 9*** *and* ***(d) noscapine****. Dashed lines denote hydrogen bonds and numbers indicate hydrogen bond lengths in Å. Hydrophobic interactions are shown as arcs with radial spokes. The figure was made using LIGPLOT. The residues within 5 Å distance from the docked ligands were only shown in the figures.*

5.3.2. N-imidazopyridine-noscapinoids revealed high free energy of binding with tubulin

The predictive binding free energy ($\Delta G_{bind,PB(GB)}$) of noscapine and its N-imidazopyridine-noscapinoids, **7-11** with tubulin according to MM-PBSA is collated in Table 5.2. Energy values were calculated as the average value out of 1000 snapshots generated from the last 2 ns of the MD trajectory for each tubulin-noscapinoid complex. It was revealed that the N-imidazopyridine-noscapinoids, **7-11** have a high binding

affinity with tubulin compared to the noscapine. The derivative, N-5-Bromoimidazopyridine-noscapine **(9)** showed the highest binding energy of -183.79 KJ/mol. Both the intermolecular van der Waals (ΔE_{vdw}) and the electrostatic (ΔE_{ele}) interactions are significant contributors to the binding, whereas the polar solvation terms (ΔG_{polar}) counteract binding. In contrast, solvent accessible surface area terms (ΔG_{SASA}), contribute slightly favorably.

Table 5.2. Binding free energy and its components (KJ/mol) calculated for the N-imidazopyridine-noscapinoids, **7-11** with αβ tubulin dimer**.**

Complex	ΔE_{elec} KJ/mol	ΔE_{vdw} KJ/mol	ΔG_{polar} KJ/mol	ΔG_{SASA} KJ/mol	$\Delta G_{binding}$ KJ/mol
Noscapine	-65.31 +/- 0.27	-222.50 +/- 0.51	176.94 +/ 0.32	-21.75 +/- 0.02	-132.63 +/- 0.15
7	-80.67 +/- 0.52	-246.61+/- 0.42	193.23 +/- 0.49	-36.57 +/- 0.10	-170.62 +/- 0.72
8	-78.73 +/- 0.66	-242.06+/- 0.47	191.01 +/- 1.08	-32.03 +/- 0.03	-161.81 +/- 0.91
9	-88.60 +/- 0.71	-252.63 +/-0.50	197.62 +/- 0.74	-40.18 +/- 0.04	-183.79 +/- 0.78
10	-72.72 +/- 0.43	-237.54+/- 0.35	187.64 +/- 0.25	-30.22 +/- 0.05	-152.84 +/- 0.48
11	-66.68 +/- 0.44	-231.76 +/- 0.47	176.69 +/- 0.65	-28.91+/- 0.04	-150.66 +/- 0.72

5.3.3. Predicted ADME properties of noscapine and its N-imidazopyridine-noscapinoids, 7-11

We have predicted the absorption, distribution, metabolism, and excretion (ADME) properties of noscapine and its N-imidazopyridine-noscapinoids, **7-11** using QikProp (Schrodinger software package). A number of ADME properties were predicted viz. molecular weight (MW), total solvent accessible surface area (SASA), octanol/water partition coefficient (QPlogPo/w), octanol/gas partition coefficient (QPlogPoct), water/gas partition coefficient (QPlogPw), polarizability in cubic angstroms (QPlogrz), % human oral absorption in intestine (QP%), brain/blood partition coefficient (QPlogBB), IC_{50} value for blockage of HERG K+ channel (QPlogHERG), skin permeability (QPlogKp), prediction of binding to human serum albumin (QPlogKhsa), apparent Caco-2 cell permeability in nm/sec (QPPCaco) and apparent MDCK cell permeability in nm/sec (QPPMDCK). Caco-2 cells are a model for the gut-blood barrier whereas MDCK cells are considered to be a good mimic for the blood-brain barrier. Also we evaluated the acceptability of noscapine and its N-imidazopyridine-noscapinoids, **7-11** based on the Lipinski's rule of 5 (number of violations of Lipinski's rule of five) which is essential for rational drug design. It was interesting to found that noscapine and its N-imidazopyridine-noscapinoids, **7-11** revealed significant values for

the properties analysed and qualified all the drug like characteristic based on Lipinski's rule of 5 (Table 5.3).

Table 5.3. A list of properties calculated for Noscapine and N-imidazopyridine-noscapinoids by Qikprop simulation and used for the ADME screening of the drug molecules. It was found that noscapine and its N-imidazopyridine-noscapinoids **7–11** satisfied all the properties essential for ADME screening.

Sl No	ADME Screening	7	8	9	10	11	Noscapine	Recommended values
1	MW.	587.58	608.44	608.44	563.99	543.57	413.42	130-725
2	SASA	856.44	748.17	772.45	787.75	801.82	597.02	300-1000
3	Accpt HB	12.25	10.25	10.25	10.25	10.25	8.75	2.0-20.0
4	QPpolrz	57.49	51.86	52.78	53.41	53.97	39.09	13.0-70.0
5	QPlogPoct	26.58	23.55	23.75	23.88	23.57	17.81	8.0-35
6	QPlogPw	15.06	12.54	12.65	12.86	12.72	10.08	4.0-45.0
7	QPlogPo/w	2.82	3.54	3.64	3.70	3.54	1.79	-2.0-6.5
8	QPlogHERG	-6.96	-6.01	-6.31	-6.61	-6.64	-4.42	Below -5.0
9	QPPCaco	150.7	670.2	585.0	541.8	571.4	777.7	< 25 poor > 500 great
10	QPlogBB	-0.79	0.27	0.18	0.12	-0.039	0.33	-3.0-1.2
11	QPPMDCK	70.80	917.73	790.29	699.29	298.91	417.06	< 25 poor >500 great
12	QPlogKp	-4.50	-3.37	-3.48	-3.46	-3.49	-3.95	-8.0- -1.0
13	QPlogKhsa	-0.18	-0.05	0.008	0.038	0.093	-0.49	-1.5-1.5
14	Rule of Five (No. of violations)	2	3	2	2	2	3	Maximum is 4

5.3.4. Newly designed noscapinoids inhibits proliferation of MCF-7 and MDAMB-231

All the N-imidazopyridine-noscapinoids, **7-11** including the parent compound, noscapine were tested for their anti-proliferative activity in two human breast adenocarcinoma cells, MCF-7 (estrogen- and progesterone- receptor positive) and MDAMB-231 (estrogen- and progesterone- receptor negative). All the N-imidazopyridine-noscapinoids, **7-11** exhibited potent cytotoxic activity in comparison to noscapine using both the cell lines at increasing concentrations (Figure 5.10). The IC_{50} values for **7-11** for both the cell lines are collated in Table 5.4. The IC_{50} value of noscapine and its N-imidazopyridine derivatives for both the cancer cell lines was found to be statistically significant compared to untreated cells ($p < 0.05$). Surprisingly noscapine and its N-imidazopyridine derivatives **7-11** inhibited proliferation of normal healthy cells with IC_{50} value > 1500 µM, indicating that these compounds were not toxic to normal healthy cells (Table 5.4 and Figure 5.11). N-5-Bromoimidazopyridine-noscapine **(9)** showed promising antiproliferative activity using both the cell lines (IC_{50}

value is 5.3 and 7.8 μM against MCF-7 and MDAMB-231) and was selected for the detailed investigation. The close IC_{50} values obtained using MCF-7 and MDA-MB-231 suggesting that these noscapinoids inhibit the proliferation of cancer cells independent of hormone receptor status. Although a significant correlation on the sensitivity of cancer cells to these analogs cannot yet be established at this stage, it is evident that tubulin represents a potential target for these compounds.

Table 5.4. IC_{50} values of N-imidazopyridine derivatives of noscapine using two human breast adenocarcinoma cell lines, MCF-7 and MDA-MB-231 as well as a normal cell line (293T). All the novel derivatives were found to have improved antiproliferative activity compared to noscapine without affecting the normal healthy cell line. The IC_{50} values between treated and untreated cells were found to be statistically significant ($p < 0.05$) using student t-test.

	IC_{50} (μM)					
	Noscapine	**7**	**8**	**9**	**10**	**11**
MCF-7	28.7±2.3*	13.2±1.5*	11.2±1.8*	5.3±0.7*	7.4±0.8*	9.8±0.9*
MDAMB-231	34.0±3.2*	17.3±1.6*	17.2±1.3*	7.8±0.9*	10.3±0.7*	9.9±0.6*
293T	1609±7.2*	1625±5.4*	2199±8.6*	2125±4.9*	1958±5.3*	2041±6.2*

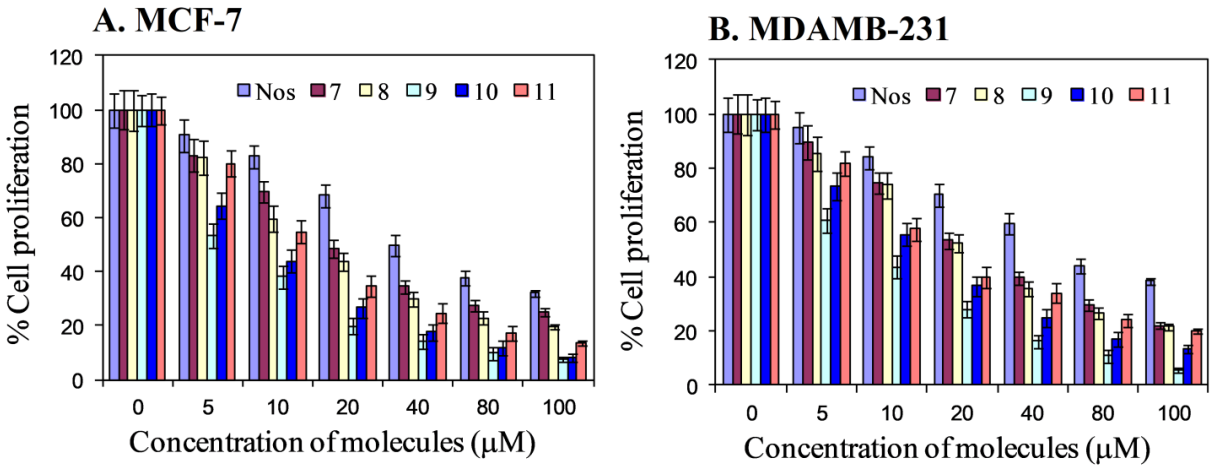

Figure 5.10*. The N-imidazopyridine-noscapinoids* ***7-11*** *have more antiproliferative activity compared to noscapine using human breast cancer cells. Both (A) MCF-7 and (B) MDA-MB-231cells were treated with noscapine and its imidazopyridine-noscapinoids,* ***7-11****, for 72 h. Each value represents the average of 3 independent experiments.*

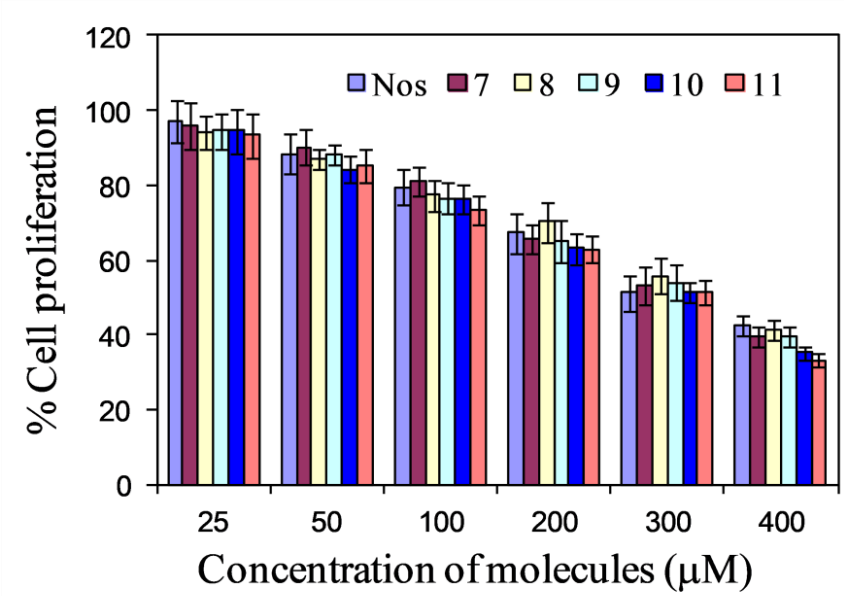

Figure 5.11*. Effect of noscapine and its N-imidazopyridine-noscapinoids* ***7-11*** *(25–400 µM) on the cell viability of normal healthy cell (293T).*

5.3.5. N-Imidazopyridine-noscapinoids, 7-11 inhibits proliferation of primary breast tumor cells

We next want to evaluate whether the N-imidazopyridine-noscapinoids, **7-11** could also inhibit the proliferation of primary tumor cells directly isolated from the patients. We have obtained the surgically removed breast tumor samples from 04 patients with different stages of breast cancer and processed the samples to isolate the primary cancer cells. All these primary breast cancer cells were treated with increasing concentrations of the noscapinoids to determine their IC_{50} value. The IC_{50} values for the test compounds are collated in Table 5.5. The IC_{50} value ranges from 40.7 to 45.1 µM for noscapine, 13.9 to 20.0 µM for **7,** 7.9 to 11.2 µM for **8**, 4.6 to 5.2 µM for **9**, 6.3 to 8.5 µM for **10**, and 5.8 to 9.7 µM for **11** using a panel of primary breast cancer cells (Table 5.5). All the N-imidazopyridine-noscapinoids developed exhibited potent cytotoxic activity in comparison to noscapine using all the primary breast cancer cells at increasing concentration (Figure 5.12).

Table 5.5. IC_{50} values of N-imidazopyridine-noscapinoids, **7-11** using primary breast cancer cells isolated from breast tumor tissue of different patients. All the noscapinoids were found to have improved antiproliferative activity compared to noscapine. The IC_{50} values between treated and untreated cells were found to be statistically significant ($p < 0.05$) using student t-test.

	IC_{50} (μM)					
Patients No.	**Noscapine**	**7**	**8**	**9**	**10**	**11**
1	43.0±3.7*	20.0±2.5*	11.2±1.5*	5.0±0.6*	7.3±0.8*	9.4±1.5*
2	44.5±3.5*	13.9±1.7*	7.9±1.2*	5.1±0.9*	6.8±1.1*	5.8±0.8*
3	45.1±3.8*	16.7±1.8*	10.0±1.5*	5.2±0.7*	8.5±1.4*	9.7±1.3*
4	40.7±3.5*	16.2±1.8*	8.5±1.1*	4.6±0.5*	6.3±0.8*	7.4±0.7*

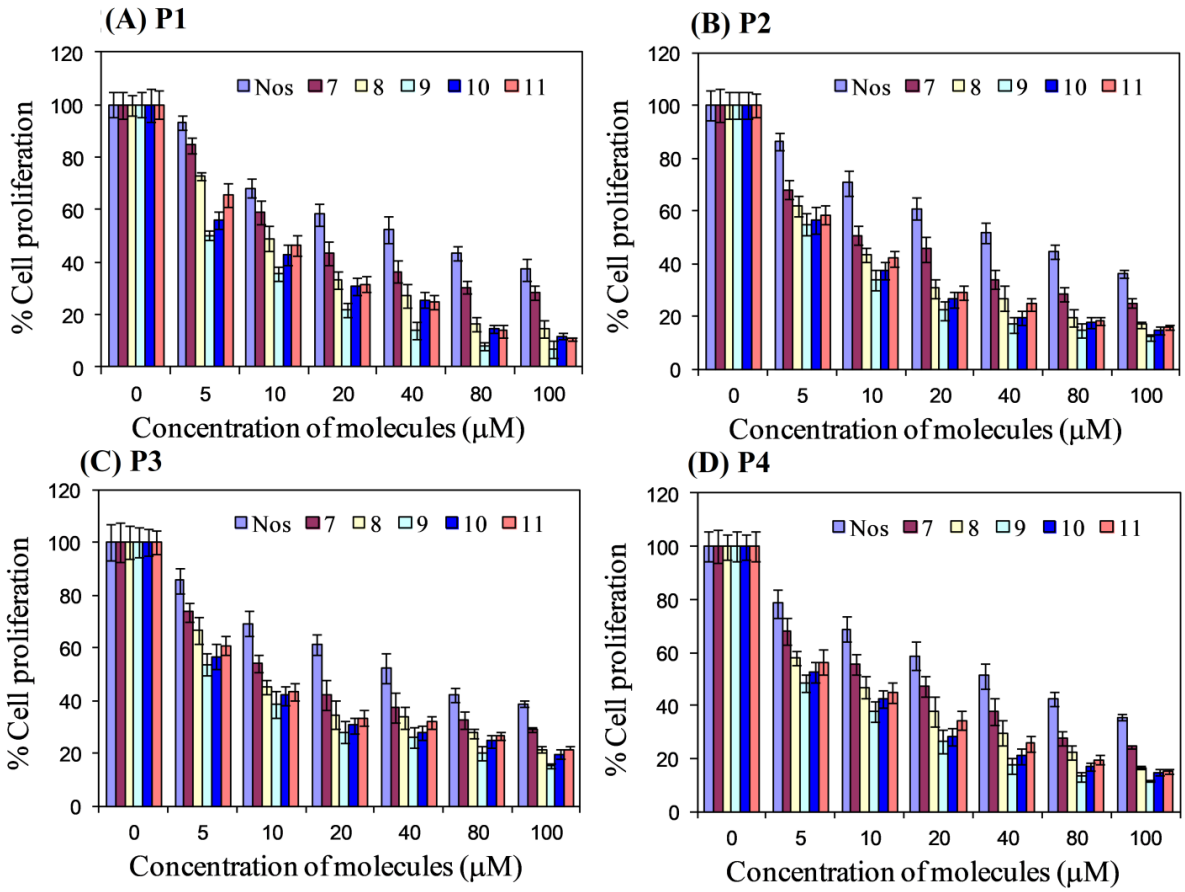

Figure: 5.12: *The N-imidazopyridine-noscapinoids,* ***7-11*** *inhibits proliferation of a panel of human primary breast tumor cells more effectively compared to noscapine. All the cells treated with N-imidazopyridine-noscapinoids,* ***7-11*** *for 72 h. Each value represents the average of 3 independent experiments.*

5.3.6. N-5-Bromoimidazopyridine-noscapine (9) induced apoptosis to cancer cells

We tested the induction of apoptotic cell death to breast cancer cell (MDA-MB-231) by N-5-Bromoimidazopyridine-noscapine **(9)**. During apoptosis, there is alteration

of lipid composition of cell membrane, in which the phosphatidyserine, translocates to the outer leaflet from the inner leaflet. The presence of phosphatidyserine on the outer membrane is detected by annexin V binding. Similarly, the cell-impermeant DNA-binding fluorescent dye, propidium iodide, can only enter the cells when it is at the stage of late apoptosis when membrane permeability is compromised. Both the fluorescent dyes were used to quantitate the population of early and late apoptotic cells by FACS. The percentage of early apoptotic and late apoptotic cells using MDA-MB-231 cell lines for the treatment of N-5-Bromoimidazopyridine-noscapine **(9)** with a IC_{50} concentration (7.8 µM) for 72 h is collated in Figure 5.13. After 72 h of culture, the control untreated cell culture contained only very few early apoptotic (2%) and late apoptotic cells (3%), which were considered as the background cell death due to regular trauma during cell culture (Figure 5.13a). In contrast, the percentage of early apoptotic cells (15%) and late apoptotic cells (20% and 15% necrotic cells) with treatments of N-5-Bromoimidazopyridine-noscapine **(9)** was found to be significantly high compared to controlled untreated cells (Figure 5.13b).

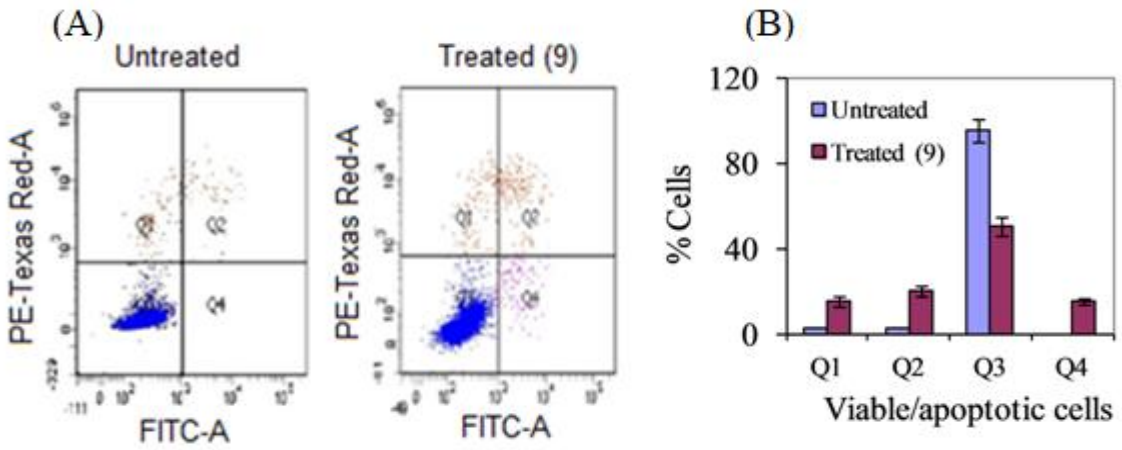

***Figure 5.13**: Flow cytometry analysis of apoptotic cells using MDAMB-231 cells treated with N-5-Bromoimidazopyridine-noscapine **(9)** with IC_{50} concentration (7.8 µM) for 72 hours and compared with non treated control cells. Alexa Fluor 488 conjugate of Annexin-V was used, in combination with the non-vital dye propidium iodide (PI), to distinguish among three sub-populations: PI-negative and Alexa Fluor 488-negative viable cells with intact membrane and preserved amino-phospholipid asymmetry (PI-, Alexa Fluor 488-), PI-negative and Alexa Fluor 488-positive early apoptotic cells with intact cellular membrane exposing phosphatidylserine (PI-, Alexa Fluor 488+), and PI-positive and Alexa Fluor 488-positive late apoptotic cells with compromised asymmetry and membrane permeability (PI+, Alexa Fluor 488+). Representative results of three*

independent experiments. (B) Percentage of viable (Q3), early apoptotic (Q1), late apoptotic (Q2) and necrotic (Q4) cell measured by flow cytometry.

5.3.7. Detection of apoptosis with treatment of 5-Bromoimidazopyridine-noscapine (9)

Membrane blebbing, cellular shrinkage, chromatin condensation and formation of apoptotic bodies are always the main morphological changes during apoptosis. Therefore, we performed cellular studies using AO, EtBr and HO (Hoechst 33342) to further confirm the induction of apoptosis by N-5-Bromoimidazopyridine-noscapine (**9**). MDA-MB-231 treated cells underwent apoptosis as demonstrated by the staining of the treated cells with these dyes (Figure 5.14). Specifically, the untreated cells were observed to have normal cell morphology. In contrast, the treated cells underwent several features of apoptosis such as membrane blebbing, numerous fragmented nuclei, and appearance of apoptotic bodies.

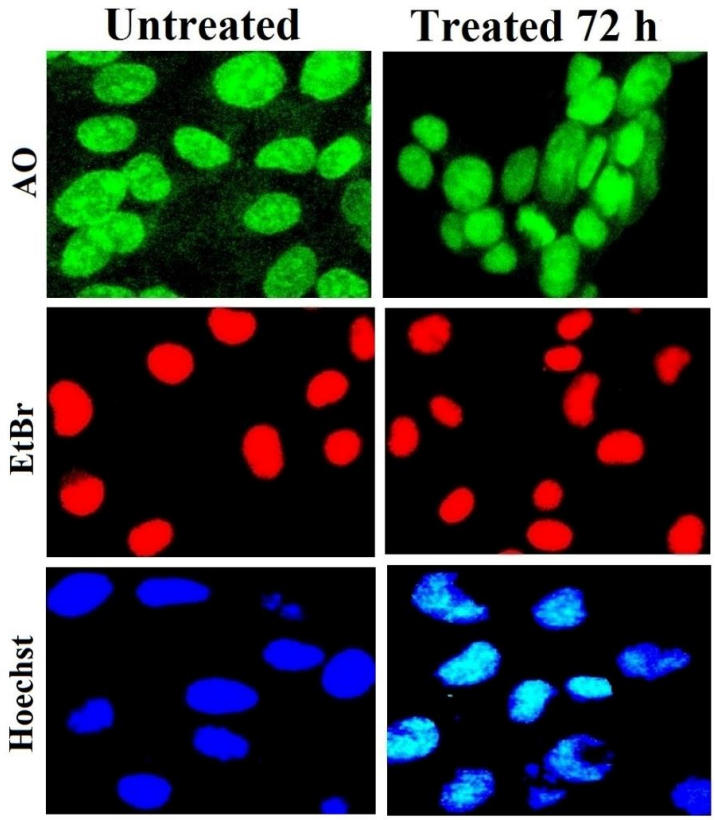

***Figure 5.14**: The changes in morphological characters such as chromatin condensation, plasma membrane blebbing and appearance of small, apoptotic bodies indicated the apoptotic cells. Panels show morphological features of cells stained with AO, EtBr and Hoechst from untreated cells and cells treated with IC_{50} concentration (5.3 μM) of N-5-Bromoimidazopyridine-noscapine **(9)** for 72 hours using fluorescence microscopy. The apoptotic cancer cells were evident after 72 hours of drug treatment.*

5.3.8. Effects of N-5-Bromoimidazopyridine-noscapine (9) on ROS accumulation in MDA-MB-231 cells

To further investigate the mechanism of induction of apoptosis in cancer cells, we found that N-5-Bromoimidazopyridine-noscapine **(9)** elevated ROS levels. Using DCFDA as the molecular probe, the ROS level was analyzed. When MDA-MB-231 cells were treated with **9**, the green fluorescence was more intense compared to untreated cells (Figure 5.15a). We found that **9** significantly elevated ROS levels in MDA-MB-231 cells as measured by fluorescent intensity, indicating that ROS might have a function in inducing apoptosis (Figure 5.15b).

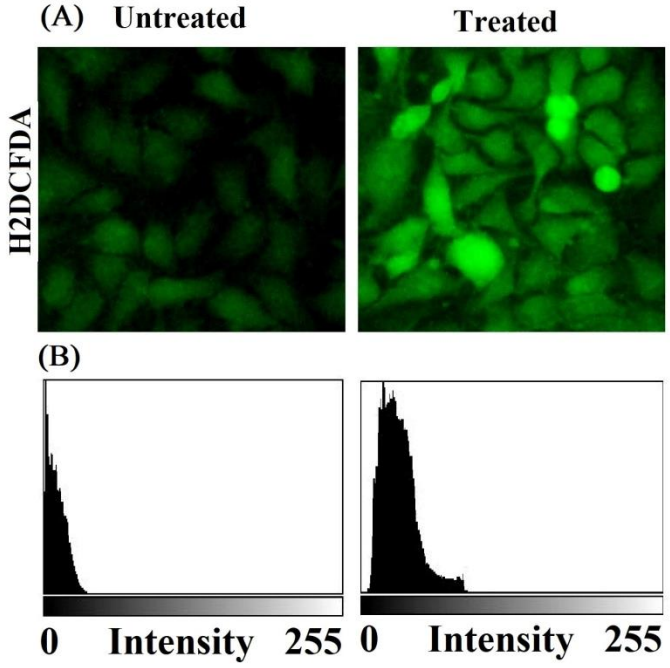

Figure 5.15: *(A) Treatment with N-5-Bromoimidazopyridine-noscapine* ***(9)*** *at its IC_{50} concentration (7.8 µM) increases the ROS level in MDAMB-231 cells compared to untreated cells as measured by the fluorescent dye DCFDA. (B) The fluorescent intensity was measured using Image J.*

5.3.9. N-5-Bromoimidazopyridine-noscapine (9) alter the cell cycle profile and cause mitotic arrest at G2/M phase

To elucidate the process of induction of cell death, we examined the effect of N-5-Bromoimidazopyridine-noscapine **(9)** with its IC_{50} concentration (7.8 µM) on the interference of cell cycle progression of MDA-MB-231 by FACS analysis and represented in Figure 5.16. Accumulation of fluorescently labelled DNA in a cell is a good indicator to access the interference of cell cycle progression and cell death. A cell with 2N DNA content represents the G1 phase while 4N DNA content represents G2 and

M phases. Cells in the process of DNA duplication between 2N and 4N peaks represent S phase. Cells with less than 2N DNA represent apoptosis cells in which the DNA are degraded to different extents. It was found that treatment of MDA-MB-231 cells for 72 h with the test compounds led to significant perturbations of the cell cycle profile at 7.8 µM. FACS analysis revealed high accumulation of cells in the G2/M phase at 72 h of treatment of N-5-Bromoimidazopyridine-noscapine **(9)** compared to untreated cells. In contrast to G2/M block, a characteristic hypodiploid DNA content peak (sub-G1) was seen to rise at 72 hours of drug treatment. The increased number of cells with hypodiploid DNA content reflects more dying cells.

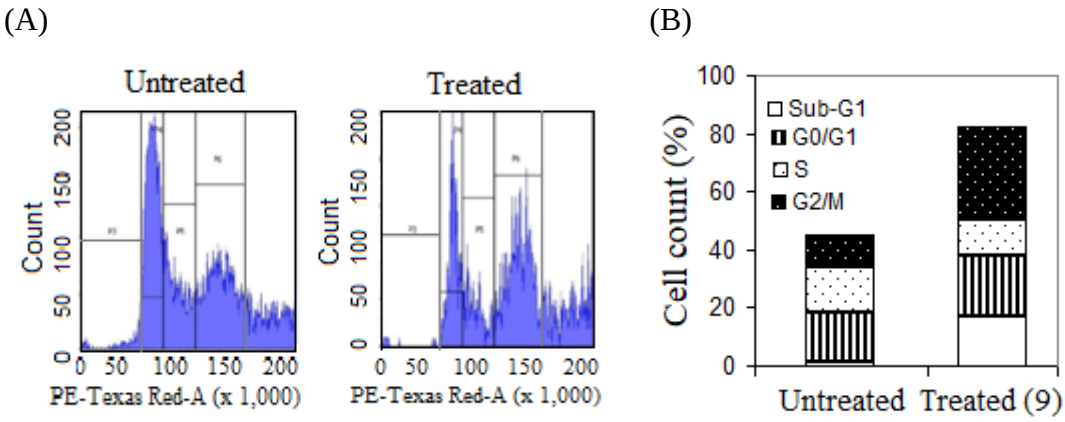

Figure 5.16: *Treatment with N-5-Bromoimidazopyridine-noscapine* ***(9)*** *at its* IC_{50} *concentration (7.8 µM) perturb cell cycle progression at G2/M phase followed by the appearance of a hypodiploid (sub-G1) DNA peak that indicate apoptotic cells. Panels A demonstrated the analyses of cell cycle progression, determined by flow cytometry in MDAMB-231 cells treated with 25 µM concentration of noscapine and its N-imidazopyridine-noscapinoids for 72 hours. Panel B represent the percentage of cells at different phases of cell cycle.*

5.3.10. Effects of N-5-Bromoimidazopyridine-noscapine (9) on mitochondrial membrane potential (ΔΨm)

Mitochondria are thought to be the major pathway for apoptosis. The induction of apoptosis is closely related to the collapse of mitochondrial membrane potential (ΔΨm). Thus we have measured the loss of mitochondrial membrane potential (ΔΨm) in MDA-MB-231 cells treated with N-5-Bromoimidazopyridine-noscapine **(9)** using DAPI, JC-1, and Rhodamine 123 dyes. When MDA-MB-231 cells were treated with **9**, JC-1 red fluorescence, Rhodamine-123 green fluorescence, and DAPI blue fluorescence in treated cells were more intense compared to untreated cells (Figure 5.17A). The compound, **9**

significantly increased the loss of mitochondrial membrane potential ($\Delta\Psi m$) in MDA-MB-231 cells (Figure 5.17B) compared to untreated cells.

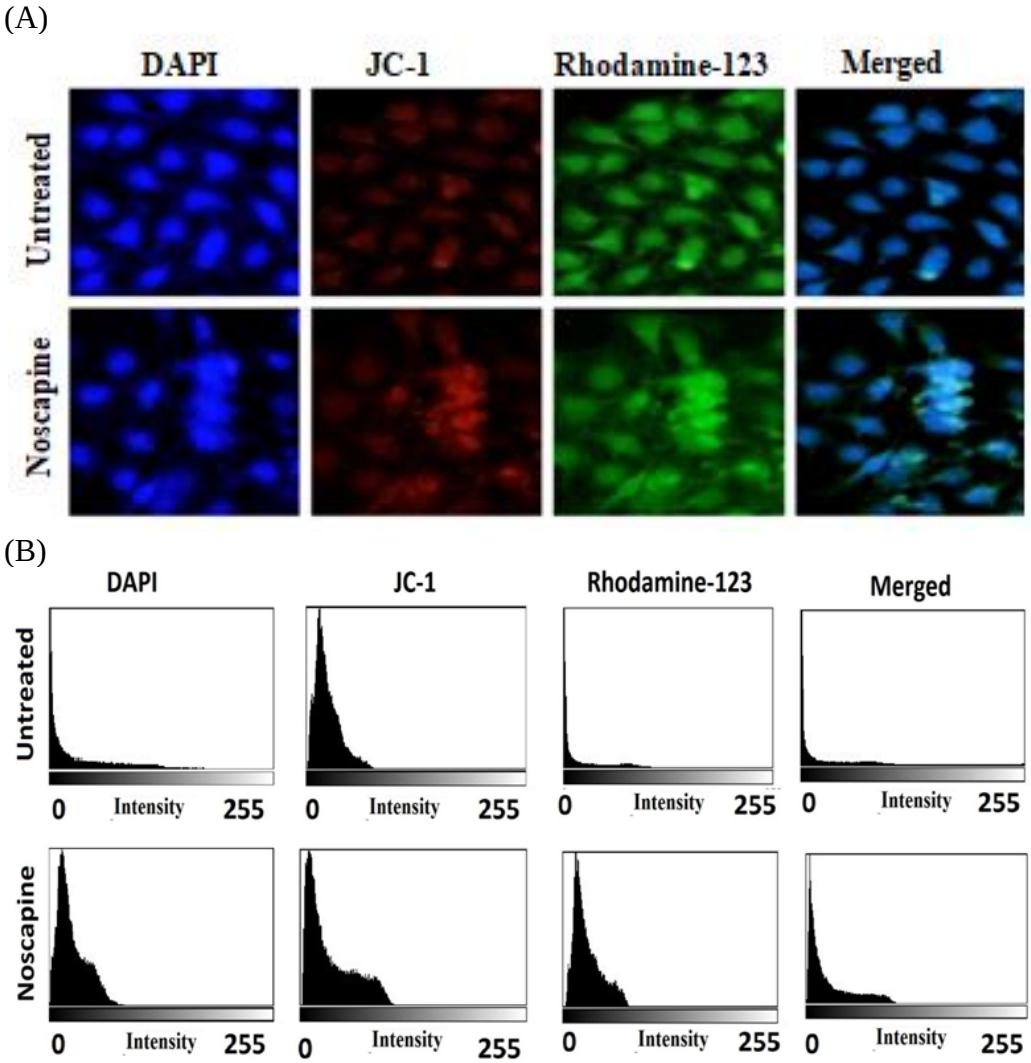

Figure 5.17. *(A) Effect of N-5-Bromoimidazopyridine-noscapine* ***(9)*** *on mitochondrial membrane potential as visualized using different fluorescent dyes, DAPI, JC-I and Rhodamine 123. (B) The fluorescent intensity was measured using Image J.*

5.3.11. Reduction in tumor volume with the treatment of N-5-Bromoimidazopyridine-noscapine (9) against MCF-7 xenograft model

Treatment with N-5-Bromoimidazopyridine-noscapine **(9)** at a concentration of 50 µM/day considerably decreased tumor volume in comparison to control ($P < 0.001$) (Figure 5.18A). Tumor volume was reduced to 809 mm^3 from the tumour size of the untreated control group with tumor volume 1479 mm^3 on day 40 post tumour implantation. On 40^{th} day mice were sacrificed and tumours were removed and weighted. All untreated mice developed solid tumours in sizes ranging from 4.8 to 11.2 g (mean 7.9 ± 2.0 g). Whereas, among the treated groups the tumor size was significantly regressed

and showed only small palpable tumors. Compared to untreated control mice, inhibition of tumor growth by **9** was statistically significant ($p < 0.001$). In addition, we did not observe any apparent weight loss after drug treatment compared to the control group of mice (Figure 5.18B).

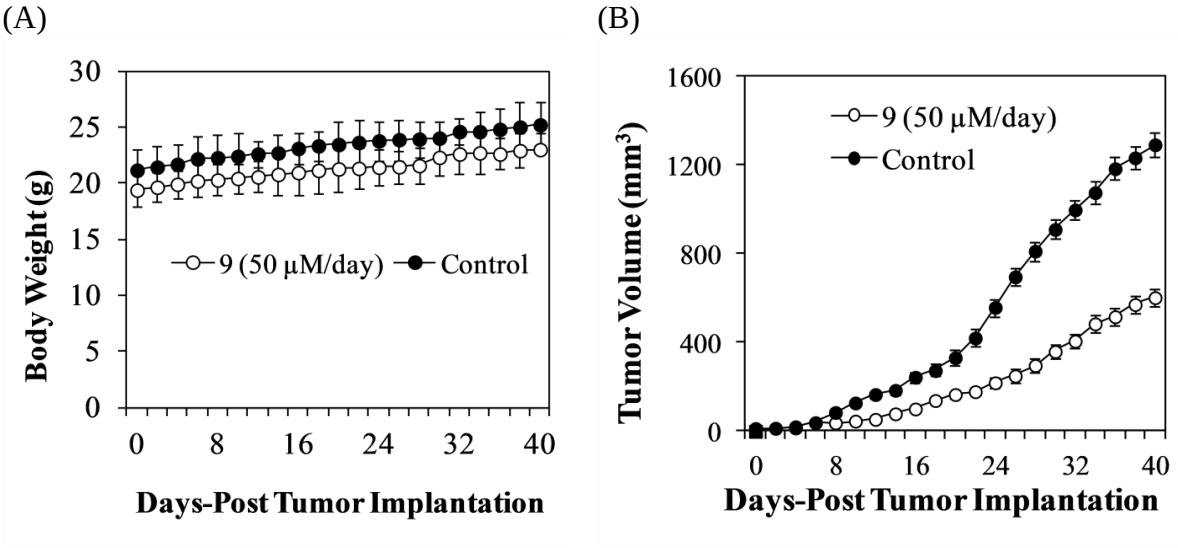

Figure 5.18: *(A) Effect of N-5-Bromoimidazopyridine-noscapine* ***(9)*** *on the body weight of mice. No difference in body weight was noticed between the treated and untreated mice. (B) Progression in tumor growth on human MCF-7 xenograft mice with the treatment of* ***9****. The tumor growth was significantly inhibited by* ***9*** *compared to untreated group.*

5.3.12. Treatment of N-5-Bromoimidazopyridine-noscapine (9) does not cause any detectable toxicity

The severe side effects during chemotherapeutics are a major concern in the treatment of cancer patients. Tubulin binding agents, for example, vinca alkaloids and taxanes, while clinically approved, are known to cause adverse side effects (Rowinsky *et al.,* 1997). As a result, there is a need to identify a drug regimen that is both safe and well-tolerated. We examined the liver, kidney, heart, and lungs of tumor-bearing mice to see if N-5-Bromoimidazopyridine-noscapine **(9)** causes toxicity to normal tissues. Treatment with **9** fails to reveal any detectable pathological abnormalities in normal tissues involved in normal cell proliferation. H&E staining of paraffin-embedded 5.0 micron-thick sections of the liver, kidney, lung, and heart is shown at 200x magnification in Figure 5.19. The hepatic lobular architecture was normal. Normal glomeruli, proximal and distal tubules, interstitium, and blood vessels were found in the kidneys. Among the groups, the heart muscle exhibited normal morphology. Normal alveoli and bronchial

airways have been seen in the lung tissue. Furthermore, we observed no differences in hematological parameters between treated and control animals (Table 5.6 and 5.7).

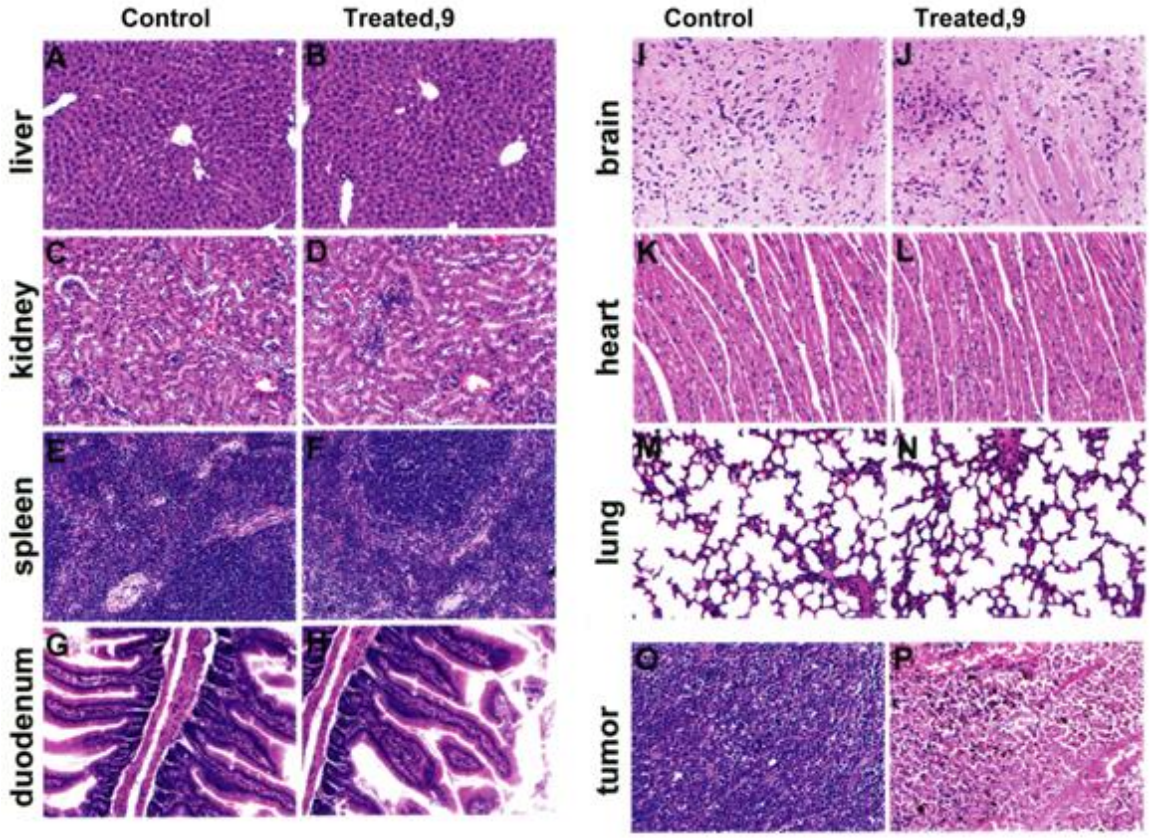

Figure 5.19: *Panels represent H&E staining of paraffin-embedded 5 micron-thick sections of the liver, kidney, spleen, lung, heart, duodenum and brain at magnifications 200x and 400x. The liver showed normal hepatic lobular architecture. The kidneys revealed normal glomeruli, proximal and distal tubules, interstitium, and blood vessels. The splenic follicles and vascular sinusoids were indistinguishable between the 9-treated and vehicle-treated control groups. The lung tissue showed normal alveoli and the heart muscle showed normal morphology among the two groups. Microsections of brain did not reveal any infracted areas. The cerebral cortex, gray and white matters appeared normal. The gut showed normal mucosa, submucosa and muscularis mucosa.*

Table 5.6. Hematological parameters, WBC count (WBC), monocytes (MON), eosinophils (EOS), RBC count (RBC), haemoglobin concentration (HB),Hematocrit(HCT), mean corpuscular volume (MCV), mean corpuscular hemoglobin (MCH), mean corpuscular hemoglobin concentration (MCHC) and platelet count between the treated (50 µM/day) and control groups.

Parameter	Treated (50 µM/day)	Control
WBC (10^3/µl)	3.6 ± 2.8	3.2 ± 2.1
MON(%)	0.6 ± 0.01	0.5 ± 0.08
EOS(%)	0.8 ± 0.09	0.7 ± 0.08
RBC(10^6/µl)	4.49 ± 0.5	4.6 ± 0.7
HB(g/dl)	15.5 ± 0.4	15.6 ± 0.5
HCT(%)	42.5 ± 1.2	43.1 ± 0.8
MCV(fL)	64.7 ± 0.7	61.8 ± 0.5
MCH(pg/cell)	28.2 ± 0.5	27.9 ± 0.7
MCHC(g/dl)	32.9 ± 0.4	33.5 ± 0.8
Platelet(10^3/µl)	91.2 ± 5.1	97.5 ± 3.5

Table 5.7. Organ functions and Serun Glucose, Serum Ca,NA,K, and Cl levels between the treated (50 µM/day) and control groups.

Parameter	Acute (50 µM/day)	Control(0)
AST(U/L)	102.3 ± 6.8	101.6 ± 8.5
ALT(U/L)	30.5 ± 6.5	31.6 ± 6.7
ALK PHOS(U/L)	80.4 ± 5.4	80.6 ± 4.4
BUN(mg/dl)	11.4 ± 1.6	10.5 ± 1.8
Creatinine(mg/dl)	0.62 ± 0.06	0.52 ± 0.04
Bilirubin Total(mg/dl)	0.53 ± 0.06	0.71 ± 0.05
Bilirubin Direct(mg/dl)	0.29 ± 0.03	0.25 ± 0.08
Bilirubin Indirect(mg/dl)	3.4 ± 0.24	3.1 ± 0.3
Albumin(g/dl)	4.25 ± 0.28	4.37 ± 0.45
Total protein(g/dl)	6.62 ± 0.32	6.94 ± 0.17
Glucose(mg/dl)	97.2 ± 6.5	97.6 ± 3.5
Ca(mg/dl)	10.2 ± 0.6	10.1 ± 0.6
Na(mEq/L)	142.6 ± 0.6	142.9 ± 0.7
K(mEq/L)	3.9 ± 0.6	3.9 ± 0.1
Cl(mEq/L)	102.5 ± 5.6	101.1 ± 5.9

5.4. Conclusion

In conclusion, we have strategically designed a panel of N-imidazopyridine-noscapinoids of natural lead molecule, noscapine, to accelerate its anticancer activity. We have also provided the simplest methods for the direct and regioselective modification of noscapine scaffold to produce the N-imidazopyridine-noscapinoids in high yields. All the five derivatives developed have shown increased antiproliferative activity to cancer cells based on our extensive molecular modeling and cellular study using two human breast cancer cell lines, MCF-7 and MDA-MB-231, and a panel of primary breast cancer cells without affecting normal healthy cells. The most promising compound, N-5-Bromoimidazopyridine-noscapine **(9)** also revealed significant reduction in the volume of implanted tumor based on *in vivo* xenograft mice model without any toxic effects to vital organs. Therefore, these novel compounds may prove efficacious in the treatment of breast carcinoma and other types of cancers.

Appendix

A5.1: ^{1}H NMR of N-imidazopyridine noscapinoid, 7

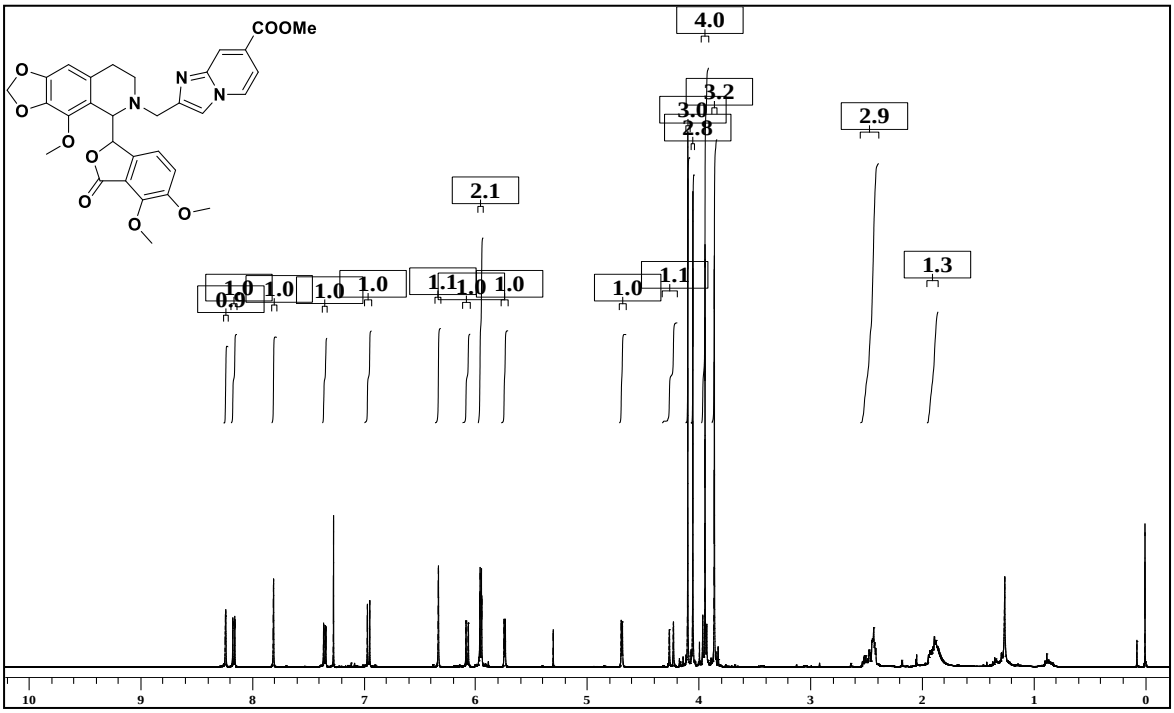

A5.2: ^{13}C NMR of N-imidazopyridine noscapinoid, 7

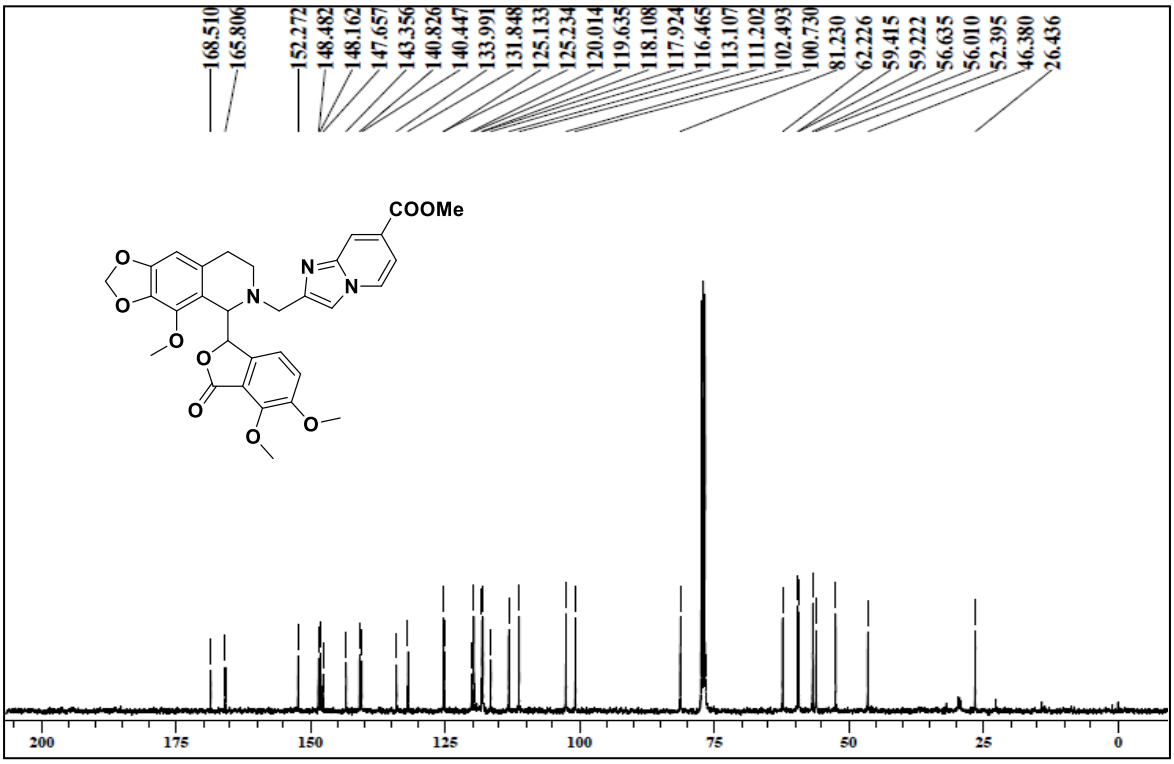

A5.3: HRMS of N-imidazopyridine noscapinoid, 7

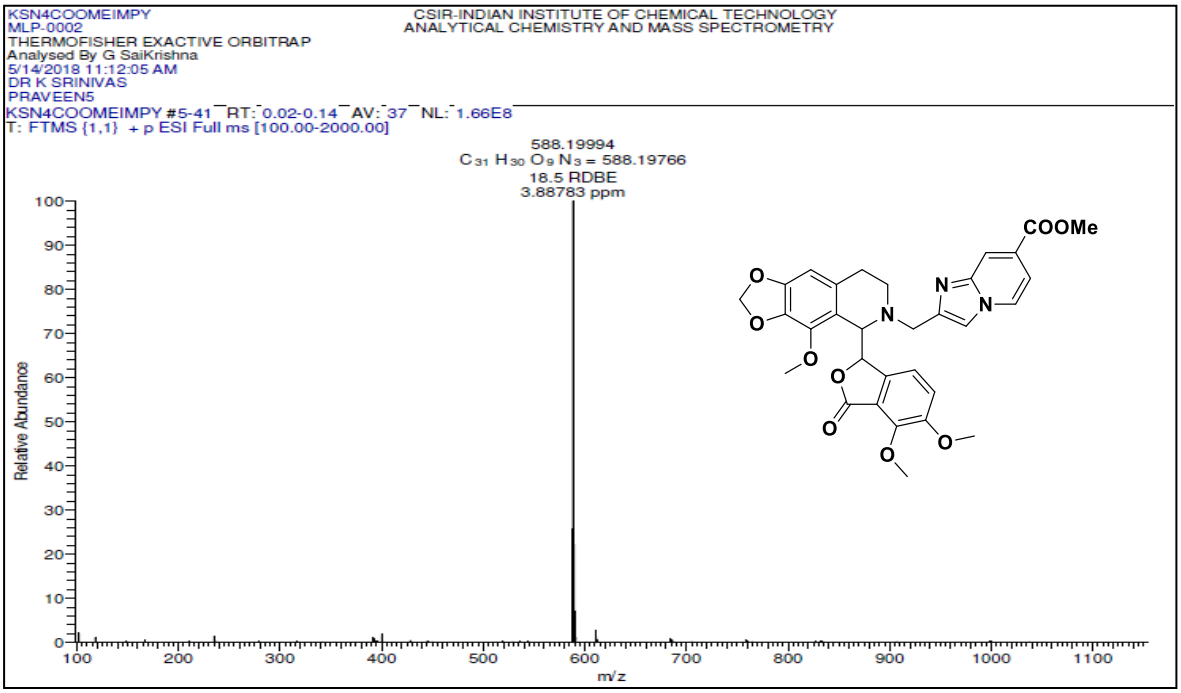

A5.4: ^{1}H NMR of N-imidazopyridine noscapinoid, 8

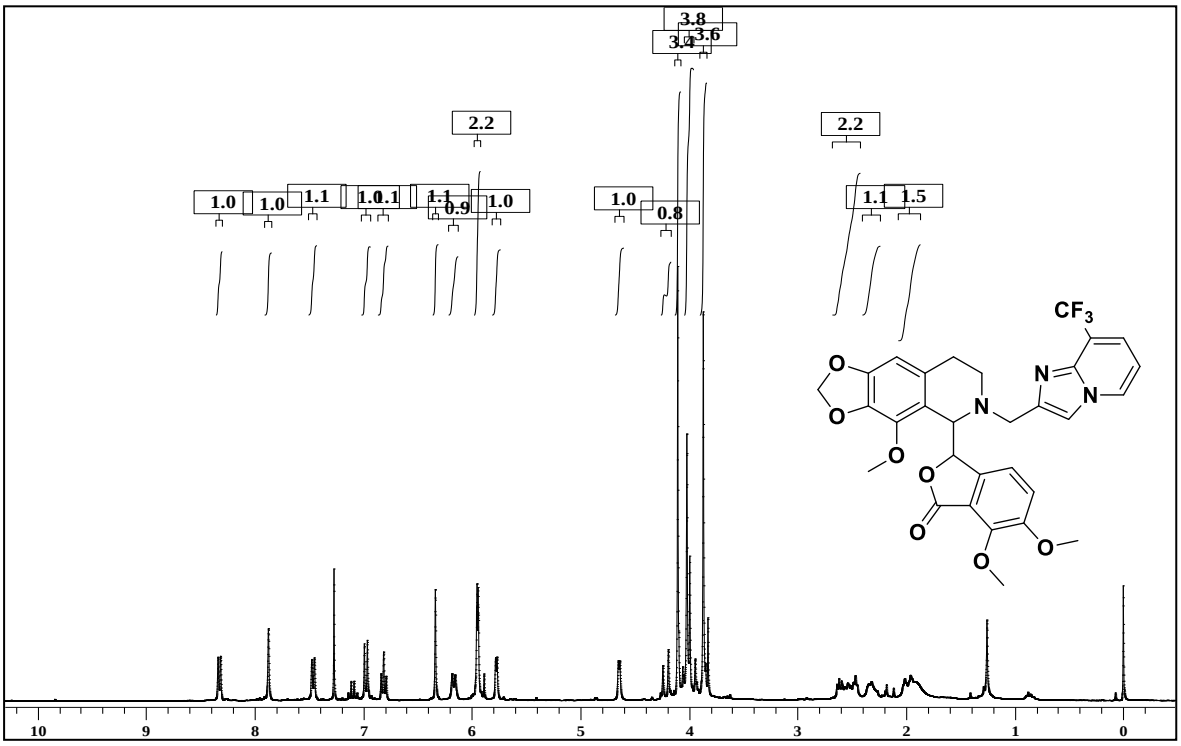

A5.5: ^{13}C NMR of N-imidazopyridine noscapinoid, 8

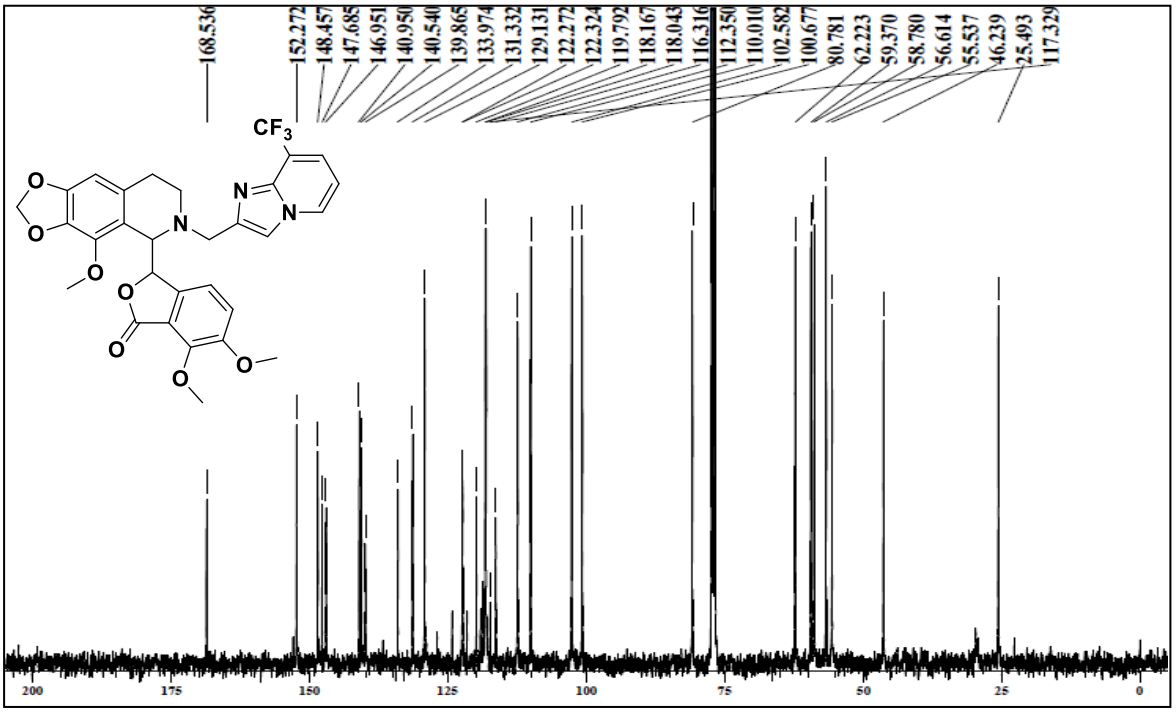

A5.6: HRMS of N-imidazopyridine noscapinoid, 8

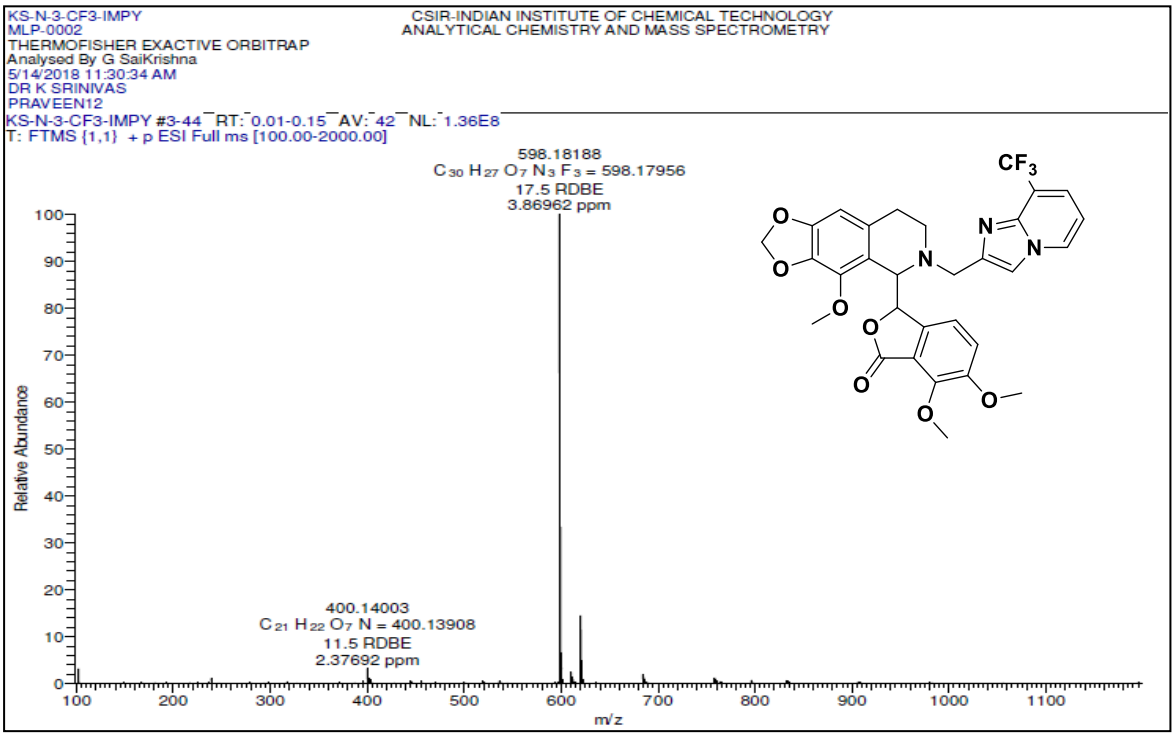

A5.7: ^{1}H NMR of N-imidazopyridine noscapinoid, 9

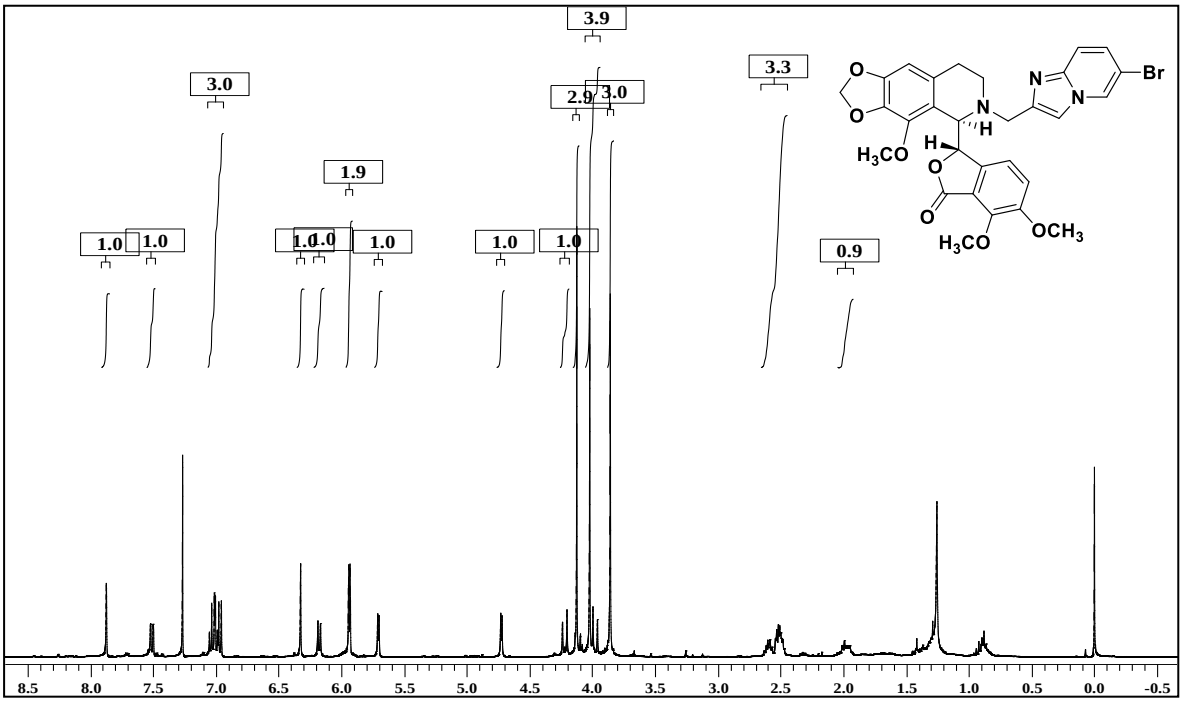

A5.8: ^{13}C NMR of N-imidazopyridine noscapinoid, 9

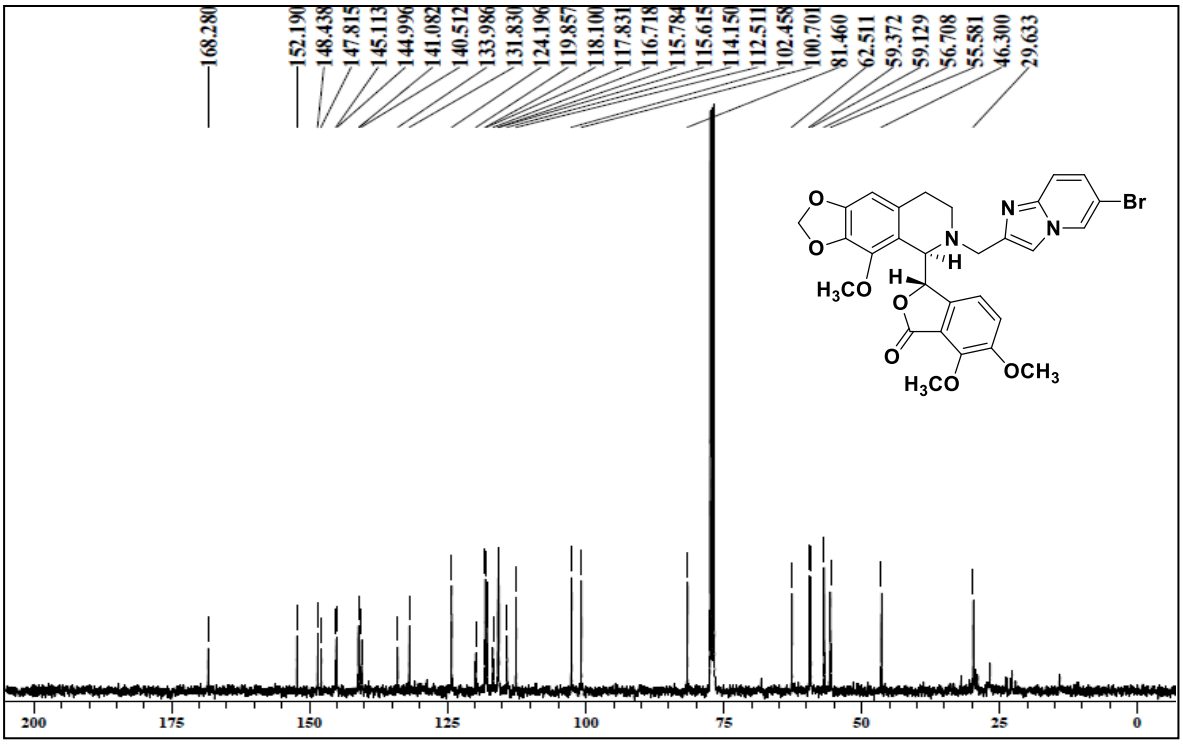

A5.9: HRMS of N-imidazopyridine noscapinoid, 9

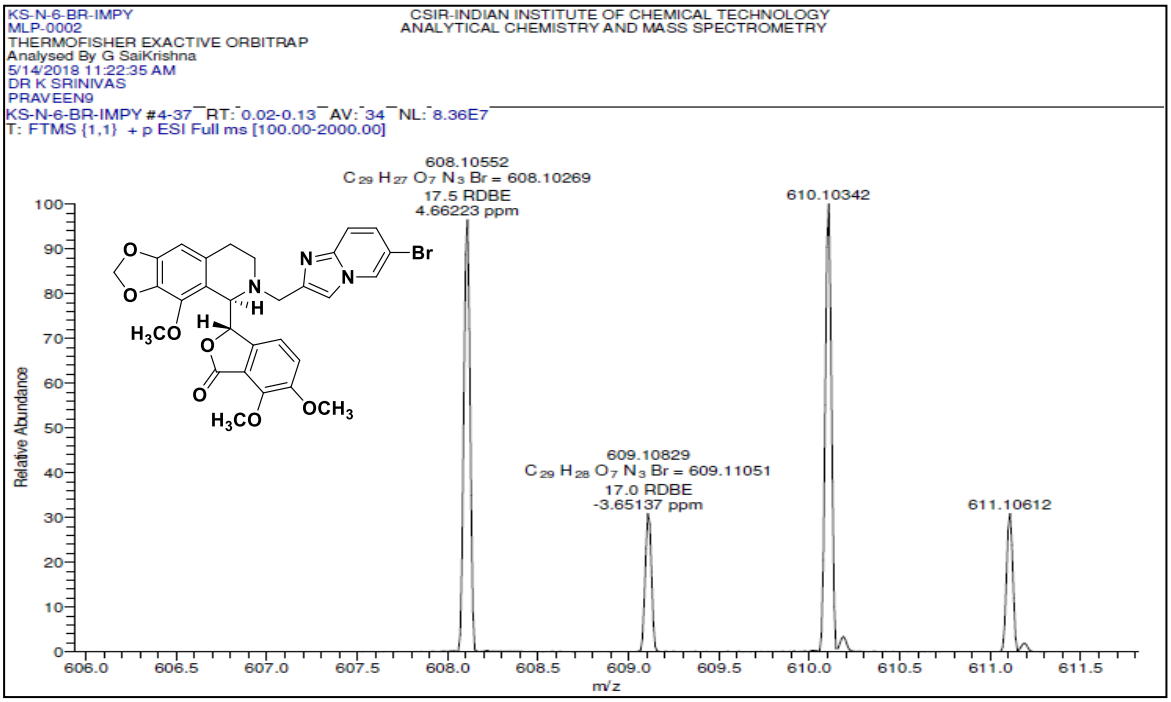

A5.10: ^{1}H NMR of N-imidazopyridine noscapinoid, 10

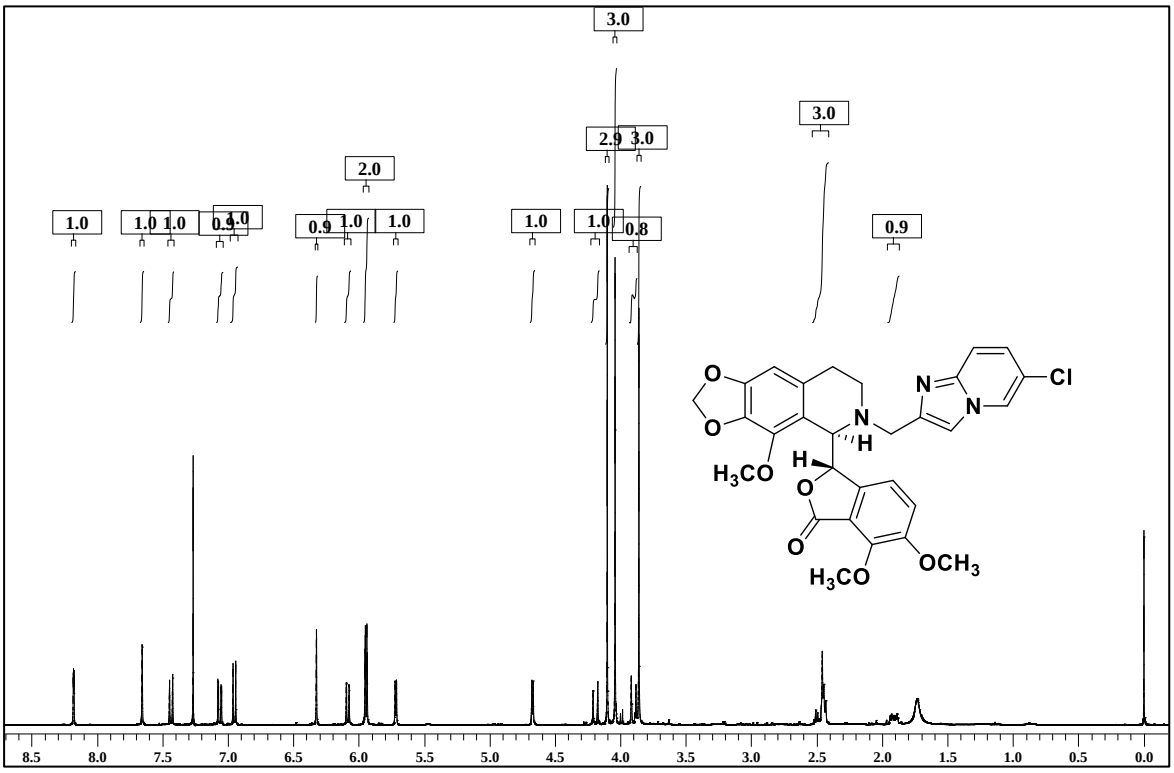

A5.11: ^{13}C NMR of N-imidazopyridine noscapinoid, 10

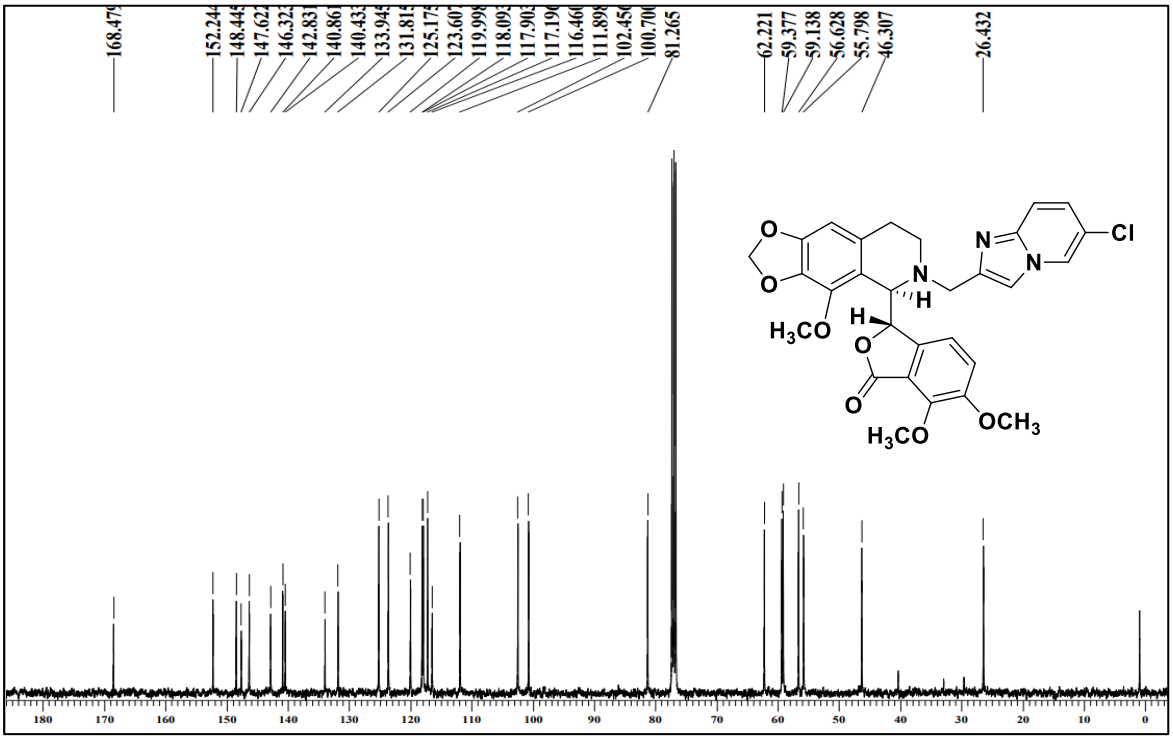

A5.12: HRMS of N-imidazopyridine noscapinoid, 10

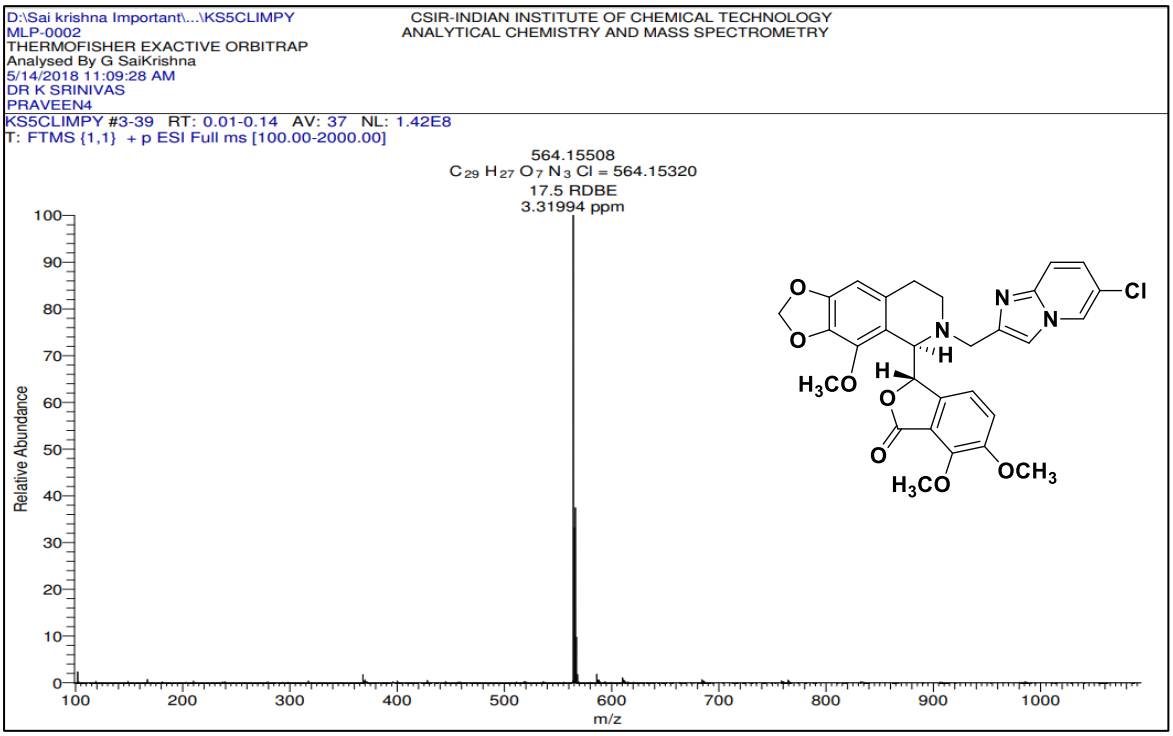

A5.13: ^{1}H NMR of N-imidazopyridine noscapinoid, 11

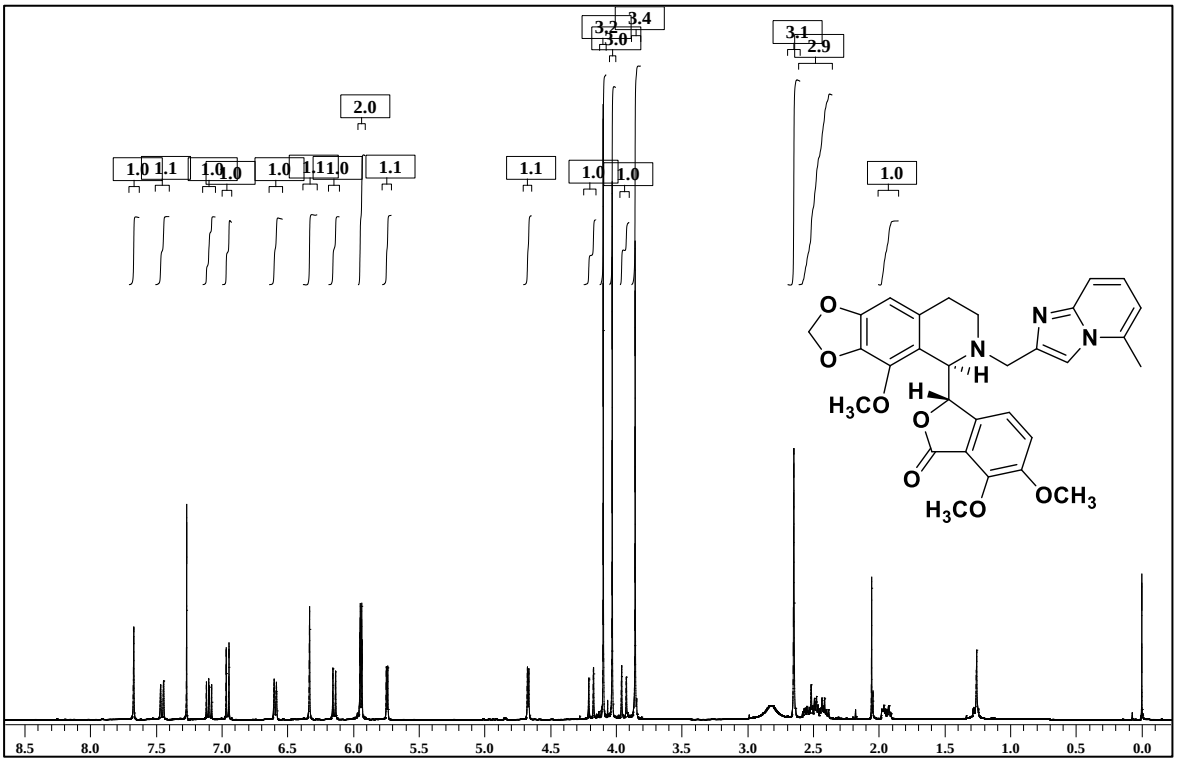

A5.14: ^{13}C NMR of N-imidazopyridine noscapinoid, 11

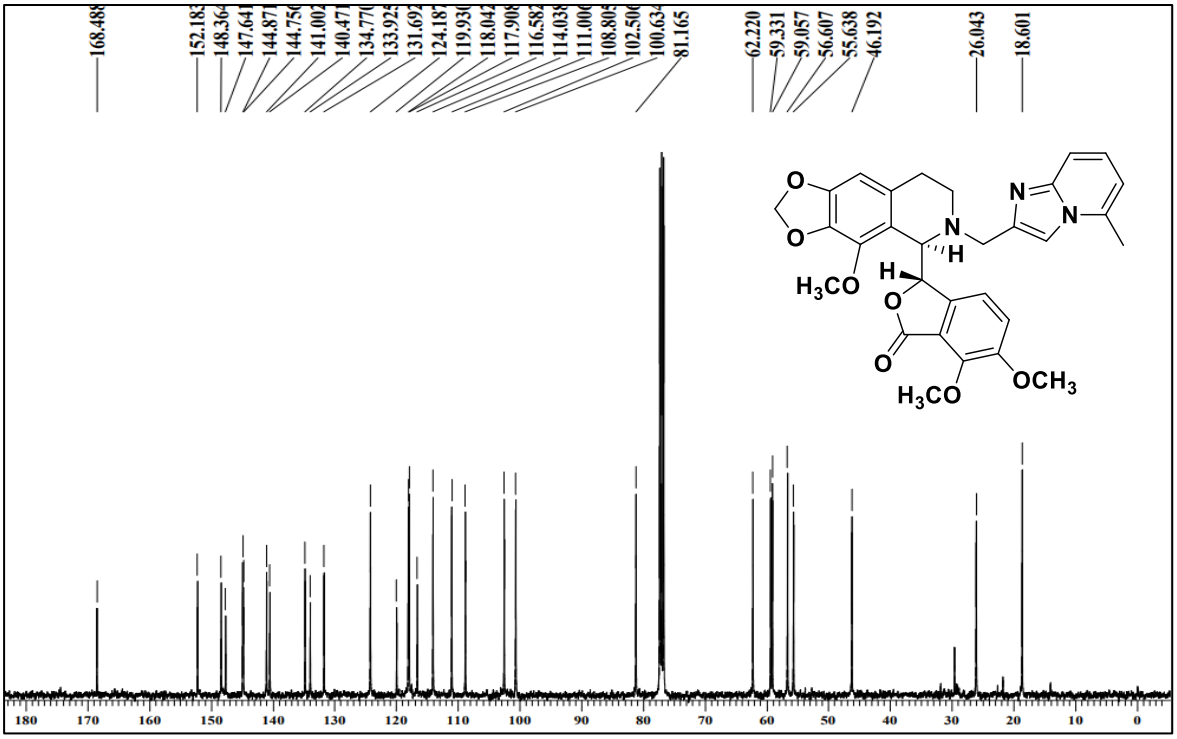

A5.15: HRMS of N-imidazopyridine noscapinoid, 11

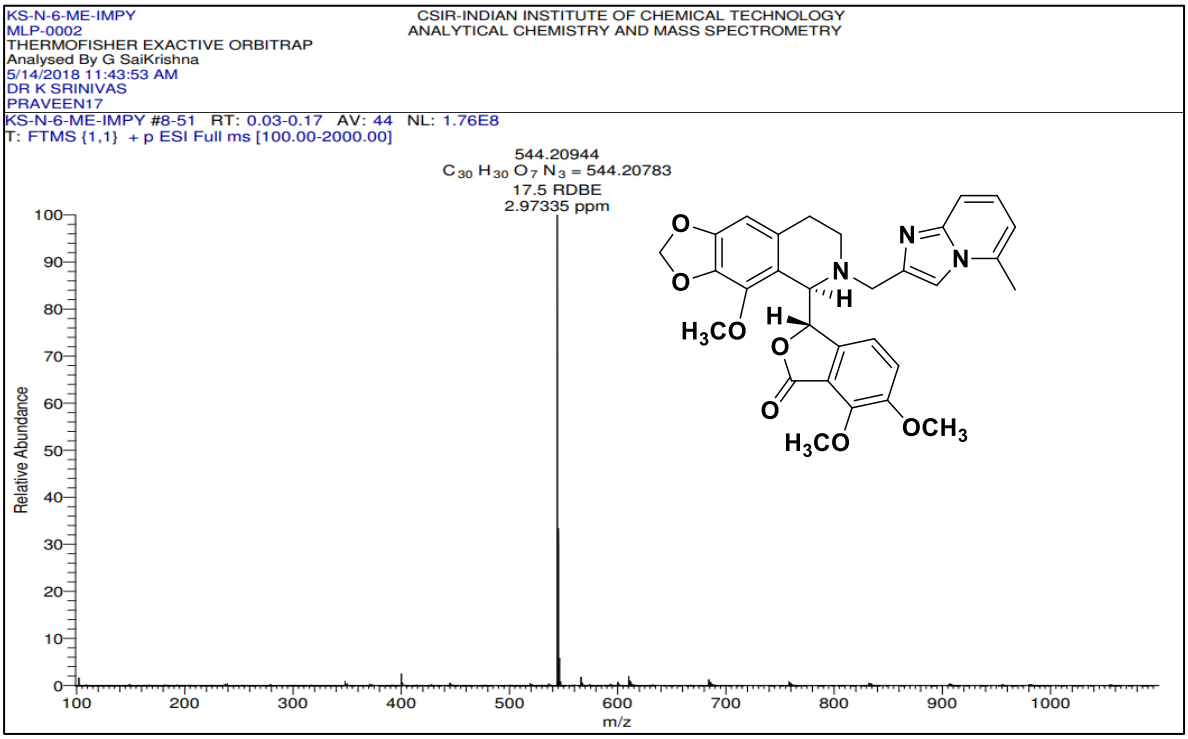

Table A5.16-A5.19: Geometry of hydrogen bonds and hydrophobic interaction of N-imidazopyridine noscapinoid, **7-9** and the lead molecule, noscapine with the binding site residues of tubulin.

Table A5.16			**Table A5.17**		
(a) 7_Tubulin			**(b) 8_Tubulin**		
Hydrogen bonding			**Hydrogen bonding**		
Hydrogen Donor (D)	**Hydrogen Acceptor (A)**	**Distance (D-A) in Å**	**Hydrogen Donor (D)**	**Hydrogen Acceptor (A)**	**Distance (D-A) in Å**
LYS B 352 NZ	900 O5	3.73	LYS B 35 NZ	900 O5	2.91
GLN B 247 N	990 O8	3.29			
Hydrophobic interaction			**Hydrophobic interaction**		
7	**Tubulin**	**Distance**	**8**	**Tubulin**	**Distance**
C10	ILE B 378 CD1	4.76	O2	ILE B 378 CD1	4.97
O1	ILE B 378 CD1	3.58	C10	ILE B 378 CD1	3.66
C9	ILE B 378 CD1	4.19	O1	ILE B 378 CD1	3.12
C1	ILE B 378 CD1	4.23	C9	ILE B 378 CD1	4.13
C31	ASP B 357 OD2	4.54	C1	ILE B 378 CD1	4.72
O9	VAL B 355 CG2	4.85	O1	ILE B 378 CG1	4.56
O9	VAL B 355 CG1	4.91	C28	VAL B 355 CB	4.89
O9	VAL B 355 CB	4.05	C29	VAL B 355 O	3.61
C30	VAL B 355 CB	4.4	C28	VAL B 355 O	4.05
C28	VAL B 355 CB	4.84	C25	VAL B 355 O	4.73
C31	VAL B 355 O	3.27	C29	VAL B 355 C	4.49
C30	VAL B 355 O	3.08	C28	VAL B 355 C	4.82
C29	VAL B 355 O	3.73	C29	VAL B 355 CA	4.71
C28	VAL B 355 O	3.53	C28	VAL B 355 CA	4.71
C27	VAL B 355 O	4.53	C29	VAL B 355 N	3.8
C25	VAL B 355 O	4.84	C28	VAL B 355 N	3.81
O9	VAL B 355 C	4.43	C27	VAL B 355 N	4.52
C31	VAL B 355 C	4.35	C25	VAL B 355 N	4.48
O8	VAL B 355 C	4.09	N3	ALA B 354 CB	3.53
C30	VAL B 355 C	4.09	N2	ALA B 354 CB	4.76

C29	VAL B 355 C	4.66	C29	ALA B 354 CB	3.96
C28	VAL B 355 C	4.42	C28	ALA B 354 CB	4.5
O9	VAL B 355 CA	4.5	C27	ALA B 354 CB	4.66
O8	VAL B 355 CA	4.86	C26	ALA B 354 CB	4.23
C30	VAL B 355 CA	4.43	N1	ALA B 354 CB	3.67
C28	VAL B 355 CA	4.55	C25	ALA B 354 CB	3.52
C27	VAL B 355 CA	4.89	C24	ALA B 354 CB	3.76
C30	VAL B 355 N	4.12	C23	ALA B 354 CB	3.66
C29	VAL B 355 N	4.15	C22	ALA B 354 CB	4.3
C28	VAL B 355 N	3.77	C7	ALA B 354 CB	3.68
C27	VAL B 355 N	3.9	C6	ALA B 354 CB	4.06
C26	VAL B 355 N	4.4	C3	ALA B 354 CB	4.89
C25	VAL B 355 N	4.57	C29	ALA B 354 C	4.5
N3	ALA B 354 CB	3.66	C28	ALA B 354 C	4.52
N2	ALA B 354 CB	4.32	C27	ALA B 354 C	4.89
C29	ALA B 354 CB	4.09	C25	ALA B 354 C	4.81
C28	ALA B 354 CB	4.54	N3	ALA B 354 CA	4.49
C27	ALA B 354 CB	4.48	C29	ALA B 354 CA	4.11
C26	ALA B 354 CB	3.97	C28	ALA B 354 CA	4.17
N1	ALA B 354 CB	3.47	C27	ALA B 354 CA	4.18
C25	ALA B 354 CB	3.51	C26	ALA B 354 CA	4.08
C24	ALA B 354 CB	3.53	N1	ALA B 354 CA	4.01
C23	ALA B 354 CB	3.68	C25	ALA B 354 CA	4.02
C22	ALA B 354 CB	4.56	C24	ALA B 354 CA	4.46
C7	ALA B 354 CB	4.03	C23	ALA B 354 CA	4.74
C6	ALA B 354 CB	3.91	C7	ALA B 354 CA	4.92
C29	ALA B 354 C	4.83	C26	ALA B 354 N	4.76
C28	ALA B 354 C	4.61	C7	ALA B 354 N	4.93
C27	ALA B 354 C	4.47	C28	THR B 353 O	4.96
C26	ALA B 354 C	4.57	C27	THR B 353 O	4.08
N1	ALA B 354 C	4.76	C26	THR B 353 O	3.56
C25	ALA B 354 C	4.87	C25	THR B 353 O	4.91
N3	ALA B 354 CA	4.63	C24	THR B 353 O	4.35
C29	ALA B 354 CA	4.43	C6	THR B 353 O	4.98
C28	ALA B 354 CA	4.39	C27	THR B 353 C	4.95
C27	ALA B 354 CA	4	C26	THR B 353 C	4.55
C26	ALA B 354 CA	3.64	N1	THR B 353 C	4.88
N1	ALA B 354 CA	3.68	C24	LYS B 352 NZ	4.61
C25	ALA B 354 CA	4.05	C21	LYS B 352 NZ	4.48
C24	ALA B 354 CA	4.02	C15	LYS B 352 NZ	4.92
C23	ALA B 354 CA	4.64	C13	LYS B 352 NZ	3.96
C26	ALA B 354 N	4.45	N2	LYS B 352 CE	4.81
C24	ALA B 354 N	4.6	C26	LYS B 352 CE	4.32
C27	THR B 353 O	4.47	N1	LYS B 352 CE	4.48
C26	THR B 353 O	3.49	C24	LYS B 352 CE	3.91
C25	THR B 353 O	4.9	C21	LYS B 352 CE	4.69
C24	THR B 353 O	3.69	O6	LYS B 352 CE	4.2
C23	THR B 353 O	4.84	O5	LYS B 352 CE	3.28
C26	THR B 353 C	4.37	C16	LYS B 352 CE	4.84
N1	THR B 353 C	4.6	C15	LYS B 352 CE	4.68
C24	THR B 353 C	4.49	C13	LYS B 352 CE	4.01
C24	LYS B 352 NZ	4.43	O4	LYS B 352 CE	4.86
C22	LYS B 352 NZ	4.91	C6	LYS B 352 CE	4.22
C21	LYS B 352 NZ	4.27	C21	LYS B 352 CD	4.06
C13	LYS B 352 NZ	4.51	O6	LYS B 352 CD	3.43
C26	LYS B 352 CE	4.94	O5	LYS B 352 CD	3.76
N1	LYS B 352 CE	4.6	C16	LYS B 352 CD	4.32
C24	LYS B 352 CE	3.59	C15	LYS B 352 CD	4.62
C23	LYS B 352 CE	4.38	C13	LYS B 352 CD	4.39
C22	LYS B 352 CE	4.35	C6	LYS B 352 CD	4.67

C21	LYS B 352 CE	4.3	C21	LYS B 352 CG	4.37
O6	LYS B 352 CE	4.68	C20	LYS B 352 CG	4.96
O5	LYS B 352 CE	4.22	O7	LYS B 352 CG	4.84
C15	LYS B 352 CE	4.93	O6	LYS B 352 CG	3.28
C13	LYS B 352 CE	4.63	O5	LYS B 352 CG	4.23
C6	LYS B 352 CE	4.94	C17	LYS B 352 CG	4.56
C24	LYS B 352 CD	4.78	C16	LYS B 352 CG	3.86
C21	LYS B 352 CD	3.52	C15	LYS B 352 CG	4.26
O6	LYS B 352 CD	4.3	C13	LYS B 352 CG	4.44
O5	LYS B 352 CD	4.82	C7	LYS B 352 CG	4.71
C16	LYS B 352 CD	4.68	C6	LYS B 352 CG	3.88
C24	LYS B 352 CG	4.75	C21	LYS B 352 CB	4.42
C21	LYS B 352 CG	3.75	C20	LYS B 352 CB	4.02
C20	LYS B 352 CG	4.86	O7	LYS B 352 CB	4.09
O6	LYS B 352 CG	4.44	O6	LYS B 352 CB	3.29
C17	LYS B 352 CG	4.7	C17	LYS B 352 CB	4.26
C16	LYS B 352 CG	4.39	C16	LYS B 352 CB	3.95
C15	LYS B 352 CG	4.7	C15	LYS B 352 CB	4.79
C6	LYS B 352 CG	4.27	C6	LYS B 352 CB	4.95
C21	LYS B 352 CB	3.75	O6	LYS B 352 CA	4.77
C20	LYS B 352 CB	3.93	C20	LYS B 352 N	4.69
O7	LYS B 352 CB	4.47	C20	ASN B 350 O	4
O6	LYS B 352 CB	4.7	C20	ASN B 350 C	4.77
C17	LYS B 352 CB	4.53	O1	ILE B 318 CD1	3.91
C16	LYS B 352 CB	4.63	C9	ILE B 318 CD1	4.25
C20	LYS B 352 CA	4.97	C1	ILE B 318 CD1	3.83
C20	LYS B 352 N	4.65	O1	ILE B 318 CG1	4.3
C20	ASN B 350 O	4.28	C9	ILE B 318 CG1	4.28
O9	MET B 325 CE	3.18	C7	ILE B 318 CG1	4.6
C31	MET B 325 CE	4.89	C3	ILE B 318 CG1	4.53
C30	MET B 325 CE	4.37	C1	ILE B 318 CG1	3.58
O9	MET B 325 SD	4.08	C7	ALA B 317 O	4.53
O1	ILE B 318 CD1	4.75	O7	ALA B 316 CB	3.92
C9	ILE B 318 CD1	4.67	C19	ALA B 316 CB	4.56
C7	ILE B 318 CD1	4.59	C18	ALA B 316 CB	3.78
C3	ILE B 318 CD1	4.73	C17	ALA B 316 CB	4.17
C1	ILE B 318 CD1	3.86	C9	ALA B 316 CB	4.82
C9	ILE B 318 CG1	4.74	C7	ALA B 316 CB	4.84
C7	ILE B 318 CG1	3.96	C3	ALA B 316 CB	4.75
C3	ILE B 318 CG1	4.32	C1	ALA B 316 CB	4.29
C1	ILE B 318 CG1	3.8	O7	ALA B 316 CA	4.43
C7	ALA B 317 O	4.45	C18	ALA B 316 CA	4.93
C20	ALA B 316 CB	4.14	C17	ALA B 316 CA	4.96
O7	ALA B 316 CB	4.98	C20	VAL B 315 O	3.88
C19	ALA B 316 CB	4.28	C17	VAL B 315 O	4.95
C18	ALA B 316 CB	3.87	C20	VAL B 315 C	4.65
C17	ALA B 316 CB	4.75	O7	VAL B 315 C	4.38
C7	ALA B 316 CB	4.49	C20	THR B 314 CB	4.75
C3	ALA B 316 CB	4.71	C20	MET B 259 SD	4.28
C1	ALA B 316 CB	4.51	O7	MET B 259 SD	3.52
C20	ALA B 316 CA	4.44	C18	MET B 259 SD	4.08
C18	ALA B 316 CA	4.99	C17	MET B 259 SD	4.34
C20	ALA B 316 N	4.45	C20	MET B 259 CG	4.88
C20	VAL B 315 O	3.41	O7	MET B 259 CG	4
C20	VAL B 315 C	4.05	C19	MET B 259 CG	4.73
C20	VAL B 315 N	4.74	C18	MET B 259 CG	3.74
C20	THR B 314 CB	4.81	C17	MET B 259 CG	4.36
C20	MET B 259 SD	3.59	O7	MET B 259 CA	4.93
O7	MET B 259 SD	4.27	C20	MET B 259 N	4.82
C18	MET B 259 SD	4.23	C18	MET B 259 N	4.94

C17	MET B 259 SD	4.77	C17	MET B 259 N	4.97
C20	MET B 259 CG	4.3	C21	ASN B 258 D2	3.99
O7	MET B 259 CG	4.38	C16	ASN B 258 D2	4.64
C19	MET B 259 CG	4.85	C15	ASN B 258 D2	4.53
C18	MET B 259 CG	3.92	C13	ASN B 258 ND2	4.62
C17	MET B 259 CG	4.61	C21	ASN B 258 OD1	3.84
O7	MET B 259 CA	4.86	C21	ASN B 258 CG	3.59
C20	MET B 259 N	4.85	O6	ASN B 258 CG	4.57
C17	MET B 259 N	4.88	C17	ASN B 258 CG	4.94
C21	ASN B 258 D2	4.64	C16	ASN B 258 CG	4.49
C17	ASN B 258 D2	4.67	C15	ASN B 258 CG	4.79
C16	ASN B 258 ND2	3.97	C21	ASN B 258 CB	3.63
C15	ASN B 258 ND2	4.38	C20	ASN B 258 CB	4.1
C13	ASN B 258 ND2	4.53	O7	ASN B 258 CB	4.25
C21	ASN B 258 OD1	4.47	O6	ASN B 258 CB	4.22
C16	ASN B 258 OD1	4.83	C19	ASN B 258 CB	4.97
C21	ASN B 258 CG	4.22	C18	ASN B 258 CB	4.46
O7	ASN B 258 CG	4.29	C17	ASN B 258 CB	3.93
O6	ASN B 258 CG	3.43	C16	ASN B 258 CB	3.91
C17	ASN B 258 CG	4.4	C15	ASN B 258 CB	4.47
C16	ASN B 258 CG	3.99	C14	ASN B 258 CB	4.97
C15	ASN B 258 CG	4.79	C20	ASN B 258 O	3.68
C21	ASN B 258 CB	4.11	C17	ASN B 258 O	4.86
C20	ASN B 258 CB	4.49	C20	ASN B 258 C	4.2
O7	ASN B 258 CB	3.19	O7	ASN B 258 C	4.42
O6	ASN B 258 CB	3.43	C17	ASN B 258 C	4.74
C18	ASN B 258 CB	4.37	C20	ASN B 258 CA	4.77
C17	ASN B 258 CB	3.47	C17	ASN B 258 CA	4.99
C16	ASN B 258 CB	3.56	O2	LEU B 255 D2	3.51
C15	ASN B 258 CB	4.54	C10	LEU B 255 D2	3.52
C20	ASN B 258 O	4.12	O1	LEU B 255 D2	4.75
C17	ASN B 258 O	4.77	C8	LEU B 255 D2	4.44
C20	ASN B 258 C	4.49	C19	LEU B 255 D1	3.72
O7	ASN B 258 C	3.78	C18	LEU B 255 CD1	3.86
C17	ASN B 258 C	4.57	O3	LEU B 255 CD1	4.78
O7	ASN B 258 CA	4.11	O2	LEU B 255 D1	3.77
O6	ASN B 258 CA	4.93	C10	LEU B 255 D1	3.71
C17	ASN B 258 CA	4.64	O1	LEU B 255 CD1	4.31
O2	LEU B 255 CD2	3.76	C9	LEU B 255 D1	4.26
C10	LEU B 255 CD2	3.75	C8	LEU B 255 D1	3.92
O1	LEU B 255 CD2	4.19	C2	LEU B 255 D1	4.45
C9	LEU B 255 CD2	4.61	C19	LEU B 255 CG	4.65
C8	LEU B 255 CD2	4.37	O3	LEU B 255 CG	4.83
C19	LEU B 255 CD1	3.84	O2	LEU B 255 CG	3.94
C18	LEU B 255 CD1	4.07	C10	LEU B 255 CG	4.14
C14	LEU B 255 CD1	5	C8	LEU B 255 CG	4.45
O2	LEU B 255 CD1	4.44	C2	LEU B 255 CG	4.9
C10	LEU B 255 CD1	4.6	C19	LEU B 255 CB	4.36
O1	LEU B 255 CD1	4.32	C11	LEU B 255 CB	4.77
C9	LEU B 255 CD1	4.17	O3	LEU B 255 CB	4
C8	LEU B 255 CD1	4.26	O2	LEU B 255 CB	4.08
C2	LEU B 255 CD1	4.79	C10	LEU B 255 CB	4.76
C1	LEU B 255 CD1	4.65	C8	LEU B 255 CB	4.45
C19	LEU B 255 CG	4.84	C2	LEU B 255 CB	4.47
C11	LEU B 255 CG	4.85	C19	LEU B 255 O	4.54
O2	LEU B 255 CG	4.35	C18	LEU B 255 O	4.35
C10	LEU B 255 CG	4.65	C19	LEU B 255 C	4.7
O1	LEU B 255 CG	4.82	C18	LEU B 255 C	4.88
C9	LEU B 255 CG	4.84	C19	LEU B 255 CA	3.79
C8	LEU B 255 CG	4.57	C18	LEU B 255 CA	4.38

C19	LEU B 255 CB	4.62	C14	LEU B 255 CA	4.46
C11	LEU B 255 CB	3.8	C12	LEU B 255 CA	4.89
O3	LEU B 255 CB	4.76	O3	LEU B 255 CA	4.4
O2	LEU B 255 CB	4.29	C2	LEU B 255 CA	4.91
C8	LEU B 255 CB	4.48	C19	LEU B 255 N	4.35
C2	LEU B 255 CB	4.66	C14	LEU B 255 N	4.6
C19	LEU B 255 O	4.87	C12	LEU B 255 N	4.65
C18	LEU B 255 O	4.46	O4	LYS B 254 CB	4.8
C17	LEU B 255 O	4.92	C12	LYS B 254 CB	4.78
C18	LEU B 255 C	4.98	C19	LYS B 254 O	4.11
C19	LEU B 255 CA	4.13	C18	LYS B 254 O	4.65
C18	LEU B 255 CA	4.47	C16	LYS B 254 O	4.85
C14	LEU B 255 CA	4.55	C15	LYS B 254 O	4.32
C12	LEU B 255 CA	4.95	C14	LYS B 254 O	3.97
C11	LEU B 255 CA	4.34	C13	LYS B 254 O	4.74
C19	LEU B 255 N	4.71	C12	LYS B 254 O	4.3
C14	LEU B 255 N	4.69	C19	LYS B 254 C	4.58
C12	LEU B 255 N	4.76	C14	LYS B 254 C	4.5
C11	LEU B 255 N	3.98	C12	LYS B 254 C	4.53
C13	LYS B 254 CB	4.88	O3	LYS B 254 C	4.98
O4	LYS B 254 CB	4.62	C11	LEU B 252 N	4.83
C11	LYS B 254 CB	4.96	C11	ASP B 251 O	3.59
C19	LYS B 254 O	4.49	C2	ASP B 251 O	4.96
C18	LYS B 254 O	4.61	C11	ASP B 251 C	3.94
C17	LYS B 254 O	4.52	O3	ASP B 251 C	4.41
C16	LYS B 254 O	4.19	C11	ASP B 251 CA	4.08
C15	LYS B 254 O	3.99	O3	ASP B 251 CA	4.85
C14	LYS B 254 O	4.2	C11	ASP B 251 N	3.73
C13	LYS B 254 O	4.35	N2	ALA B 250 CB	4.23
C12	LYS B 254 O	4.64	C22	ALA B 250 CB	4.19
C19	LYS B 254 C	4.95	O4	ALA B 250 CB	3.78
C15	LYS B 254 C	4.72	C12	ALA B 250 CB	3.57
C14	LYS B 254 C	4.66	C11	ALA B 250 CB	3.47
C13	LYS B 254 C	4.92	O3	ALA B 250 CB	3.49
O4	LYS B 254 C	4.92	C5	ALA B 250 CB	3.44
C12	LYS B 254 C	4.77	C4	ALA B 250 CB	4.4
C11	LYS B 254 C	4.78	C2	ALA B 250 CB	4.39
C11	LEU B 252 CA	4.73	C11	ALA B 250 O	3.55
C11	LEU B 252 N	4.13	C11	ALA B 250 C	3.52
C11	ASP B 251 O	2.57	O3	ALA B 250 C	4.3
C2	ASP B 251 O	4.87	C11	ALA B 250 CA	4.12
C11	ASP B 251 C	3.18	O3	ALA B 250 CA	4.53
O3	ASP B 251 C	4.48	C5	ALA B 250 CA	4.97
C11	ASP B 251 CA	3.65	C24	LEU B 248 D2	4.94
O3	ASP B 251 CA	4.67	O5	LEU B 248 D2	3.69
C11	ASP B 251 N	3.36	C13	LEU B 248 CD2	4.36
N2	ALA B 250 CB	4.56	O4	LEU B 248 CD2	4.26
C22	ALA B 250 CB	4.44	O5	LEU B 248 CG	4.88
C14	ALA B 250 CB	4.88	O4	LEU B 248 CG	4.81
C13	ALA B 250 CB	4.43	N1	LEU B 248 CB	4.58
O4	ALA B 250 CB	3.2	C24	LEU B 248 CB	4.32
C12	ALA B 250 CB	3.44	C23	LEU B 248 CB	4.69
C11	ALA B 250 CB	3.5	C25	LEU B 248 O	4.55
O3	ALA B 250 CB	3.25	C24	LEU B 248 O	4.45
C5	ALA B 250 CB	3.58	C23	LEU B 248 O	3.84
C4	ALA B 250 CB	4.47	C22	LEU B 248 O	4.06
C2	ALA B 250 CB	4.32	N3	LEU B 248 C	4.88
C11	ALA B 250 O	3.91	C23	LEU B 248 C	4.83
C11	ALA B 250 C	3.55	C29	LEU B 248 N	4.78
O3	ALA B 250 C	3.87	C26	LEU B 248 N	4.96

O4	ALA B 250 CA	4.65	C25	LEU B 248 N	4.4
C12	ALA B 250 CA	4.95	C24	LEU B 248 N	4.83
C11	ALA B 250 CA	4.14	C23	LEU B 248 N	4.95
O3	ALA B 250 CA	4.18	C29	GLN B 247 CG	4.97
C22	LEU B 248 CD2	4.78	C28	GLN B 247 CG	4.29
O5	LEU B 248 CD2	3.38	C27	GLN B 247 CG	4.54
C13	LEU B 248 CD2	4.27	C29	GLN B 247 CB	4.14
O4	LEU B 248 CD2	4.52	C28	GLN B 247 CB	3.79
C22	LEU B 248 CG	4.9	C27	GLN B 247 CB	3.98
O5	LEU B 248 CG	4.4	C26	GLN B 247 CB	4.53
O4	LEU B 248 CG	4.88	N1	GLN B 247 CB	4.8
N3	LEU B 248 CB	4.68	C25	GLN B 247 CB	4.58
N1	LEU B 248 CB	4.96	C29	GLN B 247 CA	4.62
C25	LEU B 248 CB	4.95	C28	GLN B 247 CA	4.71
C24	LEU B 248 CB	4.71	C25	GLN B 247 CA	4.97
C23	LEU B 248 CB	4.53	C29	GLN B 247 N	3.94
C22	LEU B 248 CB	4.8	C28	GLN B 247 N	4.36
C29	LEU B 248 O	4.93	C25	GLN B 247 N	4.44
C25	LEU B 248 O	4.47	C29	GLY B 246 C	4.69
C23	LEU B 248 O	4.17	N3	GLY B 246 CA	4.84
C22	LEU B 248 O	4.36	C29	GLY B 246 CA	4.47
N3	LEU B 248 C	4.65	C25	GLY B 246 CA	4.97
N3	LEU B 248 CA	4.84	C11	LEU B 242 D2	3.18
C29	LEU B 248 N	4.5	O3	LEU B 242 D2	4.41
C25	LEU B 248 N	4.38	O2	LEU B 242 CD2	4.47
O9	GLN B 247 CG	3.92	O2	LEU B 242 CD1	4.63
C31	GLN B 247 CG	4.87	C11	LEU B 242 CG	3.91
O8	GLN B 247 CG	4.39	O2	LEU B 242 CG	4.35
C30	GLN B 247 CG	3.99	C11	LEU B 242 CB	4.9
C28	GLN B 247 CG	4.34	C11	LEU B 242 CA	4.68
C27	GLN B 247 CG	4.46	C11	LEU B 242 N	4.35
O9	GLN B 247 CB	4.25	N3	CYS B 241 SG	4.09
O8	GLN B 247 CB	4.2	N2	CYS B 241 SG	4.75
C30	GLN B 247 CB	3.88	C23	CYS B 241 SG	4.27
C29	GLN B 247 CB	4.16	C22	CYS B 241 SG	3.86
C28	GLN B 247 CB	3.77	C9	CYS B 241 SG	4.78
C27	GLN B 247 CB	3.99	C7	CYS B 241 SG	3.99
C26	GLN B 247 CB	4.53	C6	CYS B 241 SG	4.9
N1	GLN B 247 CB	4.83	C4	CYS B 241 SG	4.48
C25	GLN B 247 CB	4.65	C3	CYS B 241 SG	3.94
O8	GLN B 247 CA	4.33	C1	CYS B 241 SG	4.09
C30	GLN B 247 CA	4.48	N3	CYS B 241 CB	4.82
C29	GLN B 247 CA	4.45	N2	CYS B 241 CB	4.7
C28	GLN B 247 CA	4.46	C23	CYS B 241 CB	4.76
C31	GLN B 247 N	4.04	C22	CYS B 241 CB	3.87
C30	GLN B 247 N	3.8	C11	CYS B 241 CB	4.24
C29	GLN B 247 N	3.67	O3	CYS B 241 CB	4.6
C28	GLN B 247 N	3.9	O2	CYS B 241 CB	4.88
C27	GLN B 247 N	4.87	O1	CYS B 241 CB	4.98
C25	GLN B 247 N	4.5	C9	CYS B 241 CB	4.23
C31	GLY B 246 C	4.45	C8	CYS B 241 CB	4.16
O8	GLY B 246 C	3.88	C7	CYS B 241 CB	4.49
C30	GLY B 246 C	4.7	C5	CYS B 241 CB	4.56
C29	GLY B 246 C	4.31	C4	CYS B 241 CB	3.87
C28	GLY B 246 C	4.83	C3	CYS B 241 CB	3.87
C31	GLY B 246 CA	3.94	C2	CYS B 241 CB	3.97
O8	GLY B 246 CA	3.45	C1	CYS B 241 CB	4.03
C30	GLY B 246 CA	4.52	C11	CYS B 241 O	3.81
C29	GLY B 246 CA	4.05	C11	CYS B 241 C	4.07
C28	GLY B 246 CA	4.72	C11	CYS B 241 CA	4.8

C31	GLY B 246 N	4.99	C10	VAL B 238 CB	4.84
C31	PRO B 245 O	4.69	O1	VAL B 238 CB	4.74
C11	LEU B 242 CD2	3.52	C10	VAL B 238 O	3.26
O3	LEU B 242 CD2	3.95	C9	VAL B 238 O	4.83
O2	LEU B 242 CD2	3.58	C10	VAL B 238 C	4.15
C10	LEU B 242 CD2	4.46	O1	VAL B 238 C	4.24
C8	LEU B 242 CD2	4.5	C10	VAL B 238 CA	4.63
C2	LEU B 242 CD2	4.7	O1	VAL B 238 CA	4.36
O2	LEU B 242 CD1	3.81	C10	TYR B 202 OH	3.41
C10	LEU B 242 CD1	3.85	C10	TYR B 202 CZ	4.78
C11	LEU B 242 CG	4.49	C21	VAL A 181 G2	3.97
O3	LEU B 242 CG	4.57	C20	VAL A 181 G2	3.51
O2	LEU B 242 CG	3.46	O7	VAL A 181 CG2	4.84
C10	LEU B 242 CG	3.9	O6	VAL A 181 CG2	4.61
C8	LEU B 242 CG	4.46	C21	VAL A 181 CB	4.87
C2	LEU B 242 CG	4.98	C20	VAL A 181 CB	4.98
O2	LEU B 242 CB	4.82	C21	VAL A 181 CA	4.8
C8	LEU B 242 N	4.97	C21	VAL A 181 N	3.73
N3	CYS B 241 SG	4.34	C21	ALA A 180 CB	4.35
N2	CYS B 241 SG	4.12	C21	ALA A 180 O	4.92
C23	CYS B 241 SG	4.8	C21	ALA A 180 C	3.92
C22	CYS B 241 SG	4.99	C21	ALA A 180 CA	3.45
C7	CYS B 241 SG	3.79	O6	ALA A 180 CA	4.79
C6	CYS B 241 SG	4.44	O5	ALA A 180 CA	4.61
C5	CYS B 241 SG	4.63	C21	ALA A 180 N	4.22
C4	CYS B 241 SG	4.25	C21	THR A 179 O	3.43
C3	CYS B 241 SG	3.98	C13	THR A 179 O	4.96
C2	CYS B 241 SG	4.85	C21	THR A 179 C	4.25
C1	CYS B 241 SG	4.44	O5	THR A 179 C	4.47
N3	CYS B 241 CB	4.96	C28	SER A 178 OG	4.97
N2	CYS B 241 CB	4.15	C27	SER A 178 OG	3.67
O3	CYS B 241 CB	3.96	C26	SER A 178 OG	3.18
O2	CYS B 241 CB	4.78	C24	SER A 178 OG	4.66
C9	CYS B 241 CB	4.26	C27	SER A 178 CB	4.98
C8	CYS B 241 CB	4.01	C26	SER A 178 CB	4.35
C7	CYS B 241 CB	4.21			
C6	CYS B 241 CB	4.83			
C5	CYS B 241 CB	4.06			
C4	CYS B 241 CB	3.52			
C3	CYS B 241 CB	3.74			
C2	CYS B 241 CB	3.62			
C1	CYS B 241 CB	4.12			
C11	CYS B 241 O	4.91			
C2	CYS B 241 O	4.62			
O3	CYS B 241 C	4.25			
O2	CYS B 241 C	4.95			
C8	CYS B 241 C	4.82			
C2	CYS B 241 C	4.58			
O3	CYS B 241 CA	4.77			
C8	CYS B 241 CA	4.89			
C4	CYS B 241 CA	4.89			
C2	CYS B 241 CA	4.69			
C10	THR B 239 CA	4.52			
C10	THR B 239 N	4.48			
O1	VAL B 238 CB	4.52			
C10	VAL B 238 O	2.71			
C9	VAL B 238 O	4.21			
C8	VAL B 238 O	4.69			
O2	VAL B 238 C	4.99			
C10	VAL B 238 C	3.72			

O1	VAL B 238 C	3.7			
C9	VAL B 238 C	4.83			
C10	VAL B 238 CA	4.62			
O1	VAL B 238 CA	4.14			
C10	TYR B 202 OH	3.7			
C9	TYR B 202 OH	4.89			
C21	VAL A 181 CG2	4.05			
C20	VAL A 181 CG2	4.46			
O7	VAL A 181 CG2	4.15			
O6	VAL A 181 CG2	4.8			
C21	VAL A 181 N	4.11			
C21	ALA A 180 CB	4.92			
O6	ALA A 180 CB	4.59			
C21	ALA A 180 C	4.27			
O6	ALA A 180 C	4.7			
C21	ALA A 180 CA	3.9			
O6	ALA A 180 CA	3.97			
O5	ALA A 180 CA	4.89			
C21	ALA A 180 N	4.53			
C21	THR A 179 O	3.39			
C21	THR A 179 C	4.35			
O6	THR A 179 C	4.79			
C27	SER A 178 OG	4.51			
C26	SER A 178 OG	3.69			
C24	SER A 178 OG	4.29			
C26	SER A 178 CB	4.95			
C28	SER A 178 CA				
Table A5.18			**Table A5.19**		
(c) 9_Tubulin			**(d) Noscapine_Tubulin**		
Hydrogen bonding			**Hydrogen bonding**		
Hydrogen Donor (D)	**Hydrogen Acceptor (A)**	**Distance (D-A) in Å**	**Hydrogen Donor (D)**	**Hydrogen Acceptor (A)**	**Distance (D-A) in Å**
LYS B 352 NZ	900 O5	2.99	LYS B 352 NZ	900 O6	3.62
			900 N1	LEU B 248 O	3.24
Hydrophobic interaction			**Hydrophobic interaction**		
O2	ILE B 378 CD1	4.89	C21	ILE B 378 CD1	4.43
C10	ILE B 378 CD1	3.62	C2	CYS B 356 N	4.85
O1	ILE B 378 CD1	3.13	C10	VAL B 355 G2	4.85
C9	ILE B 378 CD1	4.2	C10	VAL B 355 CB	4.4
C1	ILE B 378 CD1	4.81	O1	VAL B 355 CB	4.15
O1	ILE B 378 CG1	4.54	C9	VAL B 355 CB	4.7
C28	VAL B 355 CB	4.82	C10	VAL B 355 O	4.29
C29	VAL B 355 O	3.68	C9	VAL B 355 O	3.12
C28	VAL B 355 O	3.96	C8	VAL B 355 O	4.27
C25	VAL B 355 O	4.84	C7	VAL B 355 O	4.18
C29	VAL B 355 C	4.55	C4	VAL B 355 O	4.83
C28	VAL B 355 C	4.72	C3	VAL B 355 O	3.74
C29	VAL B 355 CA	4.78	C2	VAL B 355 O	2.75
C28	VAL B 355 CA	4.62	C10	VAL B 355 C	4.99
C29	VAL B 355 N	3.86	O1	VAL B 355 C	4.09
C28	VAL B 355 N	3.71	C9	VAL B 355 C	4.09
C27	VAL B 355 N	4.41	C7	VAL B 355 C	4.98
C25	VAL B 355 N	4.6	C3	VAL B 355 C	4.63
N3	ALA B 354 CB	3.67	C2	VAL B 355 C	3.82
N2	ALA B 354 CB	4.85	C10	VAL B 355 CA	4.76
C29	ALA B 354 CB	3.95	O1	VAL B 355 CA	4.27
C28	ALA B 354 CB	4.41	C9	VAL B 355 CA	4.37
C27	ALA B 354 CB	4.61	C2	VAL B 355 CA	4.5
C26	ALA B 354 CB	4.28	C10	VAL B 355 N	4.23
N1	ALA B 354 CB	3.77	C9	VAL B 355 N	3.72

C25	ALA B 354 CB	3.61	C8	VAL B 355 N	4.07
C24	ALA B 354 CB	3.89	C4	VAL B 355 N	4.82
C23	ALA B 354 CB	3.8	C3	VAL B 355 N	4.43
C22	ALA B 354 CB	4.4	C2	VAL B 355 N	3.96
C7	ALA B 354 CB	3.58	C1	VAL B 355 N	4.63
C6	ALA B 354 CB	4.13	N1	ALA B 354 CB	4.61
C3	ALA B 354 CB	4.8	C22	ALA B 354 CB	4.15
C29	ALA B 354 C	4.54	O7	ALA B 354 CB	4.38
C28	ALA B 354 C	4.43	O5	ALA B 354 CB	4.73
C27	ALA B 354 C	4.79	C19	ALA B 354 CB	3.47
C25	ALA B 354 C	4.92	C18	ALA B 354 CB	4.52
N3	ALA B 354 CA	4.62	C14	ALA B 354 CB	3.98
C29	ALA B 354 CA	4.13	C12	ALA B 354 CB	3.82
C28	ALA B 354 CA	4.09	C9	ALA B 354 CB	4.68
C27	ALA B 354 CA	4.11	C8	ALA B 354 CB	4.36
C26	ALA B 354 CA	4.09	C7	ALA B 354 CB	4.51
N1	ALA B 354 CA	4.08	C5	ALA B 354 CB	4.1
C25	ALA B 354 CA	4.11	C4	ALA B 354 CB	3.66
C24	ALA B 354 CA	4.55	C3	ALA B 354 CB	3.99
C23	ALA B 354 CA	4.85	C2	ALA B 354 CB	4.55
C7	ALA B 354 CA	4.81	C1	ALA B 354 CB	3.88
C27	ALA B 354 N	4.97	C9	ALA B 354 C	4.68
C26	ALA B 354 N	4.78	C8	ALA B 354 C	4.7
C7	ALA B 354 N	4.83	C2	ALA B 354 C	4.9
C28	THR B 353 O	4.95	C1	ALA B 354 C	4.97
C27	THR B 353 O	4.07	C22	ALA B 354 CA	3.96
C26	THR B 353 O	3.56	O7	ALA B 354 CA	4.55
C25	THR B 353 O	4.94	C19	ALA B 354 CA	4.85
C24	THR B 353 O	4.35	C12	ALA B 354 CA	4.86
C6	THR B 353 O	4.96	O2	ALA B 354 CA	4.67
C27	THR B 353 C	4.92	C9	ALA B 354 CA	4.59
C26	THR B 353 C	4.56	C8	ALA B 354 CA	4.2
N1	THR B 353 C	4.91	C4	ALA B 354 CA	4.39
C24	LYS B 352 NZ	4.48	C3	ALA B 354 CA	4.7
C21	LYS B 352 NZ	4.75	C2	ALA B 354 CA	4.87
C16	LYS B 352 NZ	4.95	C1	ALA B 354 CA	4.12
C15	LYS B 352 NZ	4.85	C22	ALA B 354 N	4.4
C13	LYS B 352 NZ	4	C22	THR B 353 O	2.92
N2	LYS B 352 CE	4.67	C8	THR B 353 O	4.93
C26	LYS B 352 CE	4.38	C1	THR B 353 O	4.63
N1	LYS B 352 CE	4.43	C22	THR B 353 C	3.99
C24	LYS B 352 CE	3.81	C22	LYS B 352 NZ	4.41
C23	LYS B 352 CE	4.97	C13	LYS B 352 NZ	3.95
C21	LYS B 352 CE	4.84	C22	LYS B 352 CE	3.58
O6	LYS B 352 CE	3.89	O7	LYS B 352 CE	4.2
O5	LYS B 352 CE	3.44	O6	LYS B 352 CE	3.8
C16	LYS B 352 CE	4.63	C15	LYS B 352 CE	4.43
C15	LYS B 352 CE	4.64	C14	LYS B 352 CE	4.75
C13	LYS B 352 CE	4.11	C13	LYS B 352 CE	3.73
C6	LYS B 352 CE	4.13	O3	LYS B 352 CE	3.66
C21	LYS B 352 CD	4.04	C12	LYS B 352 CE	4.32
O6	LYS B 352 CD	3.18	C22	LYS B 352 CD	4.71
O5	LYS B 352 CD	3.97	O6	LYS B 352 CD	4.63
C16	LYS B 352 CD	4.14	C13	LYS B 352 CD	4.66
C15	LYS B 352 CD	4.61	O3	LYS B 352 CD	4.87
C13	LYS B 352 CD	4.53	C22	LYS B 352 CG	4.95
C6	LYS B 352 CD	4.57	O6	LYS B 352 CG	4.87
N2	LYS B 352 CG	4.95	C16	LYS B 352 CG	4.68
C21	LYS B 352 CG	4.25	C15	LYS B 352 CG	4.59
O7	LYS B 352 CG	4.24	C14	LYS B 352 CG	4.88

O6	LYS B 352 CG	3.12	C13	LYS B 352 CG	4.65
O5	LYS B 352 CG	4.46	O3	LYS B 352 CG	4.95
C17	LYS B 352 CG	4.27	C10	MET B 325 CE	3.7
C16	LYS B 352 CG	3.72	O1	MET B 325 CE	4.04
C15	LYS B 352 CG	4.29	C10	MET B 325 SD	4.02
C13	LYS B 352 CG	4.62	O1	MET B 325 SD	4.88
C7	LYS B 352 CG	4.61	C21	ILE B 318 CD1	3.62
C6	LYS B 352 CG	3.79	O5	ILE B 318 CD1	3.74
C21	LYS B 352 CB	4.12	C21	ILE B 318 CG1	3.43
C20	LYS B 352 CB	4.65	O5	ILE B 318 CG1	3.36
O7	LYS B 352 CB	3.49	C19	ILE B 318 CG1	4.87
O6	LYS B 352 CB	3.26	C18	ILE B 318 CG1	4.55
C17	LYS B 352 CB	4.01	C21	ILE B 318 CB	4.93
C16	LYS B 352 CB	3.88	O5	ILE B 318 CB	4.76
C15	LYS B 352 CB	4.85	O5	ALA B 317 C	4.88
C6	LYS B 352 CB	4.86	C21	ALA B 316 CB	4.58
O7	LYS B 352 CA	4.69	C20	ALA B 316 CB	3.56
O6	LYS B 352 CA	4.74	O5	ALA B 316 CB	3.97
C20	ASN B 350 O	4.36	O4	ALA B 316 CB	3.39
O1	ILE B 318 CD1	3.74	C18	ALA B 316 CB	4.51
C9	ILE B 318 CD1	4.18	C17	ALA B 316 CB	4.26
C1	ILE B 318 CD1	3.85	O5	ALA B 316 C	4.79
O1	ILE B 318 CG1	4.12	C20	ALA B 316 CA	4.83
C9	ILE B 318 CG1	4.18	O5	ALA B 316 CA	4.83
C7	ILE B 318 CG1	4.68	O4	ALA B 316 CA	4.69
C3	ILE B 318 CG1	4.54	C20	MET B 259 SD	4.43
C1	ILE B 318 CG1	3.57	C20	MET B 259 CG	4.08
C7	ALA B 317 O	4.52	C20	LEU B 255 D1	3.54
C20	ALA B 316 CB	4.66	O4	LEU B 255 CD1	3.75
O7	ALA B 316 CB	4.01	C17	LEU B 255 D1	4.94
C19	ALA B 316 CB	4.52	C20	LEU B 255 CG	4.74
C18	ALA B 316 CB	3.74	O4	LEU B 255 CG	4.96
C17	ALA B 316 CB	4.23	C20	LEU B 255 CB	4.79
O1	ALA B 316 CB	4.97	C20	LEU B 255 O	4.66
C9	ALA B 316 CB	4.74	C20	LEU B 255 CA	4.33
C7	ALA B 316 CB	4.93	O4	LEU B 255 CA	4.96
C3	ALA B 316 CB	4.71	C20	LYS B 254 O	4.89
C1	ALA B 316 CB	4.22	N1	ALA B 250 CB	4.58
O7	ALA B 316 CA	4.39	O6	ALA B 250 CB	4.53
C18	ALA B 316 CA	4.85	C16	ALA B 250 CB	4.78
C17	ALA B 316 CA	4.96	C15	ALA B 250 CB	4.4
C20	ALA B 316 N	4.93	C14	ALA B 250 CB	4.88
C20	VAL B 315 O	3.94	C13	ALA B 250 CB	4.37
C17	VAL B 315 O	4.91	O3	ALA B 250 CB	4.81
C20	VAL B 315 C	4.49	C11	ALA B 250 CB	3.14
O7	VAL B 315 C	4.41	C11	ALA B 250 O	4.83
C20	VAL B 315 N	4.81	C11	ALA B 250 C	4.82
C20	THR B 314 CG2	4.87	C11	ALA B 250 CA	4.06
C20	THR B 314 G1	4.9	C11	ALA B 250 N	3.84
C20	THR B 314 CB	4.35	C11	ASN B 249 O	4.97
C20	MET B 259 SD	3.41	C11	ASN B 249 C	4.34
O7	MET B 259 SD	4.06	C11	ASN B 249 CA	4.7
C18	MET B 259 SD	4.13	C11	ASN B 249 N	4.79
C17	MET B 259 SD	4.58	O6	LEU B 248 D2	3.24
C20	MET B 259 CG	3.94	C13	LEU B 248 D2	3.79
O7	MET B 259 CG	4.61	O3	LEU B 248 D2	3.7
C19	MET B 259 CG	4.72	O6	LEU B 248 CG	4.03
C18	MET B 259 CG	3.88	C13	LEU B 248 CG	4.29
C17	MET B 259 CG	4.65	O3	LEU B 248 CG	3.93
C20	MET B 259 CB	4.75	O7	LEU B 248 CB	4.19

C20	MET B 259 CA	4.32	O6	LEU B 248 CB	4.72
C20	MET B 259 N	4.11	C13	LEU B 248 CB	4.62
C21	ASN B 258 D2	4.37	O3	LEU B 248 CB	3.8
C16	ASN B 258 D2	4.66	C12	LEU B 248 CB	4.71
C15	ASN B 258 D2	4.49	C5	LEU B 248 CB	4.39
C14	ASN B 258 ND2	4.99	C4	LEU B 248 CB	4.93
C13	ASN B 258 ND2	4.54	C1	LEU B 248 CB	4.82
C21	ASN B 258 D1	4.02	C13	LEU B 248 O	4.91
C21	ASN B 258 CG	3.82	C12	LEU B 248 O	4.29
O6	ASN B 258 CG	4.69	C11	LEU B 248 O	2.84
C17	ASN B 258 CG	4.98	C7	LEU B 248 O	4.55
C16	ASN B 258 CG	4.55	C6	LEU B 248 O	3.36
C15	ASN B 258 CG	4.79	C5	LEU B 248 O	3.25
C21	ASN B 258 CB	3.69	C4	LEU B 248 O	4.05
C20	ASN B 258 CB	3.96	C3	LEU B 248 O	4.56
O7	ASN B 258 CB	4.47	C1	LEU B 248 O	4.83
O6	ASN B 258 CB	4.43	N1	LEU B 248 C	4.45
C19	ASN B 258 CB	4.9	O3	LEU B 248 C	4.76
C18	ASN B 258 CB	4.46	C11	LEU B 248 C	4.02
C17	ASN B 258 CB	4.04	C6	LEU B 248 C	4.52
C16	ASN B 258 CB	4.04	C5	LEU B 248 C	4.26
C15	ASN B 258 CB	4.5	C4	LEU B 248 C	4.91
C14	ASN B 258 CB	4.93	O7	LEU B 248 CA	4.81
C20	ASN B 258 O	3.32	O3	LEU B 248 CA	4.76
C20	ASN B 258 C	3.71	C5	LEU B 248 CA	4.57
O7	ASN B 258 C	4.86	C4	LEU B 248 CA	4.94
C17	ASN B 258 C	4.95	C8	LEU B 248 N	4.75
C21	ASN B 258 CA	4.99	C5	LEU B 248 N	4.39
C20	ASN B 258 CA	4.48	C4	LEU B 248 N	4.29
C11	LEU B 255 CD2	4.94	C3	LEU B 248 N	4.82
O2	LEU B 255 CD2	3.61	C1	LEU B 248 N	4.24
C10	LEU B 255 CD2	3.8	O2	GLN B 247 CD	4.98
O1	LEU B 255 CD2	4.92	O2	GLN B 247 CG	3.85
C8	LEU B 255 CD2	4.57	C10	GLN B 247 CG	3.8
C19	LEU B 255 CD1	3.79	O1	GLN B 247 CG	4.03
C18	LEU B 255 CD1	4.08	C9	GLN B 247 CG	4.44
O3	LEU B 255 CD1	4.83	C8	GLN B 247 CG	4.36
O2	LEU B 255 CD1	3.76	O7	GLN B 247 CB	4.4
C10	LEU B 255 CD1	3.91	O2	GLN B 247 CB	3.53
O1	LEU B 255 CD1	4.38	C10	GLN B 247 CB	3.93
C9	LEU B 255 CD1	4.35	O1	GLN B 247 CB	4.01
C8	LEU B 255 CD1	3.98	C9	GLN B 247 CB	3.91
C2	LEU B 255 CD1	4.49	C8	GLN B 247 CB	3.65
C19	LEU B 255 CG	4.72	C4	GLN B 247 CB	4.86
C11	LEU B 255 CG	4.94	C2	GLN B 247 CB	4.62
O3	LEU B 255 CG	4.92	C1	GLN B 247 CB	4.12
O2	LEU B 255 CG	4	O2	GLN B 247 CA	4.74
C10	LEU B 255 CG	4.39	O1	GLN B 247 CA	4.75
C8	LEU B 255 CG	4.55	C9	GLN B 247 CA	4.47
C2	LEU B 255 CG	4.97	C8	GLN B 247 CA	4.48
C19	LEU B 255 CB	4.44	C2	GLN B 247 CA	4.73
C11	LEU B 255 CB	4.09	C1	GLN B 247 CA	4.72
O3	LEU B 255 CB	4.1	C10	GLN B 247 N	4.87
O2	LEU B 255 CB	4.15	C9	GLN B 247 N	3.76
C10	LEU B 255 CB	4.98	C8	GLN B 247 N	4.13
C8	LEU B 255 CB	4.54	C7	GLN B 247 N	4.75
C2	LEU B 255 CB	4.54	C6	GLN B 247 N	4.97
C19	LEU B 255 O	4.55	C4	GLN B 247 N	4.38
C18	LEU B 255 O	4.54	C3	GLN B 247 N	4.04
C19	LEU B 255 C	4.74	C2	GLN B 247 N	3.66

C19	LEU B 255 CA	3.85	C1	GLN B 247 N	4.4
C18	LEU B 255 CA	4.58	C9	GLY B 246 C	4.6
C14	LEU B 255 CA	4.47	C7	GLY B 246 C	4.58
C12	LEU B 255 CA	4.82	C6	GLY B 246 C	4.62
C11	LEU B 255 CA	4.8	C4	GLY B 246 C	4.84
O3	LEU B 255 CA	4.43	C3	GLY B 246 C	4.3
C2	LEU B 255 CA	4.94	C2	GLY B 246 C	4.1
C19	LEU B 255 N	4.41	O1	GLY B 246 CA	4.97
C14	LEU B 255 N	4.59	C9	GLY B 246 CA	4.38
C12	LEU B 255 N	4.57	C7	GLY B 246 CA	3.63
C11	LEU B 255 N	4.6	C6	GLY B 246 CA	3.92
O4	LYS B 254 CB	4.61	C4	GLY B 246 CA	4.63
C12	LYS B 254 CB	4.7	C3	GLY B 246 CA	3.71
C19	LYS B 254 O	4.13	C2	GLY B 246 CA	3.49
C18	LYS B 254 O	4.75	C7	GLY B 246 N	4.29
C16	LYS B 254 O	4.93	C6	GLY B 246 N	4.34
C15	LYS B 254 O	4.31	C3	GLY B 246 N	4.78
C14	LYS B 254 O	3.94	C2	GLY B 246 N	4.73
C13	LYS B 254 O	4.67	C7	PRO B 245 O	4.23
C12	LYS B 254 O	4.22	C6	PRO B 245 O	4.81
C19	LYS B 254 C	4.62	C3	PRO B 245 O	5
C14	LYS B 254 C	4.47	C2	PRO B 245 O	4.75
O4	LYS B 254 C	4.86	C7	PRO B 245 C	4.56
C12	LYS B 254 C	4.44	C6	PRO B 245 C	4.78
O3	LYS B 254 C	4.96	C7	PHE B 244 O	4.91
C11	LEU B 252 N	4.46	C6	PHE B 244 O	4.68
C11	ASP B 251 O	3.19	N1	CYS B 241 SG	3.55
C11	ASP B 251 C	3.65	C21	CYS B 241 SG	4.06
O3	ASP B 251 C	4.54	O5	CYS B 241 SG	4.05
C11	ASP B 251 CA	4.05	C19	CYS B 241 SG	3.4
O3	ASP B 251 CA	4.95	C18	CYS B 241 SG	4.12
C11	ASP B 251 N	3.85	C14	CYS B 241 SG	4.26
N2	ALA B 250 CB	4.24	C12	CYS B 241 SG	4.72
C22	ALA B 250 CB	4.12	C11	CYS B 241 SG	4.39
O4	ALA B 250 CB	3.68	C7	CYS B 241 SG	3.56
C12	ALA B 250 CB	3.55	C6	CYS B 241 SG	3.78
C11	ALA B 250 CB	3.85	C5	CYS B 241 SG	4.4
O3	ALA B 250 CB	3.39	C4	CYS B 241 SG	4.69
C5	ALA B 250 CB	3.46	C3	CYS B 241 SG	4.41
C4	ALA B 250 CB	4.41	N1	CYS B 241 CB	3.54
C2	ALA B 250 CB	4.37	C21	CYS B 241 CB	3.89
C11	ALA B 250 O	4.01	O5	CYS B 241 CB	4.36
C11	ALA B 250 C	3.88	C19	CYS B 241 CB	3.84
O3	ALA B 250 C	4.33	C18	CYS B 241 CB	4.28
C11	ALA B 250 CA	4.52	C14	CYS B 241 CB	4.49
O3	ALA B 250 CA	4.49	C11	CYS B 241 CB	3.76
C5	ALA B 250 CA	4.99	C7	CYS B 241 CB	4.21
C24	LEU B 248 CD2	4.82	C6	CYS B 241 CB	3.8
O5	LEU B 248 CD2	3.52	C5	CYS B 241 CB	4.8
C13	LEU B 248 CD2	4.25	C11	CYS B 241 O	3.75
O4	LEU B 248 CD2	4.27	C6	CYS B 241 O	4.05
C24	LEU B 248 CG	4.92	N1	CYS B 241 C	4.84
O5	LEU B 248 CG	4.71	C11	CYS B 241 C	4.54
O4	LEU B 248 CG	4.8	C6	CYS B 241 C	4.58
N3	LEU B 248 CB	4.88	N1	CYS B 241 CA	4.38
N1	LEU B 248 CB	4.52	C11	CYS B 241 CA	4.54
C25	LEU B 248 CB	4.9	C7	CYS B 241 CA	4.48
C24	LEU B 248 CB	4.21	C6	CYS B 241 CA	4.13
C23	LEU B 248 CB	4.51	C6	ARG B 48 NH1	4.97
C25	LEU B 248 O	4.46	C22	SER A 178 OG	3.07

C24	LEU B 248 O	4.45	C8	SER A 178 OG	4.77
C23	LEU B 248 O	3.76	C1	SER A 178 OG	4.49
C22	LEU B 248 O	3.99	C22	SER A 178 CB	4.21
N3	LEU B 248 C	4.7	O7	SER A 178 CB	4.29
C23	LEU B 248 C	4.72			
N3	LEU B 248 CA	4.93			
C24	LEU B 248 CA	4.94			
C23	LEU B 248 CA	4.93			
C29	LEU B 248 N	4.72			
C26	LEU B 248 N	5			
C25	LEU B 248 N	4.3			
C24	LEU B 248 N	4.76			
C23	LEU B 248 N	4.83			
C29	GLN B 247 CG	4.99			
C28	GLN B 247 CG	4.39			
C27	GLN B 247 CG	4.57			
C29	GLN B 247 CB	4.14			
C28	GLN B 247 CB	3.87			
C27	GLN B 247 CB	4.03			
C26	GLN B 247 CB	4.49			
N1	GLN B 247 CB	4.73			
C25	GLN B 247 CB	4.52			
C29	GLN B 247 CA	4.6			
C28	GLN B 247 CA	4.77			
C25	GLN B 247 CA	4.91			
C29	GLN B 247 N	3.92			
C28	GLN B 247 N	4.39			
C25	GLN B 247 N	4.4			
C29	GLY B 246 C	4.66			
N3	GLY B 246 CA	4.85			
C29	GLY B 246 CA	4.45			
C25	GLY B 246 CA	4.97			
C11	LEU B 242 CD2	3.18			
O3	LEU B 242 CD2	4.58			
O2	LEU B 242 CD2	4.59			
C11	LEU B 242 CD1	4.86			
O2	LEU B 242 CD1	4.77			
C11	LEU B 242 CG	3.95			
O2	LEU B 242 CG	4.46			
C11	LEU B 242 N	4.81			
N3	CYS B 241 SG	4.23			
N2	CYS B 241 SG	4.93			
C23	CYS B 241 SG	4.47			
C22	CYS B 241 SG	4.08			
C9	CYS B 241 SG	4.66			
C7	CYS B 241 SG	4.02			
C4	CYS B 241 SG	4.5			
C3	CYS B 241 SG	3.97			
C2	CYS B 241 SG	4.99			
C1	CYS B 241 SG	4.08			
N3	CYS B 241 CB	4.91			
N2	CYS B 241 CB	4.88			
C23	CYS B 241 CB	4.93			
C22	CYS B 241 CB	4.08			
C11	CYS B 241 CB	4.73			
O3	CYS B 241 CB	4.56			
O2	CYS B 241 CB	4.79			
O1	CYS B 241 CB	4.91			
C9	CYS B 241 CB	4.16			
C8	CYS B 241 CB	4.09			

C7	CYS B 241 CB	4.55			
C5	CYS B 241 CB	4.65			
C4	CYS B 241 CB	3.93			
C3	CYS B 241 CB	3.95			
C2	CYS B 241 CB	3.97			
C1	CYS B 241 CB	4.07			
C11	CYS B 241 O	4.47			
C11	CYS B 241 C	4.64			
C10	VAL B 238 CB	4.77			
O1	VAL B 238 CB	4.85			
C10	VAL B 238 O	3.21			
C9	VAL B 238 O	4.98			
C10	VAL B 238 C	4.03			
O1	VAL B 238 C	4.37			
C10	VAL B 238 CA	4.49			
O1	VAL B 238 CA	4.45			
C10	TYR B 202 OH	3.57			
C10	TYR B 202 CZ	4.93			
C21	VAL A 181 CG2	3.57			
C20	VAL A 181 CG2	4.07			
O7	VAL A 181 CG2	4.77			
O6	VAL A 181 CG2	4.82			
C21	VAL A 181 CB	4.59			
C21	VAL A 181 CA	4.64			
C21	VAL A 181 N	3.7			
C21	ALA A 180 CB	4.73			
C21	ALA A 180 O	4.96			
C21	ALA A 180 C	4.01			
C21	ALA A 180 CA	3.75			
O6	ALA A 180 CA	4.7			
O5	ALA A 180 CA	4.59			
C21	ALA A 180 N	4.54			
C21	THR A 179 O	3.62			
C13	THR A 179 O	4.99			
C21	THR A 179 C	4.5			
O6	THR A 179 C	4.94			
O5	THR A 179 C	4.49			
C27	SER A 178 OG	3.79			
C26	SER A 178 OG	3.15			
C24	SER A 178 OG	4.5			
C26	SER A 178 CB	4.34			
N1	SER A 178 CB	4.94			

CHAPTER 6

In silico inspired design of urea noscapine congeners as anticancer agent: chemical synthesis and experimental evaluation based on in vitro using breast cancer cells and in vivo using xenograft mice model

6.1. Introduction

Tubulin remains a promising target for anti-cancer therapy. This is well validated by the already approved clinically used drug classes such as toxoids and vincas. Microtubule-targeted therapeutics that are now in clinical trials have proven to be effective chemotherapeutic agents in the treatment of a variety of human cancers. However, because of their lack of selectivity for cancer cells, these agents are highly toxic. As a result, there is an urgent need for drugs that are selective in their function, have minimal side effects, and have better pharmacological properties.

Noscapine, an opium-derived phthalide isoquinoline alkaloid drug known as a safe antitussive due to its ability to cross the blood-brain barrier. Despite it bind to opioid receptor it lacks hypnotic or euphoric properties which makes it non-addictive. It has been reported to bind stoichiometrically to tubulin dimer, block cell cycle progression at the G2/M transition and cause cancer cell death (Ye *et al.*, 1998). Since its identification as an anticancer drug, numerous synthetic derivatives of noscapine (known as noscapinoids) have been created with better therapeutic indices and pharmacological characteristics (Anderson *et al.,* 2005; Zhou *et al.*, 2005; Zhou *et al.*, 2003; Aneja *et al.*, 2006b; Naik *et al.*, 2011a; Santoshi *et al.,* 2011; Manchukonda *et al.,* 2013; Santoshi *et al.,* 2015). Some analogues of noscapine have also been reported to trigger apoptosis and DNA damages by ROS dependent manner but independent of caspases (Karna *et al.*, 2010; Pannu *et al.,* 2012). Microtubule (MT)-interacting agents of this novel class differ from presently utilized anti-MT (MT-over polymerizing taxanes and MT-depolymerizing vincas) as the compounds have different therapeutic approaches. Although they decrease MT dynamics, noscapinoids do not affect the general organization/integrity or the post-mitotic activities of MTs (Naik *et al.,* 2011b; Zhou *et al.*, 2002a; Landen *et al.*, 2002; Joshi *et al.,* 2010). These drugs have a different effect on cancer cells than they do on normally dividing cells (which just stop mitosis when drugs are exposed), and their pharmacokinetics are better (clearance in 6-10 hours, Aneja *et al.,* 2007a; Aneja *et al.*, 2010a) and it sends cancer cells into apoptosis while healthy cells go back to division as usual (Landen *et al.*, 2002; Landen *et al.*, 2004). They are poor substrates for drug efflux pumps (polyglycoproteins and MDR-related proteins) (Zhou *et al.,* 2005) that play a role in drug resistance. They bind tubulin at a different location than taxanes (Checchi *et al.*, 2003; Naik *et al.,* 2011a), increased taxane treatment and toxicities to taxane-resistant cancer cells. They don't appear to be harmful to the immune system or the nervous system. (Aneja *et al.,* 2010b). Noscapine was found to inhibit the growth of murine

lymphoma, melanoma, and human breast cancers transplanted in nude mice with low or no damage to critical organs or hematological parameters.

This research aims to generate a new class of noscapinoids by selectively connecting the urea pharmacophore to the noscapine scaffold and screening the potential derivatives. These compounds were subsequently chemically synthesized and their anticancer efficacy was confirmed by cellular activity, utilizing two human breast cancer cell lines, MCF-7 and MDA-MB-231, as well as a panel of primary breast cancer cells from patients. These novel derivatives were found to bind tubulin heterodimer with enhanced binding affinity, efficiently suppress cancer cell growth, and cause cancer cells to go into selective G2/M arrest.

6.2. Materials and Methods

6.2.1. Designing of urea congeners of noscapine

Urea noscapine congeners have gained significant interest by chemists and biologists due to their wide range of biological activities, such as anticonvulsant activity, colchicine-binding antagonist, and CXCR3 antagonist (Shimshoni *et al.,* 2007; Fortin *et al.,* 2007; Watson *et al.,* 2008). It was also reported that anticancer drugs with fragments of aryl-urea such as sorafenib (**1**), lenvatinib (**2**), tivozanib (**3**), etc. (Figure 6.1) are already in the clinic. These anticancer drugs effectively inhibit cell proliferation of human hepatocellular carcinoma, advanced renal cell carcinoma, lung cancer, leukemia, prostate cancer, and other malignant neoplasms (Cowey, 2013; Keating, 2017; Frampton, 2016; Džolić *et al.,* 2016). In addition, the conjugation of urea pharmacophore helps in improving the pharmacological and pharmacokinetic profiles of some drugs (Mounetou *et al.,* 2001; Fortin *et al.,* 2007; Li *et al.,* 2009; Viswas *et al.,* 2019; El-Naggar *et al.,* 2018). Therefore, we strategically coupled the urea pharmacophore at the C-9 position of noscapine scaffold to develop a panel of urea noscapine congeners (Figure 6.2).

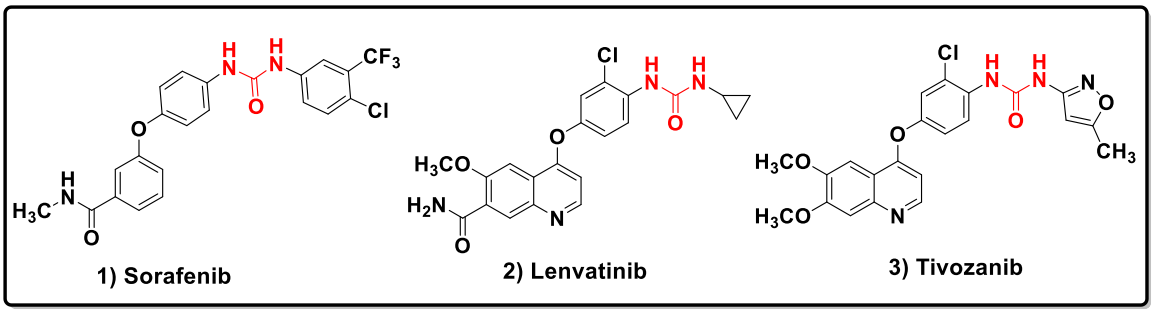

Figure 6.1: *Anticancer drugs in the clinic with urea pharmacophore.*

(A)

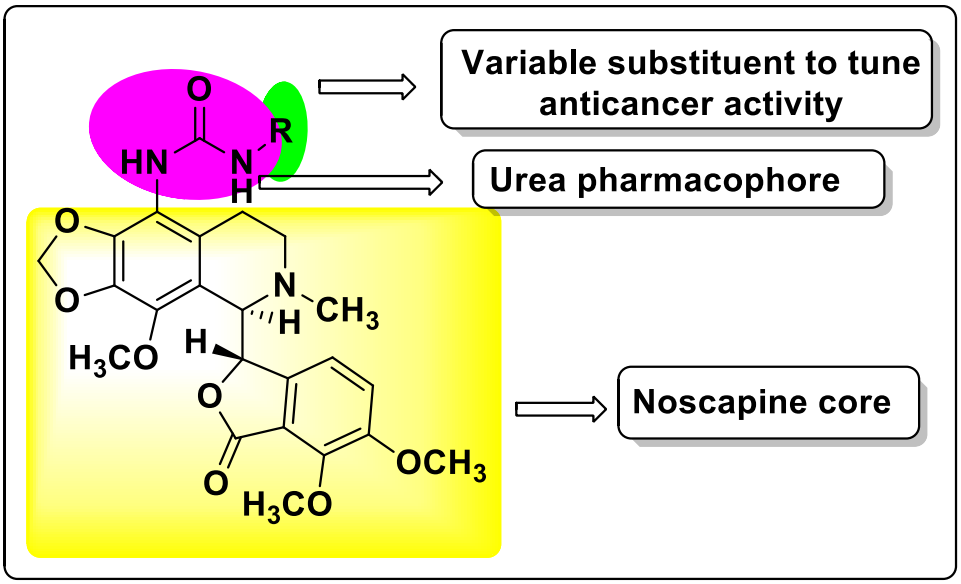

(B)

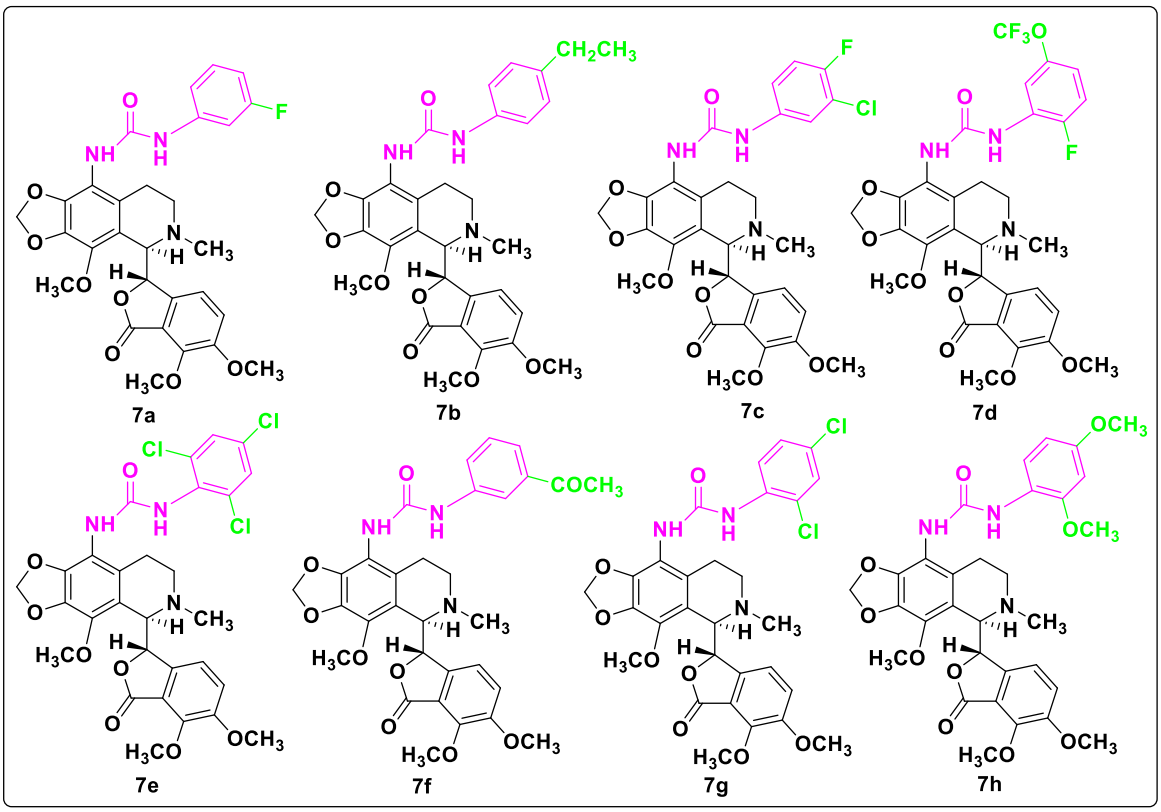

Figure 6.2: *(A) General scheme for strategic development of urea noscapine congeners by substitution of various functional groups at C-9 position of the noscapine scaffold. (B) The functional groups substituted to the scaffold structure to generate a panel of 8 urea noscapine congeners.*

6.2.2. Protein preparation

The PDB structure (PDB ID: 6Y6D; Oliva *et al.*, 2020) of tubulin heterodimer was used in the study. Although the crystal structure of tubulin has been generated at high resolution (2.20 Å), it has certain errors like missing hydrogen atoms and missing side chain atoms of some amino acids. The missing hydrogen atoms were added and the structure was preprocessed using a multistep procedure of protein preparation wizard (Schrödinger, Inc., NY). The missing side chain atoms of the amino acids were identified using Prime side chain prediction tool and repaired using Prime (Schrödinger, Inc., NY). Furthermore, the structure was refined by energy minimization using Macromodel (Schrodinger) and OPLS 2005 force field. Polak-Ribiere Conjugate Gradient (PRCG) algorithm with an energy gradient of 0.01 kcal/mol was used for the energy minimization.

6.2.3. Preparation of molecular structure of urea noscapine congeners

The molecular structure of urea noscapine congeners **7a-7h** (Figure 6.2B) were built using ChemDraw and imported into Maestro (Schrödinger package). The molecular structures were energy minimized using Macromodel (Schrödinger package) and OPLS 2005 force field with PRCG algorithm (energy gradient of 0.001). The structures were geometric optimized using hybrid density functional theory (DFT) with Becke's three-parameter exchange potential and the Lee-Yang-Parr correlation functional (B3LYP) with basis set 6-31G* using Jaguar (Schrödinger, package). Further, the various conformations were generated using Ligprep (Schrödinger package).

6.2.4. Molecular docking of urea noscapine congeners

The prepared structures of urea noscapine congeners **7a-7h** were docked with αβ-tubulin heterodimer using Glide (Schrödinger package) as reported previously (Naik *et al*, 2011a). Glide grid-receptor generation program was used to create a grid box of size 20Å x 20Å x 20Å at the centroid of the co-crystal ligand, amino-noscapine. All the molecules **7a-7h** were docked into the binding site using Glide XP (extra precision) and their binding poses were evaluated using a Glide XP_{Score} function (Friesner *et al.*, 2004; Halgren *et al.*, 2004). The single best conformation for each ligand was considered for further analysis.

6.2.5. Molecular dynamics simulation

Molecular dynamics (MD) simulation of the complexes of tubulin and urea noscapine congeners **7a-7h** in the presence of GTP, GDP and magnesium were carried

out using GROMACS 2019.2 package (Abraham *et al.,* 2015). The docked conformation of the complex with the lowest minimum docking score was taken as the initial conformation for MD simulation. The protein was processed by Gromacs with AMBER 999SB force field (Hornak *et al.,* 2006) to generate coordinates and topology files. Parameters for all the 3 ligands (GTP, GDP and **7a-7h**) were estimated using a general amber force field (GAFF) (Wang *et al.,* 2004) implemented in antechamber program of Amber 18. All atomic point charges were calculated using AM1-BCC charge model (Jakalian *et al.,* 2002). Topologies and internal coordinates for all ligands were generated using tleap program of Amber 18 and ACPYPE software (Sousa da Silva and Vranken, 2012). The complex was solvated with a tip3p water model in a truncated octahedron box with the distance of 12 Å between the atoms of protein and the wall of the box. Counter ions at physiological ionic strength (0.15 M) neutralized the system. Energy minimization was performed using the Steepest descent method of 10000 steps to release conflicting contacts. After applying position restraints of 10 kcal/Å^2 on protein and ligands, NVT equilibration of 500 ps run was done at 300 K, followed by NPT equilibration of 500 ps with Parrinello-Rahman barostat at reference pressure of 1 bar. After equilibration, production MD run was performed for 100 ns with a time step of 2 fs. Particle-mesh Ewald algorithm (PME) was used for long-range electrostatic interactions. Short-range electrostatics and van der Waals cut offs were set at 10 Å. The bonds were constrained using a shake algorithm (Ryckaert *et al.,* 1977) and a modified Berendsen thermostat was used to regulate the temperature of the system. The atomic coordinates were recorded every 20 ps during the MD simulation. Gromacs tools were used to analyze trajectories for Root Mean Square Deviation (RMSD), Radius of gyration (Rg) and Root Mean Square Fluctuation (RMSF). All plots were generated using GRACE software. The complex with the lowest minimum total energy from the MD trajectory was used to elucidate the binding mode of the ligand.

6.2.6. Prediction of binding free energy using MM-PBSA technique

Predicted binding free energy of urea noscapine congeners **7a-7h** with tubulin was calculated based on Molecular Mechanics Poisson-Boltzmann Surface Area (MM-PBSA) (Kollman *et al.*, 2000). From the last 10 ns of MD trajectory, 500 snapshots were extracted with a time step of 20 ps and the ensemble average of the $\Delta G_{bind,pred}$ was determined using g_mmpbsa tool (Kumari *et al.,* 2014) as follows:

$$\Delta G_{bind,pred} = \Delta G_{complex} - [\Delta G_{Rec} + \Delta G_{lig}]$$

$$G = E_{gas} + G_{sol} - TS.$$

$$E_{gas} = E_{int} + E_{ele} + E_{vdw}$$

$$G_{sol} = G_{PB(GB)} + G_{sol\text{-}np}$$

$$G_{sol\text{-}np} = \gamma SAS$$

Where, G is Gibbs free energy, E_{gas} is the gas phase energy calculated as the sum of internal energy (E_{int}), energy generated as a result of the electrostatic interaction (E_{ele}) and the van der Waals interaction (E_{vdw}). G_{sol} is the solvation free energy calculated as the sum of polar (G_{PB}) and nonpolar contributions ($G_{sol\text{-}np}$). Polar interaction contribution (G_{PB}) was calculated as the summation of electrostatic contribution (E_{ele}) and polar solvation contribution (G_{PB}). The nonpolar solvation contribution ($G_{sol\text{-}np}$) is approximated as linearly dependent on the solvent accessible surface area (SAS) and γ is the surface tension constant that was set to 0.0072 kcal mol^{-1} $Å^{-2}$. Inspired by the high predicted binding affinity with tubulin compared to noscapine based on the docking score and the predictive free energy of binding using MM-PBSA, we have chemically synthesised a panel of urea noscapine congeners **7a-7h** for their experimental validation.

6.2.7. Predicted ADME properties

The QikProp program (Schrodinger package) was used to predict a set of 44 ADME (absorption, distribution, metabolism, and excretion) properties of urea noscapine congeners. Some properties having zero values were manually deleted. The program also evaluates the acceptability of the compounds based on the Lipinski's rule of 5 (number of violations of Lipinski's rule of five) which is essential for rational drug design. Poor absorption or permeation are more likely when a ligand molecule violates Lipinski's rule of five i.e., has more than 5 hydrogen bond donors, the molecular weight is over 500, the log P is over 5 and the sum of N's and O's is over 10.

6.2.8. Chemical synthesis of urea noscapine congeners

The urea noscapine congeners **7a-7h** were chemically synthesized by strategically coupling isocyanates with 9-aminonoscapine. In general, chemical synthesis of noscapine derivatives is a bit tricky due to the presence of a highly sensitive C-C bond connecting two heterocyclic phthalide and isoquinoline units in the scaffold. We have optimized the reaction conditions for the synthesis of urea-noscapine conjugates without affecting the sensitive C-C bond. The synthetic scheme is depicted below. Using natural

α-noscapine **(4)** as starting material, 9-bromonoscapine **(5)** was synthesized (Figure 6.3) in excellent yield (90%) using bromine water (48% aq. HBr) by modifying the reaction conditions described in the literature (Aneja *et al.,* 2006a; Verma *et al.,* 2006; Aneja *et al.,* 2006b). It was further converted to 9-aminonoscapine **(6)** with CuI, Sodiumazide, L-Proline in DMSO at 135 ^{o}C for 3 h in 62% yield (Figure 6.3). The reaction scheme used here is different from our previously reported facile synthesis of 9-aminonoscapine (Manchukonda *et al.,* 2012). The reaction conditions embraced do not influence the sensitive C-C bond. Approximately weighed alkyl/aryl isocyanate (**7a-h**) (1.2 mmol) were added to the solution of 9-aminonoscapine, **6** (1.0 mmol) in DCM (10 mL), and stirred for 12 h at room temperature. After the completion of the reaction (judged by TLC), the contents were washed with brine solution. The organic layer was collected and passed through a Na_2SO_4 bed and later removed under reduced pressure. The crude residue was chromatographed over a triethylamine silica bed, using pet.ether/ethyl acetate (3:2) as eluents, to give pure compounds **7a-h** as solid products (65-90%, Figure 6.4). All the intermediate and final products obtained were structurally characterized by IR, ^{1}H & ^{13}C NMR spectroscopy and mass spectrometry techniques (Appendix 6.1 - 6.24).

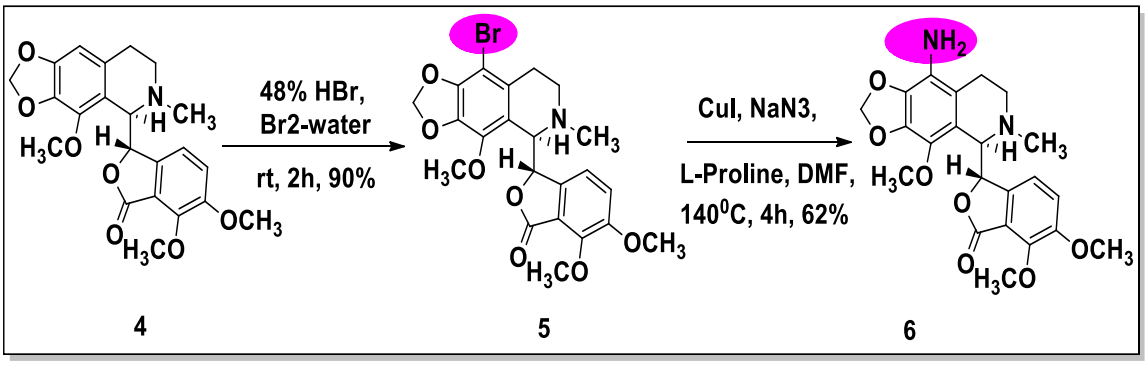

Figure 6.3: *Reaction Scheme 1: Chemical synthesis of 9-bromonoscapine (3) and 9-aminonoscapine (6) using noscapine as starting material.*

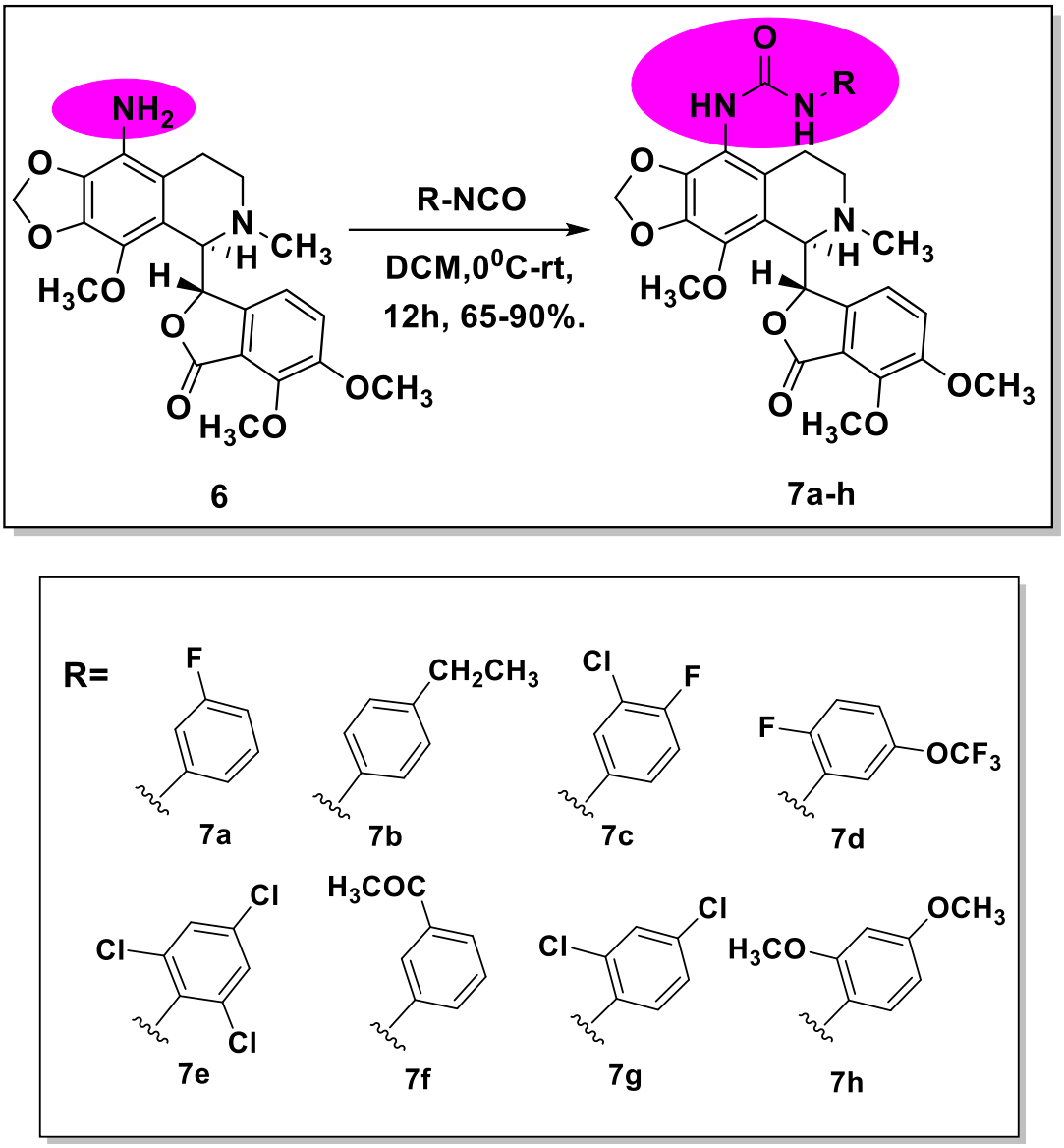

Figure 6.4: *Reaction Scheme 2: Chemical synthesis of urea noscapine congeners* ***7a-7h*** *by coupling of alkyl/aryl isocyanates with 9-aminonoscapine.*

1-((R)-5-((S)-4,5-dimethoxy-3-oxo-1,3-dihydroisobenzofuran-1-yl)-4-methoxy-6-methyl-5,6,7,8-tetrahydro-[1,3]dioxolo[4,5-g]isoquinolin-9-yl)-3-(3 fluorophenyl)urea (7a):

Nature: White solid. mp: 209-211 °C. IR (KBr): 3315, 2929, 2803, 1765, 1624, 1604, 1559, 1495, 1448, 1273, 1034, 1010, 972, 867, 770, 683, 519, 454 cm^{-1}. ^1H NMR (500 MHz, $CDCl_3$): δ 7.95 (bs, 1H, -NH), 7.35 (d, *J* = 11.1 Hz, 1H, Ar-H), 7.15-7.06 (m, 2H, Ar-H), 7.02 (d, *J* = 7.9 Hz, 1H, Ar-H), 6.94 (bs, 1H, -NH), 6.64 (t, *J* = 8.08 Hz, 1H, Ar-H), 6.51 (d, *J* = 8.0 Hz, 1H, Ar-H), 5.89 (d, *J* = 3.8 Hz, 2H, O-CH_2-O), 5.53 (d, *J* = 4.1 Hz, 1H, Ar-CH, (C_3- phthalide)), 4.36 (d, *J* = 4.1 Hz, 1H, Ar-CH, (C_5'- isoquinoline)), 4.04 (s, 3H, -OCH_3), 3.87 (s, 3H, -OCH_3), 3.82 (s, 3H, -OCH_3), 2.77-2.66 (m, 1H, -CHH- N-CH_3 (C_7'-isoquinoline)), 2.58-2.46 (m, 4H, -CHH-N- CH_3 (C_7'-isoquinoline), -

N-CH_3), 2.42-2.29 (m, 1H, Ar- CHH (C_8'-isoquinoline)), 2.07-1.89 (m, 1H, Ar-CHH (C_8'-isoquinoline)). ^{13}C NMR (75 MHz, $CDCl_3$): δ 168.4, 164.1, 161.7, 153.9, 152.2, 147.3, 144.7, 140.9, 140.7 (d, J_C-F= 11.0 Hz), 139.4 (d, J_C-F= 19.8 Hz), 134.1, 129.7(d, J_C-F=9.5Hz), 129.4, 119.0, 118.2, 114.4, 114.0, 111.3, 109.3(d, J_C-F=21.2Hz), 106.5(d, J_C-F= 25.6 Hz), 101.4, 81.5, 62.1, 61.0, 59.1, 56.6, 48.2, 44.7, 22.6. MS (ESI-MS) *m/z:* 566 $[M+H]^+$ HRMS (ESI) : Calcd for $C_{29}H_{29}FN_3O_8$ $[M+H]^+$: 566.19332, found: 566.19555.

1-((R)-5-((S)-4,5-dimethoxy-3-oxo-1,3-dihydroisobenzofuran-1-yl)-4-methoxy-6-methyl-5,6,7,8-tetrahydro-[1,3]dioxolo[4,5-g]isoquinolin-9-yl)-3-(4-ethylphenyl)urea (7b):

Nature: White solid. mp: 216-218 °C. IR (KBr): 3299, 2932, 2794, 1765, 1621, 1554, 1497, 1445, 1274, 1035, 1010, 971, 938, 819, 678 cm^{-1}. ^{1}H NMR (400 MHz, $CDCl_3$): δ 7.37 (bs, 1H, -NH), 7.24 (d, *J* = 8.3Hz, 2H, Ar-H), 7.08-6.98 (m, 3H, Ar-H), 6.66 (bs, 1H, -NH), 6.40 (d, *J* = 8.1 Hz, 1H, Ar-H), 5.89 (s, 2H, O-CH_2-O), 5.51 (d, *J* = 4.0 Hz, 1H, Ar-H, (C3-phthalide)), 4.34 (d, *J* = 4.0 Hz, 1H, Ar-H, (C_5'-isoquinoline)), 4.04 (s, 3H, -OCH_3), 3.92 (s, 3H, -OCH_3), 3.76 (s, 3H, -OCH_3), 2.70-2.61 (m, 1H, -C*H*H-*N*-CH_3 (C_7'-isoquinoline)), 2.60-2.47 (m, 6H, -CH*H*-*N*-CH_3 (C_7'-isoquinoline), -*N*-C*H*$_3$, -C*H*$_2$-CH_3), 2.37-2.28 (m, 1H, Ar-C*H*H (C_8'-isoquinolone)), 1.96-1.86 (m, 1H, Ar-CH*H* (C_8'-isoquinoline)), 1.17 (t, *J*= 7.58 Hz, 3H, -CH_2-C*H*$_3$). ^{13}C NMR (100 MHz, $CDCl_3$): δ 168.4, 154.4, 152.1, 147.3, 144.5, 141.0, 139.3X2, 136.1, 134.1, 130.0, 128.1, 120.2, 119.4, 118.8, 118.0, 117.1, 111.4, 101.3, 81.8, 62.1, 60.9, 59.2, 56.5, 48.9, 45.5, 28.1, 22.5, 15.6. MS (ESI-MS) *m/z:* 576 $[M+H]^+$ HRMS (ESI): Calcd for $C_{31}H_{34}N_3O_9$. $[M+H]^+$: 576.23404, found: 576.23376.

1-(3-chloro-4-fluorophenyl)-3-((R)-5-((S)-4,5-dimethoxy-3-oxo-1,3-dihydroisobenzofuran-1-yl)-4-methoxy-6-methyl-5,6,7,8-tetrahydro-[1,3]dioxolo[4,5-g]isoquinolin-9-yl)urea (7c):

Nature: White solid. mp: 216-218 °C. IR (KBr): 3314, 2941, 1764, 1620, 1557, 1499, 1447, 1269, 1213, 1037, 880, 796 cm^{-1}. ^{1}H NMR (300 MHz, DMSO): δ 8.53 (bs, 1H, -NH), 7.83 (dd, *J* = 2.4, 6.8 Hz, 1H, Ar- H), 7.39 (s, 1H, -NH), 7.19-7.11 (m, 2H, Ar-H), 7.03 (t, *J* = 8.8 Hz, 1H, Ar-H), 6.35 (d, *J*= 8.2 Hz, 1H, Ar-H), 6.00 (s, 2H, O-CH2-O), 5.51 (d, *J* = 4.1 Hz, 1H, Ar-CH, (C3-phthalide)), 4.39 (d, *J*= 4.1 Hz, 1H, Ar-CH, (C5' isoquinoline)), 4.03 (s, 6H, 2x -OCH3), 3.88 (s, 3H, -OCH3), 2,69-2,56 (m, 1H,-C*H*H-*N*-CH3 (C7'-isoquinoline)), 2.55-2.42 (m, 4H, -CH*H*-*N*-CH3 (C7'- isoquinoline), -*N*-C*H*3),

2.37-2.26 (m, 1H, Ar-C*H*H (C8'- isoquinoline)), 1.88-1.7 (m, 1H, Ar-CH*H* (C8'-isoquinoline)). ^{13}C NMR (75 MHz, $CDCl_3$): δ 167.7, 154.2, 153.2, 151.5, 151.0, 146.5, 143.6, 140.2, 138.4, 136.2, 133.7, 129.8, 119.9, 119.7, 119.0, 118.4 (d, *J*C-F = 20.3 Hz), 117.3 (d, *J*C-F = 6.6 Hz), 116.5, 115.8 (d, *J*C-F = 21.4 Hz), 111.5, 100.7, 81.4, 61.5, 60.3, 58.9, 56.0, 49.0, 45.6, 22.8. MS (ESI-MS) *m/z:* 600 $[M+H]^+$. HRMS (ESI): Calcd for $C_{29}H_{28}ClFN_3O_8$ $[M+H]^+$: 600.15435, found: 600.15492.

1-((R)-5-((S)-4,5-dimethoxy-3-oxo-1,3-dihydroisobenzofuran-1-yl)-4-methoxy-6-methyl-5,6,7,8-tetrahydro-[1,3]dioxolo[4,5-g]isoquinolin-9-yl)-3-(4-isopropylphenyl)urea (7d):

Nature: White solid. mp: 233-235 °C. IR (KBr): 3277, 2955, 2793, 1761, 1622, 1557, 1497, 1445, 1272, 1036, 1010, 972, 815, 672cm^{-1}. ^{1}H NMR (400 MHz, $CDCl_3$ δ 7.25 (d, *J* = 8.4 Hz, 2H, Ar-H), 7.09 (d, *J* = 8.4 Hz, 2H, Ar-H), 7.00 (d, *J* = 8.3 Hz, 1H, Ar-H), 6.56 (bs, 1H, -NH), 6.40 (d, *J* = 8.3 Hz, 1H, Ar-H), 5.90 (s, 2H, O- CH2-O), 5.51 (d, *J* = 4.0 Hz, 1H, Ar-CH, (C3- phthalide)), 4.35(d, *J* = 4.0 Hz, 1H, Ar-CH, (C5'-isoquinoline)), 4.04 (s, 3H, CH3), 3.91(s, 3H, -OCH3), 3.75 (s, 3H, -OCH3), 2.88-2.77 (m, 1H, -C*H*(CH3)2), 2.72-2.62 (m, 1H, -C*H*H-*N*-CH3 (C7'-isoquinoline)), 2.59-2.47 (m, 4H, -CH*H*-*N*-CH3 (C7'-isoquinoline), -*N*- C*H*3), 2.39-2.29 (m, 1H, Ar-C*H*H (C8'-isoquinoline)), 1.98-1.86 (m, 1H, Ar-CH*H* (C8'-isoquinoline)), 1.19 (d, *J* = 6.8 Hz, 6H, -CH(C*H*3)2). ^{13}C NMR (100 MHz, $CDCl_3$): δ 168.4, 154.4, 152.1, 147.2, 144.6, 143.9, 141.0, 139.3, 136.2, 134.1, 130.0, 126.7, 120.1, 119.4, 118.8, 118.0, 117.1, 111.4, 101.3, 81.9, 62.1, 60.9, 59.2, 56.5, 48.9, 45.6, 33.3, 23.9, 22.6. MS (ESI-MS) *m/z:* 590 $[M+H]^+$. HRMS (ESI): Calcd for $C_{32}H_{36}N_3O_8$ $[M+H]^+$: 590.24973, found: 590.24969.

1-((R)-5-((S)-4,5-dimethoxy-3-oxo-1,3-dihydroisobenzofuran-1-yl)-4-methoxy-6-methyl-5,6,7,8-tetrahydro-[1,3]dioxolo[4,5-g]isoquinolin-9-yl)-3-(2,4,6-trichlorophenyl)urea (7e):

Nature: White solid. mp: 125-127°C. IR (KBr): 3368, 2925, 2805, 1757, 1713, 1659, 1496, 1441, 1270, 1200, 1034, 789, 747 cm^{-1}. ^{1}H NMR (400 MHz, $CDCl_3$): δ 7.31 (s, 2H, Ar-H), 6.99 (d, *J* = 8.3 Hz, 1H, Ar-H), 6.47 (d, *J* = 8.3 Hz, 1H, Ar-H), 5.93 (s, 2H, O-CH2-O), 5.49 (d, *J* = 4.1 Hz, 1H, Ar-CH, (C3-phthalide)), 4.33 (d, *J* = 4.1 Hz, 1H, Ar-CH, (C5'-isoquinoline)), 4.05 (s, 3H, -OCH3), 3.92 (s, 3H, -OCH3), 3.79 (s, 3H, -OCH3), 2.84- 2.75 (m, 1H, -C*H*H-*N*-CH3 (C7'-isoquinoline)), 2.70- 2.58 (m, 1H, -CH*H*-*N*-CH3 (C7'-isoquinoline)), 2.51 (s, 3H, *N*-C*H*3), 2.48-2.39 (m, 1H, Ar-C*H*H (C8'isoquinoline)), 2.12-2.02 (m,1H, Ar-CH*H* (C8'- isoquinoline)). ^{13}C NMR (100

MHz, $CDCl_3$): δ 165.3, 160.2, 151.1, 150.0, 144.6, 142.5, 138.6, 136.6, 132.9, 132.3, 131.2, 129.4, 128.2, 126.0, 117.2, 116.6, 114.2, 110.5, 99.3, 79.3, 59.5, 58.7, 57.3, 54.4, 47.0, 43.7, 20.6. MS (ESI-MS) *m/z:* 652 $[M+H]^+$. HRMS (ESI): Calcd for $C_{29}H_{27}Cl_3N_3O_8$ $[M+H]^+$: 650.08582, found: 650.08880.

1-(3-acetylphenyl)-3-((R)-5-((S)-4,5-dimethoxy-3-oxo-1,3-dihydroisobenzofuran-1-yl)-4-methoxy-6-methyl-5,6,7,8-tetrahydro-[1,3]dioxolo[4,5-g]isoquinolin-9-yl)urea (7f):

Nature: White solid. mp: 207-209°C. IR (KBr): 3371, 3303, 2931, 1760, 1681, 1621, 1554, 1491, 1443, 1274, 1215, 1034, 938, 785, 689, 587cm^{-1}. ^1H NMR (400 MHz, DMSO): δ 8.96 (bs, 1H, -NH), 8.11 (t, *J* = 1.7 Hz, 1H, Ar-H), 7.83 (bs, 1H, -NH), 7.69-7.64 (m, 1H, Ar-H), 7.59-7.53 (m, 1H, Ar-H), 7.41 (t, *J* = 7.9 Hz, 1H, Ar-H), 7.21 (d, *J* = 8.3 Hz, 1H, Ar-H), 6.40 (d, *J*= 8.3 Hz, 1H, Ar-H), 6.05 (d, *J* = 5.7 Hz, 2H, O-CH_2-O), 5.49 (d, *J*= 4.2 Hz, 1H, Ar-CH, (C_3-phthalide)), 4.26 (d, *J* = 4.2 Hz, 1H, Ar-CH, (C_5'-isoquinoline)), 3.96 (s, 3H, -OCH_3), 3.87 (s, 3H, - OCH_3), 3.79 (s, 3H, -OCH_3), 2.66-2.53 (m, 4H, -CH*H*- *N*-CH_3 (C_7' isoquinoline), -*N*-C*H*$_3$), 2.48-2.39 (m, 4H, -C*H*H-*N*-CH_3 (C_7'-isoquinoline), -CO-C*H*$_3$), 2.32-2.22 (m, 1H, Ar-C*H*H (C_8'-isoquinoline)), 1.82-1.72 (m, 1H, Ar-CH*H* (C_8'-isoquinoline)). ^{13}C NMR (125 MHz, $CDCl_3$): δ 197.7, 167.1, 153.2, 151.8, 146.4, 144.2, 140.5, 140.4, 138.4, 137.2, 134.1, 129.6, 128.9, 122.5, 121.6, 119.1, 119.0, 118.4, 117.1, 116.5, 112.4, 101.2, 81.1, 61.4, 60.5, 59.3, 56.3, 48.6, 45.4, 26.6, 22.4. MS (ESI-MS) *m/z:* 590 $[M+H]^+$. HRMS (ESI): Calcd for $C_{31}H_{32}N_3O_9$ $[M+H]^+$: 590.21331, found: 590.21328

1-(2,4-dichlorophenyl)-3-((R)-5-((S)-4,5-dimethoxy-3-oxo-1,3-dihydroisobenzofuran-1-yl)-4-methoxy-6-methyl-5,6,7,8-tetrahydro-[1,3]dioxolo[4,5-g]isoquinolin-9-yl)urea (7g):

Nature: White solid. mp: 109-111°C. IR (KBr): 3339, 2935, 2797, 1746, 1701, 1525, 1444, 1270, 1209, 1043, 1007, 972, 790 cm^{-1}. ^1H NMR (500 MHz, $CDCl_3$): δ 8.21 (d, *J* = 9.0 Hz, 1H, Ar-H), 7.34-7.30 (m, 2H, Ar- H), 7.19 (dd, *J* = 2.4, 9.0 Hz, 1H, Ar-H), 6.99 (d, *J* = 8.2 Hz, 1H, Ar-H), 6.74 (bs, 1H, -NH), 6.43 (d, *J* = 8.2 Hz, 1H, Ar-H), 5.97 (dd, *J* = 1.2, 4.2 Hz, 2H, O-CH_2-O), 5.51 (d, *J*= 4.4 Hz, 1H, Ar-CH, (C_3-phthalide)), 4.35 (d, *J* = 4.4 Hz, 1H, Ar-CH, (C_5'-isoquinoline)), 4.06 (s, 3H, -OCH_3), 3.99 (s, 3H, -OCH_3), 3.80 (s, 3H, -OCH_3), 2.77- 2.70 (m, 1H, -C*H*H-N-CH_3 (C_7'-isoquinoline)), 2.63- 2.55 (m, 1H, -CH*H*-*N*-CH_3 (C_7'-isoquinoline)), 2.51 (s, 3H, *N*-C*H*$_3$), 2.44-2.38 (m, 1H, Ar-C*H*H (C_8'- isoquinoline)), 1.99-1.92 (m, 1H, Ar-CH*H*

(C8'-isoquinoline)). ^{13}C NMR (125 MHz, $CDCl_3$): δ 168.5, 153.5, 152.0, 147.3, 144.5, 141.0, 139.6, 134.3, 134.1, 129.7, 128.4, 127.5, 127.4, 123.0, 121.8, 119.2, 118.7, 117.9, 117.3, 110.8, 101.3, 81.7, 62.0, 60.7, 59.2, 56.4, 48.6, 45.4, 22.2. MS (ESI-MS) *m/z:* 616 $[M+H]^+$. HRMS (ESI): Calcd for $C_{29}H_{28}Cl_2N_3O_8$ $[M+H]^+$: 616.12480, found: 616.12572

1-((R)-5-((S)-4,5-dimethoxy-3-oxo-1,3-dihydroisobenzofuran-1-yl)-4-methoxy-6-methyl-5,6,7,8-tetrahydro-[1,3]dioxolo[4,5-g]isoquinolin-9-yl)-3-(2,4-dimethoxyphenyl)urea (7h):

Nature: White solid. mp: 109-111°C. IR (KBr): 3333, 2940, 2841, 1759, 1617, 1536, 1498, 1450, 1271, 1209, 1123, 1037, 934, 827, 726cm^{-1}. ^{1}H NMR (500 MHz, $CDCl_3$): δ 7.90 (d, *J* = 9.4 Hz, 1H, Ar-H), 6.93 (d, *J* = 8.2 Hz, 1H, Ar-H), 6.82 (bs, 1H, -NH), 6.49-6.44 (m, 2H, Ar-H), 6.34 (d, *J* = 8.2 Hz, 1H. Ar-H), 6.08 (bs, 1H, -NH), 5.97 (dd, *J* = 1.3, 3.6 Hz, 2H, O-CH_2-O), 5.52 (d, *J* = 4.1 Hz,1H, Ar-CH, (C3-phthalide)), 4.38 (d, *J* = 4.1 Hz, 1H, Ar-CH, (C5'-isoquinoline)), 4.07 (s, 3H, -OCH_3), 4.02 (s, 3H, -OCH_3), 3.78 (s, 3H, -OCH_3), 3.76-3.74 (m, 6H, 2 x -OCH_3), 2.74-2.66 (m, 1H, C*H*H-*N*-CH_3 (C7' isoquinoline)), 2.62-2.54 (m, 1H, -CH*H*-*N*-CH_3 (C7'- isoquinoline)), 2.52 (s, 3H, *N*-C*H*3), 2.40-2.32 (m, 1H, Ar-C*H*H (C8'-isoquinoline)), 1.95-1.85 (m, 1H, Ar-CH*H*(C8'-isoquinoline)). ^{13}C NMR (125 MHz, $CDCl_3$): δ 168.1, 156.2, 154.2, 152.1, 149.9, 147.4, 144.5, 140.9, 139.6, 134.2, 130.2, 121.2, 119.5, 118.4, 117.8, 117.6, 111.3, 103.4, 101.3, 98.7, 81.6, 62.1, 60.8, 59.3, 56.4, 55.8, 55.5, 49.0, 45.7, 22.6. MS (ESI-MS) *m/z:* 608 $[M+H]^+$. HRMS (ESI): Calcd for $C_{31}H_{34}N_3O_{10}$. $[M+H]^+$: 608.22387, found: 608.22432

6.2.9. Cell culture and reagents

All the chemicals and reagents for cell culture, including the lead compound noscapine were purchased from Sigma. MCF-7 and MDA-MB-231 human breast cancer cell lines were acquired from the National Center for Cell Science in Pune, Maharashtra, India's cell repository. The urea noscapine congeners **7a-7h** were synthesized, processed using dimethyl sulfoxide (DMSO) and kept at 4 °C until needed. The cells were cultured in Dulbecco's modified Eagle medium (DMEM, Sigma-Aldrich) with 10% fetal bovine serum (FBS) and antibiotics at 37 °C, 5% CO_2, and 95% humidity. Cells with 70-80% confluence were subcultured by trypsinization for bioassays.

6.2.10. In vitro cell proliferation assay using MCF-7 and MDA-MB-231 cell lines

The cell proliferation experiment was carried out in 96-well plates as previously described, utilizing two human breast cancer cell lines, MCF-7 and MDA-MB-231 (Naik et al, 2011b). Briefly, cells were cultured at 37 °C in a humidified environment with 5% CO_2 in culture media supplemented with 10% fetal bovine serum, 1% penicillin/streptomycin, and 2 mM l-glutamine. In 96-well plates, suspension cells were used at a density of 5 x 10^3 cells per well and were treated with noscapine and its urea congeners **7a-7h** in a gradient concentration of 5 µM to 100 µM. Next, the cells were fixed in trichloracetic acid (50%) before being stained with Sulforhodamine B (0.4% in 1%) solution. Once the cells had been cleaned with 1% acetic acid, the dye that had remained unbound was removed. To remove the protein-bound dye, 10 mM Tris base was used. An optical density at 564 nm was measured with a SPECTRAmax PLUS 384 microplate spectrophotometer. The IC_{50} values, which denote the concentration of drug needed to kill 50% of cells, were determined.

6.2.11. Primary breast cancer cells (PBCs) culture and in vitro cell proliferation assay

In an aseptic environment condition, primary breast cancer cells were collected from four different individuals with various stages of breast cancer. The tumor tissues were treated with 0.25 percent trypsin and filtered using a 70 micron filter before being centrifuged at 2000 rpm for 3 minutes in serum-free media. The filtered cells were collected, plated in T25 flasks, and cultured with complete DMEM media, supplemented with 10% FBS and 1% penstrip (combination of penicillin and streptomycin) at 37 °C under 5% CO_2. A fresh media was added every 3-4 days, and additional passaging was carried out under the same circumstances as described above. The cultures were kept at sub-confluence between three and eight passes to ensure homogenous cell type. Prior to any experimental treatments, cells were allowed to attain 80-90 percent confluence. After the primary cells had reached confluence, they were plated in 96-well plates at a density of 2000 cells per well using DMEM as the usual growth medium (low glucose). The cells were kept at 37 ^oC in a humidified environment with 5% CO_2 and exposed to a gradient of concentrations of noscapine and its urea congeners **7a-7h** (5 µM to 100 µM) for 72 hours. The sulforhodamine B (SRB) test was used to measure cell proliferation with a colorimeter. SRB-exposed cells were washed to remove unbound dye and 1mM tris, and absorbance (optical density) recorded with a microplate reader (Molecular Devices, Sunnyvale, CA) at a wavelength of 564 nm. When plotting the percentage of cells that survived against drug concentration, the IC_{50} value was discovered.

6.2.12. Flow cytometry analysis of cell cycle progression

DMEM with 4.5 g/L glucose and L-glutamine, 10% fetal bovine serum, and 1% penicillin/streptomycin was used to sustain MDA-MB-231 cells. Cells were cultured at a temperature of 37 °C in a 5% CO_2 environment. One of the promising urea noscapine congener, **7g** was dissolve in a 1% phosphate buffer saline and used to treat cells. Flow cytometry was used to analyze cells collected after 24 and 48 hours and then analyzed using the data obtained from the experiment. For this experiment, 2 x 10^6 cells were centrifuged, twice rinsed in ice-cold PBS, and then fixed in 70 percent ethanol. The cell pellets were kept in tubes at -20 ^oC for 24 hours. After that, the cells were centrifuged at 1000 x g for 10 minutes, and the supernatant was discarded. Next, cells were cleaned with 5 ml of PBS and incubated for 45 minutes in the dark with 0.5% Propidium Iodide in 0.6% Triton-X in PBS and 0.5% RNase A. The cell cycle was tracked using a flow cytometer (BD FACS Aria-III).

6.2.13. Flow cytometry analysis for apoptosis assay

Choline phospholipids (phosphatidylcholine, sphingomyelin) are found on the exterior leaflet of the lipid bilayer under physiological conditions, whereas aminophospholipids (phosphatidylserine, phosphatidylethanolamine) are only found on the cytoplasmic surface of the lipid bilayer. When phosphatidylserine (PS) is exposed on the outer leaflet of the membrane during apoptosis, this asymmetry is disrupted. The detection of PS using fluorochrome-tagged 36 KDa anticoagulant protein Annexin V allows for an accurate assessment of apoptotic incidence. This probe reversibly binds to phosphatidylserine residues only in the presence of mM concentration of divalent calcium ions. The Annexin-V-FITC apoptosis detection technique was used using Apoptosis detection kit (Sigma –Aldrich, USA) according to the manufacturer's instructions to detect Apoptosis in cancer cells. The Apoptotic Index (AI) of the breast cancer cell lines MCF-7 and MDAMB-231 was assessed using a formula that divides the proportion of apoptotic cells by the total number of cells. On a 12-well culture plate, 3 x 10^4 cells were seeded and cultured in full media for 24 hours. To determine the induction of apoptosis, the cells were incubated with the most promising derivative of the series **7g** at its IC_{50} concentration for 48 hours. Typhinized cells were stained with surface marker antibodies (biotin-conjugated Annexin V, FITC-conjugated streptavidin) and propidium iodide (PI). The cells were suspended in 1X binding buffer and treated with an Annexin V FITC conjugate for 20 minutes at room temperature in the dark. Data from a flow cytometer using PI excitation at 488 nm and emission at 530 nm was obtained. There

were four types of apoptotic/necrotic cells detected and their percentages determined: those that were still alive (Annexin V+/PI+), those that had already started to die (Annexin V+/PI), and those that had already died (Annexin V+/PI+).

6.2.14. Hoechst, Acridine orange (AO) & ethidium bromide (Etbr) staining

Fluorescence microscopy was used to examine the cell morphology after staining with hoechst, acridine orange and ethidium bromide (Nikon Eclipse Ts2R-FL). Poly-L-lysine-coated coverslips in 6-well plates were used to culture MDA-MB-231 cells, and the urea noscapine congener **7g** was added to the cells for 72 hours. After incubation, coverslips were fixed in cold methanol, rinsed with PBS, stained with hoechst, acridine orange and ethidium bromide and mounted on slides. An inverted fluorescence microscope was used to obtain these images (Nikon Eclipse Ts2R-FL). Changes in the morphology of apoptotic cells vs untreated cells were identified. Cells that have undergone apoptosis were recognized by characteristics associated with that process (e.g. nuclear condensation, formation of membrane blebs and apoptotic bodies).

6.2.15. Detection of Apoptosis by TUNEL assay

Induction of apoptosis to MDA-MB-231 cells with the treatment of **7g** was studied by the TUNEL assay. DNA fragmentation was analyzed with the Apo BrdU TUNEL assay kit from Invitrogen (Carlbad, CA, USA), using fluorescence microscopy. Briefly, cells were grown on 12 well plate and treated with **7g** at IC_{50} concentration. Cells were detached from culture plates centrifuged and pellet was collected. DNA strand break was identified by an Alexa Fluor 488 dye-labelled anti-BrdU antibody. The result displayed a green nuclear fluorescence image.

6.2.16. ROS detection

Increase of intracellular ROS is a quiescent component to damage nucleic acid, cellular lipid membrane, and organelles, which induces apoptosis in cancer cells. The intracellular ROS concentration were analyzed by using the H2DCFDA method. Briefly MDA-MB-231 cells were seeded in 6 well plate containing cover glass and treated with **7g** for 48 hours. In the control, low green fluorescence was observed, whereas in the treated bright green fluorescence was observed after staining and visualization with a fluorescence microscope (Nikon Eclipse Ts2R-FL). The results display the significantly rise in intracellular ROS in the treated cells.

6.2.17. Measurement of mitochondrial membrane potential

The effect of urea noscapine congener, **7g** on mitochondrial membrane potential was detected by using the probe rhodamine-123, JC-1 stain and DAPI stain. Briefly, cells were seeded in 12 well plate followed by treatment with **7g** for 48 hours and stained with rhodamine-123 (15 µg/ml), JC-1 stain (10 µg/ml) and DAPI (10 µg/ml) for 10 minutes at room temperature and visualized. The image was captured using inverted fluorescence microscope (Nikon Eclipse Ts2R-FL). In the untreated cell with rhodamine-123 stained, light green fluorescence was observed, whereas bright green fluorescence was observed in the treated cell. In the case of JC-1 stain, light red fluorescence was detected in untreated cells, whereas in treated cells, bright red fluorescence was observed. Similarly, in DAPI stain, relatively light blue and morphologically similar cells were observed, whereas in treated cells, bright blue with changes in morphological features of cells was observed.

6.2.18. In vivo antitumor effect against MCF-7 breast tumors

The Institutional Animal Ethics Committee approved the study of National Institute of Pharmaceutical Education and Research (NIPER), Hyderabad (1548/PO/Re/2011/CPCSEA). BALB/c athymic nude female mice of 8 to 10 weeks were housed in the Animal Care Facility. The mice were implanted with 1 x 10^6 human epithelial breast adenocarcinoma MCF-7 cells in 0.2 ml of PBS, subcutaneously into the anterior flank. When the implanted tumour was palpable, (7-10 days) treatment of the test compound (**7g**) was administrated by oral gavage. The mice were randomly divided into 2 groups. Group-1 (control) consisted of 5 animals that received daily gavage of vehicle solution (acidified water, pH 4.0) only, Group-2 consisted of 5 animals were treated with **7g** (50 µM/day). Tumor volumes were estimated on alternate days by measuring tumours in three transverse direction diameters with vernier calipers and calculating their volume as Π/6 (length x width x height) (Tomayko and Reynolds, 1989). The control group of mice was euthanized on day 30 owing to their large tumour volumes and served as the endpoint for control animals. Accordingly, this endpoint was used to evaluate tumour size in untreated mice with those administered with **7g**.

6.2.19. Histopathological and hematological analyses

On day 30, both the treated and untreated mice received an overdose (0.2 ml) of 3.5 percent chloral hydrate, blood was drawn from the heart, and CBC analysis was conducted using a CBC analyzer (CDC Technologies, Oxford CT). Following that, the

animals were perfused with a 3% paraformaldehyde and 2% glutaraldehyde combination in PBS (pH 7.4). The vital organs like liver, kidney, lung and heart, and tumour were extracted and analyzed for histological investigation. Tissues were mounted in paraffin, sectioned, and stained with hematoxylin and eosin. The tissues were observed under the microscope for toxicity evaluation.

6.3. Results and Discussion

6.3.1. Urea noscapine congeners accomodated well inside the binding cavity

The eight urea noscapine congeners, **7a-7h** designed in the study and the lead molecule, noscapine, were docked using Glide XP onto the noscapinoid binding site (Oliva et al, 2020) at the interface between α- and β- tubulin. All these molecules were found to fit nicely inside the binding site. Their binding affinity with tubulin is also evaluated using Glide XP_{score} function (Friesner *et al.*, 2004; Halgren *et al.*, 2004). The noscapinoids, **7c-7h** revealed improved docking scores ranging from -9.647 to -6.411 kcal/mol compared to noscapine (docking score is -5.213 kcal/mol) (Table 6.1). The docked complexes of these ligands with tubulin were considered for MD simulation of 100 ns to observe the stability of the complex. The convergence of the MD trajectories was monitored by plotting the root mean square deviation (RMSD) and radius of gyration (Rg) of the backbone C_α atoms with respect to time. The relative fluctuation of the RMSD (0.02 to 0.024 nm) and Rg (2.965 to 2.972 nm) was minimal, suggesting the system's stability (Figure 6.5 and 6.6). Furthermore, the root mean square fluctuations (RMSF) of the residues of tubulin in the bound form with ligands and in the free form were calculated to reveal the flexibility of these residues (Figure 6.7a & 6.7b). It was observed that the RMSF values of the residues in the bound and free form were minimum (0.02 to 0.04 nm) for both α- and β- tubulin, indicating that the residues were more rigid. Overall, the urea derivatives of noscapine **7a-7h** were well accommodated inside the binding site, at the interface between α- and β- tubulin (Figure 6.8). However, their binding modes inside the binding cavity are distinct as shown in the ligplot (Figure 6.9). The differences in binding modes of these noscapinoids are due to various substitutions of functional groups in the scaffold structure and because of differential contribution in binding free energy of amino acids involved in the interactions. As shown in the figure, the most potent urea derivative of noscapine 7g in terms of docking score interacts more intensely with the residues of tubulin than other derivatives. Its binding involved 03 hydrogen bond (Figure 6.9b). Besides hydrogen bonding, a good number of

hydrophobic interactions were involved in binding of **7a-7h** with binding site residues (Appendix table A6.25-A6.28).

Table 6.1: Results of molecular docking of urea congeners of noscapine (**7a-7h**) with tubulin. All the 8 noscapinoids were found to docked well within the binding site. However, only 6 noscapinoids bind with high affinity compared to the lead molecule, noscapine.

Ligands ID	GlideXP$_{score}$ (Kcal/mol)	Glide$_{lipo}$ (Kcal/mol)	Glide$_{evdw}$ (Kcal/mol)	Glide$_{ecoul}$ (Kcal/mol)	Glide $_{emodel}$ (Kcal/mol)	Glide$_{energy}$ (Kcal/mol)
7a	-2.837	-2.837	-15.428	-9.654	40.063	-25.082
7b	-3.193	-7.001	-34.377	-2.928	122.939	-37.306
7c	-6.419	-6.850	-53.968	-2.730	-67.616	-56.699
7d	-7.096	-7.750	-59.412	-4.128	-55.026	-63.541
7e	-6.411	-6.411	-32.753	-5.576	115.302	-38.329
7f	-8.145	-7.915	-57.261	-4.583	-93.547	-61.844
7g	-9.647	-7.347	-53.729	-4.706	-90.844	-58.436
7h	-7.919	-8.276	-67.063	-6.678	-109.602	-73.742
Noscapine	-5.213	-2.543	-33.660	-2.941	-22.080	-41.676

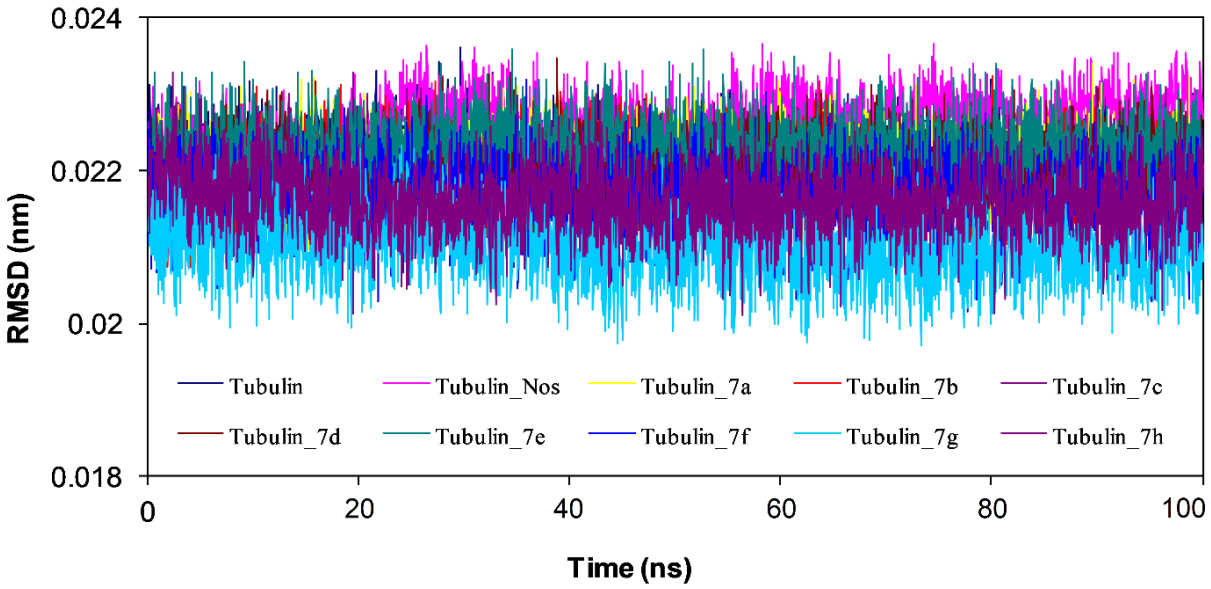

Figure 6.5: *Root mean square deviations (RMSD) of Cα carbon atoms of tubulin only and in complex with urea noscapine congeners (**7a-7h**) during 100 ns of MD simulation. The relative fluctuation in the RMSD of the Cα atoms is very small (0.02 to 0.024 nm.) for the entire duration of the simulation. The time step of 20 ps was used during the simulation that generated 5,000 frames.*

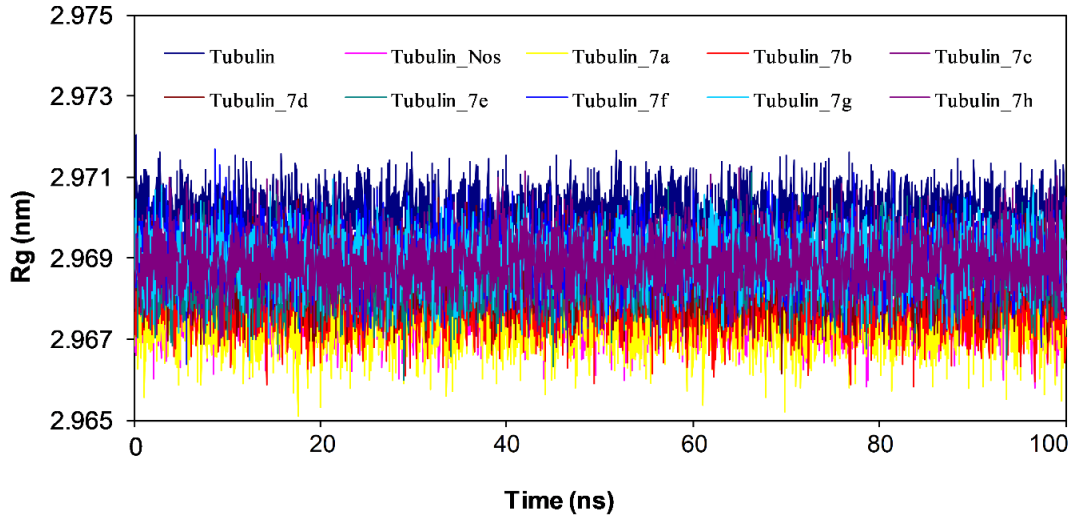

Figure 6.6: *Time evolution of radius of gyration of the tubulin and in complex with urea noscapine congeners (**7a-7h**) over a period of 100 ns of MD simulation. All the molecular systems were found to be stable for the entire duration of the simulation.*

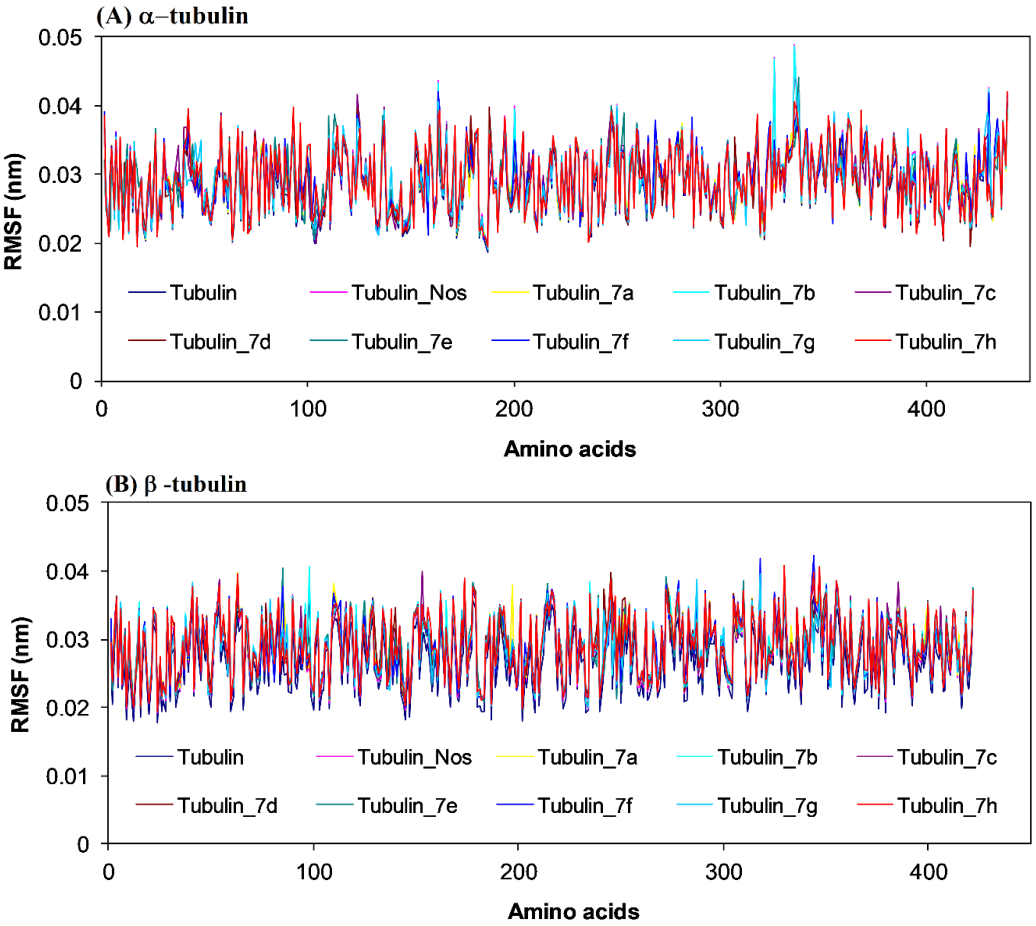

Figure 6.7a&b: *Root mean square fluctuation (RMSF) of the residues of tubulin of the docked ligands in the bound form and in the unbound form of tubulin heterodimer. Different levels of flexibility of these residues were noticed in the free and bound form of tubulin with ligands. All the amino acids showed very low fluctuation (0.02 to 0.04 nm) indicating that most of the residues were rigid both in free and bound form of tubulin.*

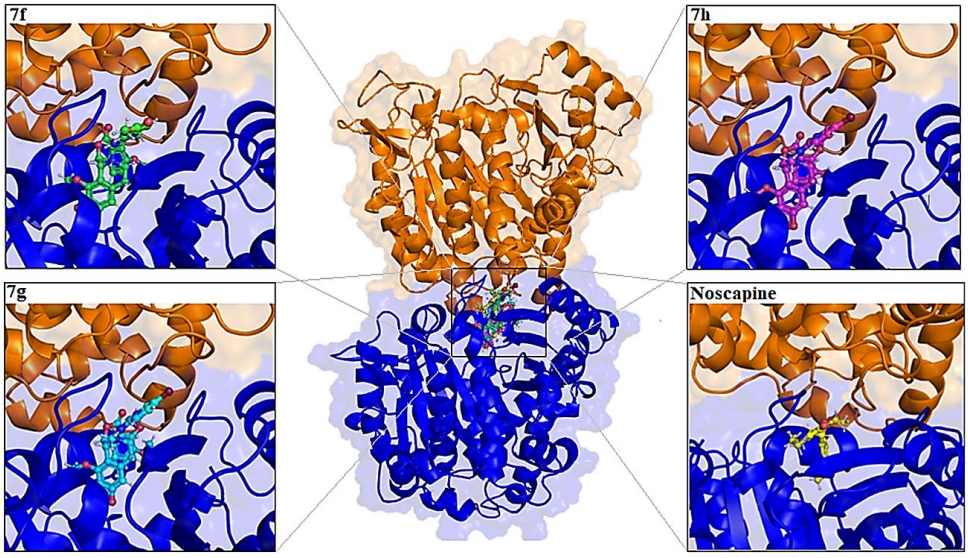

Figure 6.8: *The newly designed urea noscapine congeners (**7f-7h**) are well accommodated inside the noscapine binding site at the interface of α- and β- tubulin. The binding site is represented as macromodel surface according to α- and β- tubulin (α-tubulin is represented in blue colour and β-tubulin is represented in brown colour).*

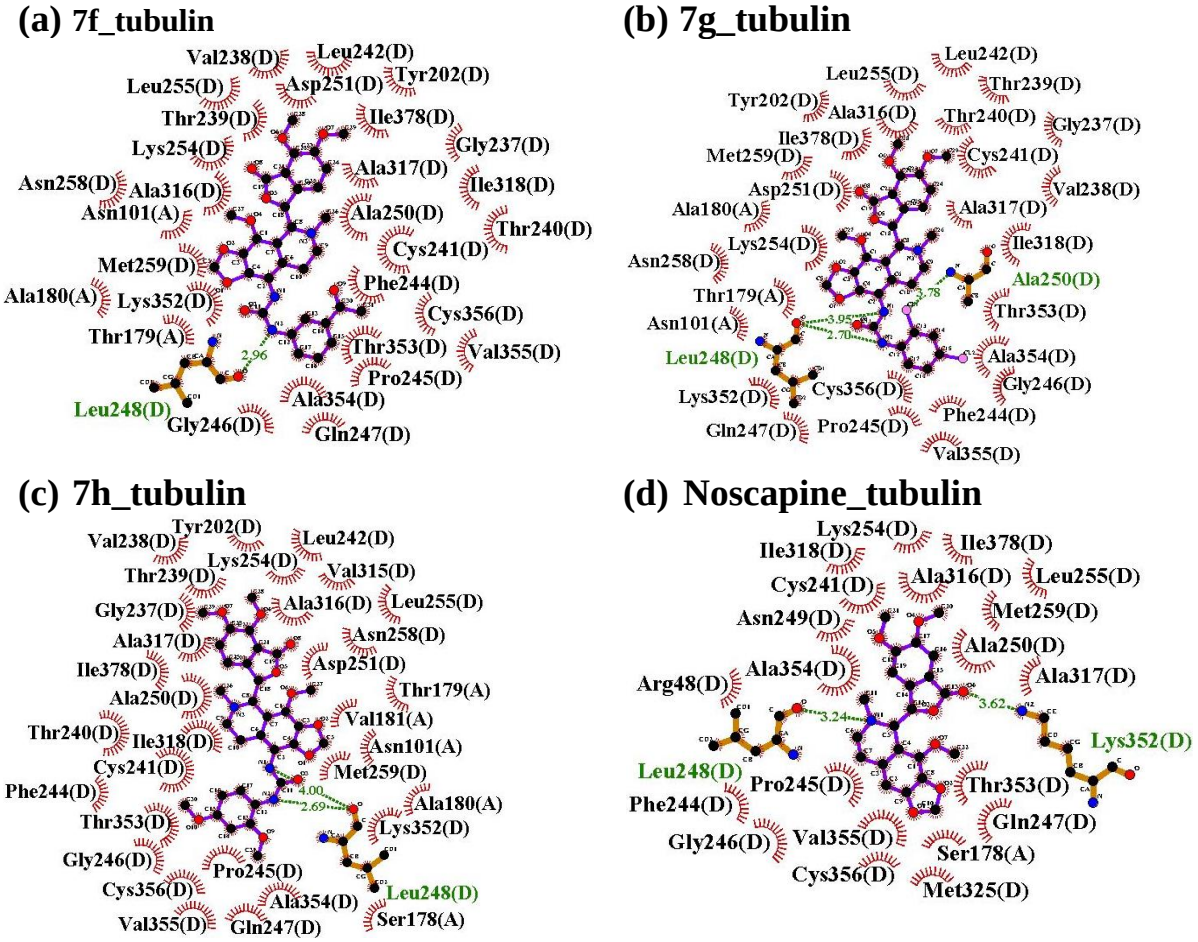

Figure 6.9: *Two dimensional representation of interaction observed between the binding site residues of tubulin with urea noscapine congeners, **(a) 7f, (b) 7g, (c) 7h** and **(d)***

***Noscapine**. Dashed lines denote hydrogen bonds and numbers indicate hydrogen bond lengths in Å. Hydrophobic interactions are shown as arcs with radial spokes. The figure was made using LIGPLOT. The residues within 5 Å distance from the docked ligands were only shown in the figures.*

6.3.2. Urea noscapine congeners (7a-7h) revealed high binding affinity with tubulin

The predictive binding affinity ($\Delta G_{bind,PB}$) of noscapine and its urea congeners, **7a-7h** with tubulin according to MM-PBSA is collated in Table 6.2. Energy values were calculated as the average value out of 1000 snapshots generated from the last 2 ns of the MD trajectory for each tubulin-noscapinoid complex. It was revealed that the urea noscapine congeners, **7a-7h** have a high binding affinity with tubulin compared to the noscapine. The derivative, **7g** showed the highest binding energy of -186.3 KJ/mol. Both the intermolecular van der Waals (ΔE_{vdw}) and the electrostatic (ΔE_{ele}) interactions were significant contributors to the binding, whereas the polar solvation terms (ΔG_{polar}) counteract binding. In contrast, solvent accessible surface area terms (ΔG_{SASA}), contribute slightly favorably.

Table 6.2: Predicted binding free energy and its components (KJ/mol) of urea noscapine congeners with αβ tubulin dimer**.**

Complex	ΔE_{elec} KJ/mol	ΔE_{vdw} KJ/mol	ΔG_{polar} KJ/mol	ΔG_{SASA} KJ/mol	$\Delta G_{binding}$ KJ/mol
Noscapine	-65.31 +/- 0.28	-222.5 +/- 0.51	176.9 +/ 0.33	-21.75 +/- 0.03	-132.6 +/- 0.16
7a	-67.42 +/- 0.11	-235.1 +/-0.62	179.2 +/- 0.51	-35.40 +/- 0.01	-158.7 +/- 0.58
7b	-72.44 +/- 0.87	-239.3+/- 0.56	185.8 +/- 0.84	-39.52 +/- 0.05	-165.5 +/- 0.88
7c	-68.10 +/- 0.58	-238.2+/- 0.32	182.5 +/- 0.15	-33.48 +/- 0.09	-157.3 +/- 0.82
7d	-60.21 +/- 0.29	-219.8+/- 0.25	160.3 +/- 0.19	-21.20 +/- 0.02	-140.9 +/- 0.37
7e	-64.12 +/- 0.64	-229.7 +/- 0.52	165.9 +/- 0.78	-36.12 +/- 0.08	-164.0 +/- 0.89
7f	-80.11 +/- 0.53	-246.1 +/- 0.28	190.0 +/- 0.74	-42.29 +/- 0.01	-178.5 +/- 0.63
7g	-84.75 +/- 0.79	-249.7 +/- 0.49	194.9 +/- 0.61	-46.12 +/- 0.04	-186.3 +/- 0.26
7h	-78.29 +/- 0.60	-241.0 +/- 0.89	189.3 +/- 0.22	-40.05 +/- 0.04	-170.1 +/- 0.68

6.3.3. Predicted ADME properties of noscapine and its urea congeners, 7a-7h

We have predicted the absorption, distribution, metabolism, and excretion (ADME) properties of noscapine and its urea congeners, **7a-7h** using QikProp (Schrodinger software package). A number of ADME properties were predicted viz. molecular weight (MW), total solvent accessible surface area (SASA), octanol/water

partition coefficient (QPlogPo/w), octanol/gas partition coefficient (QPlogPoct), water/gas partition coefficient (QPlogPw), polarizability in cubic angstroms (QPlogPo/w), % human oral absorption in intestine (QP%), brain/blood partition coefficient (QPlogBB), IC_{50} value for blockage of HERG K+ channel (QPlogHERG), skin permeability (QPlogKp), prediction of binding to human serum albumin (QPlogKhsa), apparent Caco-2 cell permeability in nm/sec (QPPCaco) and apparent MDCK cell permeability in nm/sec (QPPMDCK). Caco-2 cells are a model for the gut-blood barrier whereas MDCK cells are considered to be a good mimic for the blood-brain barrier. Also we evaluated the acceptability of noscapine and its urea congeners **7a-7h** based on the Lipinski's rule of 5 (number of violations of Lipinski's rule of five) which is essential for rational drug design. It was interesting that noscapine and its urea congeners, 7a-7h revealed significant values for the properties analyzed and qualified all the drug-like characteristics based on Lipinski's rule of 5 (Table 6.3).

Table 6.3. A list of properties calculated for Noscapine and its urea congeners **7a-7h** by Qikprop simulation and used for the ADME screening of the drug molecules. It was found that noscapine and its urea congeners **7a-7h** satisfied all the properties essential for ADME screening.

ADME Screening	**7a**	**7b**	**7c**	**7d**	**7e**	**7f**	**7g**	**7h**	**Nos**	**Recommended values**
MW	565.5	575.6	599.9	649.5	650.9	589.6	616.4	607.6	413.4	130-725
SASA	847.7	795.4	823.4	873.2	841.8	835.3	773.6	846.2	597.0	300-1000
Accpt HB	10.75	10.75	10.75	10.75	10.75	13.7	11.7	12.25	8.75	2.0-20.0
QPpolrz	55.95	55.09	55.23	58.20	57.40	56.17	54.08	57.24	39.01	13.0-70.0
QPlogPoct	27.50	27.30	27.53	28.59	28.40	29.97	28.48	28.39	17.81	8.0-35
QPlogPw	17.8	17.37	17.84	17.65	17.84	20.62	18.15	18.09	10.08	4.0-45.0
QPlogPo/w	3.00	3.04	3.30	3.97	4.07	1.65	2.91	2.85	1.79	-2.0-6.5
QPlogHEG	-5.71	-4.68	-5.08	-5.52	-4.85	-5.04	-4.86	-4.86	-4.42	Below -5.0
QPPCaco	134.4	217.7	173.5	184.6	255.7	41.38	144.5	249.8	777.7	< 25 poor > 500 great
QPlogBB	-0.56	-0.31	-0.14	-0.17	0.26	-1.25	-0.24	-0.41	0.33	-3.0-1.2
QPPMDCK	153.8	159.4	525.0	837.8	2128	27.45	411.1	167.9	417.1	< 25 poor >500 great
QPlogKp	-4.47	-4.02	-4.33	-4.15	-4.06	-5.18	-4.30	-4.03	-3.95	-8.0- -1.0
QPlogKhsa	0.18	0.20	0.2	0.35	0.36	-0.32	-0.01	0.05	-0.49	-1.5-1.5
Rule of Five (No. of violations)	2	2	2	2	2	2	2	2	3	Maximum is 4

6.3.4. Urea noscapine congeners inhibited proliferation of cancer cells without affecting the normal cells

The effects of urea noscapine congeners **7a-7h** and the lead molecule, noscapine with increasing concentrations (0-100 µM) were analyzed for their anti-proliferative activity in two human breast adenocarcinoma cells, MCF-7 (estrogen- and progesterone-

receptor positive) and MDA-MB-231 (estrogen- and progesterone- receptor negative) using MTT assay (Figure 6.10A and 6.10B). All the urea noscapine congeners **7a-h** exhibited potent cytotoxic activity in comparison to noscapine using both the cell lines. The IC_{50} values for the tested compounds for both the cell lines are collated in Table 6.4. The IC_{50} value for the urea noscapine congeners **7a-h** ranges from 38.2 to 4.77 µM was significantly less than the lead molecule, noscapine (IC_{50} value is 39.67 µM) for MCF-7 cells. Parenthetically, a similar modest IC_{50} value ranges from 48.45 to 6.56 µM were measured for urea noscapine congeners, **7a-h** compared to noscapine (IC_{50} value is 53.99 µM) for MDA-MB-231 cells. The IC_{50} value of noscapine and its urea congeners for both the cancer cell lines was found to be statistically significant compared to untreated cells ($p < 0.05$). Surprisingly noscapine and its urea congeners **7a-7h** inhibited proliferation of normal healthy cells with IC_{50} value > 285 µM, indicating that these compounds were not toxic to normal healthy cells (Table 6.4 and Figure 6.11). The compound **7g** was found to be the most promising among the library based on IC_{50} value and was selected for the detailed investigation.

Table 6.4: IC_{50} values of urea noscapine congeners using two human breast adenocarcinoma cell lines, MCF-7 and MDA-MB-231 as well as a normal cell line (HEK). All the novel derivatives were found to have improved antiproliferative activity compared to noscapine without affecting the normal healthy cell line. The IC_{50} values between treated and untreated cells were found to be statistically significant ($p < 0.05$) using student t-test.

	IC_{50} (µM)		
	MCF-7	**MDA-MB-231**	**HEK**
Noscapine	39.67±2.38*	53.99±4.53*	229.2±12.3*
7a	37.87±3.62*	48.45±3.47*	291.9±10.5*
7b	38.2±4.21*	45.71±2.69*	290.0±11.4*
7c	32.68±3.48*	35.22±3.57*	285.4±15.3*
7d	36.07±3.19*	48.05±4.15*	293.9±12.8*
7e	27.66±2.94*	35.68±3.68*	293.2±12.8*
7f	29.50±2.43*	33.21±2.72*	305.8±11.8*
7g	4.77±0.87*	6.56±0.68*	337.8±16.8*
7h	17.51±1.62*	20.45±1.61*	305.8±13.8*

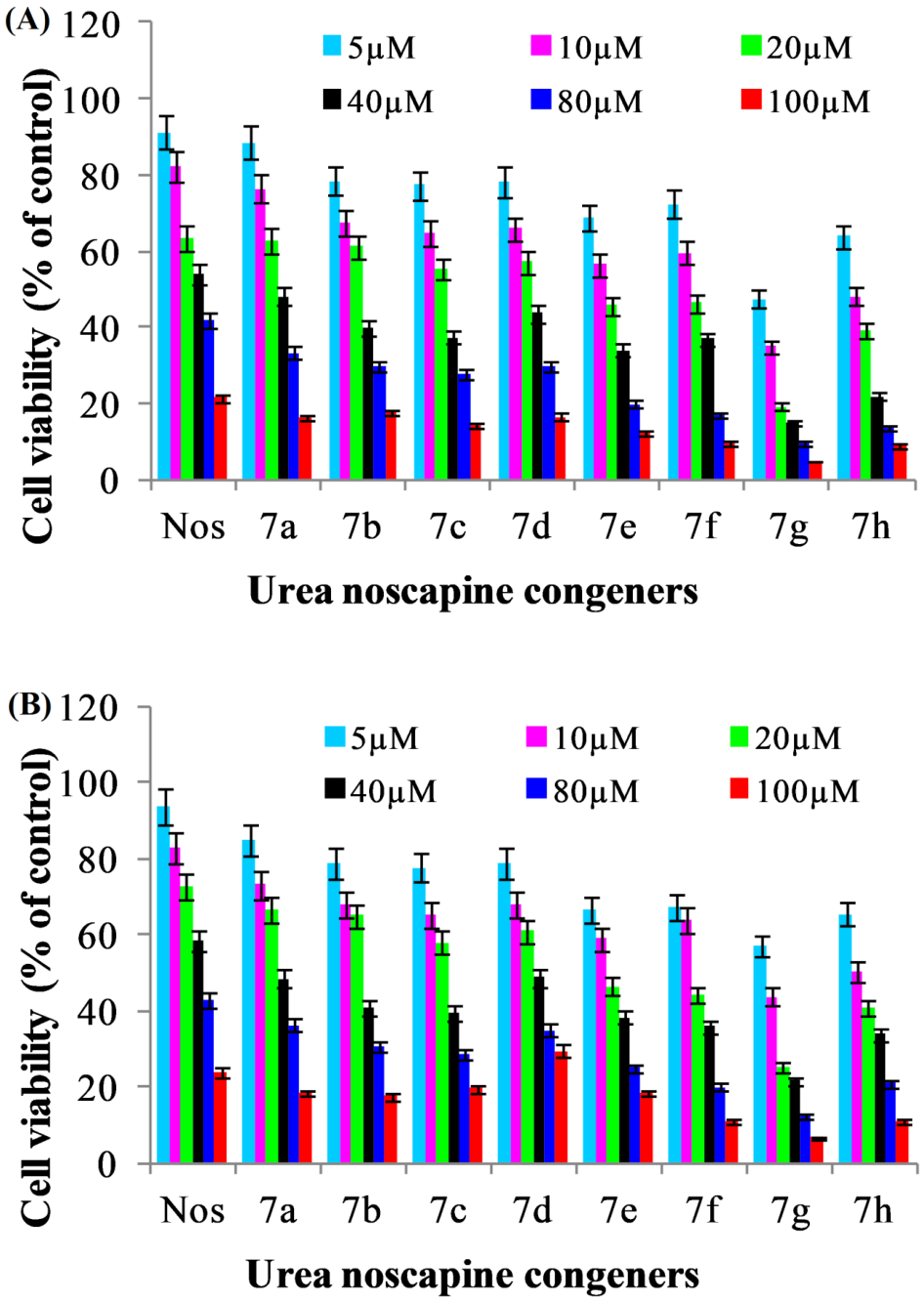

Figure 6.10: *The urea noscapine congeners* ***7a-7h*** *have more antiproliferative activity compared to noscapine using human breast cancer cells. Both (A) MCF-7 and (B) MDAMB-231cells were treated with noscapine and its urea congeners,* ***7a-7h****, for 72 h. Each value represents the average of 3 independent experiments.*

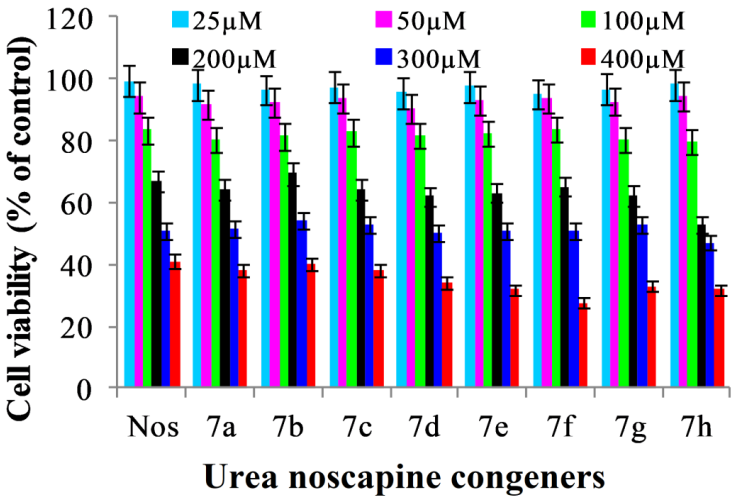

***Figure 6.11**: Effect of noscapine and its urea congeners **7a-7h** (25–400 µM) on the cell viability of normal healthy cell (HEK).*

6.3.5. Urea noscapine congeners, 7g inhibits proliferation of primary tumor cells

We next evaluated the sensitivity of primary cancer cells directly isolated from eight different patients with different stages of breast cancer with the treatment of the most promising urea congener of noscapine, **7g.** The primary breast cancer cells were treated with increasing concentrations (0-100 µM) of **7g** and its antiproliferative activity was measured using MTT assay. The compound significantly inhibited the proliferation of primary tumor cells compared to the untreated cells (Figure 6.12). The IC_{50} values range from 14.61 to 27.63 µM for all the eight primary tumor cells. The molecule **7g** exhibited potent cytotoxic activity in comparison to noscapine using all the primary breast cancer cells at increasing concentration (Figure 6.12).

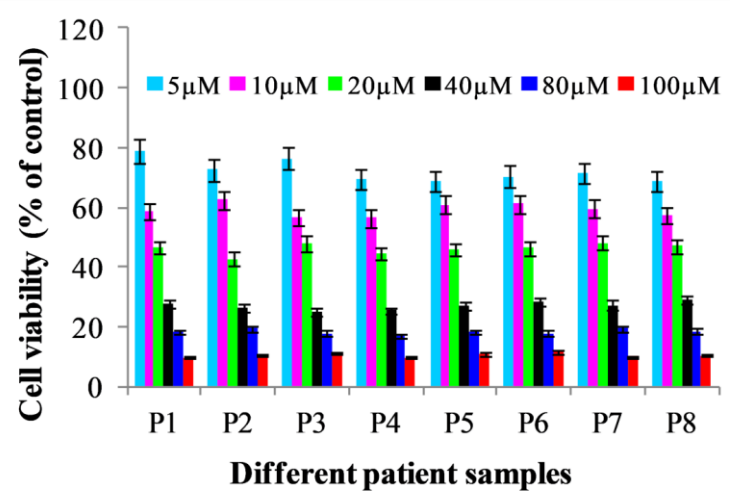

***Figure 6.12:** The urea noscapine congener **7g** inhibits proliferation of a panel of human primary breast tumor cells more effectively compared to noscapine. All the cells treated with 7**g** for 72 h. Each value represents the average of 3 independent experiments.*

6.3.6. Detection of apoptosis with the treatment of noscapine and its urea congeners

Membrane blebbing, cellular shrinkage, chromatin condensation and formation of apoptotic bodies are always the main morphological changes during apoptosis. Therefore, we performed cellular studies using AO, EtBr, and HO (Hoechst 33342) to confirm the induction of apoptosis by **7g**. MDA-MB-231 cells treated with IC_{50} concentration (6.56 µM) of **7g** underwent apoptosis as demonstrated by staining of the treated cells with these dyes (Figure 6.13). Specifically, the untreated cells were observed to have normal cell morphology, whereas, the treated cells underwent several features of apoptosis such as membrane blebbing, numerous fragmented nuclei, and appearance of apoptotic bodies.

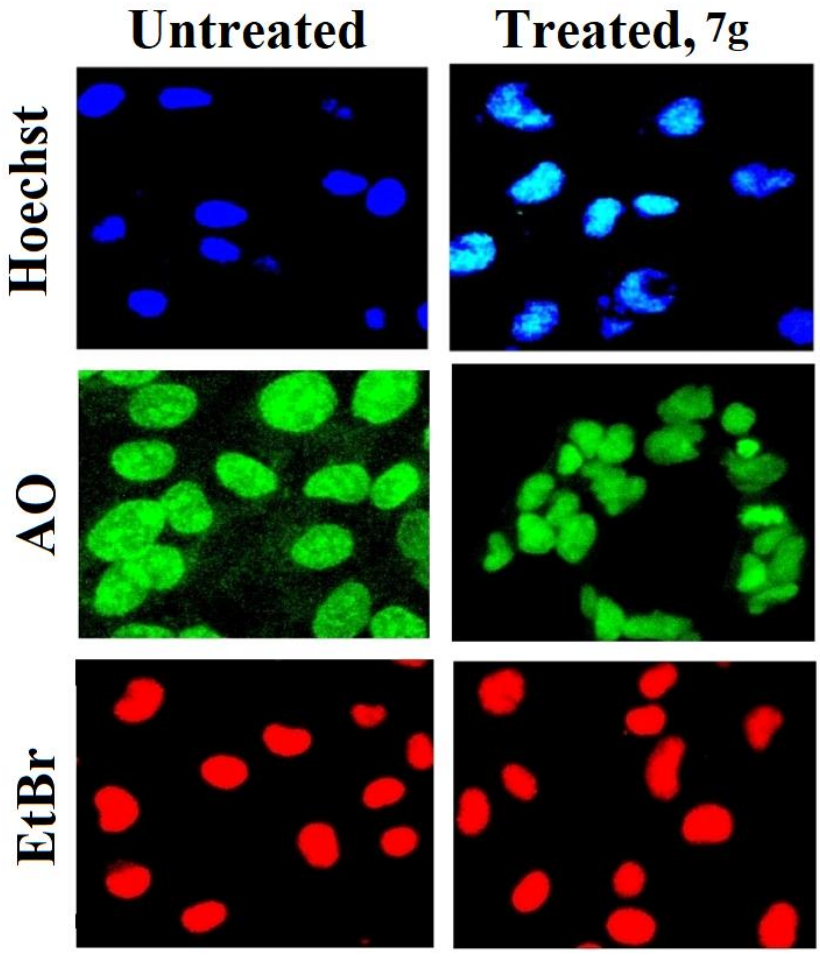

Figure 6.13: *The changes in morphological characters such as chromatin condensation, plasma membrane blebbing and appearance of small, apoptotic bodies indicated the apoptotic cells. Panels show morphological features of cells stained with AO, EtBr and Hoechst from untreated cells and cells treated with IC_{50} concentration (6.56 µM) of urea noscapine congener* ***(7g)*** *for 72 hours using fluorescence microscopy. The apoptotic cancer cells were evident after 72 hours of drug treatment*.

6.3.7. Urea noscapine congener 7g induced cell death in MDA-MB-231 cells

We approached to determine the induction of cell death to MDA-MB-231 cells with the treatment of **7g**. The apoptotic cells were quantified by FACS analysis using Annexin/FITC fluorescent dyes. The percentage of early apoptotic and late apoptotic cells using MDA-MB-231 cells at IC_{50} concentration (6.56 µM) after 72 h is collated in figure 6.14.

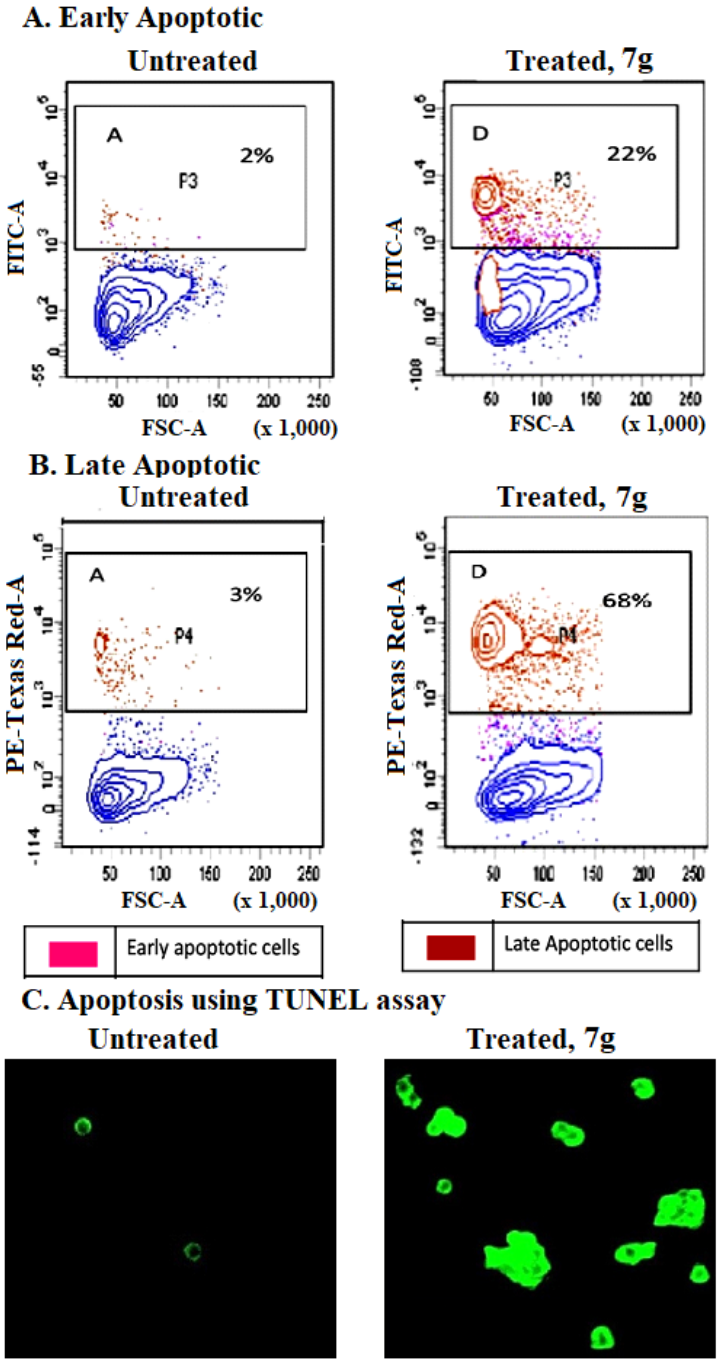

Figure 6.14: *(A & B): The control untreated cells contained only very few early apoptotic (2%) and late apoptotic cells (3%), which were considered as the background cell death due to regular trauma during cell culture. In contrast, the percentage of early*

*apoptotic cells of 22% and late apoptotic cells of 68% were noticed with the treatment of **7g** and were found to be significantly high compared to controlled untreated cells. (C): Further, TUNEL assay was performed to investigate induction of apoptosis to MDA-MB-231. Results showed that treatment with **7g** increased the number of TUNEL positive nucleus, indicating cell death.*

6.3.8. Effects of urea noscapine congener 7g on ROS accumulation in MDA-MB-231

To further investigate the mechanism of induction of apoptosis to cancer cells, we found that **7g** elevated ROS levels. Using DCFDA as the molecular probe, the ROS level was analyzed. When MDA-MB-231 cells were treated with **7g** (6.56 µM), the green fluorescence was more intense compared to untreated cells (Figure 6.15). We found that **7g** significantly elevated ROS level in MDAMB-231 cells as measured by fluorescent intensity, indicating that ROS might have a function in the induction of apoptosis (Figure 6.15). MDA-MB-231 cells treated with H_2O_2 (10 µM) also showed a substantial amount of ROS inside the cells and were labeled with more intense green fluorescence.

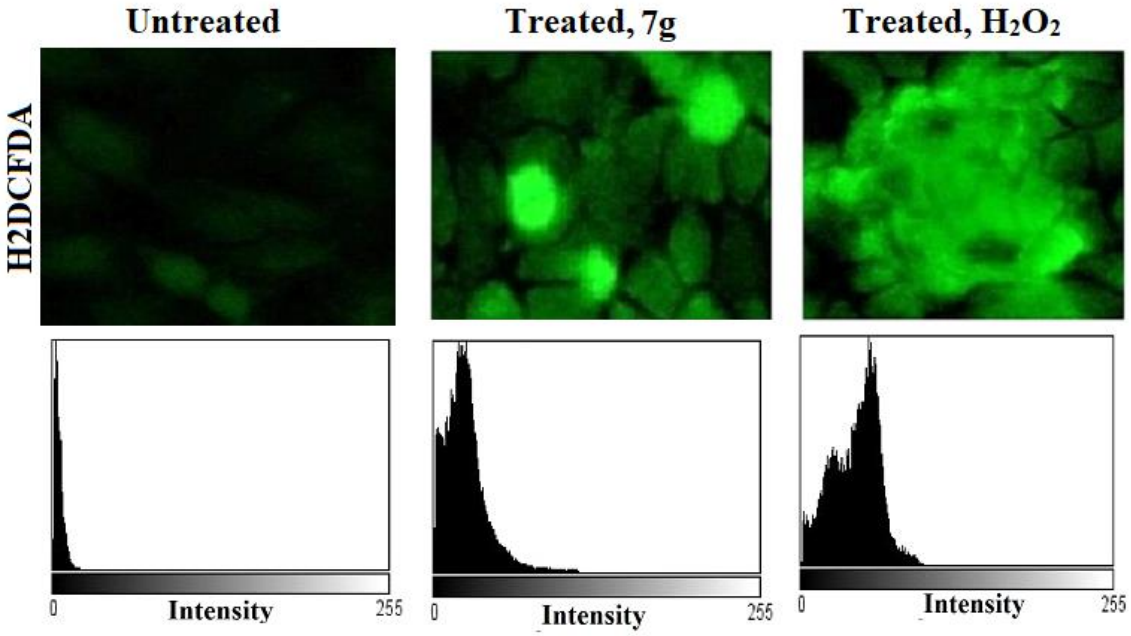

***Figure 6.15:** Treatment with **7g** increases the intracellular ROS production as imaged and estimated using an oxidation sensitive fluorophore, DCFDA. The H2O2 is taken as a reference for comparative purpose.*

6.3.9. Urea noscapine congener alter the cell cycle profile and cause mitotic arrest at G_2/M phase

We examined the effect of **7g** with its IC_{50} concentration (6.56 µM) on the cell cycle profile of MDA-MB-231 based on FACS analysis. Treatment of MDA-MB-231 cells for 72 h led to significant perturbations of the cell cycle profile. FACS analysis revealed a high accumulation of cells in the G2/M phase compared to untreated cells (Figure 6. 16). In contrast to G2/M block, a characteristic hypodiploid DNA content peak (sub-G1) was seen to rise at 72 h of drug treatment. The progressive generation of cells having hypodiploid DNA content reflects fragmented DNA indicating dying cells.

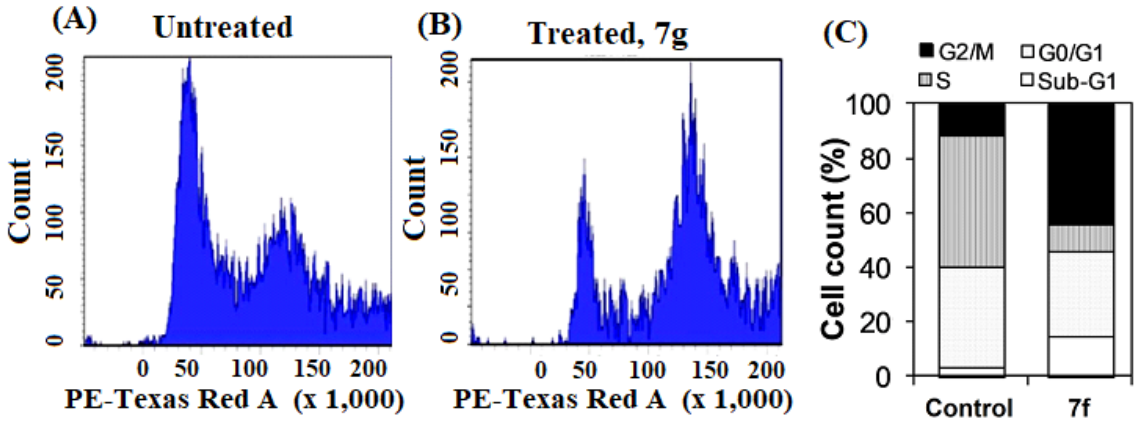

Figure 6.16: *Treatment with urea noscapine congener,* ***7g*** *at its IC_{50} concentration (6.56 µM) perturb cell cycle progression at G2/M phase followed by the appearance of a hypodiploid (sub-G1) DNA peak that indicates apoptotic cells. Panels A demonstrated the analyses of cell cycle progression, determined by flow cytometry in MDA-MB-231 cells treated with* ***7g*** *for 72 hours. Panel B represents the percentage of cells at different phases of cell cycle.*

6.3.10. Effects of noscapine and its urea congener on mitochondrial membrane potential ($\Delta\Psi m$)

Mitochondria are thought to be the major pathway for apoptosis. The induction of apoptosis is closely related to the collapse of mitochondrial membrane potential ($\Delta\Psi m$). Thus, we measured the loss of mitochondrial membrane potential ($\Delta\Psi m$) in MDA-MB-231 cells treated with **7g** using DAPI, JC-1, and Rhodamine 123 dyes. When MDA-MB-231 cells were treated with **7g**, JC-1 red fluorescence, Rhodamine-123 green fluorescence, and DAPI blue fluorescence in treated cells were more intense compared to untreated cells (Figure 6.17). In addition, the urea noscapine congener, **7g** significantly increased the loss of mitochondrial membrane potential ($\Delta\Psi m$) in MDAMB-231 cells (Figure 6.17) compared to untreated cells.

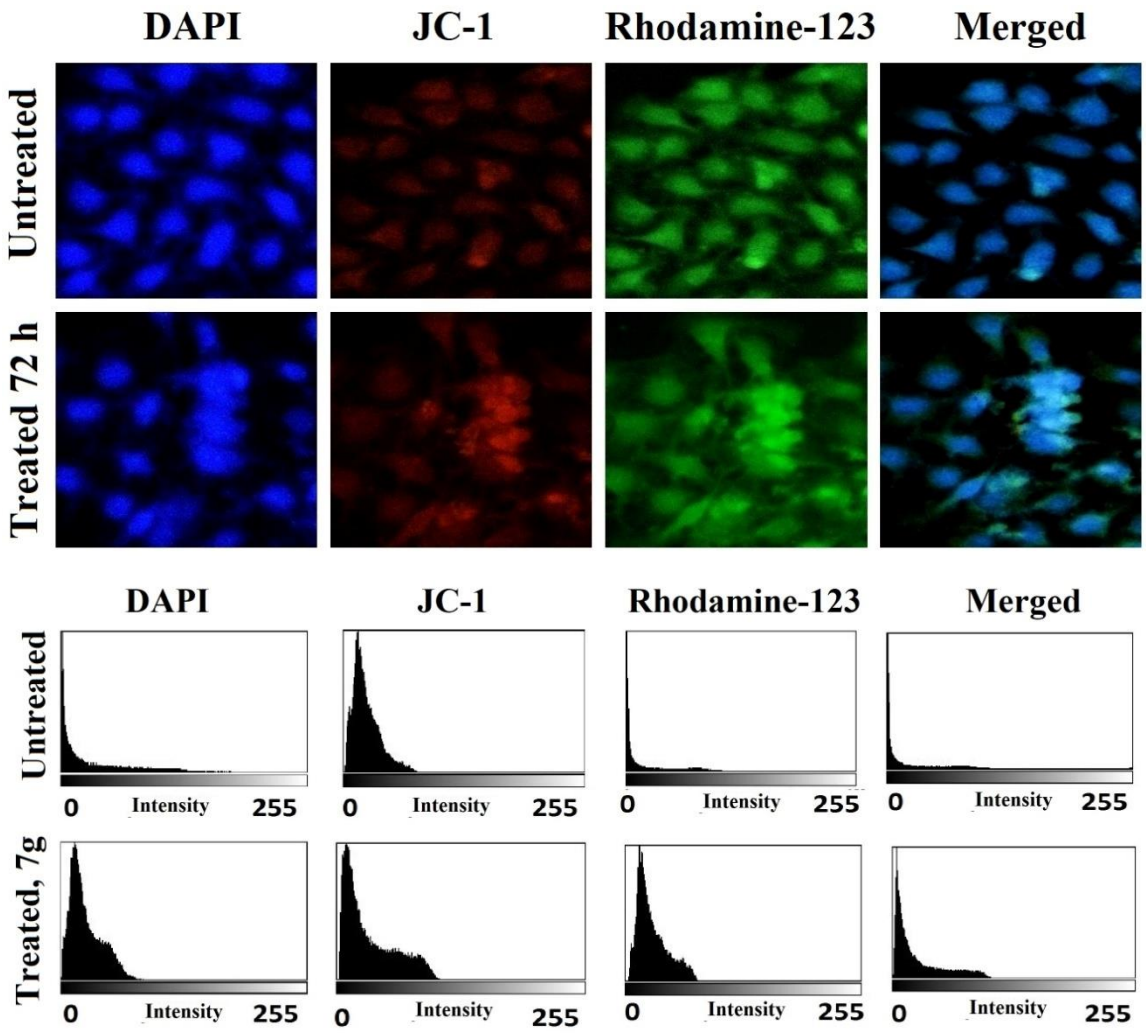

Figure 6.17: *(A) Effect of urea noscapine congener* ***7g*** *on mitochondrial membrane potential as visualized using different fluorescent dyes, DAPI, JC-I and Rhodamine 123. (B) The fluorescent intensity was measured using Image J.*

6.3.11. Reduction in tumor volume with the treatment of 7g against MCF-7 xenograft model

Treatment with **7g** (50 µM/day) considerably decreased tumor volume in comparison to control ($P < 0.001$) (Figure 6.18). Tumor volume was reduced to 0.34 cm^3 from the tumour size of the untreated control group with tumor volume 1.63 cm^3 on day 30 post tumour implantation. On 30^{th} day mice were sacrificed and tumours were removed and weighted. All untreated mice developed solid tumours in sizes ranging from 4.5 to 11.9 g (mean 7.4 ± 2.3 g). Whereas, among the treated groups the tumor size was significantly regressed and showed only small palpable tumors. Compared to untreated control mice, inhibition of tumor growth by **7g** was statistically significant ($p < 0.001$). In addition, we did not observe any apparent weight loss after drug treatment compared to the control group of mice (Fig. 6.19).

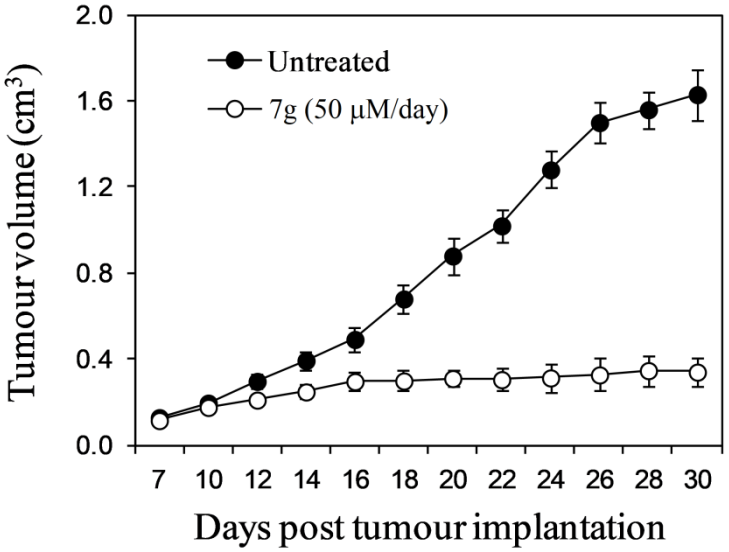

Figure 6.18. *Effect of urea noscapine congener,* ***7g*** *on the progression in tumor growth on human MCF-7 xenograft mice. The tumor growth was significantly inhibited by* ***9*** *compared to untreated group.*

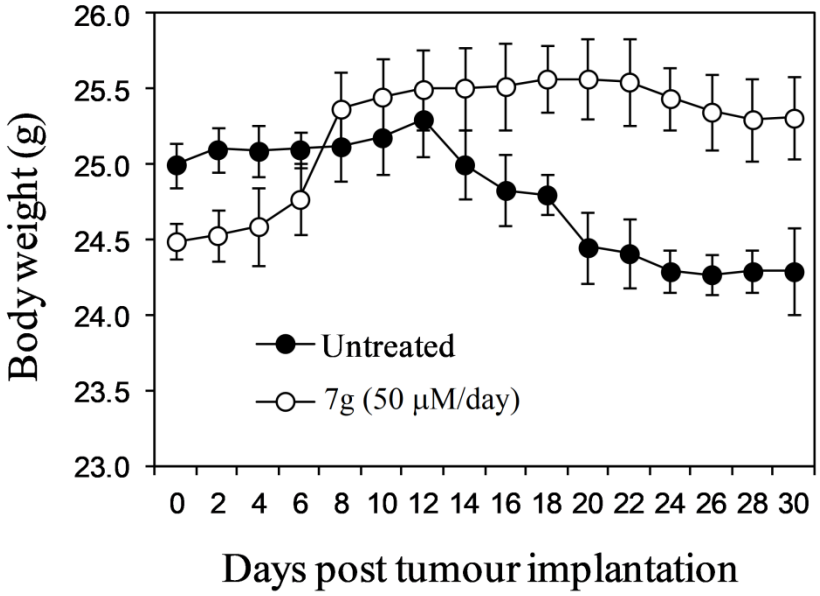

Figure 6.19. *Effect of urea noscapine congener,* ***7g*** *on the body weight of mice. No significant difference in body weight was noticed between the treated and untreated mice.*

6.3.12. Treatment of 7g does not cause any detectable toxicity

The severe side effects during chemotherapeutics are a major concern in the treatment of cancer patients. Tubulin binding agents, for example, vinca alkaloids and taxanes, while clinically approved, are known to cause adverse side effects (Rowinsky *et al.,* 1997). As a result, there is a need to identify a drug regimen that is both safe and

well-tolerated. We examined the liver, kidney, brain and lungs of tumour-bearing mice to see if **7g** causes toxicity to normal tissues. Treatment with **7g** fails to reveal any detectable pathological abnormalities in normal tissues involved in normal cell proliferation. H&E staining of paraffin-embedded 5.0 micron-thick sections of the liver, kidney, lung, and brain is shown at 200x magnification in Figure 6.20. The hepatic lobular architecture was normal. Normal glomeruli, proximal and distal tubules, interstitium, and blood vessels were found in the kidneys. Normal alveoli and bronchial airways have been seen in the lung tissue. Furthermore, we observed no differences in hematological parameters between treated and control animals (Table 6.5.and 6.6).

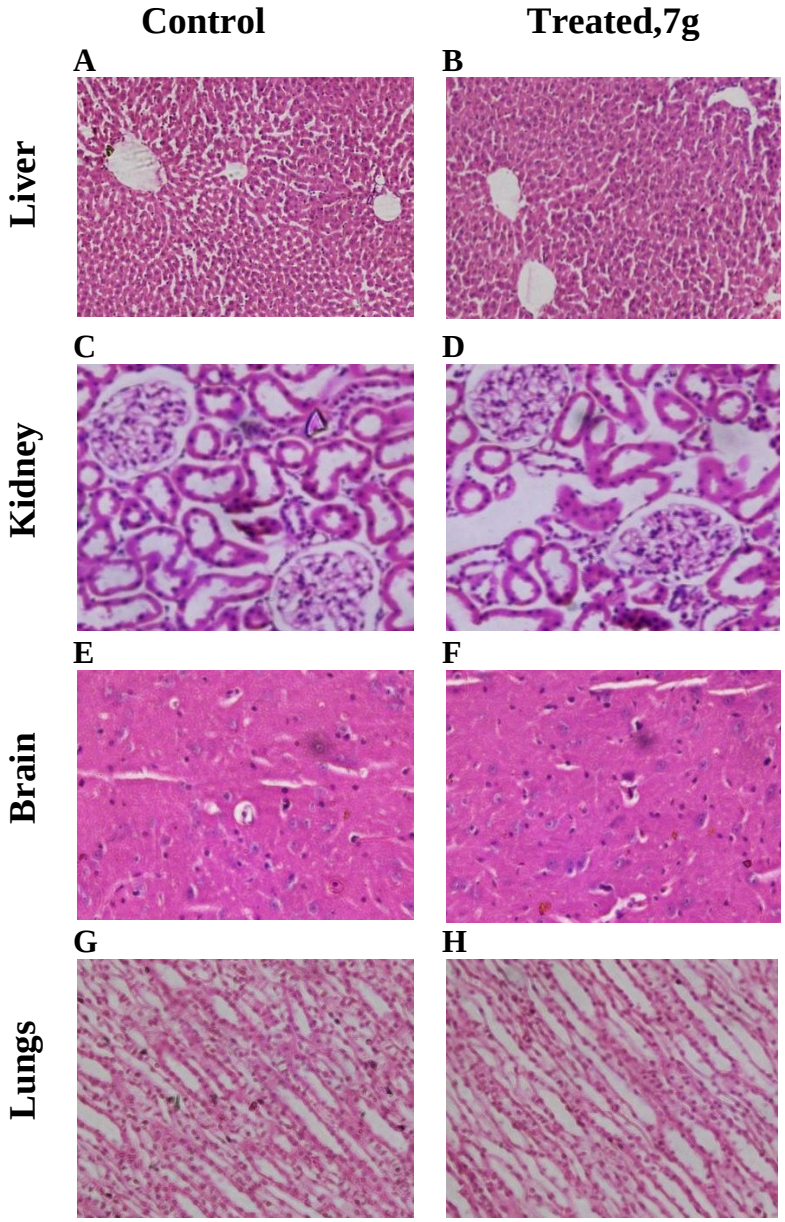

Figure 6.20: *Panels represent H&E staining of paraffin-embedded 5 micron-thick sections of the liver, kidney, lung, and brain at magnifications 200x and 400x. The liver showed normal hepatic lobular architecture. The kidneys revealed normal glomeruli,*

proximal and distal tubules, interstitium, and blood vessels. The splenic follicles and vascular sinusoids were indistinguishable between the 7g-treated and vehicle-treated control groups. The lung tissue showed normal alveoli among the two groups. Microsections of brain did not reveal any infracted areas. The cerebral cortex, gray and white matters appeared normal.

Table 6.5: Hematological parameters, WBC count (WBC), monocytes (MON), eosinophils (EOS), RBC count (RBC), haemoglobin concentration (HB), Hematocrit (HCT), mean corpuscular volume (MCV), mean corpuscular hemoglobin (MCH), mean corpuscular hemoglobin concentration (MCHC) and platelet count between the treated (50 µM/day) and control groups.

Parameter	Treated (50 µM/day)	Control
WBC (10^3/µl)	3.9 ± 1.8	3.5 ± 2.6
MON (%)	0.4 ± 0.06	0.3 ± 0.03
EOS (%)	0.9 ± 0.06	0.8 ± 0.04
RBC (10^6/µl)	6.29 ± 0.7	5.1 ± 0.3
HB (g/dl)	14.6 ± 0.1	16.8 ± 0.4
HCT (%)	39.5 ± 0.9	41.9 ± 0.3
MCV (fL)	58.2 ± 0.9	53.6 ± 0.6
MCH (pg/cell)	29.7 ± 0.6	28.2 ± 0.8
MCHC (g/dl)	34.4 ± 0.8	35.8 ± 0.2
Platelet (10^3/µl)	89.7 ± 2.6	95.1 ± 7.3

Table 6.6: Organ functions and Serun Glucose, Serum Ca,NA,K, and Cl levels between the treated (50 µM/day) and control groups.

Parameter	Acute (50 µM/day)	Control (0)
AST (U/L)	106.8 ± 4.3	105.2 ± 6.4
ALT (U/L)	28.2 ± 3.2	29.9 ± 3.5
ALK PHOS (U/L)	78.5 ± 6.9	78.9 ± 5.8
BUN (mg/dl)	12.1 ± 2.6	10.9 ± 2.8
Creatinine (mg/dl)	0.64 ± 0.08	0.54 ± 0.06
Bilirubin Total (mg/dl)	0.56 ± 0.04	0.73 ± 0.03
Bilirubin Direct (mg/dl)	0.32 ± 0.02	0.28 ± 0.06
Bilirubin Indirect (mg/dl)	3.8 ± 0.29	3.5 ± 0.3
Albumin (g/dl)	5.19 ± 0.22	5.31 ± 0.41
Total protein (g/dl)	6.56 ± 0.28	6.88 ± 0.15
Glucose (mg/dl)	98.3 ± 5.2	98.7 ± 3.2
Ca (mg/dl)	9.8 ± 0.4	9.6 ± 0.4
Na (mEq/L)	144.6 ± 0.4	144.9 ± 0.5
K (mEq/L)	3.6 ± 0.8	3.6 ± 0.3
Cl (mEq/L)	106.7 ± 4.3	105.3 ± 4.6

6.6. Conclusion

In conclusion, we have strategically developed potent derivatives of the natural lead molecule noscapine in quest of increasing its anticancer activity. We have also provided the simplest methods for direct and regioselective modification of the noscapine scaffold to produce the urea noscapine congeners in high yields. All the derivatives screened out based on molecular docking have shown increased predicted binding affinity with tubulin. Further, it was experimentally demonstrated that these derivatives also bind to tubulin with high affinity. Their anticancer activity was evaluated using two human breast cancer cell lines (MCF-7 and MDA-MB-231) as well as a panel of primary breast tumour cells. All the derivatives revealed improved anticancer activity compared to noscapine without affecting the normal healthy cells. Therefore, these novel compounds may prove efficacious not only in the treatment of breast carcinoma but also for other types of cancer.

Appendix

A6.1: ^{1}H NMR of Urea congener, 7a

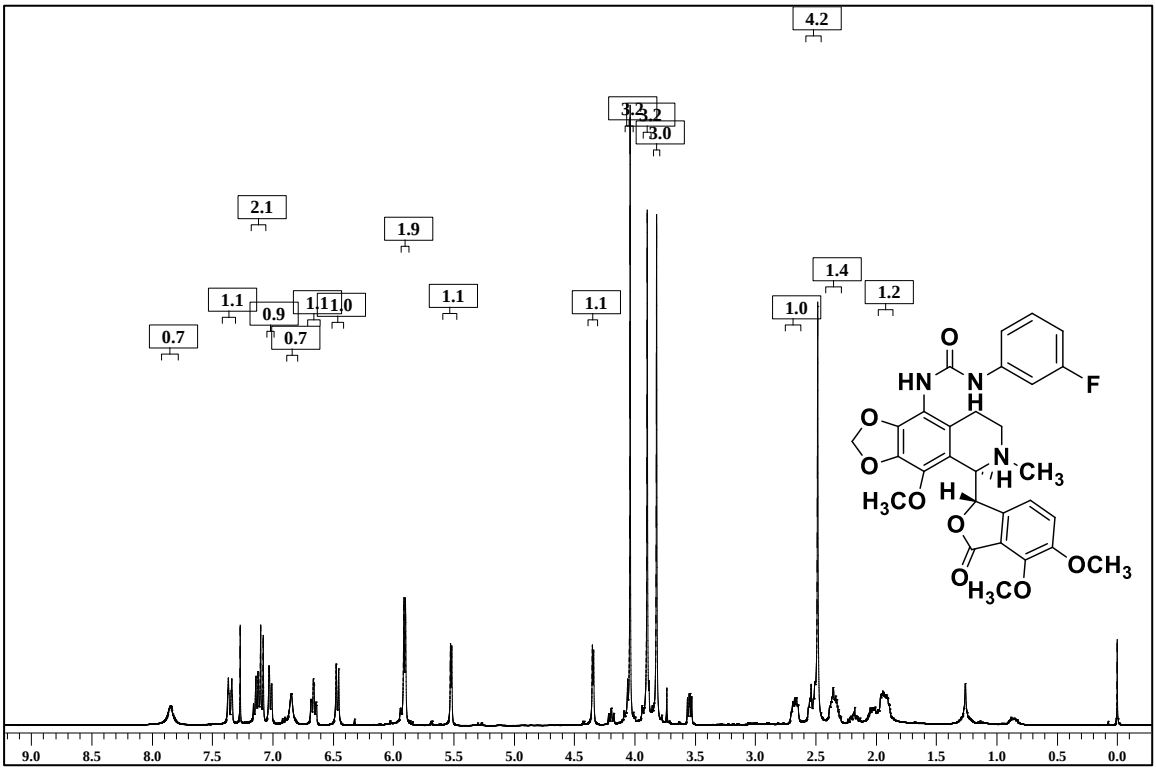

A6.2: ^{13}C NMR of Urea congener, 7a

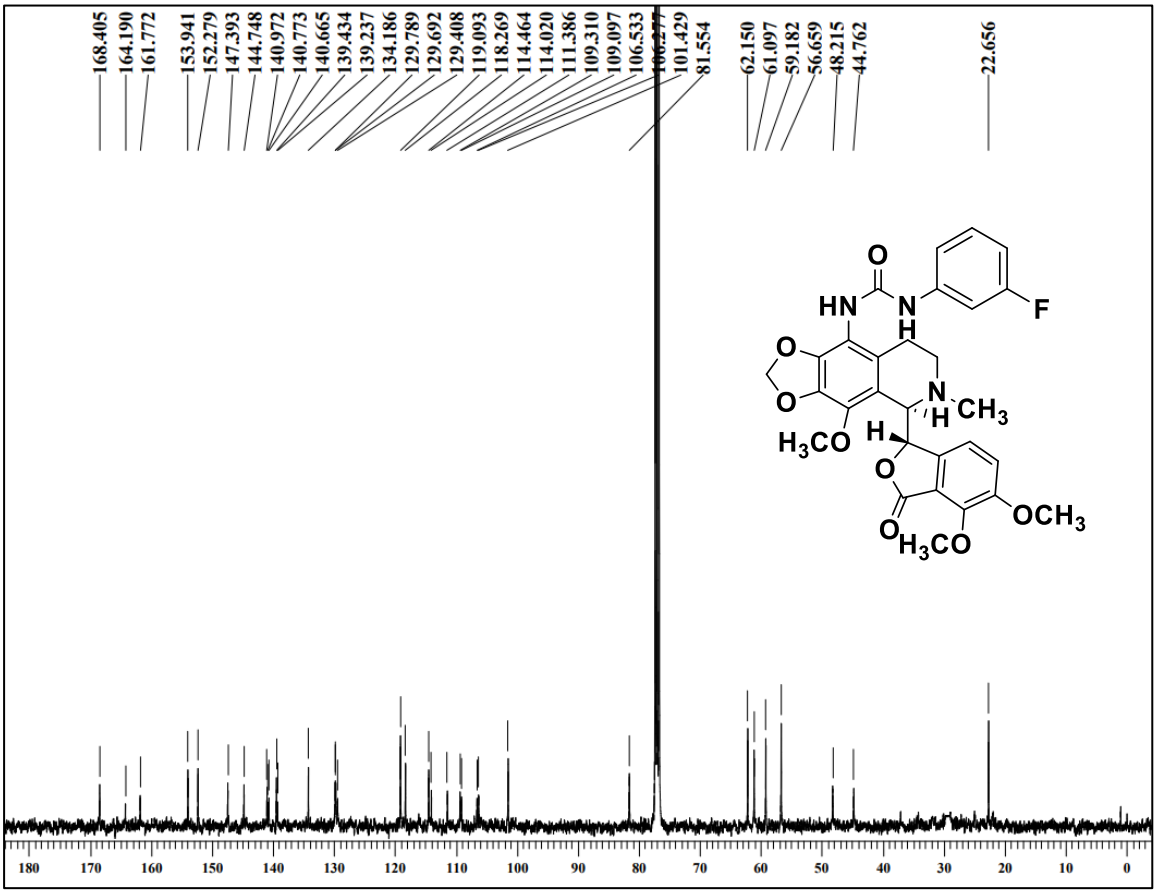

A6.3: HRMS of Urea congener, 7a

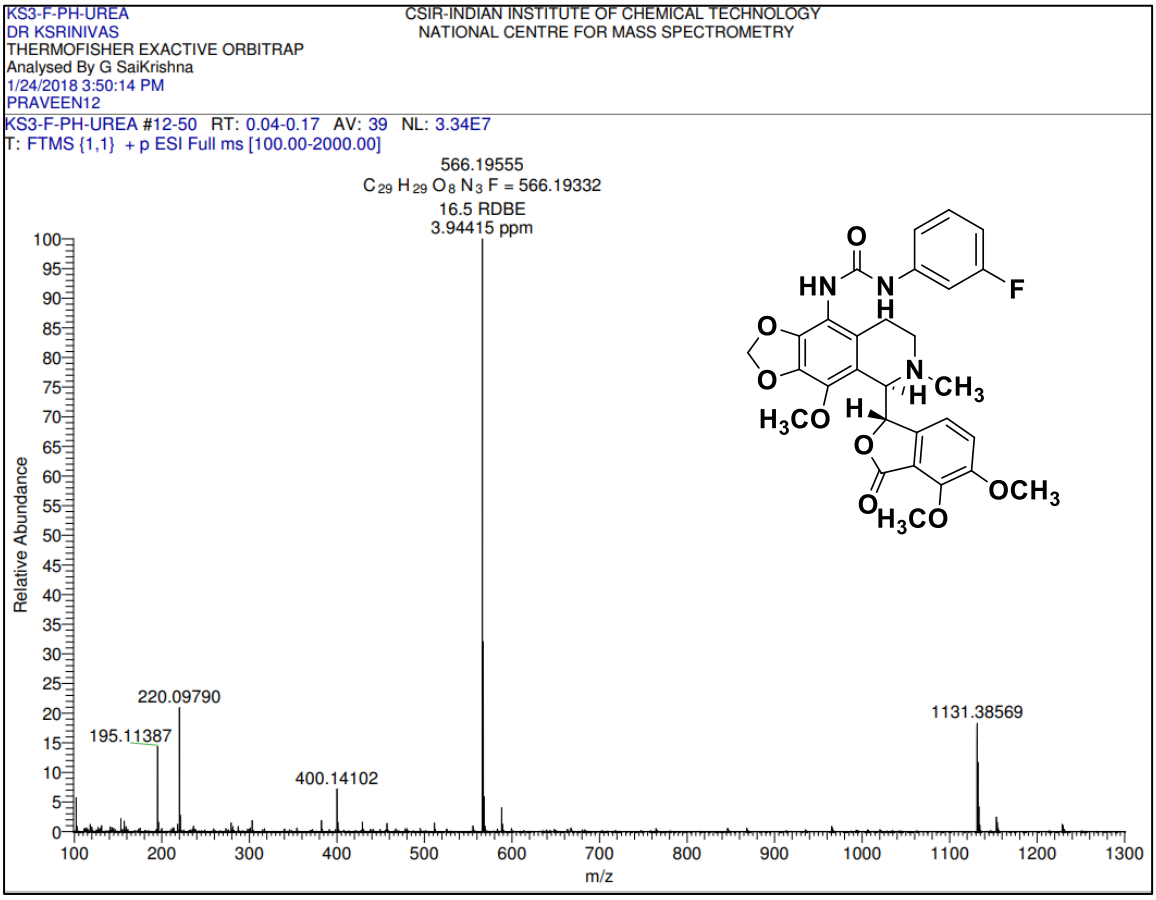

A6.4: ^{1}H NMR of Urea congener, 7b

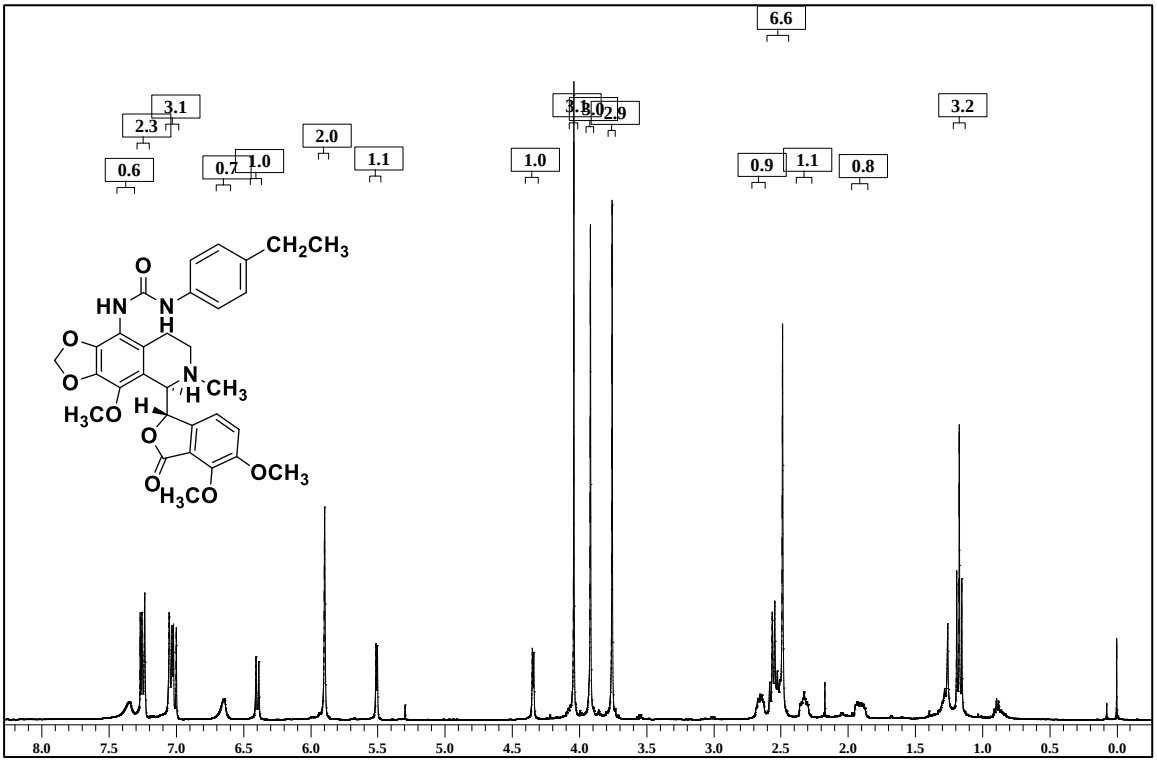

A6.5: ^{13}C NMR of Urea congener, 7b

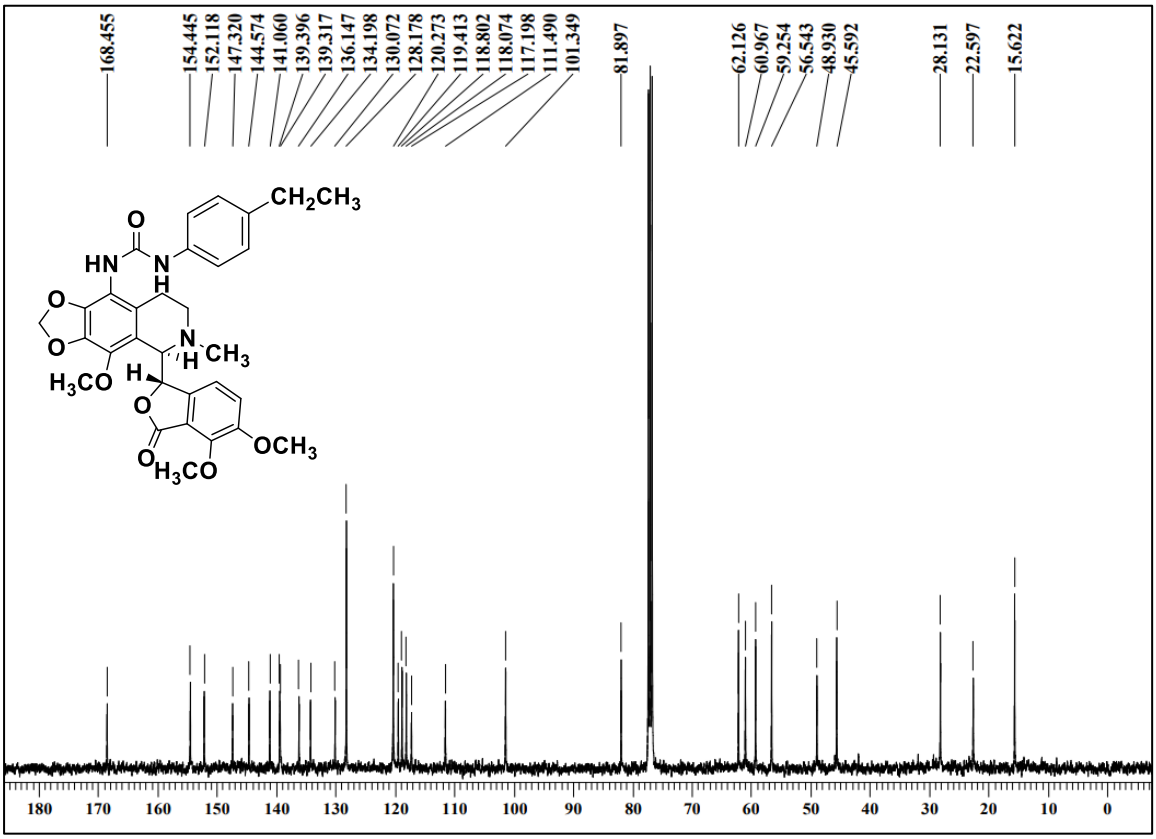

A6.6: HRMS of Urea congener, 7b

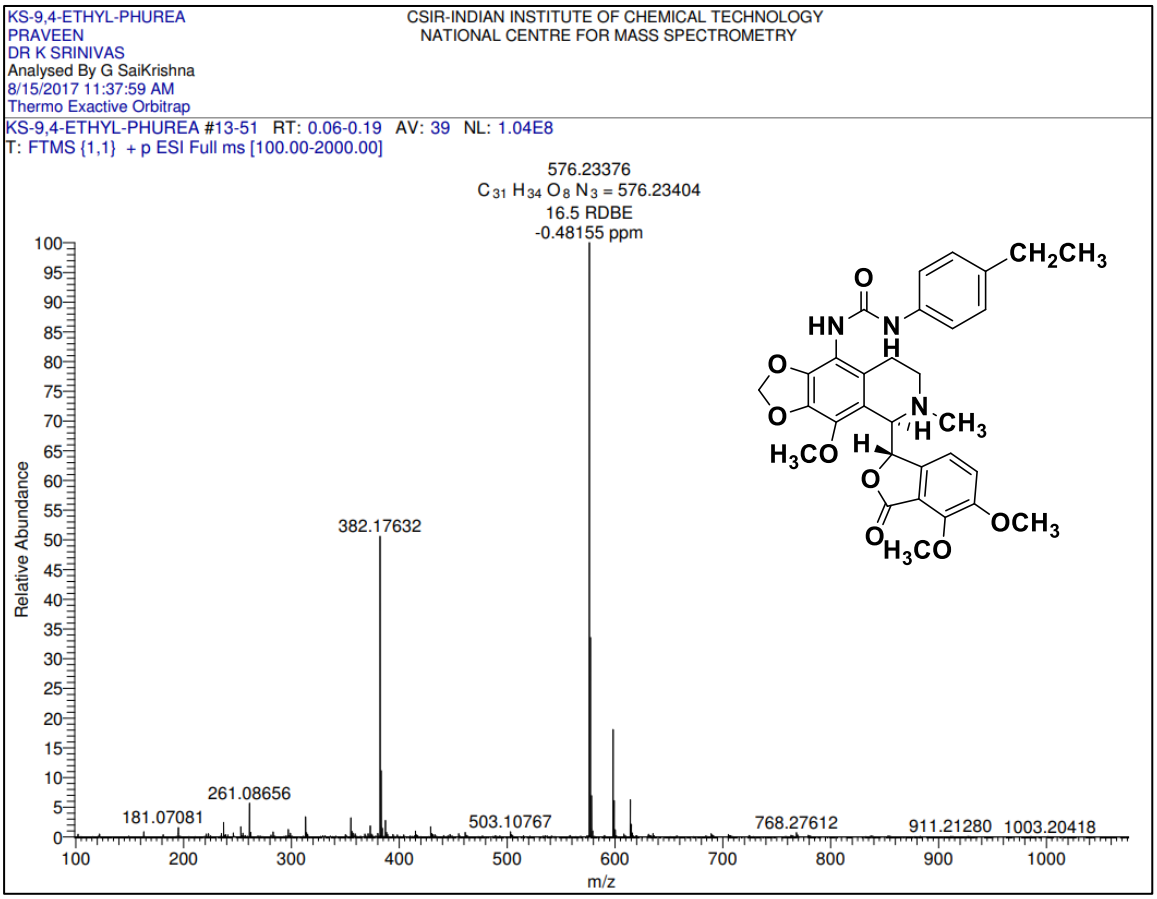

A6.7: ^{1}H NMR of Urea congener, 7c

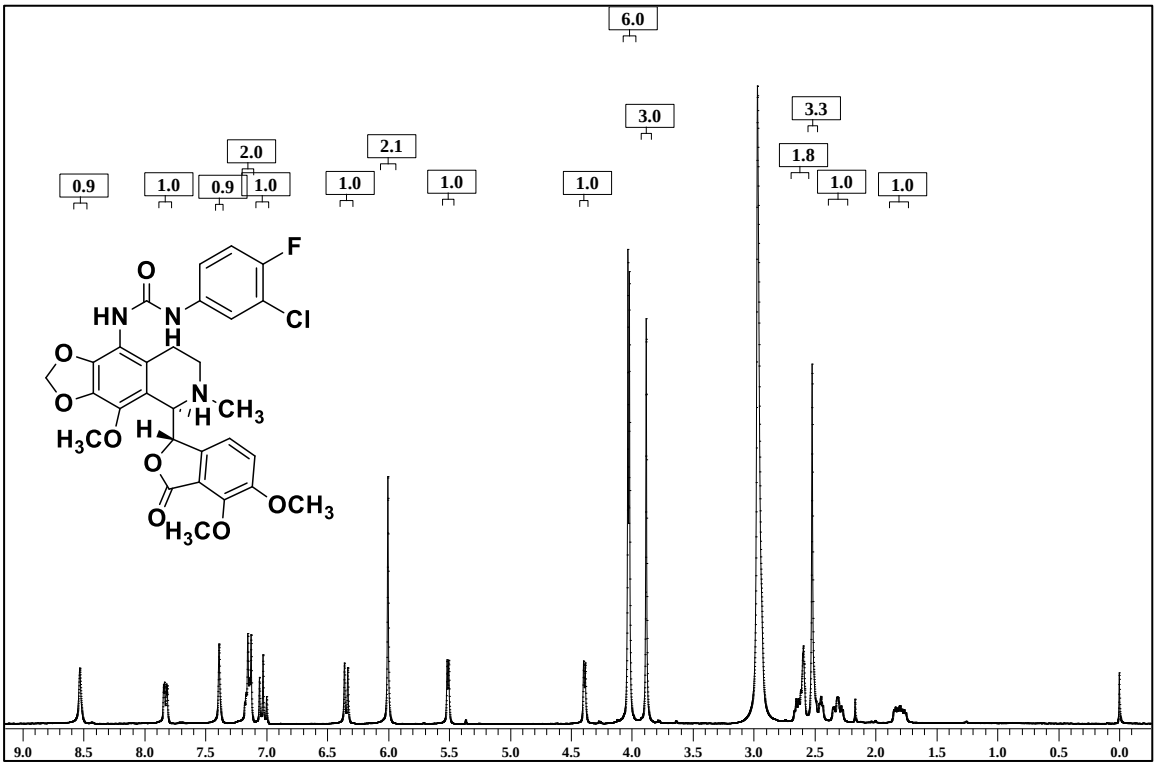

A6.8: ^{13}C NMR of Urea congener, 7c

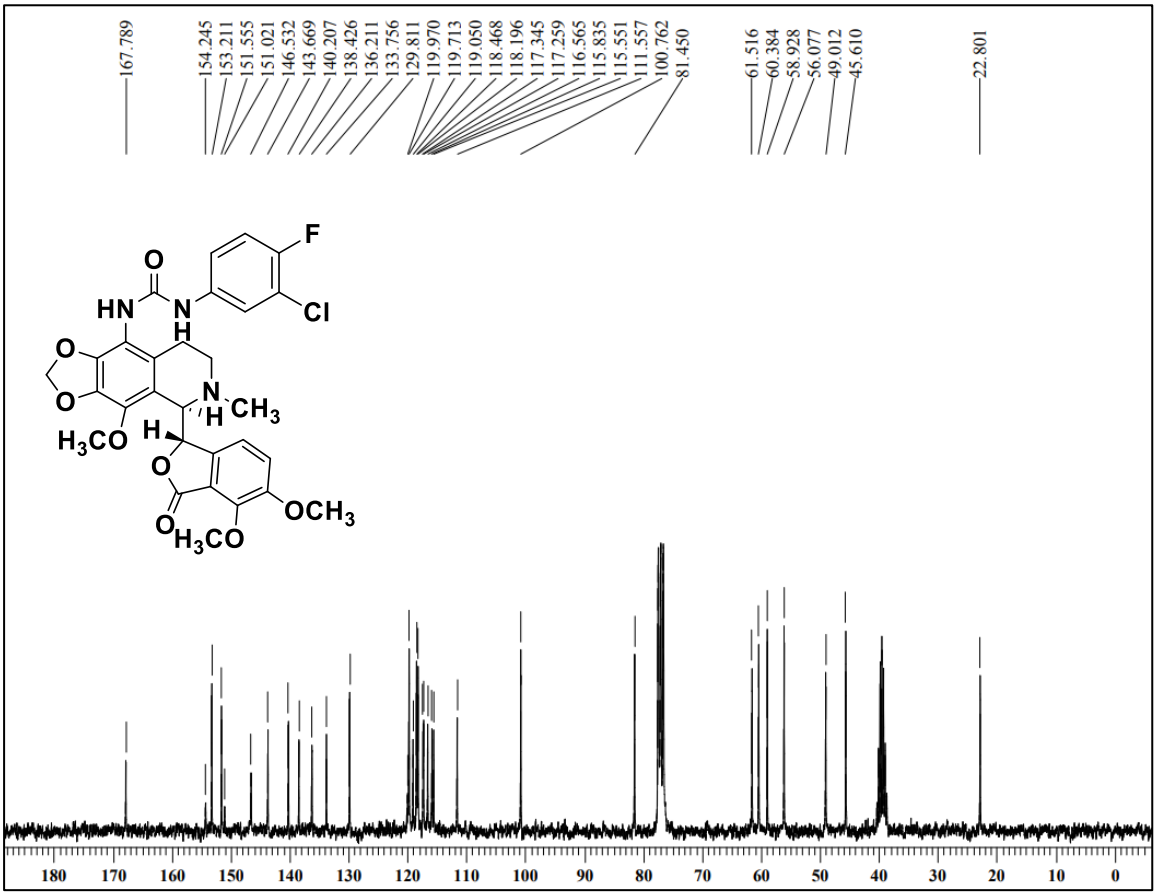

A6.9: HRMS of Urea congener, 7c

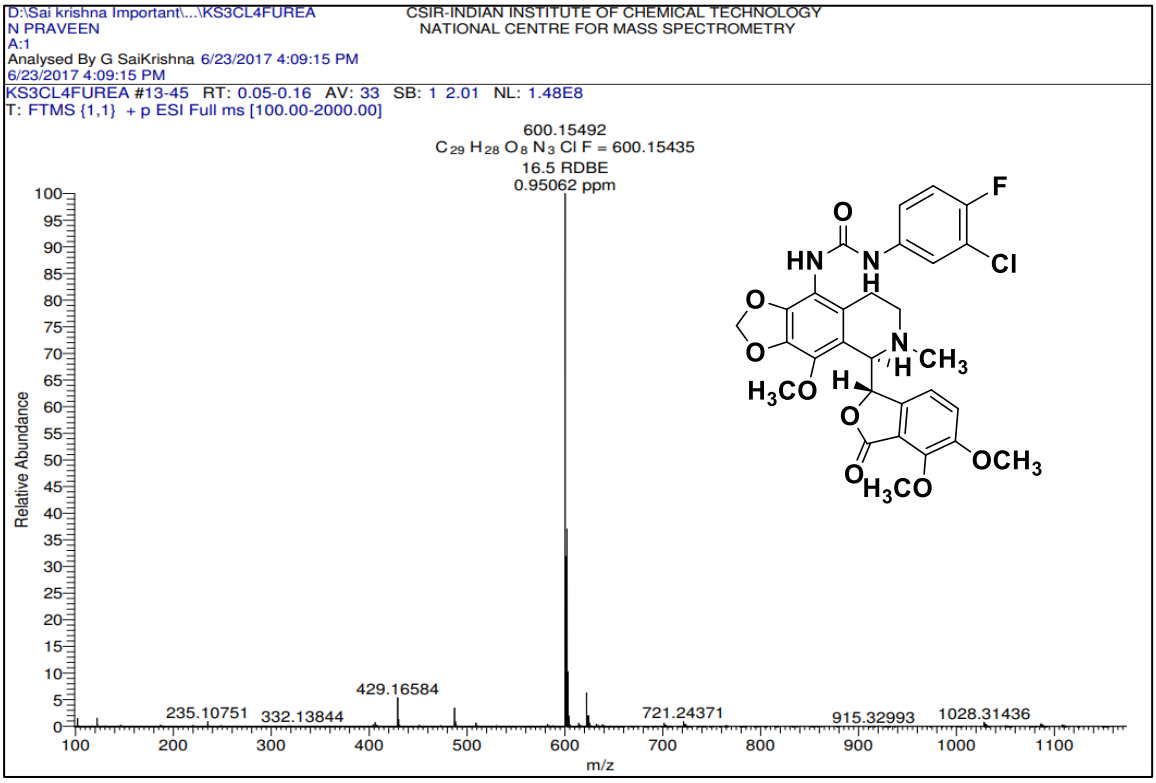

A6.10: ^{1}H NMR of Urea congener, 7d

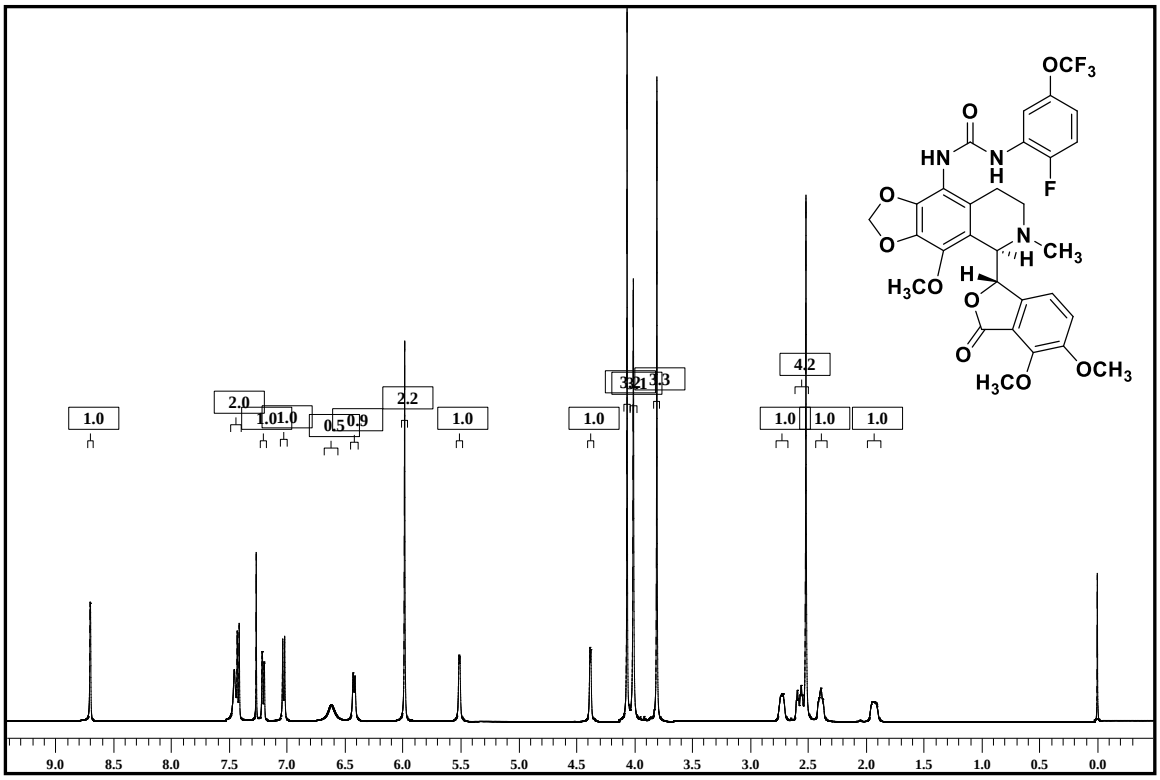

A6.11: ^{13}C NMR of Urea congener, 7d

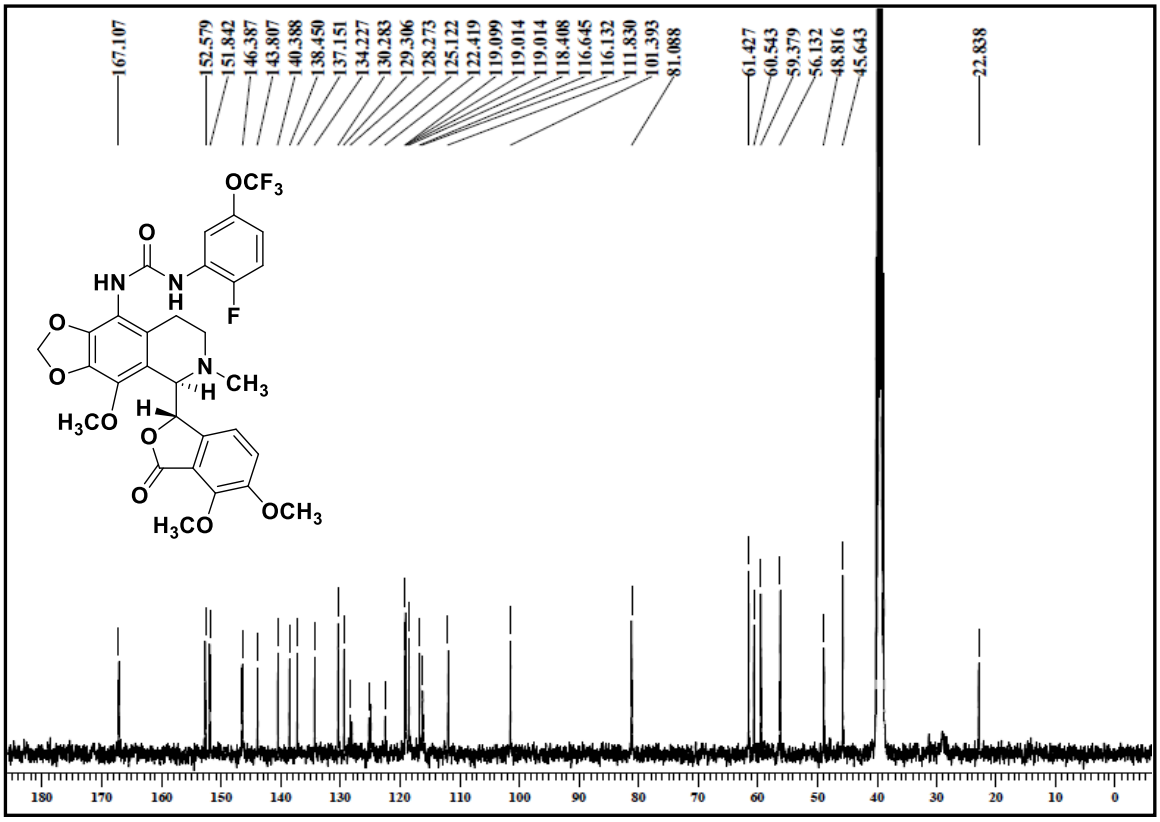

A6.12: HRMS of Urea congener, 7d

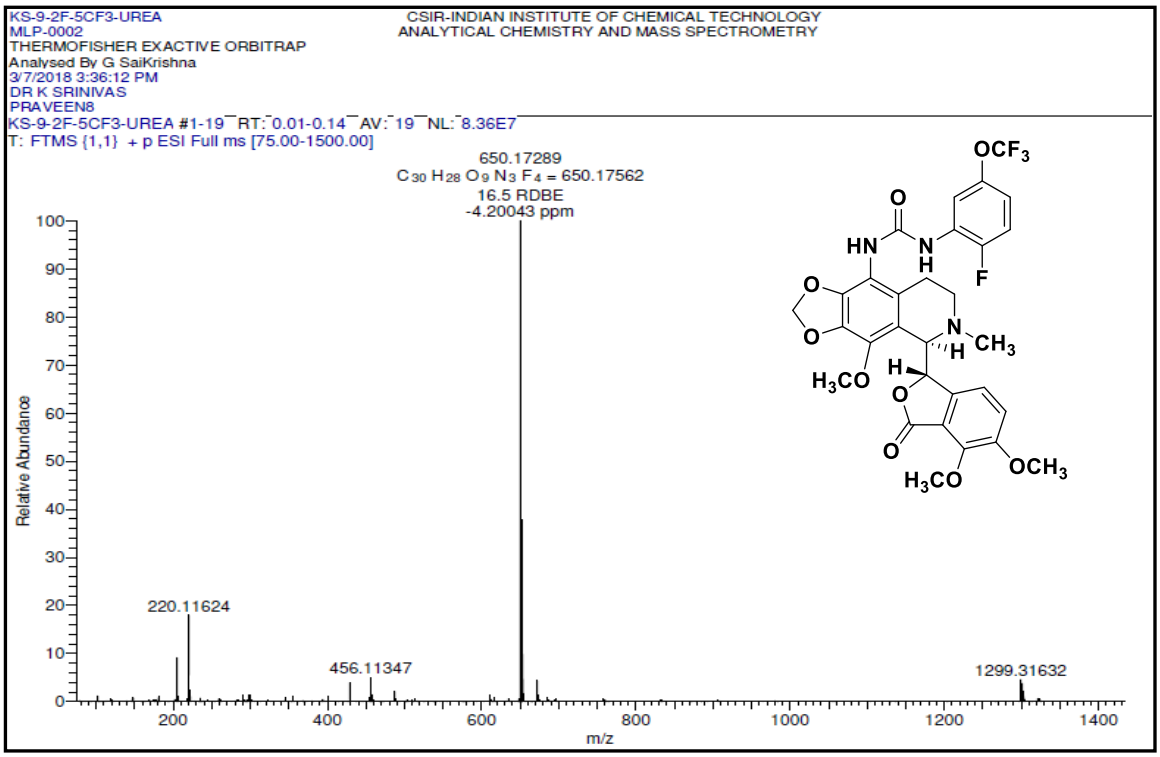

A6.13: ^{1}H NMR of Urea congener, 7e

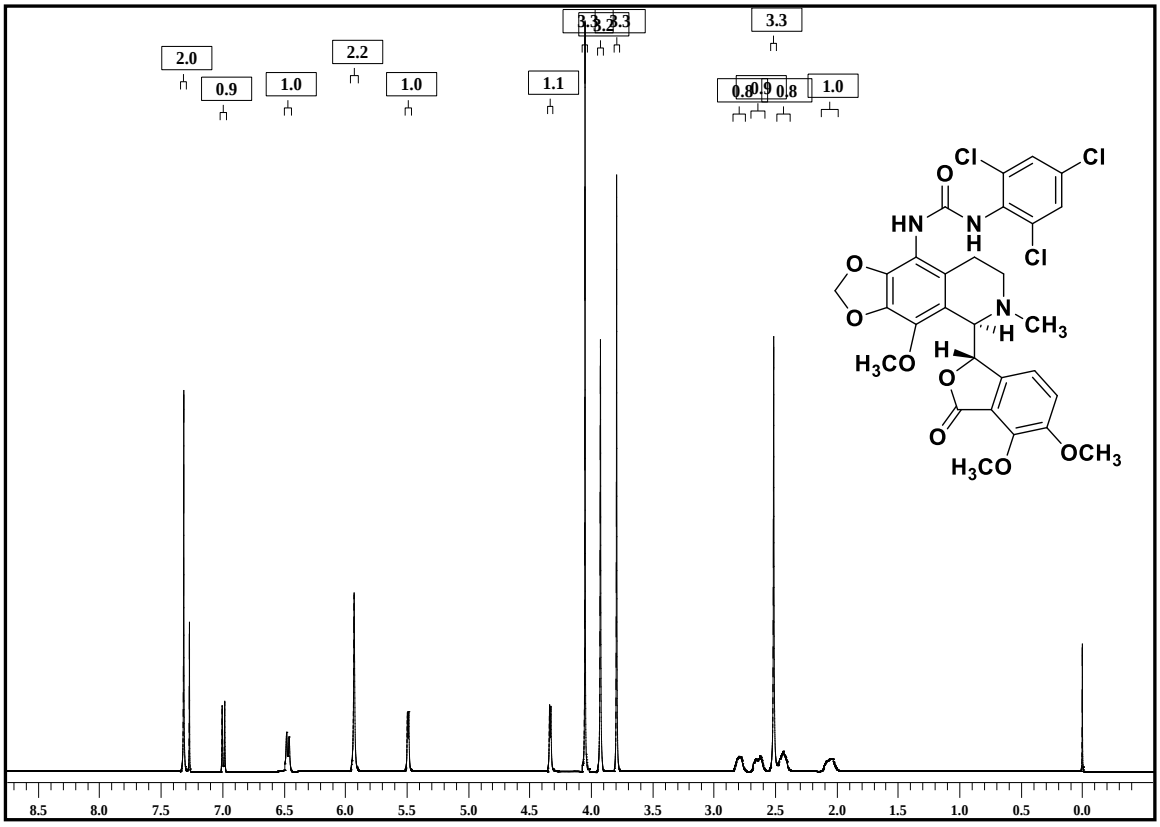

A6.14: ^{13}C NMR of Urea congener, 7e

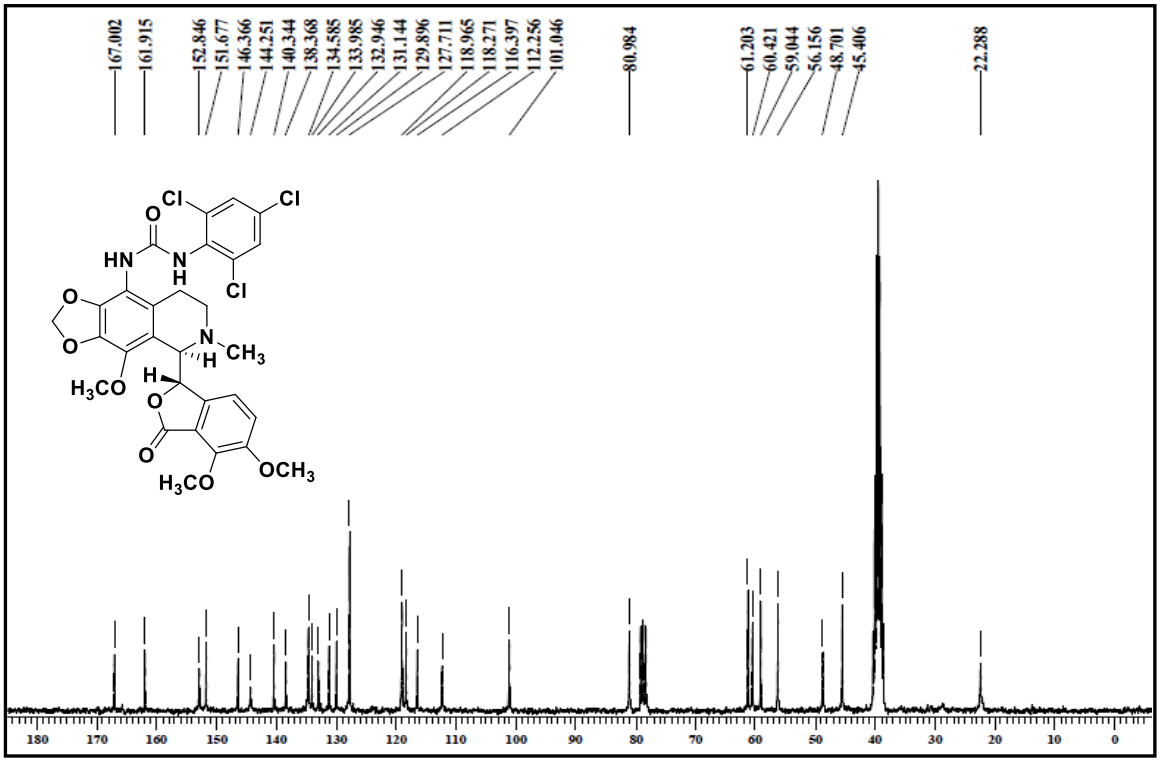

A6.15: HRMS Urea congener, 7e

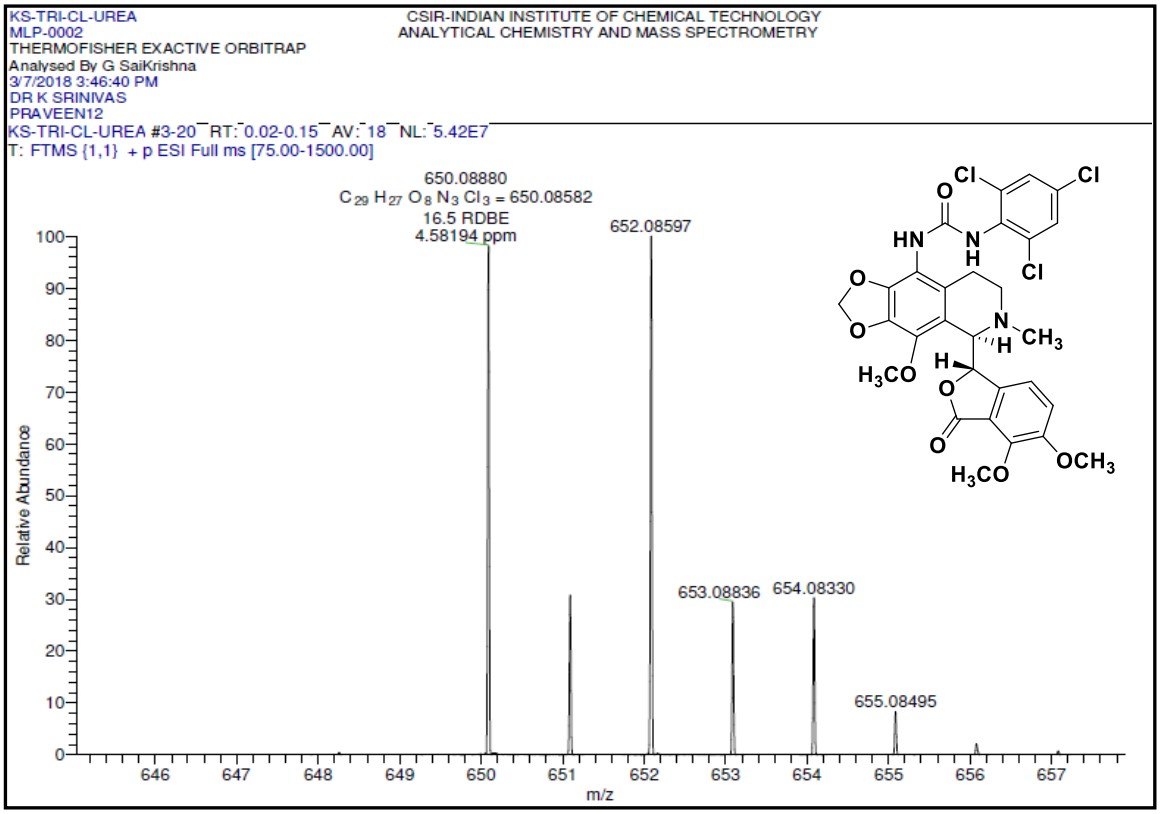

A6.16: ^{1}H NMR of Urea congener, 7f

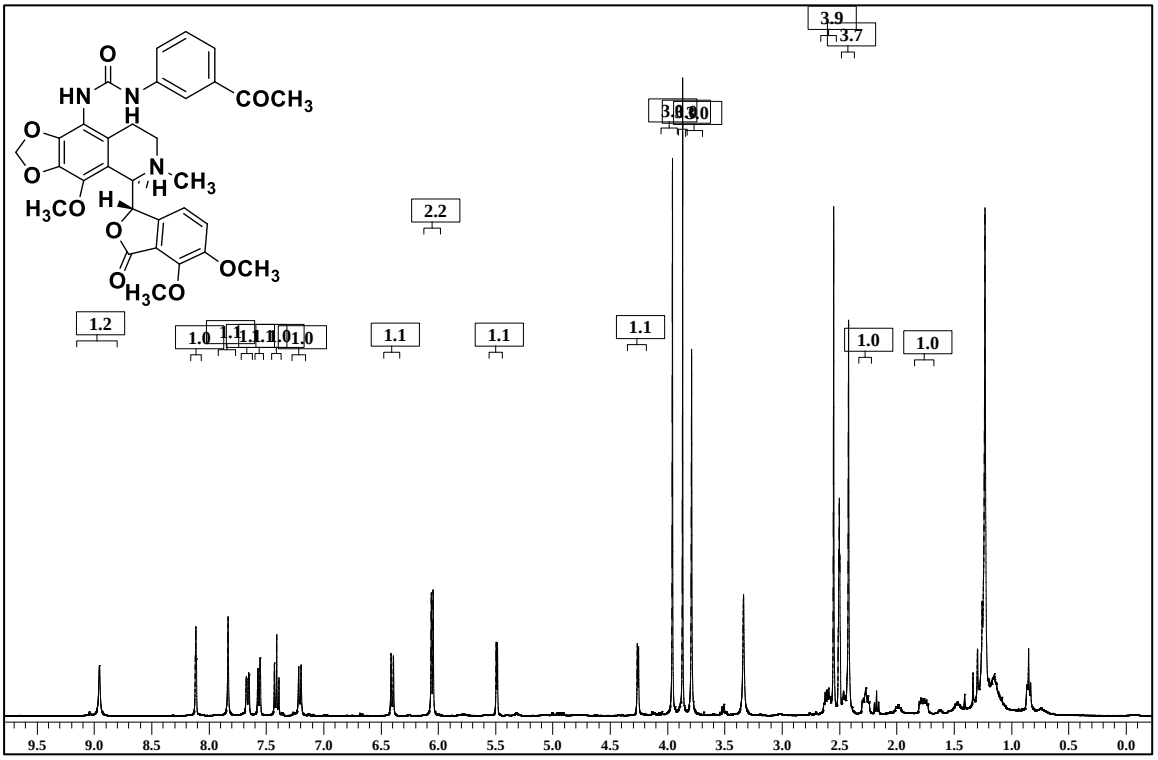

A6.17: ^{13}C NMR of Urea congener, 7f

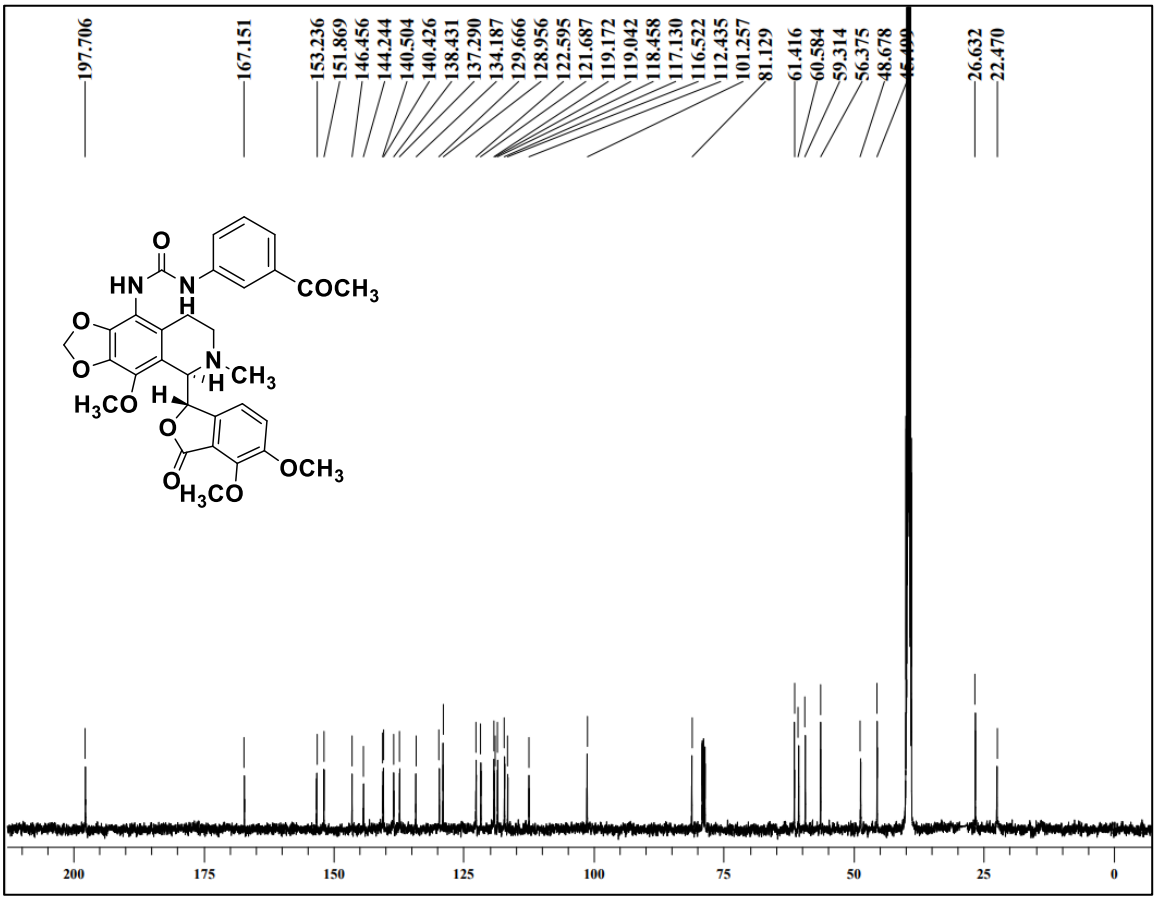

A6.18: HRMS Urea congener, 7f

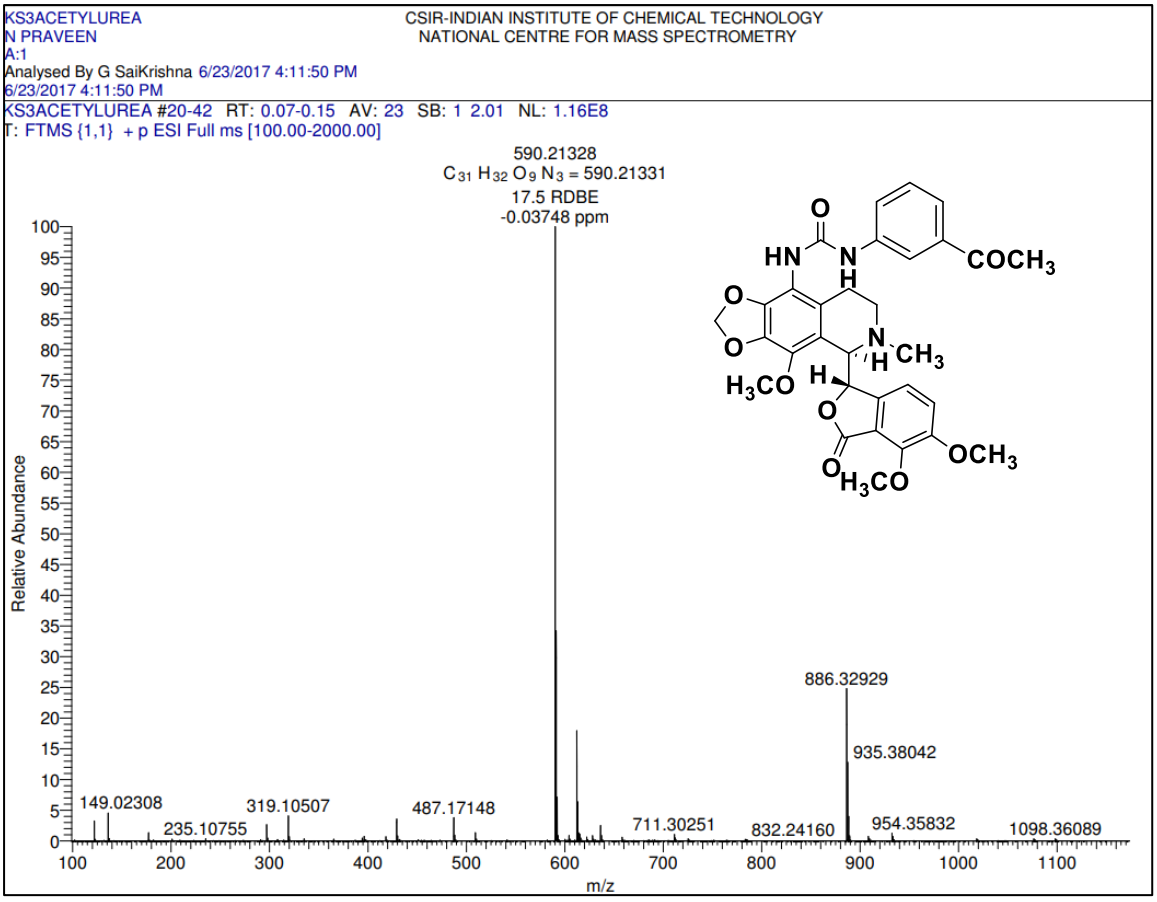

A6.19: ^{1}H NMR of Urea congener, 7g

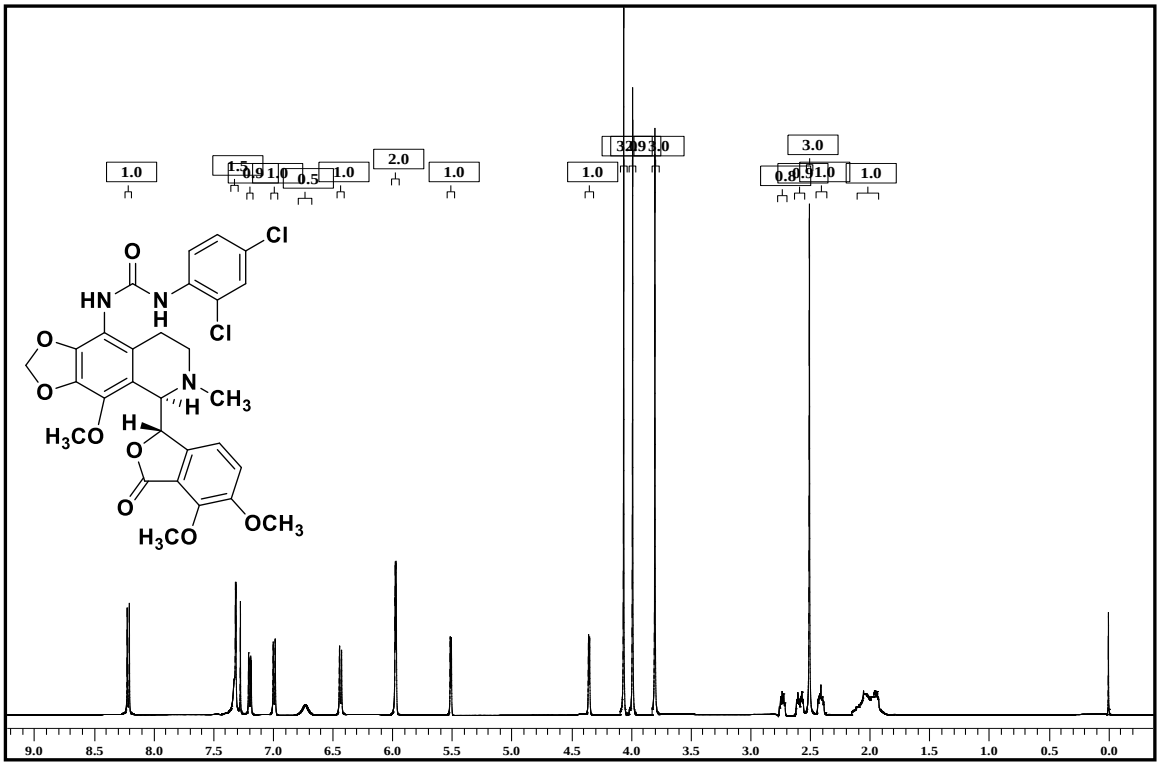

A6.20: ^{13}C NMR of Urea congener, 7g

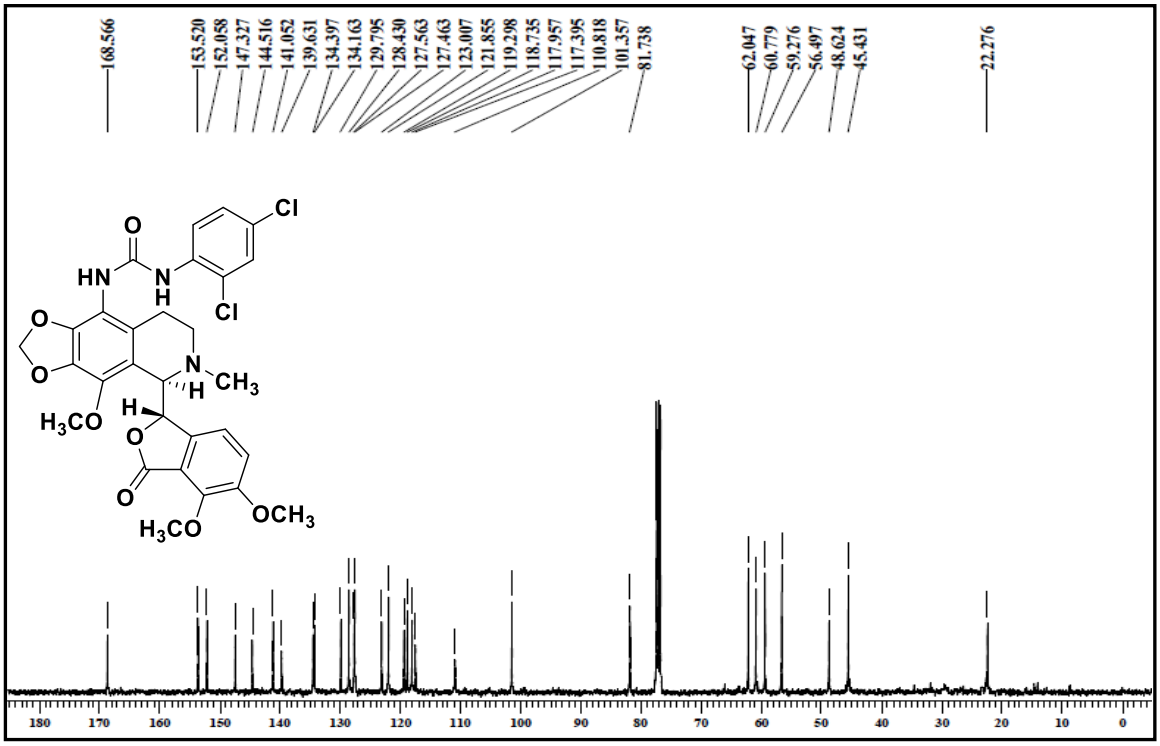

A6.21: HRMS Urea congener, 7g

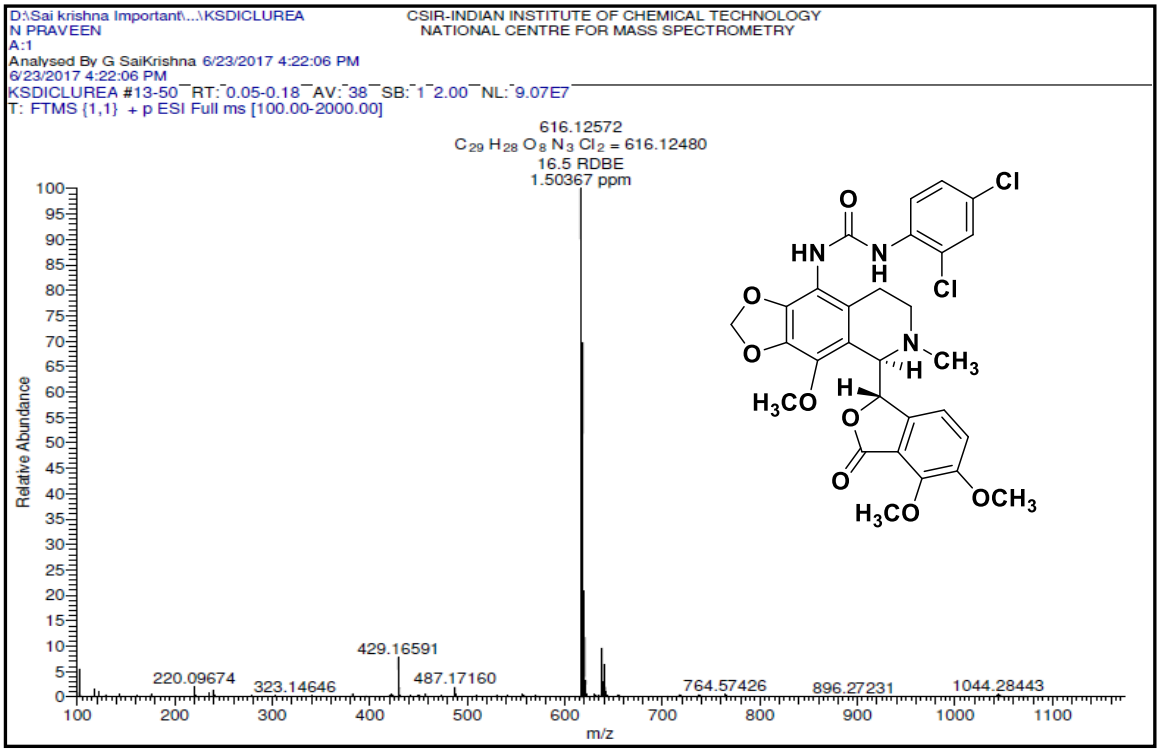

A6.22: ^{1}H NMR of Urea congener, 7h

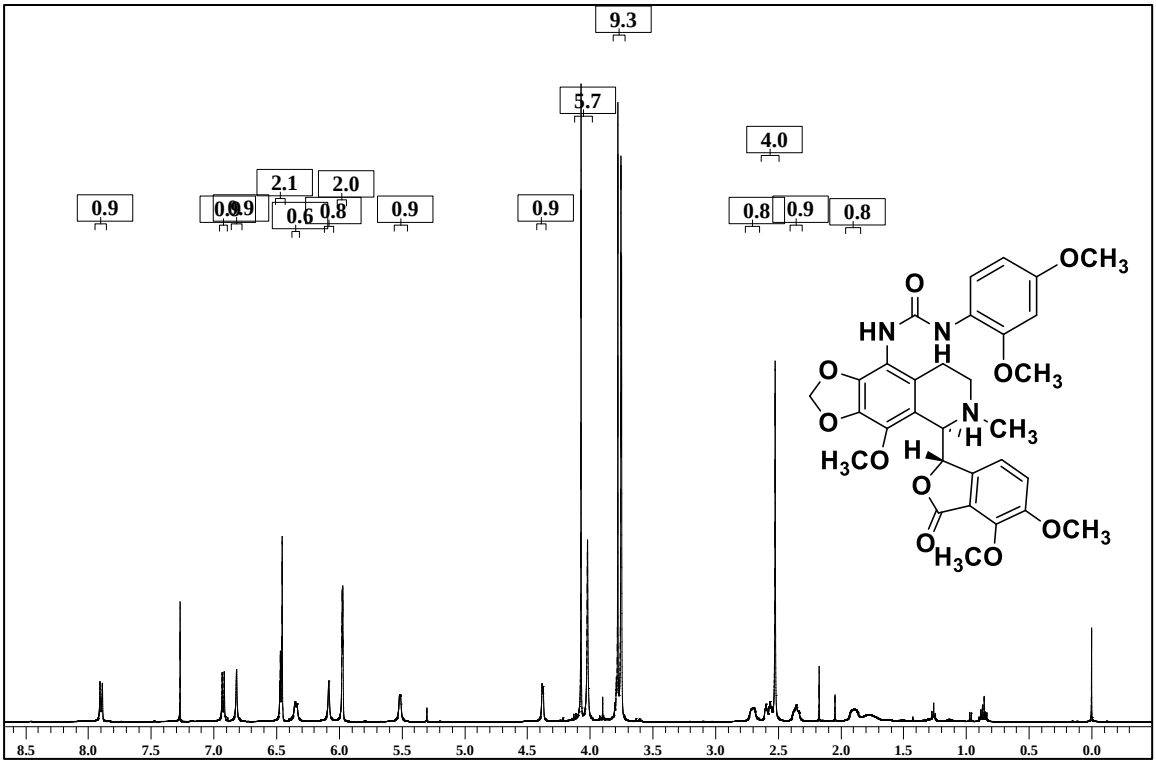

A6.23: ^{13}C NMR of Urea congener, 7h

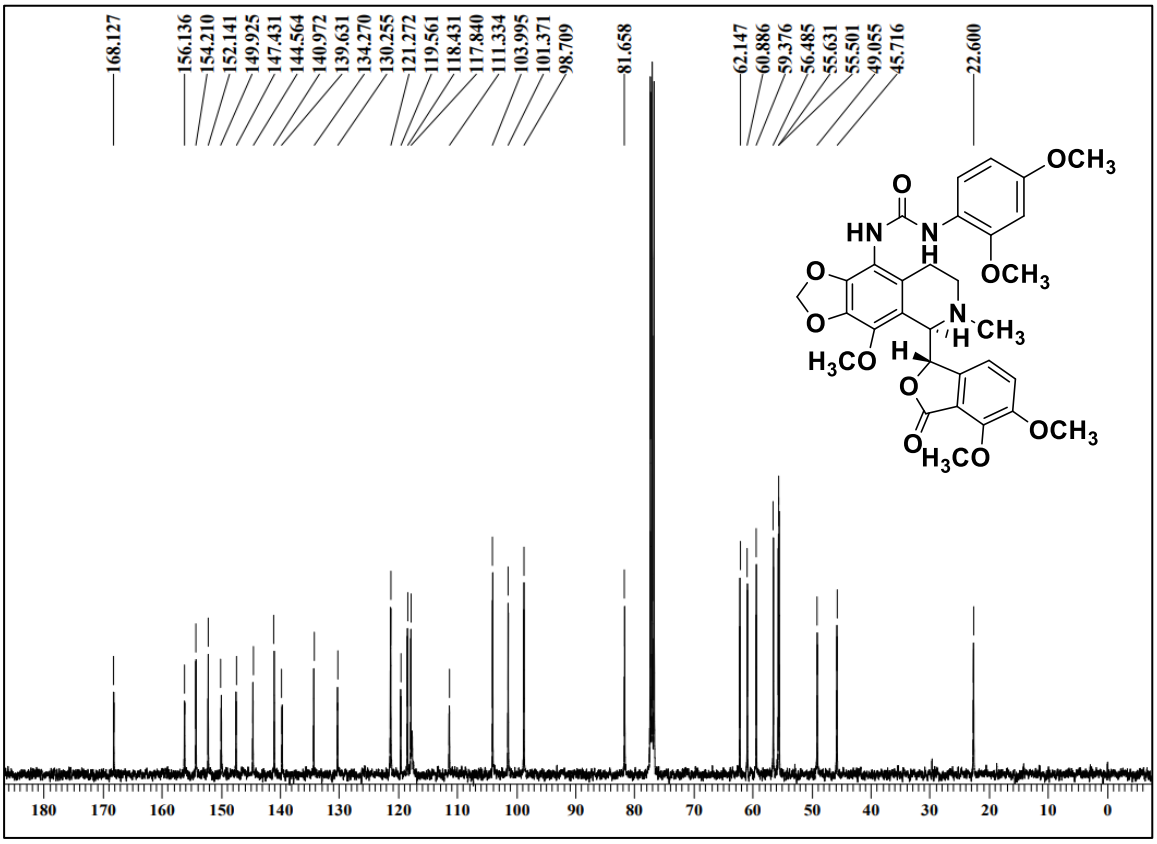

A6.24: HRMS Urea congener, 7h

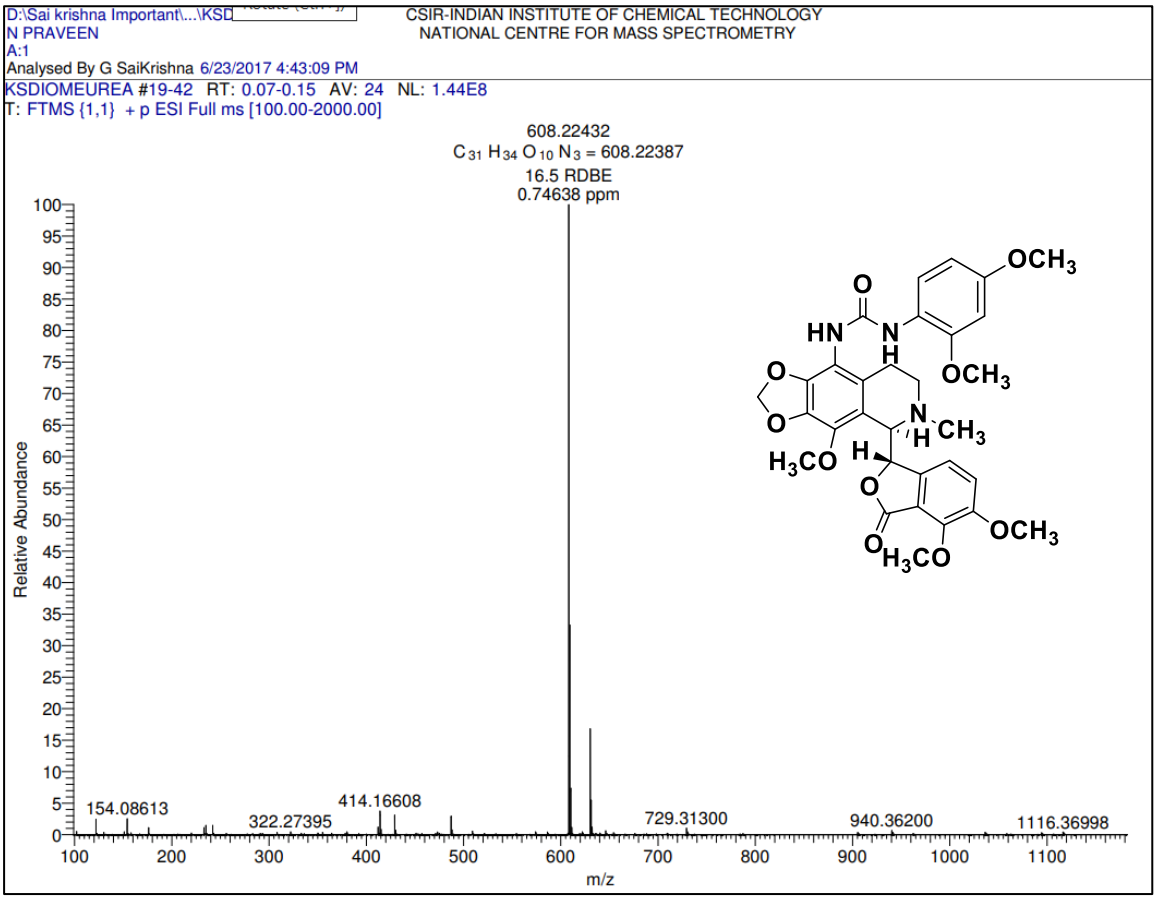

Table A6.25-A6.28: Geometry of hydrogen bonds and hydrophobic interaction of urea congeners, **7f-7h** and the lead molecule, noscapine with the binding site residues of tubulin.

Table A6.25			**Table A6.26**		
(a) 7f_Tubulin			**(b) 7g_Tubulin**		
Hydrogen bonding			**Hydrogen bonding**		
Hydrogen Donor (D)	**Hydrogen Acceptor (A)**	**Distance (D-A) in Å**	**Hydrogen Donor (D)**	**Hydrogen Acceptor (A)**	**Distance (D-A) in Å**
900 N2	LEU B 248 O	2.96	ALA B 250 N	900 CL1	3.78
			900 N2	LEU B 248 O	2.70
			900 N1	EU B 248 O	3.95
Hydrophobic interaction			**Hydrophobic interaction**		
7f	**Tubulin**	**Distance**	**7g**	**Tubulin**	**Distance**
C25	ILE B 378 CD1	3.5	C25	ILE B 378 CD1	3.57
C24	ILE B 378 CD1	3.42	C24	ILE B 378 CD1	3.48
C23	ILE B 378 CD1	4.57	C23	ILE B 378 CD1	4.62
C20	ILE B 378 CD1	4.7	C20	ILE B 378 CD1	4.75
C25	ILE B 378 CG1	4.78	C25	ILE B 378 CG1	4.84
C24	ILE B 378 CG1	4.81	C24	ILE B 378 CG1	4.87
C31	CYS B 356 SG	3.96	C15	CYS B 356 CA	4.92
C31	CYS B 356 CB	3.22	C16	CYS B 356 N	4.83
C30	CYS B 356 CB	4.72	C15	CYS B 356 N	4.87
C31	CYS B 356 C	4.89	C17	VAL B 355 O	4.33
C31	CYS B 356 CA	3.4	C16	VAL B 355 O	3.11
C30	CYS B 356 CA	4.82	C15	VAL B 355 O	3.55
C31	CYS B 356 N	3.58	C14	VAL B 355 O	4.95
C30	CYS B 356 N	4.93	C16	VAL B 355 C	3.97
C15	CYS B 356 N	4.87	C15	VAL B 355 C	4.36
C31	VAL B 355 O	3.12	C16	VAL B 355 CA	4.65
C30	VAL B 355 O	3.89	C17	VAL B 355 N	4.52
C17	VAL B 355 O	4.86	C16	VAL B 355 N	3.96
C16	VAL B 355 O	3.63	C15	VAL B 355 N	4.9
C15	VAL B 355 O	2.87	N3	ALA B 354 CB	4.71
C14	VAL B 355 O	3.7	C26	ALA B 354 CB	3.96
C13	VAL B 355 O	4.9	C17	ALA B 354 CB	3.58
C31	VAL B 355 C	3.56	C16	ALA B 354 CB	3.83
C30	VAL B 355 C	4.61	C15	ALA B 354 CB	4.67
C16	VAL B 355 C	4.64	C12	ALA B 354 CB	4.24
C15	VAL B 355 C	3.94	N2	ALA B 354 CB	4.76
C14	VAL B 355 C	4.58	O3	ALA B 354 CB	3.66
C31	VAL B 355 CA	4.78	C11	ALA B 354 CB	4.44
C15	VAL B 355 CA	4.71	C10	ALA B 354 CB	3.94
C31	VAL B 355 N	4.76	C9	ALA B 354 CB	4.2
C17	VAL B 355 N	4.96	C17	ALA B 354 C	4.94
C16	VAL B 355 N	4.29	C16	ALA B 354 C	4.66
C15	VAL B 355 N	4.18	C26	ALA B 354 CA	4.76
C14	VAL B 355 N	4.79	C17	ALA B 354 CA	4.34
N3	ALA B 354 CB	4.84	C16	ALA B 354 CA	4.5
C26	ALA B 354 CB	4.18	O3	ALA B 354 CA	4.34
C17	ALA B 354 CB	4.39	C26	ALA B 354 N	4.23
C16	ALA B 354 CB	4.6	C26	THR B 353 O	4.8
C15	ALA B 354 CB	4.6	C26	THR B 353 C	4.38
C14	ALA B 354 CB	4.4	O3	THR B 353 C	4.8
C13	ALA B 354 CB	4.17	C26	THR B 353 CA	4.69
C12	ALA B 354 CB	4.15	C26	THR B 353 N	4.62
N2	ALA B 354 CB	4.63	C11	LYS B 352 NZ	4.68
O3	ALA B 354 CB	3.71	C6	LYS B 352 NZ	4.97
C11	ALA B 354 CB	4.38	C5	LYS B 352 NZ	3.59
C10	ALA B 354 CB	3.93	C4	LYS B 352 NZ	3.43

C9	ALA B 354 CB	4.24	C3	LYS B 352 NZ	3.9
C26	ALA B 354 CA	4.96	C2	LYS B 352 NZ	4.06
C17	ALA B 354 CA	4.77	C1	LYS B 352 NZ	4.83
C16	ALA B 354 CA	4.8	O3	LYS B 352 CE	3.57
C12	ALA B 354 CA	4.97	C11	LYS B 352 CE	4.2
O3	ALA B 354 CA	4.32	N1	LYS B 352 CE	4.08
C26	ALA B 354 N	4.41	C7	LYS B 352 CE	4.58
C26	THR B 353 O	4.95	C6	LYS B 352 CE	4.27
C26	THR B 353 C	4.53	O2	LYS B 352 CE	4.35
O3	THR B 353 C	4.56	C5	LYS B 352 CE	4.35
C26	THR B 353 CA	4.78	O1	LYS B 352 CE	3.87
C26	THR B 353 N	4.66	C4	LYS B 352 CE	3.48
C11	LYS B 352 NZ	4.4	C3	LYS B 352 CE	3.85
C6	LYS B 352 NZ	4.98	C2	LYS B 352 CE	3.71
C5	LYS B 352 NZ	3.69	C1	LYS B 352 CE	4.39
C4	LYS B 352 NZ	3.45	O4	LYS B 352 CD	4.74
C3	LYS B 352 NZ	4.01	O3	LYS B 352 CD	4.74
C2	LYS B 352 NZ	4.03	C7	LYS B 352 CD	4.6
C1	LYS B 352 NZ	4.96	C6	LYS B 352 CD	4.75
O3	LYS B 352 CE	3.21	O2	LYS B 352 CD	4.31
C11	LYS B 352 CE	3.88	C5	LYS B 352 CD	4.65
N1	LYS B 352 CE	3.93	O1	LYS B 352 CD	4.6
C7	LYS B 352 CE	4.67	C4	LYS B 352 CD	4.15
C6	LYS B 352 CE	4.27	C3	LYS B 352 CD	4
O2	LYS B 352 CE	4.5	C2	LYS B 352 CD	4.52
C5	LYS B 352 CE	4.43	C1	LYS B 352 CD	4.24
O1	LYS B 352 CE	3.87	N3	LYS B 352 CG	4.73
C4	LYS B 352 CE	3.49	C26	LYS B 352 CG	3.94
C3	LYS B 352 CE	3.97	O4	LYS B 352 CG	4.1
C2	LYS B 352 CE	3.66	O3	LYS B 352 CG	4.66
C1	LYS B 352 CE	4.53	C10	LYS B 352 CG	4.9
O4	LYS B 352 CD	4.95	C8	LYS B 352 CG	4.33
O3	LYS B 352 CD	4.35	C7	LYS B 352 CG	3.77
C7	LYS B 352 CD	4.67	C6	LYS B 352 CG	4.14
C6	LYS B 352 CD	4.72	O2	LYS B 352 CG	4.59
O2	LYS B 352 CD	4.44	C4	LYS B 352 CG	4.32
C5	LYS B 352 CD	4.72	C3	LYS B 352 CG	3.99
O1	LYS B 352 CD	4.58	C2	LYS B 352 CG	4.38
C4	LYS B 352 CD	4.12	C1	LYS B 352 CG	3.71
C3	LYS B 352 CD	4.09	C26	LYS B 352 CB	4.31
C2	LYS B 352 CD	4.44	O4	LYS B 352 CB	4.11
C1	LYS B 352 CD	4.37	C8	LYS B 352 CB	4.62
N3	LYS B 352 CG	4.76	C7	LYS B 352 CB	4.44
C26	LYS B 352 CG	3.95	C3	LYS B 352 CB	4.76
O4	LYS B 352 CG	4.32	C1	LYS B 352 CB	4.22
O3	LYS B 352 CG	4.28	C26	LYS B 352 O	4.08
C10	LYS B 352 CG	4.8	C26	LYS B 352 C	4.35
C8	LYS B 352 CG	4.44	N3	ILE B 318 CD1	4.76
C7	LYS B 352 CG	3.84	C26	ILE B 318 CD1	4.89
C6	LYS B 352 CG	4.09	C25	ILE B 318 CD1	3.93
O2	LYS B 352 CG	4.7	C24	ILE B 318 CD1	3.79
C4	LYS B 352 CG	4.28	C23	ILE B 318 CD1	4.99
C3	LYS B 352 CG	4.06	N3	ILE B 318 CG1	4.45
C2	LYS B 352 CG	4.29	C29	ILE B 318 CG1	4.89
C1	LYS B 352 CG	3.83	C26	ILE B 318 CG1	4.47
C26	LYS B 352 CB	4.25	C25	ILE B 318 CG1	4.21
O4	LYS B 352 CB	4.32	C24	ILE B 318 CG1	4.02
C8	LYS B 352 CB	4.7	C23	ILE B 318 CG1	4.97
C7	LYS B 352 CB	4.47	C9	ILE B 318 CG1	4.42
C3	LYS B 352 CB	4.8	C26	ILE B 318 N	4.94

C1	LYS B 352 CB	4.31	C26	ALA B 317 O	3.27
C26	LYS B 352 O	4.03	C26	ALA B 317 C	4.04
C26	LYS B 352 C	4.33	C26	ALA B 317 CA	4.56
C26	LYS B 352 CA	4.98	C26	ALA B 317 N	3.8
N3	ILE B 318 CD1	4.75	N3	ALA B 316 CB	3.49
C29	ILE B 318 CD1	4.75	C27	ALA B 316 CB	4.74
C26	ILE B 318 CD1	4.86	C26	ALA B 316 CB	3.68
C25	ILE B 318 CD1	3.94	C25	ALA B 316 CB	3.76
C24	ILE B 318 CD1	3.74	C20	ALA B 316 CB	4.07
C23	ILE B 318 CD1	4.92	O5	ALA B 316 CB	4.96
N3	ILE B 318 CG1	4.48	C18	ALA B 316 CB	3.61
C29	ILE B 318 CG1	4.47	O4	ALA B 316 CB	4.74
C26	ILE B 318 CG1	4.51	C9	ALA B 316 CB	4.88
C25	ILE B 318 CG1	4.25	C8	ALA B 316 CB	3.37
C24	ILE B 318 CG1	3.99	C7	ALA B 316 CB	4.76
C23	ILE B 318 CG1	4.9	C26	ALA B 316 O	4.84
C9	ILE B 318 CG1	4.4	N3	ALA B 316 C	4.56
C26	ILE B 318 N	4.98	C26	ALA B 316 C	4.02
C26	ALA B 317 O	3.35	N3	ALA B 316 CA	4.27
C9	ALA B 317 O	4.98	C26	ALA B 316 CA	3.9
C26	ALA B 317 C	4.07	C18	ALA B 316 CA	4.94
C26	ALA B 317 CA	4.51	C8	ALA B 316 CA	4.33
C26	ALA B 317 N	3.7	C27	MET B 259 SD	4.57
N3	ALA B 316 CB	3.37	C27	MET B 259 CG	4.09
C27	ALA B 316 CB	4.83	C27	MET B 259 N	4.52
C26	ALA B 316 CB	3.46	C27	ASN B 258 ND2	4.62
C25	ALA B 316 CB	3.76	C5	ASN B 258 ND2	3.69
C20	ALA B 316 CB	4.11	C3	ASN B 258 ND2	4.54
C18	ALA B 316 CB	3.69	C5	ASN B 258 OD1	4.63
O4	ALA B 316 CB	4.75	C27	ASN B 258 CG	4.48
C9	ALA B 316 CB	4.79	O4	ASN B 258 CG	4.74
C8	ALA B 316 CB	3.32	O2	ASN B 258 CG	3.77
C7	ALA B 316 CB	4.7	C5	ASN B 258 CG	4.2
C26	ALA B 316 O	4.69	C3	ASN B 258 CG	4.9
N3	ALA B 316 C	4.51	C27	ASN B 258 CB	3.46
C26	ALA B 316 C	3.87	O4	ASN B 258 CB	4
N3	ALA B 316 CA	4.18	O2	ASN B 258 CB	4.01
C26	ALA B 316 CA	3.71	C5	ASN B 258 CB	4.87
C8	ALA B 316 CA	4.33	C3	ASN B 258 CB	4.89
C27	MET B 259 SD	4.58	C1	ASN B 258 CB	4.89
C27	MET B 259 CG	4.01	C27	ASN B 258 O	4.87
C18	MET B 259 CG	4.98	C27	ASN B 258 C	4.45
C27	MET B 259 N	4.44	C27	ASN B 258 CA	4.52
C27	ASN B 258 ND2	4.58	O6	LEU B 255 CD2	4.66
C5	ASN B 258 ND2	3.58	C23	LEU B 255 CD2	4.71
C3	ASN B 258 ND2	4.45	C22	LEU B 255 CD2	4.45
C5	ASN B 258 OD1	4.54	C21	LEU B 255 CD2	4.57
C27	ASN B 258 CG	4.47	C20	LEU B 255 CD2	4.96
O4	ASN B 258 CG	4.64	C19	LEU B 25 CD2	4.96
O2	ASN B 258 CG	3.64	C27	LEU B 255 CD1	4.49
C5	ASN B 258 CG	4.1	O8	LEU B 255 CD1	4.47
C3	ASN B 258 CG	4.81	C25	LEU B 255 CD1	3.93
C27	ASN B 258 CB	3.44	C24	LEU B 255 CD1	4.48
O4	ASN B 258 CB	3.87	C23	LEU B 255 CD1	4.65
O2	ASN B 258 CB	3.88	C22	LEU B 255 CD1	4.27
C5	ASN B 258 CB	4.77	C21	LEU B 255 CD1	3.63
C3	ASN B 258 CB	4.78	C20	LEU B 255 CD1	3.46
C1	ASN B 258 CB	4.78	C19	LEU B 255 CD1	3.8
C27	ASN B 258 O	4.89	O5	LEU B 255 CD1	3.74
C27	ASN B 258 C	4.41	C18	LEU B 255 CD1	3.59

C27	ASN B 258 CA	4.47	O8	LEU B 255 CG	4.52
O6	LEU B 255 CD2	4.84	O6	LEU B 255 CG	4.91
C23	LEU B 255 CD2	4.76	C22	LEU B 255 CG	4.58
C22	LEU B 255 CD2	4.51	C21	LEU B 255 CG	4.23
C21	LEU B 255 CD2	4.56	C20	LEU B 255 CG	4.51
C20	LEU B 255 CD2	4.88	C19	LEU B 255 CG	4.23
C19	LEU B 255 CD2	4.97	O5	LEU B 255 CG	4.53
C27	LEU B 255 CD1	4.32	C18	LEU B 255 CG	4.76
O8	LEU B 255 CD1	4.63	O8	LEU B 255 CB	3.49
C25	LEU B 255 CD1	3.87	O6	LEU B 255 CB	4.42
C24	LEU B 255 CD1	4.5	C22	LEU B 255 CB	4.42
C23	LEU B 255 CD1	4.72	C21	LEU B 255 CB	4.03
C22	LEU B 255 CD1	4.35	C20	LEU B 255 CB	4.68
C21	LEU B 255 CD1	3.66	C19	LEU B 255 CB	3.6
C20	LEU B 255 CD1	3.4	O5	LEU B 255 CB	4.11
C19	LEU B 255 CD1	3.87	C18	LEU B 255 CB	4.8
O5	LEU B 255 CD1	3.73	C27	LEU B 255 O	4.1
C18	LEU B 255 CD1	3.49	C27	LEU B 255 C	4.65
C8	LEU B 255 CD1	4.91	O8	LEU B 255 C	4.93
O8	LEU B 255 CG	4.68	O5	LEU B 255 C	4.92
C22	LEU B 255 CG	4.67	C27	LEU B 255 CA	4.26
C21	LEU B 255 CG	4.25	O8	LEU B 255 CA	3.42
C20	LEU B 255 CG	4.45	C21	LEU B 255 CA	4.52
C19	LEU B 255 CG	4.29	C19	LEU B 255 CA	3.63
O5	LEU B 255 CG	4.48	O5	LEU B 255 CA	3.76
C18	LEU B 255 CG	4.64	C18	LEU B 255 CA	4.68
O8	LEU B 255 CB	3.66	C27	LEU B 255 N	4.87
O6	LEU B 255 CB	4.65	C21	LEU B 255 N	4.98
C22	LEU B 255 CB	4.54	C19	LEU B 255 N	3.85
C21	LEU B 255 CB	4.06	O8	LYS B 254 CB	4.33
C20	LEU B 255 CB	4.62	C27	LYS B 254 O	3.92
C19	LEU B 255 CB	3.65	C19	LYS B 254 O	4.57
O5	LEU B 255 CB	4.03	C3	LYS B 254 O	4.83
C18	LEU B 255 CB	4.67	C1	LYS B 254 O	4.94
C27	LEU B 255 O	3.89	C27	LYS B 254 C	4.78
C27	LEU B 255 C	4.42	O8	LYS B 254 C	3.72
O5	LEU B 255 C	4.92	C19	LYS B 254 C	4.44
C27	LEU B 255 CA	4.03	O5	LYS B 254 C	4.53
O8	LEU B 255 CA	3.67	O8	LYS B 254 CA	4.57
C21	LEU B 255 CA	4.58	C28	ASP B 251 O	3.95
C19	LEU B 255 CA	3.73	C19	ASP B 251 O	4.47
O5	LEU B 255 CA	3.72	C28	ASP B 251 C	4.31
C18	LEU B 255 CA	4.57	O8	ASP B 251 C	4.45
C27	LEU B 255 N	4.65	O6	ASP B 251 C	4.6
C19	LEU B 255 N	3.93	C28	ASP B 251 CA	4.4
O8	LYS B 254 CB	4.44	C28	ASP B 251 N	3.98
C27	LYS B 254 O	3.75	C28	ALA B 250 CB	3.43
C19	LYS B 254 O	4.7	O8	ALA B 250 CB	3.47
C5	LYS B 254 O	4.98	O6	ALA B 250 CB	4.79
C3	LYS B 254 O	4.72	C19	ALA B 250 CB	4.33
C1	LYS B 254 O	4.81	N2	ALA B 250 CB	4.77
C27	LYS B 254 C	4.59	N1	ALA B 250 CB	4.22
O8	LYS B 254 C	3.96	C6	ALA B 250 CB	4.93
C19	LYS B 254 C	4.54	C4	ALA B 250 CB	4.98
O5	LYS B 254 C	4.5	C2	ALA B 250 CB	4.51
O8	LYS B 254 CA	4.75	C28	ALA B 250 O	3.64
C28	ASP B 251 O	4.21	C28	ALA B 250 C	3.66
C19	ASP B 251 O	4.42	O8	ALA B 250 C	4.62
C28	ASP B 251 C	4.59	O6	ALA B 250 C	4.87
O8	ASP B 251 C	4.4	C28	ALA B 250 CA	4.16

O6	ASP B 251 C	4.77	O8	ALA B 250 CA	4.6
C28	ASP B 251 CA	4.65	N2	LEU B 248 CD2	4.87
O8	ASP B 251 CA	4.94	C11	LEU B 248 CD2	4.39
C28	ASP B 251 N	4.19	N1	LEU B 248 CD2	3.7
C28	ALA B 250 CB	3.44	C5	LEU B 248 CD2	3.92
O8	ALA B 250 CB	3.3	O1	LEU B 248 CD2	2.77
O6	ALA B 250 CB	4.8	C4	LEU B 248 CD2	3.71
C19	ALA B 250 CB	4.25	C3	LEU B 248 CD2	4.84
N1	ALA B 250 CB	4.36	C2	LEU B 248 CD2	4.2
C6	ALA B 250 CB	4.99	O1	LEU B 248 CD1	4.97
C2	ALA B 250 CB	4.59	N2	LEU B 248 CG	4.4
C28	ALA B 250 O	3.75	C11	LEU B 248 CG	4.37
C28	ALA B 250 C	3.8	N1	LEU B 248 CG	3.85
O8	ALA B 250 C	4.43	O1	LEU B 248 CG	3.97
O6	ALA B 250 C	4.9	C4	LEU B 248 CG	4.6
C28	ALA B 250 CA	4.24	C2	LEU B 248 CG	4.73
O8	ALA B 250 CA	4.44	C12	LEU B 248 CB	4.81
N2	LEU B 248 CD2	4.69	N2	LEU B 248 CB	3.75
O3	LEU B 248 CD2	4.99	O3	LEU B 248 CB	4.6
C11	LEU B 248 CD2	4.34	C11	LEU B 248 CB	3.92
N1	LEU B 248 CD2	3.73	N1	LEU B 248 CB	3.9
C5	LEU B 248 CD2	4	O1	LEU B 248 CB	4.92
O1	LEU B 248 CD2	2.85	C17	LEU B 248 O	4.3
C4	LEU B 248 CD2	3.78	C14	LEU B 248 O	4.37
C3	LEU B 248 CD2	4.93	C13	LEU B 248 O	3.23
C2	LEU B 248 CD2	4.26	C12	LEU B 248 O	3.19
N2	LEU B 248 CG	4.31	C11	LEU B 248 O	3.77
C11	LEU B 248 CG	4.42	C13	LEU B 248 C	4.41
N1	LEU B 248 CG	3.94	C12	LEU B 248 C	4.26
O1	LEU B 248 CG	4.05	N2	LEU B 248 C	3.67
C4	LEU B 248 CG	4.68	C11	LEU B 248 C	4.56
C2	LEU B 248 CG	4.81	N1	LEU B 248 C	4.64
C17	LEU B 248 CB	4.62	C12	LEU B 248 CA	4.69
C12	LEU B 248 CB	4.39	N2	LEU B 248 CA	3.99
N2	LEU B 248 CB	3.58	C11	LEU B 248 CA	4.62
O3	LEU B 248 CB	4.75	N1	LEU B 248 CA	4.81
C11	LEU B 248 CB	3.96	C17	LEU B 248 N	4.62
N1	LEU B 248 CB	3.98	C13	LEU B 248 N	4.98
O1	LEU B 248 CB	5	C12	LEU B 248 N	4.33
C17	LEU B 248 O	4.26	C11	LEU B 248 N	4.72
C14	LEU B 248 O	4.69	C17	GLN B 247 N	4.35
C13	LEU B 248 O	3.67	C16	GLN B 247 N	4.42
C12	LEU B 248 O	3.4	C15	GLN B 247 N	4.83
C11	LEU B 248 O	4.04	C12	GLN B 247 N	4.7
C17	LEU B 248 C	4.86	C17	GLY B 246 C	4.72
C13	LEU B 248 C	4.73	C16	GLY B 246 C	4.65
C12	LEU B 248 C	4.28	C15	GLY B 246 C	4.65
N2	LEU B 248 C	3.81	C14	GLY B 246 C	4.73
C11	LEU B 248 C	4.78	C13	GLY B 246 C	4.81
N1	LEU B 248 C	4.77	C12	GLY B 246 C	4.82
C17	LEU B 248 CA	4.58	C17	GLY B 246 CA	4.34
C12	LEU B 248 CA	4.38	C16	GLY B 246 CA	3.87
N2	LEU B 248 CA	3.94	C15	GLY B 246 CA	3.54
C11	LEU B 248 CA	4.75	C14	GLY B 246 CA	3.71
N1	LEU B 248 CA	4.91	C13	GLY B 246 CA	4.19
C17	LEU B 248 N	3.67	C12	GLY B 246 CA	4.5
C16	LEU B 248 N	4.41	C16	GLY B 246 N	4.89
C13	LEU B 248 N	4.7	C15	GLY B 246 N	4.18
C12	LEU B 248 N	3.85	C14	GLY B 246 N	4.05
C11	LEU B 248 N	4.83	C13	GLY B 246 N	4.67

C17	GLN B 247 CG	4.88	C16	PRO B 245 O	4.79
C16	GLN B 247 CG	4.57	C15	PRO B 245 O	3.77
C17	GLN B 247 CB	3.72	C14	PRO B 245 O	4.02
C16	GLN B 247 CB	3.73	C15	PRO B 245 C	4.29
C15	GLN B 247 CB	4.84	C14	PRO B 245 C	4.22
C12	GLN B 247 CB	4.83	C15	PHE B 244 O	4.81
C17	GLN B 247 C	4.4	C14	PHE B 244 O	4.11
C16	GLN B 247 C	4.81	C28	LEU B 242 CD2	3.4
C12	GLN B 247 C	4.86	O7	LEU B 242 CD2	4.7
C17	GLN B 247 CA	4.07	O6	LEU B 242 CD2	3.2
C16	GLN B 247 CA	4.05	C22	LEU B 242 CD2	4.5
C15	GLN B 247 CA	4.82	C29	LEU B 242 CD1	4.71
C12	GLN B 247 CA	4.86	O7	LEU B 242 CD1	4.22
C17	GLN B 247 N	3.6	O6	LEU B 242 CD1	4.31
C16	GLN B 247 N	3.27	C29	LEU B 242 CG	4.15
C15	GLN B 247 N	3.68	C28	LEU B 242 CG	4.02
C14	GLN B 247 N	4.32	O7	LEU B 242 CG	3.9
C13	GLN B 247 N	4.57	O6	LEU B 242 CG	3.48
C12	GLN B 247 N	4.27	C23	LEU B 242 CG	4.67
C30	GLY B 246 C	4.97	C22	LEU B 242 CG	4.53
C17	GLY B 246 C	4.35	C29	LEU B 242 CB	4.64
C16	GLY B 246 C	4.01	C28	LEU B 242 CB	4.93
C15	GLY B 246 C	3.98	O7	LEU B 242 CB	4.84
C14	GLY B 246 C	4.3	O6	LEU B 242 CB	4.68
C13	GLY B 246 C	4.61	C29	LEU B 242 CA	4.69
C12	GLY B 246 C	4.65	C28	LEU B 242 CA	4.63
C31	GLY B 246 CA	4.72	O6	LEU B 242 CA	4.76
O9	GLY B 246 CA	3.82	C29	LEU B 242 N	3.54
C30	GLY B 246 CA	3.73	C28	LEU B 242 N	4.19
C17	GLY B 246 CA	4.42	C23	LEU B 242 N	4.98
C16	GLY B 246 CA	3.82	C22	LEU B 242 N	4.99
C15	GLY B 246 CA	3.26	N3	CYS B 241 SG	4.93
C14	GLY B 246 CA	3.41	C29	CYS B 241 SG	4.35
C13	GLY B 246 CA	4.06	C23	CYS B 241 SG	4.94
C12	GLY B 246 CA	4.54	C17	CYS B 241 SG	4.38
C30	GLY B 246 N	4.13	C16	CYS B 241 SG	4.21
C15	GLY B 246 N	4.43	C15	CYS B 241 SG	3.77
C14	GLY B 246 N	4.26	C14	CYS B 241 SG	3.5
C13	GLY B 246 N	4.88	C13	CYS B 241 SG	3.71
C31	PRO B 245 O	3.81	C12	CYS B 241 SG	4.14
C30	PRO B 245 O	3.47	N2	CYS B 241 SG	4.98
C15	PRO B 245 O	4.43	C10	CYS B 241 SG	4.02
C14	PRO B 245 O	4.24	C9	CYS B 241 SG	3.7
C31	PRO B 245 C	4.72	C29	CYS B 241 CB	3.33
O9	PRO B 245 C	3.59	C28	CYS B 241 CB	3.87
C30	PRO B 245 C	4.04	O7	CYS B 241 CB	4.09
C15	PRO B 245 C	4.88	O6	CYS B 241 CB	4.13
C14	PRO B 245 C	4.6	C24	CYS B 241 CB	4.56
O9	PRO B 245 CA	4.55	C23	CYS B 241 CB	3.95
O9	PHE B 244 CB	4.86	C22	CYS B 241 CB	3.97
C31	PHE B 244 O	4.86	C21	CYS B 241 CB	4.59
C30	PHE B 244 O	4.22	C15	CYS B 241 CB	4.58
O9	PHE B 244 C	3.99	C14	CYS B 241 CB	3.74
C30	PHE B 244 C	4.96	C13	CYS B 241 CB	3.74
O9	PHE B 244 CA	4.89	C12	CYS B 241 CB	4.57
C28	LEU B 242 CD2	3.58	C10	CYS B 241 CB	4.25
O7	LEU B 242 CD2	4.81	C9	CYS B 241 CB	3.92
O6	LEU B 242 CD2	3.22	C29	CYS B 241 O	4.8
C22	LEU B 242 CD2	4.49	C28	CYS B 241 O	3.58
O7	LEU B 242 CD1	4.29	C14	CYS B 241 O	4.19

O6	LEU B 242 D1	4.31	C13	CYS B 241 O	4.14
C29	LEU B 242 CG	4.66	C29	CYS B 241 C	3.77
C28	LEU B 242 CG	4.12	C28	CYS B 241 C	3.82
O7	LEU B 242 CG	3.98	O7	CYS B 241 C	4.55
O6	LEU B 242 CG	3.43	O6	CYS B 241 C	4.21
C23	LEU B 242 CG	4.69	C23	CYS B 241 C	4.94
C22	LEU B 242 CG	4.48	C22	CYS B 241 C	4.79
C28	LEU B 242 CB	4.99	C14	CYS B 241 C	4.49
O7	LEU B 242 CB	4.88	C13	CYS B 241 C	4.68
O6	LEU B 242 CB	4.58	C29	CYS B 241 CA	3.38
C28	LEU B 242 CA	4.63	C28	CYS B 241 CA	4.48
O6	LEU B 242 CA	4.62	O7	CYS B 241 CA	4.43
C29	LEU B 242 N	4.07	O6	CYS B 241 CA	4.72
C28	LEU B 242 N	4.11	C23	CYS B 241 CA	4.74
C23	LEU B 242 N	4.97	C22	CYS B 241 CA	4.88
C22	LEU B 242 N	4.9	C15	CYS B 241 CA	4.69
C31	CYS B 241 SG	3.78	C14	CYS B 241 CA	3.81
O9	CYS B 241 SG	3.82	C13	CYS B 241 CA	4.21
C30	CYS B 241 SG	3.6	C29	CYS B 241 N	2.84
C29	CYS B 241 SG	4.39	C23	CYS B 241 N	4.79
C23	CYS B 241 SG	4.92	C14	CYS B 241 N	4.87
C14	CYS B 241 SG	4.01	C29	THR B 240 CB	4.65
C13	CYS B 241 SG	3.83	C29	THR B 240 O	4.83
C12	CYS B 241 SG	4.85	C29	THR B 240 C	3.77
C10	CYS B 241 SG	4.07	C29	THR B 240 CA	4
C9	CYS B 241 SG	3.77	C29	THR B 240 N	3.28
C31	CYS B 241 CB	4.81	C29	THR B 239 CB	4.87
O9	CYS B 241 CB	3.94	C29	THR B 239 O	3.87
C30	CYS B 241 CB	4.27	C29	THR B 239 C	3.28
C29	CYS B 241 CB	3.6	O7	THR B 239 C	4.24
C28	CYS B 241 CB	3.61	C29	THR B 239 CA	3.38
O7	CYS B 241 CB	4.07	O7	THR B 239 CA	3.86
O6	CYS B 241 CB	3.91	C29	THR B 239 N	3.45
C24	CYS B 241 CB	4.6	C29	VAL B 238 O	3.29
C23	CYS B 241 CB	3.95	C24	VAL B 238 O	4.07
C22	CYS B 241 CB	3.89	C23	VAL B 238 O	3.77
C21	CYS B 241 CB	4.53	C22	VAL B 238 O	4.93
C14	CYS B 241 CB	4.82	C29	VAL B 238 C	3.39
C13	CYS B 241 CB	4.39	O7	VAL B 238 C	3.32
C10	CYS B 241 CB	4.33	C24	VAL B 238 C	4.54
C9	CYS B 241 CB	4	C23	VAL B 238 C	4.41
C28	CYS B 241 O	3.45	C29	VAL B 238 CA	4.25
O9	CYS B 241 C	4.2	O7	VAL B 238 CA	4.21
C29	CYS B 241 C	4.26	C24	VAL B 238 CA	4.67
C28	CYS B 241 C	3.67	C23	VAL B 238 CA	5
O7	CYS B 241 C	4.55	C29	GLY B 237 O	4.09
O6	CYS B 241 C	4	C29	GLY B 237 C	4.94
C23	CYS B 241 C	4.94	C24	TYR B 202 OH	4.76
C22	CYS B 241 C	4.72	C23	TYR B 202 OH	4.89
C31	CYS B 241 CA	4.61	O2	ALA A 180 CB	4.45
O9	CYS B 241 CA	3.53	C5	ALA A 180 CB	3.74
C30	CYS B 241 CA	4.18	O1	ALA A 180 CB	4.89
C29	CYS B 241 CA	3.72	O2	ALA A 180 C	4.98
C28	CYS B 241 CA	4.27	C5	ALA A 180 C	4.74
O7	CYS B 241 CA	4.39	O2	ALA A 180 CA	3.97
O6	CYS B 241 CA	4.49	C5	ALA A 180 CA	3.42
C23	CYS B 241 CA	4.72	O1	ALA A 180 CA	4.61
C22	CYS B 241 CA	4.79	C5	ALA A 180 N	3.65
C31	CYS B 241 N	4.89	C5	THR A 179 O	3.53
C30	CYS B 241 N	4.9	C4	THR A 179 O	4.91

C29	CYS B 241 N	3.05	C3	THR A 179 O	4.66
C23	CYS B 241 N	4.74	O2	THR A 179 C	4.6
C31	THR B 240 CG2	4.6	C5	THR A 179 C	3.87
C29	THR B 240 CB	4.48	O1	THR A 179 C	4.47
C31	THR B 240 O	4.83	C5	ASN A 101 OD1	4.08
C30	THR B 240 O	5	C5	ASN A 101 CG	4.78
O9	THR B 240 C	4.73			
C29	THR B 240 C	3.93			
C29	THR B 240 CA	3.99			
C29	THR B 240 N	3.22			
C29	THR B 239 CB	4.92			
C29	THR B 239 O	4.12			
C29	THR B 239 C	3.38			
O7	THR B 239 C	4.14			
C29	THR B 239 CA	3.4			
O7	THR B 239 CA	3.78			
C29	THR B 239 N	3.23			
C23	THR B 239 N	4.99			
C29	VAL B 238 CB	4.99			
O7	VAL B 238 CB	4.96			
C29	VAL B 238 O	3.1			
C24	VAL B 238 O	4.03			
C23	VAL B 238 O	3.69			
C22	VAL B 238 O	4.84			
C29	VAL B 238 C	3.08			
O7	VAL B 238 C	3.23			
C24	VAL B 238 C	4.49			
C23	VAL B 238 C	4.31			
C29	VAL B 238 CA	3.78			
O7	VAL B 238 CA	4.1			
C24	VAL B 238 CA	4.6			
C23	VAL B 238 CA	4.89			
C29	VAL B 238 N	4.54			
C29	GLY B 237 O	3.58			
C29	GLY B 237 C	4.44			
C24	TYR B 202 OH	4.73			
C23	TYR B 202 OH	4.86			
O2	ALA A 180 CB	4.45			
C5	ALA A 180 CB	3.72			
O1	ALA A 180 CB	4.86			
C5	ALA A 180 C	4.73			
O2	ALA A 180 CA	4			
C5	ALA A 180 CA	3.42			
O1	ALA A 180 CA	4.56			
C5	ALA A 180 N	3.69			
C5	THR A 179 O	3.6			
C4	THR A 179 O	4.89			
C3	THR A 179 O	4.72			
O2	THR A 179 C	4.71			

Table A6.27

(c) 7h_Tubulin

Hydrogen bonding		
Hydrogen Donor (D	**Hydrogen Acceptor (A)**	**Distance (D-A) in Å**
900 N2	LEU B 248 O	2.69
900 N1	LEU B 248 O	4.00
Hydrophobic interaction		
7h	**Tubulin**	**Distance**
C25	ILE B 378 CD1	3.4
C24	ILE B 378 CD1	3.5

Table A6.28

(d) Noscapine_Tubulin

Hydrogen bonding		
Hydrogen Donor (D	**Hydrogen Acceptor (A)**	**Distance (D-A) in Å**
LYS B 352 NZ	900 O6	3.62
900 N1	LEU B 248 O	3.24
Hydrophobic interaction		
Noscapine	**Tubulin**	**Distance**
C21	ILE B 378 CD1	4.43
C2	CYS B 356 N	4.85

C23	ILE B 378 CD1	4.76	C10	VAL B 355 CG2	4.85
C20	ILE B 378 CD1	4.6	C10	VAL B 355 CB	4.4
C25	ILE B 378 CG1	4.71	O1	VAL B 355 CB	4.15
C24	ILE B 378 CG1	4.91	C9	VAL B 355 CB	4.7
C30	CYS B 356 SG	3.84	C10	VAL B 355 O	4.29
O10	CYS B 356 SG	4.46	C9	VAL B 355 O	3.12
C30	CYS B 356 CB	3.77	C8	VAL B 355 O	4.27
O10	CYS B 356 CB	3.87	C7	VAL B 355 O	4.18
C30	CYS B 356 CA	4.24	C4	VAL B 355 O	4.83
O10	CYS B 356 CA	3.89	C3	VAL B 355 O	3.74
C30	CYS B 356 N	4.78	C2	VAL B 355 O	2.75
C14	CYS B 356 N	4.97	C10	VAL B 355 C	4.99
C31	VAL B 355 O	4.04	O1	VAL B 355 C	4.09
C30	VAL B 355 O	4.39	C9	VAL B 355 C	4.09
C15	VAL B 355 O	3.7	C7	VAL B 355 C	4.98
C14	VAL B 355 O	3.24	C3	VAL B 355 C	4.63
C13	VAL B 355 O	4.43	C2	VAL B 355 C	3.82
C31	VAL B 355 C	4.8	C10	VAL B 355 CA	4.76
C30	VAL B 355 C	4.91	O1	VAL B 355 CA	4.27
O10	VAL B 355 C	3.87	C9	VAL B 355 CA	4.37
C15	VAL B 355 C	4.49	C2	VAL B 355 CA	4.5
C14	VAL B 355 C	4.1	C10	VAL B 355 N	4.23
C31	VAL B 355 CA	4.74	C9	VAL B 355 N	3.72
C14	VAL B 355 CA	4.77	C8	VAL B 355 N	4.07
C31	VAL B 355 N	3.74	C4	VAL B 355 N	4.82
C15	VAL B 355 N	4.95	C3	VAL B 355 N	4.43
C14	VAL B 355 N	4.06	C2	VAL B 355 N	3.96
C13	VAL B 355 N	4.61	C1	VAL B 355 N	4.63
N3	ALA B 354 CB	4.57	N1	ALA B 354 CB	4.61
C31	ALA B 354 CB	4.07	C22	ALA B 354 CB	4.15
O9	ALA B 354 CB	3.69	O7	ALA B 354 CB	4.38
C26	ALA B 354 CB	3.97	O5	ALA B 354 CB	4.73
C15	ALA B 354 CB	4.58	C19	ALA B 354 CB	3.47
C14	ALA B 354 CB	3.85	C18	ALA B 354 CB	4.52
C13	ALA B 354 CB	3.68	C14	ALA B 354 CB	3.98
C12	ALA B 354 CB	4.29	C12	ALA B 354 CB	3.82
N2	ALA B 354 CB	4.82	C9	ALA B 354 CB	4.68
O3	ALA B 354 CB	3.76	C8	ALA B 354 CB	4.36
C11	ALA B 354 CB	4.53	C7	ALA B 354 CB	4.51
C10	ALA B 354 CB	3.85	C5	ALA B 354 CB	4.1
C9	ALA B 354 CB	3.91	C4	ALA B 354 CB	3.66
C31	ALA B 354 C	4.37	C3	ALA B 354 CB	3.99
O9	ALA B 354 C	4.79	C2	ALA B 354 CB	4.55
C14	ALA B 354 C	4.73	C1	ALA B 354 CB	3.88
C31	ALA B 354 CA	3.9	C9	ALA B 354 C	4.68
O9	ALA B 354 CA	4	C8	ALA B 354 C	4.7
C26	ALA B 354 CA	4.69	C2	ALA B 354 C	4.9
C14	ALA B 354 CA	4.54	C1	ALA B 354 C	4.97
C13	ALA B 354 CA	4.41	C22	ALA B 354 CA	3.96
O3	ALA B 354 CA	4.44	O7	ALA B 354 CA	4.55
C26	ALA B 354 N	4.09	C19	ALA B 354 CA	4.85
C31	THR B 353 O	4.77	C12	ALA B 354 CA	4.86
C26	THR B 353 O	4.6	O2	ALA B 354 CA	4.67
C26	THR B 353 C	4.18	C9	ALA B 354 CA	4.59
O3	THR B 353 C	4.83	C8	ALA B 354 CA	4.2
C26	THR B 353 CA	4.45	C4	ALA B 354 CA	4.39
C26	THR B 353 N	4.35	C3	ALA B 354 CA	4.7
C11	LYS B 352 NZ	4.58	C2	ALA B 354 CA	4.87
C5	LYS B 352 NZ	3.74	C1	ALA B 354 CA	4.12
C4	LYS B 352 NZ	3.65	C22	ALA B 354 N	4.4

C3	LYS B 352 NZ	4.14	C22	THR B 353 O	2.92
C2	LYS B 352 NZ	4.14	C8	THR B 353 O	4.93
O3	LYS B 352 CE	3.46	C1	THR B 353 O	4.63
C11	LYS B 352 CE	4.11	C22	THR B 353 C	3.99
N1	LYS B 352 CE	4.1	C22	LYS B 352 NZ	4.41
C7	LYS B 352 CE	4.66	C13	LYS B 352 NZ	3.95
C6	LYS B 352 CE	4.32	C22	LYS B 352 CE	3.58
O2	LYS B 352 CE	4.56	O7	LYS B 352 CE	4.2
C5	LYS B 352 CE	4.42	O6	LYS B 352 CE	3.8
O1	LYS B 352 CE	3.94	C15	LYS B 352 CE	4.43
C4	LYS B 352 CE	3.65	C14	LYS B 352 CE	4.75
C3	LYS B 352 CE	4.05	C13	LYS B 352 CE	3.73
C2	LYS B 352 CE	3.76	O3	LYS B 352 CE	3.66
C1	LYS B 352 CE	4.53	C12	LYS B 352 CE	4.32
C27	LYS B 352 CD	4.54	C22	LYS B 352 CD	4.71
O4	LYS B 352 CD	4.9	O6	LYS B 352 CD	4.63
O3	LYS B 352 CD	4.64	C13	LYS B 352 CD	4.66
C7	LYS B 352 CD	4.65	O3	LYS B 352 CD	4.87
C6	LYS B 352 CD	4.76	C22	LYS B 352 CG	4.95
O2	LYS B 352 CD	4.55	O6	LYS B 352 CG	4.87
C5	LYS B 352 CD	4.79	C16	LYS B 352 CG	4.68
O1	LYS B 352 CD	4.7	C15	LYS B 352 CG	4.59
C4	LYS B 352 CD	4.25	C14	LYS B 352 CG	4.88
C3	LYS B 352 CD	4.14	C13	LYS B 352 CG	4.65
C2	LYS B 352 CD	4.54	O3	LYS B 352 CG	4.95
C1	LYS B 352 CD	4.33	C10	MET B 325 CE	3.7
N3	LYS B 352 CG	4.64	O1	MET B 325 CE	4.04
C27	LYS B 352 CG	4.05	C10	MET B 325 SD	4.02
C26	LYS B 352 CG	3.73	O1	MET B 325 SD	4.88
O4	LYS B 352 CG	4.17	C21	ILE B 318 CD1	3.62
O3	LYS B 352 CG	4.57	O5	ILE B 318 CD1	3.74
C10	LYS B 352 CG	4.89	C21	ILE B 318 CG1	3.43
C8	LYS B 352 CG	4.41	O5	ILE B 318 CG1	3.36
C7	LYS B 352 CG	3.78	C19	ILE B 318 CG1	4.87
C6	LYS B 352 CG	4.1	C18	ILE B 318 CG1	4.55
O2	LYS B 352 CG	4.77	C21	ILE B 318 CB	4.93
C4	LYS B 352 CG	4.34	O5	ILE B 318 CB	4.76
C3	LYS B 352 CG	4.04	O5	ALA B 317 C	4.88
C2	LYS B 352 CG	4.36	C21	ALA B 316 CB	4.58
C1	LYS B 352 CG	3.72	C20	ALA B 316 CB	3.56
C27	LYS B 352 CB	3.7	O5	ALA B 316 CB	3.97
C26	LYS B 352 CB	4.08	O4	ALA B 316 CB	3.39
O4	LYS B 352 CB	4.11	C18	ALA B 316 CB	4.51
C8	LYS B 352 CB	4.67	C17	ALA B 316 CB	4.26
C7	LYS B 352 CB	4.41	O5	ALA B 316 C	4.79
C3	LYS B 352 CB	4.76	C20	ALA B 316 CA	4.83
C1	LYS B 352 CB	4.17	O5	ALA B 316 CA	4.83
C26	LYS B 352 O	3.84	O4	ALA B 316 CA	4.69
C26	LYS B 352 C	4.08	C20	MET B 259 SD	4.43
C26	LYS B 352 CA	4.77	C20	MET B 259 CG	4.08
N3	ILE B 318 CD1	4.68	C20	LEU B 255 CD1	3.54
C29	ILE B 318 CD1	4.95	O4	LEU B 255 CD1	3.75
C25	ILE B 318 CD1	3.91	C17	LEU B 255 CD1	4.94
C24	ILE B 318 CD1	3.93	C20	LEU B 255 CG	4.74
C9	ILE B 318 CD1	4.85	O4	LEU B 255 CG	4.96
N3	ILE B 318 CG1	4.36	C20	LEU B 255 CB	4.79
C29	ILE B 318 CG1	4.62	C20	LEU B 255 O	4.66
C26	ILE B 318 CG1	4.64	C20	LEU B 255 CA	4.33
C25	ILE B 318 CG1	4.24	O4	LEU B 255 CA	4.96
C24	ILE B 318 CG1	4.17	C20	LYS B 254 O	4.89

C9	ILE B 318 CG1	4.14	N1	ALA B 250 CB	4.58
C26	ILE B 318 N	4.96	O6	ALA B 250 CB	4.53
C26	ALA B 317 O	3.2	C16	ALA B 250 CB	4.78
C9	ALA B 317 O	4.66	C15	ALA B 250 CB	4.4
N3	ALA B 317 C	4.82	C14	ALA B 250 CB	4.88
C26	ALA B 317 C	4	C13	ALA B 250 CB	4.37
C26	ALA B 317 CA	4.48	O3	ALA B 250 CB	4.81
C26	ALA B 317 N	3.7	C11	ALA B 250 CB	3.14
N3	ALA B 316 CB	3.45	C11	ALA B 250 O	4.83
C26	ALA B 316 CB	3.72	C11	ALA B 250 C	4.82
C25	ALA B 316 CB	3.91	C11	ALA B 250 CA	4.06
C20	ALA B 316 CB	4.07	C11	ALA B 250 N	3.84
O5	ALA B 316 CB	4.73	C11	ASN B 249 O	4.97
C18	ALA B 316 CB	3.4	C11	ASN B 249 C	4.34
O4	ALA B 316 CB	4.43	C11	ASN B 249 CA	4.7
C9	ALA B 316 CB	4.83	C11	ASN B 249 N	4.79
C8	ALA B 316 CB	3.25	O6	LEU B 248 CD2	3.24
C7	ALA B 316 CB	4.6	C13	LEU B 248 CD2	3.79
C26	ALA B 316 O	4.86	O3	LEU B 248 CD2	3.7
N3	ALA B 316 C	4.41	O6	LEU B 248 CG	4.03
C26	ALA B 316 C	3.99	C13	LEU B 248 CG	4.29
C8	ALA B 316 C	4.95	O3	LEU B 248 CG	3.93
N3	ALA B 316 CA	4.16	O7	LEU B 248 CB	4.19
C26	ALA B 316 CA	3.85	O6	LEU B 248 CB	4.72
C18	ALA B 316 CA	4.76	C13	LEU B 248 CB	4.62
C8	ALA B 316 CA	4.22	O3	LEU B 248 CB	3.8
C27	VAL B 315 O	4.99	C12	LEU B 248 CB	4.71
O4	MET B 259 SD	4.99	C5	LEU B 248 CB	4.39
C18	MET B 259 CG	4.92	C4	LEU B 248 CB	4.93
O4	MET B 259 CG	4.96	C1	LEU B 248 CB	4.82
C27	ASN B 258 ND2	4.89	C13	LEU B 248 O	4.91
C5	ASN B 258 ND2	3.69	C12	LEU B 248 O	4.29
C3	ASN B 258 ND2	4.5	C11	LEU B 248 O	2.84
C5	ASN B 258 OD1	4.83	C7	LEU B 248 O	4.55
C27	ASN B 258 CG	4.41	C6	LEU B 248 O	3.36
O4	ASN B 258 CG	4.94	C5	LEU B 248 O	3.25
O2	ASN B 258 CG	3.68	C4	LEU B 248 O	4.05
C5	ASN B 258 CG	4.3	C3	LEU B 248 O	4.56
C3	ASN B 258 CG	4.84	C1	LEU B 248 O	4.83
C27	ASN B 258 CB	3.63	N1	LEU B 248 C	4.45
O4	ASN B 258 CB	4.11	O3	LEU B 248 C	4.76
O2	ASN B 258 CB	3.9	C11	LEU B 248 C	4.02
C5	ASN B 258 CB	4.92	C6	LEU B 248 C	4.52
C3	ASN B 258 CB	4.76	C5	LEU B 248 C	4.26
C1	ASN B 258 CB	4.88	C4	LEU B 248 C	4.91
C27	ASN B 258 O	4.64	O7	LEU B 248 CA	4.81
C27	ASN B 258 C	4.73	O3	LEU B 248 CA	4.76
C27	ASN B 258 CA	4.81	C5	LEU B 248 CA	4.57
O6	LEU B 255 CD2	4.73	C4	LEU B 248 CA	4.94
C24	LEU B 255 CD2	4.93	C8	LEU B 248 N	4.75
C23	LEU B 255 D2	4.7	C5	LEU B 248 N	4.39
C22	LEU B 255 D2	4.45	C4	LEU B 248 N	4.29
C21	LEU B 255 CD2	4.56	C3	LEU B 248 N	4.82
C20	LEU B 255 CD2	4.9	C1	LEU B 248 N	4.24
C19	LEU B 255 CD2	4.91	O2	GLN B 247 CD	4.98
O8	LEU B 255 CD1	4.46	O2	GLN B 247 CG	3.85
C25	LEU B 255 CD1	3.87	C10	GLN B 247 CG	3.8
C24	LEU B 255 CD1	4.48	O1	GLN B 247 CG	4.03
C23	LEU B 255 CD1	4.71	C9	GLN B 247 CG	4.44
C22	LEU B 255 CD1	4.29	C8	GLN B 247 CG	4.36

C21	LEU B 255 CD1	3.62	O7	GLN B 247 CB	4.4
C20	LEU B 255 CD1	3.44	O2	GLN B 247 CB	3.53
C19	LEU B 255 CD1	3.7	C10	GLN B 247 CB	3.93
O5	LEU B 255 CD1	3.43	O1	GLN B 247 CB	4.01
C18	LEU B 255 CD1	3.49	C9	GLN B 247 CB	3.91
O8	LEU B 255 CG	4.57	C8	GLN B 247 CB	3.65
O6	LEU B 255 CG	4.96	C4	GLN B 247 CB	4.86
C25	LEU B 255 CG	4.98	C2	GLN B 247 CB	4.62
C22	LEU B 255 CG	4.58	C1	GLN B 247 CB	4.12
C21	LEU B 255 CG	4.23	O2	GLN B 247 CA	4.74
C20	LEU B 255 CG	4.49	O1	GLN B 247 CA	4.75
C19	LEU B 255 CG	4.17	C9	GLN B 247 CA	4.47
O5	LEU B 255 CG	4.29	C8	GLN B 247 CA	4.48
C18	LEU B 255 CG	4.72	C2	GLN B 247 CA	4.73
O8	LEU B 255 CB	3.58	C1	GLN B 247 CA	4.72
O6	LEU B 255 CB	4.44	C10	GLN B 247 N	4.87
C22	LEU B 255 CB	4.4	C9	GLN B 247 N	3.76
C21	LEU B 255 CB	4.05	C8	GLN B 247 N	4.13
C20	LEU B 255 CB	4.7	C7	GLN B 247 N	4.75
C19	LEU B 255 CB	3.59	C6	GLN B 247 N	4.97
O5	LEU B 255 CB	3.97	C4	GLN B 247 N	4.38
C18	LEU B 255 CB	4.84	C3	GLN B 247 N	4.04
O8	LEU B 255 C	4.97	C2	GLN B 247 N	3.66
O5	LEU B 255 C	4.8	C1	GLN B 247 N	4.4
O8	LEU B 255 CA	3.47	C9	GLY B 246 C	4.6
C21	LEU B 255 CA	4.55	C7	GLY B 246 C	4.58
C19	LEU B 255 CA	3.62	C6	GLY B 246 C	4.62
O5	LEU B 255 CA	3.68	C4	GLY B 246 C	4.84
C18	LEU B 255 CA	4.79	C3	GLY B 246 C	4.3
C19	LEU B 255 N	3.89	C2	GLY B 246 C	4.1
O8	LYS B 254 CB	4.4	O1	GLY B 246 CA	4.97
C19	LYS B 254 O	4.6	C9	GLY B 246 CA	4.38
C5	LYS B 254 O	4.83	C7	GLY B 246 CA	3.63
C3	LYS B 254 O	4.68	C6	GLY B 246 CA	3.92
C1	LYS B 254 O	4.97	C4	GLY B 246 CA	4.63
O8	LYS B 254 C	3.77	C3	GLY B 246 CA	3.71
C19	LYS B 254 C	4.49	C2	GLY B 246 CA	3.49
O5	LYS B 254 C	4.64	C7	GLY B 246 N	4.29
O8	LYS B 254 CA	4.65	C6	GLY B 246 N	4.34
C28	ASP B 251 O	4.24	C3	GLY B 246 N	4.78
C19	ASP B 251 O	4.56	C2	GLY B 246 N	4.73
C28	ASP B 251 C	4.55	C7	PRO B 245 O	4.23
O8	ASP B 251 C	4.64	C6	PRO B 245 O	4.81
O6	ASP B 251 C	4.55	C3	PRO B 245 O	5
C28	ASP B 251 CA	4.56	C2	PRO B 245 O	4.75
O6	ASP B 251 CA	4.97	C7	PRO B 245 C	4.56
C28	ASP B 251 N	4.13	C6	PRO B 245 C	4.78
C28	ALA B 250 CB	3.5	C7	PHE B 244 O	4.91
O8	ALA B 250 CB	3.49	C6	PHE B 244 O	4.68
O6	ALA B 250 CB	4.69	N1	CYS B 241 SG	3.55
C19	ALA B 250 CB	4.46	C21	CYS B 241 SG	4.06
N2	ALA B 250 CB	4.75	O5	CYS B 241 SG	4.05
N1	ALA B 250 CB	4.17	C19	CYS B 241 SG	3.4
C4	ALA B 250 CB	4.91	C18	CYS B 241 SG	4.12
C2	ALA B 250 CB	4.52	C14	CYS B 241 SG	4.26
C28	ALA B 250 O	3.6	C12	CYS B 241 SG	4.72
C28	ALA B 250 C	3.71	C11	CYS B 241 SG	4.39
O8	ALA B 250 C	4.74	C7	CYS B 241 SG	3.56
O6	ALA B 250 C	4.77	C6	CYS B 241 SG	3.78
C28	ALA B 250 CA	4.21	C5	CYS B 241 SG	4.4

O8	ALA B 250 CA	4.67	C4	CYS B 241 SG	4.69
N2	LEU B 248 CD2	4.73	C3	CYS B 241 SG	4.41
O3	LEU B 248 CD2	4.9	N1	CYS B 241 CB	3.54
C11	LEU B 248 CD2	4.28	C21	CYS B 241 CB	3.89
N1	LEU B 248 CD2	3.71	O5	CYS B 241 CB	4.36
C5	LEU B 248 CD2	3.8	C19	CYS B 241 CB	3.84
O1	LEU B 248 CD2	2.89	C18	CYS B 241 CB	4.28
C4	LEU B 248 CD2	3.94	C14	CYS B 241 CB	4.49
C2	LEU B 248 CD2	4.33	C11	CYS B 241 CB	3.76
N2	LEU B 248 CG	4.28	C7	CYS B 241 CB	4.21
C11	LEU B 248 CG	4.28	C6	CYS B 241 CB	3.8
N1	LEU B 248 CG	3.88	C5	CYS B 241 CB	4.8
O1	LEU B 248 CG	3.94	C11	CYS B 241 O	3.75
C4	LEU B 248 CG	4.8	C6	CYS B 241 O	4.05
C2	LEU B 248 CG	4.85	N1	CYS B 241 C	4.84
C12	LEU B 248 CB	4.62	C11	CYS B 241 C	4.54
N2	LEU B 248 CB	3.64	C6	CYS B 241 C	4.58
O3	LEU B 248 CB	4.55	N1	CYS B 241 CA	4.38
C11	LEU B 248 CB	3.85	C11	CYS B 241 CA	4.54
N1	LEU B 248 CB	3.97	C7	CYS B 241 CA	4.48
O1	LEU B 248 CB	4.85	C6	CYS B 241 CA	4.13
C17	LEU B 248 O	3.07	C6	ARG B 48 NH1	4.97
C16	LEU B 248 O	4.19	C22	SER A 178 OG	3.07
C13	LEU B 248 O	4.2	C8	SER A 178 OG	4.77
C12	LEU B 248 O	3.09	C1	SER A 178 OG	4.49
C11	LEU B 248 O	3.78	C22	SER A 178 CB	4.21
C17	LEU B 248 C	4.26	O7	SER A 178 CB	4.29
C12	LEU B 248 C	4.14			
N2	LEU B 248 C	3.63			
C11	LEU B 248 C	4.55			
N1	LEU B 248 C	4.69			
C12	LEU B 248 CA	4.54			
N2	LEU B 248 CA	3.92			
C11	LEU B 248 CA	4.59			
N1	LEU B 248 CA	4.87			
C17	LEU B 248 N	4.84			
C13	LEU B 248 N	4.46			
C12	LEU B 248 N	4.18			
C11	LEU B 248 N	4.72			
C31	GLN B 247 CG	4.65			
C31	GLN B 247 CB	3.97			
O9	GLN B 247 CB	4.28			
C13	GLN B 247 CB	4.9			
C31	GLN B 247 CA	4.77			
O9	GLN B 247 CA	4.8			
C31	GLN B 247 N	4.36			
C15	GLN B 247 N	4.88			
C14	GLN B 247 N	4.36			
C13	GLN B 247 N	4.24			
C12	GLN B 247 N	4.66			
C17	GLY B 246 C	4.83			
C16	GLY B 246 C	4.77			
C15	GLY B 246 C	4.7			
C14	GLY B 246 C	4.58			
C13	GLY B 246 C	4.65			
C12	GLY B 246 C	4.81			
C30	GLY B 246 CA	4.48			
O10	GLY B 246 CA	3.96			
C17	GLY B 246 CA	4.28			
C16	GLY B 246 CA	3.82			

C15	GLY B 246 CA	3.62			
C14	GLY B 246 CA	3.83			
C13	GLY B 246 CA	4.31			
C12	GLY B 246 CA	4.55			
C30	GLY B 246 N	4.44			
C17	GLY B 246 N	4.79			
C16	GLY B 246 N	4.17			
C15	GLY B 246 N	4.25			
C14	GLY B 246 N	4.86			
C30	PRO B 245 O	2.99			
C16	PRO B 245 O	4.23			
C15	PRO B 245 O	3.91			
C14	PRO B 245 O	4.81			
C30	PRO B 245 C	3.82			
O10	PRO B 245 C	4.12			
C16	PRO B 245 C	4.39			
C15	PRO B 245 C	4.38			
C30	PRO B 245 CA	4.76			
C30	PRO B 245 N	4.57			
C30	PHE B 244 CB	3.9			
C30	PHE B 244 O	3.44			
C16	PHE B 244 O	4.23			
C15	PHE B 244 O	4.82			
C30	PHE B 244 C	3.9			
C30	PHE B 244 CA	4.43			
C30	PHE B 244 N	4.88			
C28	LEU B 242 CD2	3.4			
O7	LEU B 242 D2	4.37			
O6	LEU B 242 CD2	3.18			
C23	LEU B 242 CD2	4.93			
C22	LEU B 242 CD2	4.45			
C29	LEU B 242 CD1	4.94			
O7	LEU B 242 CD1	4.05			
O6	LEU B 242 CD1	4.36			
C23	LEU B 242 CD1	4.97			
C29	LEU B 242 CG	4.43			
C28	LEU B 242 CG	3.93			
O7	LEU B 242 CG	3.59			
O6	LEU B 242 CG	3.5			
C23	LEU B 242 CG	4.52			
C22	LEU B 242 CG	4.49			
C29	LEU B 242 CB	4.94			
C28	LEU B 242 CB	4.77			
O7	LEU B 242 CB	4.5			
O6	LEU B 242 CB	4.69			
C29	LEU B 242 CA	4.99			
C28	LEU B 242 CA	4.4			
O7	LEU B 242 CA	4.76			
O6	LEU B 242 CA	4.74			
C29	LEU B 242 N	3.83			
C28	LEU B 242 N	3.91			
C23	LEU B 242 N	4.85			
C22	LEU B 242 N	4.97			
N3	CYS B 241 SG	4.93			
C30	CYS B 241 SG	4.16			
O10	CYS B 241 SG	4.01			
C29	CYS B 241 SG	4.32			
C23	CYS B 241 SG	4.95			
C17	CYS B 241 SG	3.8			
C16	CYS B 241 SG	3.45			

C15	CYS B 241 SG	3.63			
C14	CYS B 241 SG	4.21			
C13	CYS B 241 SG	4.53			
C12	CYS B 241 SG	4.31			
C10	CYS B 241 SG	3.94			
C9	CYS B 241 SG	3.58			
C30	CYS B 241 CB	4.65			
O10	CYS B 241 CB	4.89			
C29	CYS B 241 CB	3.42			
C28	CYS B 241 CB	3.59			
O7	CYS B 241 CB	3.79			
O6	CYS B 241 CB	4.11			
C24	CYS B 241 CB	4.58			
C23	CYS B 241 CB	3.9			
C22	CYS B 241 CB	3.98			
C21	CYS B 241 CB	4.58			
C17	CYS B 241 CB	3.82			
C16	CYS B 241 CB	3.64			
C15	CYS B 241 CB	4.41			
C12	CYS B 241 CB	4.72			
C10	CYS B 241 CB	4.21			
C9	CYS B 241 CB	3.97			
C28	CYS B 241 O	3.27			
C17	CYS B 241 O	4.22			
C16	CYS B 241 O	4.09			
C30	CYS B 241 C	4.97			
C29	CYS B 241 C	4.02			
C28	CYS B 241 C	3.5			
O7	CYS B 241 C	4.13			
O6	CYS B 241 C	4.18			
C23	CYS B 241 C	4.82			
C22	CYS B 241 C	4.77			
C17	CYS B 241 C	4.79			
C16	CYS B 241 C	4.43			
C30	CYS B 241 CA	4.03			
O10	CYS B 241 CA	4.71			
C29	CYS B 241 CA	3.54			
C28	CYS B 241 CA	4.17			
O7	CYS B 241 CA	4.09			
O6	CYS B 241 CA	4.7			
C23	CYS B 241 CA	4.66			
C22	CYS B 241 CA	4.88			
C17	CYS B 241 CA	4.35			
C16	CYS B 241 CA	3.78			
C15	CYS B 241 CA	4.56			
C30	CYS B 241 N	4.38			
C29	CYS B 241 N	2.95			
C23	CYS B 241 N	4.73			
C16	CYS B 241 N	4.88			
C30	THR B 240 CG2	4.5			
C29	THR B 240 CB	4.58			
C30	THR B 240 O	3.83			
C29	THR B 240 O	4.97			
C30	THR B 240 C	4.34			
C29	THR B 240 C	3.88			
O7	THR B 240 C	4.92			
C29	THR B 240 CA	4.03			
C29	THR B 240 N	3.29			
C29	THR B 239 CB	4.95			
C29	THR B 239 O	4.05			

C29	THR B 239 C	3.39			
O7	THR B 239 C	4.14			
C29	THR B 239 CA	3.44			
O7	THR B 239 CA	3.88			
C29	THR B 239 N	3.38			
C29	VAL B 238 O	3.21			
C24	VAL B 238 O	3.84			
C23	VAL B 238 O	3.76			
C22	VAL B 238 O	4.96			
C29	VAL B 238 C	3.26			
O7	VAL B 238 C	3.63			
C24	VAL B 238 C	4.34			
C23	VAL B 238 C	4.41			
C29	VAL B 238 CA	4.03			
O7	VAL B 238 CA	4.57			
C24	VAL B 238 CA	4.53			
C29	VAL B 238 N	4.8			
C29	GLY B 237 O	3.85			
C29	GLY B 237 C	4.71			
C24	TYR B 202 OH	4.59			
C23	TYR B 202 OH	4.93			
C27	VAL A 181 CG2	4.38			
O2	ALA A 180 CB	4.55			
C5	ALA A 180 CB	4.08			
O2	ALA A 180 CA	4.16			
C5	ALA A 180 CA	3.85			
C5	ALA A 180 N	4.07			
C5	THR A 179 O	3.93			
C3	THR A 179 O	4.87			
O2	THR A 179 C	4.86			
C5	THR A 179 C	4.28			
O1	THR A 179 C	4.97			
C31	SER A 178 OG	4.98			
C5	ASN A 101 OD1	4.01			
C5	ASN A 101 CG	4.81			

Conclusion

Conclusion and Future Direction

Microtubules have long been considered an ideal target for anticancer drugs because of the essential role they play in mitosis, forming the dynamic spindle apparatus. As such, there is a wide variety of compounds currently in clinical use and in development that act as antimitotic agents by altering microtubule dynamics. Despite the initial impressive response by these MT binding drugs such as taxanes and vinca alkaloids, their potential is somewhat restricted by the development of multi drug resistance, toxicity, hypersensitivity and limited bioavailability. Therefore, there is a continual need to develop novel drugs that are efficacious, well-tolerated, non-toxic, orally available, can overcome resistance to other chemotherapeutic and display better pharmacologic profiles. Noscapine (an opium alkaloid) has shown great potential as a microtubule binding anti-cancer agent. Noscapine alters tubulin dynamics and leads to programmed cell death and its relatively non-toxic profile, oral availability and efficiency against various drug resistant cell lines indicates its potential as a chemotherapeutic agent for the treatment of human cancers to treat various malignancies in the clinic. Furthermore, it was found to be effective against a wide variety of cancer cells (according to the NC 60 cell line screen) but the effective concentration was found to be in high micromolar ranges. Thus, the paramount goal is to develop a more potent derivative of noscapine by structural modifications.

In pursuit of developing novel potent derivatives of the natural lead molecule noscapine, we have strategically developed five new class of noscapinoids in a quest of increasing its anticancer activity. Towards this end the scaffold structure of noscapine has been substituted with active pharmacophore such as arylimino groups (Schiff bases), N-aryl methyl, 1,3-diynyl, imidazo[1,2-*a*] pyridine and urea group at the C-9 position based on *in silico* combinatorial approach and followed by screening of potent derivatives based on combine approach of molecular docking, molecular dynamics simulation and LIE-SGB/MM-GBSA/MM-PBSA determination of binding free energy. We have primarily focused on these functional groups because they are recognized as key pharmacophores in several anticancer drugs utilized in the clinic. We have also provided the simplest methods for direct and regioselective modification of the noscapine scaffold to produce the new classes of noscapine derivatives in high yields. All the noscapinoids developed were experimentally demonstrated to bind to tubulin with high affinity. Their anticancer activity was evaluated using two human breast cancer cell lines (MCF-7 and MDA-MB-231) as well as a panel of primary breast tumor cells. All the noscapinoids revealed improved

antiproliferative activity to cancer cells, perturbed DNA synthesis, delayed the cell cycle progression at S phase and G2M phase as well as induced apoptosis in cancer cells compared to noscapine without affecting the normal healthy cells. In vivo toxicological evaluation of promising derivatives of noscapine from the two different classes effectively regress the tumor volume in the xenograft mice and failed to reveal any toxicities in the vital organs like liver, kidney, spleen, lung, heart, brain and duodenum. Also, there was no significant difference in hematological and blood biochemical parameters between the treated and untreated groups.

Hence the newly designed noscapinoids of different classes are safe and effective anticancer drug with a potential for the oral treatment of cancer and holds great promise for further clinical studies. Our data thus generate compelling evidence that these analogues indicate a great potential for further preclinical and clinical evaluation.

References

Abraham, M. J., Murtola, T., Schulz, R., Páll, S., Smith, J. C., Hess, B., & Lindahl, E. (2015). GROMACS: High performance molecular simulations through multi-level parallelism from laptops to supercomputers. *SoftwareX*, *1*, 19-25.

Ali, I., Haque, A., Saleem, K., & Hsieh, M. F. (2013). Curcumin-I Knoevenagel's condensates and their Schiff's bases as anticancer agents: synthesis, pharmacological and simulation studies. *Bioorganic & medicinal chemistry*, *21*, 3808–3820.

Allen, C., & Borisy, G. G. (1974). Structural polarity and directional growth of microtubules of Chlamydomonas flagella. *Journal of molecular biology*, *90*, 381–402.

Almirante, L., Polo, L., Mugnaini, A., Provinciali, E., Rugarli, P., Biancotti, A., Gamba, A., & Murmann, W. (1965). Derivatives of imidazole. I. Synthesis and reactions of imidazo [1, 2-α] pyridines with analgesic, antiinflammatory, antipyretic, and anticonvulsant activity. *Journal of medicinal chemistry*, *8*, 305-312.

American Cancer Society. https://www.cancer.org/. Last accessed: August 2021

Amos, L., & Klug, A. (1974). Arrangement of subunits in flagellar microtubules. *Journal of cell science*, *14*, 523–549.

Anderson, J. T., Ting, A. E., Boozer, S., Brunden, K. R., Crumrine, C., Danzig, J., Dent, T., Faga, L., Harrington, J. J., Hodnick, W. F., Murphy, S. M., Pawlowski, G., Perry, R., Raber, A., Rundlett, S. E., Stricker-Krongrad, A., Wang, J., & Bennani, Y. L. (2005b). Identification of novel and improved antimitotic agents derived from noscapine. *Journal of medicinal chemistry*, *48*, 7096–7098.

Anderson, J. T., Ting, A. E., Boozer, S., Brunden, K. R., Danzig, J., Dent, T., Harrington, J. J., Murphy, S. M., Perry, R., Raber, A., Rundlett, S. E., Wang, J., Wang, N., & Bennani, Y. L. (2005a). Discovery of S-phase arresting agents derived from noscapine. *Journal of medicinal chemistry*, *48*, 2756–2758.

Aneja, R., Asress, S., Dhiman, N., Awasthi, A., Rida, P. C., Arora, S. K., Zhou, J., Glass, J. D., & Joshi, H. C. (2010a). Non-toxic melanoma therapy by a novel tubulin-binding agent. *International journal of cancer*, *126*, 256–265.

Aneja, R., Dhiman, N., Idnani, J., Awasthi, A., Arora, S. K., Chandra, R., & Joshi, H. C. (2007a). Preclinical pharmacokinetics and bioavailability of noscapine, a tubulin-binding anticancer agent. *Cancer chemotherapy and pharmacology*, *60*, 831–839.

Aneja, R., Kalia, V., Ahmed, R., & Joshi, H. C. (2007b). Nonimmunosuppressive chemotherapy: EM011-treated mice mount normal T-cell responses to an acute lymphocytic choriomeningitis virus infection. *Molecular cancer therapeutics*, *6*, 2891–2899.

Aneja, R., Lopus, M., Zhou, J., Vangapandu, S. N., Ghaleb, A., Yao, J., Nettles, J. H., Zhou, B., Gupta, M., Panda, D., Chandra, R., & Joshi, H. C. (2006d). Rational design of the microtubule-targeting anti-breast cancer drug EM015. *Cancer research*, *66*, 3782–3791.

Aneja, R., Miyagi, T., Karna, P., Ezell, T., Shukla, D., Vij Gupta, M., Yates, C., Chinni, S. R., Zhau, H., Chung, L. W., & Joshi, H. C. (2010b). A novel microtubule-modulating agent induces mitochondrially driven caspase-dependent apoptosis via mitotic checkpoint activation in human prostate cancer cells. *European journal of cancer (Oxford, England: 1990)*, *46*(9), 1668–1678.

Aneja, R., Vangapandu, S. N., & Joshi, H. C. (2006c). Synthesis and biological evaluation of a cyclic ether fluorinated noscapine analog. *Bioorganic & medicinal chemistry*, *14*, 8352–8358.

Aneja, R., Vangapandu, S. N., Lopus, M., Chandra, R., Panda, D., & Joshi, H. C. (2006b). Development of a novel nitro-derivative of noscapine for the potential treatment of drug-resistant ovarian cancer and T-cell lymphoma. *Molecular pharmacology*, *69*, 1801–1809.

Aneja, R., Vangapandu, S. N., Lopus, M., Viswesarappa, V. G., Dhiman, N., Verma, A., Chandra, R., Panda, D., & Joshi, H. C. (2006a). Synthesis of microtubule-interfering halogenated noscapine analogs that perturb mitosis in cancer cells followed by cell death. *Biochemical pharmacology*, *72*, 415–426.

Beck, A. D. (1993). Density-functional thermochemistry. III. The role of exact exchange. *J. Chem. Phys*, *98*, 5648-6.

Belmont, L. D., Hyman, A. A., Sawin, K. E., & Mitchison, T. J. (1990). Real-time visualization of cell cycle-dependent changes in microtubule dynamics in cytoplasmic extracts. *Cell*, *62*, 579–589.

Berendsen, H. J., van der Spoel, D., & van Drunen, R. (1995). GROMACS: a message-passing parallel molecular dynamics implementation. *Computer physics communications*, *91*, 43-56.

Betty Smoot PT, D. P. T. S., Meredith Wampler PT, D. P. T. S., & Topp, K. S. (2009). Breast cancer treatments and complications: implications for rehabilitation. *Rehabilitation Oncology*, *27*, 16.

Bhalla, K., Ibrado, A. M., Tourkina, E., Tang, C., Mahoney, M. E., & Huang, Y. (1993). Taxol induces internucleosomal DNA fragmentation associated with programmed cell death in human myeloid leukemia cells. *Leukemia*, *7*, 563–568.

Bhardwaj, V. K., & Purohit, R. (2021). Targeting the protein-protein interface pocket of Aurora-A-TPX2 complex: rational drug design and validation. *Journal of biomolecular structure & dynamics*, *39*, 3882–3891.

Bhardwaj, V. K., Singh, R., Sharma, J., Das, P., & Purohit, R. (2020). Structural based study to identify new potential inhibitors for dual specificity tyrosine-phosphorylation-regulated kinase. *Computer methods and programs in biomedicine*, *194*, 105494.

Bhushan, A., Gonsalves, A., & Menon, J. U. (2021). Current State of Breast Cancer Diagnosis, Treatment, and Theranostics. *Pharmaceutics*, *13*, 723.

Binkley, J. S., Pople, J. A., & Hehre, W. J. (1980). Self-consistent molecular orbital methods. 21. Small split-valence basis sets for first-row elements. *Journal of the American Chemical Society*, 102, 939-947.

Bissery, M. C., Guénard, D., Guéritte-Voegelein, F., & Lavelle, F. (1991). Experimental antitumor activity of taxotere (RP 56976, NSC 628503), a taxol analogue. *Cancer research*, *51*, 4845–4852.

Boerner, R. J., & Moller, H. J. (1997). Saripidem-a new treatment for panic disorders. *Psychopharmakotherapie*, *4*, 145-148.

Bonfoco, E., Ceccatelli, S., Manzo, L., & Nicotera, P. (1995). Colchicine induces apoptosis in cerebellar granule cells. *Experimental cell research*, *218*, 189–200.

Borisy, G. G., & Taylor, E. W. (1967a). The mechanism of action of colchicine. Binding of colchincine-3H to cellular protein. *The Journal of cell biology*, *34*, 525–533.

Borisy, G. G., & Taylor, E. W. (1967b). The mechanism of action of colchicine. Colchicine binding to sea urchin eggs and the mitotic apparatus. *The Journal of cell biology*, *34*(2), 535–548.

Bradford M. M. (1976). A rapid and sensitive method for the quantitation of microgram quantities of protein utilizing the principle of protein-dye binding. *Analytical biochemistry*, *72*, 248–254.

Bradley, G., & Ling, V. (1994). P-glycoprotein, multidrug resistance and tumor progression. *Cancer metastasis reviews*, *13*, 223–233.

Bray, F., Ferlay, J., Soerjomataram, I., Siegel, R. L., Torre, L. A., & Jemal, A. (2018). Global cancer statistics 2018: GLOBOCAN estimates of incidence and mortality worldwide for 36 cancers in 185 countries. *CA: a cancer journal for clinicians*, *68*, 394–424.

Burkhart, C. A., Kavallaris, M., & Band Horwitz, S. (2001). The role of beta-tubulin isotypes in resistance to antimitotic drugs. *Biochimica et biophysica acta*, *1471*, O1–O9.

Burns R. G. (1991). Alpha-, beta-, and gamma-tubulins: sequence comparisons and structural constraints. *Cell motility and the cytoskeleton*, *20*, 181–189.

Checchi, P. M., Nettles, J. H., Zhou, J., Snyder, J. P., & Joshi, H. C. (2003). Microtubule-interacting drugs for cancer treatment. *Trends in pharmacological sciences*, *24*, 361–365.

Chopra, R. N., Mukherjee, B., & Dikshit, B. B. (1930). Narcotine: its pharmacological action and therapeutic uses. *Indian J Med Res*, *18*, 35-49.

Couty, F. and G. Evanoff in Comprehensive heterocyclic chemistry III. (2008). Vol. 11, eds AR Katritzky, CA Ramsden, EFV Scriven, RJK Taylor.

Cowey, C. L. (2013). Profile of tivozanib and its potential for the treatment of advanced renal cell carcinoma. *Drug design, development and therapy*, *7*, 519.

Crown, J., & O'Leary, M. (2000). The taxanes: an update. *Lancet (London, England)*, *355*, 1176–1178.

Dahlström, B., Mellstrand, T., Löfdahl, C. G., & Johansson, M. (1982). Pharmacokinetic properties of noscapine. *European journal of clinical pharmacology*, *22*, 535–539.

Dash, S. G., Kantevari, S., & Naik, P. K. (2021). Combination Regimen of Amino-Noscapine and Docetaxel for Evaluation of Anticancer Activity. *Analytical Chemistry Letters*, 11, 215-229.

Dash, S. G., Suri, C., Nagireddy, P., Kantevari, S., & Naik, P. K. (2021). Rational design of 9-vinyl-phenyl Noscapine as potent tubulin binding anticancer agent and evaluation of the effects of its combination on Docetaxel. *Journal of biomolecular structure & dynamics*, *39*, 5276–5289.

David-Pfeuty, T., Erickson, H. P., & Pantaloni, D. (1977). Guanosinetriphosphatase activity of tubulin associated with microtubule assembly. *Proceedings of the National Academy of Sciences of the United States of America*, *74*, 5372–5376.

Debono, A. J., Mistry, S. J., Xie, J., Muthiah, D., Phillips, J., Ventura, S., Callaghan, R., Pouton, C. W., Capuano, B., & Scammells, P. J. (2014). The synthesis and biological evaluation of multifunctionalised derivatives of noscapine as cytotoxic agents. *ChemMedChem*, *9*, 399–410.

DeBono, A. J., Xie, J. H., Ventura, S., Pouton, C. W., Capuano, B., & Scammells, P. J. (2012). Synthesis and biological evaluation of N-substituted noscapine analogues. *ChemMedChem*, *7*, 2122–2133.

Devine, S. M., Yong, C., Amenuvegbe, D., Aurelio, L., Muthiah, D., Pouton, C., Callaghan, R., Capuano, B., & Scammells, P. J. (2018). Synthesis and Pharmacological Evaluation of Noscapine-Inspired 5-Substituted Tetrahydroisoquinolines as Cytotoxic Agents. *Journal of medicinal chemistry*, *61*, 8444–8456.

DSouza, N. D., Murthy, N. S., & Aras, R. Y. (2013). Projection of burden of cancer mortality for India, 2011-2026. *Asian Pacific Journal of Cancer Prevention*, *14*, 4387-4392.

Dustin, P. (1984). Microtubule poisons. In *Microtubules* (pp. 171-233). Springer, Berlin, Heidelberg.

Džolić, Z. R., Perković, I., Pavelić, S. K., Sedić, M., Ilić, N., Schols, D., & Zorc, B. (2016). Design, synthesis, and cytostatic activity of novel pyrazine sorafenib analogs. *Medicinal Chemistry Research*, *25*(12), 2729-2741.

Empey, D. W., Laitinen, L. A., Young, G. A., Bye, C. E., & Hughes, D. T. (1979). Comparison of the antitussive effects of codeine phosphate 20 mg, dextromethorphan 30 mg and noscapine 30 mg using citric acid-induced cough in normal subjects. *European journal of clinical pharmacology*, *16*, 393–397.

Fan, J., Griffiths, A. D., Lockhart, A., Cross, R. A., & Amos, L. A. (1996a). Microtubule minus ends can be labelled with a phage display antibody specific to alpha-tubulin. *Journal of molecular biology*, *259*, 325–33.

Fan, J., Griffiths, A. D., Lockhart, A., Cross, R. A., & Amos, L. A. (1996b). Microtubule minus ends can be labelled with a phage display antibody specific to alpha-tubulin. *Journal of molecular biology*, *259*, 325–330.

Fan, W., Miller III, M. C., Cheng, L., & Willingham, M. C. (1998). Taxol-induced apoptosis may occur via a signaling pathway independent of microtubule bundling and cell cycle arrest. *Microscopy and Microanalysis*, *4*, 1042-1043.

Fisher, M. H., & Lusi, A. (1972). Imidazo [1, 2-a] pyridine anthelmintic and antifungal agents. *Journal of Medicinal Chemistry*, *15*, 982-985.

Fortin, J. S., Lacroix, J., Desjardins, M., Patenaude, A., Petitclerc, E., & C-Gaudreault, R. (2007). Alkylation potency and protein specificity of aromatic urea derivatives and bioisosteres as potential irreversible antagonists of the colchicine-binding site. *Bioorganic & medicinal chemistry*, *15*, 4456–4469.

Frampton, J. E. (2016). Lenvatinib: a review in refractory thyroid cancer. *Targeted oncology*, *11*(1), 115-122.

Friesner, R. A., Banks, J. L., Murphy, R. B., Halgren, T. A., Klicic, J. J., Mainz, D. T., Repasky, M. P., Knoll, E. H., Shelley, M., Perry, J. K., Shaw, D. E., Francis, P., & Shenkin, P. S. (2004). Glide: a new approach for rapid, accurate docking and scoring. 1. Method and assessment of docking accuracy. *Journal of medicinal chemistry*, *47*, 1739–1749.

Garcia, M., Jemal, A. W. E. C. M. H. Y. S. R. T. M. J., Ward, E. M., Center, M. M., Hao, Y., Siegel, R. L., & Thun, M. J. (2007). Global cancer facts & figures 2007. *Atlanta, GA: American cancer society*, *1*, 52.

Giannakakou, P., Sackett, D. L., Kang, Y. K., Zhan, Z., Buters, J. T., Fojo, T., & Poruchynsky, M. S. (1997). Paclitaxel-resistant human ovarian cancer cells have mutant beta-tubulins that exhibit impaired paclitaxel-driven polymerization. *The Journal of biological chemistry*, *272*, 17118–17125.

Giordano, S. H., Buzdar, A. U., & Hortobagyi, G. N. (2002). Breast cancer in men. *Annals of internal medicine*, *137*, 678–68.

Gómez-Raposo, C., Zambrana Tévar, F., Sereno Moyano, M., López Gómez, M., & Casado, E. (2010). Male breast cancer. *Cancer treatment reviews*, *36*, 451–457.

Gordon, M. S., Binkley, J. S., Pople, J. A., Pietro, W. J., & Hehre, W. J. (1982). Self-consistent molecular-orbital methods. 22. Small split-valence basis sets for second-row elements. *Journal of the American Chemical Society*, *104*, 2797-2803.

Gottesman, M. M., & Pastan, I. (1993). Biochemistry of multidrug resistance mediated by the multidrug transporter. *Annual review of biochemistry*, *62*, 385–427.

Gudmundsson, K.; Boggs, S. D. PCT Int. Appl. WO 2006026703, 2006; CAN 2006, 144, 274.

Haikala, V., Sothmann, A., & Marvola, M. (1986). Comparative bioavailability and pharmacokinetics of noscapine hydrogen embonate and noscapine hydrochloride. *European journal of clinical pharmacology*, *31*, 367–369.

Halgren, T. A., Murphy, R. B., Friesner, R. A., Beard, H. S., Frye, L. L., Pollard, W. T., & Banks, J. L. (2004). Glide: a new approach for rapid, accurate docking and scoring. 2. Enrichment factors in database screening. *Journal of medicinal chemistry*, *47*, 1750–1759.

Hamdouchi, C., de Blas, J., del Prado, M., Gruber, J., Heinz, B. A., & Vance, L. (1999). 2-Amino-3-substituted-6-[(E)-1-phenyl-2-(N-methylcarbamoyl) vinyl] imidazo [1, 2-a] pyridines as a novel class of inhibitors of human rhinovirus: stereospecific synthesis and antiviral activity. *Journal of medicinal chemistry*, *42*, 50-59.

Hamel, E., & Lin, C. M. (1981). Glutamate-induced polymerization of tubulin: characteristics of the reaction and application to the large-scale purification of tubulin. *Archives of biochemistry and biophysics*, *209*, 29–40.

Harbeck, N., Penault-Llorca, F., Cortes, J., Gnant, M., Houssami, N., Poortmans, P., Ruddy, K., Tsang, J., & Cardoso, F. (2019). Breast cancer. *Nature reviews. Disease primers*, *5*, 66.

Hartwell, L. H., & Weinert, T. A. (1989). Checkpoints: controls that ensure the order of cell cycle events. *Science (New York, N.Y.)*, *246*, 629–634.

Heald, R., McLoughlin, M., & McKeon, F. (1993). Human wee1 maintains mitotic timing by protecting the nucleus from cytoplasmically activated Cdc2 kinase. *Cell*, *74*, 463–474.

Hornak, V., Abel, R., Okur, A., Strockbine, B., Roitberg, A., & Simmerling, C. (2006). Comparison of multiple Amber force fields and development of improved protein backbone parameters. *Proteins: Structure, Function, and Bioinformatics*, *65*, 712-725.

Hou, T., Wang, J., Li, Y., & Wang, W. (2011). Assessing the performance of the molecular mechanics/Poisson Boltzmann surface area and molecular

mechanics/generalized Born surface area methods. II. The accuracy of ranking poses generated from docking. *Journal of computational chemistry*, *32*(5), 866–877.

Jain, N., Yada, D., Shaik, T. B., Vasantha, G., Reddy, P. S., Kalivendi, S. V., & Sreedhar, B. (2011). Synthesis and antitumor evaluation of nitrovinyl biphenyls: anticancer agents based on allocolchicines. *ChemMedChem*, *6*, 859–868.

Jakalian, A., Jack, D. B., & Bayly, C. I. (2002). Fast, efficient generation of high-quality atomic charges. AM1-BCC model: II. Parameterization and validation. *Journal of computational chemistry*, *23*, 1623-1641.

Jensen, L. N., Christrup, L. L., Jacobsen, L., Bonde, J., & Bundgaard, H. (1992). Relative bioavailability in man of noscapine administered in lozenges and mixture. *Acta pharmaceutica Nordica*, *4*, 309–312.

Jordan, M. A. & Wilson, L. in *Methods in Cell Biology, in Mitosis and Meiosis* Vol. **61** (ed. Rieder, C. L.) 267–295 (Academic, New York, 1998).

Jordan, M. A., & Wilson, L. (1999). The use and action of drugs in analyzing mitosis. *Methods in cell biology*, *61*, 267–295.

Joshi H. C. (1998). Microtubule dynamics in living cells. *Current opinion in cell biology*, *10*, 35–44.

Joshi, H. C., Salil, A., Bughani, U., & Naik, P. (2010). Noscapinoids: A new class of anticancer drugs demand biotechnological intervention. *Medicinal Plant Biotechnology*, 303-320.

Kaminski, J. J., & Doweyko, A. M. (1997). Antiulcer agents. 6. Analysis of the in vitro biochemical and in vivo gastric antisecretory activity of substituted imidazo [1, 2-a] pyridines and related analogues using comparative molecular field analysis and hypothetical active site lattice methodologies. *Journal of medicinal chemistry*, *40*, 427-436.

Karlsson, M. O., Dahlström, B., Eckernäs, S. A., Johansson, M., & Alm, A. T. (1990). Pharmacokinetics of oral noscapine. *European journal of clinical pharmacology*, *39*, 275–279.

Karna, P., Zughaier, S., Pannu, V., Simmons, R., Narayan, S., & Aneja, R. (2010). Induction of reactive oxygen species-mediated autophagy by a novel microtubule-modulating agent. *The Journal of biological chemistry*, *285*, 18737–18748.

Kavanagh, J. J., & Kudelka, A. P. (1993). Systemic therapy for gynecologic cancer. *Current opinion in oncology*, *5*, 891–899.

Kawamura, K. I., Grabowski, D., Weizer, K., Bukowski, R., & Ganapathi, R. (1996). Modulation of vinblastine cytotoxicity by dilantin (phenytoin) or the protein phosphatase inhibitor okadaic acid involves the potentiation of anti-mitotic effects and induction of apoptosis in human tumour cells. *British journal of cancer*, *73*, 183–188.

Ke, Y., Ye, K., Grossniklaus, H. E., Archer, D. R., Joshi, H. C., & Kapp, J. A. (2000). Noscapine inhibits tumor growth with little toxicity to normal tissues or inhibition of immune responses. *Cancer immunology, immunotherapy: CII*, *49*, 217–225.

Keating, G. M. (2017). Sorafenib: a review in hepatocellular carcinoma. *Targeted oncology*, *12*(2), 243-253.

Kelly, S. M., Jess, T. J., & Price, N. C. (2005). How to study proteins by circular dichroism. *Biochimica et biophysica acta*, *1751*, 119–139.

King, K. L., & Cidlowski, J. A. (1995). Cell cycle and apoptosis: common pathways to life and death. *Journal of cellular biochemistry*, *58*, 175–180.

Kollman, P. A., Massova, I., Reyes, C., Kuhn, B., Huo, S., Chong, L., Lee, M., Lee, T., Duan, Y., Wang, W., Donini, O., Cieplak, P., Srinivasan, J., Case, D. A., & Cheatham, T. E., 3rd (2000). Calculating structures and free energies of complex molecules: combining molecular mechanics and continuum models. *Accounts of chemical research*, *33*, 889–897.

Krishna, R., & Mayer, L. D. (2000). Multidrug resistance (MDR) in cancer: mechanisms, reversal using modulators of MDR and the role of MDR modulators in influencing the pharmacokinetics of anticancer drugs. *European Journal of Pharmaceutical Sciences*, 11, 265-283.

Kumari, R., Kumar, R., Open-Source Drug Discovery Consortium, & Lynn, A. (2014). g_mmpbsa□ A GROMACS tool for high-throughput MM-PBSA calculations. *Journal of chemical information and modeling*, *54*, 1951-1962.

Landen, J. W., Hau, V., Wang, M., Davis, T., Ciliax, B., Wainer, B. H., Van Meir, E. G., Glass, J. D., Joshi, H. C., & Archer, D. R. (2004). Noscapine crosses the blood-brain barrier and inhibits glioblastoma growth. *Clinical cancer research: an official journal of the American Association for Cancer Research*, *10*, 5187–5201.

Landen, J. W., Lang, R., McMahon, S. J., Rusan, N. M., Yvon, A. M., Adams, A. W., Sorcinelli, M. D., Campbell, R., Bonaccorsi, P., Ansel, J. C., Archer, D. R., Wadsworth, P., Armstrong, C. A., & Joshi, H. C. (2002). Noscapine alters microtubule dynamics in living cells and inhibits the progression of melanoma. *Cancer research*, *62*, 4109–4114.

Langer, S. Z., Arbilla, S., Benavides, J., & Scatton, B. (1990). Zolpidem and alpidem: two imidazopyridines with selectivity for omega 1-and omega 3-receptor subtypes. *Advances in biochemical psychopharmacology*, *46*, 61-72.

Lee, C. J., Liang, X., Wu, Q., Najeeb, J., Zhao, J., Gopalaswamy, R., Titecat, M., Sebbane, F., Lemaitre, N., Toone, E. J., & Zhou, P. (2016). Drug design from the cryptic inhibitor envelope. *Nature communications*, *7*, 10638.

Lee, C., Yang, W., & Parr, R. G. (1988). Development of the Colle-Salvetti correlation-energy formula into a functional of the electron density. *Physical review. B, Condensed matter*, *37*, 785–789.

Li, H. Q., Lv, P. C., Yan, T., & Zhu, H. L. (2009). Urea derivatives as anticancer agents. *Anti-cancer agents in medicinal chemistry*, *9*(4), 471–480.

Liang, X., Gopalaswamy, R., Navas, F., 3rd, Toone, E. J., & Zhou, P. (2016). A Scalable Synthesis of the Difluoromethyl-allo-threonyl Hydroxamate-Based LpxC Inhibitor LPC-058. *The Journal of organic chemistry*, *81*, 4393–4398.

Lieu, C. H., Chang, Y. N., & Lai, Y. K. (1997). Dual cytotoxic mechanisms of submicromolar taxol on human leukemia HL-60 cells. *Biochemical pharmacology*, *53*, 1587–1596.

Liu, J., and Chen, Q. (2010). HuaxueJinzhan, 22, 631.

Logan, G. J., Dabbs, D. J., Lucas, P. C., Jankowitz, R. C., Brown, D. D., Clark, B. Z., Oesterreich, S., & McAuliffe, P. F. (2015). Molecular drivers of lobular carcinoma in situ. *Breast cancer research: BCR*, *17*, 76.

Long, B. H., & Fairchild, C. R. (1994). Paclitaxel inhibits progression of mitotic cells to G1 phase by interference with spindle formation without affecting other microtubule functions during anaphase and telephase. *Cancer research*, *54*, 4355–4361.

Lopus, M., & Naik, P. K. (2015). Taking aim at a dynamic target: Noscapinoids as microtubule-targeted cancer therapeutics. *Pharmacological reports: PR*, *67*, 56–62.

Lukong K. E. (2017). Understanding breast cancer - The long and winding road. *BBA clinical*, *7*, 64–77.

MacNeal, R. K., & Purich, D. L. (1978). Stoichiometry and role of GTP hydrolysis in bovine neurotubule assembly. *The Journal of biological chemistry*, *253*, 4683–4687.

Malvia, S., Bagadi, S. A., Dubey, U. S., & Saxena, S. (2017). Epidemiology of breast cancer in Indian women. *Asia-Pacific journal of clinical oncology*, *13*, 289–295.

Manchukonda, N. K., Naik, P. K., Santoshi, S., Lopus, M., Joseph, S., Sridhar, B., & Kantevari, S. (2013). Rational design, synthesis, and biological evaluation of third generation α-noscapine analogues as potent tubulin binding anti-cancer agents. *PloS one*, *8*, e77970.

Manchukonda, N. K., Naik, P. K., Sridhar, B., & Kantevari, S. (2014). Synthesis and biological evaluation of novel biaryl type α-noscapine congeners. *Bioorganic & medicinal chemistry letters*, *24*, 5752–5757.

Manchukonda, N. K., Sridhar, B., Naik, P. K., Joshi, H. C., & Kantevari, S. (2012). Copper (I) mediated facile synthesis of potent tubulin polymerization inhibitor, 9-amino-α-noscapine from natural α-noscapine. *Bioorganic & medicinal chemistry letters*, *22*, 2983-2987.

Mandelkow, E. M., Schultheiss, R., Rapp, R., Müller, M., & Mandelkow, E. (1986). On the surface lattice of microtubules: helix starts, protofilament number, seam, and handedness. *The Journal of cell biology*, *102*, 1067–1073.

Margolis, R. L., & Wilson, L. (1978). Opposite end assembly and disassembly of microtubules at steady state in vitro. *Cell*, *13*, 1–8.

Massova, I., & Kollman, P. A. (2000). Combined molecular mechanical and continuum solvent approach (MM-PBSA/GBSA) to predict ligand binding. *Perspectives in drug discovery and design*, *18*, 113-135.

Mathur, P., Sathishkumar, K., Chaturvedi, M., Das, P., Sudarshan, K. L., Santhappan, S., Nallasamy, V., John, A., Narasimhan, S., Roselind, F. S., & ICMR-NCDIR-NCRP Investigator Group (2020). Cancer Statistics, 2020: Report From National Cancer Registry Programme, India. *JCO global oncology*, *6*, 1063–1075.

Maughan, K. L., Lutterbie, M. A., & Ham, P. S. (2010). Treatment of breast cancer. *American family physician*, *81*, 1339–1346.

Mazia D (1961). Mitosis. In "The Cell" (J. Brachet and A. E. Mirsky, eds.), Vol. 3, pp. 77-142. Academic Press, New York.

McIntosh J. R. (1991). Structural and mechanical control of mitotic progression. *Cold Spring Harbor symposia on quantitative biology*, *56*, 613–619.

Meher, R. K., Nagireddy, P., Pragyandipta, P., Kantevari, S., Singh, S. K., Kumar, V., & Naik, P. K. (2021). *Insilico* design of novel tubulin binding 9-arylimino derivatives of noscapine, their chemical synthesis and cellular activity as potent anticancer agents against breast cancer. *Journal of biomolecular structure & dynamics*, 1–12.

Milas, L., Hunter, N. R., Kurdoglu, B., Mason, K. A., Meyn, R. E., Stephens, L. C., & Peters, L. J. (1995). Kinetics of mitotic arrest and apoptosis in murine mammary and ovarian tumors treated with taxol. *Cancer chemotherapy and pharmacology*, *35*, 297–303.

Miller, M. C., 3rd, Johnson, K. R., Willingham, M. C., & Fan, W. (1999). Apoptotic cell death induced by baccatin III, a precursor of paclitaxel, may occur without G (2)/M arrest. *Cancer chemotherapy and pharmacology*, *44*, 444–452.

Mishra, K. B., Tiwari, N., Bose, P., Singh, R., Rawat, A. K., Singh, S. K., Mishra, R.C., Singh, R. K., & Tiwari, V. K. (2019). Design, synthesis and Pharmacological evaluation of Noscapine Glycoconjugates. *ChemistrySelect*, *4*, 2644-2648.

Mishra, R. C., Karna, P., Gundala, S. R., Pannu, V., Stanton, R. A., Gupta, K. K., Robinson, M. H., Lopus, M., Wilson, L., Henary, M., & Aneja, R. (2011). Second generation benzofuranone ring substituted noscapine analogs: synthesis and biological evaluation. *Biochemical pharmacology*, *82*, 110–121.

Mitchison, T., & Kirschner, M. (1984a). Dynamic instability of microtubule growth. *Nature*, *312*, 237–242.

Mitchison, T., & Kirschner, M. (1984b). Microtubule assembly nucleated by isolated centrosomes. *Nature*, *312*, 232–237.

Mounetou, E., Legault, J., Lacroix, J., & C-Gaudreault, R. (2001). Antimitotic antitumor agents: synthesis, structure-activity relationships, and biological characterization of N-aryl-N'-(2-chloroethyl) ureas as new selective alkylating agents. *Journal of medicinal chemistry*, *44*, 694–702.

Nagireddy, P. K. R., Kommalapati, V. K., Siva Krishna, V., Sriram, D., Tangutur, A. D., & Kantevari, S. (2019). Imidazo [2, 1-b] thiazole-coupled natural noscapine derivatives as anticancer agents. *ACS omega*, *4*, 19382-19398.

Nagireddy, P. K. R., Kumar, D., Kommalapati, V. K., Pedapati, R. K., Kojja, V., Tangutur, A. D., & Kantevari, S. (2021). 9-Ethynyl noscapine induces G2/M arrest and apoptosis by disrupting tubulin polymerization in cervical cancer. *Drug Development Research*.

Naik, P. K., Chatterji, B. P., Vangapandu, S. N., Aneja, R., Chandra, R., Kanteveri, S., & Joshi, H. C. (2011a). Rational design, synthesis and biological evaluations of amino-noscapine: a high affinity tubulin-binding noscapinoid. *Journal of computer-aided molecular design*, *25*, 443–454.

Naik, P. K., Lopus, M., Aneja, R., Vangapandu, S. N., & Joshi, H. C. (2012). In silico inspired design and synthesis of a novel tubulin-binding anti-cancer drug: folate conjugated noscapine (Targetin). *Journal of computer-aided molecular design*, *26*, 233–247.

Naik, P. K., Santoshi, S., Rai, A., & Joshi, H. C. (2011b). Molecular modelling and competition binding study of Br-noscapine and colchicine provide insight into noscapinoid-tubulin binding site. *Journal of molecular graphics & modelling*, *29*, 947–955.

Nambiar, N., Nagireddy, P., Pedapati, R., Kantevari, S., & Lopus, M. (2020). Tubulin- and ROS-dependent antiproliferative mechanism of a potent analogue of noscapine, N-propargyl noscapine. *Life sciences*, *258*, 118238.

National Cancer Institute. Available from: https://www.cancer.gov/about-cancer/understanding/statistics Last accessed August 2021

National Cancer Institute. Available from: https://www.cancer.gov/about-cancer/treatment/drugs/breast. Last accessed September 2021

Nounou, M. I., ElAmrawy, F., Ahmed, N., Abdelraouf, K., Goda, S., & Syed-Sha-Qhattal, H. (2015). Breast Cancer: Conventional Diagnosis and Treatment Modalities and Recent Patents and Technologies. *Breast cancer: basic and clinical research*, *9*, 17–34.

Oliva, M. A., Prota, A. E., Rodríguez-Salarichs, J., Bennani, Y. L., Jiménez-Barbero, J., Bargsten, K., Canales, Á., Steinmetz, M. O., & Díaz, J. F. (2020). Structural Basis of Noscapine Activation for Tubulin Binding. *Journal of medicinal chemistry*, *63*, 8495–8501.

Panda, D., Chakrabarti, G., Hudson, J., Pigg, K., Miller, H. P., Wilson, L., & Himes, R. H. (2000). Suppression of microtubule dynamic instability and treadmilling by deuterium oxide. *Biochemistry*, *39*, 5075–5081.

Pannu, V., Rida, P. C., Ogden, A., Clewley, R., Cheng, A., Karna, P., Lopus, M., Mishra, R. C., Zhou, J., & Aneja, R. (2012). Induction of robust de novo centrosome amplification, high-grade spindle multipolarity and metaphase catastrophe: a novel chemotherapeutic approach. *Cell death & disease*, *3*, e346.

Patel, A. K., Meher, R. K., Nagireddy, P. K., Pragyandipta, P., Pedapati, R. K., Kantevari, S., & Naik, P. K. (2021). 9-Arylimino noscapinoids as potent tubulin binding anticancer agent: chemical synthesis and cellular evaluation against breast tumour cells. *SAR and QSAR in environmental research*, *32*, 269–291.

Patel, A. K., Meher, R. K., Reddy, P. K., Pedapati, R. K., Pragyandipta, P., Kantevari, S., Naik, M. R., & Naik, P. K. (2021). Rational design, chemical synthesis and cellular evaluation of novel 1,3-diynyl derivatives of noscapine as potent tubulin binding anticancer agents. *Journal of molecular graphics & modelling*, *106*, 107933.

Pelicano, H., Carney, D., & Huang, P. (2004). ROS stress in cancer cells and therapeutic implications. *Drug resistance updates: reviews and commentaries in antimicrobial and anticancer chemotherapy*, *7*, 97–110.

Pilleron, S., Soto-Perez-de-Celis, E., Vignat, J., Ferlay, J., Soerjomataram, I., Bray, F., & Sarfati, D. (2021). Estimated global cancer incidence in the oldest adults in 2018 and projections to 2050. *International journal of cancer*, *148*, 601-608.

Rahmanian-Devin, P., Baradaran Rahimi, V., Jaafari, M. R., Golmohammadzadeh, S., Sanei-Far, Z., & Askari, V. R. (2021). Noscapine, an Emerging Medication for Different Diseases: A Mechanistic Review. *Evidence-based complementary and alternative medicine: eCAM*, *2021*, 8402517.

Report of National Cancer Registry Programme 2020, ICMR (2012-2016). https://www.ncdirindia.org/All_Reports/Report_2020/default.aspx. Last accessed August 2021

Rival, Y., Grassy, G., & Michel, G. (1992). Synthesis and antibacterial activity of some Imidazo [1, 2-α] pyrimidine derivatives. *Chemical and pharmaceutical bulletin*, *40*, 1170-1176.

Rival, Y., Grassy, G., Taudou, A., & Ecalle, R. (1991). Antifungal activity in vitro of some imidazo [1, 2-a] pyrimidine derivatives. *European journal of medicinal chemistry*, *26*, 13-18.

Rowinsky E. K. (1997). The development and clinical utility of the taxane class of antimicrotubule chemotherapy agents. *Annual review of medicine*, *48*, 353–374.

Rudner, A. D., & Murray, A. W. (1996). The spindle assembly checkpoint. *Current opinion in cell biology*, *8*, 773–780.

Russell, P., & Nurse, P. (1986). cdc25+ functions as an inducer in the mitotic control of fission yeast. *Cell*, *45*, 145–153.

Russell, P., & Nurse, P. (1987). Negative regulation of mitosis by wee1+, a gene encoding a protein kinase homolog. *Cell*, *49*, 559–567.

Ryckaert, J. P., Ciccotti, G., & Berendsen, H. J. (1977). Numerical integration of the cartesian equations of motion of a system with constraints: molecular dynamics of n-alkanes. *Journal of computational physics*, *23*, 327-341.

Sajadian, S., Vatankhah, M., Majdzadeh, M., Kouhsari, S. M., Ghahremani, M. H., & Ostad, S. N. (2015). Cell cycle arrest and apoptogenic properties of opium alkaloids noscapine and papaverine on breast cancer stem cells. *Toxicology mechanisms and methods*, *25*, 388–395.

Santoshi, S., & Naik, P. K. (2014). Molecular insight of isotypes specific β-tubulin interaction of tubulin heterodimer with noscapinoids. *Journal of computer-aided molecular design*, *28*, 751–763.

Santoshi, S., Manchukonda, N. K., Suri, C., Sharma, M., Sridhar, B., Joseph, S., Lopus, M., Kantevari, S., Baitharu, I., & Naik, P. K. (2015). Rational design of biaryl pharmacophore inserted noscapine derivatives as potent tubulin binding anticancer agents. *Journal of computer-aided molecular design*, *29*, 249–270.

Santoshi, S., Naik, P. K., & Joshi, H. C. (2011). Rational design of novel anti-microtubule agent (9-azido-noscapine) from quantitative structure activity relationship (QSAR) evaluation of noscapinoids. *Journal of biomolecular screening*, *16*, 1047–1058.

Saranath, D., & Khanna, A. (2014). Current status of cancer burden: global and Indian scenario. *Biomed Res J*, *1*, 1-5.

Saxton, W. M., Stemple, D. L., Leslie, R. J., Salmon, E. D., Zavortink, M., & McIntosh, J. R. (1984). Tubulin dynamics in cultured mammalian cells. *The Journal of cell biology*, *99*, 2175–2186.

Schiff, P. B., & Horwitz, S. B. (1980). Taxol stabilizes microtubules in mouse fibroblast cells. *Proceedings of the National Academy of Sciences of the United States of America*, *77*, 1561–1565.

Schulze, E., & Kirschner, M. (1986). Microtubule dynamics in interphase cells. *The Journal of cell biology*, *102*, 1020–1031.

Shen, W., Liang, B., Yin, J., Li, X., & Cheng, J. (2015). Noscapine Increases the Sensitivity of Drug-Resistant Ovarian Cancer Cell Line SKOV3/DDP to Cisplatin by Regulating Cell Cycle and Activating Apoptotic Pathways. *Cell biochemistry and biophysics*, *72*, 203–213.

Shimshoni, J. A., Bialer, M., Wlodarczyk, B., Finnell, R. H., & Yagen, B. (2007). Potent anticonvulsant urea derivatives of constitutional isomers of valproic acid. *Journal of medicinal chemistry*, *50*, 6419–6427.

Shin, H. R., Carlos, M. C., & Varghese, C. (2012). Cancer control in the Asia Pacific region: current status and concerns. *Japanese journal of clinical oncology*, *42*, 867-881.

Sondhi, S. M., Arya, S., Rani, R., Kumar, N., & Roy, P. (2012). Synthesis, anti-inflammatory and anticancer activity evaluation of some mono-and bis-Schiff's bases. *Medicinal Chemistry Research*, *21*, 3620-3628.

Song, Y. H., & Mandelkow, E. (1995). The anatomy of flagellar microtubules: polarity, seam, junctions, and lattice. *The Journal of cell biology*, *128*, 81–94.

Sousa da Silva, A. W., & Vranken, W. F. (2012). ACPYPE-Antechamber python parser interface. *BMC research notes*, *5*, 1-8.

Spiegelman, B. M., Penningroth, S. M., & Kirschner, M. W. (1977). Turnover of tubulin and the N site GTP in Chinese hamster ovary cells. *Cell*, *12*, 587–600.

Sun, H., Li, Y., Shen, M., Tian, S., Xu, L., Pan, P., Guan, Y., & Hou, T. (2014). Assessing the performance of MM/PBSA and MM/GBSA methods. 5. Improved docking performance using high solute dielectric constant MM/GBSA and MM/PBSA rescoring. *Physical chemistry chemical physics: PCCP*, *16*, 22035–22045.

Theiss, C., & Meller, K. (2000). Taxol impairs anterograde axonal transport of microinjected horseradish peroxidase in dorsal root ganglia neurons in vitro. *Cell and tissue research*, *299*, 213-224.

Tomayko, M. M., & Reynolds, C. P. (1989). Determination of subcutaneous tumor size in athymic (nude) mice. *Cancer chemotherapy and pharmacology*, *24*, 148-154.

Topp, K. S., Tanner, K. D., & Levine, J. D. (2000). Damage to the cytoskeleton of large diameter sensory neurons and myelinated axons in vincristine-induced painful peripheral neuropathy in the rat. *Journal of Comparative Neurology*, *424*, 563-576.

van Tellingen, O., Sips, J. H., Beijnen, J. H., Bult, A., & Nooijen, W. J. (1992). Pharmacology, bio-analysis and pharmacokinetics of the vinca alkaloids and semi-synthetic derivatives (review). *Anticancer research*, *12*, 1699–1715.

Verma, A. K., Bansal, S., Singh, J., Tiwari, R. K., Kasi Sankar, V., Tandon, V., & Chandra, R. (2006). Synthesis and in vitro cytotoxicity of haloderivatives of noscapine. *Bioorganic & medicinal chemistry*, *14*, 6733–6736.

Viswas, R. S., Pundir, S., & Lee, H. (2019). Design and synthesis of 4-piperazinyl quinoline derived urea/thioureas for anti-breast cancer activity by a hybrid pharmacophore approach. *Journal of enzyme inhibition and medicinal chemistry*, *34*, 620–630.

Wahl, A. F., Donaldson, K. L., Fairchild, C., Lee, F. Y., Foster, S. A., Demers, G. W., & Galloway, D. A. (1996). Loss of normal p53 function confers sensitization to Taxol by increasing G2/M arrest and apoptosis. *Nature medicine*, *2*, 72–79.

Walker, R. A., O'Brien, E. T., Pryer, N. K., Soboeiro, M. F., Voter, W. A., Erickson, H. P., & Salmon, E. D. (1988). Dynamic instability of individual microtubules analyzed by video light microscopy: rate constants and transition frequencies. *The Journal of cell biology*, *107*, 1437–1448.

Wallace, A. C., Laskowski, R. A., & Thornton, J. M. (1995). LIGPLOT: a program to generate schematic diagrams of protein-ligand interactions. *Protein engineering*, *8*, 127–134.

Wang, H., Hu, Y., Li, H., Xie, Y., Wang, X., & Wan, W. (2020). Preliminary study on identification of estrogen receptor-positive breast cancer subtypes based on dynamic contrast-enhanced magnetic resonance imaging (DCE-MRI) texture analysis. *Gland surgery*, *9*, 622–628.

Wang, J., Wolf, R. M., Caldwell, J. W., Kollman, P. A., & Case, D. A. (2004). Development and testing of a general amber force field. *Journal of computational chemistry*, *25*, 1157-1174.

Watson, R. J., Allen, D. R., Birch, H. L., Chapman, G. A., Galvin, F. C., Jopling, L. A., Knight, R. L., Meier, D., Oliver, K., Meissner, J. W., Owen, D. A., Thomas, E. J., Tremayne, N., & Williams, S. C. (2008). Development of CXCR3 antagonists. Part 3: Tropenyl and homotropenyl-piperidine urea derivatives. *Bioorganic & medicinal chemistry letters*, *18*, 147–151.

Weis, A., Katebzadeh, K., Söderhjelm, P., Nilsson, I., & Ryde, U. (2006). Ligand affinities predicted with the MM/PBSA method: dependence on the simulation method and the force field. *Journal of medicinal chemistry*, *49*, 6596–6606.

Weisenberg, R. C., Borisy, G. G., & Taylor, E. W. (1968). The colchicine-binding protein of mammalian brain and its relation to microtubules. *Biochemistry*, *7*, 4466–4479.

Wells W. A. (1996). The spindle-assembly checkpoint: aiming for a perfect mitosis, every time. *Trends in cell biology*, *6*, 228–234.

Winter, C. A., & Flataker, L. (1954). Antitussive compounds: testing methods and results. *Journal of Pharmacology and Experimental Therapeutics*, *112*, 99-108.

Woods, C. M., Zhu, J., McQueney, P. A., Bollag, D., & Lazarides, E. (1995). Taxol-induced mitotic block triggers rapid onset of a p53-independent apoptotic pathway. *Molecular medicine (Cambridge, Mass.)*, *1*, 506–526.

World Health Organization, IARC, GLOBOCAN. Available from: https://gco.iarc.fr/. Last accessed August 2021

Xu, L., Sun, H., Li, Y., Wang, J., & Hou, T. (2013). Assessing the performance of MM/PBSA and MM/GBSA methods. 3. The impact of force fields and ligand charge models. *The journal of physical chemistry. B*, *117*, 8408–8421.

Ye, K., Ke, Y., Keshava, N., Shanks, J., Kapp, J. A., Tekmal, R. R., Petros, J., & Joshi, H. C. (1998). Opium alkaloid noscapine is an antitumor agent that arrests metaphase and induces apoptosis in dividing cells. *Proceedings of the National Academy of Sciences of the United States of America*, *95*, 1601–1606.

Ye, K., Zhou, J., Landen, J. W., Bradbury, E. M., & Joshi, H. C. (2001). Sustained activation of p34(cdc2) is required for noscapine-induced apoptosis. *The Journal of biological chemistry*, *276*, 46697–46700.

Zhou, J., & Giannakakou, P. (2005). Targeting microtubules for cancer chemotherapy. *Current Medicinal Chemistry-Anti-Cancer Agents*, *5*, 65-71.

Zhou, J., Gupta, K., Aggarwal, S., Aneja, R., Chandra, R., Panda, D., & Joshi, H. C. (2003). Brominated derivatives of noscapine are potent microtubule-interfering agents that perturb mitosis and inhibit cell proliferation. *Molecular pharmacology*, *63*, 799–807.

Zhou, J., Gupta, K., Yao, J., Ye, K., Panda, D., Giannakakou, P., & Joshi, H. C. (2002b). Paclitaxel-resistant human ovarian cancer cells undergo c-Jun NH2-terminal kinase-mediated apoptosis in response to noscapine. *The Journal of biological chemistry*, *277*, 39777–39785.

Zhou, J., Liu, J., & Chen, Q. (2009). YoujiHuaxue, 29, 1708.

Zhou, J., Liu, M., Aneja, R., Chandra, R., Lage, H., & Joshi, H. C. (2006). Reversal of P-glycoprotein-mediated multidrug resistance in cancer cells by the c-Jun NH2-terminal kinase. *Cancer research*, *66*, 445–452.

Zhou, J., Panda, D., Landen, J. W., Wilson, L., & Joshi, H. C. (2002a). Minor alteration of microtubule dynamics causes loss of tension across kinetochore pairs and activates the spindle checkpoint. *The Journal of biological chemistry*, *277*, 17200–17208.

Zhou, R., Friesner, R. A., Ghosh, A., Rizzo, R. C., Jorgensen, W. L., & Levy, R. M. (2001). New linear interaction method for binding affinity calculations using a continuum solvent model. *The Journal of Physical Chemistry B*, *105*, 10388-10397.

List of Publications

1. **Pragyandipta, P**., Meher, R. K., Naik, M. R., Nagireddy, P. K., Pedapati, R. K., Kantevari, S., & Naik, P. K. (2021). In-Silico-Inspired Design of 1, 3-Diynyl Congeners of Noscapine as Promising Tubulin-Binding Anticancer Agent: Chemical Synthesis and Cellular Activity with Breast Cancer Cell Lines. *ChemistrySelect*, *6*(14), 3500-351.

2. **Pragyandipta, P**., Meher, R. K., Reddy, P. K., Pedaparti, R., Kantevari, S., & Naik, P. K. (2022). Structure Based Design of Tubulin Binding 9-Arylimino Noscapinoids: Chemical Synthesis and Experimental Validation Against Breast Cancer Cell Lines. *Analytical Chemistry Letters*, *12*(1), 29-43.

3. Patel, A. K., Meher, R. K., Reddy, P. K., Pedapati, R. K., **Pragyandipta, P**., Kantevari, S., Naik, M. R., & Naik, P. K. (2021). Rational design, chemical synthesis and cellular evaluation of novel 1,3-diynyl derivatives of noscapine as potent tubulin binding anticancer agents. *Journal of molecular graphics & modelling*, *106*, 107933.

4. Meher, R. K., Nagireddy, P., **Pragyandipta, P**., Kantevari, S., Singh, S. K., Kumar, V., & Naik, P. K. (2021). *Insilico* design of novel tubulin binding 9-arylimino derivatives of noscapine, their chemical synthesis and cellular activity as potent anticancer agents against breast cancer. *Journal of biomolecular structure & dynamics*, 1–12.

5. Meher, R. K., **Pragyandipta, P**., Pedapati, R. K., Nagireddy, P., Kantevari, S., Nayek, A. K., & Naik, P. K. (2021). Rational design of novel N-alkyl amine analogues of noscapine, their chemical synthesis and cellular activity as potent anticancer agents. *Chemical biology & drug design*, *98*(3), 445–465.

6. Patel, A. K., Meher, R. K., Nagireddy, P. K., **Pragyandipta, P**., Pedapati, R. K., Kantevari, S., & Naik, P. K. (2021). 9-Arylimino noscapinoids as potent tubulin binding anticancer agent: chemical synthesis and cellular evaluation against breast tumour cells. *SAR and QSAR in environmental research*, *32*(4), 269–291.

7. Meher, R. K., **Pragyandipta, P**., Reddy, P. K., Pedaparti, R., Kantevari, S., & Naik, P. K. (2021). Development of 1,3-diynyl derivatives of noscapine as potent tubulin binding anticancer agents for the management of breast cancer. *Journal of biomolecular structure & dynamics*, 1–18.

8. **Pragyandipta, P**., Reddy, P. K., Pedaparti, R., Kantevari, S., Bastia, B., Kantevari, S., & Naik, P. K. (2022). Development of 9-(N-Arylmethylamino) derivatives of noscapine: The Tubulin Binding Anticancer Agent for the Treatment of Breast Cancer. (Under Review in Applied Biochemistry and Biotechnology Journal)

9. **Pragyandipta, P**., Pedapati, R., Mir, SH., Reddy, P. K., Kantevari, S and Naik, P.K (2022) Rational design of N-imidazopyridine derivatives of noscapine as promising tubulin binding anticancer agents: chemical synthesis and cellular evaluation. Submitted to Drug Development Research

10. **Pragyandipta, P**., Pedapati, R., Mir, SH., Reddy, P. K., Kantevari, S and Naik, P.K (2022) (2022) Rational design of novel a-noscapine urea congeners as potent tubulin binding anticancer agents. chemical synthesis and cellular evaluation. Submitted to Chemico-Biological Interactions

Conference/Seminar Presentation

1. **Pratyush Pragyandipta** and Pradeep Kumar Naik. "Progress Toward the Development of Noscapine and Noscapinoids for the Management of Breast Cancer." Poster Presentation in Odisha Research Conclave on 14th November, 2021 jointly organized by Odisha State Higher Education council and Utkal University.
2. **Pratyush Pragyandipta** and Pradeep Kumar naik. "Targeted delivery of novel derivative of noscapine specifically to tumor cells for the management of breast cancer." Oral Presentation in National Conference on Current Research Trends in Biotechnology, Bioinformatics and Intellectual Property Management from 3rd to 4th March, 2020 organized by Department of Biotechnology and Bioinformatics, Sambalpur University
3. **Pratyush Pragyandipta** and Pradeep Kumar Naik. "In silico inspired design of promising derivatives of noscapine and their extensive preclinical evaluation as tubulin-binding anticancer agents." Oral Presentation in National Seminar on Harnessing Science & Technology for a better future from 23rd to 24th November, 2019 jointly organized by Odisha Environmental Society, Bhubaneswar and Siksha 'O' Anusandhan (Deemed to be University).
4. **Pratyush Pragyandipta** and Pradeep Kumar Naik. "Development of novel Noscapinoids and Preclinical Efficacy Evaluation for human breast cancer management." Presented a paper in UGC Sponsored National Seminar on Recent Advances on Molecules of Chemical & Biological Importance from organized by Municipal College, Rourkela from 6th to 7th February, 2018 Organized by Municipal College, Rourkela.

Received: 3 April 2021 | Revised: 30 April 2021 | Accepted: 23 May 2021

DOI: 10.1111/cbdd.13901

RESEARCH ARTICLE

WILEY

Rational design of novel *N*-alkyl amine analogues of noscapine, their chemical synthesis and cellular activity as potent anticancer agents

Rajesh Kumar Meher[1] | **Pratyush Pragyandipta**[1] | **Ravi K. Pedapati**[2] | **Praveen K. R. Nagireddy**[2] | **Srinivas Kantevari**[2] | **Arnab K. Nayek**[1] | **Pradeep K. Naik**[1]

[1]Department of Biotechnology and Bioinformatics, Centre of Excellence in Natural Products and Therapeutics, Sambalpur University, Sambalpur, India

[2]Fluoro and Agrochemicals Division, CSIR-Indian Institute of Chemical Technology, Hyderabad, India

Correspondence
Pradeep K. Naik, Department of Biotechnology and Bioinformatics, Centre of Excellence in Natural Products and Therapeutics, Sambalpur University, Sambalpur, India.
Email: pknaik1973@suniv.ac.in

Funding information
Indian Council of Medical Research (ICMR), Govt. of India, Grant/Award Number: 5/13/13/2019/NCD-III

Abstract

The scaffold structure of noscapine (an antitussive plant alkaloid) was modified by inducting *N*-aryl methyl pharmacophore at C-9 position of the isoquinoline ring to rationally design and screened three novel 9-(*N*-arylmethylamino) noscapinoids, **15–17** with robust binding affinity with tubulin. The selected 9-(*N*-arylmethylamino) noscapinoids revealed improved predicted binding energy of −6.694 kcal/mol for **15**, −7.118 kcal/mol for **16** and −7.732 kcal/mol for **17**, respectively in comparison to the lead molecule (−5.135 kcal/mol). These novel derivatives were chemically synthesized and validated their anticancer activity based on cellular studies using two human breast adenocarcinoma, MCF-7 and MDA-MB-231, as well as with a panel of primary breast tumor cells. These derivatives inhibited cellular proliferation in all the cancer cells that ranged between 3.2 and 32.2 μM, which is 11.9 to 1.8 fold lower than that of noscapine. These novel derivatives effectively arrest the cell cycle in the G2/M phase followed by apoptosis and appearance of apoptotic cells. Thus, we conclude that 9-(*N*-arylmethyl amino) noscapinoids, **15–17** have a high probability to be a novel therapeutic agent for breast cancers.

KEYWORDS

anticancer agents, breast cancer, *N*-arylmethylamino-noscapinoids, noscapine, tubulin binding

1 | INTRODUCTION

Noscapine is an opium alkaloid. It is non-narcotic, non-sedative and does not produce elation or addiction (Martindale, 1977). In the clinic, it has been used as orally available, safe antitussive drug for over 40 years. The ability of noscapine to bind microtubule, suppressing its dynamic instability and thereby inhibiting cell proliferation as well as induction of apoptosis encouraged a number of investigators to examine its anticancer potential (Jordan & Wilson, 2004; Landen et al., 2002; Ye et al., 1998; Zhou, Gupta, et al., 2002). Toward increment of its anticancer potential, a number of synthetic derivatives were synthesized and evaluated (Landen et al., 2002, 2004; Ye et al., 1998; Zhou et al., 2003; Zhou, Panda, et al., 2002). Interestingly, unlike the classic microtubule-targeted agents, taxanes (that over polymerizes microtubules and bundles them) and vincas (that depolymerizes microtubules), noscapine and its derivatives do not significantly alter the polymer and monomer ratio of microtubules and were known as a "kindler" microtubule poison. From clinical prospective, noscapine is also very unique from many other microtubule-targeted agents in a sense that it is lacking of substantial cytotoxicity to normal cells. It is also demonstrated to have very little or no toxicity to healthy volunteers (Dahlström et al., 1982; Jensen et al., 1992; Karlsson

Journal of Molecular Graphics and Modelling 106 (2021) 107933

Contents lists available at ScienceDirect

Journal of Molecular Graphics and Modelling

journal homepage: www.elsevier.com/locate/jmgm

Rational design, chemical synthesis and cellular evaluation of novel 1,3-diynyl derivatives of noscapine as potent tubulin binding anticancer agents

Amiya Kumar Patel [a], Rajesh Kumar Meher [a], Praveen Kumar Reddy [b], Ravi Kumar Pedapati [b], Pratyush Pragyandipta [a], Srinivas Kantevari [b], Manas Ranjan Naik [c], Pradeep Kumar Naik [a,*]

[a] Centre of Excellence in Natural Products and Therapeutics, Department of Biotechnology and Bioinformatics, Sambalpur University, Jyoti Vihar, Burla, Sambalpur-768019, Odisha, India
[b] Fluoro and Agrochemicals Division, CSIR-Indian Institute of Chemical Technology, Hyderabad 500 007, India
[c] Department of Pharmacology, SLN Medical College, Koraput-764020, Odisha, India

ARTICLE INFO

Keywords:
Noscapine
1, 3-Diynyl-noscapinoids
Tubulin binding
Anticancer agents
Breast cancer

ABSTRACT

We present a new class of derivatives of noscapine, 1,3-diynyl-noscapinoids of an antitussive plant alkaloid, noscapine based on our *in silico* efforts that binds tubulin and displays anticancer activity against a panel of breast cancer cells. Structure-activity analyses pointed the C-9 position of the isoquinoline ring which was modified by coupling of 1,3-diynyl structural motifs to rationally design and screened a series of novel 1,3-diynyl-noscapinoids (**20–22**) with robust binding affinity with tubulin. The selected 1,3-diynyl-noscapinoids, **20–22** revealed improved predicted binding energy of −6.568 kcal/mol for **20**, -7.367 kcal/mol for **21** and -7.922 kcal/mol for **22**, respectively in comparison to the lead molecule (−5.246 kcal/mol). These novel derivatives were chemically synthesized and validated their anticancer activity based on cellular studies using two human breast adenocarcinoma, MCF-7 and MDAMB-231, as well as with a panel of primary breast cancer cells isolated from patients. Interestingly, all these derivatives inhibited cellular proliferation in all the cancer cells that ranged between 6.2 to 38.9 μM, which is 6.7 to 1.5 fold lower than that of noscapine. Unlike previously reported derivatives of noscapine that arrests cells in the S-phase, these novel derivatives effectively inhibit proliferation of cancer cells, arrests cell cycle in the G2/M-phase followed by apoptosis and appearance of apoptotic cells. Thus, we conclude that 1,3-diynyl-noscapinoids have great potential to be a novel therapeutic agent for breast cancers.

1. Introduction

Currently available breast cancer chemotherapeutic regimens have been encumbered by poor selectivity because most antiproliferative drugs are toxic not only to tumor cells but also to body's non-neoplastic cells [1–5]. This unsatisfactory situation has driven intensive research over the last few decades towards more specific and less toxic anticancer drugs. Noscapine, a safe anti-tussive agent, is an excellent choice of drug to use however, because of the nature of its action; it is not harmful to healthy cells [6,7]. It is also well tolerated in humans and has been shown to be non-toxic in healthy volunteers including pregnant mothers [8–10]. Noscapine, has been discovered as a novel selective tubulin-binding anticancer drug that does not change the steady state monomer/polymer ratio of tubulin over a wide range of concentrations. This is a unique edge over currently-available antimicrotubule drugs that either inhibit microtubule disassembly (taxanes, epothilone) or inhibit tubulin assembly (vincas, eribulin, estramustine, drug-antibody complexes with dolastatin 10 and maytansine analogs) and hence cause various debilitating toxicities such as leucocytopenias, diarrhea, alopecia and peripheral neuropathies [4,5,11]. Owing to absence of extreme effects on microtubules, noscapine does not cause any hemo-, immuno- and neuronal toxicity. The basis for not killing healthy cells seems to be that noscapine subtly attenuates microtubule dynamics just enough to activate the mitotic checkpoints in normal cells, and halts their cell-cycle reversibly until the drug is cleared by metabolism and excretion [12]. Whereas, cancer cells upon noscapine treatment do not halt for long durations due to mutational lesions in their checkpoint mechanisms; instead they continue to traverse the cell-cycle without cell

* Corresponding author.
E-mail addresses: pknaik1973@gmail.com, pknaik1973@suniv.ac.in (P.K. Naik).

https://doi.org/10.1016/j.jmgm.2021.107933
Received 14 November 2020; Received in revised form 29 March 2021; Accepted 19 April 2021
Available online 5 May 2021

Medicinal Chemistry & Drug Discovery

In-Silico-Inspired Design of 1,3-Diynyl Congeners of Noscapine as Promising Tubulin-Binding Anticancer Agent: Chemical Synthesis and Cellular Activity with Breast Cancer Cell Lines

Pratyush Pragyandipta,[a] Rajesh K. Meher,[a] Manas R. Naik,[b] Praveen K. R. Nagireddy,[c] Ravi K Pedapati,[c] Srinivas Kantevari,*[c] and Pradeep K. Naik*[a]

A panel of 1,3-diynyl-noscapinoids (**20**–**22**) were strategically designed to increase the anticancer activity of the lead molecule, noscapine. Structure-activity analyses revealed strong predicted free energy of binding ($\Delta G_{bind,pred}$) of −6.694, −7.294 and −7.468 kcal/mol, for **20**–**22** respectively compared to noscapine (experimental free energy of binding ($\Delta G_{bind,expt}$) is −5.246 kcal/mol). These novel derivatives were demonstrated to bind tubulin by fluorescence quenching assay and Far-UV circular dichroism. Further, they were tested to exhibit potent cytotoxic activity compared to noscapine using two human breast cancer cell lines. The IC_{50} value for noscapine, **20**, **21** and **22** has been derived to be 35.2, 27.3, 18.7 and 12.7 μM using MCF7 and 39.6, 31.4, 22.5 and 16.1 μM using MDAMB-231. These derivatives were found to arrest cell cycle in the G2/M-phase followed by apoptosis and appearance of TUNEL-positive cells. Thus, we conclude that 1,3-diynyl derivatives of noscapine have great potential to be a novel therapeutic agent for breast cancers.

Introduction

Microtubules (MTs) play a significant role in many of the cellular functions including cell division. Therefore, it has been used as a suitable drug target for the development of chemotherapeutic drugs against rapidly dividing cancer cells. The effectiveness of MT targeting drugs has been confirmed by the clinical use of vinca alkaloids and taxanes for the treatment of a wide variety of human cancers. However, these anti-MT agents are known to induce undesired, dose-limiting toxicities in patients.[1,2] The clinical success of taxanes has impelled world-wide to search for natural compounds targeted to MT but with improved characteristics. In quest for finding such a compound, without having any side effects, noscapine (an opium alkaloid) was discovered that binds tubulin dimer with a 1:1 stoichiometry, arrests a variety of mammalian cells in mitosis and causes apoptosis.[3] It has been used as a cough suppressant since the mid 1950s and illustrating a good safety profile. It is also found to be well-tolerated in humans without having any severe toxicity.[4,5,6] Furthermore, it inhibits the proliferation of cancer cells of different tissue origin and regresses effectively the implanted tumor in animal models without any side effects.[3,7–10] The minimal side effect of noscapine is due to its selectivity in killing the cancer cells without hampering the normal healthy cells. It was revealed that normal healthy cells respond to noscapine (or its tested derivatives) treatment by arresting mitosis for long period of time, at least 12 to 24 hours. However, if noscapine exposure is removed prior to this time period by replenishing with fresh drug free culture medium, the arrested cells resume the progression of the normal mitosis producing viable daughter cells.[7] This innovative research has prodded a huge enthusiasm for the scientific world to use noscapine and its synthetic analogues for the therapy of malignancy.

In order to enhance the anti-proliferative activity of noscapine we have tried to develop a new series of its derivatives (called diyne derivatives) by strategically modifying its scaffold structure and supported by our in silico efforts. These derivatives were then chemically synthesized and validated their anti-proliferative activity to cancer cells using two human carcinoma cell lines, MCF-7 and MDAMB-231. The novel derivatives were found to bind tubulin heterodimer with increased binding affinity, inhibit proliferation of neoplastic cell and causes selective G2/M arrest in cancer cells. The mitotic catastrophe in cancer cells is then followed by induction of apoptosis.

[a] *P. Pragyandipta, R. K. Meher, Prof. P. K. Naik*
Centre of Excellence in Natural Products and Therapeutics, Department of Biotechnology and Bioinformatics, Sambalpur University, Jyoti Vihar, Burla, Sambalpur-768019, Odisha, India
Phone No.: +91-9479268802
E-mail: pknaik1973@suniv.ac.in
[b] *M. R. Naik*
Department of Pharmacology, SLN Medical College Koraput-464020 Odisha, India
[c] *P. K. R. Nagireddy, R. K Pedapati, Dr. S. Kantevari*
Fluoro and Agrochemicals Division, CSIR-Indian Institute of Chemical Technology, Hyderabad 500 007, India
E-mail: ksrinivas@iict.res.in

Supporting information for this article is available on the WWW under https://doi.org/10.1002/slct.202004723

JOURNAL OF BIOMOLECULAR STRUCTURE AND DYNAMICS
https://doi.org/10.1080/07391102.2021.1982008

Development of 1,3-diynyl derivatives of noscapine as potent tubulin binding anticancer agents for the management of breast cancer

Rajesh Kumar Meher[a], Pratyush Pragyandipta[a], Praveen Kumar Reddy[b], Ravikumar Pedaparti[b], Srinivas Kantevari[b] and Pradeep K. Naik[a]

[a]Centre of Excellence in Natural C and Therapeutics, Department of Biotechnology and Bioinformatics, Sambalpur University, Sambalpur, Odisha, India; [b]Fluoro and Agrochemicals Division, CSIR-Indian Institute of Chemical Technology, Hyderabad, India

Communicated by Ramaswamy H. Sarma

ABSTRACT

We developed 1,3-diynyl derivatives of noscapine (an opium alkaloid) through *in silico* combinatorial approach and screened out a panel of promising derivatives that bind tubulin and display anticancer activity. The selected derivatives such as 9-4-^{t}Bu-Ph-Diyne **(20p)**, 9-3,4-Di-Cl-Diyne **(20k)** and 9-3,4-Di-F-Diyne **(22s)** noscapinoids revealed improved predicted binding energy of −6.676 kcal/mol for **20p**, −7.294 kcal/mol for **20k** and −7.750 kcal/mol for **20s** respectively in comparison to noscapine (−5.246 kcal/mol). These 1,3-diynyl derivatives **(20p, 29k** and **20s)** were strategically synthesized in high yields by regioselective modification of noscapine scaffold and HPLC purified (purity is >96%). The decrease in intrinsic fluorescence of purified tubulin to 8.39%, 17.39% and 25.47% by **20p, 20k** and **20s** respectively, compared to control suggests their binding capability to tubulin. Their cytotoxicity activity was validated based on cellular studies using two human breast adenocarcinoma (MCF-7 and MDA-MB-231), a panel of primary breast tumor cells and one normal human embryonic kidney cell (293 T). The 1,3-diynyl noscapinoids, **20p, 20k** and **20s** inhibited cellular proliferation in all the cancer cells that ranged between 6.2 and 38.9 μM, without affecting the normal healthy cells (cytotoxicity is <5% at 100 μM). Further, these novel derivatives arrest cell cycle in the G2/M-phase, followed by induction of apoptosis to cancer cells. Thus, we conclude that 1,3-diynyl-noscapinoids have great potential to be a novel therapeutic agent for breast cancers.

ARTICLE HISTORY
Received 8 July 2021
Accepted 13 September 2021

KEYWORDS
Noscapine; 1, 3-diynyl-noscapinoids; tubulin binding; anticancer agents; breast cancer

Introduction

Currently available breast cancer chemotherapeutic regimens have been plagued with serious toxicity (peripheral neuropathies, gastrointestinal toxicity, myelosuppression, and immunosuppression) owing to their non-selective action and extreme over polymerizing or depolymerizing effects on microtubules (Crown & O'Leary, 2000; Pace et al., 1996; Rowinsky & Donechwer, 1991; Theiss & Meller, 2000; Topp et al., 2000). This unsatisfactory situation has driven intensive research over the last few decades to find novel tubulin binding anticancer agents that are more specific to cancer cells without having severe side effects. Noscapine, a safe anti-tussive drug, is an excellent choice of drug to use and because of the nature of its action; it is not harmful to healthy cells or healthy volunteers including pregnant mothers (Dahlström et al., 1982; Jensen et al., 1992; Karlsson et al., 1990; Ye et al., 1998; Zhou et al., 2006). It was found that noscapine binds stoichiometrically to tubulin (one noscapine molecule for each $\alpha\beta$-tubulin dimer), modifies tubulin compliance and arrests mammalian cells at the mitotic phase (Lettre, 1954). However, unlike vinca alkaloids and taxanes, it does not induce over-polymerization, depolymerization or any change in the general interphase microtubule organization. Because of its subtle effect on the kinetic parameters of dynamic instability of microtubules, it inhibits mitosis at prometaphase and induces apoptosis, specifically to cancer cells without affecting normal cells (Warolin, 1999). Further, in comparison to the other microtubule binding drugs such as taxanes and vinca alkaloids, noscapine offers various advantages in cancer treatment. It arrests a variety of mammalian cells including drug resistant variants in mitosis and targets them for apoptosis (Jordan et al., 1993; Karlsson et al., 1990; Wang et al., 2005). It is a poor substrate for drug pumps (poly glycoproteins and MDR-related proteins) which constitute a major cause of drug resistance (Karlsson et al., 1990). It inhibits the progression of murine melanoma, lymphoma, glioblastoma and human breast tumors implanted in nude mice, without any detectable toxicity (Jordan et al., 1993; Karlsson et al., 1990; Wang et al., 2005). It doesn't cause any immunological and neurological toxicity. It is orally administered and hence is devoid of any anaphylactic reactions (Jordan et al., 1993; Karlsson et al., 1990; Wang et al., 2005). It shows a mean bioavailability of ~30–32% over a dose range of 10 mg/kg to 300 mg/kg in mice (Wang et al., 2005). However, noscapine has low cytotoxicity. The values of IC_{50} remain within the high micromolar ranges (~21.1 to 100 μM)

CONTACT Pradeep Kumar Naik pknaik1973@suniv.ac.in Centre of Excellence in Natural Products and Therapeutics, Department of Biotechnology and Bioinformatics, Sambalpur University, Sambalpur, Odisha, India

Supplemental data for this article can be accessed online at https://doi.org/10.1080/07391102.2021.1982008.

SAR AND QSAR IN ENVIRONMENTAL RESEARCH
https://doi.org/10.1080/1062936X.2021.1891567

Taylor & Francis
Taylor & Francis Group

9-Arylimino noscapinoids as potent tubulin binding anticancer agent: chemical synthesis and cellular evaluation against breast tumour cells

A.K. Patel[a], R.K. Meher[a], P.K. Nagireddy[b], P. Pragyandipta[a], R.K. Pedapati[b], S. Kantevari[b], and P.K. Naik[a]*

[a]Centre of Excellence in Natural Products and Therapeutics, Department of Biotechnology and Bioinformatics, Sambalpur University, Burla, Sambalpur, India; [b]Fluoro and Agrochemicals Division, CSIR-Indian Institute of Chemical Technology, Hyderabad, India

ABSTRACT

A library of 9-arylimino derivatives of noscapine was developed by coupling of Schiff base containing imine groups. Virtual screening using molecular docking with tubulin revealed three molecules, 12–14 that bind with high affinity. An improved predicted free energy of binding (FEB) of −5.390, −6.506 and −6.679 kcal/mol for the molecules 12–14 was found compared to noscapine (−5.135 kcal/mol). Furthermore, molecular dynamics simulation in combination with Molecular Mechanics Poisson-Boltzmann Surface Area (MM-PBSA) revealed robust binding free energy of −166.03, −169.75 and −170.63 kcal/mol for the molecules 12, 13 and 14, respectively. These derivatives were strategically synthesized and experimentally validated for their anticancer activity. Tubulin binding assay revealed substantial binding of molecules 12–14 with purified tubulin. Further, their anticancer activity was demonstrated using two cancer cell lines (MCF-7 and MDAMB-231) and a panel of primary breast tumour cells. All these derivatives inhibited cellular proliferation in all the cancer cells that ranged between 30.1 and 5.8 μM, which is 1.7 to 7.52 fold lower than that of noscapine. Further, these novel derivatives arrest cell cycle in the G2/M-phase followed by induction of apoptosis. Thus, 9-arylimino noscapinoids 12–14 have a great potential to be a novel therapeutic agent for breast cancers.

ARTICLE HISTORY
Received 12 November 2020
Accepted 14 February 2021

KEYWORDS
Noscapine; 9-arylimino noscapinoids; tubulin binding; anticancer agents; breast cancer

Introduction

Microtubule dynamics is absolutely crucial for the mitotic cell division of the cells. Interference with microtubule dynamics often leads to programmed cell death and thus microtubule-binding drugs are currently used to treat various malignancies in the clinic [1]. Although useful, currently used microtubule drugs such as *Vinca* alkaloids and taxanes are limited due to their undesirable toxicity [2–5]. The wonderful promise of taxol in managing breast cancers justifies further effort to discover novel mitotic inhibitors that may have fewer side effects and that can be easily administered.

CONTACT P.K. Naik pknaik1973@gmail.com
Supplementary data for this article can be accessed at: https://dx.doi.org/10.1080/1062936X.2021.1891567

Analytical Chemistry Letters
https://www.tandfonline.com/loi/tacl

Taylor & Francis
Taylor & Francis Group

ISSN: 2229-7928 (Print); ISSN: 2230-7532 (Online)

Article

Structure Based Design of Tubulin Binding 9-Arylimino Noscapinoids: Chemical Synthesis and Experimental Validation Against Breast Cancer Cell Lines

Pratyush Pragyandipta [1], Rajesh Kumar Meher [1], Praveen Kumar Reddy [2], Ravikumar Pedaparti [2], Srinivas Kantevari [2] and Pradeep K. Naik [1]*

[1] Centre of Excellence in Natural Products and Therapeutics, Department of Biotechnology and Bioinformatics, Sambalpur University, Jyoti Vihar, Burla, Sambalpur-768019, Odisha, India

[2] Fluoro and Agrochemicals Division, CSIR-Indian Institute of Chemical Technology, Hyderabad 500007, India

* *Corresponding Author: pknaik1973@suniv.ac.in (Pradeep K. Naik)*

Received 29 August 2021; Received in revised form 15 November 2021; Accepted 16 November 2021Volorumq

Abstract: A novel class of noscapine derivatives known as 9-arylimino noscapinoids was designed by substituting arylimino groups (Schiff bases) at the C-9 position. These molecules were docked with αβ-tubulin complex and a panel of three top scoring molecules, 4-6 based on docking score were screened out. These molecules bind tubulin with robust predicted binding energy of -37.24 kcal/mol and -45.41 kcal/mol for 4, -39.73 kcal/mol and -47.74 kcal/mol for 5, and -43.62 kcal/mol and -49.72 kcal/mol for 6 respectively compared to noscapine (-34.47 kcal/mol and -40.27 kcal/mol) using molecular mechanics/Poisson-Boltzmann surface area (MM/PBSA) and molecular mechanics/generalized Born surface area (MM/GBSA). These three molecules were chemically synthesized and demonstrated experimentally to bind tubulin with high affinity compared to noscapine. The anti-proliferative activity of 4-6 revealed inhibitory concentration (IC_{50} value) in between 3.6 to 32.6 μM using MCF-7 and MDA-MB-231 human breast cancer cell lines and a group of primary breast tumor cells. All three molecules were shown to inhibit the mitotic progression at the G2/M phase and induce apoptosis to cancer cells at a different level. Thus, we conclude that 9-arylimino noscapinoids 4-6 have tremendous potential as chemotherapeutic agents for the treatment of breast cancer.

Keywords: 9-arylimino noscapinoids; Anticancer agents; Breast cancer; Molecular docking; Noscapine; Tubulin targeting.

Introduction

Microtubule-interacting drugs, for example, taxols and vinca alkaloids have been used in the clinic for the treatment of various malignancies. However, these drugs are known to cause severe dose-dependent toxicities in patients such as peripheral neuropathy, systemic toxicity, and allergic reactions [1,2]. More importantly, patients are developing resistance against taxol. Thus, the wonderful promise of taxol in managing breast cancers justifies further efforts to discover novel mitotic inhibitors. Better yet, it would be additionally useful if other novel anti-mitotic agents have fewer side effects and are easily administered. In a quest of finding such compounds, the natural compounds were screened and noscapine (an opium alkaloid that is in the clinic as a safe anti-tussive drug)

DOI: 10.1080/22297928.2021.2009029

JOURNAL OF BIOMOLECULAR STRUCTURE AND DYNAMICS
https://doi.org/10.1080/07391102.2021.1889668

Taylor & Francis
Taylor & Francis Group

In silico design of novel tubulin binding 9-arylimino derivatives of noscapine, their chemical synthesis and cellular activity as potent anticancer agents against breast cancer

Rajesh Kumar Meher[a], Praveen Kumar Reddy Nagireddy[b], Pratyush Pragyandipta[a], Srinivas Kantevari[b], Satyandra Kumar Singh[c], Vijay Kumar[d] and Pradeep K. Naik[a]

[a]Department of Biotechnology and Bioinformatics, Centre of Excellence in Natural Products and Therapeutics, Sambalpur University, Sambalpur, India; [b]Organic Chemistry Division-II (CPC Division), CSIR-Indian Institute of Chemical Technology, Hyderabad, India; [c]Center For Advance Research, Stem Cell and Tissue Culture Laboratory, King George's Medical University, Lucknow, India; [d]Department of Surgical Oncology, King Georgès Medical University, Lucknow, India

Communicated by Ramaswamy H. Sarma

ABSTRACT

We present a series of 9-arylimino derivatives of noscapine (an antitussive plant alkaloid) that binds to tubulin and displaying anticancer activity against a panel of breast cancer cells. These compounds were rationally designed by coupling of Schiff base containing imine groups at position-9 of the isoquinoline ring of noscapine. Based on a combination of Glide docking and free energy of binding (FEB) calculation, we have screened a panel of three 9-compounds, **12–14** with improved binding affinity with tubulin compared to noscapine. The predicted FEB is −6.166 kcal/mol for **12**, −6.411 kcal/mol for **13** and −7.512 kcal/mol for **14**. In contrast, the predicted FRB of noscapine is −5.135 kcal/mol. These novel derivatives were strategically synthesized and validated their anticancer activity based on cellular studies using two human breast adenocarcinoma, MCF-7 and MDAMB-231, as well as with a panel of primary breast tumor cells isolated from patients. Interestingly, all these derivatives inhibited cellular proliferation in all the cancer cells that ranged between 3.6 and 26.4 μM, which is 11.02–2.03 fold lower than that of noscapine. Unlike previously reported derivatives of noscapine that arrest cells in the S-phase, these novel derivatives effectively inhibit proliferation of cancer cells, arrest the cell cycle in the G2/M-phase and induced apoptosis. Thus, we conclude that 9-arylimino derivatives of noscapine have great potential to be a novel therapeutic agent for breast cancers.

ARTICLE HISTORY
Received 1 November 2020
Accepted 6 February 2021

KEYWORDS
Noscapine; 9-arylimino noscapinoids; tubulin binding; anticancer agents; breast cancer

Introduction

Chemotherapy remains the current method of therapy for metastatic cancer, in that, along with DNA binding drugs, microtubule (MT)-interacting drugs, for example, taxanes, vinca alkaloids, estramustine, halaven and ixempra are utilized for the treatment of localized and metastatic breast cancers. However, these medications possess severe toxicities such as leucocytopenias, diarrhea, alopecia, peripheral neuropathies, etc., resulting in poor quality of life (Kavanagh & Kudelka, 1993; Rowinsky & Donehower, 1991). The wonderful promise of taxol in managing breast cancers justifies further effort to discover novel mitotic inhibitors that may have less side effects and that can be easily administered.

In a quest of finding such molecule, by rational screening of natural compounds, noscapine (an opium alkaloid, non-narcotic, orally available, safe antitussive drug for over 40 years) was discovered. It binds to tubulin heterodimer with a 1:1 stoichiometry, alters the secondary structure of tubulin and arrests the dividing cells at mitosis (Ye et al., 1998). However, the cancer cells selectively undergo apoptosis because of the compromised cell cycle checkpoints, without hampering the normal dividing cells. The careful real-time observation of individual polymerizing MTs *in vitro* and tracking the plus end growth over time revealed that noscapine affected MT-dynamics primarily by enhancing the time period that MTs spend in an attenuated pause state rather than engaging into active depolymerization and repolymerization (Zhou et al., 2002). Because noscapine only affects MT dynamics, cellular functions that do not require exquisite control of MT dynamics may not be interrupted. Noscapine, therefore, has no detectable neurotoxic effect on the histologies of peripheral nerves (Landen et al., 2004). It has favorable pharmacokinetics *in vivo* (clearance within ∼10 h) (Jordan & Wilson, 1998) and has no significant side effects (Ke et al., 2000; Landen et al., 2002). *In vitro* as well as mouse xenograft models have shown that noscapine and its analogs are useful in treatment of cancer of different tissue origin (Ke et al., 2000; Ye et al., 1998; Zhou et al., 2003). These properties enable its therapeutic use at high concentrations (∼150–300 mg/kg body weight) in murine models of

CONTACT Pradeep K. Naik pknaik1973@gmail.com; pknaik1973@suniv.ac.in Centre of Excellence in Natural Products and Therapeutics, Department of Biotechnology and Bioinformatics, Sambalpur University, Jyoti Vihar, Burla, Sambalpur 768019, Odisha, India

Supplemental data for this article can be accessed online at https://doi.org/10.1080/07391102.2021.1889668.